

DEVELOPING SMALL MOLECULE LIGANDS FOR THE STUDY OF BROMODOMAIN-HISTONE INTERACTIONS

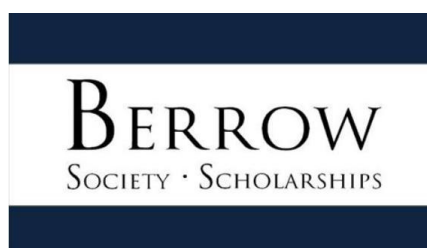


A thesis submitted for the degree of
Doctor of Philosophy in Organic Chemistry

Michael Brand

Lincoln College, University of Oxford

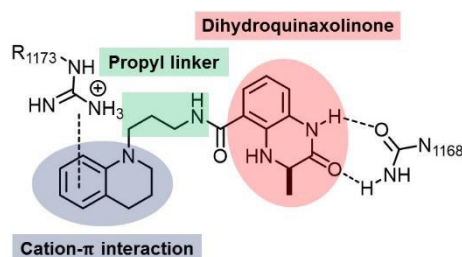
Supervisor: Prof. Stuart J. Conway



Developing small molecule ligands for the study of bromodomain-histone interactions

Dynamic changes in DNA methylation, and post-translational modifications on histone proteins which DNA wraps around, form the basis of epigenetic transfer of information. The histone code refers to different combinations of epigenetic marks, each mediating transcription in a specific manner. Bromodomains are acetyl-lysine readers of the histone protein which interact selectively with acetylated lysine residues on histones. This protein-protein interaction alters gene expression levels, causing specific downstream effects. The human bromodomain family consists of 61 unique proteins, which are divided into eight subfamilies based on sequence similarity. Most research has been focused on the bromodomain and extra C-terminal (BET) family, which has yielded 14 compounds currently in clinical trials. However, only a few selective ligands and no compounds in clinical trials have been reported for other bromodomain families.

Herein is reported, an extensive structure activity relationship of a potent CREBBP bromodomain ligand. The focus was on the cation- π interaction between R1173 and the tetrahydroquinaxolinone, and a good correlation between the computationally calculated electrostatic surface



potential and the CREBBP bromodomain binding affinity was observed. Attempts to increase the selectivity of the ligand over the BET bromodomain were unsuccessful. The stability of the dihydroquinaxolinone headgroup was optimised by ring size expansion, which maintained CREBBP affinity and binding mode – the latter of which was confirmed by X-Ray crystallography. The propyl linker was modified by introducing a *gem*-difluoro group, and due to the conformational effect of the gauche-gauche interaction, a 3-fold affinity increase was observed.

A second project in this dissertation reports the development of a small, modular photo-affinity based probe based on a 3,5-dimethylisoxazole acetyl lysine mimic. This probe could be crosslinked to purified bromodomain proteins with up to 30% efficiency and subsequently modified *via* CuAAC chemistry to attach a fluorophore or biotin tag. The probe can crosslink to BRD4(1), CREBBP, WDR9(2) and the parasitic bromodomain TcBDF3.



SCHOOL OF CHEMISTRY

DECLARATION OF AUTHORSHIP

Name: Michael Brand

Candidate number: 686826

College: Lincoln College

Supervisor: Prof. Stuart J. Conway

Title of thesis: Developing small molecule ligands for the study of bromodomain-histone interactions.

Word count: _____

Please tick to confirm the following:

I have read and understood the University's disciplinary regulations concerning conduct in examinations and, in particular, the regulations on plagiarism.

I have read and understood the Education Committee's information and guidance on academic good practice and plagiarism at www.admin.ox.ac.uk/edc/goodpractice.

The dissertation I am submitting is entirely my own work except where otherwise indicated.

It has not been submitted, either partially or in full, for another Honour School or qualification of this University (except where the Special Regulations for the subject permit this), or for a qualification at any other institution.

I have clearly indicated the presence of all material I have quoted from other sources, including any diagrams, charts, tables or graphs.

I have clearly indicated the presence of all paraphrased material with appropriate references.

I have acknowledged appropriately any assistance I have received in addition to that provided by my supervisor.

I have not copied from the work of any other candidate.

I have not used the services of any agency providing specimen, model or ghostwritten work in the preparation of this dissertation.

I agree to retain an electronic copy of this work until the publication of my final examination result, except where submission in hand-written format is permitted.

I agree to make any such electronic copy available to the examiners should it be necessary to confirm my word count or to check for plagiarism.

Candidate's signature: Date:

Table of Content

Acknowledgments	viii
Abbreviations	x
1 Introduction	1
1.1 Epigenetics	2
1.1.1 Post Translational Modifications.....	2
1.1.2 Histone Modifications	2
1.1.3 Epigenetic drugs.....	4
1.2 Bromodomains	5
1.2.1 Bromodomain introduction.....	5
1.2.2 Bromodomain structure	6
1.2.3 Bromodomain as drug target.....	7
1.3 CREBBP	8
1.3.1 CREBBP functions.....	8
1.3.2 CREBBP dysfunction in human diseases	9
1.3.3 CREBBP as drug target.....	10
1.4 Current CREBBP bromodomain ligands	10
1.4.1 Early research	10
1.4.2 Optimisation of potent CREBBP ligands	13
1.4.3 Comparison of the small molecule binding modes in CREBBP.....	20
1.5 Project aims	21

2 Optimisation of the dihydroquinoxalinone acetyl lysine mimic ..	23
2.1 Introduction and aims	24
2.2 Synthesis of the 6-membered dihydroquinoxalinone (R)-12	25
2.3 7-membered DHQ analogues (R/S)-26 and 27	27
2.3.1 Computational approach.....	27
2.3.2 Synthesis of (R/S)-26 and 27	29
2.3.3 Stability study of (R)-12 and (R)-26	34
2.4 Biological evaluation of (R)-12, (R/S)-26 and 27	35
2.4.1 Affinities for the CREBBP and BRD4(1) bromodomain	35
2.4.2 ¹⁹ F- NMR on fluorine labelled tryptophan on CREBBP and BRD4(1)...	40
2.4.3 X-ray crystallography.....	43
2.5 Conclusion and discussion	44
3 Structure activity relationship of the cation-π interaction	47
3.1 Introduction and aims	48
3.2 Introduction to cation-π interactions	49
3.3 Electrostatic surface potential of THQ derivatives.....	51
3.4 Synthesis of first generation THQ analogues.....	54
3.4.1 Retrosynthetic analysis	54
3.4.2 Synthesis of the THQ building blocks 72 and 73.....	54
3.4.3 Synthesis of the THQ analogues 86-88 and 96-97	55
3.4.4 Biophysical analysis of 86-88 and 96-97 binding to CREBBP	58

3.5 Second generation of THQ analogues	60
3.5.1 Rationale	60
3.5.2 Synthesis of compounds 98-107	62
3.5.3 Biophysical analysis of 98-107 binding to CREBBP bromodomain	66
3.6 Conclusion.....	69
4 Propyl linker rigidification to increase CREBBP potency.....	71
4.1 Aims	72
4.2 Gem-difluoro propyl linker	72
4.2.1 Rationale	72
4.2.2 Synthesis of the <i>gem</i> -difluorinated compound 141	74
4.2.3 Conformational analysis of the <i>gem</i> -difluorinated compound 141	78
4.2.4 Biological evaluation of 141	79
4.2.5 X-ray crystallography.....	81
4.3 Conclusion.....	82
5 Development of photoaffinity labelling probes for bromodomains	83
5.1 Aims	84
5.2 Introduction	84
5.2.1 Activity based profiling	84
5.2.2 Photo-affinity groups	85
5.2.3 Ligation chemistry.....	86
5.2.4 Examples of ABPs applied to epigenetic proteins	87

5.3 First generation photoaffinity probes	89
5.3.1 Rationale.....	89
5.3.2 Synthesis of the first generation probe	90
5.3.2.1 Synthesis of the benzophenone 168	90
5.3.2.2 Synthesis of the diazirine	93
5.3.3 Biological evaluation	96
5.3.3.1 BRD4(1) affinities of compounds 168 and 184	96
5.2.3.2 Crosslinking experiments with 168 and 184	96
5.4 Second generation photoaffinity probes	99
5.4.1 Rationale.....	99
5.4.2 Synthesis of the second generation probes	100
5.4.2.1 Synthesis of the benzophenone 185	100
5.4.2.2 Synthesis of the diazirine 186	101
5.4.3 Biological evaluation	102
5.4.3.1 BRD4(1) affinities of compounds 185 and 186	102
5.4.3.2 Crosslinking experiments on purified bromodomains.....	103
5.4.3.2 Crosslinking experiments on cell lysates	108
5.5 Conclusion	109
6 Summary	111
7 Experimental Section.....	115
7.1 General experimental	115
7.1.1 Physical methods	115
7.1.2 Biochemical and biophysical methods	115
7.1.3 Synthetic methods	124
7.2 General Procedures	127

7.3 Chapter 2 Procedures	130
7.4 Chapter 3 Procedures	152
7.5 Chapter 4 Procedures	200
7.6 Chapter 5 Procedures	211
Bibliography	233
Appendix.....	247
A Brief description and optimisation of the biophysical assays	248
A1 Differential scanning fluorimetry	248
A2 AlphaScreen™	249
A3 Isothermal Calorimetry	250
B ITC data	254
B1 CREBBP bromodomain	254
B2 BRD4(1) bromodomain	259
C CPMG-NMR data.....	261
D X-ray Crystallisation data.....	264
E Stability of compound 186 in cell lysate	266
F NMR spectra of novel compounds.....	267
G Permission for reprinted figures	429

Acknowledgment

I am very grateful to my supervisor Prof Stuart J. Conway for giving me the opportunity to be part of his research group. I am thankful for his continuous support throughout my DPhil studies and keeping me going when times were difficult.

Thanks to Dr Timothy Rooney for his DPhil work, which provided me with a good starting point for my dissertation.

I have been lucky to be able to collaborate with and receive help from many wonderful people. Dr Oleg Fedorov, Prof. Panagis Filippakopoulos and Dr Sarah Picaud (Structural Genomics Consortium) who provided me with AlphaScreen™ affinity data and protein X-ray crystal structures, which was very helpful for the progress of my project; Dr Anthony Chan for providing me with plenty of purified bromodomain proteins and helping with SDS-PAGE and Western-blot; Prof. Timothy Claridge for training me on the AVC700 and helping me to interpret the CPMG-NMR data; Dr David Staunton for training me on the ITC, DSF and MST and his continuous advice; Gabriella Perell and Prof. William Pomerantz (University of Minnesota) for running selected compounds on ¹⁹F labelled CREBBP and BRD4(1) bromodomains; Larissa See for providing me with AlphaScreen™ affinity data for the photoaffinity probes; Wilian A. Cortopassi and his supervisor Prof. Robert Paton for all the computational simulations. I really enjoyed this fruitful collaboration and working with you all – many thanks!

I would like to thank my working colleague and friend Alex Saunders, who made the time at work as well as outside an even more pleasant experience; Dr Liam O'Connor for providing me with the RKO cell lysate and his good music taste in G11. I am also grateful to Dr Lingbing Kong for all the enjoyable chats about science and life. I wish him all the best for his future career and hope he will soon find a lectureship position. To Sarah Collins, I will never forget the amazing chocolate cake you did, and of course it was always fun having you around. It was a pleasure having lunches and dinners with Charles Evans at either University or Lincoln College. Thanks to Amelie Joffrin for organising the group schedule and organising the group business. To the group members who joined more recently – Corentine (Coco) Laurin, Catherine Haslam, Larissa See – thanks for making the lab atmosphere enjoyable and to Dr Ewen Cadler for his help on NMR problems. I also wish Dr James Clayton and Mus Morgulu success on the continuation of the CREBBP project.

To those that welcomed and trained me when I first joined the group, Dr Sonia Diab, Dr Corinna Kaul, Dr Diane Swallow, Dr Angelina Sekirnik, Dr Laura Jennings, Dr Brian Wilson,

Dr Sam Greyer, and Dr David Hewings. I will always appreciate your kind help and making the start in Oxford easier.

I was lucky to work with smart and humorous Part II and visiting Master students throughout my studies. I especially enjoyed supervising Sophie Willis and Eva Herrlinger and answering many of their challenging questions.

To Alex Saunders, Sarah Collins, Larissa See, Lingbing Kong, Charles Evans, Corentine Laurin, Catherine Haslam and Anthony Chan – thanks for proofreading parts of my thesis; to my supervisor Stuart for proofreading the entire thesis and providing plenty of helpful feedback.

I would also like to acknowledge the NMR service, mass spectrometry service, stores and the workshop team from the Chemistry Research Laboratory who helped the department run like a well-oiled machine.

I must express my gratitude to Pei Jin, my girlfriend, for listening about all my scientific problems and her continued support. I was amazed by her willingness to proof read part of my dissertation. Without you it would have been much more difficult. Also many thanks to my parents Maria and Daniel, my brother and his wife Christian and Nicole for the encouragement.

Finally, I would like to thank Marquise the Amodio and Lincoln College for awarding me the Lord Florey Berrow Scholarship.

List of Abbreviations

ABP	Activity based probe
AcCl	Acetyl chloride
AcOH	Acetic acid
AML	Acute myeloid leukaemia
BCP	Bromodomain containing protein
BET	Bromodomain and extra terminal domain
BnBr	Benzyl bromide
Boc	<i>tert</i> -Butyloxycarbonyl
Boc ₂ O	Di- <i>tert</i> -butyl pyrocarbonate
BRD4	Bromodomain-containing protein 4
CPMG-NMR	Car-Purcell-Meiboom-Gill - NMR
CREBBP	Cyclic adenosine monophosphate-response element-binding protein (CREB) binding protein
CTCL	Cutaneous T cell lymphoma
CuAAC	Copper catalysed alkyne azide cycloaddition
DBU	1,8-Diazabicyclo[5.4.0]undec-7-ene
DFT	Density functional theory
DHQ	Dihydroquinaxolinone
DIPA	<i>N,N</i> -Diisopropylamine
DIPEA	<i>N,N</i> -Diisopropylethylamine
DMF	<i>N,N</i> -Dimethylformamide
DMSO	Dimethyl sulfoxide
DNA	Deoxyribonucleic acid
DNMT1	DNA methyltransferase 1
DSF	Differential scanning fluorimetry
ee	Enantiomeric excess
EP300	E1A binding protein p300
ESP	Electrostatic surface potential
Et ₂ O	Diethyl ether
Et ₃ N	Triethylamine
EtOAc	Ethyl acetate
EtOH	Ethanol
FDA	Food and Drug administration
FRAP	Fluorescence recovery after photobleaching

GE	Group efficiency
HAT	Histone acetyl transferase
HDAC	Histone deacetylase
HEPES	4-(2-Hydroxyethyl)-1-piperazineethanesulfonic acid
HMBC	Heteronuclear multiple bond correlation
HPLC	High performance liquid chromatography
HRP	Horseradish peroxidase
HSQC	Heteronuclear single quantum coherence
IC ₅₀	Half maximal inhibitory concentration
ITC	Isothermal calorimetry
KAc	Acetylated lysine
K _D	Dissociation constant
LDA	Lithium diisopropylamide
LE	Ligand efficiency
<i>m</i> CPBA	meta-Chloroperoxybenzoic acid
MD	Molecular Dynamics
MDS	Myelodysplastic syndrome
MeI	Iodomethane
MeOH	Methanol
mRNA	Messenger ribonucleic acid
MS	Mass spectrometry
MsCl	Methanesulfonyl chloride
<i>n</i> BuLi	<i>n</i> -Butyl lithium
NF-κB	Nuclear factor kappa-light-chain-enhancer of activated B cells
NMP	<i>N</i> -Methyl pyrrolidone
NMR	Nuclear magnetic resonance
PCAF	P300/CBP-associated factor
PCC	Pyridinium chlorochromate
PEG	Polyethylene glycol
PHD	Plant homeodomain
PHIP(2)	PH-interacting protein, 2nd bromodomain
PhMgBr	Phenylmagnesium bromide
PI3PK	Phosphatidylinositol-3-kinase
PPh ₃	Triphenyl phosphine
PPI	Protein-protein interaction
PTCL	Peripheral T cell lymphoma

PTM	Post translational modification
p-TsOH	<i>p</i> -Toluenesulfonic acid
PyBOP	Benzotriazol-1-yl-oxytripyrrolidinophosphonium hexafluorophosphate
QM	Quantum mechanics
RP	Reversed-phase
RTS	Rubinstein-Taybi Syndrome
RuPhos	2-Dicyclohexylphosphino-2',6'-diisopropoxybiphenyl
SAR	Structure activity relationship
SDS PAGE	Sodium dodecyl sulfate polyacrylamide gel electrophoresis
SGC	Structural Genomics Consortium
S _N Ar	Nucleophilic aromatic substitution
SPAAC	Strain-promoted alkyne-azide cycloaddition
<i>T</i> ₂	Spin-spin relaxation time
TBTA	Tris(benzyltriazolylmethyl)amine
<i>t</i> BuOK	Potassium <i>tert</i> -butoxide
TcBDF3	Bromodomain factor 3 in <i>Trypanosoma cruzi</i>
TCEP	tris(2-Carboxyethyl)phosphine
TEMPO	2,2,6,6-Tetramethylpiperidin-1-yl)oxyl
TFA	Trifluoroacetic acid
THF	Tetrahydrofuran
THP	Tetrahydropyran
THQ	Tetrahydroquinolinone
TR-FRET	Time-resolved fluorescence resonance energy transfer
TRIS	<i>Tris</i> (Hydroxymethyl)aminomethane
UV	Ultraviolet light
<i>v</i> _{1/2}	Peak half width

Chapter 1

Introduction

1. Introduction

1.1 Epigenetics

Epigenetics refers to heritable changes in gene expression or cellular phenotype transmitted without variation in the underlying DNA sequence.¹ Instead, the phenotype is altered by changes in the chromatin conformation, regulated by DNA methylation or post-translational modifications on the histone proteins. This controls the accessibility of the transcriptional machinery, which is recruited through reader domains.²⁻⁵ These markers lead to a number of biological effects that are not fully explored nor understood, and as such are of great interest.

1.1.1 Post-Translational Modifications

Post translational modifications (PTMs) are functional groups that are covalently attached to residues on proteins. These modifications are installed by enzymes, after the protein is synthesised by the ribosome, using information encoded in the mRNA sequence.⁶ Post-translation modification is dynamic and reversible, diversifying the information encoded by the genome at any one time by controlling which genes are expressed and to what levels. Common PTMs include reversible phosphorylation on serine, threonine, histidine and tyrosine side chains, acetylation on the ϵ -amine lysine, and in rare cases, serine and threonine, and methylation on lysine and arginine.⁷

1.1.2 Histone Modifications

Histone proteins consist of an H2A-H2B dimer and an H3-H4 tetramer.⁸ In the nucleus, the negative charge of the DNA phosphate backbone facilitates its interaction with positively charged histone proteins, causing DNA to wrap tightly around the histones in 1.7 super-helical turns per nucleosome particle that is stabilised by electrostatic interactions (Figure 1.1).⁷ This structure blocks the access of RNA polymerase, transcription factors, and cofactors to the DNA, and prevents the expression of genes encoded in this tightly bound region, also referred to as the heterochromatin region.⁹ To loosen the inactive

heterochromatin structure to the transcriptionally active euchromatin structure, the N-terminal tail of histones undergo acetylation and lose their negative charge, thus weakening their interaction with the DNA.⁹ In case of the post-translational methylation of the histones, the DNA will be even tighter bound to the histone protein complex. Combinations of different PTMs on histones regulate the accessibility of genes located in proximity, and hence control the expression of these genes. These combinations translate into a number of phenotypes, including those linked to diseases, such as inflammation and cancer.⁹ This dynamic process is also known as the histone code and referred to as the “write, read, erase” concept.¹⁰ There are numerous reviews on histone-modifying enzymes^{9,11,12} and in this dissertation the focus is on acetylation of lysines found in histones.

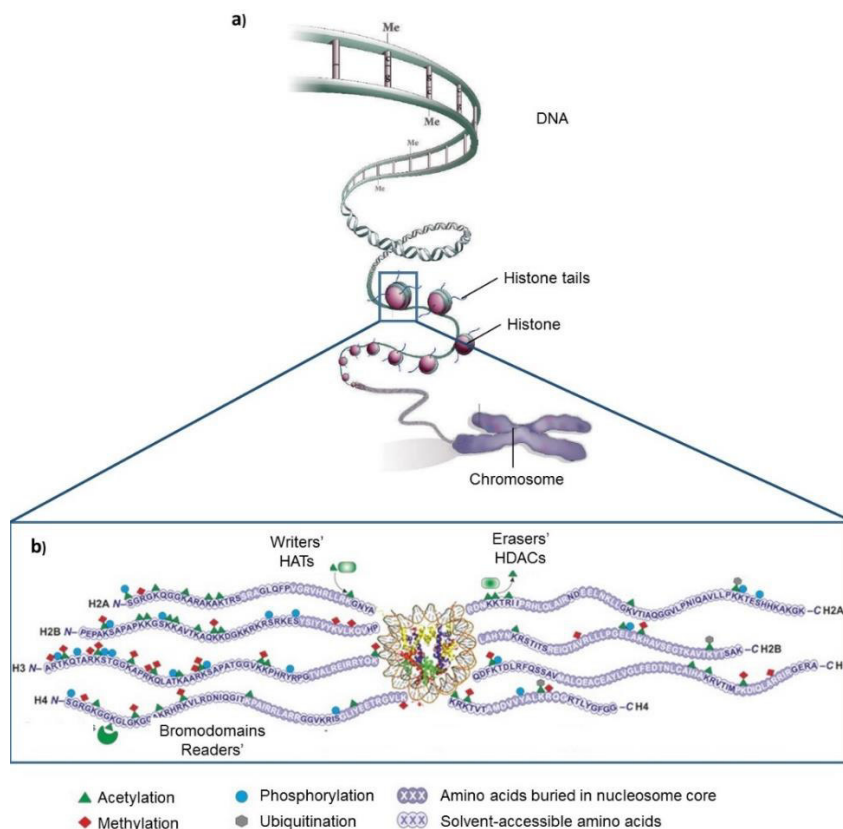


Figure 1.1 a) Chromosomes are compact structures comprising DNA wrapped around histone proteins forming electrostatic interactions. Figure adapted by permission from Macmillan Publishers Ltd: Nature,¹³ copyright (2006). b) Post-translational modifications of histone tails such as acetylation, phosphorylation, methylation or ubiquitination change the interactions between DNA and histones, thus altering the accessibility of transcription machineries to modulate gene expression. Figure adapted by permission from Future Science,⁵ copyright (2014).

The first reported lysine histone modification was by Allfrey and coworkers in 1964 where they demonstrated lysine acetylation and methylation.^{14,15} Acetylation of lysine residues on histone proteins is a dynamic process that involves three different proteins. Histone Acetyl Transferases (HATs) are responsible for acetylation of the lysines, whereas Histone Deacetylases (HDACs) remove the acetylation mark (Figure 1.2).^{16,17} Bromodomains recognise acetylated lysines (KAc) and are present in a total of 46 diverse nuclear and cytoplasmic human proteins.³

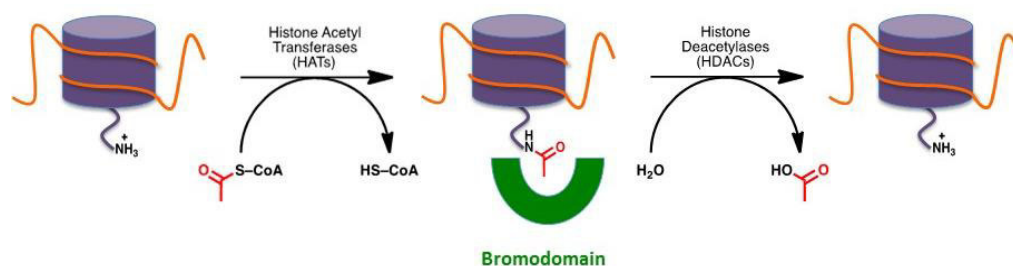


Figure 1.2 Schematic overview of the dynamic process of the lysine acetylation of the histones. Acetylation by histone acetyltransferases (HATs) or deacetylation by histone deacetylases (HDACs) can either weaken or strengthen the electrostatic interactions between DNA and histones, respectively, thus altering the access of transcription machineries to allow gene expression. The bromodomain selectively recognises acetylated lysine and recruits transcription factors to the chromatin. Figure provided with permission by Dr Laura Jennings.

1.1.3 Epigenetic drugs

In the last ten years, there has been much progress in the development of epigenetic drugs. Vidaza™ was the first epigenetic drug approved by the FDA.^{18,19} Vidaza™ is an irreversible DNA methyltransferase 1 (DNMT1) inhibitor used for the treatment of acute myeloid leukaemia (AML) and myelodysplastic syndrome (MDS).¹⁸ More recently, three HDAC inhibitors were approved for clinical treatment of cutaneous T cell lymphoma (CTCL) and peripheral T cell lymphoma (PTCL).²⁰ This recent progress demonstrates that targeting epigenetic proteins is a promising alternative compared to the traditional treatments that target effector proteins.

1.2 Bromodomains

1.2.1 Bromodomain introduction

The first bromodomain-containing protein (BCP) was discovered in the early 90s and was named after the drosophila gene *brahma*, the species from which it was first isolated.^{21,22} Haynes *et al.* speculated in the paper:²¹

"We speculate that the hydrophobic surfaces of the helices and the invariant hydrophobic residues could serve as sites of intramolecular or intermolecular protein-protein interaction. Such interactions could influence the assembly or activity of multicomponent complexes involved in transcription activation or other cellular processes."

Over the next quarter of the century the authors were proven correct.

There are now 61 known human bromodomains, identified by a genome-wide analysis found in 46 different proteins (Figure 1.3).²³ The bromodomains are divided into 8 different families according their sequence homology and structural similarity.

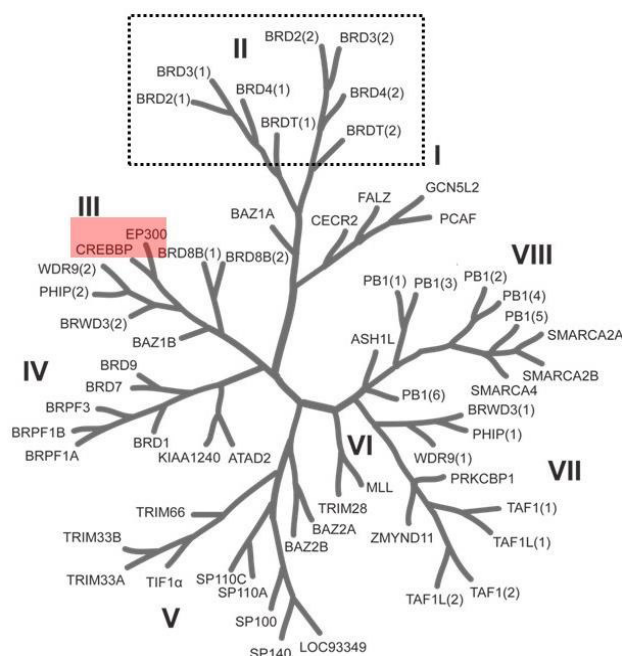


Figure 1.3 Phylogenetic tree of the 61 bromodomains, divided into 8 families according to sequence similarity. The BET bromodomain family is highlighted with a dashed box. The CREBBP and EP300 bromodomain are highlighted in a red box. Reprinted with permission from Journal of Medicinal Chemistry.⁴ Copyright (2013) American Chemical Society.

To date, most research has focused on the family II, also known as the bromodomain and extra terminal domain (BET). However, since 2014, research on non-BET bromodomains has become more commonplace.²⁴ The main focus on this dissertation will be on the non-BET-bromodomain, cyclic adenosine monophosphate-response element-binding protein binding protein (CREBBP), and its close homolog E1A binding protein p300 (EP300). In the following section, the importance of this bromodomain and the discovery of early ligands will be discussed in more detail.

1.2.2 Bromodomain structure

The bromodomains are small, well-conserved domains (~110 amino acid residues) that selectively bind to ϵ -*N*-acetylated lysine. They are formed of four left-handed α -helices (α_Z , α_A , α_B & α_C), which are connected by two loop regions (ZA & BC) (Figure 1.4).²³

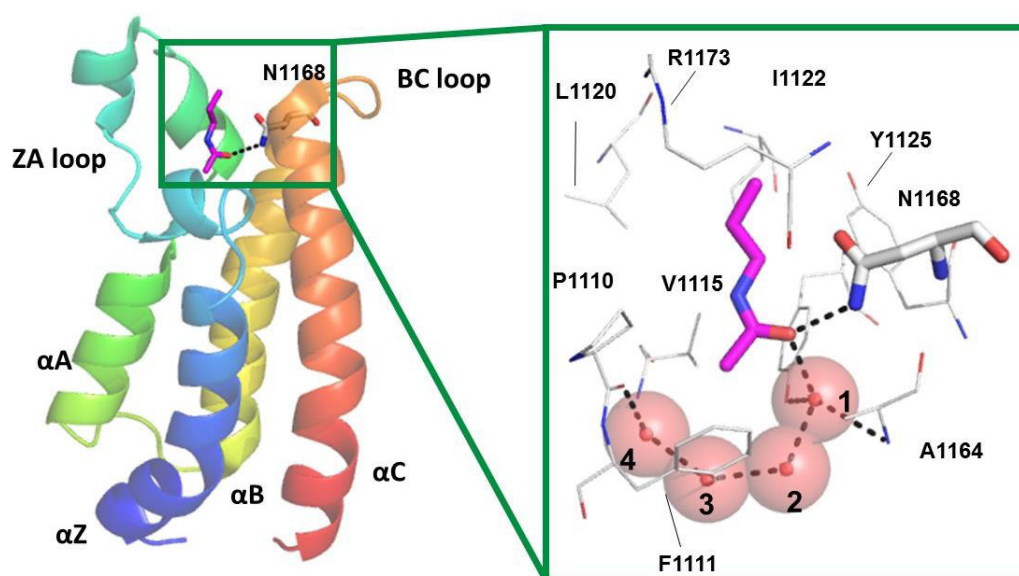


Figure 1.4 Structure of the CREBBP bromodomain. a) The CREBBP bromodomain crystal structure in complex with acetylated lysine (PDB: 3P1C). b) KAc binding pocket, showing the key interaction of acetylated lysine (carbon = magenta). The conserved water molecules in the binding site are shown as red spheres (labelled as 1-4).

There is a low sequence homology for the ZA and BC loops.²³ The well-defined KAc binding pocket consists of mainly hydrophobic amino acids and an asparagine residue (Figure 1.4b).^{23,25} Most of the bromodomains contain this asparagine residue (48), which is a crucial recognition pattern for the protein-protein interaction (PPI) with acetylated lysine

of the histone tail as well as the design for small molecule ligands. The acetylated lysine forms a hydrogen bond to the asparagine residue (N1168), as well as a water mediated hydrogen bond to the conserved water molecule (H₂O 1, Figure 1.4) in the hydrophobic pocket. In all bromodomains, except PB1(5), there are four conserved water molecules inside the KAc binding pocket, and some bromodomains also contain an additional two water molecules in the ZA channel. In the CREBBP bromodomain there is one basic amino acid, an arginine (R1173), close to the KAc binding pocket (Figure 1.4). This can be an important handle for the design of small molecule ligands.

1.2.3 Bromodomains as drug target

Overexpression of BCPs is often implicated in diseases, such as cancer and inflammation, therefore bromodomains are an exciting therapeutic target.²⁶ Unlike most PPIs,²⁷ the bromodomain has a defined binding domain, which makes them more druggable by small molecules. Computational analysis of the 61 bromodomains revealed that family I and II bromodomains are the most druggable, whereas bromodomains in family V-VIII are more difficult to develop ligands for.²⁸

Since the discovery of the benzodiazapine BET bromodomain ligands (+)-JQ1 (**1**)²⁹ and I-BET762,³⁰ research on bromodomain ligands has exploded (Figure 1.5). Much research has been performed on the development of BET bromodomains, where ligands were found to exhibit antitumor activity, reduction of inflammation, treatment for viral infections, and male contraception.^{3-5,24,31} To date, 21 human clinical trials of 14 BET bromodomain ligands are currently in process, with RVX-208 (**4**) already recruiting for Phase III in order to treat cardiovascular diseases (NCT02586155).^{32,33} However, to our knowledge, no non-BET bromodomain ligands are yet in clinical trials.

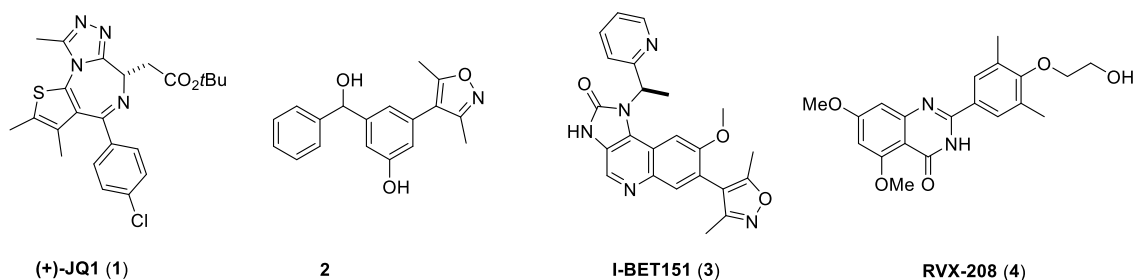


Figure 1.5 Selection of some BET bromodomain ligands.

1.3 CREBBP

1.3.1 CREBBP functions

CREBBP is acetyltransferase enzyme composed of 2414 amino acids, which contains a KIX domain, a bromodomain, a PHD finger, and enzymatic HAT domains (Figure 1.6). This protein contains a high sequence homology (61%) to p300, and hence it is often referred to CREBBP/p300.⁷ In the bromodomain region there is a 97% sequence similarity between CREBBP and p300, which potentially makes it difficult to develop selective probes for either bromodomain.⁷ CREBBP/p300 are transcriptional coactivators for a number of important genes. Over 400 different protein interaction partners are known, which reflects the importance of CREBBP/p300 as key proteins in gene regulatory networks.³⁴ Around 100 of these interactions are involved as CREBBP/p300 acetylation substrates.^{6,7} Furthermore, the CREBBP protein is associated with acetylation of the DNA damage response protein p53, which is linked with cancer.^{35,36} Furthermore it was found that homozygous and heterozygous mice lacking the CREBBP and/or p300 genes did not survive beyond the embryonic stage, indicating the importance of these proteins.^{37,38}

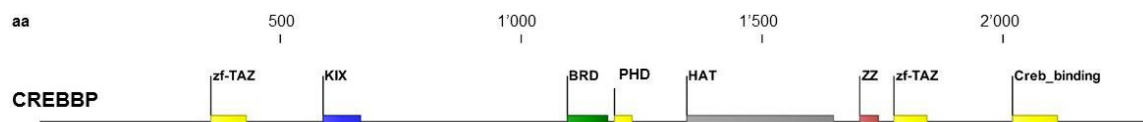


Figure 1.6 CREBBP protein sequence domains highlighted using Pfam version 29.³⁹

1.3.2 CREBBP dysfunction in human diseases

Cancer

The controlled activity of lysine acetyltransferases is essential for maintaining cellular integrity, as for example the loss of p300 and CREBBP activity has been associated with carcinogenesis.⁴⁰ A genetic screen of cancer cell lines including colon, breast, ovarian, leukaemia, lung, melanoma, renal, prostate and central nervous system cancer cell lines performed at the National Cancer Institute in America detected the deletion of DNA regions encoding for p300 and CREBBP.⁴¹ Furthermore, genetic mutations encoding truncated and non-functional p300 proteins have been detected in tumour tissues isolated from patients and in cancer cell lines.⁴⁰ In addition, mutations in p300 and CREBBP causing the loss of lysine acetyltransferase activity, or suppressed expression and activity of p300 and CREBBP has also been observed.⁴² In cancers such as B cell lymphoma,⁴² a critical role of p300 and CREBBP in tumour suppression was identified, making lysine acetyltransferases good targets for cancer therapies.

Inflammation

Cells produce inflammatory cytokines such as tumour necrosis factor- α (TNF α) in response to pathogenic infections.⁴³ CREBBP facilitates signalling pathways downstream of TNF α by mediating the recruitment of proteins forming the transcriptional machinery and the binding of transcription factors NF- κ B and AP-1 to enhancers of their target genes.^{43,44} This activates the expression of target genes involved in activation and recruitment of immune cells to clear off the invading pathogens.

Neurodegenerative disease

Rubinstein-Taybi Syndrome (RTS) is a rare genetic disorder disease characterised by facial abnormalities, short stature, broad thumbs, broad big toes, and learning difficulties.⁴⁵ This disease is associated with partial deficiency of the CREBBP protein.

Further studies revealed that 56% of RTS patients can be accounted to CREBBP mutations and 5% to a p300 mutation.^{7,46} Another study demonstrated that cells from these patients show reduced histone acetylation.⁴⁷ This observation confirms that mutation of the CREBBP gene results in histone acetylation deficiency. Furthermore, treating these patients' cell lines with HDAC inhibitors reversed the hypoacetylation, indicating a potential therapy.⁴⁷

Haploinsufficient CREBBP^{+/-} mice show common RTS symptoms, including growth retardation and facial anomalies.^{48,49} These findings indicate clearly that CREBBP is a major factor for RTS.

1.3.3 CREBBP as drug target

Given the pivotal role of the CREBBP/p300 proteins and their association with diseases such as cancer, inflammation, and neurodegenerative diseases, it is important to design new, selective chemical probes. These compounds will enable the study of the biological role of these proteins by inhibiting individual domains, and could aid drug development by validation of a new target protein. This approach is especially relevant as gene knockout experiments for CREBBP are lethal at the embryonic stage.

1.4 Current CREBBP bromodomain ligands

1.4.1 Early research

The pioneers in the development of CREBBP bromodomain ligands were Zhou and co-workers. Having solved an NMR structure of a truncated K382Ac p53 peptide bound to the CREBBP bromodomain,⁵⁰ they started a structure-based screening of ligands disrupting the p53-CREBBP bromodomain interaction.⁵¹ By screening a library of 200 compounds by 2D ¹H-¹⁵N HSQC NMR, they found 14 binding fragments, of which 13 were selective for the CREBBP bromodomain over the PCAF bromodomain. The ligand binding site was predicted by docking experiments, in combination with the chemical shift patterns of the 2D NMR spectra, to be the KAc binding pocket. The highest affinity ligand was MS7972 (5)

(Table 1.1) with a dissociation constant of 19.6 μM . The authors demonstrated that MS7972 (**5**) can modulate the p53 protein in a cell-based assay.⁵¹ A second screening campaign tested 3000 ligands using a similar approach to that employed in the discovery of MS7972 (**5**). In this study, the azobenzene was seen to be a privileged scaffold.⁵² Subsequently, this scaffold was further optimised by a structure activity relationship and tested by a cellular assay measuring the p53 activation in human osteosarcoma cells, which resulted in the active compound, Ischemin (**6**) (Table 1.1). The binding mode was evaluated using NMR techniques. The crucial interaction observed by NMR was the hydrogen bonding of the phenol in **6** to conserved N1168, and an electrostatic interaction between R1173 and the sulfonic acid in **6** (Figure 1.7a).⁵²

Additionally, Gerano-Navarro *et al.* designed a cyclic peptide (**7**) based on the linear p53 peptide sequence binding to the KAc binding site in the CREBBP bromodomain using molecular dynamic simulations.⁵³ They showed the importance of the β -turn of the linear peptide sequence, by forming a cyclic peptide **7** *via* a disulfide bond of the cysteines, and increased the potency 24-fold compared to the linear p53 peptide (Table 1.1). The cyclic peptide **7** reduced the endogenous doxorubicin-induced p53-CREBBP binding *in vitro*.

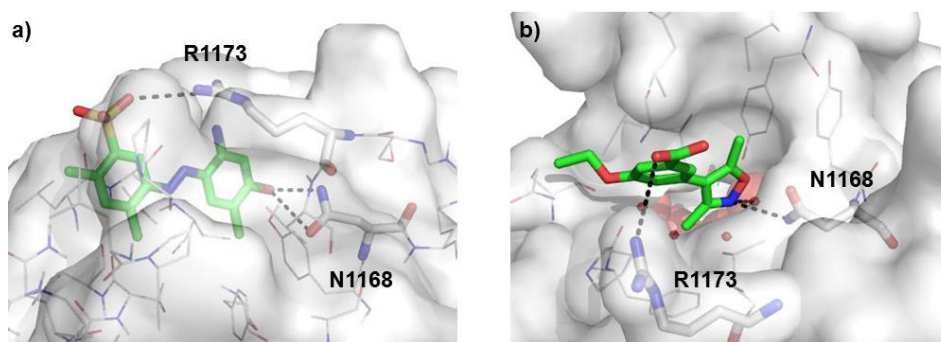


Figure 1.7 a) NMR crystal structure of CREBBP in complex with Ischemin (**6**) (PDB: 4L84)⁵⁴ with the important interactions highlighted as dashed lines. b) X-ray crystal structure of CREBBP in complex with **8** (PDB: 3SVH)⁵⁴. R1173 and N1168 are highlighted in bold.

Hewings *et al.* developed dimethylisoxazole bromodomain ligands for the BET family and they observed that these compounds also bind well to CREBBP bromodomain.⁵⁵ The X-ray crystal structure of **8** with CREBBP show that the carboxylic acid might form an

electrostatic interaction with R1173, giving rise to a potential feature for increasing selectivity of CREBBP ligands (Figure 1.7b).

Table 1.1 Overview of the first CREBBP bromodomain ligands with affinity data shown.

CREBBP ligands	CREBBP affinities
MS7972 (5)	$K_D = 19.6 \mu\text{M}$ (tryptophan fluorescence) ⁵¹
Ischemin (6)	$K_D = 19 \mu\text{M}$ (tryptophan fluorescence) ⁵² $IC_{50} = 5.0 \mu\text{M}$ (cellular assay)
7	$IC_{50} = 8.0 \mu\text{M}$ (fluorescence polarisation) ⁵³
8	$K_D = 32 \mu\text{M}$ (AlphaScreen™) ⁵⁵

1.4.2 Optimisation of potent CREBBP ligands

Since the discovery of the first BET bromodomain ligands and their interesting biological effects, the interest in non-BET bromodomain inhibitors has increased. The focus in this section is the discussion of the optimisation of potent CREBBP ligands.

Dihydroquinaxolinone

The dihydroquinaxolinone ligand was discovered by Rooney and co-workers.⁵⁶ The discovery of the potent dihydroquinaxolinone (*R*)-**12** started from a fragment-based screening approach, resulting from the observation of *N*-methyl pyrrolidone (NMP, **9**) as a ligand efficient ligand for the CREBBP bromodomain (Figure 1.8a).⁵⁶⁻⁵⁸ Screening of NMP analogues identified 3,4-dihydro-3-methyl-2(1*H*)-quinazolinone and benzoxazinone **10** as an efficient ligand. However, the 3,4-dihydro-3-methyl-2(1*H*)-quinazolinone headgroup is unstable and prone to oxidation on the benzylic carbon and hence the work focussed on the optimisation of **10**.⁵⁵ X-Ray crystal structures of **10** bound to the CREBBP bromodomain showed the carboxylic acid of **10** points towards the ZA channel.⁵⁶ Amide couplings with amine linkers connected to an aromatic ring were performed, but only slight affinity increases were observed. Rooney was concerned the interaction of the ether oxygen with the carbonyl backbone of P1110 may be unfavourable. Furthermore, he noticed that the internal hydrogen bond of the amide to the benzoxazinone in **11** resulted in the wrong direction of the linker (Figure 1.8a).^{56,57} Subsequently, the oxygen of the benzoxazinone **10** was changed to the amine, resulting in the internal hydrogen bond being inverted (Figure 1.8a). This led to the discovery of the dihydroquinaxolinone (DHQ) ligand (*R*)-**12** for the CREBBP bromodomain. The important interactions were two hydrogen bonds of the DHQ amide to N1168, and a cation- π interaction between the tetrahydroquinolinone (THQ) and R1173 (Figure 1.8b and c). This cation- π interaction in the CREBBP bromodomain was observed for the first time during the development of (*R*)-**12**.⁵⁶ The compound (*R*)-**12** is selective over multiple bromodomains and has a 4-fold

selectivity over the BET bromodomain BRD4(1). Furthermore, activity in fluorescence recovery after photobleaching (FRAP) assay was demonstrated in U2OS cells.⁵⁶

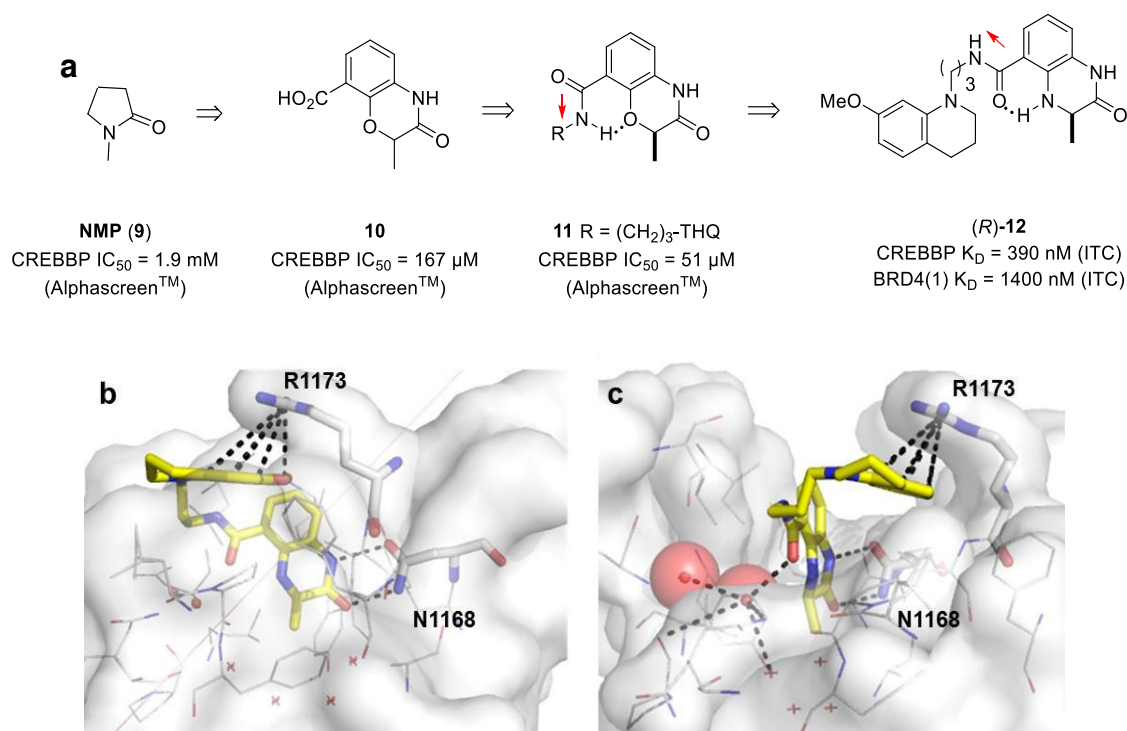


Figure 1.8 a) Overview of the optimisation of the NMP fragment **9** to the potent CREBBP ligand (*R*)-**12**. b) and c) Two views of the crystal structure of (*R*)-**12** (carbon = yellow) in complex with the CREBBP bromodomain (PDB: 4NYX)⁵⁴ highlighting the important interactions with the ligand and the protein. The conserved water molecules are shown as red spheres.

3,5-Dimethylisoxazole

The 3,5-dimethylisoxazole is an acetyl lysine mimic head group used for many BET bromodomain ligands.^{55,59-61} Hay *et al.* started the project from the unselective, but potent, 3,5-dimethylisoxazole CREBBP ligand **13**, which forms a hydrogen bond to the conserved N1168 (Figure 1.9).^{62,63} A library of over 100 substituted aryl bromides of substituted benzimidazole fragments were purchased, and Suzuki reactions were performed on the 3,5-dimethylisoxazole to yield the most promising compound **14** (Figure 1.9). Further optimisation of the two substituents yielded a potent and moderately selective CREBBP ligand **15**. Changing the substituents of the methoxy-benzene ring and introduction of the (*S*)-methyl group next to the morpholine resulted in a slightly more potent CREBBP ligand, with 40-fold selectivity over the BET bromodomains (Figure 1.9). The X-ray crystal

structure of CREBBP in complex with **16** revealed the dimethylisoxazole forms one hydrogen bond to N1168, and a water mediated-hydrogen bond to P1110. They also observed a cation- π interaction between R1173 and the electron-rich aromatic ring (Figure 1.9). This compound **16** showed an increased recovery time in a fluorescence recovery after photobleaching (FRAP) assay on a GFP-CREBBP bromodomain construct in HeLa cells. Phenotypic analysis of **16** in a BioMAP profile on primary hematopoietic cells revealed that it has a different phenotype compared to the BRD4 bromodomain ligands at low compound concentrations (0.1-1.1 μM), however, at 10 μM it exhibits a similar phenotypic profile to (+)-JQ1.⁶⁴ This indicates a 40-fold selectivity over BRD4 is not sufficient to overcome the strong BRD4 phenotype, and consequently more selective ligands are desired.

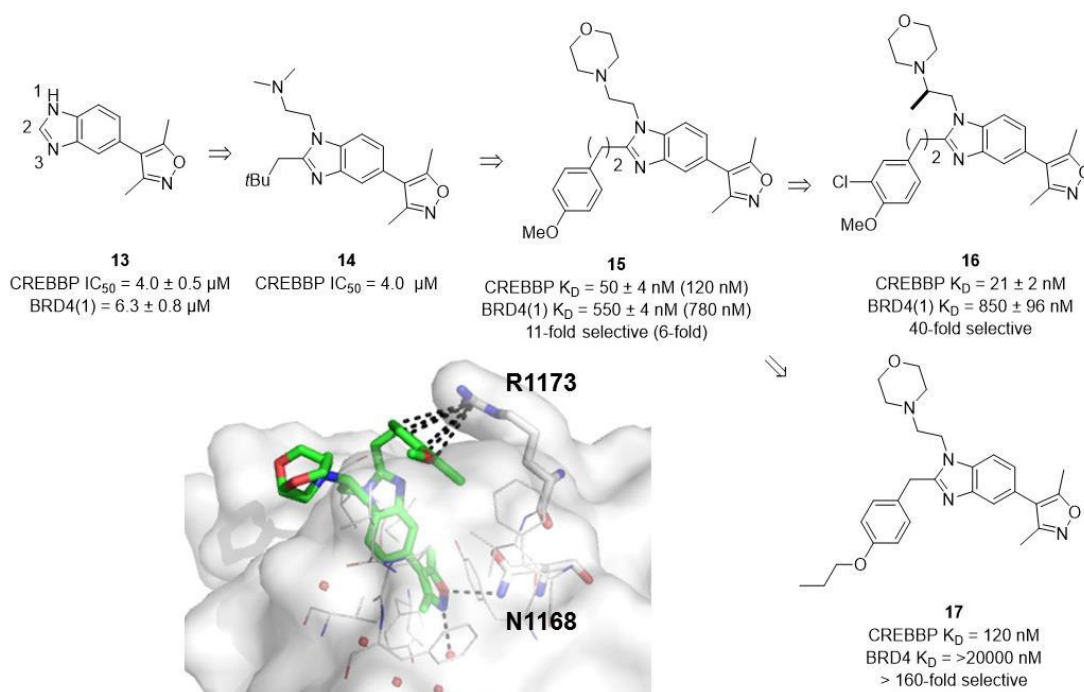


Figure 1.9 Overview of the optimisation of the unselective 3,5-dimethylisoxazole **13** to selective CREBBP ligands **16** and **17**. The X-ray crystal structure of **16** (carbon = green) in complex with the CREBBP bromodomain is highlighting the important interactions (PDB: 4NR7).⁵⁴

Pfizer developed a selective CREBBP ligand **17** based on Hay's moderately selective ligand **15**, supported by X-ray crystal structures of CREBBP and BRD4.⁶⁵ By increasing the size of the methoxy to a propoxy substituent on the benzyl group, they maintained the CREBBP

bromodomain affinity, whereas no BRD4 interaction was observed by ITC, resulting in a valuable and selective probe (Figure 1.9). This compound did not show any cytotoxicity on primary macrophage cells, indicating that it does not have a BRD4 phenotype. Furthermore, they demonstrated that the single cell transcriptional profiling is significantly different to the BET inhibitor I-BET151 (**3**).⁶⁵

Benzoxazepine CREBBP ligand

The Structural Genomics Consortium (SGC) developed a 36-fold selective and cellularly active CREBBP bromodomain ligand, I-CBP112 (**18**) (Figure 1.10a).^{66,67} The X-ray crystal structure reveals the key interactions were the hydrogen bond of the acyl group with N1168 and the conserved water molecule, as well as a cation- π interaction of the electron-rich aromatic ring with R1173 (Figure 1.10b and c). The methyl-piperidine group is likely to act as a solubilising group, and increasing the selectivity over the BET bromodomains. I-CBP112 (**18**), despite only having 36-fold selectivity over the BET bromodomains, did result in a distinctive non-BET phenotype using four hematopoietic cocultures.⁶⁶

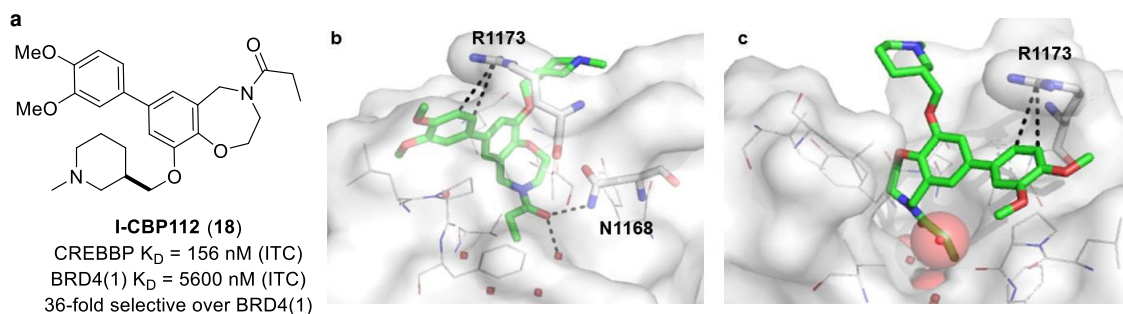


Figure 1.10 a) Structure of I-CBP112. b) and c) The X-ray crystal structure of **18** (carbon = green) in complex with the CREBBP bromodomain, highlighting the important interactions (PDB: 4NR6)⁵⁴.

A FRAP assay demonstrated chromatin can get displaced from the bromodomain by using **18**. Furthermore, I-CBP112 (**18**) was shown to significantly reduce the clonogenic growth in 12 human cell lines.⁶⁶ This compound is a very promising structure to further evaluate in different biological systems.

Popp *et al.* performed an SAR around the I-CBP112 scaffold investigating different acyl groups, solubility groups, and electron rich aromatic rings to increase the cation- π

interaction. However, no compound with increased affinity and selectivity over **18** was discovered.^{68,69}

Acylbenzene

The discovery of the selective compound **21**, was initiated by a computational high-throughput compound docking into two different CREBBP X-ray crystal structures using two million compounds (Figure 1.11).⁷⁰ Molecular dynamic simulations were performed on the promising docking poses, and 17 fragments were subsequently tested on CREBBP, resulting in two promising compounds, one of which is **19**.⁷¹ Subsequently, three acetyl benzene analogues were purchased resulting in the ligand efficient, and potent (5 μM) CREBBP ligand **20**. The affinity increase can be attributed to an electrostatic interaction between the carboxylic acid of **20** and R1173. An SAR study of **20** revealed that the ethoxy substituent is important for the affinity to CREBBP as it forms a hydrophobic interaction in the KAc binding site. The fumaric acid moiety was replaced by benzoic acid, resulting in an increased affinity value. Finally, a small SAR study of this fragment resulted in a potent CREBBP ligand **21** (K_D 300 nM), which is selective over the BET bromodomain. In cell-based assays, compound **21** showed a cell growth reduction of leukemic cell lines.⁷¹ This compound is a valuable tool for further biological studies on the CREBBP bromodomain.

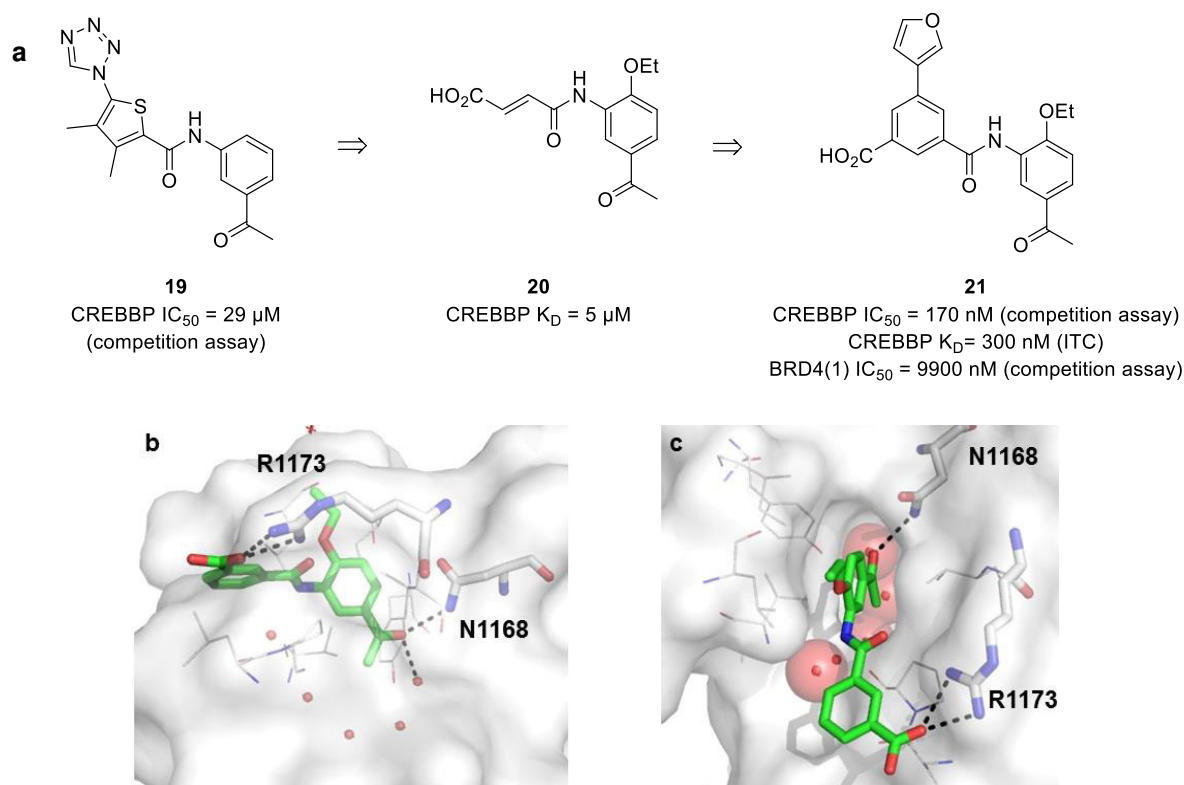


Figure 1.11 a) Overview of the hit **19** to lead optimisation of a potent and selective CREBBP ligand **21**. b) and c) X-ray crystal structure of **21** (carbon = green) in complex with the CREBBP bromodomain (PDB: 4TQN)⁵⁴ highlighting the important interactions with the ligand and the protein. The conserved water molecules are shown as red spheres.

Acylpiperidine

Recently, a collaboration between Genentech, Constellation, and Wuxi resulted in the selective CREBBP *in vivo* probe GNE-272 (**24**) with good pharmacokinetic properties.⁷² Fragment **22** was identified using differential scanning fluorimetry by screening a lead-like compound set (Figure 1.12). They further validated this compound by time-resolved fluorescence resonance energy transfer (TR-FRET) on CREBBP and BRD4(1) and observed an IC₅₀ of 0.62 μM on CREBBP and 100-fold selectivity over the BRD4(1) bromodomain.⁷² The X-ray crystal structure (PDB: 5KTU)⁵⁴ of this ligand revealed hydrogen bonding between the acyl amide carbonyl of **22** and N1168, and a water-mediated hydrogen bond to P1110 *via* the conserved water molecule in the KAc binding pocket. The benzyl group of **22** points into the hydrophobic LPF shelf. An extensive SAR study of this ligand **22** was performed. The acetyl amide group is the most potent acetyl lysine mimic headgroup.

Either decreasing the electron density of the acetyl group, or increasing the size, resulted in lower CREBBP bromodomain affinity. Adding a carboxamide substituent on the aniline increased the CREBBP affinity 5-fold. Small substituents were attached on the pyrazole. Hydrophobic substituents increased the binding affinity. The most potent ligand was **23** with an IC_{50} value of $0.03 \mu\text{M}$ for CREBBP, and over 100-fold selectivity over the BET bromodomains (Figure 1.12).⁷² At this stage, the authors focused on optimising the pharmacokinetic properties. The amide substituent on **23** contributed to a low *in vitro* permeability, and the cyclopropyl substituent is metabolised quickly. This issues were solved by replacing the cyclopropyl group with a tetrahydrofuran, and substituting the amide with the pyrazole isostere. Furthermore, a fluorine atom was incorporated on the 2-position at the aniline to decrease the basicity and reduce the compound glucuronidation resulting in a potent, selective compound **24** with improved pharmacokinetics (Figure 1.12).

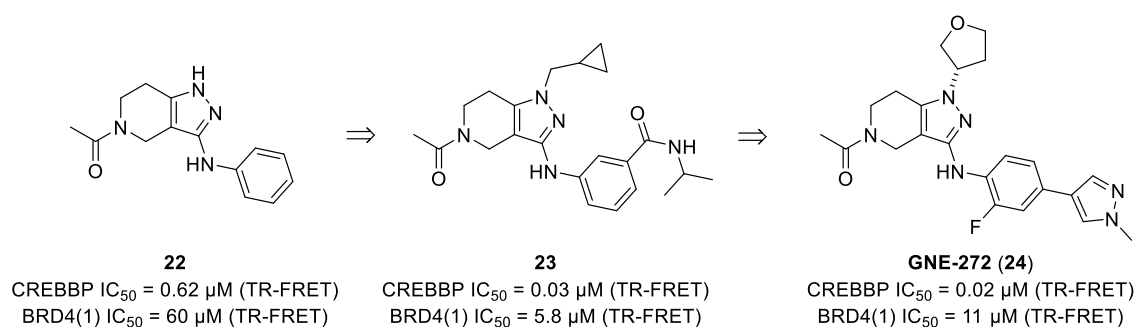


Figure 1.12 Optimisation process of the fragment **22** to the selective CREBBP *in vivo* probe GNE-272 (**24**).

Compound **24** was tested by a BromoScan assay on 35 different human bromodomains and was 160-fold selective over the BET family. **24** was tested on haematological cancer cell lines and reduced the expression of the *MYC* oncogene in a dose-dependent manner. Furthermore, this compound is antiproliferative on a broad panel of blood cancer cell lines.⁷² In an *in vivo* experiment, treating MOLM-16 xenograft mice with **24** showed a dose-dependent tumour growth inhibition with 46%, 65% and 102% at 12.5, 25 and

50 mg/kg, respectively.⁷² This result clearly indicates that selective CREBBP bromodomain ligands show a good potential as future cancer therapeutics.

1.4.3 Comparison of the small molecule binding modes in CREBBP

Having discussed the SAR of multiple CREBBP ligands, a few common interactions were observed. All potent small molecules ligands form a hydrogen bond to N1168 and a water-mediated hydrogen bond to P1110 (Figure 1.13). The KAc mimic headgroups are diverse, with a dimethylisoxazole (**16** and **17**), dihydroquinaxolinone ((*R*)-**12**) or acyl amides (**18** and **24**) being used, showing different groups can be tolerated in the hydrophobic KAc binding pocket.

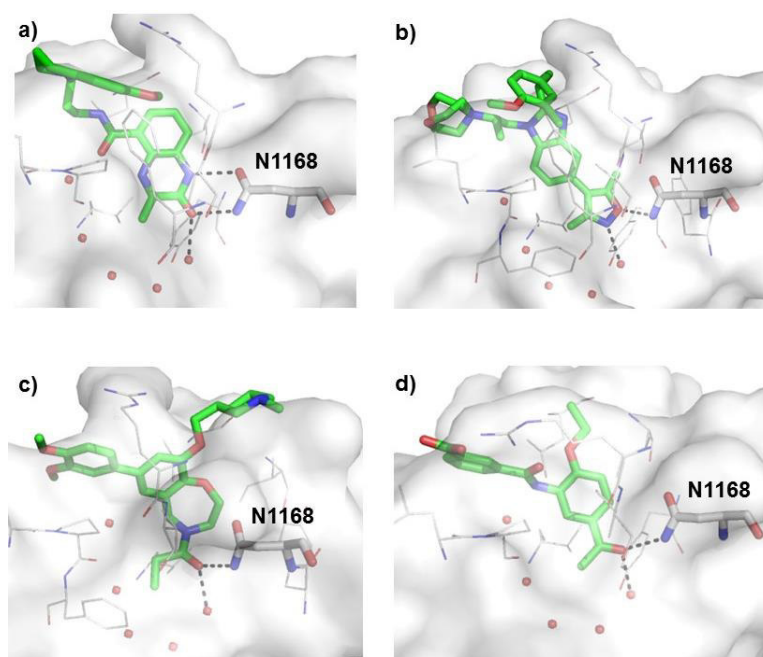


Figure 1.13 Analysis of the CREBBP KAc mimic a) (*R*)-**12** (carbon = green) (PDB: 4NYX)⁵⁴, b) **16** (carbon = green) (PDB: 4NR7)⁵⁴, c) **18** (carbon = green) (PDB: 4NR6)⁵⁴ and d) **21** (carbon = green) (PDB: 4TQN)⁵⁴ to N1168. The conserved water molecules are indicated as red spheres and N1168 is highlighted as sticks.

The other common interaction involves R1173. The ligands (*R*)-**12**, I-CBP112 (**18**), **16** and **17** form a cation- π interaction between R1173 and the electron-rich aromatic ring (Figure 1.14a-c). **21** has an electrostatic interaction between the carboxylic acid and R1173 (Figure 1.14d).

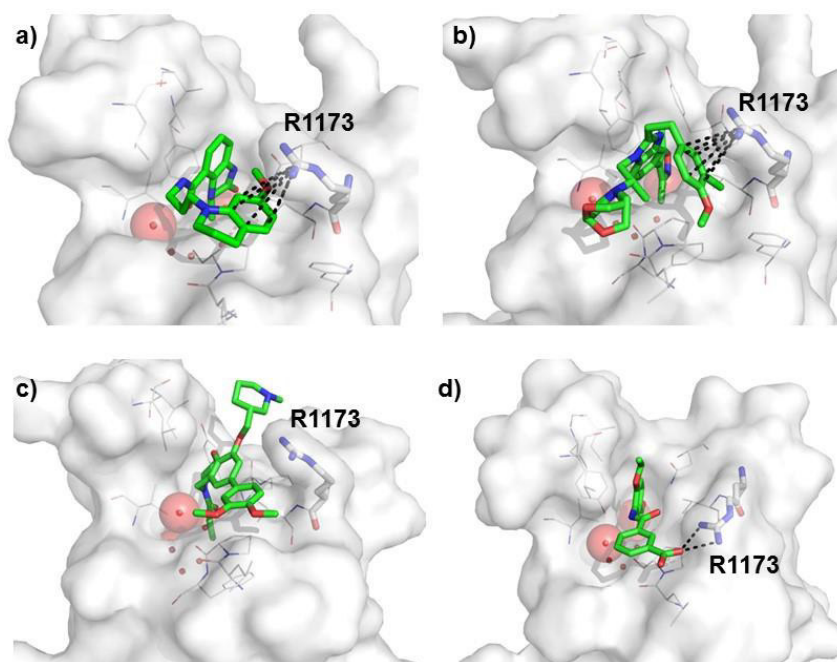


Figure 1.14 Analysis of the interaction between R1173 and the potent CREBBP ligands a) (*R*)-**12** (carbon = green) (PDB: 4NYX), b) **16** (carbon = green) (PDB: 4NR7), c) **18** (carbon = green) (PDB: 4NR6) and d) **21** (carbon = green) (PDB: 4TQN) to N1168. The conserved water molecules are indicated as red spheres and R1173 is highlighted as sticks.

Other ways to increase the ligand selectivity of CREBBP over the BET bromodomains was by attaching solvent-exposed, bulky groups on the ligand, such as the morpholine for **16** (Figure 1.14b), propoxy ether for **17**, or the piperidine moiety for I-CBP112 (**18**) (Figure 1.14c). These groups are thought to cause a steric clash with the BRD4 bromodomain and results in decreased affinity.

1.5 Project aim

At the commencement of the discovery and optimisation of CREBBP ligands by Dr T. Rooney, there were no potent and selective CREBBP inhibitors reported. Dr T. Rooney in the course of his studies discovered a potent CREBBP ligand (*R*)-**12** with a novel cation- π interaction previously not observed in this system.^{56,57} The main focus of this dissertation is the study of the cation- π interaction between the THQ and R1173. Also, the ligand selectivity between CREBBP and the BET bromodomain family will be investigated.

Furthermore, the compound stability of the dihydroquinaxolinone acetyl lysine mimic should be optimised, while maintaining the CREBBP affinity.

A second related project was on the development of a two-step photo-affinity probe for bromodomains, which will be introduced in more detail in Chapter 5.

Chapter 2

Optimisation of the dihydroquinoxalinone acetyl lysine mimic.

2. Optimisation of the dihydroquinoxalinone acetyl lysine mimic

2.1 Introduction and aims

The dihydroquinoxalinone (DHQ) fragment **25** was discovered in our group as a ligand efficient acetyl-lysine mimic (KAc), which forms two hydrogen bonds to N1168.⁵⁶ Fragment **25** was further optimised to give a potent CREBBP ligand (*R*)-**12** (Figure 2.1). The optimised ligand contained a propyl linker which directs the tetrahydroquinolinone (THQ) towards R1173 to form a cation- π interaction (Figure 2.1).

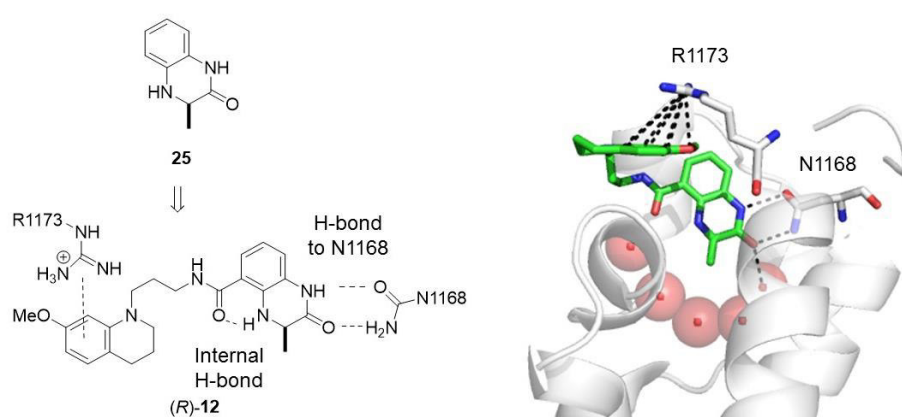


Figure 2.1 Schematic overview of the binding interactions of the compound (*R*)-**12** in complex with the CREBBP bromodomain. The dihydroquinoxalinone forms two hydrogen bonds to N1168 and the THQ forms a cation- π interaction with the positively charged R1173. The internal hydrogen bond between the aniline and the carbonyl amide linker is important in setting up the correct vector for the linker. The crystal structure of the compound (*R*)-**12** in CREBBP bromodomain (PDB: 4NYX)⁵⁴ is shown on the right. The conserved water molecules are shown as red spheres.

The drawback of the dihydroquinoxalinone headgroup is the moderate stability to oxidation. Therefore, we aimed to optimise this fragment towards a more stable, KAc mimic, by expanding the 6-membered DHQ ring to the 7-membered DHQ ring analogues ((*R/S*)-**26** and **27**) to prevent oxidation (Figure 2.2).

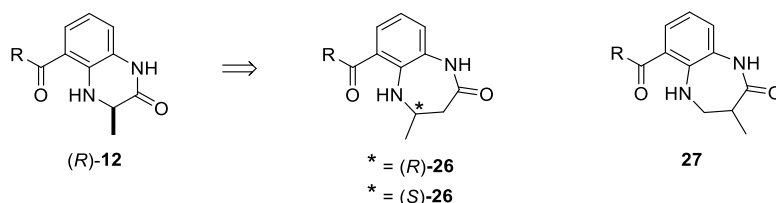
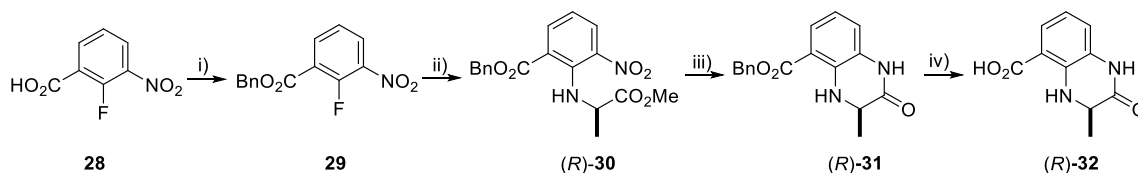


Figure 2.2 Proposed stable DHQ fragments by ring expansion. R = 7-MeO-THQ-(CH₂)₃NH-.

2.2 Synthesis of the 6-membered dihydroquinoxalinone (*R*)-12

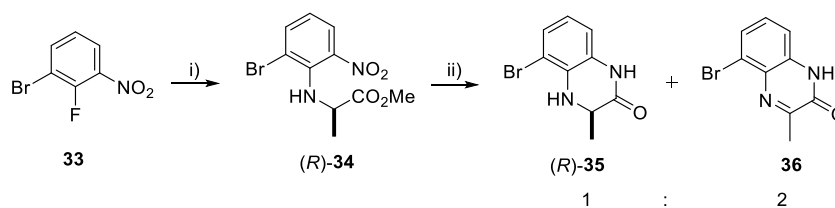
The 6-membered dihydroquinoxalinone (*R*)-12 was synthesised as reference compound for comparison to the ring extended analogues ((*R/S*)-26, 27) according to the optimised conditions from Dr Timothy Rooney starting from 2-fluoro-3-nitrobenzoic acid **28** (Scheme 2.1).⁵⁶



Scheme 2.1 Synthesis of the dihydroquinoxalinone scaffold (*R*)-32. *Reagents and conditions:* i) BnBr, K₂CO₃, DMF, 60 °C, 3 h, 93%; ii) D-Alanine methyl ester hydrochloride, Cs₂CO₃, toluene, 85 °C, 18 h, 90%; iii) Zn, NH₄Cl, DMF, rt, 25 h, 82%; iv) 10% (w/w) Pd/C, H₂, EtOAc, rt, 99%.

The carboxylic acid of **28** was protected by benzylation in 93% yield to afford **29**. The nucleophilic aromatic substitution of **29**, with D-alanine methyl ester works well on the electron-poor aromatic ring, and compound (*R*)-**30** was isolated in 90% yield. The nitro reduction of (*R*)-**30** with Zn and ammonium chloride, followed by *in situ* cyclisation, gave the dihydroquinoxalinone (*R*)-**31**. The deprotection of the benzyl ester by hydrogenolysis gave the key intermediate (*R*)-**32**, in excellent yield.

In addition to the 7-carboxy-DHQ derivative (*R*)-**32**, a brominated fragment was synthesised to enable the installation of other linkers to the KAc headgroup (Scheme 2.2). The nucleophilic aromatic substitution on **33** using caesium carbonate resulted in a complex mixture of products. However, upon changing the base to DIPEA, (*R*)-**34** was isolated in 96% yield (Scheme 2.2). The reduction of the aromatic bromide (*R*)-**34** was avoided using the Béchamp condition, with Fe(0) and acetic acid. The reaction was complete in 2 hours and the isolated crude material (*R*)-**35** was fairly clean (Figure 2.3a).



Scheme 2.2 Synthesis of the 7-Br DHQ. *Reagents and conditions:* i) D-Alanine methyl ester hydrochloride, DIPEA, DMF, 85 °C, 18 h, 96%; ii) Fe, AcOH, EtOH, 50 °C, 2 h. Compound unstable.

The crude material was purified by crystallisation from isopropanol and the obtained ^1H NMR spectrum contained the oxidised compound **36** in a 2:1 ratio to the desired 7-Br-DHQ (*R*)-**35** (Figure 2.3b). This demonstrates that (*R*)-**35** is an unstable intermediate. In contrast, (*R*)-**32** is more stable, even at elevated temperature (see Chapter 2.3.3). This difference is potentially due to the predicted hydrogen bonding of the aniline amine to the carbonyl, and hence the oxidation potential of compound (*R*)-**35** is increased.

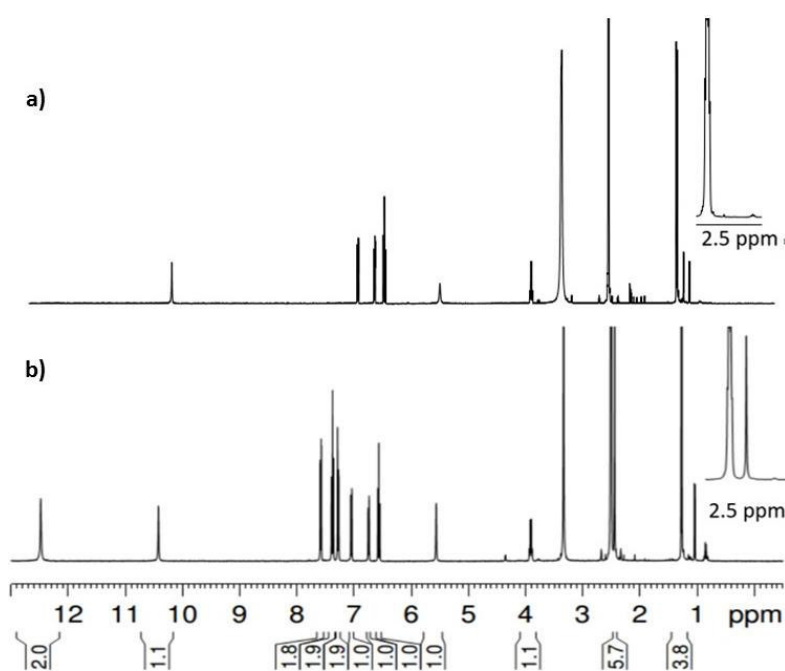
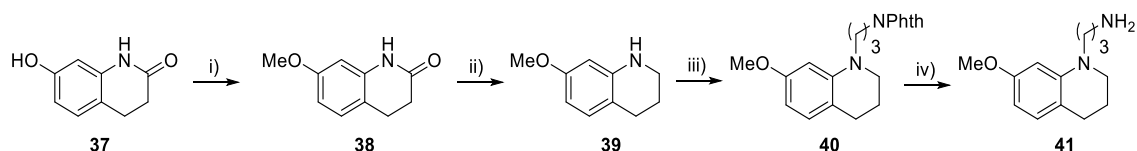


Figure 2.3 ^1H NMR spectra of the crude compound (*R*)-**35** (a) and the recrystallised compound **36** (b) in D_6 -DMSO. The expanded region at 2.5 ppm shows the CH_3 signal of **36** next to the D_5 -DMSO.

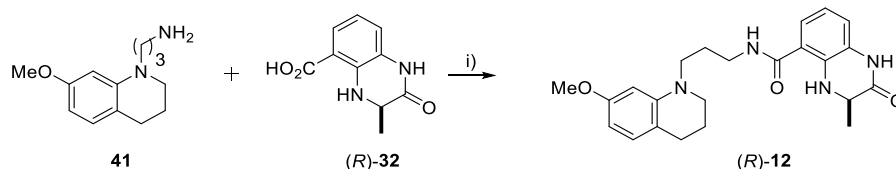
The synthesis of the 7-methoxy-tetrahydroquinoline (7-MeO-THQ)-propyl amine **41** was performed by following the literature starting from 7-hydroxy-3,4-dihydroquinolin-2(1*H*)-one **37** (Scheme 2.3).^{56,57} The phenol of **37** was methylated using iodomethane, and **38**

was isolated in 50% yield. The amide reduction of **38** with lithium aluminium hydride yielded the 7-MeO-THQ **39** in 97%. Subsequently, the amine **39** was reacted with *N*-(3-bromopropyl) phthalimide, to attach the *N*-propyl linker, followed by the phthalimide deprotection with hydrazine (Scheme 2.3) to give **41**. The crude material was purified via an acid-base extraction to give **41** in high purity.



Scheme 2.3 Synthesis of the THQ linker **41**. *Reagents and conditions:* i) MeI, K₂CO₃, DMF, 60 °C, 17 h, 50%; ii) LiAlH₄, THF, rt, 97%; iii) K₂CO₃, *N*-(3-bromopropyl) phthalimide, DMF, 85 °C, 18 h, 60%; iv) hydrazine monohydrate, MeOH, CH₂Cl₂, 70 °C, 2 h, 96%.

The final step in the synthesis of (*R*)-**12** was an amide coupling with 7-MeO-THQ propyl amine **41** and the DHQ carboxylic acid (*R*)-**32** using PyBOP to afford compound (*R*)-**12** in 77% yield (Scheme 2.4).



Scheme 2.4 The amide coupling of **41** and (*R*)-**32** to afford (*R*)-**12**: *Reagents and conditions:* i) PyBOP, Et₃N, DMF, 20 °C, 15 h, 77%.

2.3 7-membered ring DHQ analogues (*R/S*)-26 and 27

2.3.1 Computational approach

To establish whether the expanded DHQ ring could be accommodated in the CREBBP bromodomain KAc binding pocket, docking experiments into the *apo*-CREBBP X-ray crystal structure (PDB: 3P1C)⁵⁴ were performed. Subsequently, extended molecular dynamic simulations were employed using the Amber forcefield to determine if the cation- π interaction between the THQ and R1173 would be retained. These experiments were

carried out in collaboration with Wilian A. Cortopassi in the group of Prof. Robert S. Paton (University of Oxford).

To validate the computational method, compound (*R*)-**12** was docked into the *apo* X-ray crystal structure of CREBBP (Figure 2.4), using AutoDock Vina.⁷³ The lowest energy conformation of the docking experiment was used for the quantum mechanics (QM) calculations, which were performed over 120 ns. The calculations showed that the lowest energy conformation is obtained after 40 ns, and a constant root mean square deviation of 1.3 Å is reached (Figure 2.4c). The average structure by QM calculation of the 6-membered DHQ headgroup (blue) matches well with the crystal structure (PDB: 4NYX,⁵⁴ yellow) (Figure 2.4b). The DHQ sits deeper in the binding pocket using the computational approach compared to the X-ray crystal structure. The propyl linker with the THQ is differently aligned between the computationally and the experimentally determined structures, but both of the protein-ligand complexes form the electrostatic driven cation- π interaction.

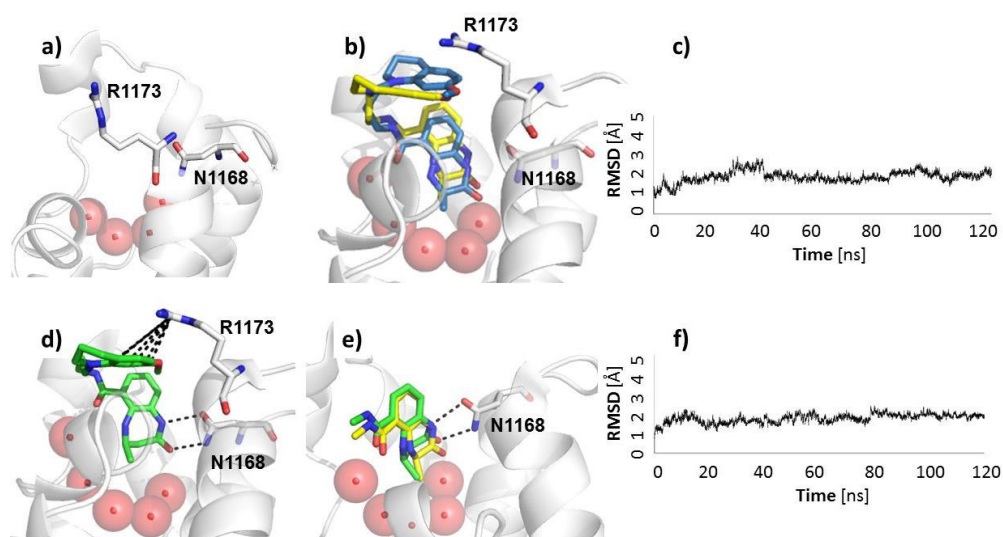


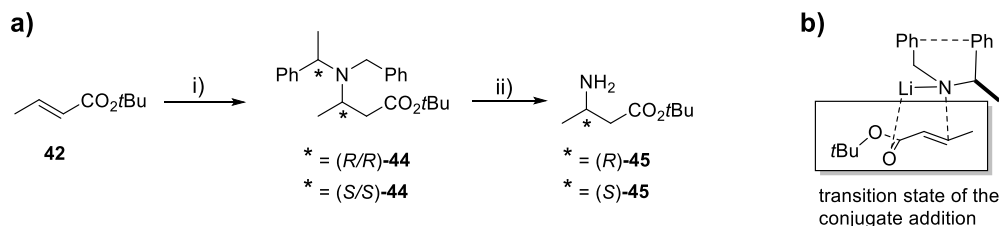
Figure 2.4 a) The *apo* X-ray crystal structure of the CREBBP bromodomain (PDB: 3P1C)⁵⁴ highlighting the key amino acids N1168 and R1173 (carbon = grey). The conserved water molecules in the binding pocket are shown as red spheres. b) Overlaid structures of the molecular dynamics (carbon = blue) and X-ray crystal structure of (*R*)-**12** (carbon = yellow). Root mean square deviation (RMSD) over 120 ns of the quantum mechanics calculations for (*R*)-**12** (c) and (*R*)-**26** (f). (d) Simulated structure of (*R*)-**26** by molecular dynamics (carbon = green) and the overlaid 6- and 7-membered DHQ headgroup are shown (e).

The same method was performed for the 7-membered analogue (*R*)-**26**. The simulated molecular dynamic structure of the 7-membered ring (Figure 2.4d and e) matches well with the 6-membered analogue. The hydrogen bonds between the DHQ amide and N1168, as well as the internal hydrogen bond of the DHQ amine to the carbonyl linker were observed. Additionally, the cation- π interaction between R1173 and the THQ is present, as during the MD simulations this interaction is formed. The computational data clearly indicates that the 7-membered DHQ ring (*R*)-**26** is a promising analogue of (*R*)-**12** with regards to the binding profile towards CREBBP. Consequently, the 7-membered DHQ analogues (*R/S*)-**26** and **27** should be synthesised.

2.3.2 Synthesis of (*R/S*)-**26** and **27**

β -Alanine is an important building block for the synthesis of the 7-membered ring DHQ fragment. The enantiopure β -alanine can be synthesised by an Arndt-Eistert rearrangement⁷⁴ or diastereoselective PtO₂ catalysed hydrogenation under high pressure.⁷⁵ To avoid using the toxic diazomethane or high pressurised reactions, the conjugate addition of a chiral lithium amide onto crotonic acid by Davies *et al.* shows a good alternative approach with a high substrate scope.^{76,77} Furthermore, having a *tert*-butyl ester is helpful in enabling orthogonal ester hydrolysis at a later stage in the synthesis.

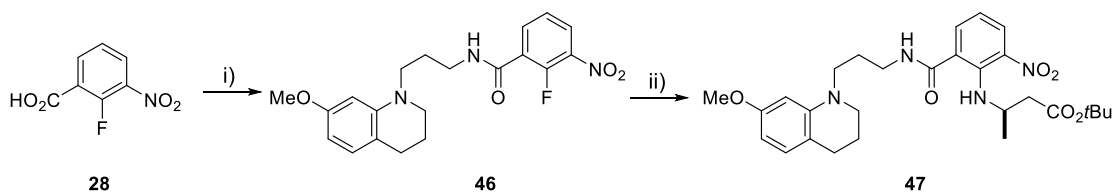
The synthesis towards the enantiopure (*R*)-**45** started with the conjugate addition of the lithium amide of (*R*)-*N*-benzyl-*N*-(α -methylbenzyl)amide (*R*)-**43** to the crotonic acid *tert*-butyl ester **42** (Scheme 2.5a). This reaction proceeded in 84% yield and high enantioselectivity. The high enantioselectivity results from the proposed butterfly transition state of the chiral auxiliary (Scheme 2.5b). Computational calculations demonstrated the π - π stacking of the phenyl rings rigidifies the conformation of (*R*)-*N*-benzyl-*N*-(α -methylbenzyl)amide and can only attack on the *re* face of the crotonic acid resulting in the *R/R* compound (Scheme 2.5b).⁷⁸



Scheme 2.5 a) Enantioselective synthesis of the (*R*) and the (*S*) β -alanine **45** according to S. Davies *et al.* Reagents and conditions: i) 1) *n*BuLi, (*R*)- or (*S*)-*N*-benzyl-*N*-(α -methylbenzyl)amide (*R*)-**43** or (*S*)-**43** THF, -78°C , 2) **42**, -78°C , 2 h, 3) 10% NH_4Cl (aq), 84% for (*R/R*)-**44** and 69% for (*S/S*)-**44**; ii) $\text{Pd}(\text{OH})_2$, MeOH, AcOH, H_2O , 91% for (*R*)-**45** and 79% for (*S*)-**45**. b) The proposed transition state of the conjugate addition is shown resulting in a single diastereomeric product.⁷⁸

The hydrogenolysis of (*R*)-**44** worked well using literature procedure⁷⁹ to give (*R*)-**45**. The synthesis for the (*S*)-enantiomer worked in good yields using the same conditions.

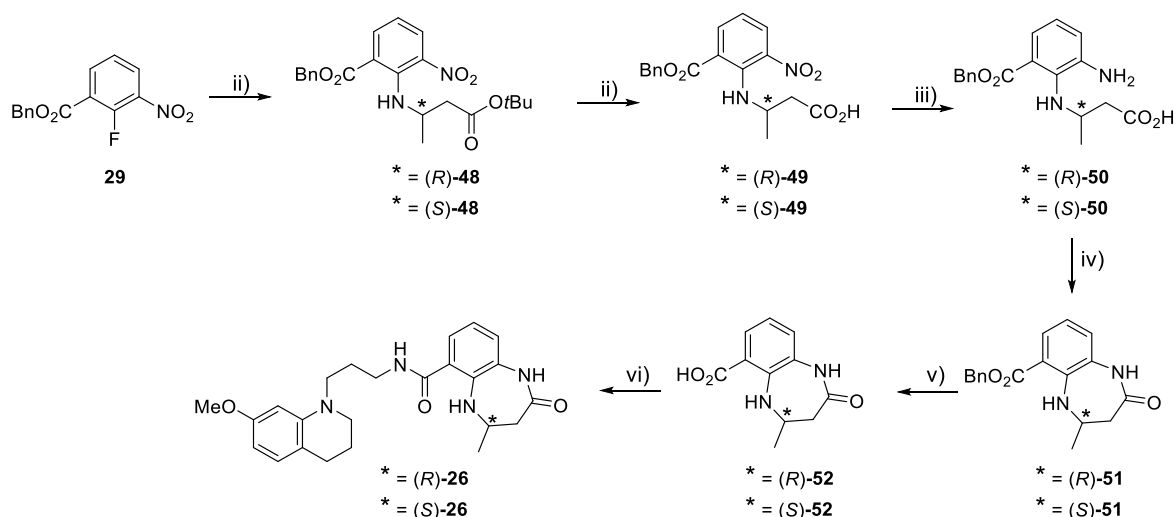
To shorten the synthesis compared to the previous route for (*R*)-**12**, it was thought to form the DHQ ring system at a later stage. Therefore the amide coupling with 7-MeO-THQ (**41**) was first performed on **28** to give **46** in moderate yield (Scheme 2.6). Subsequently, the $\text{S}_{\text{N}}\text{Ar}$ was performed with the chiral β -amino acid (*R*)-**45**. During the reaction, unidentified by-products were formed and the purification was difficult, and yielded only a small amount of impure **47**.



Scheme 2.6 Amide coupling of the carboxylic acid **28** and 7-MeO-THQ-propyl amine **41** followed by the $\text{S}_{\text{N}}\text{Ar}$. Reagents and conditions: i) PyBOP, **41**, Et_3N , DMF, 20°C , 15 h, ii) (*R*)-**45**, Cs_2CO_3 , toluene, 85°C , 18 h.

It was decided that rather than optimising the conditions for these two reactions, it would be better to synthesise the benzyl-protected 7-membered DHQ fragment **51**. The nucleophilic aromatic substitution with (*R*)-**45** worked in excellent yield to afford (*R*)-**48** (Scheme 2.7). The nitro reduction of (*R*)-**48**, with Zn and ammonium chloride, went to completion, but the 7-membered ring cyclises less well compared to the 6-membered analogue (*R*)-**30**. Consequently, an amide coupling strategy was pursued. The *tert*-butyl

ester of (*R/R*)-**48** was hydrolysed with formic acid in a first attempt, but the deprotection of the *tert*-butyl ester was slow and incomplete. By changing to the more acidic trifluoroacetic acid, the deprotection of (*R*)-**48** went to completion in two hours. Compound (*R*)-**49** was taken directly onto the nitro group reduction using Zn and ammonium chloride. Instead of purifying the zwitterionic species (*R*)-**50**, the reaction mixture was filtered through Celite®, the pH adjusted to 9, and PyBOP added for the DHQ ring formation to afford (*R*)-**51** in a yield of 67% over 3 steps (Scheme 2.7). The final two steps were a hydrogenolysis of the benzyl ester, followed by an amide coupling to obtain (*R*)-**26**. The overall yield of the (*R*)-enantiomer was 31% over 8 steps. (*S*)-**26** was synthesised using the same conditions as the (*R*)-enantiomer, and an overall yield of 8% was achieved.



Scheme 2.7 Enantioselective synthesis of the 7-membered DHQ ring derivatives (*R/S*)-**26**. *Reagents and conditions:* i) Cs_2CO_3 , (*R*)-**45** or (*S*)-**45**, toluene, 85 °C, 14 h, 97% for (*R*) and 83% for (*S*), ii) TFA/dichloromethane 1:1, 20 °C, 2 h, iii) Zn, NH_4Cl , DMF, 20 °C, 15 h, iv) PyBOP, Et_3N , DMF, 67% over 3 steps for (*R*) and 65% for (*S*), v) H_2 , Pd/C, MeOH, 20 °C, 15 h, vi) PyBOP, **41**, Et_3N , DMF, 68% over 2 steps for (*R*) and 26% for (*S*).

The optical rotation for (*R*)-**26** measured -21.0 , whereas that for the (*S*) enantiomer was $+21.4$. Besides the good match it was important to prove the stereochemistry by chiral HPLC. It was difficult to separate the enantiomers on

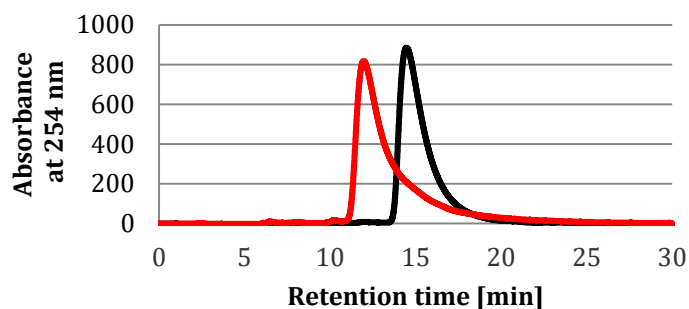
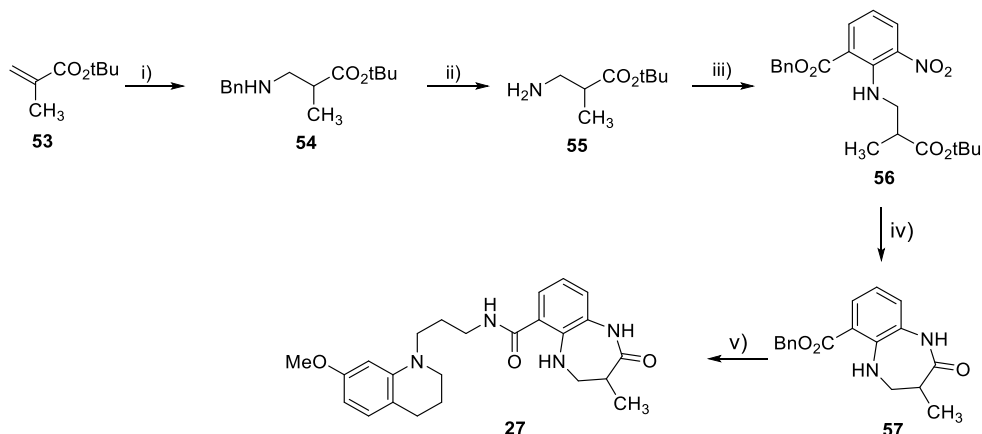


Figure 2.5 Chiral HPLC traces of (*R*)-**26** (black line) and (*S*)-**26** (red) performed on an AD-H Chiralpak® column eluting with 50% IPA in hexane.

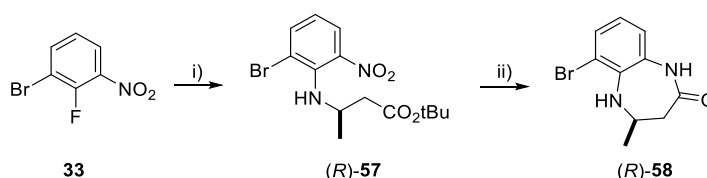
the AD-H Chiralpak® column as the elution profile of the compounds were broad. Addition of either triethylamine or trifluoroacetic acid did not improve the separation. The best separation was achieved with an isocratic elution of 50% isopropanol in hexane (Figure 2.5). It clearly shows that (*R*)-**26** (black line) is enantiomerically pure. It can be assumed that the (*S*)-**26** is also enantiomerically pure because the optical rotation value is inverted.

In order to obtain the regioisomer of the 7-membered DHQ **26**, the racemic β^2 -amino acid is essential. The synthesis of the racemic β^2 -amino acid was attempted using the lithium amide chemistry involving dibenzylamine and *tert*-butyl methyl acrylate, according to the synthesis above. However, multimeric species formed during the addition of the acrylate to the lithium amide, and none of the desired product could be isolated. An alternative approach involved the conjugate addition of dibenzylamine onto *tert*-butyl methyl acrylate **53** in the presence of DBU, but surprisingly no conversion was observed at 90 °C. By changing the nucleophile to the less sterically demanding benzyl amine the reaction worked in 37% yield (Scheme 2.8). The yield was increased to 51% by performing the conjugate addition in solvent-free conditions. The secondary amine of **54** was deprotected by hydrogenolysis with $\text{Pd}(\text{OH})_2$ to afford the racemic *tert*-butyl protected β^2 amino acid **55**. The nucleophilic aromatic substitution, the cyclisation of the DHQ ring, and the amide couplings were performed in the same manner as for the regioisomer (*R/S*)-**26** to afford the desired racemic 7-membered DHQ compound **27** (Scheme 2.8).



Scheme 2.8 Synthesis of the racemic β^2 -DHQ **27**. *Reagents and conditions:* i) BnNH_2 , DBU, 90°C , 16 h, 51%; ii) $\text{Pd}(\text{OH})_2$, MeOH, AcOH, H_2O , 20°C , 16 h; iii) Cs_2CO_3 , **29**, toluene, 85°C , 14 h, 96% over 2 steps; iv) 1) TFA/dichloromethane 1:1, 20°C , 2 h, 2) Zn, NH_4Cl , DMF, 20°C , 15 h; 3) PyBOP, Et_3N , DMF, 10% over 3 steps; v) 1) H_2 , Pd/C, MeOH, 20°C , 15 h; 2) PyBOP, **41**, Et_3N , DMF, 34% over 2 steps.

The bromide substituted 7-membered DHQ (*R*)-**58** was also synthesised as it can be used as a good building block for attaching different linkers (Scheme 2.9). The conditions used were the same as those for the 6-membered analogue (*R*)-**34** via a nucleophilic aromatic substitution on **33**, followed by the nitro reduction with Fe(0) in acetic acid (Scheme 2.9). Again, the 7-membered ring did not cyclise spontaneously at 50°C . By changing the proton source from acetic acid to trifluoroacetic acid, the desired fragment (*R*)-**58** was obtained in 35% yield. The *tert*-butyl ester of (*R*)-**57** is likely too sterically hindered to cyclise with the aniline, which might be the reason why trifluoroacetic acid is needed as proton source for the reduction and deprotection of the ester followed by the ring formation. The crude material was crystallised in isopropanol to afford the compound (*R*)-**58** in high purity.



Scheme 2.9 Synthesis of the 7-Br 7-membered DHQ (*R*)-**58**. *Reagents and conditions:* i) (*R*)-**45**, DIPEA, DMF, 85°C , 18 h, 96%; ii) Fe(0), TFA, 50°C , 2 h, 35%.

2.3.3 Stability study of (*R*)-12 and (*R*)-26

The 7-Br-DHQ compound (*R*)-35 was extremely unstable at elevated temperature, whereas the 7-membered ring analogue (*R*)-58 seemed stable under the same crystallisation conditions. To systematically study the stability of the 6-membered DHQ compound (*R*)-12 in comparison to the 7-membered analogue (*R*)-26, the compounds were stirred in D₆-DMSO at 50 °C over 5 days, and monitored by ¹H NMR analysis (Figure 2.6). After 20 hours, the oxidised compound 59 was detectable by the appearance of the singlet peak corresponding to the CH₃-protons of the quinoxalinone (Figure 2.6).

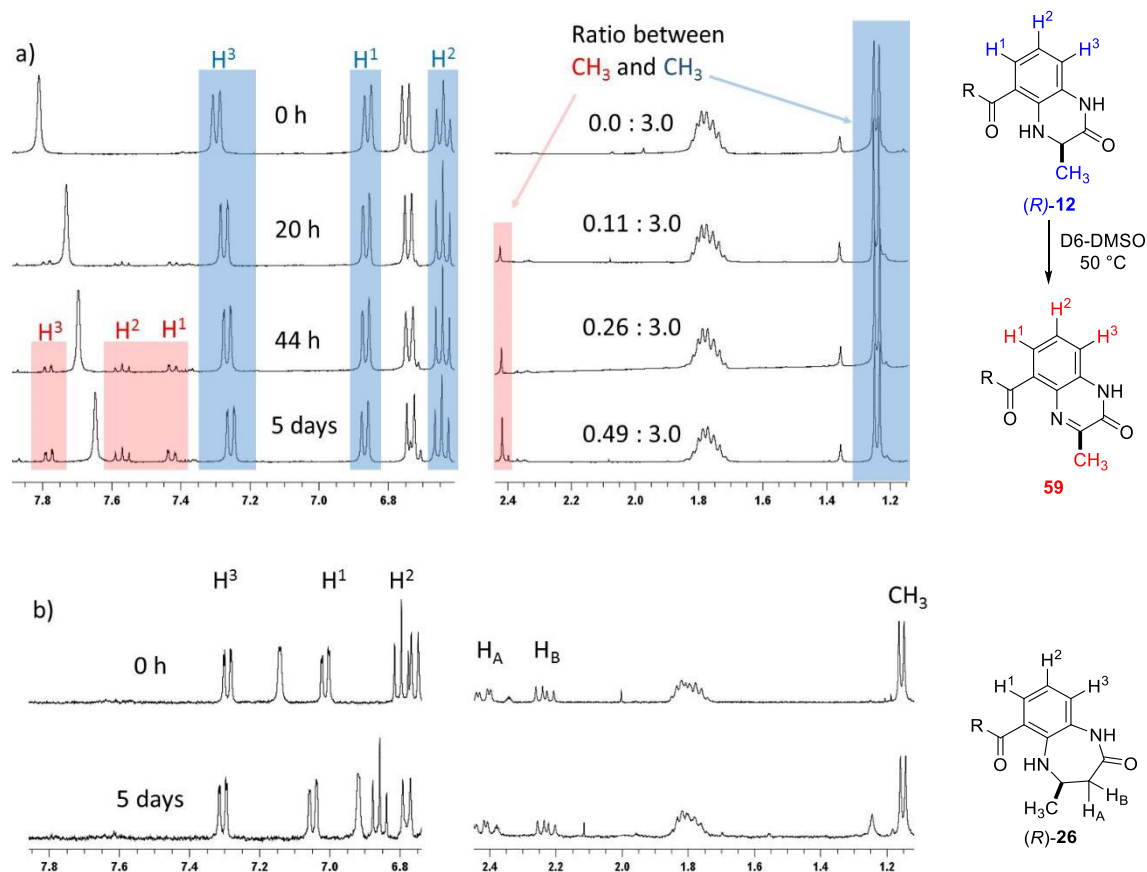


Figure 2.6 Stability monitoring of the 6-membered DHQ (*R*)-12 (a) and the 7-membered ring analogue (*R*)-26 (b) by ¹H NMR over 5 days. R = 7-MeO-THQ-(CH₂)₂NH.

Also, at the aromatic region 3 new signals belonging to the oxidised DHQ 59 appeared: three doublets of doublets (7.8, 7.6 and 7.4 ppm) (Figure 2.6a). These signals increased in intensity over 5 days resulting in 14% of the quinoxalinone 59. In comparison to the 7-Br DHQ (*R*)-35, this compound is still fairly stable. The 7-membered ring DHQ (*R*)-26 did not

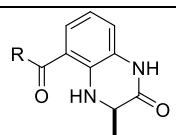
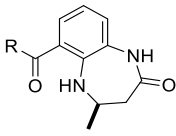
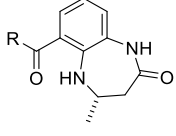
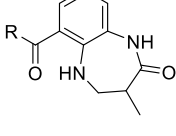
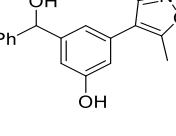
undergo in any oxidation and was stable as had been hypothesised (Figure 2.6b) and it indicates a great improvement regarding stability.

2.4 Biological evaluation of (*R*)-**12**, (*R/S*)-**26** and **27**

2.4.1 Affinities for CREBBP and BRD4 bromodomain

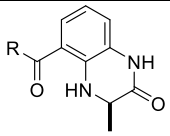
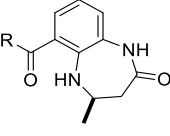
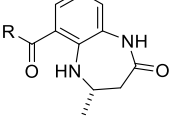
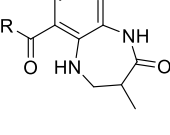
In order to evaluate the affinities and selectivities of the DHQ derivatives ((*R*)-**12**, (*R*)-**26**, (*S*)-**26** and **27**), differential scanning fluorimetry (DSF, Appendix A1) was performed using the CREBBP and BRD4(1) bromodomains (Table 2.1). The 6-membered ring compound (*R*)-**12** showed a thermal shift of 3.4 °C with CREBBP. The 6-membered ring compound (*R*)-**12** stabilised the CREBBP bromodomain, showing a thermal shift of 3.4 C. To our delight, the protein's stability was greater when treated with the 7-membered ring compound (*R*)-**26** ($\Delta T_m = 5.1$ C), whilst its enantiomer (*S*)-**26** showed no stabilisation ($\Delta T_m = 0.2$ C). The higher melting temperature of (*R*)-**26** compared to the starting compound could be due to a combination of a higher affinity and the more hydrophobic nature of the compound.⁸⁰ The racemic mixture of the α -methylated DHQ 7-membered ring **27** showed a lower protein stabilisation compared to (*R*)-**12**, indicating a lower CREBBP affinity. On the BET bromodomain BRD4(1), no significant protein stabilisation was observed for all the DHQ derivatives ((*R*)-**12**, (*R*)-**26**, (*S*)-**26** and **27**). In contrast, positive control compound **2** (BRD4(1) $IC_{50} = 382$ nM)⁵⁹ stabilised the protein with a thermal shift of 5.6 C. This is surprising, since (*R*)-**12** is reported to have an IC_{50} value of 1.2 μ M for BRD4(1).⁵⁶

Table 2.1 DSF data measured on the CREBBP and BRD4(1) bromodomains using 2 μ M of bromodomain, 10 μ M ligand and 5 \times SYPRO orange. R = 7-MeO-THQ-propylamine. (n = 4)

Compounds		ΔT_M CREBBP [$^{\circ}$ C]	ΔT_M BRD4(1) [$^{\circ}$ C]
(R)-12		3.4 ± 0.2	1.0 ± 0.5
(R)-26		5.1 ± 0.2	0.5 ± 0.2
(S)-26		0.2 ± 0.8	0.1 ± 0.2
27		1.7 ± 1.3	-0.4 ± 1.4
2		3.1 ± 0.7	5.6 ± 1.7

To obtain quantitative data, AlphaScreenTM assays (Appendix A2) were kindly performed on the CREBBP bromodomain by Dr Oleg Fedorov at the Structural Genomics Consortium (Oxford, UK). The trend observed by DSF was in good agreement with the IC₅₀ values obtained from the AlphaScreenTM assay. The 6-membered DHQ (R)-12 and the 7-membered (R)-26 showed similar affinity, whereas no ligand binding was observed for (S)-26 (Table 2.2). This is a striking result, demonstrating that altering the stereochemistry of the methyl group changes a potent ligand to an inactive compound. This compound could serve as an important negative control for future biological work. In comparison, changing the stereochemistry of (R)-12 only results in a 8-fold decrease in CREBBP affinity.^{56,57}

Table 2.2 Affinity of the DHQ analogues (*R*)-**12**, (*R/S*)-**26** and **27** on the CREBBP bromodomain. Measured by AlphaScreen™ R = 7-MeO-THQ-propylamine.

Compounds		IC ₅₀ CREBBP [μM] (n = 6)
(<i>R</i>)- 12		1.6 ± 0.5
(<i>R</i>)- 26		1.4 ± 0.2
(<i>S</i>)- 26		> 50
27		10.2 ± 3.3

The racemic β²-DHQ analogue **27** also showed a lower potency of 10 μM. This is likely because the (*R*)-enantiomer has a higher affinity than the (*S*)-enantiomer, and hence the racemic mixture showed a decreased potency. It was noted that, in this assay, the IC₅₀ value of compound (*R*)-**12** was significantly lower compared to the previously published affinity determined by AlphaScreen™ (IC₅₀ 323 nM).⁵⁶ This shows some of the drawbacks of the AlphaScreen™ assay. This technique results in the correct trend of binding affinities if the compounds are measured on the same plate, however the reproducibility of quantitative data can be problematic.⁸¹

The promising compounds (*R*)-**26** and (*S*)-**26** and the reference compound (*R*)-**12** were measured by isothermal titration calorimetry (ITC, Appendix A3) on the CREBBP bromodomain (Figure 2.7). The published CREBBP affinity of (*R*)-**12** was reproduced with a K_D of 470 nM (Figure 2.7a). The 7-membered DHQ analogue (*R*)-**26** showed a slightly lower affinity (903 nM) compared to the 6-membered ring analogue (*R*)-**12** (Figure 2.7b).

More importantly, (*S*)-**26** did not show any affinity by ITC and confirms the previously observed trends obtained by DSF and AlphaScreen™ (Figure 2.7c).

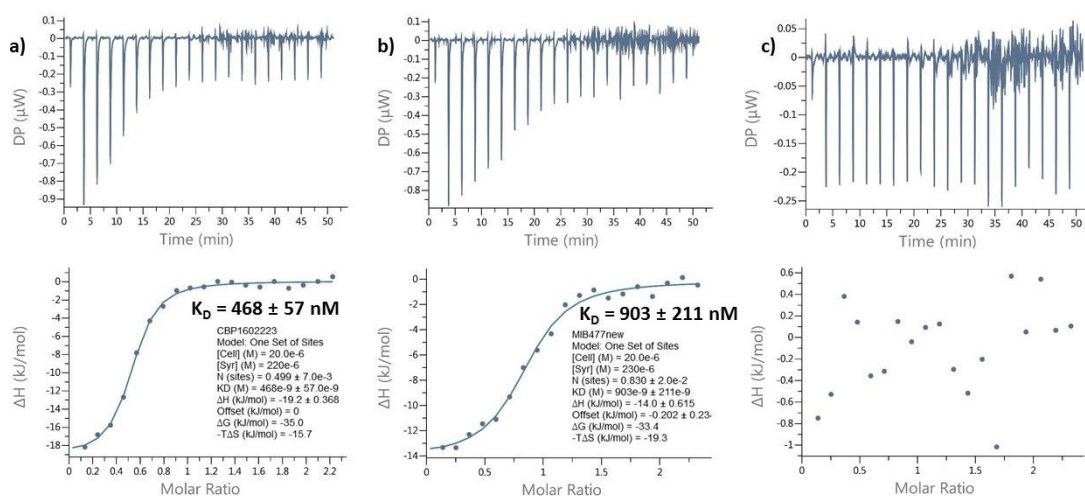


Figure 2.7 ITC measurements of (a) (*R*)-**12** and the 7-membered analogues (b) (*R*)-**26** and (c) (*S*)-**26** on the CREBBP bromodomain.

The dissociation constant of compounds (*R*)-**12** and (*R*)-**26** were then determined for the BET bromodomain BRD4(1) (Figure 2.8). Both compounds showed a low μM affinity for the BET bromodomain, resulting in only a 2 to 5-fold selectivity for CREBBP over BRD4(1), which is not sufficient for a probe.

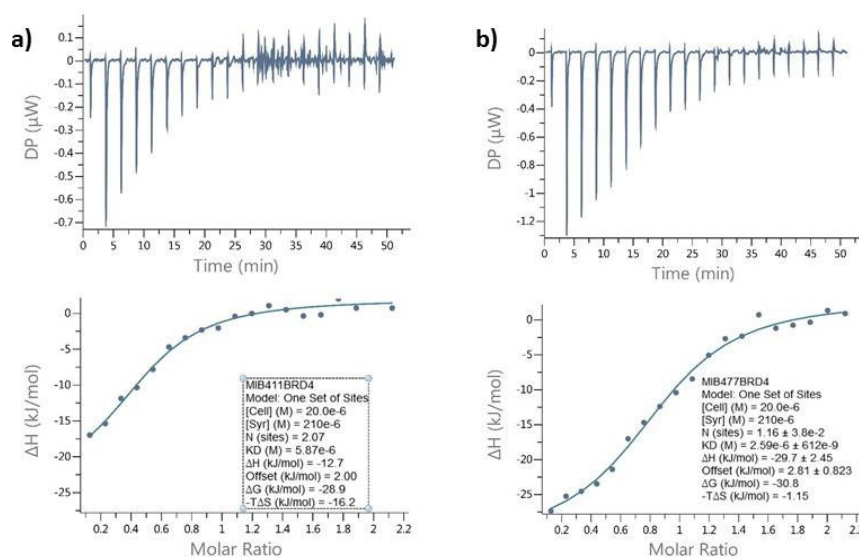


Figure 2.8 ITC measurements of (a) (*R*)-**12** and the 7-membered analogues (b) (*R*)-**26** on the BRD4(1) bromodomain.

To confirm the CREBBP bromodomain affinity of compounds (*R*)-**12** and (*R*)-**26**, Car-Purcell-Meiboom-Gill (CPMG)-NMR was performed.⁸² This technique can be used to obtain quantitative binding data by titrating protein into a ligand solution and observing the peak broadening of the ligand signal.

The peak half width ($\nu_{1/2}$) of an NMR signal correlates with the reciprocal value of the spin-spin relaxation time (T_2) upon protein binding (Figure 2.9, Eq. 1). The spin-spin

relaxation time (T_2) of small molecules is longer lived as compared to macromolecules because the tumbling rate decreases with increasing size. This means ligand binding to the protein results in a decrease in the T_2 relaxation time and a broader signal. The signal broadening can be quantified by measuring the relative peak height of the ligand to an internal standard that does not bind to the protein. Fumaric acid was chosen as internal standard because it gives a distinct singlet peak at 6.38 ppm, which does not interfere with the ligand and protein signals. CREBBP bromodomain was titrated into a solution of either (*R*)-**12** (a) or (*R*)-**26** (b) containing the internal standard fumaric acid (Figure 2.10). The broadening of the methoxy signal of (*R*)-**12** was observed upon addition of 1 μ M CREBBP bromodomain (Figure 2.10a). The decrease in peak height can be observed with increasing protein concentration and the methoxy peak of (*R*)-**12** completely vanishes after adding 10 μ M of the CREBBP bromodomain protein. The small molecule signals of (*R*)-**12** were recovered when the solution of the ligand in 10 μ M protein was denatured at 95 °C, confirming the binding specificity. A K_D value of 400 nM for (*R*)-**12** was extracted,

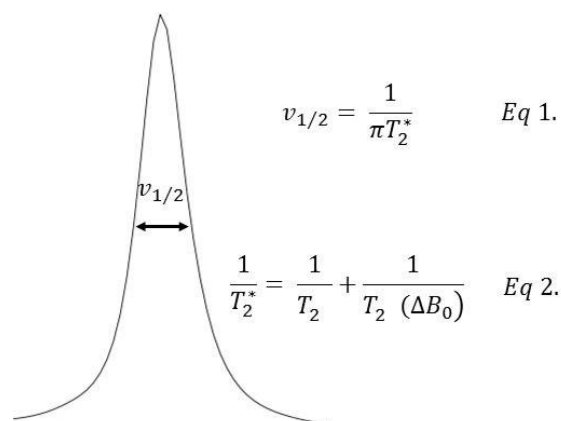


Figure 2.9 Visual representation of the peak half width ($\nu_{1/2}$) and the mathematical correlation of the spin-spin (transverse) relaxation time T_2^* (Eq. 1). The observed T_2^* is a combination of the genuine relaxation process T_2 and the relaxation process caused by field inhomogeneity (ΔB_0) (Eq. 2).

which is in good agreement with the ITC results (Figure 2.10c). The same experiment was performed with (*R*)-**26** and the relative peak height decreased slightly slower (Figure 2.10b and c) compared to (*R*)-**12**, which indicates a weaker affinity. A dissociation constant of 520 nM was calculated, which is slightly more potent compared to dissociation constant of 900 nM, measured by ITC.

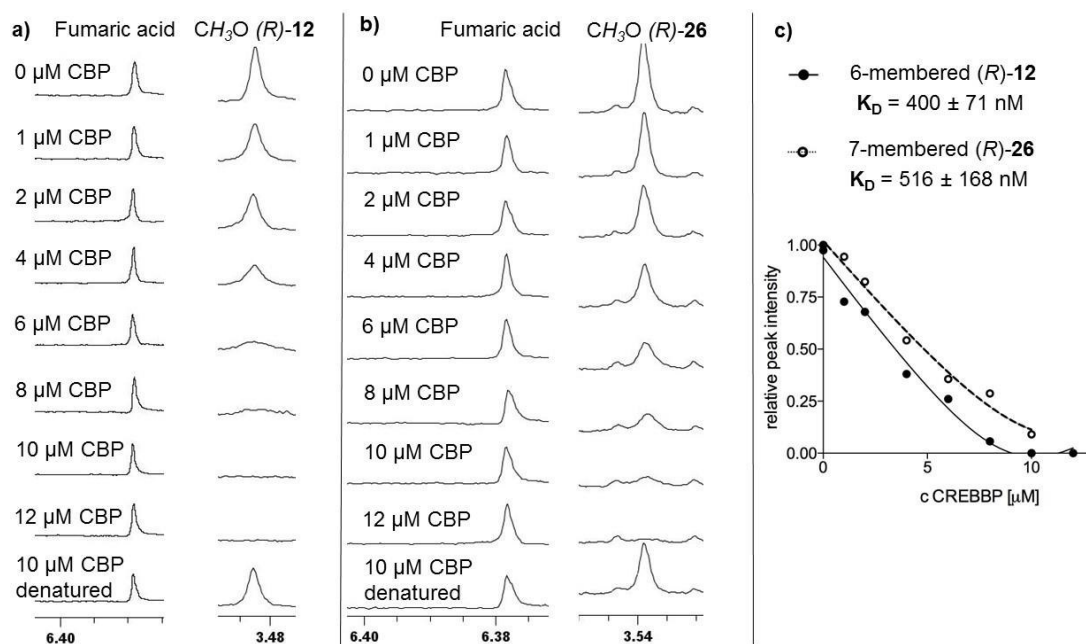


Figure 2.10 Titration spectra of the CREBBP bromodomain into 20 μM (a) (*R*)-**12** and (b) (*R*)-**26** showing the signal of the internal standard fumaric acid and the methoxy-THQ group. c) The relative peak height is plotted against the CREBBP concentration. the K_D value was determined according to Dalvit.⁸² The full NMR spectra are shown in Appendix C.

2.4.2 ¹⁹F- NMR on fluorine labelled tryptophan on CREBBP and BRD4(1)

¹⁹F-labelled NMR studies are a powerful method to obtain binding information between a ligand and the protein.⁸³ Incorporating ¹⁹F nuclei into a protein enables sensitive measurements of structural changes upon ligand binding. The advantage is that the fluorine nuclei do not interfere with any other signals of the protein as fluorine atoms are not present in natural biomolecules. Furthermore, the fluorine-19 nuclei has a similar magnetogyric ratio to the proton nuclei and with a 100% natural abundance it possesses

almost the same sensitivity as ^1H NMR.⁸⁴ This means short measurement times are required to obtain a good data.

Pomerantz and co-workers expressed ^{19}F -labelled tryptophan BRD4(1) and BPTF bromodomains and demonstrated that the wild type and the ^{19}F -labelled protein showed similar affinities to the BET ligand (+)-JQ1 (**1**).^{85,86} Subsequently, they performed fluorine NMR studies of the fluorinated protein and observed a big chemical shift of the fluorinated W81 residue upon binding of (+)-JQ1 (**1**) (Figure 2.11). Furthermore, they demonstrated that this technique can be used to detect weak binders and is a good orthogonal binding technique to ITC or CPMG-NMR.

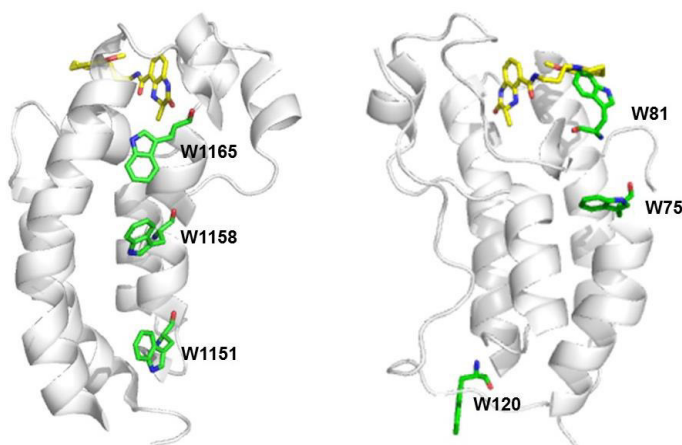


Figure 2.11 X-ray Crystal structures of the CREBBP (left, PDB: 4NYX) and the BRD4(1) bromodomain (right, PDB 4J0S) in complex with compound (*R*)-**12** (carbon = yellow). The tryptophan residues (carbon = green) are highlighted.

We were thankful to collaborate with Prof. William Pomerantz and Gabriela Perell from the University of Michigan. They expressed a CREBBP bromodomain mutant carrying three fluorinated tryptophan residues located along the α -helix B. Upon ligand binding, W1165 should show a change in chemical shift, whereas W1158 and W1151 are too far away to result in a chemical shift change (Figure 2.11).

The ^{19}F -NMR signals of the mutant CREBBP are observed between -123 and -127 ppm (Figure 2.12a and c). After the addition of $45\ \mu\text{M}$ (*R*)-**12**, the ^{19}F signal for W1165 shifted

0.5 ppm upfield (Figure 2.12a). This result confirms ligand binding to the CREBBP bromodomain. The other signals of the fluorinated tryptophan did not result in a chemical shift change. While titrating in the 7-membered DHQ (*R*)-**26** into the CREBBP bromodomain the same shift for W1165 was observed (Figure 2.12c).

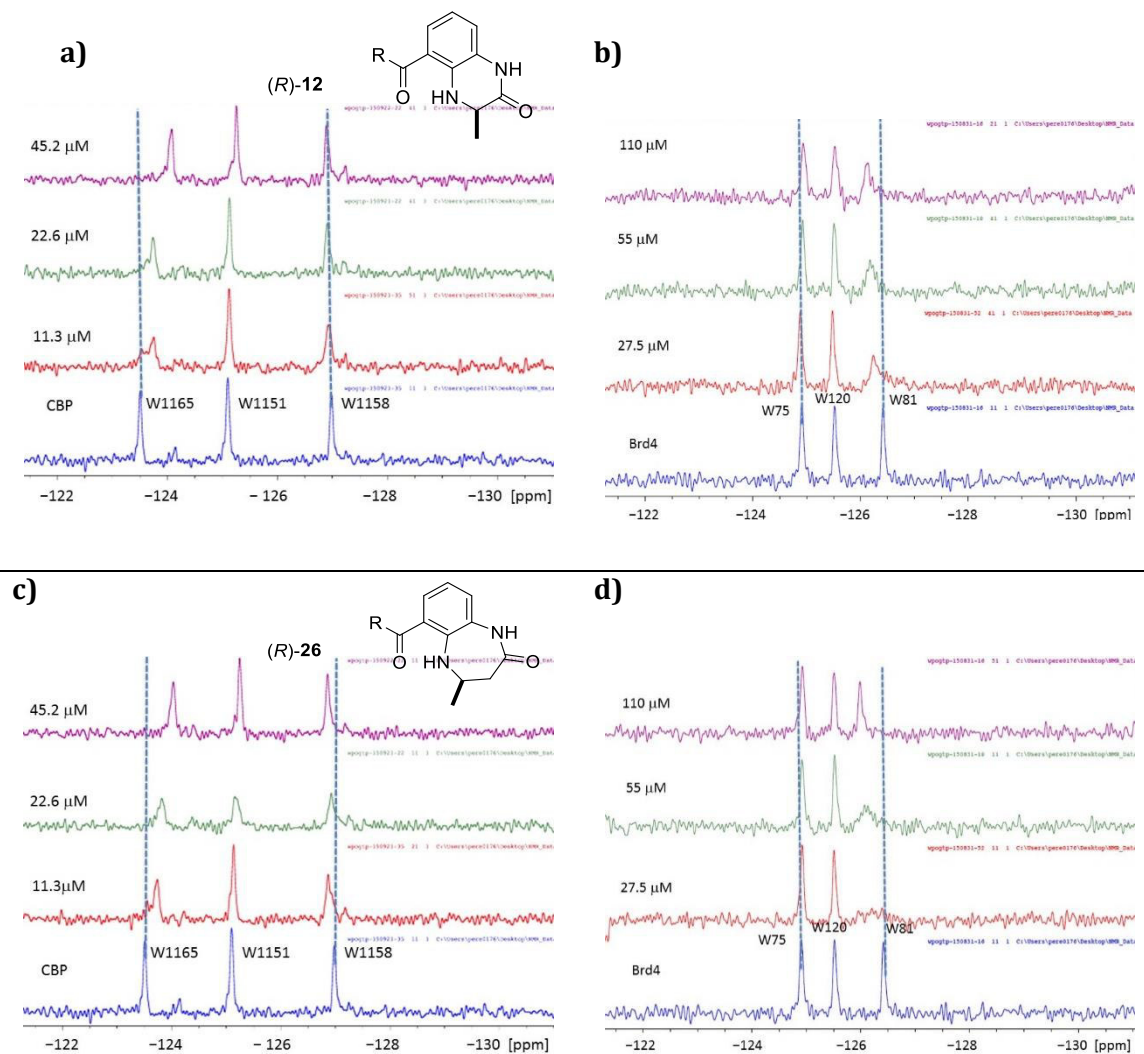


Figure 2.12 ^{19}F -NMR of the 6-membered DHQ (*R*)-**12** (a and b) and 7-membered (*R*)-**26** (c and d). On the left spectra (a and c) the mutant CREBBP bromodomains were titrated into the compound whereas on the right spectra (b and d) the mutant BRD4(1) bromodomain was used. R = 7-MeO-THQ.

More interestingly, the other fluorinated tryptophan residues (W1151 and W1158) also showed a slight shift, which indicates a structural change of the bromodomain. This observation suggests that the compound needs more space in the CREBBP binding site due

to the ring expansion of the DHQ. Consequently, the bromodomain undergoes a conformational change, which could explain the chemical shift difference.

A crystal structure of the tandem bromodomain and PHD finger of CREBBP, obtained by Zhou and co-workers, showed that the PHD finger forms an interaction along the α -helices B and C of the bromodomain.⁸⁷ As all of the fluorinated tryptophan residues are located on the α -helix B, we hypothesise that the conformational change of the bromodomain caused upon ligand binding may disrupt the domain-domain interaction between the CREBBP bromodomain and the neighbouring PHD finger, thus altering the function of CREBBP.

For the titration experiment on BRD4(1), both 6- and 7-membered DHQ analogues showed a shift of the ^{19}F signal of W81, which confirms binding to the BET bromodomain (Figure 2.12b and d). This results are in agreement with the ITC data.

2.4.3 X-ray crystallography

To further investigate the observation of the ^{19}F -NMR experiments, Dr Sarah Picaud and Prof. Panagis Filippakopoulos from the Structural Genomics Consortium obtained a co-crystal structure of the 7-membered DHQ (*R*)-**26** in CREBBP. The overlaid X-ray crystal structures of (*R*)-**26** and (*R*)-**12** in complex with CREBBP shows that both compounds have the same binding mode. The hydrogen bonds of the DHQ amide to N1168 are observed for both compounds. Furthermore, a cation- π interaction between the THQ and R1173 is present. These results are in good agreement with the molecular dynamics calculations discussed in chapter 2.3.1.

In Figure 2.13b and c, it is apparent that the 7-membered DHQ ring (*R*)-**26** requires more space in the binding pocket compared to (*R*)-**12**. Furthermore, the DHQ ring of (*R*)-**26** is slightly twisted in the binding pocket. This might result in a slightly weaker internal hydrogen bond between the aniline amine and carboxamide, which could explain the lower binding affinity. The selectivity of (*R*)-**26** over (*S*)-**26** can be explained by steric clashes in the KAc binding pocket and the *S*-enantiomer.

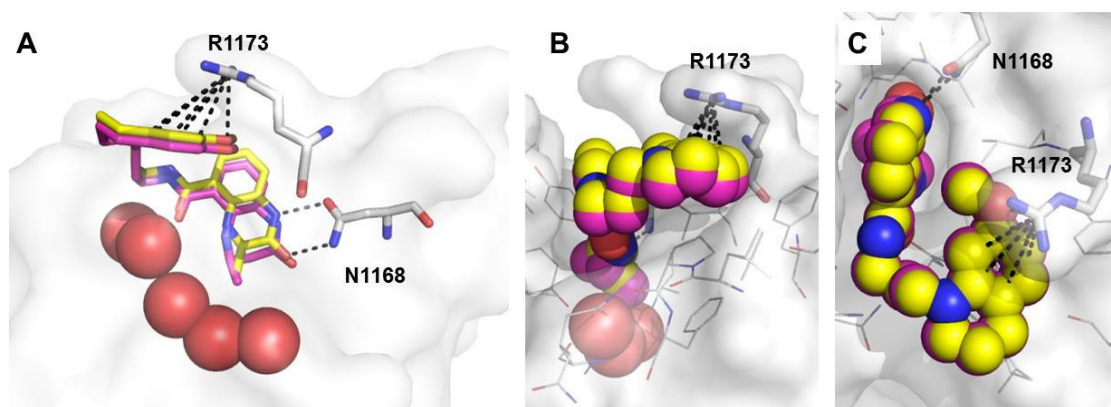


Figure 2.13 a) Overlaid crystal structure of (*R*)-**12** (carbon = yellow, PDB: 4NYX)⁵⁴ and (*R*)-**26** (carbon = purple) in the CREBBP bromodomain. The amino acid residues N1168 and R1173 are highlighted in bold and the conserved water molecules are shown as red spheres. (b) and (c) The ball representation shows more space is needed for (*R*)-**26** to fit into the KAc binding pocket.

The α -helix B of the CREBBP bromodomain X-ray crystal structures in complex with (*R*)-**12** and (*R*)-**26** seems identical, in contrast to the results from ¹⁹F-NMR experiment. This might be because the crystal structures are static whereas the NMR measurements are dynamic observations. It would be interesting to further investigate the domain-domain interaction between the CREBBP bromodomain and PHD finger.

2.5 Conclusion and discussion

A reliable and high yielding synthesis towards enantiopure (*R*)-**26** and (*S*)-**26** was developed. The ring-expanded DHQ ring of (*R*)-**26** was demonstrated to be more stable compared to (*R*)-**12**. We have shown that the ring expansion of the DHQ headgroup can be tolerated and results in a 900 nM CREBBP bromodomain ligand (*R*)-**26**. (*S*)-**26** does not show any binding affinity and could be a very useful negative control in future biological assays. The NMR study of ¹⁹F-tryptophan-labelled CREBBP indicates that (*R*)-**26** changes the α -helix B structure and might affect the domain-domain interaction between the bromodomain and the neighbouring PHD finger, but the X-ray crystal structure did not confirm this result.

This work has been published independently by Genentech and Constellation in 2016.^{88,89} Their researcher discovered the 7-membered DHQ fragment **60** by screening a fragment library. The authors optimised this hit **60** to a potent and selective CREBBP ligand **61** (Figure 2.14). The compound (*R*)-**26** was synthesised in July 2014 and it was included in my transfer of status report.

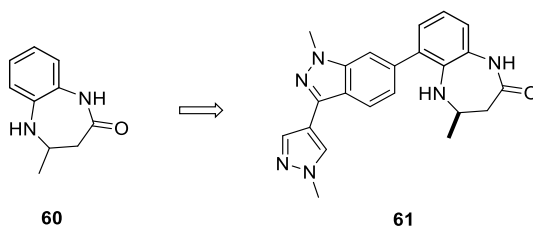


Figure 2.14 Discovery and optimisation of the potent and selective CREBBP ligand **60** by Genentech, starting from the 7-membered DHQ fragment **61**.

Chapter 3

Structure activity relationship of the cation- π interaction

3.1 Introduction and aims

The induced fit pocket on CREBBP formed by an electrostatic driven cation- π interaction between R1173 and the THQ ring of (*R*)-**12** was discovered in our group (Figure 3.1).⁵⁶ R1173 is only observed in 4 human bromodomains²³ (CREBBP, EP300, PHIP(2) and BWRD3(2)) and can be an important handle to increase ligand selectivity over

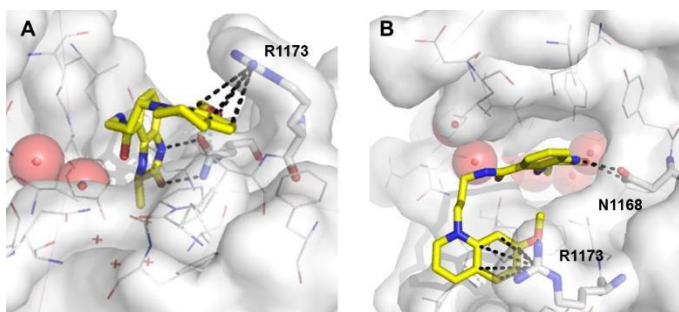


Figure 3.1 The cation- π interaction between R1173 and 7-MeO-THQ (*R*-**12**) is highlighted (PDB: 4NYX)⁵⁴ with dotted lines. The conserved water molecules are shown as red spheres.

other bromodomains. To optimise CREBBP bromodomain selectivity and potency, a structure activity relationship (SAR) analysis of the THQ group was performed. The X-ray crystal structure of (*R*)-**12** suggests only 7-position substitutions of the THQ ring are tolerated as other substitutions patterns will clash with the protein backbone (Figure 3.1).

The main aims of this chapter are to:

- Study the cation- π interaction between R1173 and the THQ.
- Compare the electrostatic surface potential (ESP) of the THQ analogues with CREBBP bromodomain affinities.
- Determine group efficiency of (*R*)-**12**.

3.2. Introduction to cation- π interactions

Cation- π interactions in proteins were first observed in the early 1990s in the active site of acetylcholine esterase.⁹⁰ The first evidence of this non-covalent interaction was the X-ray crystal structure of acetylcholine esterase, showing that the positively charged ammonium ion of acetylcholine was in proximity to 14 aromatic amino acids, and not as previously suggested to negatively charged amino acids (Figure 3.2a).⁹¹ Mutation studies of the aromatic amino acids in the binding site demonstrated that the Trp residue is extremely important for the active site, as complete enzyme activity was lost in a W86A mutant, whereas mutations of other amino acids had less of an effect. This observation underlined the importance of this cation- π interaction.⁹² Beene *et. al.* investigated reducing the electron density of tryptophans by incorporating mono-, di-, tri- and tetra-fluorinated Trp residues into the acetylcholine receptor. They observed that reduction of the electrostatic potential of the Trp residues the acetylcholine activity was substantially lowered (Figure 3.2b).⁹³

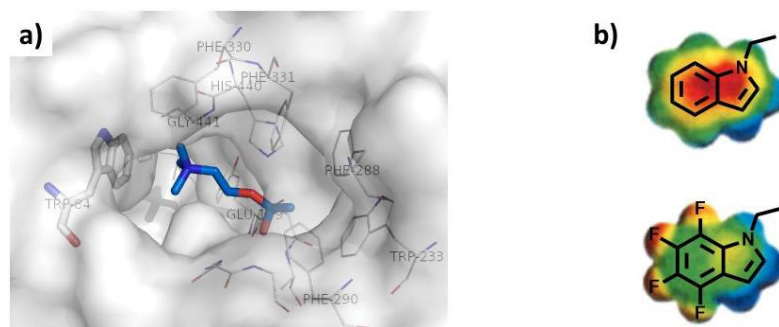


Figure 3.2 a) X-ray crystal structure (PDB: 2ACE) of the acetylcholine esterase in complex with acetylcholine (carbon = marine). The amino acid residues within 5 Å around acetylcholine are highlighted as white lines and the important Trp residue for the cation- π interaction is shown in bold. b) Electrostatic surfaces of the Trp and tetra fluorinated Trp, where blue is positive and red is negative. Adapted with permission from Beene *et al.*⁹³ Copyright (2002) American Chemical Society.

Dougherty and others established the importance of the cation- π interaction experimentally and computationally.^{90,94–97} Calculations of the binding energy between a sodium ion and substituted benzene analogues produced a good correlation between the

calculated binding energy and the electrostatic potential.⁹⁸ Further electrostatic surface potential (ESP) calculations of aromatic and heteroaromatic compounds demonstrated that amine substituents have the highest electrostatic surface potential, which means they are the most negatively polarised aromatic rings. They further discussed that Trp residues are the most prominent aromatic amino acids for cation- π interactions due to the highly negative ESP, whereas Phe residues are less involved.⁹⁹ Gallavan *et al.* studied 600 proteins of the Protein Data Bank for cation- π interactions. They observed that every 77th amino acid residue in the protein contributes towards a cation- π interaction. The prevalence of this interaction implies that it plays an important role in protein stabilisation. The most common amino acid residue pairs was the strong interaction between the Trp and Arg residues.⁹⁷

The first report of a cation- π interaction between a small molecule ligand and a protein was discovered by Sorme *et al.* in galectin-3.¹⁰⁰ During the optimisation of the low affinity β -galactoside containing disaccharide **62**, they discovered a 50-fold affinity increase by adding aromatic rings on the 3-position. A X-ray crystal structure of **63** in galactin-3 revealed that the affinity increased due an induced fit pocket, formed by a cation- π interaction between R144 and the aromatic ring (Figure 3.3).¹⁰¹

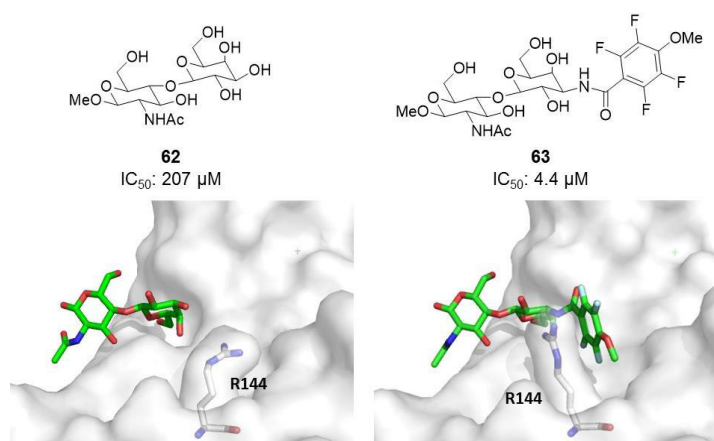


Figure 3.3 Crystal structures of the β -galactoside-containing disaccharide **XA** (carbon = green, left) in galactin-3 (PDB: 1KJL)⁵⁴ highlighting the R144 residue. The optimised β -galactoside containing disaccharide **XB** (carbon = green, right) shows an induced fit pocket and the cation- π interaction is observed (PDB: 1KJR),⁵⁴ which results in a high affinity compound.¹⁰¹

Cation- π interactions were also identified as being important for the design of potent Keap1 ligands to disrupt the PPI to Nrf2.¹⁰² As an example, the potent ligand **64** forms a cation- π interaction between R415 and the naphthalene (Figure 3.4). The other two important interactions for the binding affinity was a π - π stacking between the benzene substituent and Y334 as well as the electrostatic interaction between R483 and the carboxylic acid of **64**.¹⁰³

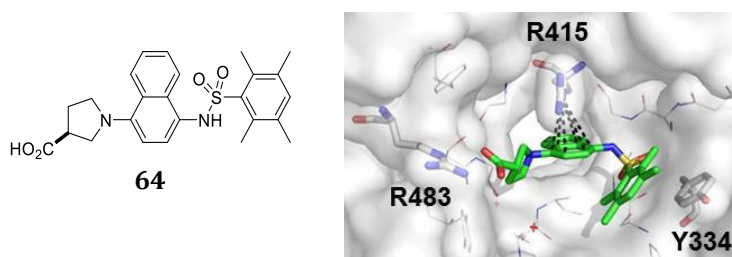


Figure 3.4 Crystal structures of **64** (carbon = green)⁵⁴ in Keap1 (PDB: 5CGJ) highlighting the residues R483, R415 and Y334. The cation- π interaction is indicated with black dotted lines.

As discussed in the introduction, Conway and coworkers observed the cation- π interaction between R1173 of the CREBBP bromodomain and the THQ ring of (*R*)-**12**. This interaction was also found to be important for the CREBBP ligands **16**, **17**, I-CBP112 (**18**), and **61**.

3.3 Electrostatic surface potential of THQ derivatives

For a strong cation- π interaction, electron-rich THQ analogues were desired for our system. A collaboration with Wilian A. Cortopassi, from the Paton group (University of Oxford), was established to identify electron-rich THQ derivatives. A computational model was developed to calculate ESP of THQ derivatives both qualitatively and quantitatively.¹⁰⁴ The model computed the ESP of the THQ-analogues, where the guanidinium residue (mimicking the asparagine) was placed parallel to the THQ at a distance of 3.5 Å (Figure 3.5). It was noted that the single variable ESP calculations (calculating only the π -system) were insufficient for a good binding energy prediction, as the electrostatic potential of the THQ substituent is important. Subsequently, a model containing calculations of the ESP of

the cation- π interaction and the cationic-electrostatic-interaction with the substituent was developed using density functional theory (DFT).¹⁰⁴

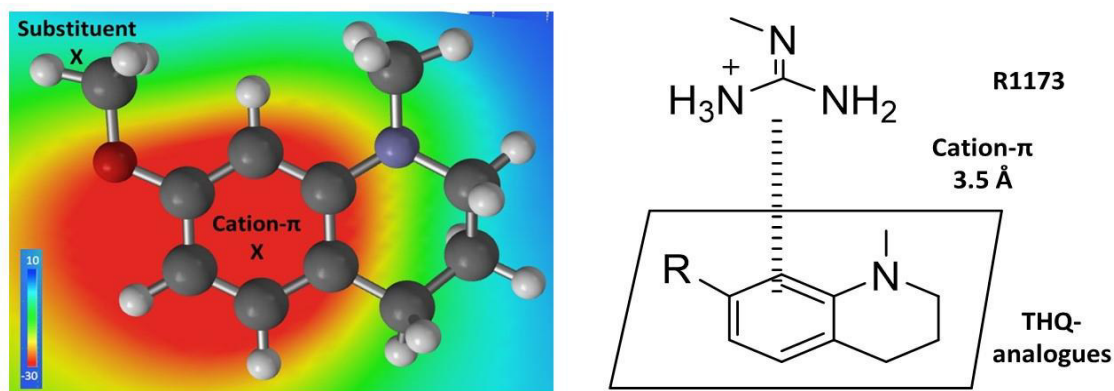


Figure 3.5 A 2D ESP isosurface generated at 3.5 Å of the 7-MeO-THQ and the guanidinium residue. Colour scale spans -30 to 10 kJ/mol, where red indicates negative polarised and blue positive polarised regions. Figure provided with permission by Willian A. Cortopassi.

Qualitative and quantitative calculation of six different 7-substituted THQ analogues (**64**-**69**) and 6-methoxyindole (**70**) were performed (Figure 3.6 and Table 3.1). With the unsubstituted THQ **64**, an electron-rich π -system was observed. By introducing the mesomerically electron donating methoxy **65** and amine **67** substituents, the electron density of the aromatic ring is increased. Furthermore the substituents also contribute to the electrostatic interaction with the guanidine residue. The acetamide **68** substituent has a lower electron density in the π -system, however, the amide is an electron-rich substituent, which enhances the electrostatic interaction with R1173. This effect means while the cation- π interaction is diminished, and the electrostatic interaction is maintained. The overall ESP of compound **68** is comparable to the methoxy substituted analogue **65**, indicating they should have similar binding affinities for the CREBBP bromodomain (Table 3.1).

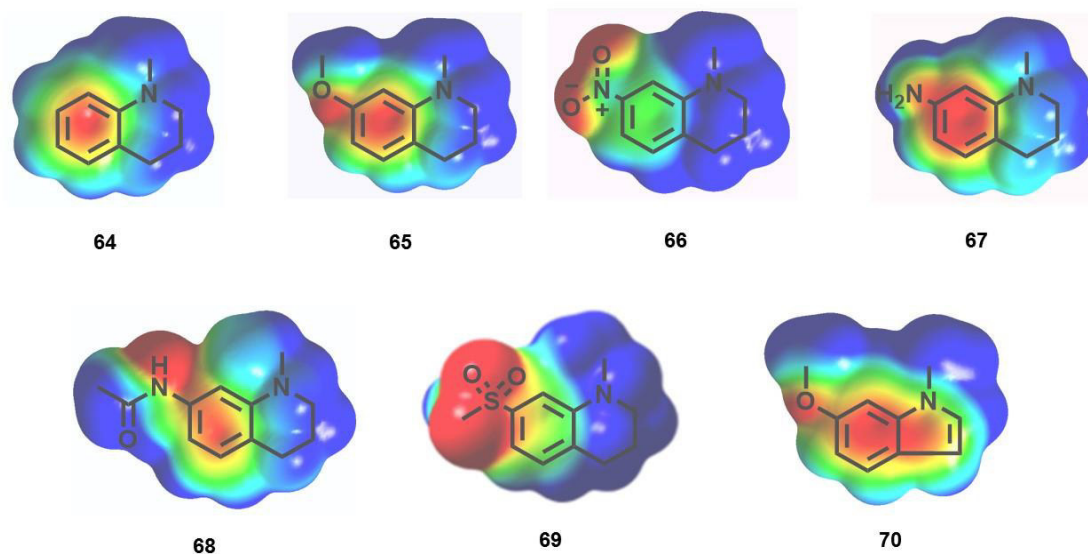


Figure 3.6 2D generated ESP isosurfaces of THQ analogues with different substituents on the 7-position. Red indicates electron dense regions whereas blue is electron deficient. The calculated values of ESP for the cation- π and the substituents are shown in the table.

Table 3.1 Calculated values of ESP for the cation- π interaction and the electrostatic interaction of the THQ **64-70**.

Compound	ESP cation- π (Hartrees)	ESP substituent (Hartrees)	ESP total (Hartrees)
64	-0.017	0	-0.017
65	-0.021	-0.013	-0.034
66	-0.004	-0.016	-0.020
67	-0.025	-0.014	-0.039
68	-0.016	-0.014	-0.030
69	N/A	N/A	N/A
70	-0.020	-0.012	-0.032

The THQ with the electron-withdrawing nitro **66** and methyl sulfone **69** substituents contain almost no electron density in the aromatic system, but they contain highly polarised substituents. The overall electrostatic potential of the nitro compound **66** has a higher overall electron density compared to the unsubstituted THQ **64** and hence should result in a stronger affinity. The 7-methoxy indole **70** shows promising electrostatics on the π -system and the substituent. The structural change of the THQ to the indole system is

unlikely to affect the binding properties. Based on these data, we decided to synthesise the discussed THQ analogues.

3.4 Synthesis of first generation THQ analogues

3.4.1 Retrosynthetic analysis

The general synthesis of the THQ analogues were based on the previous syntheses performed by Dr Timothy Rooney.⁵⁷ To obtain 7-substituted-THQ analogues (R = H, OMe, NH₂, NO₂, NHAc, SO₂Me), there was a need to protect the amine of the linker (Figure 3.7). The propyl linker can be disconnected at the THQ amine to give the THQ fragments (**39**, **71**, **73**, **74**) and the linker. 3-Bromo-*N*-propylphthalimide **72** is a cheap, commercially available building block and will be used for this synthesis. The brominated THQ **74** has a good reactive handle to introduce amines, thiols or sulfones, by transition metal-catalysed chemistry. The brominated THQ **74** and 7-NO₂-THQ **73** can be obtained by either a bromination¹⁰⁵ or nitration,¹⁰⁶ respectively, starting from THQ **71**. The synthesis of the 7-MeO-THQ **39** was discussed in Chapter 2. The 6-methoxy indole derivative can be synthesised in a similar manner as **41** starting with the commercial available 6-methoxy indole.

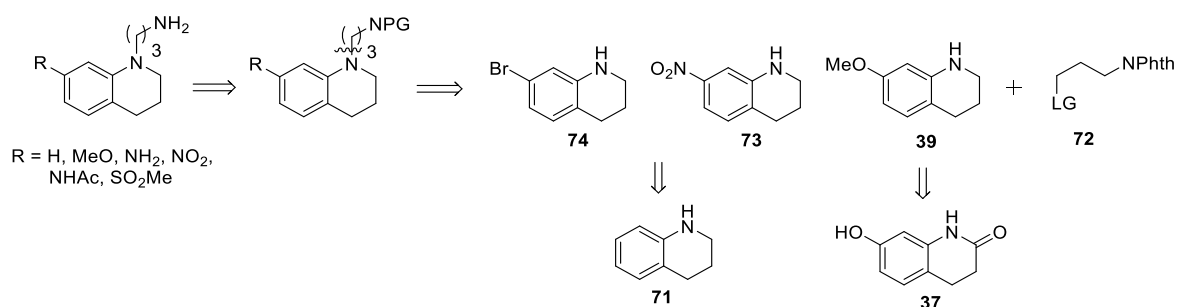
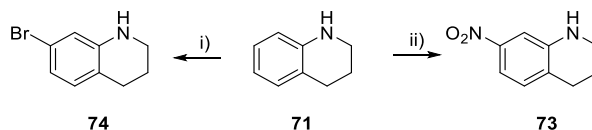


Figure 3.7 Retrosynthetic analysis to access a library of 7-substituted THQ analogues.

3.4.2 Synthesis of the THQ building blocks **72** and **73**

The bromination of THQ **71** was performed with bromine in sulfuric acid according to Kolmakov *et al.* (Scheme 3.2).¹⁰⁵ The reaction resulted in a mixture of the desired 7-

bromo- **74**, 5-bromo-, and 5,7-dibromo-THQ. Two silica gel column chromatography purifications with different eluents were necessary to isolate the pure single isomer **74** in a 17% yield. The yield was low, due to partial co-elution of the regio-isomers.



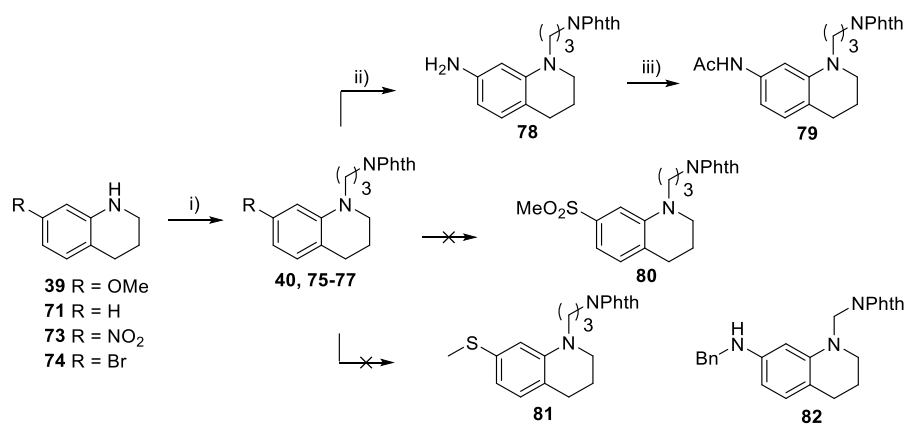
Scheme 3.2 Synthesis of 7-substituted THQ analogues **73** and **74**. *Reagents and conditions:* i) Br₂, Ag₂SO₄, H₂SO₄, 0 °C, 2 h, 17%; ii) HNO₃, H₂SO₄, -10 to 0 °C, 30 min, 46%.

The THQ **71** was nitrated using nitric acid and sulfuric acid and a mixture of the 5- and the desired 7-isomer **73** were obtained. Purifications by silica gel column chromatography enriched the desired compound **73** but could not be completely separated. A second purification using aluminium oxide as stationary phase yielded 46% of the pure 7-nitro-THQ **73**.

3.4.3 Synthesis of the THQ analogues 86-88 and 96-97

The different 7-substituted THQ analogues (**39**, **71**, **73**, **74**) were reacted with 3-bromopropyl-*N*-phthalimide (**72**) in the presence of potassium carbonate in DMF (Scheme 3.3). The unsubstituted THQ **71** and the electron-rich 7-MeO-THQ **39** were isolated in 49% and 60% yield, respectively (Table 3.2). The bromine analogue **74** showed a low conversion with only 11% isolated yield, and the electron-poor 7-nitro-THQ **73**, did not result in any product. To overcome the low reactivity of 7-NO₂-THQ **73** a more reactive electrophile was desired and/or the nucleophilicity of the THQ amine **73** has to be increased. To improve its nucleophilicity, **73** was deprotonated with sodium hydride or ^{*n*}BuLi, but still no reaction was observed. Compound **73** was reacted successfully with acetyl chloride to demonstrate its reactivity to a good electrophile. The electrophilicity of the 3-bromopropyl-*N*-phthalimide **72** was increased by introducing a better leaving group, through changing the bromide to an iodide. Repeating the previously established reaction conditions and adding NaI to the mixture resulted in a slow conversion towards **76**. After

48 hours at 85 °C, 20% of the desired compound was isolated and the remaining compound was unreacted starting material **73**. These reaction conditions were also applied to the brominated compound **74** and the yield for this system was increased to 24%. Reduction of the 7-NO₂-THQ **73** to the amine **78**, followed by acetylation resulted in the acetylated-amine-THQ **79** in 51% yield over 2 steps. The 7-Br-THQ **74** was reacted using a Cu(I)-catalysed reaction with sodium methylsulfonate and proline as ligand, to install the methyl sulfone according literature procedures,¹⁰⁷ but no conversion to **80** was observed. Other Cu(I)-catalysed reactions on the 7-Br-THQ with better nucleophiles, such as benzylamine (**82**) and methyl thiol (**81**), did not result in any conversion. Therefore, the investigation of the methyl sulfone was stopped.

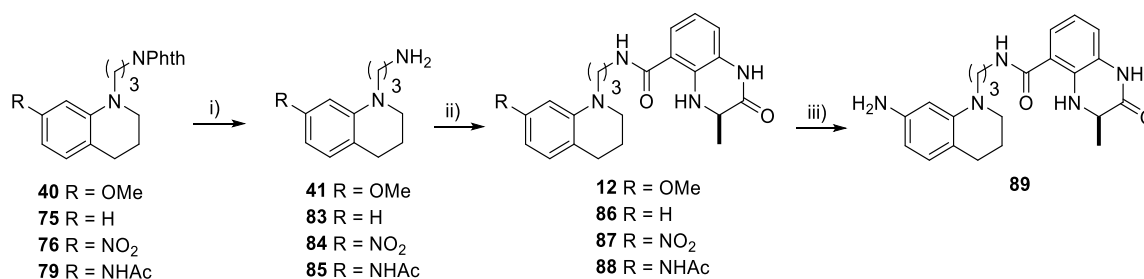


Scheme 3.3 Synthesis scheme for the introduction of different 7-substituted THQ analogues. *Reagents and conditions:* i) K₂CO₃, 3-bromopropyl-*N*-phthalimide, DMF, 85 °C, 16-48 h; 24-60% ii) R = NO₂, H₂, Pd/C, MeOH, CH₂Cl₂, rt, 3 h, 69%; iii) AcCl, Et₃N, CH₂Cl₂, 0 to rt, 1 h, 74%.

Table 3.2 Yield for the alkylation of the different 7-substituted THQ analogues (**39**, **71**, **72**, **73**) with 3-bromopropyl-*N*-phthalimide.

Entry	R	Yield in % i)	Additives
1	H	49 (75)	--
2	MeO	60 (40)	--
3	NO ₂	20 (76)	NaI
4	Br	24 (77)	NaI

The *N*-phthalimides (**40**, **75-76**, **79**) were deprotected with hydrazine and purified by an acid-base extraction to isolate the free amines (**41**, **83-85**) (Scheme 3.4, Table 3.3). The amide couplings with the 7-substituted THQ analogues (**41**, **83-85**) using the established PyBOP coupling conditions resulted in the desired compounds (**12**, **86-88**). The nitro-compound **87** was reduced to the amine **89** by a Pd/C-catalysed hydrogenolysis. This compound **89** was observed to be unstable in solution and no normal- or reversed-phase HPLC data could be obtained, despite having obtained clean ^1H and ^{13}C NMR spectra. For this reason **89** was excluded from the biological tests.



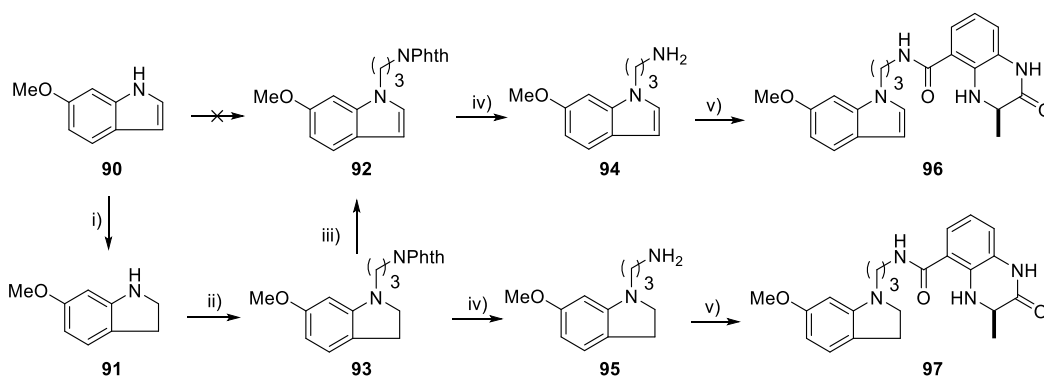
Scheme 3.4 Synthesis scheme for the 7-substituted THQ analogues (**12**, **86-88**). *Reagents and conditions:* i) Hydrazine monohydrate, MeOH, CH₂Cl₂, 70 °C, 2 h; ii) (*R*)-**32**, PyBOP, Et₃N, DMF, rt, overnight; iii) R = NO₂, H₂, Pd/C, MeOH, CH₂Cl₂, rt, 3 h, 60%.

Table 3.3 Yields for deprotection of the *N*-phthalimides (**40**, **75-76**, **79**) and the amide coupling of (*R*)-**32**.

Entry	R	Yield in % i)	Yield in % ii)
1	H	61 (83)	46 (86)
2	MeO	96 (41)	77 (12)
3	NO ₂	32 (84)	77 (87)
4	NHAc	66 (85)	62 (88)

The synthesis of the 6-methoxyindole derivative **96** commenced with compound **90** by nucleophilic substitution of the indole with 3-bromopropyl-*N*-phthalimide **72** (Scheme 3.5). However, no conversion to **92** was observed, even with addition of NaI. This lack of reactivity can be explained by the fact that the amine of the indole is even more delocalized than the 7-NO₂-THQ **73**. To increase the reactivity, the indole **90** was reduced

with borane to 2*H*-indole **91** in 82% yield. This 2*H*-indole **91** reacted well to nucleophilic substitution for the installation of the propyl linker. Consequently the 2*H*-indole **93** was oxidised with MnO₂ to **92** in 78% yield. The compounds **92** and **93** were reacted according to the previously discussed procedures to isolate the indole derivatives **96** and **97** in 47% and 49%, respectively.

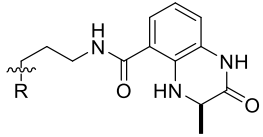
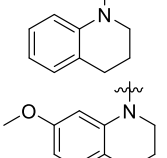
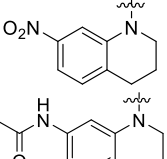
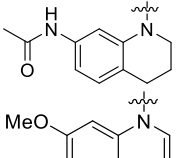
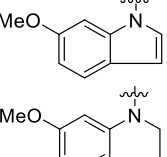
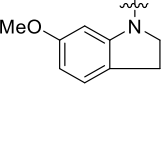


Scheme 3.5 Synthesis of the 6-substituted indole **96** and **97**. *Reagents and conditions:* i) 1) BH₃, THF 0 °C, 30 min, 2) TFA, 0 °C, 45 min, 82%; ii) K₂CO₃, **72**, DMF, 85 °C, 15 h, 69%; iii) MnO₂, CH₂Cl₂, 40 °C, 16 h, 78%; iv) Hydrazine monohydrate, MeOH, CH₂Cl₂, 70 °C, 2 h, 53% for (**94**) and 67% for (**95**); v) (*R*)-**32**, PyBOP, Et₃N, DMF, rt, overnight, 89% for (**96**) and 73% for (**97**).

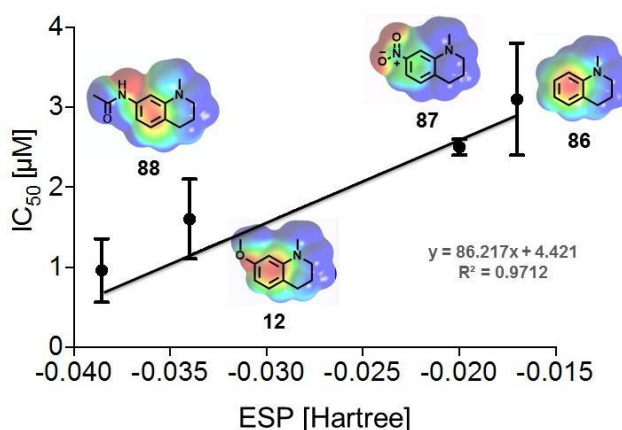
3.4.4 Biophysical analysis of **86-88** and **96-97** binding to the CREBBP bromodomain

Subsequently, the synthesised THQ derivatives (**86-88**, **96-97**) were tested using AlphaScreen™ on CREBBP, to probe the electronic effect of the cation- π interaction (Table 3.4). The unsubstituted THQ **86** showed the weakest affinity of the THQ compound series with an IC₅₀ value of 3.1 μ M. The 7-methoxy **12** and 7-acetamide- THQ **88** resulted in the most potent ligands as predicted by the ESP calculations (Table 3.4). The 7-nitro-substituted compound **87** has a slightly higher affinity compared to **86**. The indole derivatives **96** and **97** resulted in the weakest affinities in the AlphaScreen™ assay with IC₅₀ values of approximately 4.8 μ M and 5.7 μ M for the CREBBP bromodomain, respectively. The structural change of the THQ to the indole seems not tolerated, perhaps because of a potential clash with L1109 residue on the CREBBP bromodomain. The reduced CREBBP binding affinity of **96** compared to **12** was confirmed by ITC with a K_D value of 1.7 μ M.

Table 3.4 Overview of the AlphaScreen™ and ITC results on the CREBBP bromodomain with the THQ analogues **12**, **86-88** and **96-97**.

Compounds	AlphaScreen™ IC ₅₀ [μ M]	ITC CREBBP K _D [μ M]	ITC BRD4(1) K _D [μ M]
86 	3.1 ± 0.7	N/A	N/A
12 	1.6 ± 0.5	0.47 ± 0.06	3.59 ± 1.17
87 	2.5 ± 0.1	N/A	N/A
88 	1.0 ± 0.4	1.18 ± 0.24	2.35 ± 0.52
96 	4.8 ± 0.3	1.70 ± 0.44	5.36 ± 1.39
97 	5.7 ± 0.5	N/A	N/A

The comparison of the ESP with the AlphaScreen™ data for the 7-substituted THQ analogues (**12**, **86-88**) showed a good correlation, but the effect of the substituent is relatively small (Figure 3.8). An approximately 3-fold affinity increase was observed from the electron-rich analogue **12** compared to the unsubstituted THQ **86**.

**Figure 3.8** Linear regression of the electrostatic potential and the CREBBP affinity of **12**, **86-88** shows a good correlation.

The dissociation constant of the acetamide **88** was determined for the CREBBP bromodomain using ITC and CPMG-NMR analysis, giving values of 1180 nM (Appendix B1) and 869 nM (Appendix C), respectively. This shows that 7-MeO-THQ **12** is a higher affinity ligand than the 7-acetamide substituent **88**. Furthermore, the selectivity between the CREBBP and BRD4(1) bromodomain decreased from 7-fold to 2-fold between compounds **12** and **88**. This suggests having a more polarised substituent does not increase the CREBBP selectivity.

^{19}F -NMR of the fluorine-labelled tryptophan on CREBBP and BRD4(1) bromodomain in complex with ligand **88** showed a slight chemical shift on the tryptophan residues located close to the binding site (W1165 and W81, respectively) (Figure 3.9). A slow exchange rate with the CREBBP bromodomain was observed, indicating a long residence time for the ligand in the protein and hence the high affinity.

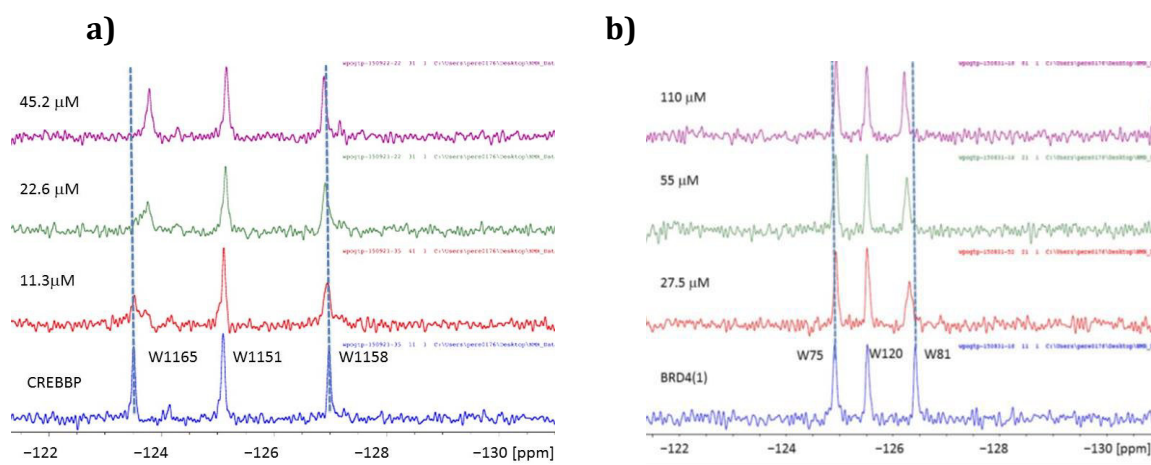


Figure 3.9 ^{19}F -NMR of the acetamide **88**. (a) **88** was titrated into mutant CREBBP bromodomain. (b) The mutant BRD4(1) bromodomain was used.

3.5 Second generation of THQ analogues

3.5.1 Rationale

The first generation compounds (**12** and **86-88**) showed a good correlation between the electrostatic surface potential and the CREBBP affinity. In a second series, we studied the importance of the THQ ring and analysed the group efficiency (GE) by disassembling the

ligand into smaller fragments, with the following analogues (Figure 3.10). The aniline **98** and the methylated aniline **99** are the smallest aromatic compounds that can interact with R1173. The 3-methoxy **100** and 3-(*n*-propoxy) anilines **101** were selected as electron-rich aromatic compounds. In particular, the propoxy substituent on **101** was chosen, as Chekler *et al.* demonstrated, an increase in CREBBP selectivity over the BET family with a similar compound **17**.⁶⁵ The 3-acetamide **102** and 3-methyl sulfone **103** have electron-rich substituents, which could enhance the electrostatic component of the interaction with R1173. The methoxy derivate **104** should confirm the importance of the R1173 interaction and a large affinity decrease is expected. The heteroatom was exchanged from an amine to an oxygen as the non-aromatic amine would be protonated at physiological pH, and might result in a different interpretation of the structure-activity relationship due to a repulsion of the ammonium ion with the positively charged R1173.

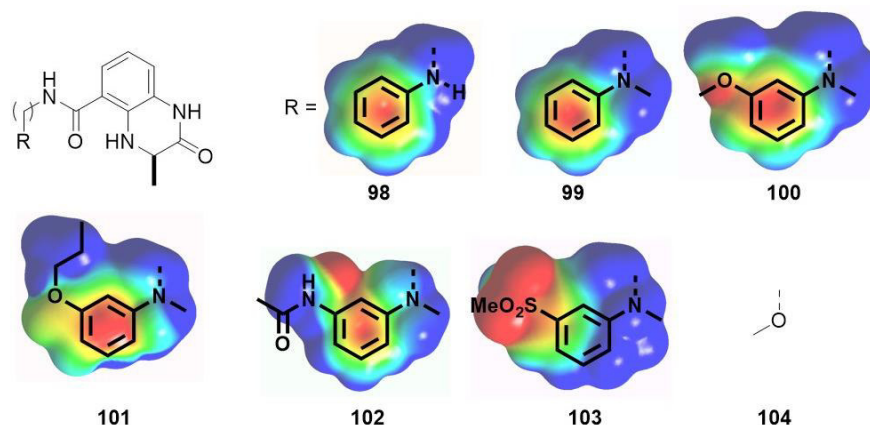


Figure 3.10 Overview of the second generation THQ derivatives **98-104** and their corresponding electrostatic potential.

We also hypothesised, that it would be possible to increase the CREBBP bromodomain affinity over the BET bromodomain, by attaching a bulky substituent on the aniline amine (Figure 3.11). The THQ amine of **12** is solvent exposed in the X-ray crystal structure and the binding should not be affected by adding a bulky substituent (Figure 3.11). In contrast, the overlaid BRD4(1) crystal structure in complex with **12** suggests the bulky aniline analogues should not be accommodated in the WPF shelf, and might clash with W81 (Figure 3.11). Therefore, the tetrahydropyran was used as the bulky substituent as it was

hypothesised to increase compound solubility. Hence the electron rich aniline derivatives **105-107** should be synthesised.

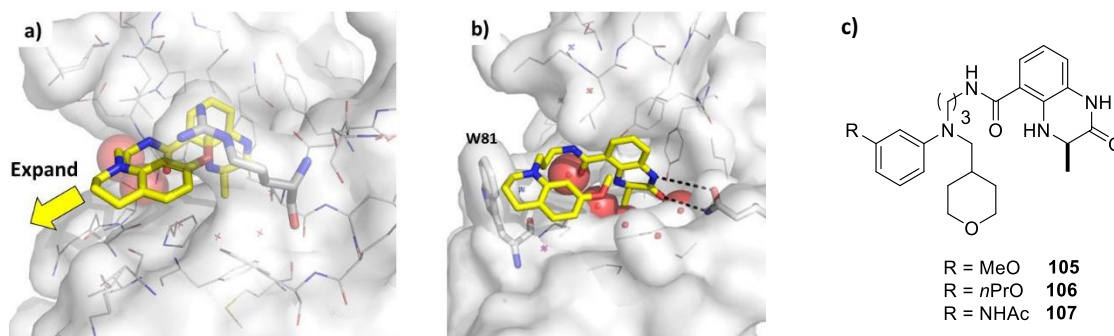
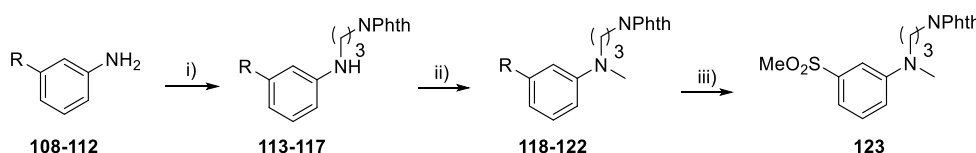


Figure 3.11 a) The X-Ray crystal structure of the CREBBP bromodomain (PDB: 4NYX)⁵⁴ in complex with **12**. b) The overlaid BRD4(1) X-Ray crystal structure (PDB: 4NR8, right)⁵⁴ with **12** is shown with the steric clash between W81 and the THQ highlighted. The yellow vector shows the bulky THP group pointing out to the solvent in the CREBBP bromodomain, whereas a steric clash in BRD4 is enforced to result in higher selectivity. c) The proposed selective CREBBP bromodomain small molecule structures **105-107**.

3.5.2 Synthesis of compounds 98-107

The aniline analogues (**118-122**) were synthesised from **108-112** using the procedure discussed in Chapter 3.4.3 (Scheme 3.6, Table 3.5). Subsequently, the secondary aniline amines were methylated in moderate yields using MeI and K₂CO₃ (Scheme 3.6, Table 3.5).



Scheme 3.6 Synthesis scheme for 7-substituted anilines analogues (**118-123**). *Reagents and conditions:* i) K₂CO₃, 3-bromopropyl-*N*-phthalimide, DMF, 85 °C, 16-19 h; ii) MeI, K₂CO₃, DMF, 85 °C, 2-8 h; iii) R = MeS, 1) *m*CPBA, CH₂Cl₂, rt, 3 h, 2) B₂(OH)₄, MeOH, rt, 14 h, 75%.

Table 3.5 Yields for the alkylation (**113-117**) and methylation (**118-122**) of the various 3-substituted aniline analogues (**108-112**). (*) Yield over two steps.

Entry	R	Yield in % i)	Yield in % ii)
1	H	47 (113)	74 (118)
2	MeO	48 (114)	48 (119)
3	<i>n</i> PrO	52 (115)	49 (120)
4	NHAc	(116)	29* (121)
5	MeS	58 (117)	71 (122)

The oxidation of the thioether **122** was problematic as both the thioether and the aniline oxidised using *m*CPBA. Kokatla and others reported the reduction of aliphatic *N*-oxides by treatment with diboron reagents at ambient temperature without affecting other substituents.^{108,109} The oxophilic nature of boron, and the large enthalpic increase by formation of two B-O bonds, makes diboron a suitable reducing agent. Applying these conditions to our substrate was successful using tetrahydroxydiboron in MeOH. Using *bis*(pinacolato)diboron, the reaction rate was slower and did not go to completion. The oxidation of the methyl thioether **122** was optimised and performed in a one-pot synthesis to isolate the desired compound **123**. The reaction was monitored by ¹H NMR. Two hours after the addition of *m*CPBA, both methyl groups of the starting material disappeared and appeared downfield (Figure 3.12). The methyl next to the *N*-oxide signal was observed at 3.9 ppm, whereas the methyl sulfone was at 3.1 ppm. After the addition of B₂(OH)₄ the *N*-oxide of **124** was reduced to **123**. After 2 hours, there was still 10% of the *N*-oxide **124** left, which was reduced completely after 15 hours. The methyl sulfone **123** was isolated in 75% yield over two steps.

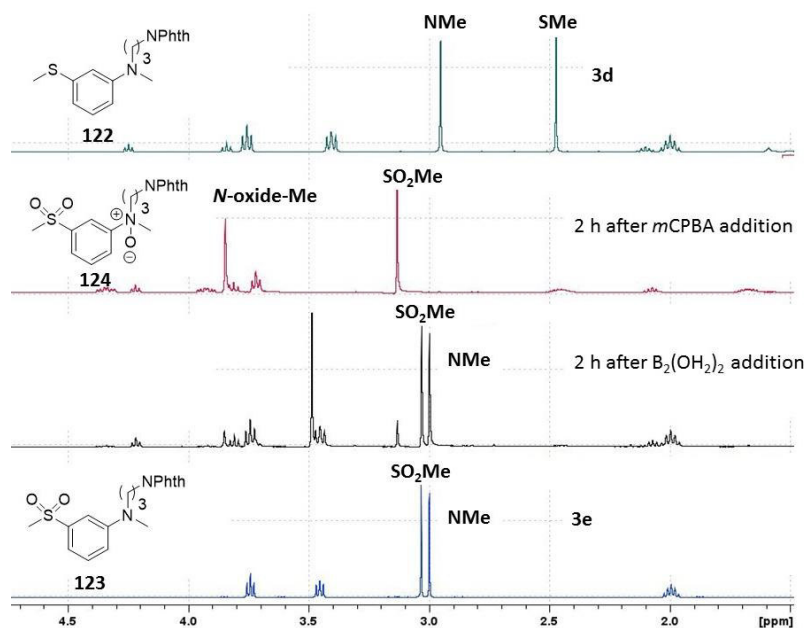
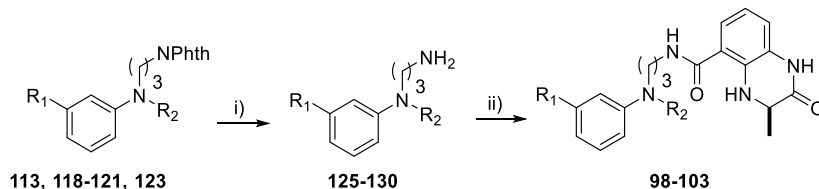


Figure 3.12 Reaction monitoring by ¹H NMR analysis of the oxidation from **122** to **123**. The CH₃ signals of the starting material **122**, intermediate **124** and product **123** are assigned.

The aniline analogues with the *N*-phthalimide linker (**113**, **118-121** and **123**) were deprotected and coupled using the previously optimised conditions to give (**98-103**) (Scheme 3.7, Table 3.6).

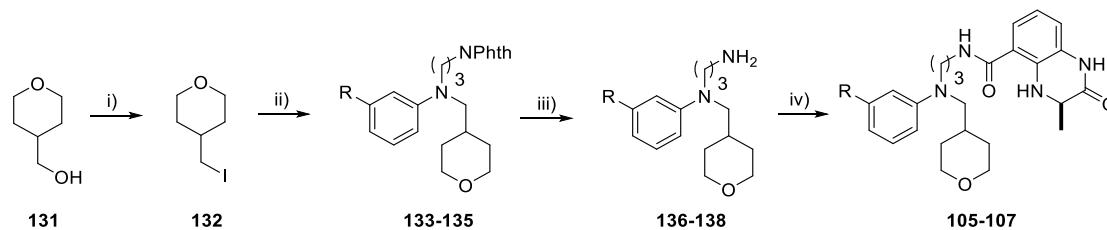


Scheme 3.7 Synthesis scheme for 7-substituted aniline-DHQ derivatives (**98-103**). *Reagents and conditions:* i) Hydrazine monohydrate, MeOH, CH₂Cl₂, 70 °C, 2 h; ii) (*R*)-**32**, PyBOP, Et₃N, DMF, rt, overnight.

Table 3.6 Yields for deprotection of the *N*-phthalimides (**125-130**) and amide coupling with (*R*)-**32** to give (**98-103**).

Entry	R ₁	R ₂	Yield i)	Yield ii)
1	H	H	96 (125)	43 (98)
2	H	CH ₃	64 (126)	47 (99)
2	MeO	CH ₃	85 (127)	49 (100)
3	<i>n</i> PrO	CH ₃	89 (128)	60 (101)
4	NHAc	CH ₃	50 (129)	62 (102)
5	MeSO ₂	CH ₃	71 (130)	61 (103)

The bulky THP electrophile **132** was synthesised starting from cyclohexylmethanol **131** by mesylation followed by iodination in 43% yield (Scheme 3.8). The alkylations of the secondary anilines were performed in a similar manner as discussed before to isolate intermediates **133-135** (Scheme 3.8 and Table 3.7). Deprotection of the *N*-phthalimides (**133-135**), followed by the amide couplings with (*R*)-**32** resulted in the desired compounds **105-107** (Scheme 3.8 and Table 3.7).

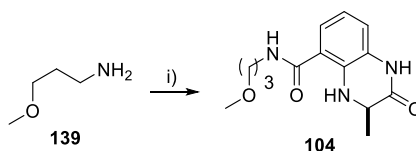


Scheme 3.8 Synthesis scheme for the electron-rich 7-substituted anilines with a THP group (**105-107**). *Reagents and conditions:* i) 1) MsCl, Et₃N, toluene, 0 to rt, 2) NaI, acetone, 60 °C, 4 h, 43%, ii) **114-116**, K₂CO₃, DMF, 85 °C, 16 h; iii) Hydrazine monohydrate, MeOH, CH₂Cl₂, 70 °C, 2 h; iv) (*R*)-**32**, PyBOP, Et₃N, DMF, rt, overnight.

Table 3.7 Yields for the synthesis of the electron-rich 7-substituted anilines with a THP group **105-107**.

Entry	R	Yield in % ii)	Yield in % iii)	Yield in % iv)
1	MeO	48 (133)	85 (136)	49 (105)
2	<i>n</i> PrO	58 (134)	51 (137)	38 (106)
3	AcNH	29 (135)	50 (138)	60 (107)

The 7-methoxy propyl linker **104** was synthesised by an amide coupling with the DHQ (*R*)-**32** and the commercial available 3-methoxy amine **139** in 82% yield (Scheme 3.9).

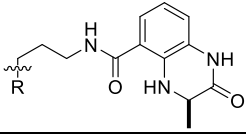
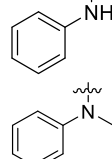
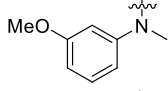
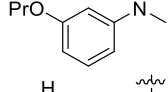
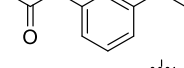
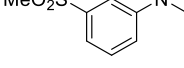
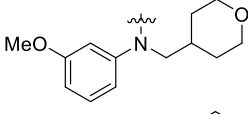
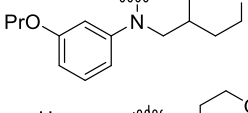
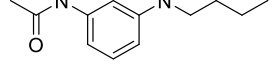


Scheme 3.9 Synthesis scheme of the amide coupling to **104**. *Reagents and conditions:* i) (*R*)-**32**, PyBOP, Et₃N, DMF, rt, 17h, 82%.

3.5.3 Biophysical analysis of 98-107 binding to the CREBBP bromodomain

Compounds **98-107** were tested on CREBBP using ITC. The ligand affinities of the ligands were in the low μM range with the exception of the non-aromatic compound **104**, which had no measurable affinity for CREBBP (Table 3.8). This confirms the importance of the cation- π interaction between the aromatic ring and R1173 residue. The 3-methoxy substituent **100** increases the affinity approximately 2-fold over the unsubstituted aniline **99**, as previously observed with the THQ analogues (**12** and **86**). This affinity increase can be attributed to higher ESP. The propoxy substituent **101**, despite having an electron-rich aromatic ring, resulted in a 5-fold decrease in affinity, indicating the increased size of the substituent is not tolerated. The electron-rich acetamide **102** and methyl sulfone **103** have similar affinities as the unsubstituted aniline **99**, despite having an electron-rich substituent. The bulky THP group on the substituted anilines (**105-107**) is well tolerated and the dissociation constants are approximately the same as with the methyl amines (**100-102**). This proves our hypothesis correct, that the THP group will not affect the CREBBP binding affinities of **100-102**. To determine the BET selectivity, the BRD4(1) bromodomain affinity was measured for the most potent CREBBP ligands **99** and **105**, which showed K_D values of 3.6 and 2.1 μM , respectively. Compound **99** has a 4-fold selectivity for the CREBBP bromodomain over the BRD4(1) bromodomain, which is similar to the values obtained for the 7-MeO-THQ substituent **12**. Adding the bulky THP group onto the aniline amine resulted in similar affinity for the BRD4(1) bromodomain, despite our hypothesis.

Table 3.8 Affinity data for compounds **98-107** on CREBBP and BRD4(1) bromodomain of the substituted aniline derivatives.

Compounds	AlphaScreen™ CREBBP	ITC CREBBP	ITC BRD4(1)
	IC ₅₀ [μ M]	K _D [μ M]	K _D [μ M]
98 	8.3 ± 1.4	N/A	N/A
99 	4.3 ± 0.3	1.98 ± 0.19	N/A
100 	N/A	0.86 ± 0.21	3.62 ± 0.74
101 	N/A	5.20 ± 2.00	N/A
102 	N/A	1.55 ± 0.40	N/A
103 	N/A	1.85 ± 0.48	N/A
104 MeO	> 50	> 10.0	N/A
105 	N/A	1.35 ± 0.25	2.08 ± 0.50
106 	N/A	2.66 ± 1.32	N/A
107 	N/A	2.10 ± 0.39	N/A

The series of compounds that had been synthesised allowed the group efficiency of compound (*R*)-**12** to be analysed. Group efficiency is a measure of a normalised binding affinity of molecules of different sizes.¹¹⁰ The binding affinity is ranked and compared by addition of the number of heavy atoms to identify important functionalities of the compound (Figure 3.13a *Eq. 1*). Large negative GE values represent important functionalities for the ligand affinity. The group efficiency and the Gibbs binding energy of the compounds were calculated with the measured dissociation constant (K_D) or the IC₅₀

for weak binding fragments (Figure 3.13a, Eq. 2). The KAc mimic head group resulted in a high group efficiency of -0.5 (Figure 3.13c).⁵⁶ The propyl methoxy linker **104** resulted in a low group efficiency, indicating that it does not contribute to the binding properties. However, addition of the aniline **99** onto the linker, resulted in a large affinity increase and a high group efficiency of -0.33 . The methoxy group of **100** had a positive effect on the GE as the electron density of the aromatic ring is increased, resulting in a stronger cation- π interaction. Rigidifying the aniline by forming the THQ (*R*)-**12** helps the aromatic ring to point towards the induced fit pocket and is represented by a group efficiency increase of -0.18 .

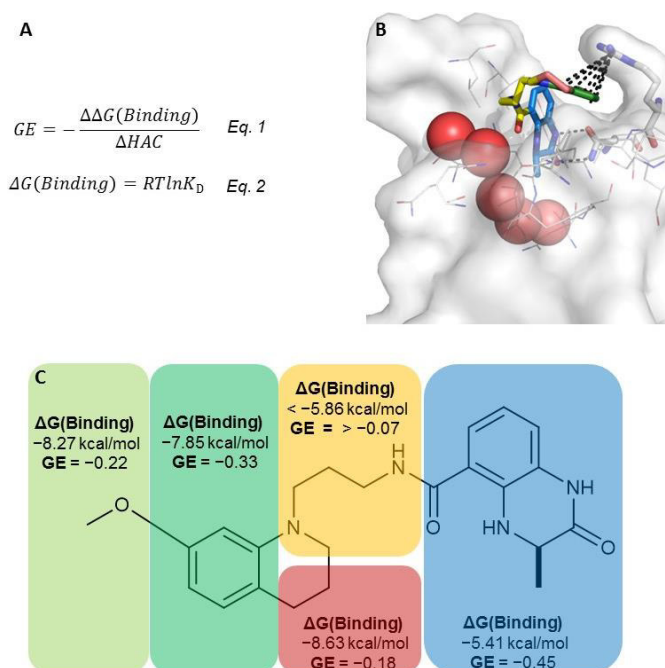


Figure 3.13 A) The group efficiency (GE) is calculated by the difference of the Gibbs binding energy ($\Delta G(\text{Binding})$) divided by the increase of heavy atom counts (HAC) (Eq. 1). The correlation of the Gibbs binding energy ($\Delta G(\text{Binding})$) with the dissociation constant (K_D). R is the gas constant and T is the temperature. B) Colour coded crystals structure of (*R*)-**12** in the CREBBP bromodomain (PDB: 4NYX) highlighting the different groups. DHQ forehead (carbon = marine), propyl linker (carbon = yellow), aniline (carbon = green) and THQ (carbon = red). C) Calculated group efficiencies for different fragments. The binding affinity of the benzoxazinone-carboxylic acid was used instead of the DHQ.

To conclude, compound (*R*)-**12** is the most ligand efficient compound tested so far. Changing the THQ substituents results in affinity loss. Also, the ring opening of the THQ reduces the GE and potency.

3.6 Conclusion

The importance of the cation- π interaction between R1173 and the THQ was studied, and a correlation between the electrostatic surface potential and the affinity on CREBBP was observed. However, the affinity difference between electron-rich and electron-poor analogues were small, resulting in a relatively flat SAR profile. It was shown that the THQ ring is essential for the compound potency. The affinity dropped substantially without aromatic ring. The most potent ligand contained a methoxy group. Other substituents are tolerated, but the affinity on the CREBBP bromodomain is decreased.

The group efficiency revealed that the 7-MeO-THQ is the highest affinity substituent. Converting the THQ ring to an aniline derivative reduces the affinity 2-fold, indicating that the rigidified conformation is beneficial. Substituting the aniline derivatives with a bulky THP group did not affect the affinity on CREBBP, but no selectivity over BRD4(1) was gained.

Chapter 4

Propyl linker rigidification to increase CREBBP potency

4.1 Aims

As discussed in the previous Chapter 3, the GE of the propyl linker was low, however, there were possible gains to be made. The crystal structure of (*R*)-**12** in CREBBP shows the propyl linker connecting the DHQ and the THQ to be twisted (Figure 4.1). If it were possible to rigidify the flexibility of the propyl linker, an increase in affinity and selectivity might be achieved. Here we discuss a strategy to rigidify the linker by introducing a *gem*-difluorinated propyl linker.

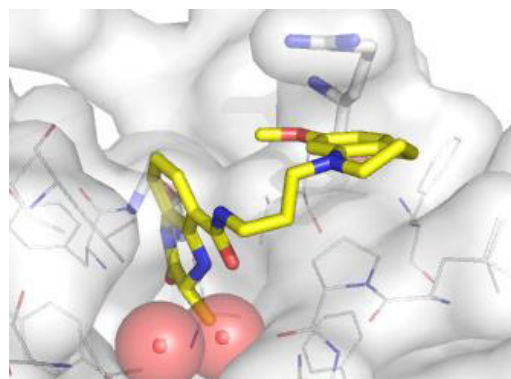


Figure 4.1 Crystal structure of (*R*)-**12** (carbon = yellow) in the CREBBP bromodomain showing the twisted propyl linker (PDB: 4NYX).⁵⁴

4.2 *Gem*-difluoro propyl linker

4.2.1 Rationale

Fluorine is commonly incorporated into drug molecules to increase their metabolic stability.^{111,112} The trend of fluorine-containing drugs has been increasing, with almost 30% of the newly approved drugs containing at least one fluorine atom.¹¹²

O'Hagan and others reported that fluorine can be used to rigidify conformations of aliphatic carbon chains.^{113,114} It was demonstrated that, in *N*- β -fluorine ethyl-amide **140**, the *gauche* conformation is preferred by 1.8 kcal/mol compared to the *anti*-conformation (Figure 4.2).^{115,116} This can be explained by the σ C-H orbital donating electrons into the very electron poor anti-bonding σ^* C-F orbital, which stabilises the conformation.

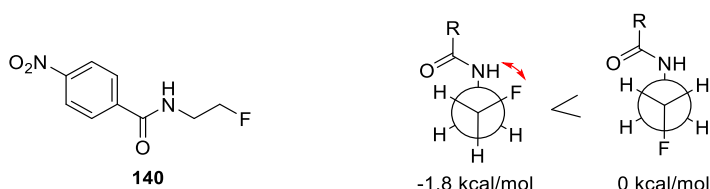


Figure 4.2 Illustration of the gauche effect of compound **140** by the Newman projection of the possible conformations. The *gauche-gauche* interactions are highlighted by a red arrow.¹¹⁵

It was hypothesised that the propyl linker of **86** could be rigidified by introducing a *gem*-difluoro group due to the *gauche-gauche* interactions (Figure 4.3). The three *gauche-gauche* interactions should stabilise the X-ray crystal structure compound conformation and result in a higher compound affinity for the CREBBP bromodomain.

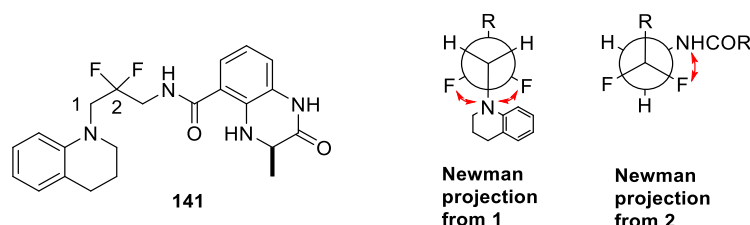


Figure 4.3 Newman projection of the difluorinated compound **141** and the *gauche-gauche* interaction according to the ligand conformation in the CREBBP bromodomain crystal structure. The *gauche-gauche* interactions are highlighted in red arrows.

The retrosynthetic analysis of the THQ *gem*-difluorinated propyl amine linker **142** shows a disconnection of the THQ **71** and the difluorinated propyl linker **145**, as previously discussed (Figure 4.4a). This compound **145** can be synthesised by reduction of the literature compound **144**, which is obtained by a 2-step synthesis starting from dibenzylamine and bromo-difluoro ethylacetate **143**.¹¹⁷ Alternatively, compound **142** could be synthesised by a functional group conversion of the ester **148** to the amine. This compound **148** can be obtained by a Reformatsky reaction using **146** and **147** according to previous literature procedures.¹¹⁷

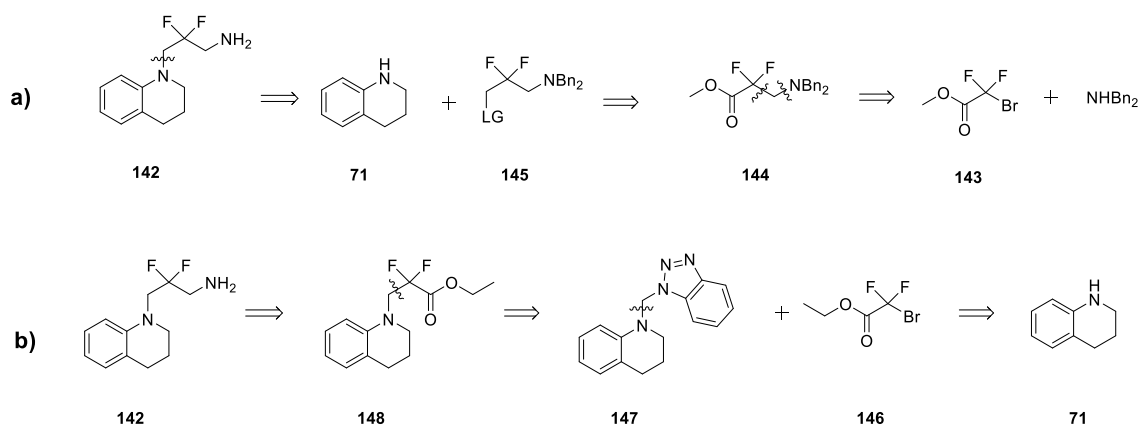
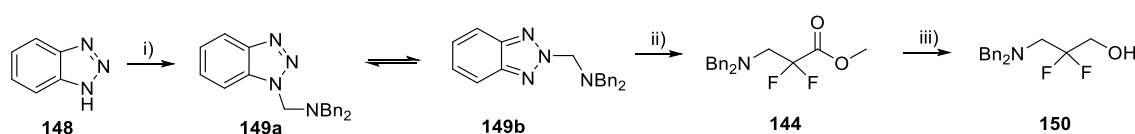


Figure 4.4 Retrosynthetic analysis of the difluorinated propyl-THQ linker **142** using disconnection strategy a) or b).

4.2.2 Synthesis of the *gem*-difluorinated compound **141**

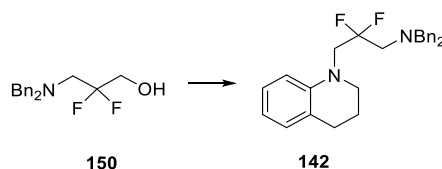
The synthesis of the *gem*-difluorinated propyl linker **142** commenced by using a Mannich reaction with 1*H*-benzotriazole **148** and dibenzylamine, giving compound **149a** in 77% yield (Scheme 4.2). In the ¹H and ¹³C NMR spectra, a mixture of the 1*H* **149a** and 2*H*-benzotriazoles **149b** isomers were observed as previously reported in the literature.¹¹⁸ The isomeric ratio between **149a** and **149b** was solvent dependent resulting in an 83:17 mixture measuring the ¹H NMR in CDCl₃ and 73:27 in benzene, respectively.



Scheme 4.2 Synthesis of the *gem*-difluoropropyl linker **150**. *Reagents and conditions:* i) Dibenzylamine, 37% CH₂O (aq.), MeOH, 40 °C, 16 h, 77%, ii) a) TMSCl, Zn, THF, rt, 10 min, b) **143**, rt, 10 min, c) **149a**, rt, 4.5 h, 33%, iii) LiAlH₄, THF, 0 °C to rt, 2 h, 83%.

The Reformatsky reaction with **143** and **149a** was performed according to a literature procedure¹¹⁷ and worked in 33% yield. Formation of the Reformatsky reagent for a longer time period and/or increasing the reaction temperature did not result in a higher yield. The ester reduction of **144** with lithium aluminium hydride went to completion within 2 hours, and the alcohol **150** was isolated in 83% yield. The alcohol **150** was mesylated followed by nucleophilic substitution with THQ (Scheme 4.3, Table 4.1, Entry 1), however, no reaction for the nucleophilic substitution was observed. This is likely because the THQ is a poor nucleophile.

Another approach was the Swern oxidation of alcohol **150** to the aldehyde followed by a reductive amination. However, no reaction for the reductive amination was observed (Table 4.1, Entry 2). The hydrogen borrowing reaction¹¹⁹ with the alcohol **150** and the THQ **71** using dichloro(*p*-cymene)ruthenium(II) did not result in any conversion either (Table 4.1, Entry 3).

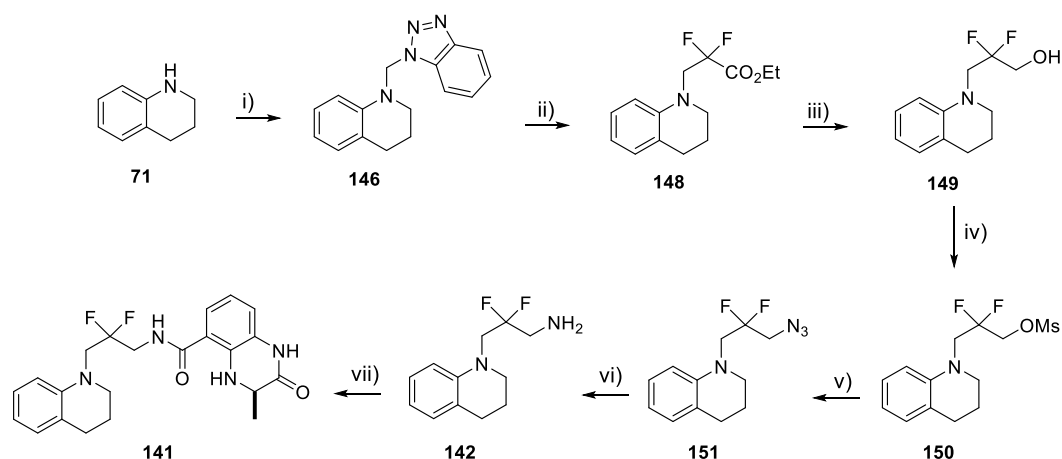


Scheme 4.3 Reaction scheme of the *gem*-difluoropropyl linker **150** to obtain the difluorinated propyl linker **142**. The reaction conditions are shown in Table 4.1.

Table 4.1 Overview of different reaction conditions to connect to difluoropropyl linker **150** to the THQ **71**.

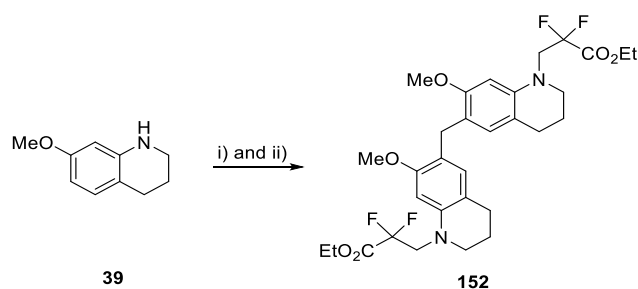
Entry	Reactions	Reagent and conditions	Result
1	Mesylate formation and S_N reaction	MsCl, Et ₃ N, CH ₂ Cl ₂ , 5 h, 20 °C 71 , DMF, K ₂ CO ₃ , 16 h, 85 °C	No product isolated.
2	Oxidation and reductive amination	1) (COCl) ₂ , DMSO, Et ₃ N, CH ₂ Cl ₂ , 2) 71 , NaBH(OAc) ₃ , (CH ₂ Cl) ₂	No product isolated.
3	Hydrogen borrowing reaction	[Ru(<i>p</i> -cymene)Cl ₂] ₂ , DPEphos, toluene, 100 °C, 17 h.	No product isolated.

As a result of no conversion, the reaction sequence was changed as the non-nucleophilic THQ **71** is more likely to react in the Mannich reaction. The THQ **71** and 1*H*-benzotriazole **148** reacted in excellent 92% yield to **146** (Scheme 4.4). The Reformatsky reaction with bromo-difluoro acetate **145** and **146** was low yielding, but the required *gem*-difluoro propyl linker was installed. The ethyl ester of **148** was reduced with LiAlH₄ to the alcohol **149**, followed by mesylate formation to give **150** (Scheme 4.4). This compound **150** was reacted with sodium azide and reduced by hydrogenolysis to isolate the THQ-*gem*-difluorinated propyl amine linker **142**. The final step involved the amide coupling between (*R*)-**32** and **142** to isolate the *gem*-difluorinated compound **141** in 68% yield (Scheme 4.4).



Scheme 4.4 Synthetic scheme for the difluorinated compound **141**: *Reagents and conditions* i) 1*H*-benzotriazole, 37% CH₂O (aq.), MeOH, Et₂O, 50 °C, 4 h, 92%; ii) 1) TMSCl, Zn, rt, 10 min; 2) BrF₂CCO₂Me, rt, 10 min; 3) **146**, 60 °C, 75 min; iii) LiAlH₄, THF, rt, 1 h, 27% over 2 steps; iv) MsCl, Et₃N, CH₂Cl₂, rt, 3 h, 97%; v) NaN₃, DMF, 110 °C, 16 h, 86%; vi) H₂, Pd/C, EtOAc, rt, 16 h, 97%; vii) (*R*)-**32**, PyBOP, Et₃N, DMF, rt, 20 h, 68%.

To obtain the more electron-rich THQ, 7-MeO-THQ **39** was reacted with the previously established procedure for the Mannich reaction. As the NMR data for this intermediate were difficult to characterise due to the 1*H*- and 2*H*-benzotriazole isomers, the crude mixture was directly taken forward to the Reformatsky reaction. The only isolated product after the 2-step synthesis was the dimerised compound **152** in 22% yield (Scheme 4.5).



Scheme 4.5 Synthetic scheme for the Mannich and Reformatsky reactions of **39**: *Reagents and conditions* i) 1*H*-Benzotriazole, 37% CH₂O (aq.), MeOH, Et₂O, 50 °C, 4 h; ii) a) TMSCl, Zn, rt, 10 min; b) BrF₂CCO₂Me, rt, 10 min; c) **155**, 60 °C, 3 h, 22% over 2 steps.

The structure of **152** was characterised using 2D-NMR analysis. Evidence for the dimer formation came from the peak heights of the aliphatic carbon signals in the ¹³C NMR (Figure 4.5a). The carbon signal at 27.6 ppm, belonging to the benzylic CH₂ group (C(15))

connecting the two THQ rings, has only half the peak height compared to the other aliphatic THQ carbon signal (Figure 4.5a). Using ^1H - ^{13}C HMBC-NMR (Figure 4.5b), the benzylic $\text{C}(15)\text{H}_2$ only correlates to aromatic carbon signals, which confirmed the structure of **152**. Furthermore, the dimeric structure was also observed by mass spectrometry analysis.

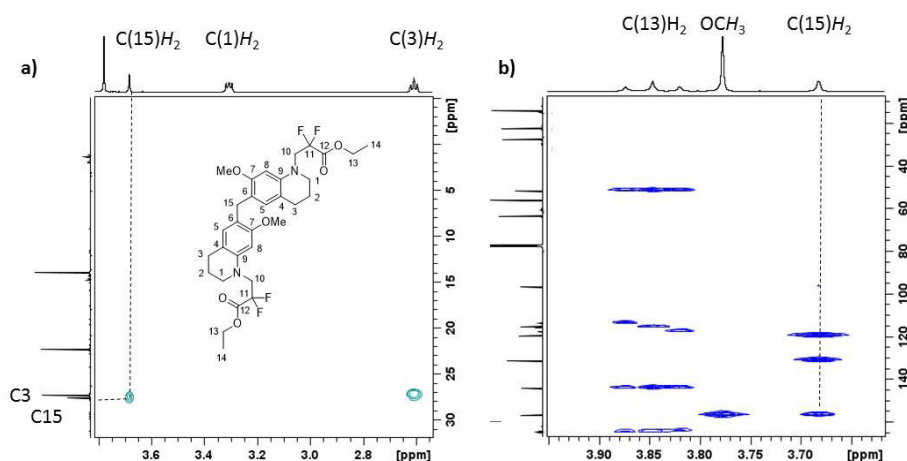


Figure 4.5 Assignment of the dimeric structure **152** using a) ^1H - ^{13}C HSQC NMR and b) ^1H - ^{13}C HMBC NMR.

To investigate the unexpected product **152**, the first step of the synthesis was further analysed, and the NMR of the intermediate characterised. The ^1H - ^{13}C HSQC-NMR spectrum of the aliphatic region revealed that the benzylic methyl group at 3.71 ppm correlates to the carbon signal at 27.8 ppm and shows this bond was formed during the first step of the synthesis. The electron-rich THQ **39** did react with reagent **153** to give the benzotriazole intermediate **154** (Figure 4.6). Subsequently, another THQ derivative **39** reacts to form the dimer **155**. The ^1H and the ^{13}C -NMR were difficult to characterise because of the observed *1H*- and *2H*-benzotriazole isomers (**155a-155c**). Katritzky *et al.* reported similar reactions with the electron-rich 1,3,5-trimethoxybenzene and **153** in a low yield. However, the authors did not comment on forming dimeric compounds.¹²⁰ To conclude, the electron-rich aromatic ring of THQ **39** is more nucleophilic compared to the THQ-amine and hence only the dimer **155** was formed. Further synthesis towards the 7-MeO-THQ *gem*-difluoro propyl linker was stopped.

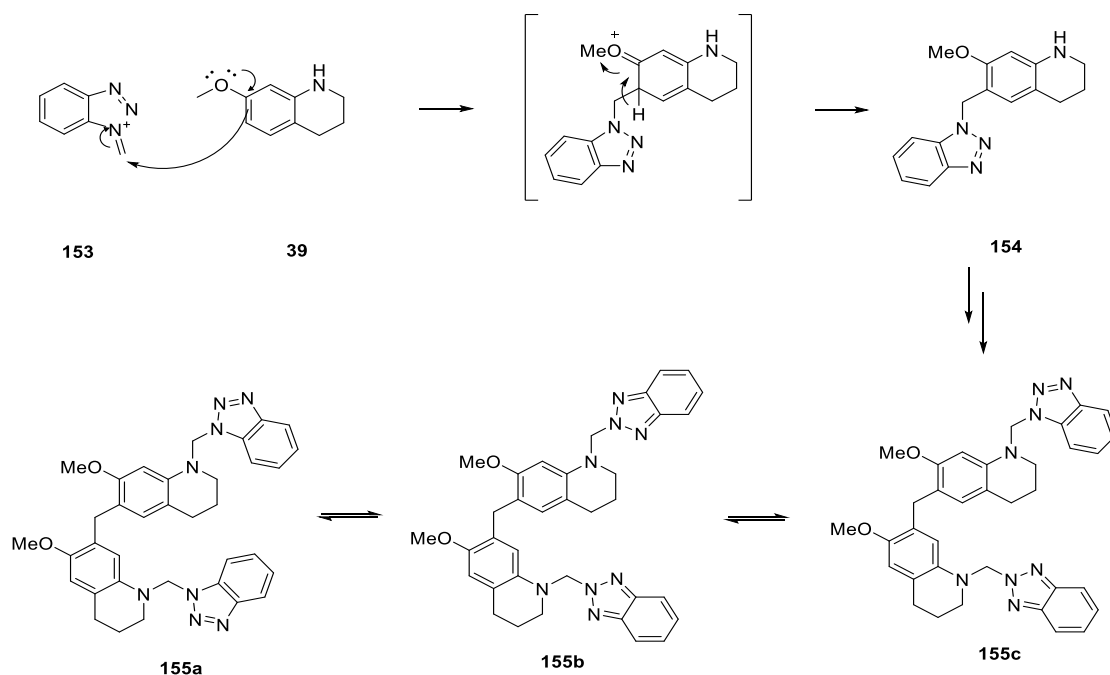


Figure 4.6 Proposed reaction mechanism for the Mannich reaction between **39** and **153**.

4.2.3 Conformational analysis of the *gem*-difluorinated small molecule **141**

To study conformational change due to the *gauche* effect, we analysed the coupling constants of compound **141** by ^{19}F -NMR. A triplet of triplets splitting pattern was observed at a chemical shift of -105.1 ppm (Figure 4.7a). Both coupling constants were 14 Hz, suggesting the preferred solution based conformation is *anti* (Figure 4.7b) and the bond is freely rotatable.

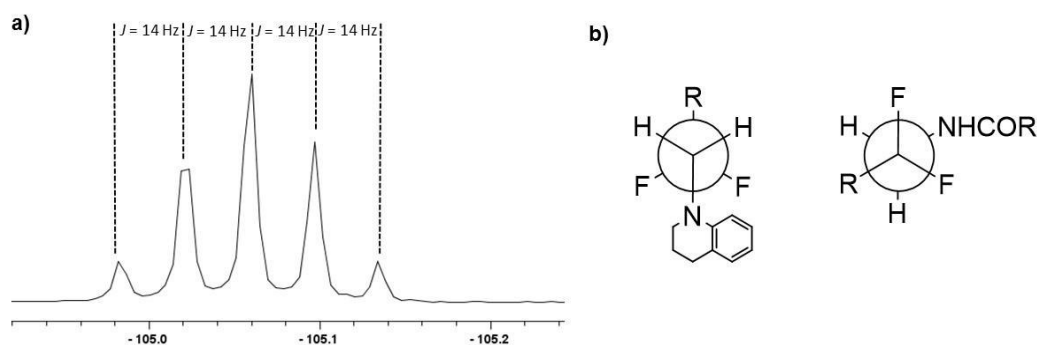


Figure 4.7 a) The ^{19}F NMR splitting pattern is a triplet of triplets with 14 Hz coupling constant each. b) Suggested solution based conformation of **141**.

A X-ray crystal structure of **141** was kindly solved by Prof. Richard Cooper (X-Ray service, Oxford (Figure 4.8) (Appendix D2). To our delight the propyl linker in the crystal structure of **141** was twisted. The THQ amine has a presumed *gauche-gauche* interaction with the fluorine F1 leading to a twisted propyl linker (Figure 4.8b). The amide (N5) is centred between the fluorine atoms and two *gauche-gauche* interactions were observed. Unfortunately, this crystal structure does not match our hypothesis, but we posit that the energy of the protein-bound conformation of the ligand is lower with the *gem*-difluorinated compound **141** compared to non-fluorinated compound **86**. Furthermore, the internal hydrogen bonding between the DHQ amine (N14) to the carbonyl (O7) is observed, as previously reported.

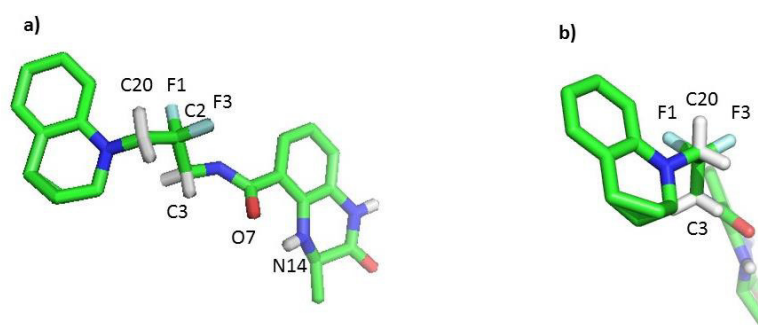


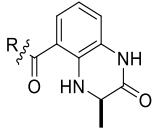
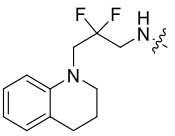
Figure 4.8 Crystal structure of **141**. Green = carbon, blue = nitrogen, red = oxygen, marine = fluorine. The C23 and C24 were disordered in a ratio of 23 to 77.

4.2.4 Biological evaluation of **141**

The synthesised *gem*-difluoro compound **141** was tested in comparison to the non-fluorinated compound **86** by differential scanning fluorimetry, AlphaScreen™, and ITC (Table 4.2). The compound solubility of the difluorinated compound **141** was problematic, but affinity data was obtained. The thermal shift on the CREBBP bromodomain with the fluorinated compound **141** measured 6 °C, which is an increase of 2 °C compared to the non-fluorinated compound **86**. This increased protein stabilisation could be attributed to a stronger binding affinity and/or increased lipophilicity of the fluorinated linker.⁸⁰ The AlphaScreen™ data, provided by Dr Oleg Fedorov, confirmed the

DSF results. The *gem*-difluorinated compound **141** has an IC₅₀ value of 1.1 μM, which is approximately a 3-fold affinity increase compared to **86**. The dissociation constant of **141** was determined by an ITC experiment with 920 nM.

Table 4.2 Overview of the DSF, the AlphaScreen™ and ITC results on the CREBBP bromodomain with the *gem*- difluorinated propyl linker **141** and non-fluorinated compound **86**.

Compounds	DSF CREBBP Thermal shift [° C]	CREBBP IC ₅₀ [μM]	CREBBP K _D [nM]
 86	4.3 ± 0.1	3.1 ± 0.7	N/A
 141	6.0 ± 0.3	1.1 ± 0.2	918 ± 147

Furthermore, the *gem*-difluorinated compound **141** was titrated into CREBBP or BRD4(1) with ¹⁹F-labelled tryptophan residues (Figure 4.9) (by Gabriella Perell, and Prof. William C. K. Pomerantz (University of Minnesota)). The titration experiment on the CREBBP bromodomain did not result in any chemical shifts of the labelled tryptophan residues, but the ¹⁹F signal intensity of W1165 broadened (Figure 4.9a). This is an indication of compound aggregation due to the low solubility. Compound titration into the labelled BRD4(1) bromodomain resulted in a slight chemical shift of the W81 residue, indicating binding. However, the signal intensity of W81 decreased drastically, which again confirms compound aggregation.

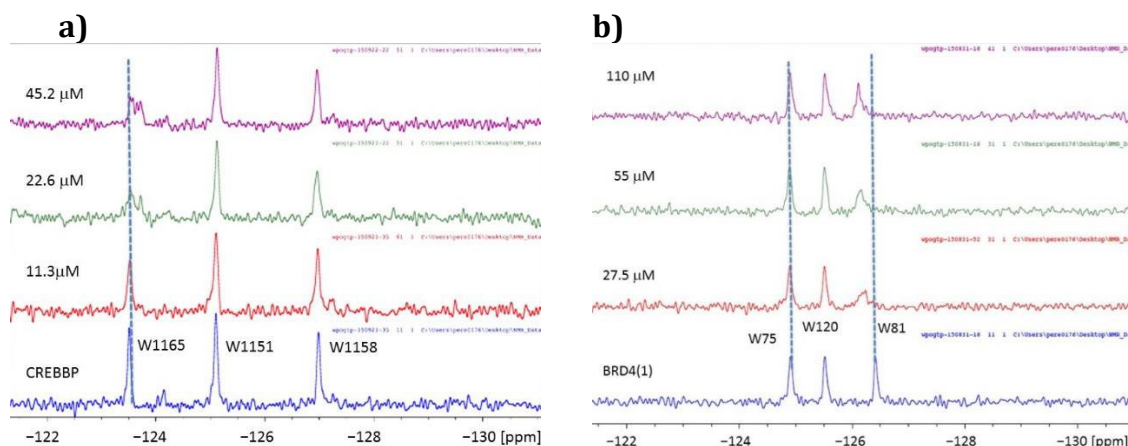


Figure 4.9 ^{19}F -NMR of the *gem*-difluorinated **142**. (a) **142** was titrated into mutant CREBBP bromodomain whereas on b) the mutant BRD4(1) bromodomain was used.

4.2.5 X-Ray crystallography

Dr Sarah Picaud and Prof. Panagis Filipiakous (SGC, Oxford) obtained a X-ray crystal structure of the CREBBP bromodomain in complex with the *gem*-difluorinated compound **141** (Appendix D1). The binding mode is the same as the previously discussed analogue (*R*)-**12**. The hydrogen bonds of the DHQ amide to the N1168 residue, and the cation- π interaction between R1173 and the THQ were observed (Figure 4.10a and b). Furthermore, there is possibly a hydrophobic interaction of the fluorine atom to P1110 (Figure 4.10a). This interaction might stabilise the twisted propyl linker and increase the compound affinity.

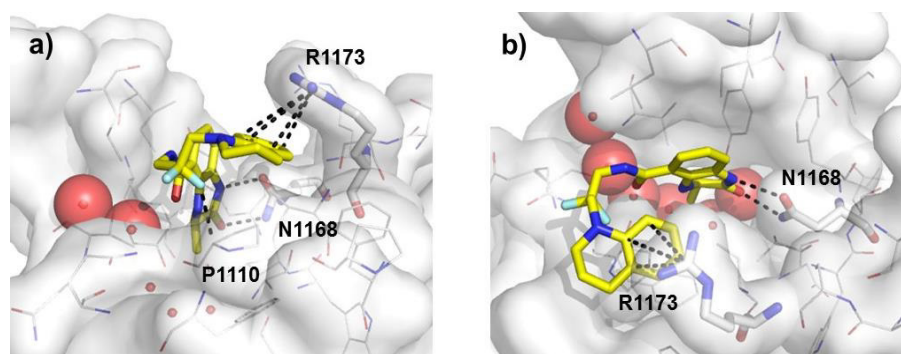


Figure 4.10 X-ray crystal structure of **141** (carbon = yellow) in the CREBBP bromodomain. The amino acid residues P1110, N1168 and R1173 are highlighted in bold and the conserved water molecules are shown as red spheres.

A second X-ray crystal structure of CREBBP in complex with **141** was solved, showing a trimeric structure of the bromodomain in complex with five molecules of **141** (Appendix

D1). Three molecules were located in each acetyl lysine binding pocket and the other two molecules are binding at the interface between two protein modules. This structure confirms the tendency of compound **141** to aggregate.

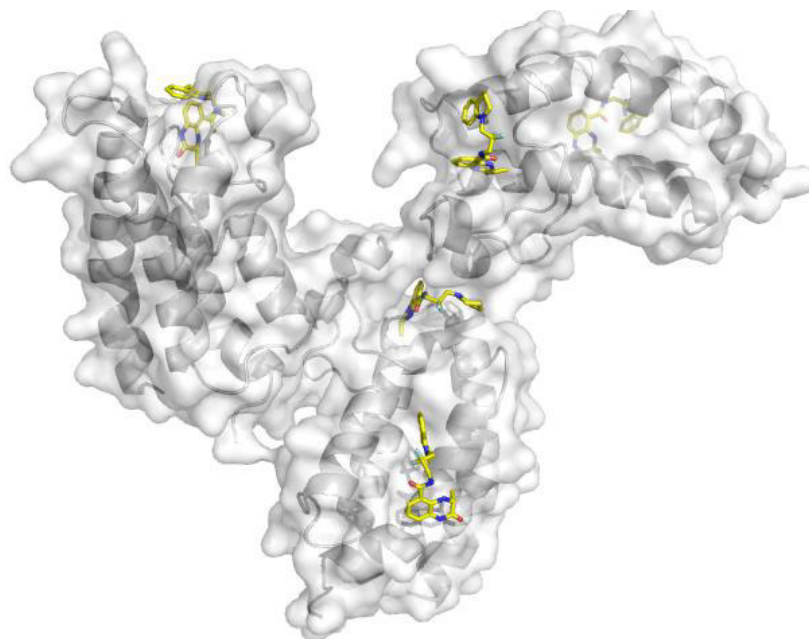


Figure 4.11 Observed trimeric bromodomain crystal structure containing five molecules of **141** (carbon = yellow).

4.3 Conclusion

A synthesis of the *gem*-difluorinated compound **141** was developed, and a small molecule crystal structure was obtained confirming the gauche-gauche interaction. Adding the *gem*-difluoro group on to the propyl linker increased the CREBBP affinity on three-fold, which could be attributed to the linker rigidification. Unfortunately, the compound solubility was decreased with the *gem*-difluorinated linker. Furthermore compound aggregation on the bromodomain was observed by the X-ray crystal structure as well as by ^{19}F NMR of the ^{19}F -labelled tryptophan residues on CREBBP. Consequently, **141** does not represent a good probe.

Chapter 5

Development of photoaffinity labelling probes for bromodomains

5.1 Aims

The 3,5-dimethylisoxazole BET bromodomain ligand **2** was developed by Hewings *et al.* and showed anti-proliferative effects on acute myeloid leukemia MV4;11 cancer cell lines ($IC_{50} = 800$ nM).⁵⁹ However, the data obtained did not conclusively demonstrate that the anti-proliferative activity of this ligand was due to its inhibitory effect on BRD4 *in vitro*.

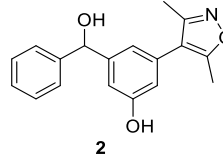


Figure 5.1 The 3,5-dimethylisoxazole ligand **2** with anti-proliferative effects on AML.

Hence, the aim of this Chapter is to develop a modular photoaffinity probe, which could assist the study of interaction partners of the 3,5-dimethylisoxazole BET bromodomain ligand **2** in a biological context. Furthermore the selectivity of this BET bromodomain ligand **2** will be studied.

5.2 Introduction

5.2.1 Activity-based profiling

Activity-based probes (ABPs) are used to identify protein targets of a ligand with a known biological activity.¹²¹⁻¹²³ An activity-based probe usually consists of a headgroup, a photo-affinity element, and a tag or ligation handle for the direct or two-step ABP, respectively (Figure 5.2a). The headgroup is essential for protein recognition. The photo-affinity element forms a covalent bond to the bound protein following UV irradiation, and hence the ligand's interaction partners can be identified. This photoaffinity element is especially important for identification of weakly binding interaction partners.¹²¹⁻¹²³ The tag of the ABP is used either for protein enrichment or visualisation of the target proteins. Usually a biotin tag is employed for pull-down experiments followed by mass spectrometry (MS) analysis. Alternatively, a fluorophore can be used for visualisation of the protein in the sodium dodecyl sulfate polyacrylamide gel electrophoresis (SDS PAGE). After the SDS-PAGE gel or mass spectrometry the interacting partners can be identified (Figure 5.2b and c).¹²² The advantage of the ligation handle over the direct tag is to have a smaller, modular

probe which can be modified after the crosslinking. Furthermore, the two-step ABP is smaller in size and less likely to interfere with the ligand binding interaction to the protein than the direct ABP.

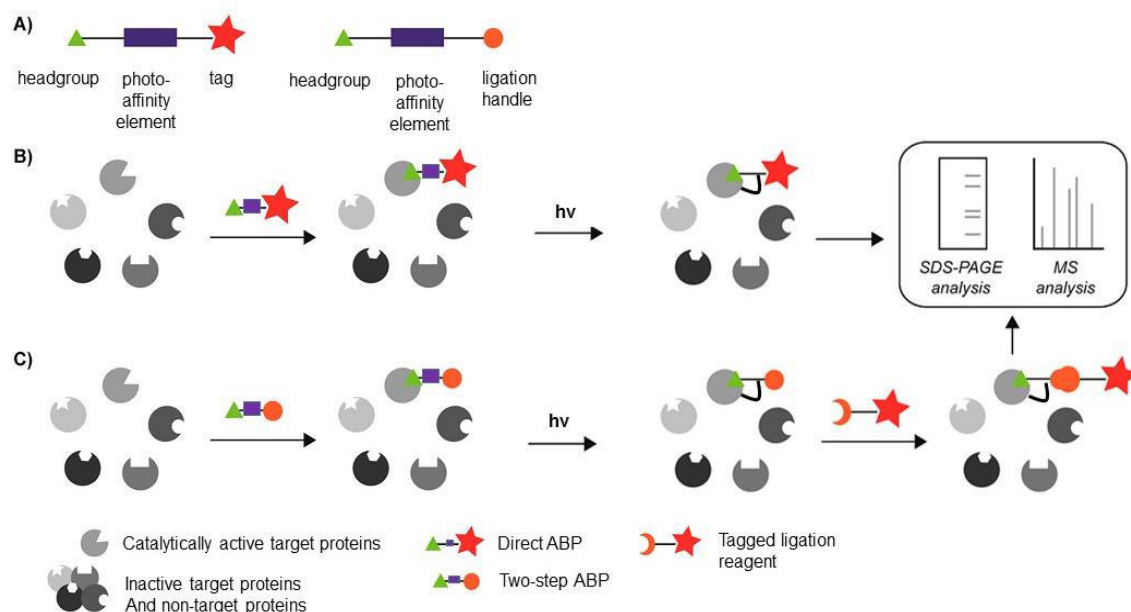


Figure 5.2 Schematic overview of an activity based probe (ABP) and the target validation. A) Composition of a direct ABP (left) or two-step ABP (right). B) and C) Schematic cartoon of the target identification of a direct ABP (B) and a two-step ABP (C). $h\nu$ is UV irradiation. Figure adapted with permission from Bioconjugate Chemistry.¹²² Copyright (2014) American Chemical Society.

5.2.2 Photo-reactive groups

The three major photo-reactive groups used for protein crosslinking are arylazides **156a**, benzophenones **157a**, and diazirines **158a** and **158d** (Figure 5.3).¹²⁴ Upon UV irradiation, the aryl azide group **156a** generates a reactive phenyl nitrene **156b** under the loss of nitrogen (Figure 5.3a). This reactive species **156b** can either crosslink with protein or undergo ketenimine **156c** formation, which results in a lower crosslinking efficiency.¹²⁴ The high energy UV irradiation (250-280 nm) needed for the aryl azide **156a** to generate the aryl nitrene **156b** can damage the proteins and cell lysates.¹²⁵ Consequently, the preferred photo-reactive groups are benzophenone **157a** and diazirines (**158a**, **158d**) as they generate the reactive species following irradiation at 350-370 nm, and the UV irradiation at these wavelengths do not damage the proteins.

The benzophenone **157a** can be readily synthesised, and hence is frequently used as a photo crosslinking group. Under UV irradiation at 350 nm the benzophenone generates a triplet carbonyl biradical **157b**, which can insert into C-H bonds of the protein (Figure 5.3b). Longer irradiation times are necessary for the benzophenone **157b** to crosslink, as the radicals are not as reactive as the aryl azide radicals **156a**. This can result in unspecific protein labelling.¹²⁶

Diazirines (**158a**, **158d**) are the smallest photo-sensitive cross linking groups, but they are synthetically more challenging to incorporate into ligands. Upon UV irradiation, the diazirine (**158a**, **158d**) forms by a loss of nitrogen a carbene (**158b**, **158e**) (Figure 5.3c). The singlet carbenes **158b** are obtained from diazirines that possess electron-donating substituents **158a**, whereas the triplet carbene **158e** is obtained from diazirines with electron-withdrawing groups **158d** (Figure 5.3c). The disadvantage of an electron-donating group on the diazirine **158a** is that the singlet carbene **158b** can photoisomerise to the diazo compound **158c** (Figure 5.3c). Therefore, to overcome this issue the more stable trifluoro diazirine **158d** is commonly used.^{124,127}

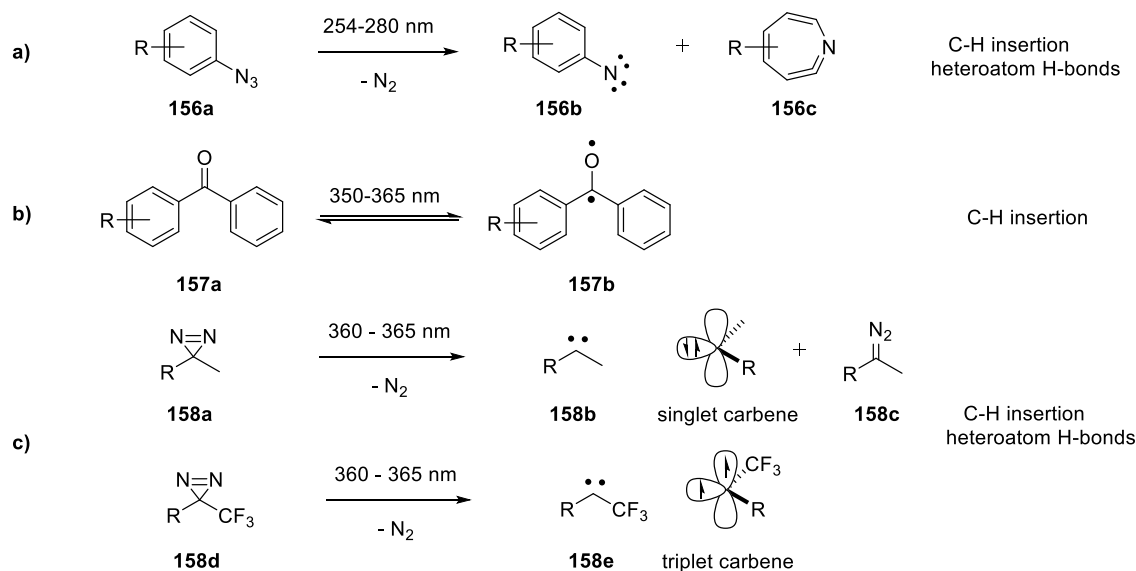


Figure 5.3 Photo crosslinking groups used in ABPs. a) Phenyl azide **156a** generating an aryl nitrene **156b** and rearranges to the ketenimine **156c**. b) Benzophenone **157a** generates the triplet biradical **157b**. c) Diazirines (**158a**, **158d**) generate either singlet (**158b**) or triplet (**158e**) carbenes under UV irradiation, depending on the substituents.

5.2.3 Ligation chemistry

Ligation chemistry for the two-step ABP is important to attach a tag of choice to the crosslinked probe. The requirement for the chemistry is that it must be modular, be high in substrate scope, high yielding, selective, and suitable for use in aqueous solution. Such conditions are met by click chemistry.¹²⁸ The Copper-catalysed alkyne azide cycloaddition (CuAAC) developed by Sharpless and others fulfils all these requirements (Figure 5.4a).¹²⁹⁻¹³¹ For example, the Cu(I)-catalysed 1,3-dipolar cyclisation using an azide **159** and alkyne **160a** has fast reaction kinetics, excellent functional group tolerance, and is extremely efficient under physiological conditions. However, a disadvantage of this reaction is the use of the copper catalyst, which is toxic to cells.¹³² To overcome this issue, Bertozzi and co-workers have developed a copper-free click reaction using a strain-promoted alkyne-azide cycloaddition (SPAAC) (Figure 5.4b).^{133,134} Due to the strain of the cyclooctanyne **161a** it reacts rapidly with azides **159** in aqueous solution.

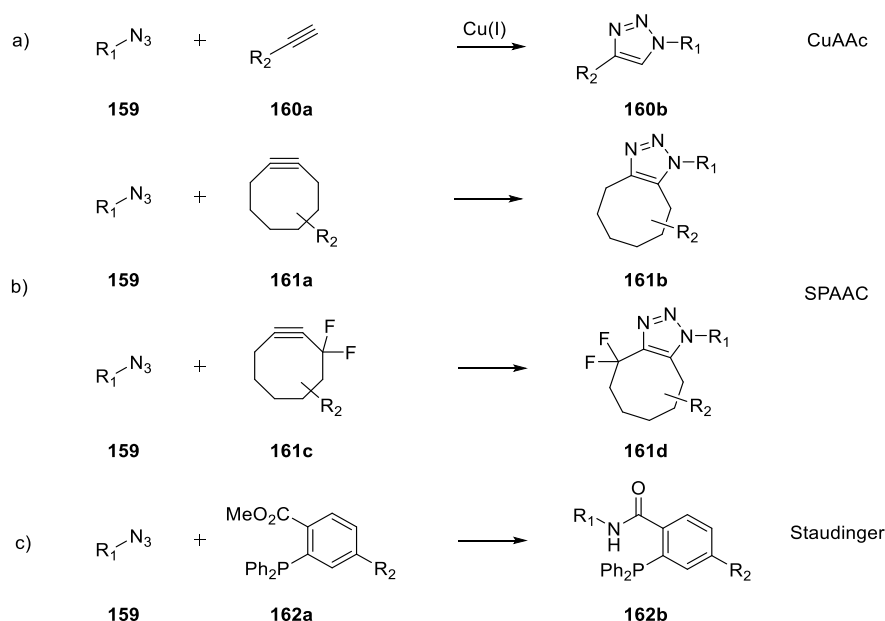


Figure 5.4 Overview of bioorthogonal ligation reactions. a) A copper-catalysed alkyne azide cycloaddition (CuAAC). b) Strain-promoted alkyne-azide cycloaddition (SPAAC). c) Staudinger ligation.

The reaction rate was further accelerated by using a *gem*-difluoro substituted cyclooctyne **161c**, and the conditions demonstrated to be useful for *in vivo* work.^{133,135} Other

biorthogonal ligation reactions include the Staudinger reactions with azides **159** and **162a** (Figure 5.4c),¹³⁶ Diels-Alder reactions,^{137,138} or Pd catalysed cross couplings,¹³⁹ which are less frequently used for ABPs.

5.2.4 Examples of ABPs applied to epigenetic proteins

ABPs have been applied to identify and study epigenetic proteins and some examples are outlined in this section.

Compound LY294002 (**163**) was published in 1994 as a selective PI3PK inhibitor.¹⁴⁰ Since then, **163** has been used as PI3PK probe, with over 8500 PubMed entries (Figure 5.5). Recent pull-down studies, however, have revealed that **163** is not a selective kinase inhibitor, and it binds to a number of different targets, one of which are the BET bromodomains.^{141,142}

Recently, Pfizer designed the pull-down probe **164**, which is based on the 3,5-dimethylisoxazole **16**.¹⁴³ The 3,5-dimethylisoxazole headgroup was substituted with a tropolone photoactivating group, without significantly affecting the CREBBP bromodomain affinity (Figure 5.5).¹⁴³ They demonstrated **164** covalently bound to purified BRD4 bromodomain in K562 cell lysate, but they were not able to detect any full length BRD4 protein.¹⁴³

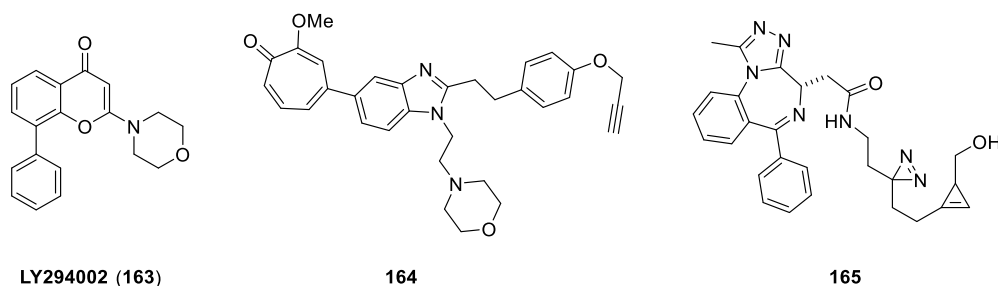


Figure 5.5 ABPs used to evaluate bromodomains as biological target.

Yao and coworkers have developed a copper-free clickable diazirine linker attached to the (+)-JQ1 analogue **165** (Figure 5.5).¹⁴⁴ This probe **165** was used to pull down full-length BRD4 in human liver cancer cell lysate HepG2. Additionally, they showed **165** pulled other

nuclear proteins out such as DDB1 and RAD23B. Furthermore they demonstrated the application of the ABP as an *in vivo* imaging agent.¹⁴⁴

Other applications of photoaffinity ligands in epigenetics have included the use of truncated modified histone proteins, with incorporated photo-affinity groups to detect post translational modifications of the binding partners.¹⁴⁵⁻¹⁴⁷

5.3 First generation photo-affinity probe

5.3.1 Rationale

The 3,5-dimethylisoxazole fragment **166** is an efficient BRD4 bromodomain ligand that was optimised to the potent bromodomain ligand **2**.^{55,59} This compound has 800 nM anti-proliferative effects on acute myeloid leukemia MV4;11 cancer cell lines.

The X-ray crystal structure of **2** bound to the first bromodomain of BRD4 (PDB: 4JOS)⁵⁴ reveals two solvent-exposed hydroxyl groups, which could be modified to attach a photoaffinity crosslinker (Figure 5.6).

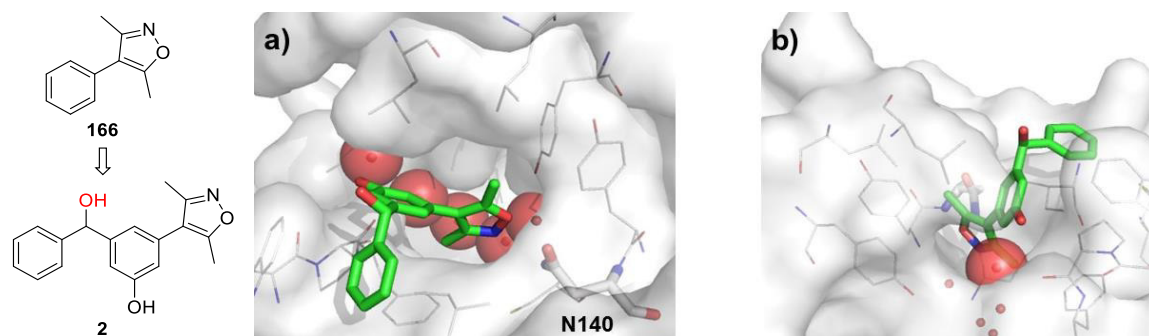


Figure 5.6 a), b) X-Ray crystal structure of **2** (carbon = green) bound to BRD4(1) (PDB: 4JOS)⁵⁴. The conserved water molecules are highlighted as red spheres.

The design of a first generation photo-affinity probe targeted inclusion of a photoaffinity group, capable of crosslinking at 360 nm, so the protein does not degrade upon UV-irradiation. For example, the benzophenone **168** is promising as the basis for a photoaffinity probe compound as previous data showed a 540 nM affinity on BRD4(1) of the non-acetylated compound.⁵⁹

Alternatively, attaching a small diazirine linker on **167** might be another strategy. Based on the X-ray crystal structure (Figure 5.6a and b), the benzylic hydroxyl group on **167** is solvent-exposed and well suited to attach a small diazirine linker. Consequently, the affinity of **169** for BRD4(1) should not be affected, making compound **169** an ideal synthetic target.

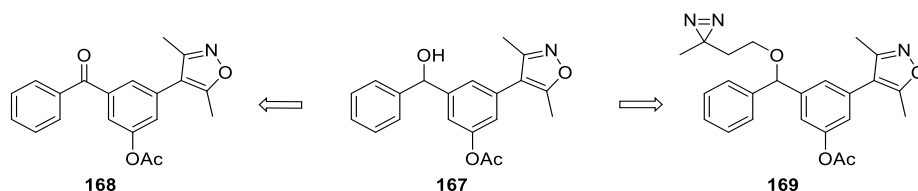


Figure 5.7 Photoaffinity probe design of the dimethyl isoxazole **167**.

The retrosynthetic analysis of **168** shows it can be obtained by oxidation from the dimethylisoxazole **167**, which could be synthesised according to Hewings⁵⁹ *et al.* starting from **170** and **171** (Figure 5.8a). The diazirine-containing dimethylisoxazole **169** could be obtained by a nucleophilic substitution of the benzylic alcohol **167** with the diazirine **174**. This short diazirine linker could be synthesised from 4-hydroxybutan-2-one **173**.

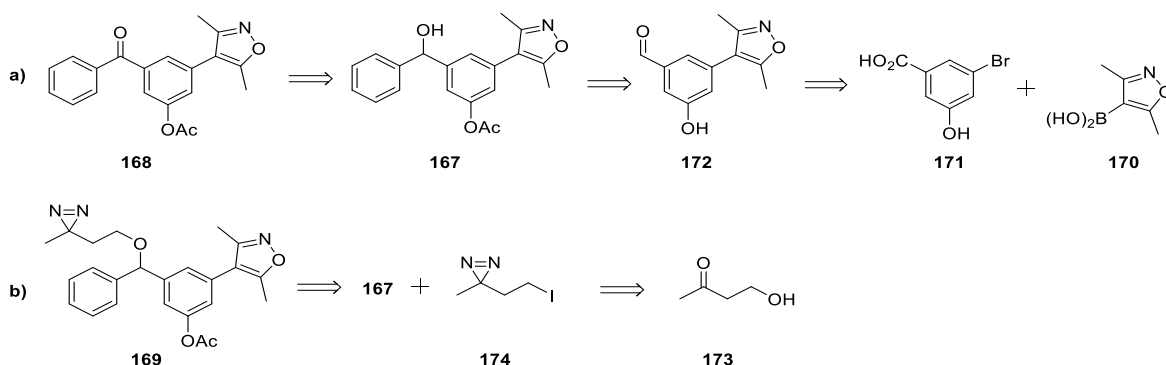


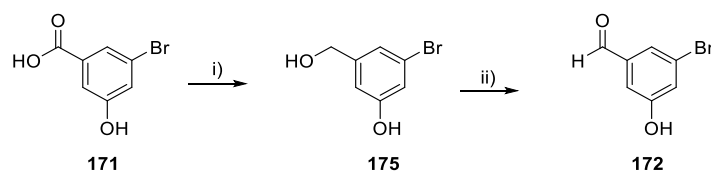
Figure 5.8 Retrosynthetic analysis of (a) the benzophenone **168** and (b) the diazirine **169** photoaffinity based probe.

5.3.2 Synthesis of the first generation probe

5.3.2.1 Synthesis of the benzophenone **168**

The synthesis of the 3,5-dimethylisoxazole ligand **168** was performed according to the literature.⁵⁹ Reduction of the carboxylic acid **171** to the alcohol **175** with borane worked

well in 95% yield (Scheme 5.2). Previous work on the oxidation of the alcohol **175** used the very toxic and environmental damaging pyridinium chlorochromate (PCC).⁵⁹ To avoid producing chromium waste, a greener alternative for the alcohol oxidation to the aldehyde was investigated (Table 5.1). The mild oxidation of the alcohol **175** to the aldehyde **172** with MnO₂ in dichloromethane resulted in a clean conversion, but the reaction rate was slow. After 9 days, 82% of the aldehyde **172** was isolated (Table 5.1, Entry 1). To increase the oxidation rate, the mild TEMPO-catalysed NaOCl oxidation developed by Anelli *et al.* was used (Table 5.1, Entry 2).¹⁴⁸ Despite having adjusted the pH to 9.5, the alcohol **175** overoxidised to the carboxylic acid **171**. Alternatively, employing the Dess-Martin-periodane oxidation on the substrate **175** did not result in any conversion (Entry 3).¹⁴⁹ To increase the reaction rate of MnO₂ reaction conditions, the temperature was increased to 40 °C and the reaction was complete after 47 hours (Entry 4). The solvent was changed to the higher boiling solvent, chloroform, and the reaction temperature increased to 70 °C. After 2 hours the reaction went to completion and 74% of the purified aldehyde **172** was isolated (Table 5.1, Entry 5).

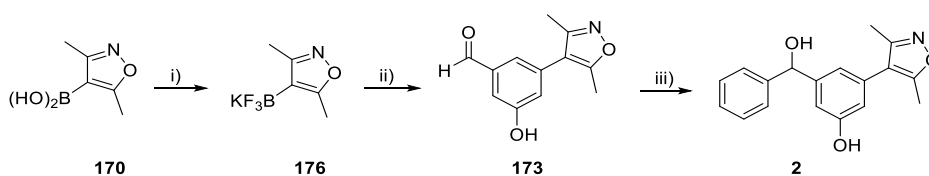


Scheme 5.2 Synthesis of 3-bromo-5-hydroxybenzaldehyde **172**. Reagents and conditions: i) BH₃, THF, 20 °C, 20 h, 95%; ii) MnO₂, CHCl₃, 70 °C, 2 h, 74%.

Table 5.1 Reaction optimisation for the oxidation of **176** to **172**.

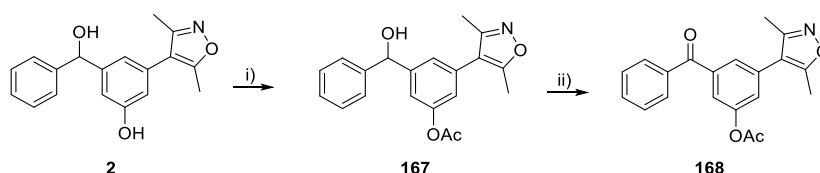
Entry	Reagents and conditions for ii)	t [h]	Comments/Yields
1	MnO ₂ , CH ₂ Cl ₂ , 20 °C	216	82%
2	TEMPO, NaOCl, KBr, NaHCO ₃ , 0 °C	1	Oxidised to CO ₂ H
3	Dess-Martin-periodane, H ₂ O, CH ₂ Cl ₂ , 20 °C	2	No conversion
4	MnO ₂ , CH ₂ Cl ₂ , 40 °C	47	70%
5	MnO ₂ , CHCl ₃ , 70 °C	2	74%

As the Suzuki coupling between **172** and (3,5-dimethylisoxazol-4-yl)boronic acid **170** results in a fast protodeborylation, the trifluoroborate **176** was needed. Lennox *et al.* demonstrated that aromatic trifluoroborates slowly release the corresponding boronic acid and hence result in less protodeborylation.¹⁵⁰ The (3,5-dimethylisoxazol-4-yl) trifluoro borate **176** was obtained by treating **170** with KHF_2 following the literature¹⁵¹ (Scheme 5.3). The desired compound **176** was purified by a Soxhlett extraction followed by a crystallisation. The Suzuki coupling between **172** and **176** using $\text{Pd}(\text{OAc})_2$ and RuPhos as the ligand resulted in 76% of the dimethylisoxazole **173**. A Grignard reaction with this intermediate **173** and phenyl magnesium bromide gave **2** in 81% yield (Scheme 5.3).



Scheme 5.3 Synthesis of the bromodomain ligand **2**. *Reagents and conditions:* i) KHF_2 , MeOH, H_2O , rt, 10 min, 83%, ii) **172**, $\text{Pd}(\text{OAc})_2$, RuPhos, Na_2CO_3 , EtOH, 70 °C, 2.5 h, 76%, iii) PhMgBr , THF, rt, 1 h, 81%.

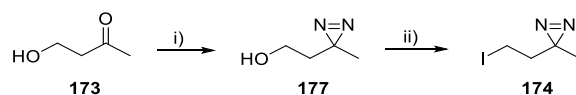
The selective acetylation of the phenol **2** worked well, following the procedure of Srivastava *et al.* and **167** was isolated in 85% yield.¹⁵² The benzylic alcohol of **167** was oxidised with PCC to the benzophenone **168** to give the desired benzophenone photo-affinity probe **168** in 36% yield.



Scheme 5.4 Synthesis of the benzophenone photo-affinity probe **168**. *Reagents and conditions:* i) Ac_2O , IPA, rt, 1 h, 85%, ii) PCC, CH_2Cl_2 , rt, 3 h, 36%.

5.3.2.2 Synthesis of the diazirine

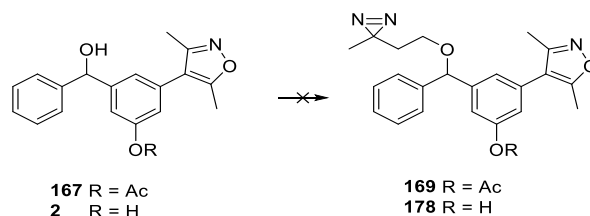
The diazirine linker **174** was synthesised according to literature procedures, starting from 4-hydroxybutan-2-one **173** (Scheme 5.5).^{153,154} The synthesis of the diazirine **174** commenced by forming the imine using liquid ammonia, followed by diaziridine formation with hydroxylamine-*O*-sulfonic acid, which subsequently was oxidised with iodine to give **177**. The crude material was purified by a Kugelrohr distillation to give **177** in 26% yield. The alcohol of **177** was converted to an iodide using an Appel reaction to obtain the electrophilic diazirine linker **174**.



Scheme 5.5 Synthesis of the diazirine linker **174**. *Reagents and conditions:* i) 1) NH_3 (l), -40°C , 3 h. 2) $\text{NH}_2\text{OSO}_3\text{H}$, MeOH, -40°C rt. 3) I_2 , Et_3N , Et_2O , 0°C , 30 min, 26%; ii) 1*H*-Imidazole, PPh_3 , I_2 , CH_2Cl_2 , 0°C , 4 h, 50%.

The alkylation of the benzylic hydroxyl group by treating **167** with sodium hydride, followed by the addition of the electrophilic diazirine **174**, did not result in any of the desired compound (Scheme 5.6, Table 5.2 Entry 1). Analysis using ^1H - ^{13}C HMBC-NMR suggested that the acetyl group migrated from the phenol to the benzylic hydroxyl group. Using the weaker base *t*BuOK, both deacetylation and acetyl group migration was observed suggesting the *O*-alkylation of **167** does not work under basic conditions (Scheme 5.6, Table 5.2, Entry 2). An alternative approach was using silver(I) oxide to mediate ether formation, but these conditions did not result in any conversion with our substrate (Table 5.2, Entry 3). Forming the mesylate of the secondary alcohol **167**, followed by a nucleophilic substitution with the deprotonated **177**, did not result in any product either (Table 5.2, Entry 4). To overcome the acetyl group migration on **167**, a test reaction for the double deprotonation of **2** using NaH was performed. After the addition of methyl iodide only *O*-alkylation on the phenolic hydroxyl was observed by ^1H - ^{13}C HMBC NMR (Table 5.2, Entry 5). It is likely that the dianion is insoluble in THF and as a result

only the single deprotonated alcohol was reacting. An alternative approach involved a Dean-Stark condensation with **177** and **167**. Some conversion of the starting material was seen, but the diazirine was unstable at this temperature and decomposed, something which has been observed in previous studies.^{155,156}

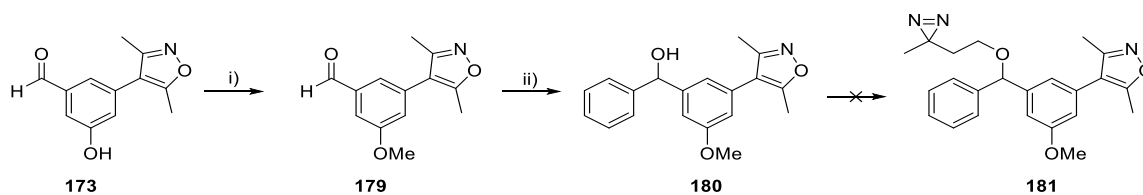


Scheme 5.6 Synthesis strategies for the installation of the diazirine linker.

Table 5.2 Different reaction conditions for the alkylation of the benzylic alcohol of **167**

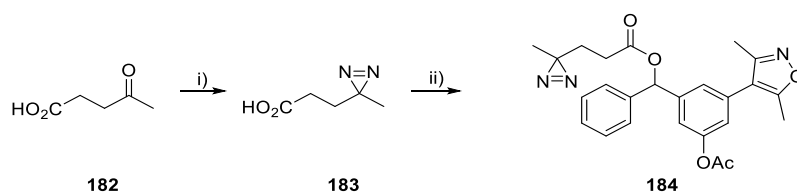
Entry	R	Reagents and conditions	Comments/Yields
1	Ac	1) NaH, DMF, 30 min, 2) 174 , 20 °C, 18 h.	Acetyl group migration
2	Ac	<i>t</i> BuOK, 174 , DMF, 60 °C, 3 h.	Acetyl group migration and deacetylation
3	Ac	Ag ₂ O, 174 , CH ₂ Cl ₂ , 20 °C, 18 h then 40 °C, 4 h.	No conversion
4	Ac	1) MsCl, Et ₃ N, CH ₂ Cl ₂ , 20 °C, 16 h, 2) 177 , NaH, THF, 0 °C, 0.5 h.	No product observed
5	H	1) <i>n</i> BuLi (2 eq.), THF, -78 °C, 2) MeI, -78 °C to 20 °C, 15 h.	Methylation on the phenolic alcohol
6	Ac	4-TsOH, 177 , toluene, 120 °C, 2 h.	The diazirine decomposed at 120 °C

To avoid the deacetylation and acetyl group migration, the methylated phenol **180** was synthesised as this compound still shows acceptable binding affinity for the BRD4 bromodomain (IC₅₀ = 1.36 μM).⁵⁹ The phenol of **173** was alkylated with MeI to give **179** in 74% yield. Subsequently, the Grignard reaction with phenyl magnesium bromide was performed, to give **180** in 99% yield (Scheme 5.7). Efforts to alkylate the benzylic alcohol of **180** with **174** using NaH as base were unsuccessful and no reaction to **181** was observed.



Scheme 5.7 Synthesis scheme towards the methylated diazirine probe **181**. Reagents and conditions: i) MeI, Cs₂CO₃, DMF, rt, 2.5 h, 74%; ii) PhMgBr, THF, rt, 1.5 h, 99%.

As the ether formation of the diazirine **174** with the 3,5-dimethylisoxazoles **167** and **180** were unsuccessful, a more reactive diazirine linker was desired. The more electrophilic diazirine linker **183** was synthesised from levulinic acid **182** following the literature procedure (Scheme 5.8).¹⁵⁷ The acid chloride of **183** was prepared using thionyl chloride, followed by the addition of the 3,5-dimethylisoxazole **167**, leading to the desired diazirine probe **184** in 68% yield.



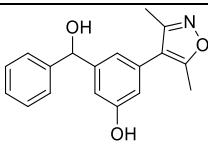
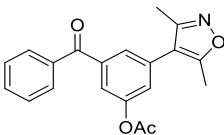
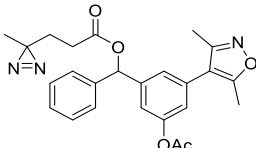
Scheme 5.8 Synthesis of the diazirine probe **184**. Reagents and conditions: i) 1) 7 M NH₃ in MeOH, 0 °C, 3 h, 2) NH₂OSO₃H, MeOH, 0 °C to rt, 3) I₂, Et₃N, , 0 °C, 30 min, 47%; ii) 1) SOCl₂, 40 °C, 15 min, 2) **183**, CH₂Cl₂, 2 h, rt, 68%.

5.3.3 Biological evaluation

5.3.3.1 BRD4(1) affinities of compounds **168** and **184**

The AlphaScreen™ IC₅₀ on BRD4(1) of the 3,5-dimethylisoxazole probes **2**, **168** and **184** were provided by Larissa See (Table 5.3). In this AlphaScreen™ assay, both of the affinity probes show a low μM BRD4(1) IC₅₀ value. Compared to compound **2**, the benzophenone probe **164** has approximately a 10-fold decrease in affinity, whereas the diazirine probe **184** shows approximately a 5-fold reduction. This observation shows that slight modifications of the compound result in a decrease of affinity, but it is still sufficient to evaluate the crosslinking efficiency of the compounds.

Table 5.3 BRD4(1) AlphaScreen™ IC₅₀ values of the first generation photo-affinity probes (**168**, **184**). In parentheses the 95% confidence level is shown.

Compound	IC ₅₀ on BRD4(1) [μM]
2 	0.24 (0.19-0.30)
168 	2.6 (1.8-3.9)
184 	1.3 (1.0-1.7)

5.3.3.2 Crosslinking experiments with compounds **168** and **184**

Next, the UV/VIS spectra of the benzophenone **168** and the diazirine **184** were measured. Both of the compounds show a minimal absorbance around 350 nm. The small absorbance of the benzophenone **168** is the n to π* transition, generating the triplet biradical, which subsequently reacts with the protein *via* a sequential abstraction-recombination mechanism. The absorbance of the diazirine **184** at 350 nm is the n to π* transition, which

subsequently generate a singlet state carbene. This can then react with the protein backbone to form a covalent bond.

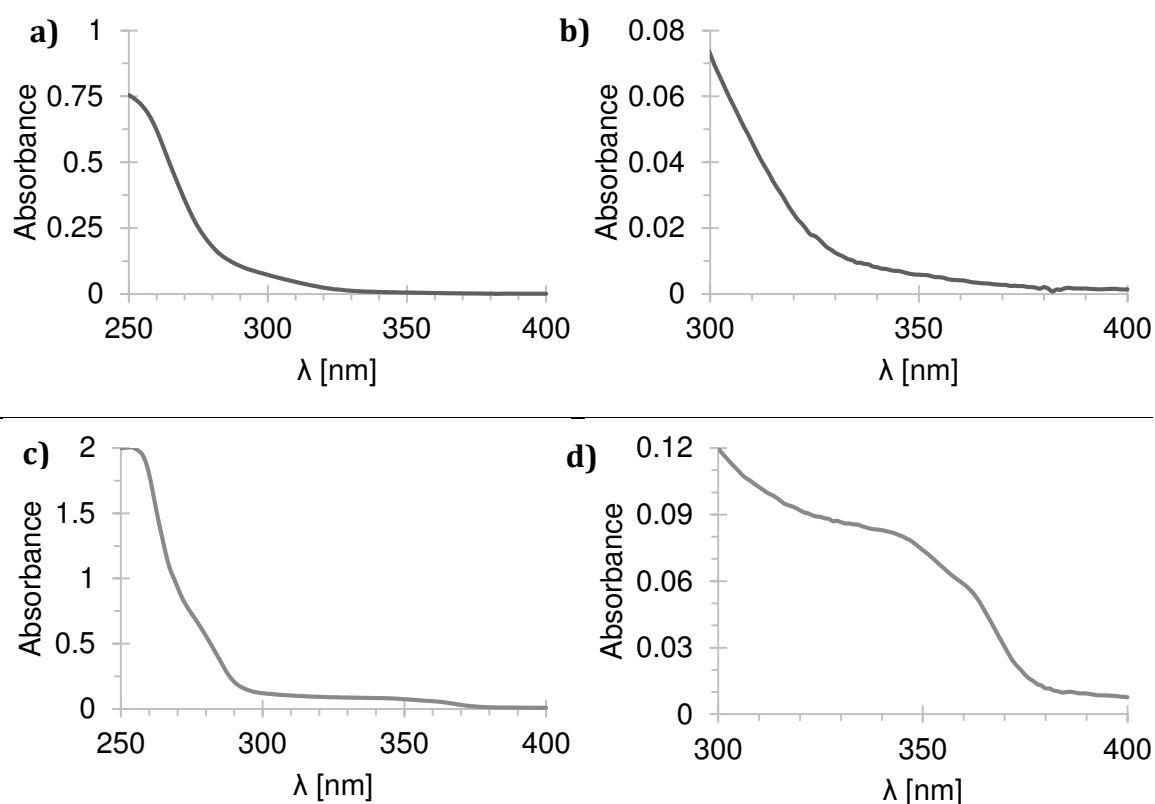


Figure 5.9 UV/VIS spectrum of 50 μ M solution of **168** (a-b) and a 1 mM solution of **184** (c-d) in MeOH. (a, c) The full absorbance spectrum is shown, whereas on the right a zoomed version (b, d) between 300 and 400 nm is shown.

Initial crosslinking experiments were performed with 10 μ M purified BRD4(1) bromodomain, and 20 μ M of the photo-affinity probe, in HEPES buffer. This solution was irradiated with eight 8 W light bulbs emitting at 350 nm for 1 hour, then analysed by LC-MS. The deconvoluted BRD4(1) bromodomain mass peak was observed at 17.54 kDa, which is in good agreement with the expected mass (Figure 5.10a). Irradiation for 60 minutes of the benzophenone probe **168** in presence of BRD4(1) bromodomain did not result in any change of the mass spectrum, suggesting no crosslinking occurred (Figure 5.10b). The diazirine probe **184** showed 30% crosslinked BRD4(1) protein after 1 hour UV irradiation, with a mass increase of 420 Dalton (Figure 5.10c).

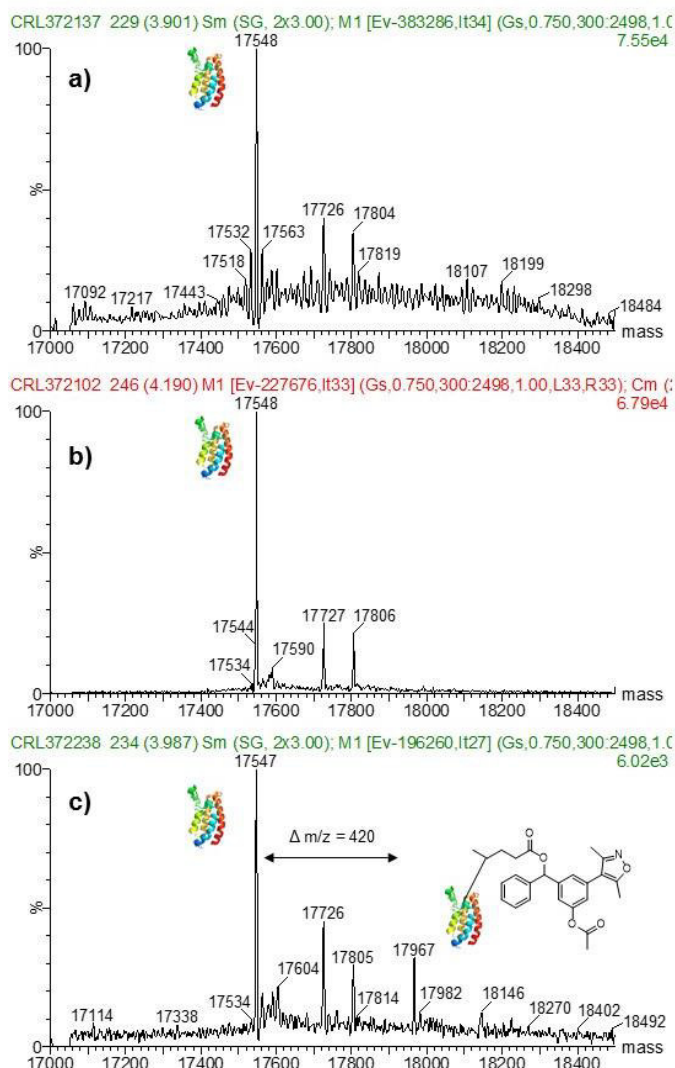


Figure 5.10 Deconvoluted protein mass spectra of (a) the BRD4(1) bromodomain, (b) UV irradiated benzophenone **168** for 1 hour in presence of BRD4(1) bromodomain. (c) UV irradiated diazirine **184** for 1 hour in BRD4(1) bromodomain.

To elucidate the cross-linking efficiency of the probes and the behaviour in different buffers, a time course experiment in TRIS and HEPES buffer were performed. Irradiation of the benzophenone **168** did not result in any crosslinking after 1 hour in either buffer. This result showed that this probe **168** is not suited for crosslinking at 350 nm. However, irradiation of the diazirine probe **184** in HEPES or TRIS buffer led to approximately 30% crosslinking to BRD4(1) after 30 min (Figure 5.11). This observations indicates that the crosslinking of the diazarine **184** is independent of the buffer conditions. In subsequent experiments only HEPES buffer was used, as the protein was stored in this buffer.

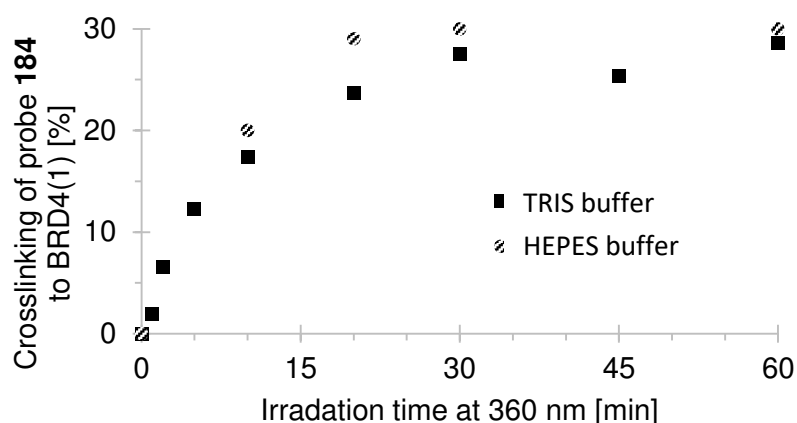


Figure 5.11 Crosslinking time course of the diazirine probe **184** in TRIS and HEPES buffer showing the amount of crosslinked BRD4(1) bromodomain (n = 1).

5.4 Second generation photo-affinity probe

5.4.1 Rationale

The second generation probes are an extension to the first generation probes (**168**, **184**) containing a modular handle, which can be modified after crosslinking to the protein.

Despite the poor crosslinking performance of the benzophenone **164**, it was thought that a modular compound based on the benzophenone scaffold (Figure 5.12) would be useful. According to the BRD4(1) X-ray crystal structure in complex with **2** (Figure 5.6), a PEG linker can be attached on the phenolic hydroxyl to add a solvent exposed linker without affecting the protein-ligand interaction. The Boc-protected amine **185** can be coupled to biotin, a fluorophore, or an alkyne functionality, to obtain a functionalised ABP.

Having demonstrated the ability of the diazirine compound **184** to crosslink to the BRD4(1) bromodomain, a modular pull-down probe with a photo-affinity tag and a clickable linker was designed **186** (Figure 5.12). The reported minimalist alkyne-containing diazirine linker¹⁵⁸ is the perfect attachment for a versatile clickable probe, as it should not change the binding affinity compared to the previous probe **184**, because the linker is solvent exposed.

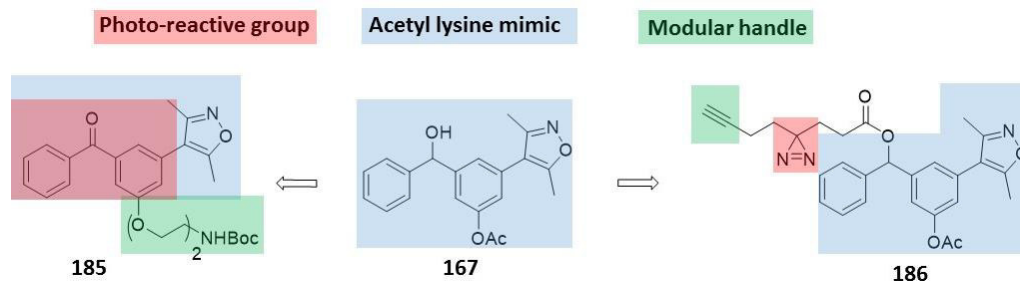
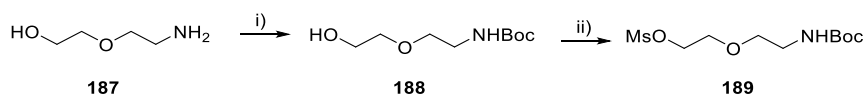


Figure 5.12 Design of the modular second generation photo-affinity probes (**185** and **186**). The photo-reactive group (red), acetyl lysine mimic (blue) and the modular handle (green) are highlighted.

5.4.2 Synthesis of the second generation probe

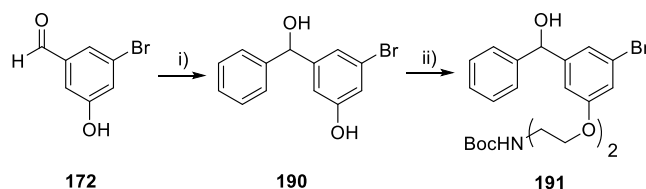
5.4.2.1 Synthesis of the benzophenone **185**

The synthesis of the PEG linker started with a Boc-protection of the amine **187** using Boc-anhydride (Scheme 5.9). **188** was then converted to the mesylate **189** in 74% yield.



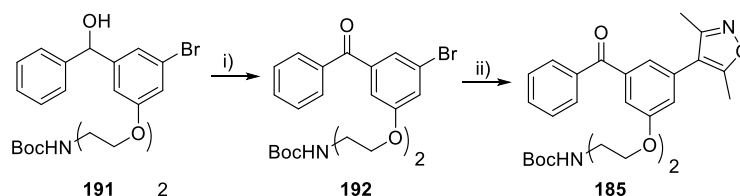
Scheme 5.9 Synthesis of the PEG linker starting from *Reagents and conditions*: i) Boc_2O , THF, rt, 3 h, 96%; ii) MsCl , Et_3N , THF, 0 to rt, 15 min, 74%.

Previous work in the group¹⁵⁹ indicated that substitution on the phenolic alcohol of **2** with PEG-linkers does not result in any conversion due to the electron withdrawing 3,5-dimethylisoxazole. However, this reaction was successful with the brominated phenol **190**. Compound **190** was obtained in a similar manner to the previously described Grignard reaction using phenyl magnesium bromide and **172** in 100% yield. The PEG linker **189** was attached to the phenolic alcohol **190** to isolate **191** in 53% yield (Scheme 5.10).



Scheme 5.10 Attachment of the PEG linker **189** to **190**: *Reagents and conditions*: i) PhMgBr , THF, rt, 1.5 h, 100%; ii) **189**, Cs_2CO_3 , DMF, 60 °C, 1 h, 53%.

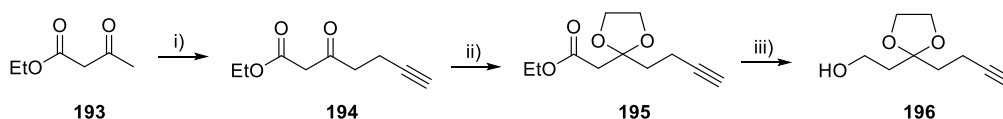
The oxidation from the benzylic alcohol **191** to the benzophenone **192** using PCC worked in 44% yield. The final step for the synthesis of compound **185** was the Suzuki coupling of **192** and **176**, which was performed in a similar manner as previously discussed yielded **185** in 67% (Scheme 5.11).



Scheme 5.11 Attachment of the PEG linker: *Reagents and conditions:* i) PCC, CH₂Cl₂, rt, 6 h, 44%, ii) **176**, Pd(OAc)₂, RuPhos, Na₂CO₃, EtOH, 70 °C, 3 h, 67%.

5.4.2.2 Synthesis of the diazirine compound **186**

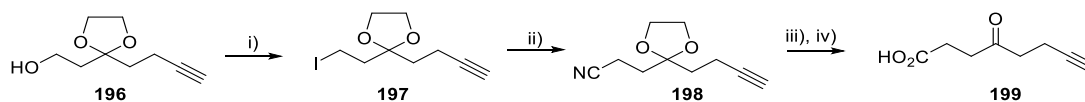
The synthesis of the diazirine cross linker **200** was based on the procedures from Liu *et al.*¹⁵⁸ The double deprotonation of **193** with LDA, followed by the selective alkylation with propargyl bromide proceeded smoothly (Scheme 5.12). Purification of **194** by distillation was necessary to separate the starting material **193** and the product **194**, as by column chromatography these compounds were co-eluting. The acetal formation to give **195** was achieved by heating **194** under reflux in toluene with a substoichiometric amount of 4-TsOH in a Dean-Stark apparatus. The ester of compound **195** was reduced using LiAlH₄ to isolate the alcohol **196**.



Scheme 5.12 i) 1) Diisopropylamine, *n*-BuLi, 30 min, -78 °C, 2) **193**, -78 °C - 0 °C, 3) propargyl bromide, 3 h, 0 °C, 56%; ii) 4-TsOH, ethylene glycol, toluene, Dean-Stark apparatus, 16 h, 110 °C; iii) LiAlH₄, THF, 3 h, 60% over 2 steps.

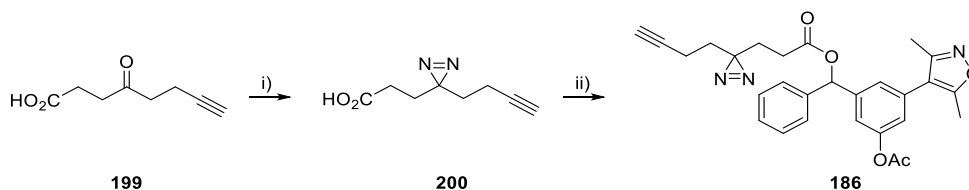
The reaction sequence was shortened from the previous reported procedure¹⁵⁸ by performing an Appel reaction on **196** to obtain **197**. Subsequently, compound **197** was reacted with potassium cyanide to introduce an additional carbon atom to give **198** in 70% yield over 2 steps. The nitrile of **198** was hydrolysed to the carboxylic acid under basic

conditions, followed by the acidic acetal hydrolysis to give propargyl levulinic acid **199** (Scheme 5.13).



Scheme 5.13 i) 1*H*-Imidazole, PPh₃, I₂, CH₂Cl₂, 1 h, 40 °C; ii) KCN, DMF, 3 h, 70 °C, 70% over 2 steps; iii) 10% NaOH (aq.), 3 h, 100 °C; iv) 5 M HCl (aq) adjusted pH to 1, 3 h, rt, 66%.

The diazirine formation of **200** was achieved by applying the conditions previously used to form the diazirine **183**. However, this reaction resulted in an unknown minor impurity, which could not be purified. By changing the reaction conditions for the imine formation using liquid ammonia, instead of 7 M ammonium in methanol, solved the problem and compound **200** was isolated in acceptable purity. The esterification of the diazirine linker **200** with the 3,5-dimethylisoxazole **167** gave compound **186** in 31% yield (Scheme 5.14).



Scheme 5.14 i) 1) NH₃, 5 h, -40 °C, 2) H₂N-OSO₃H, MeOH, -40 °C - 0 °C, 3) I₂, Et₃N, Et₂O, 0 °C, 1 h, 38%; ii) **167**, CH₂Cl₂, 2 h, rt, 31%.

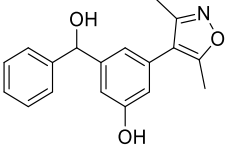
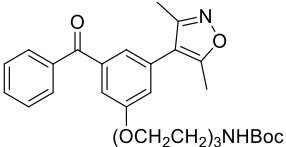
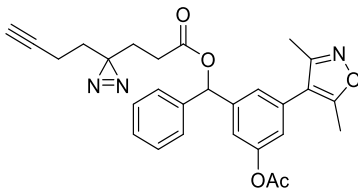
5.4.3 Biological evaluation of **185** and **186**

5.4.3.1 BRD4(1) affinities of compounds **185** and **186**

The compounds **185** and **186** were tested by AlphaScreen™ on the BRD4(1) bromodomain (Table 5.4). The benzophenone compound **185** showed a low IC₅₀ value (> 50 μM) on BRD4(1), indicating the PEG linker is not tolerated. However, the diazirine **186** is a relatively potent BRD4(1) ligand with approximately a 4-fold decrease compared

2.

Table 5.4 BRD4(1) AlphaScreen™ IC₅₀ values of the second generation photo-affinity probes (**185** and **186**). In parentheses the 95% confidence level is shown.

Compound	IC ₅₀ on BRD4(1) [μM]
2 	0.24 (0.19-0.30)
185 	> 50
186 	0.91 (0.62-1.24)

5.3.3.2 Crosslinking experiments on purified bromodomains with **186**

The UV/VIS spectrum of compound **186** shows an intense absorption band between 250 nm and 260 nm, which results from the π - π^* transition of the aromatic rings (Figure 5.13). At a shorter wavelength the n to π^* transition of the diazirine is observed with a λ_{\max} at 345 nm. The molar extinction coefficient is very low ($62 \text{ M}^{-1} \text{ cm}^{-1}$), but is in agreement with published extinction coefficient of aliphatic diazirine compounds.¹⁶⁰ The absorbance between 280 to 320 nm might indicate the presence of some diazomethane, which can be formed by decomposition of the diazirine.¹⁶¹

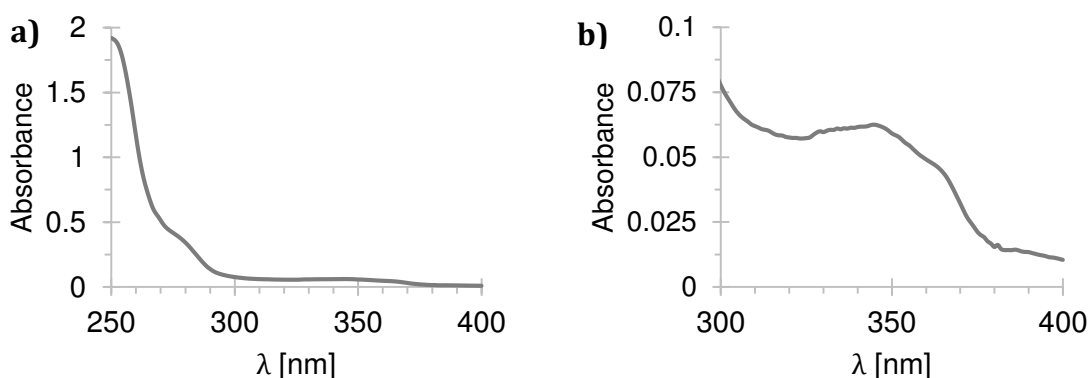


Figure 5.13 a) and b) UV/VIS spectrum of 1 mM solution of **186** in MeOH. a) the full absorbance spectrum is shown whereas b) a zoomed version between 300 and 400 nm is shown.

Crosslinking experiments between the diazirine **186** and purified BRD4(1) bromodomain were performed and analysed by mass spectrometry (Figure 5.14). Incubation of diazirine **186** with BRD4(1) did not result in any crosslinking without UV-irradiation (Figure 5.14b), but after 10 minutes of irradiation, the crosslinked protein can be clearly observed by mass spectrometry (Figure 5.14c). A time-course experiment showed that in HEPES buffer probe, **186** crosslinks with BRD4(1) after 2 minutes UV irradiation. After 20 minutes irradiation, a plateau is formed with 25% crosslinked protein observed (Figure 5.14d). Pleasingly, the crosslinking efficiency is similar to the first generation probe **184**. The selective binding in the KAc binding site of the probe **186** was confirmed by a competition experiment with 10 equivalents of the potent BRD4 ligand I-BET151 (**3**), in which no crosslinking was observed (Figure 5.14e). To modify the crosslinked protein, copper-catalysed alkyne azide cyclisation (CuAAC) with azide PEG3-biotin (**201**) was performed. The click chemistry was performed using CuSO₄, the reducing agent TCEP and the ligand TBTA.¹⁶² After 1 hour incubation at room temperature, the corresponding mass to the attached biotinylated BRD4(1) bromodomain was observed (Figure 5.14f). This experiment demonstrates a functional *in vitro* probe, which is able to crosslink to BRD4(1) bromodomain, and subsequently the linker can be modified by using CuAAC chemistry to attach a biotin linker.

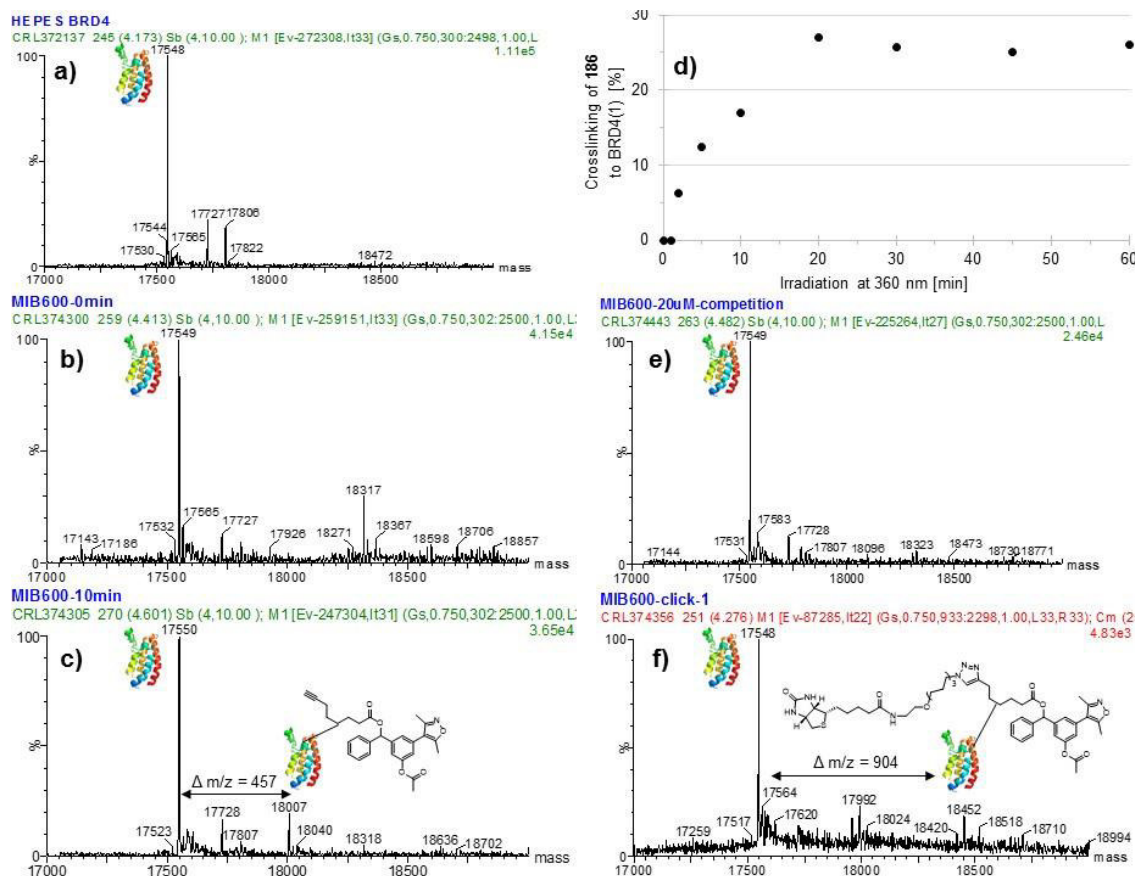


Figure 5.14 Deconvoluted protein mass spectra of (a) the BRD4(1) bromodomain, (b) incubated diazine probe **186** with BRD4(1) without UV irradiation; (c) with 10 min UV irradiation showing it only crosslinks upon UV light emission. (d) Time course of the crosslinking efficiency of the probe **186** to BRD4(1) bromodomain. (e) Competition experiment with 10 eq of I-BET151 and 1 hour UV irradiation showing the probe does not crosslink. (f) CuAAC between the cross linked protein and PEG3-biotin azide showing the mass spec adduct of the biotin azide.

In further investigations, BRD4(1) crosslinked to probe **186** was reacted with either the commercial biotin azide **201** or the fluorescent 5-carboxytetramethylrhodamine-azide **202** (Figure 5.15).

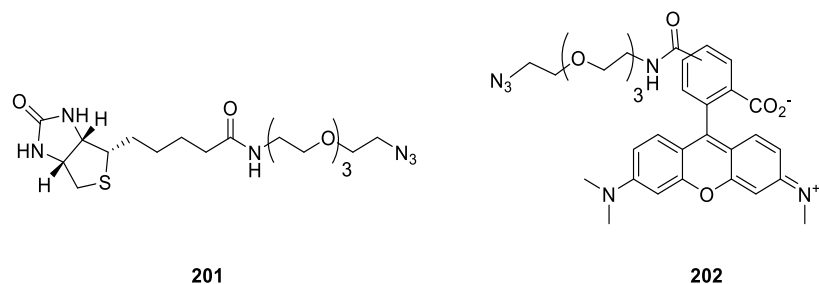


Figure 5.15 Commercially available azides containing a biotin **201** or fluorescent group **202**.

After running the SDS-PAGE, the protein band was stained using Ponceau stain. The protein seems stable under UV irradiation following CuAAC chemistry as no other bands were detected on the gel (Figure 5.16a and c). Western-blot analysis using streptavidine-HRP conjugated antibody shows the biotin adduct in lane 2 (Figure 5.16b). The other lanes also show a weak signal, which might be due to the nature of the unselective antibody. However, it clearly demonstrates that the competition experiment with (+)-JQ1 (**1**) (Lane 3), did not result in any crosslinking as well as the experiment without UV irradiation (Lane 4).

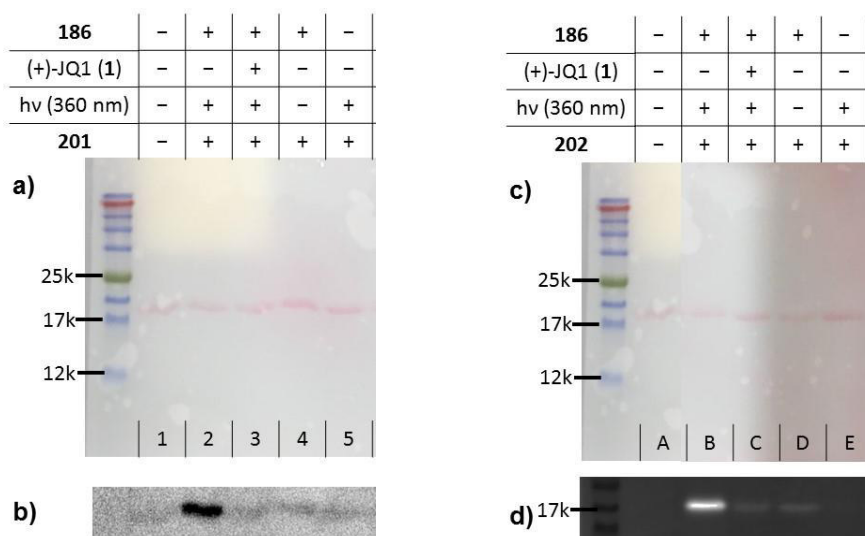


Figure 5.16 SDS-PAGE gel of purified BRD4(1) bromodomain crosslinked with probe **186**. a) and c) The membrane was visualised with Ponceau stain. b) Western-blot with streptavidine HRP 1:500 and enhanced chemiluminescence staining (ECL) staining. d) Fluorescence (Ex 532 nm, Em: 605 nm) visualisation.

Similarly, the rhodamine-labelled BRD4(1) bromodomain protein was visualised through fluorescence (Ex 532 nm, Em: 605 nm), with an intense band on lane B confirming the CuAAC chemistry worked with **202** (Figure 5.16d). The negative controls in lane C and D show very faint bands, indicating the probe might have slightly crosslinked, despite the competition with (+)-JQ1 (**1**).

To understand the selectivity of probe **186**, crosslinking to other bromodomains was studied (Figure 5.17). It was demonstrated that the probe **186** has a strong affinity to the CREBBP bromodomain. While competing the probe **185**, with the 3,5-dimethylisoxazole **2**,

the fluorescent intensity was reduced to 24% in CREBBP, demonstrating selective binding. Surprisingly, the probe **186** crosslinked weakly to the WDR9(2) bromodomain. This bromodomain does not have the conserved asparagine residue in the active site, which is the important amino acid for most of the small molecule bromodomain ligands. To our knowledge this is the first observed small molecule ligand to WDR9(2) bromodomain. Previous efforts from other groups discovered a weak ligand (112 μ M) for the atypical bromodomain PHIP(2), which also contains a threonine instead of the conserved asparagine residue.¹⁶³ No selective crosslinking was observed on the TRIM24 bromodomain with a PHD finger (Figure 5.17). Crosslinking on the family I bromodomain FALZ was observed, albeit weak. The parasitic bromodomains *TcBDF2* and *TcBDF3*, which are present in the *Trypanosoma cruzi* showed some crosslinking to the *TcBDF3*, whereas the other parasite bromodomain was unaffected. This is a very interesting observation as the BET inhibitors I-BET151 (**3**) and (+)-JQ1 (**1**) show similar efficacies to the approved drug benznidazole for Chagas disease treatment.¹⁶⁴ This might indicate that the 3,5-dimethylisoxazole ligand **2** could be a potential binding molecule for the *TcBDF3* bromodomain.

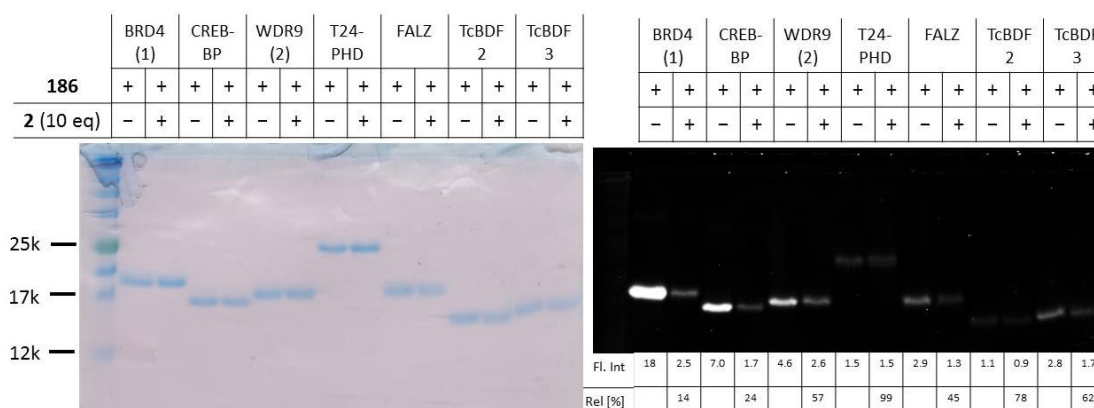


Figure 5.17 SDS PAGE gel of different crosslinked bromodomains and visualised by Coomassie blue stain (left) and fluorescence (right). The relative band intensity between the lane with and without competitor ligand (**2**) is shown.

3.4.3.3 Crosslinking experiments on cell lysates

Having established a functioning modular cross linking probe **186**, we evaluated the probe on the colon cancer cell lysate RKO, which overexpresses BRD4.¹⁶⁵ The cell lysate was kindly provided by Dr Liam O'Connor (Prof. Ester Hammond lab, Oxford). The compound was incubated for 30 minutes in the cell lysate, before it was irradiated for 20 minutes. The CuAAC with **202** was performed according the previous established method.¹⁶⁶ The Ponceau stain demonstrates that the cell lysate is not degraded under UV irradiation following the crosslinking reaction. However, no fluorescence of the crosslinked cell lysate could be detected (Figure 5.18). This could be due to a variety of reasons, such as low expression level of BRD4, detection limit of the probe is too low, failure of CuAAC chemistry, or hydrolysis of probe **202** due to esterase activity. However, the probe stability of compound **202** was analysed in *E. coli* cell lysate over 24 hours by HPLC and it was found partially stable (Appendix E). After 24 h in the *E. coli* cell lysate, still 34% of **186** was detected.

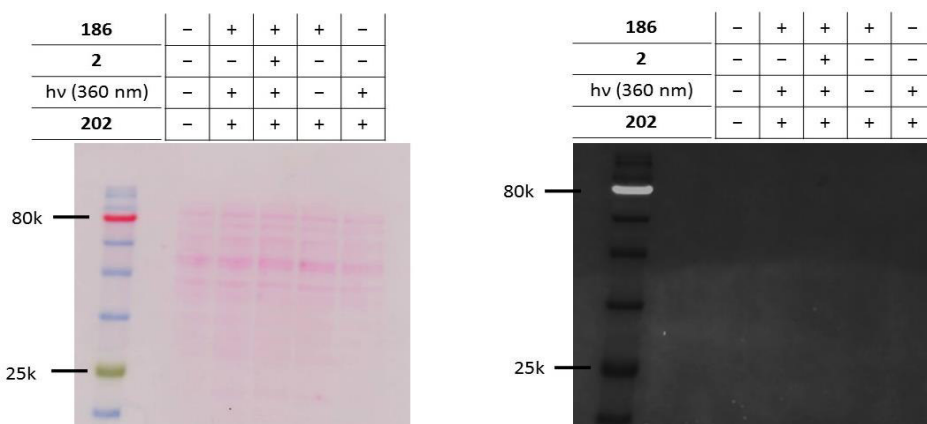


Figure 5.18 Membrane of the RKO cell lysate and visualised by Ponceau stain (left) and fluorescence (right).

In an additional experiment, the RKO cell lysate was spiked with purified BRD4(1) bromodomain and the analysis was repeated (Figure 5.19). A Western-blot using a BRD4-HRP antibody could not detect any BRD4 protein in the RKO cell lysate. This result explains why in the previous experiment, no fluorescence was detected due of a low

abundance of BRD4. However in this experiment the probe crosslinked to the purified BRD4(1) bromodomain indicating the probe is partially stable in the cell lysate and the CuAAc chemistry functional (Figure 5.19b).

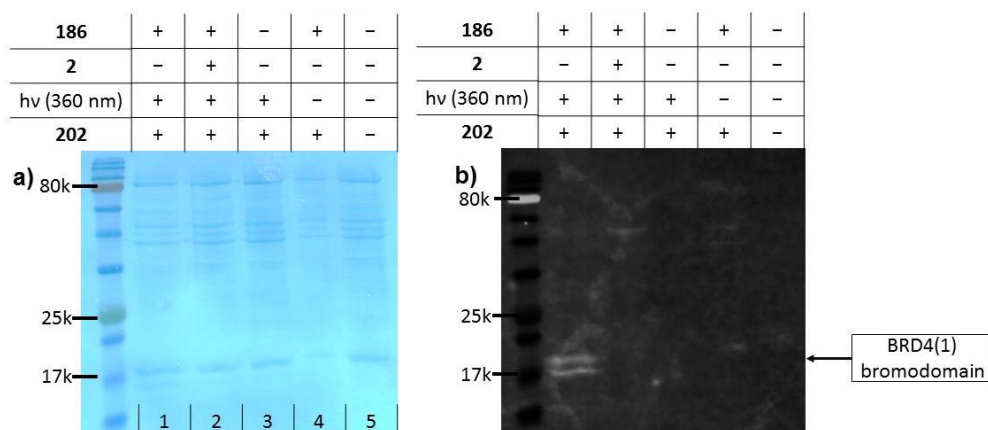


Figure 5.19 PVDF membrane of the RKO cell lysate spiked with purified BRD4(1) bromodomain and visualised by a) Coomassie blue stain and b) fluorescence.

5.5 Conclusion

Two photoaffinity probes containing a benzophenone **185** or a diazirine crosslinking group **186** were synthesised. The modular diazirine **186**, was demonstrated to be a useful probe with 30% crosslinking efficiency to the BRD4(1) bromodomain. Furthermore, new bromodomain targets for the unselective bromodomain probe **186** were discovered. The compound bound weakly to WDR9(2), an atypical human bromodomain, and the parasitic *TcBDF3* bromodomain. In order to optimise the probe stability the ester bond linking the probe and the modular linker should be changed to the amide **203** (Figure 5.20). In summary, we demonstrated that probe **186** can be a tool to evaluate biological targets of the 3,5-dimethylisoxazole **2** in either human or parasitic cell lines.

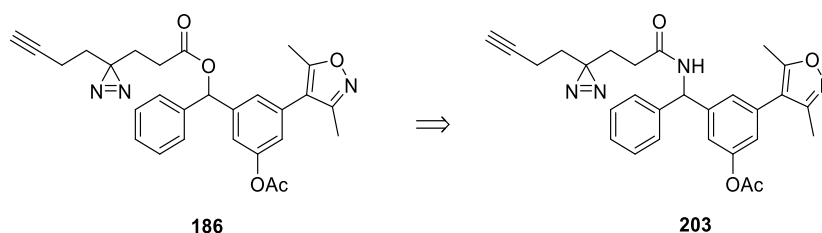


Figure 5.20 Optimisation of probe **186** to increase the stability in cell lysate.

Chapter 6

Summary

6.1 Summary

This dissertation discussed two projects on developing and understanding bromodomain ligands for CREBBP and BRD4.

Chapter 2 detailed the optimisation of the dihydroquinaxolinone acetyl lysine head group, which tends to oxidise to an aromatic compound. By expanding the 6-membered DHQ ring to a 7-membered ring a stable ligand was obtained, while maintaining a sub-micro molar affinity for the CREBBP bromodomain. Furthermore, it was shown that only the (*R*)-enantiomer has affinity to the bromodomain, whereas no affinity was observed for the (*S*)-enantiomer. The crystal structure confirmed the identical binding mode of the 6- and 7-membered DHQ ring.

Chapter 3 discussed the cation- π interaction between R1173 of the bromodomain and the THQ ring. Calculations of the electrostatic surface potential of THQ analogues with different substituents were compared to the CREBBP binding affinities and a good correlation, albeit weak, was observed. Attempts to increase the selectivity of the CREBBP ligand by adding the bulky THP substituent on the aniline were unsuccessful. The evaluation of the group efficiency of the ligand revealed that the DHQ headgroup and the THQ ring are contributing most towards the binding affinity.

Chapter 4 explored the rigidification of the propyl linker by introducing a *gem*-difluoro group, and a 3-fold affinity increase was measured. A small molecule and protein X-ray crystal structure confirmed the *gauche-gauche* effect on conformation. However, introduction of the fluorines decreased compound solubility.

Chapter 5 discussed the development of a photoaffinity labelled activity probe based on a BRD4 bromodomain ligand. Attaching a clickable diazirine linker to the ligand slightly reduced the

BRD4(1) affinity. This probe crosslinked to the BRD4(1) bromodomain in 30% efficiency. Subsequently, the crosslinked compound to BRD4(1) could be modified with either a biotin or a fluorophore tag using CuAAC. Furthermore, this compound was tested on various human and parasitic bromodomains and crosslinked to CREBBP, WDR9(2) and the parasitic bromodomain TcBDF3. The probe was further investigated in RKO colon cancer cell lysate, but no crosslinking to any cell lysate proteins could be detected, except the exogenously added BRD4(1) bromodomain.

Chapter 7

Experimental Section

7.1 General Experimental

7.1.1 Physical Methods

Molecular Dynamics (MD) and Density Functional Theory (DFT) calculations (by Wilian A. Cortopassi and Prof. Robert S. Paton (Department of Chemistry, University of Oxford): 120 ns MD simulations were performed of the 6- and 7- membered DHQ ring system using the Amber force field and following the same methodology as described in the literature.⁵⁶ Electrostatic surface potentials (ESPs) of the aniline and THQ derivative were obtained from DFT densities at the B3LYP/6- 31G(d,p) level of theory (gas and solution-phase); with B3LYP/6-31G++(d,p) and M06-2X/6- 31G(d,p). Calculations used the Solvation Model Density (SMD) and SM8 Minnesota implicit solvation models³⁸ of diethyl ether ($\epsilon = 4.24$) to mimic the hydrophobic environment of the binding site of CREBBP, with little effect upon the resulting ESP.

X-Ray crystal structure diffraction pattern (by Prof. Richard Cooper, CRL Oxford): was collected at the Oxford Diffraction (Agilent) SuperNova Diffractometer with microfocus Cu-K α radiation using standard procedures at 150 K.¹⁶⁷ The crystal structure was refined by Prof. Richard Cooper.

7.1.2 Biochemical and biophysical methods

Protein expression and purification (by Dr Anthony K. N. Chan, CRL Oxford): Briefly, the CREBBP (Addgene plasmid # 38977) and BRD4(1) bromodomain (Addgene plasmid # 38942) constructs were transformed into *E. coli* BL21 (DE3) cells for expression. The proteins were purified using Immobilized Metal Affinity Chromatography with a HisTrap™ column (GE Healthcare) followed by gel filtration chromatography with Superdex 75 resin (GE Healthcare). The protein purity was assessed by SDS-PAGE.

Differential scanning fluorimetry. Thermal melting experiments were carried out using the Mx3005p real-time PCR machine (Agilent) employing a protein concentration of 2 μ M, small molecule concentration of 10 μ M, and 5 x SyproOrange (Invitrogen, CA). Buffer

conditions were 50 mM HEPES, 500 mM NaCl, pH 7.5. The fluorescence were taken between 25-85 °C, in one degree increment, with a 30 sec hold for each step. 492 nm and 610 nm were used for excitation and emission, respectively. The melting temperature (T_M) was calculated using the Boltzmann equation (Eq. 1):

$$y=LL + \frac{UL-LL}{1+e^{\frac{Tm-x}{a}}}$$

Equation 7.1: Boltzmann equation: LL and UL minimum and maximum intensities, a corresponds to the slope of the curve

Data processing performed using Prism 6.0 (GraphPad Software, La Jolla, California, USA) and the T_M shift was calculated relative to the reference sample on the same plate. Experiments were performed in triplicates; average values are reported.

AlphaScreen™ assay (by Larissa See and Dr Oleg Federov, Oxford) on BRD4(1) was performed by Larissa See (Department of Chemistry, University of Oxford) using the following method: AlphaScreen™ buffer (25 mM HEPES, 100 mM NaCl, 0.05% w/v% CHAPS, 0.1% w/v BSA; pH 7.6) was filter sterilised through a 0.22 µm filter. Biotinylated peptides employed a final assay concentrations were: his₆BRD4(1) 20 nM, H4[1-20](KAc)₄ 4 nM, donor beads 5 µg/mL; acceptor beads 5 µg/mL; DMSO < 0.5%. Small molecules were prepared as 25 mM DMSO stock solutions with a 1:50 pre-dilution step inot buffer before addition to the assay. Data processed by fitting a four-parameter equation to calculate IC₅₀ values using Prism 6.0h (GraphPad Software, La Jolla, California, USA). Dose-response curves against BRD4 were performed in triplicate with a serial 1:2 dilutions, on a ProxiPlate-384 Plus (Perkin Elmer), which was read using a Synergy™ 2 MultiMode Microplate Reader. For incubation steps, the plate was sealed, shaken for 10 seconds at 600 rpm, and incubated at room temperature in the dark for 1 h. CREBBP affinity was measured by Dr Oleg Fedorov, (Structural Genomics Consortium, University of Oxford) as described previously.

Isothermal calorimetry. All calorimetric experiments were performed on a MicroCal iTC200 or MicroCal PEAQ-ITC Automated (Malvern) and analysed with the MicroCal

PEAQ-ITC Analysis software (Malvern 1.1.0.1262) using a single binding site model. The first data point was excluded from the analysis. BRD4(1) and CREBBP bromodomains were dialysed at 4 °C overnight in a Slide-A-Lyzer® MINI Dialysis Device (3500 MWCO; Thermo Scientific Life Technologies) into 50 mM HEPES, 150 mM NaCl containing 0.2% DMSO; pH 7.4. Proteins were centrifuged to remove aggregates (5 min, 3,000 rpm, 25 °C). Protein concentration were determined by measuring the absorbance at 280 nm using a Nanodrop® ND-1000 spectrophotometer (Nanodrop® Technologies Inc.) or a NanoDrop Lite spectrophotometer (Nanodrop® Technologies Inc.) by using the predicted protein absorbance¹⁶⁸ (CREBBP: ϵ_{280} : 26930 M⁻¹ cm⁻¹ and BRD4(1): ϵ_{280} : 28545 M⁻¹ cm⁻¹). Small molecules ligand were dissolved as 10 to 20 mM DMSO stock solution and diluted to the required concentration using dialysis buffer. The cell was stirred at 750 rpm, reference power set to 3 μ cal/sec and temperature held at 15 °C. After an initial delay of 60 sec, 20 \times 2 μ L injections (first injection 0.4 μ L) were performed with a spacing of 180 sec. Heated dilutions were measured under the same conditions and subtracted for analysis. Small molecule solutions in the calorimetric cell (250 μ L, (20 to 30 μ M)) were titrated with the protein solutions in the syringe (60 μ L, 200-300 μ M).

¹H CPMG-NMR data were obtained in collaboration with Prof. Timothy D. W Claridge (Department of Chemistry, University of Oxford). The NMRs were measured in Match NMR tube 3.0 mm (Bruker) on a Bruker AVIII 700 MHz equipped with an inversed TCI cryoprobe and data were processed and analysed using TopSpin Version 3.2. The PROJECT CPMG pulse sequence (Figure 7.1) as described by Aguilar *et al.*¹⁶⁹ was used to remove the broad resonances of the protein. The CPMG filter time was at 60 ns.

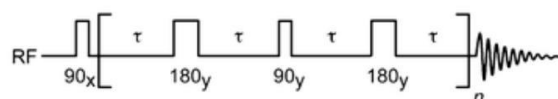


Figure 7.1: Pulse sequence for the CPMG experiment. Figure adapted with permission.¹⁶⁹

160 μL samples were made up with a constant concentration of the small molecule ligand (20 μM , from a 1 mM DMSO stock solution) and fumaric acid (20 μM) as internal standard in deuterated phosphate buffer (50 mM sodium phosphate, 150 mM NaCl, D_2O ; pH 7.4). CREBBP bromodomain was titrated into the sample until complete saturation of the ligand signal was achieved. The relative signal intensity of the ligand in comparison to the internal standard was calculated upon the addition of the CREBBP bromodomain was calculated using the shown in Equation 7.2.

$$\text{Decrease of relative peak intensity} = \frac{\frac{I(\text{sample})}{I(\text{int. std.})}}{\frac{I(\text{sample})_{c=0}}{I(\text{int. std.})_{c=0}}}$$

Equation 7.2 The equation used to calculate the decrease in signal intensity of the ligand upon addition of the CREBBP bromodomain. $I(\text{sample})_{c=0}$ and $I(\text{int. std.})_{c=0}$ are the peak heights in the absence of CREBBP whereas $I(\text{sample})$ and $I(\text{int. std.})$ are the peak heights in the presence of CREBBP at a given concentration.

The titration data was fitted using Prism 6.0 (GraphPad Software, La Jolla, California, USA) and K_D values were extracted using the equation described by Dalvit.⁸² (Equation 7.3).

$$y = A \times \frac{[P_T] + [L_T] + K_D - \sqrt{([P_T] + [L_T] + K_D)^2 - 4([P_T][L_T])}}{2[L_T]}$$

Equation 7.3 The equation used to determine K_D values from titration data, where y is the decrease in ligand signal intensity; A the maximum loss in the signal intensity; $[P_T]$ is the total protein concentration; $[L_T]$ is the total ligand concentration; K_D is the dissociation constant.

Crystallisation (by Prof. Panagis Filippakopoulos, Dr Sarah Picaud, SGC, Oxford).

Aliquots of the purified protein were set up for crystallization using a mosquito® crystallization robot (TTP Labtech, Royston UK). Coarse screens were typically setup onto Greiner 3-well plates using three different drop ratios of precipitant to protein per condition (100+50 nl, 75+75 nl and 50+100 nl). Initial hits were optimized further scaling up the drop sizes. All crystallizations were carried out using the sitting drop vapor diffusion method at 4 °C. CREBBP crystals with **141** were grown by mixing 200 nl of the

protein (10 mg/ml and 2 mM final ligand concentration) with 100 nl of reservoir solution containing 21 % PEG3350, 15 % ethylene glycol and 0.25 M sodium formate or by mixing 150 nL of protein with an equal amount of reservoir solution containing 20 % PEG3350, 10 % ethylene glycol and 0.2 M sodium acetate. CREBBP crystals with (*R*)-**26** were grown by mixing 100 nL of the protein (10 mg/ml and 2 mM final ligand concentration) with 200 nL of reservoir solution containing 20 % PEG3350, 10 % ethylene glycol and 0.2 M sodium fluoride. Diffraction quality crystals grew within a few days.

Data Collection and Structure solution (by Prof. Panagis Filippakopoulos, Dr Sarah Picaud, SGC, Oxford). All crystals were cryo-protected using the well solution supplemented with additional ethylene glycol and were flash frozen in liquid nitrogen. Data were collected at Diamond beamline I03 0.97625 Å. Indexing and integration was carried out using XDS¹⁷⁰ and scaling was performed with SCALA (MRC Laboratories, Cambridge). Initial phases were calculated by molecular replacement with PHASER¹⁷¹ using the known model of CREBBP (PDB ID 3DWY). Initial models were built by ARP/wARP¹⁷² followed by manual building in COOT.¹⁷³ Refinement was carried out in REFMAC5.¹⁷⁴ Thermal motions were analyzed using TLSMD¹⁷⁵ and hydrogen atoms were included in late refinement cycles.

Protein Observed Fluorine NMR (by Gabriella Perell, and Prof. William C. K. Pomerantz, University of Minnesota): Protein observed 1D ¹⁹F NMR samples were obtained as previously described using a frequency window of -120 to -130 ppm, a D1 of 0.7 sec and an acquisition time of 0.05 sec.⁸⁵ Small molecules stock solutions were prepared in DMSO at 20 mM. Small molecules were titrated into CREBBP or BRD4 bromodomain (protein solutions at 40-50 μM in 50 mM TRIS, 100 mM NaCl, 5% D₂O, pH 7.4) at 0.25, 0.5, 1.0, and 2.0 equivalents of protein with a final concentration of 0.5% DMSO.

Crosslinking experiments on purified bromodomains: A solution of 20 μM of the photo affinity probe was added to 10 μM of purified bromodomain in 50 mM HEPES, 150 mM NaCl; pH 7.4 buffer, and incubated for 30 min at 4 $^{\circ}\text{C}$ with or without competitor ligand. Subsequently, the mixtures were irradiated in a Luzchem LCZ-5 photoreactor equipped with eight 8 Watt lamps (Hitachi FL8BL-8, ~ 350 nm) for 0 to 60 min at 4 $^{\circ}\text{C}$.

Crosslinking experiments on RKO cell lysate: 20 μM of the crosslinking probe was incubated in 1 mg/mL RKO cell lysate (provided by Dr Liam O'Connor, Hammond lab, University of Oxford) for 30 min at 4 $^{\circ}\text{C}$ with or without competitor ligand. Subsequently, the mixtures were irradiated in a Luzchem LCZ-5 photoreactor equipped with eight 8 Watt lamps (Hitachi FL8BL-8, ~ 350 nm) for 20 min at 4 $^{\circ}\text{C}$.

Crosslinking efficiencies: The crosslinking efficiencies of the probes to purified BRD4(1) bromodomains were determined by protein liquid chromatography-mass spectrometry (LC-MS). A Waters LCT Premier XE (ESI-TOF-MS) coupled to a Waters 1525 μ Binary HPLC system using a Merck Cromolith RP18e guard cartridge as the column (5 x 2 mm) was used.

Mobile Phase: Solvent A: Water + 0.1% formic acid; Solvent B: Acetonitrile

Step length (min)	Flow rate (mL/min)	Elapsed time (min)	%A	%B
1	0.4	1	95	5
4	0.4	5	0	100
3	1	8	0	100
0.1	1	8.1	95	5

Total mass spectra were reconstructed from the ion series using the MaxEnt1 algorithm on MassLynx software (Version 4.1, Waters Inc.) by deconvolution between 16000 and 19000 Da. Crosslinking efficiencies (CE) were calculated by comparing the peak heights of

the signal from crosslinked BRD4(1) to the signal from unreacted BRD4(1) displayed in MassLynx (Equation 7.4).

$$CE [\%] = \frac{CP}{CP + BRD4(1)} \times 100$$

Equation 7.4 The equation used to determine the crosslinking efficiency (*CE*), where *CP* is the peak height of crosslinked BRD4(1) protein and *BRD4(1)* is the peak height of unreacted BRD4(1) protein.

CuAAC of the crosslinked protein: The solutions of the crosslinked proteins (50 μ L) were mixed with freshly prepared click mix solution (50 μ L) and either a 10 mM stock solution of azide-PEG3-biotin conjugate or azide-fluor 545 (1 μ L) and incubated at ambient temperature for 2 h. The click mix solution contains 1 mM CuSO₄, 1 mM *tris*(2-carboxyethyl)phosphine (TCEP), 100 μ M *tris*(benzyltriazolylmethyl)amine (TBTA) (from a 5 mM DMSO stock solution) dissolved in Milli-Q water. All chemicals were purchased from Sigma-Aldrich.

SDS-PAGE: Sodium dodecyl sulfate polyacrylamide gel was cast using Mini-PROTEAN® 3 Cell (Bio-Rad). Sodium dodecyl sulfate polyacrylamide gel electrophoresis (SDS-PAGE) was performed using Mini-PROTEAN® 3 Electrophoresis Module (Bio-Rad). The Tris-Glycine discontinuous buffer system was used in the SDS-PAGE experiments. Protein samples for SDS-PAGE was first prepared in 1 \times Laemmli sample buffer (diluted from 4 \times Laemmli sample buffer, Bio-Rad) containing 1.42 M β -mercaptoethanol (aliquoted from 14.2 M β -mercaptoethanol, Bio-Rad), and then denatured at 100 °C for 10 min. Chemicals for SDS-PAGE, Trizma® base, 30% acrylamide/bis-acrylamide solution, sodium dodecyl sulfate dust-free pellets, *N,N,N',N'*-tetramethylethane-1,2-diamine (TEMED) and ammonium persulfate (APS), were purchased from Sigma-Aldrich. Glycine was purchased from Fisher Scientific.

Western blotting: Proteins separated by SDS-PAGE were transferred onto a polyvinylidene fluoride (PVDF) membrane (Immuno-Blot® PVDF Membrane Sandwiches, Bio-Rad) using the Mini Trans-Blot® Electrophoretic Transfer Cell (Bio-Rad) operated at 100 V, 350 A for 1 h. Standard Western blotting procedures were performed according to the Bio-Rad immunodetection manual (Bio-Rad Bulletin 6219: http://www.bio-rad.com/webroot/web/pdf/lsr/literature/Bulletin_6219.pdf, accessed 19th September 2016). TBS and TTBS 10× buffers were purchased from Alfa Aesar. Non-fat milk powders (Blotting-Grade Blocker, Bio-Rad) was used for membrane blocking and antibody incubation. HRP (horseradish peroxidase)-conjugated streptavidin antibody (Insight Biotechnology) was used to detect biotinylated crosslinked proteins. Clarity™ Western ECL substrate kit (Bio-Rad) was employed and visualised using ChemiDoc™ MP System (Bio-Rad)

Protein staining: After SDS-PAGE, the gels and PVDF membranes were stained with Staining Solution (0.5% Brilliant Blue G (Sigma-Aldrich), 50% (v/v) methanol (Sigma-Aldrich), 10% (v/v) glacial acetic acid (Fisher Scientific), 40% (v/v) Milli-Q water) for 15 min. Destaining was performed with 40% (v/v) methanol, 10% (v/v) glacial acetic acid, 50% (v/v) Milli-Q water until protein bands became visible. Alternatively, proteins transferred onto PVDF membranes were stained with Ponceau S Stain (Amresco Inc.) for 15 min. Subsequently, proteins were visualised by rinsing with Milli-Q water (Merck Millipore). To completely remove the stain for Western blotting, the stained PVDF membrane was then de-stained in Blocking Solution [5% (w/v) Blotting-Grade Blocker (Bio-Rad) in 1× TBS solution (Alfa Aesar)]. The crosslinked proteins with Alexa 545 were visualised (Ex. 532 nm, Em. 605 nm) on the SDS PAGE gel using ChemiDoc™ MP System (Bio-Rad).

Probe stability in *E. coli* cell lysate: 20 µM of the ABP probe and 20 µM of the internal standard 2-naphtoic acid (Sigma-Aldrich) was incubated in 1 mg/mL *E. coli* cell lysate

(200 μ L) for 0 and 24 h at ambient temperature. Isopropanol (200 μ L) was added, sonicated for 5 min, and filtered through a Millipore 0.45 μ m microsyringe filter. The filtrates were concentrated on the lyophiliser (Christ-Alpha 2-4 LD). The residue was dissolved in 25 μ L DMSO and ran on the PerkinElmer Flexar system with a Binary LC Pump and UV/VIS LC Detector. A Dionex Acclaim[®] 120 column (C18, 5 μ m, 120 Å , 4.6 \times 150 mm) was employed, with a 5 minutes gradient of 95% H₂O/5% MeCN + 0.1% TFA (Solvent A) to 95% MeCN/5% H₂O + 0.1% TFA (Solvent B), flow rate 1.0 mL/min and detection at 254 nm. The area under the curve (AUC) of the internal standard and **186** was compared.

Step length (min)	Elapsed time (min)	%A	%B
1	1	100	0
5	11	0	100
3	14	0	100
1	15	100	0
5	20	100	0

7.1.3 Synthetic methods

¹H NMR spectra were recorded on a Bruker AVIIIHD 400 nanobay (400 MHz), Bruker AVIIIHD 500 nanobay (500 MHz) or Bruker AVII 500 with He cryoprobe (500 MHz) using CDCl₃ (unless indicated otherwise) as a reference for internal deuterium lock. The chemical shift data for each signal are given as δ_{H} in units of parts per million (ppm) relative to the NMR solvent¹⁷⁶ where δ_{H} (CDCl₃) = 7.26 ppm, δ_{H} ((CD₃)₂SO) = 2.54 ppm, δ_{H} ((CD₃)₂CO) = 2.17 ppm, and δ_{H} (C₆D₆) = 7.15 ppm. The multiplicity of each signal is indicated by: s (singlet); br s (broad singlet); d (doublet); t (triplet); q (quartet); qn (quintet), dd (doublet of doublets); or m (multiplet). The number of protons (n) for a given resonance signal is indicated by nH. Coupling constants (*J*) are quoted in Hz and are

recorded to the nearest 0.1 Hz. Identical proton coupling constants (J) are averaged in each spectrum and reported to the nearest 0.1 Hz. The coupling constants are determined by analysis using Bruker TopSpin software.

^{13}C NMR spectra were recorded on a Bruker AVIIIHD 400 nanobay (101 MHz), Bruker AVIIIHD 500 nanobay (126 MHz) or Bruker AVII 500 with He cryoprobe (126 MHz) using broadband proton decoupling and internal deuterium lock. The chemical shift data for each signal are given as δ_{C} in units of parts per million (ppm) relative to the NMR solvent where $\delta_{\text{C}}(\text{CDCl}_3) = 77.16$ ppm, $\delta_{\text{C}}(\text{D}_6\text{-DMSO}) = 39.52$ ppm, $\delta_{\text{C}}((\text{CD}_3)_2\text{CO}) = 29.84$ ppm, and $\delta_{\text{C}}(\text{C}_6\text{D}_6) = 128.06$ ppm.

^{19}F NMR spectra were recorded on a Bruker AVIIIHD 400 nanobay (400 MHz), Bruker AVIIIHD 500 nanobay (500 MHz) using a deuterium internal lock. The chemical shift data for each signal are given as δ_{F} in units of parts per million (ppm). The multiplicity of each signal is indicated by: s (singlet); d (doublet); t (triplet); q (quartet) or m (multiplet). The number of protons (n) for a given resonance signal is indicated by $n\text{H}$. Coupling constants (J) are quoted in Hz and are recorded to the nearest 0.1 Hz. Identical proton coupling constants (J) are averaged in each spectrum and reported to the nearest 0.1 Hz. The coupling constants are determined by analysis using Bruker TopSpin software.

High-resolution mass spectra were acquired on a Bruker MicroTOF spectrometer from solutions of methanol, water or acetonitrile (ESI), or a Waters GCT TOF spectrometer with a temperature-programmed solids probe inlet (FI), operating in positive or negative mode.

Low-resolution mass spectra were recorded on a Waters LCT Premier spectrometer or Agilent 6120 Quadrupole LC/MS spectrometer (ESI). m/z values are reported in Daltons and followed by their percentage abundance in parentheses.

Infrared spectra were obtained from thin films on a NaCl plate, or from thin films or solid sample using a diamond ATR module as indicated. The spectra were recorded on a Bruker Tensor 27 spectrometer. Absorption maxima are reported in wavenumbers (cm^{-1}) and are classified as broad (br), strong (s), medium (m) or weak (w).

Specific optical rotations were measured using a Perkin Elmer 341 polarimeter or Schmidt Haensch Unipol polarimeter, in cells with a path length of 1 dm. The light source was maintained at 589 nm. The concentration (c) is expressed in g/100 mL (equivalent to g/0.1 dm³). Specific rotations are denoted $[\alpha]_D^T$ and are given in implied units of 10⁻¹ deg cm² g⁻¹ (where T = ambient temperature in °C).

Melting points on recrystallised samples were determined using a Kofler hot stage microscope and are uncorrected. The solvent of crystallisation is shown in parentheses.

Analytical thin layer chromatography (TLC) was carried out on Merck silica gel 60 F₂₅₄ aluminium-supported thin layer chromatography sheets. Visualisation was by absorption of UV light (λ_{\max} 254 nm), or thermal development after dipping in an aqueous solution of potassium permanganate, potassium carbonate and sodium hydroxide or for free amines a 1 g ninhydrin solution in 150 mL ethanol.

Column chromatography was performed manually or on a Biotage SP1 system using KP-Sil™ cartridges (gradient elution) or on Merck Geduran® silica gel 60 (40-63 μm).

Analytical HPLC was carried out on a PerkinElmer Flexar system with a Binary LC Pump and UV/VIS LC Detector. For determination of compound purity, a Dionex Acclaim® 120 column (C18, 5 μm, 120 Å, 4.6 × 150 mm) was employed, with a 10 minute gradient of 95% H₂O/5% MeCN + 0.1% TFA (Solvent A) to 95% MeCN/5% H₂O + 0.1% TFA (Solvent B), flow rate 1.0 mL/min and detection at 254 nm (unless stated otherwise). Samples were injected in DMSO, isopropanol or MeOH. The method was as described below:

Step length (min)	Elapsed time (min)	%A	%B
1	1	100	0
10	11	0	100
3	14	0	100
1	15	100	0
5	20	100	0

For instable compounds Method B was used, which involved the same gradient as method A, but without TFA.

Chiral HPLC For determination of enantio-purity a Daicel ChiralPak® (AD-H, 5 μm , 120 \AA , 4.6 \times 250 mm) was used with isocratic elution of isopropanol and hexane (50:50). Samples were injected in isopropanol. Chromera software was used to determine purity and enantiomeric excess from relative peak areas of UV/VIS absorbance at 254 nm.

Anhydrous solvents were obtained under the following conditions: anhydrous DMF and anhydrous MeOH were purchased from Sigma-Aldrich UK in SureSeal™ bottles and used without further purification; anhydrous THF, CH_2Cl_2 and Et_2O were dried over activated 3 \AA molecular sieves under an argon or nitrogen atmosphere (where stated, THF was distilled from sodium and benzophenone); Na_2CO_3 was degassed by bubbling a stream of nitrogen gas through the solution for several hours with sonication before use.

Chemicals were purchased from Acros UK, Sigma-Aldrich UK, Alfa Aesar UK, Apollo Scientific or Fisher UK. Where appropriate and if not stated otherwise, all non-aqueous reactions were performed in a flame-dried flask under an inert atmosphere of nitrogen or argon.

In vacuo refers to the use of a rotary evaporator attached to a diaphragm pump.

Brine refers to a saturated aqueous solution of sodium chloride.

Petroleum ether refers to the fraction boiling between 40-60 $^\circ\text{C}$ unless otherwise stated.

7.2 General procedures

General Procedure 1 for deprotection of *N*-benzyl protected amines.

To a solution of (*R*)-*tert*-butyl 3-(benzyl((*R*)-1-phenylethyl)amino)butanoate (1.98 g, 5.60 mmol, 1.0 eq) in H_2O (3.2 mL), glacial acetic acid (2.0 mL) and MeOH (80 mL) was added 20% $\text{Pd}(\text{OH})_2/\text{C}$ (800 mg, 1.14 mmol, 0.2 eq). The system was purged with nitrogen, and then hydrogen gas was added. The suspension was stirred for 15 h under an atmosphere of hydrogen at ambient temperature. The black suspension was filtered over Celite™, dried (MgSO_4), filtered and concentrated *in vacuo*.

General Procedure 2A for preparation of phthalimide protected amines.

A mixture of the requisite aniline/ THQ derivative (200 mg, 1.23 mmol, 1.0 eq), *N*-(3-bromopropyl)phthalimide (394 mg, 1.47 mmol, 1.2 eq), NaI (220 mg, 1.47 mmol, 1.2 eq) and K₂CO₃ (203 mg, 1.47 mmol, 1.2 eq) in DMF (1.0 mL) was heated at 80 °C for 48 h. After cooling to rt the reaction mixture was diluted with EtOAc (50 mL), washed with aq. K₂CO₃ (2 M, 3 × 50 mL), brine (50 mL), dried (MgSO₄), filtered and concentrated *in vacuo*.

General Procedure 2B for preparation of phthalimide protected amines.

A mixture of the requisite aniline/ THQ derivative (200 mg, 1.23 mmol, 1.0 eq), *N*-(3-bromopropyl)phthalimide (394 mg, 1.47 mmol, 1.2 eq) and K₂CO₃ (203 mg, 1.47 mmol, 1.2 eq) in DMF (1.0 mL) was heated at 80 °C for 20 h. After cooling to ambient temperature the reaction mixture was diluted with EtOAc (50 mL), washed with 2 M aq. K₂CO₃ (3 × 50 mL), brine (50 mL), dried (MgSO₄), filtered and concentrated *in vacuo*.

General Procedure 3 for phthalimide deprotection.

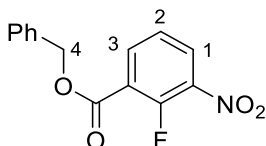
To a solution of the phthalimide (260 mg, 0.742 mmol, 1.0 eq) in CH₂Cl₂ (2 mL) and MeOH (2 mL) was added hydrazine monohydrate (65%, 144 μL, 149 mg, 3.02 mmol, 4.1 eq) and the reaction mixture heated at 70 °C for 3 h. After cooling to ambient temperature the reaction mixture was diluted with CH₂Cl₂ (20 mL), filtered through Celite® (eluent CH₂Cl₂), and concentrated *in vacuo*. Purification *via* acid base extraction was performed as follows: The crude reaction mixture was dissolved in EtOAc (10 mL) and extracted with sat aq. NH₄Cl (3 × 10 mL). The combined aqueous layers were basified with 2 M aq. NaOH and extracted with CH₂Cl₂ (3 × 25 mL). The combined organic extractions were washed with brine (20 mL), dried (Na₂SO₄), filtered, and concentrated *in vacuo*. Alternatively, a silica gel chromatography purification was performed, eluting with MeOH:CH₂Cl₂:Et₃N 10:100:1.

General Procedure 4 for coupling of carboxylic acids to amines

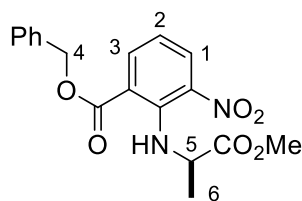
To a solution of the requisite carboxylic acid (40 mg, 0.19 mmol, 1.0 eq) and PyBOP (101 mg, 0.21 mmol, 1.1 eq) in DMF (1 mL) was added triethylamine (54 μL, 50 mg,

0.39 mmol, 2.0 eq). The reaction mixture was stirred for 10 min, then a solution of the requisite amine (0.21 mmol, 1.1 eq) in DMF (1 mL) was added and stirring continued for 19 h. The reaction mixture was diluted with EtOAc (50 mL), washed with H₂O (3 × 50 mL), brine (50 mL), dried (Mg₂SO₄), filtered, and concentrated *in vacuo*.

7.3.1 Chapter 2 Procedures

Benzyl 2-fluoro-3-nitrobenzoate (29)

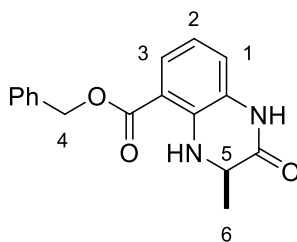
To a suspension of 2-fluoro-3-nitrobenzoic acid **28** (1.00 g, 5.40 mmol, 1.0 eq.), K_2CO_3 (1.12 g, 8.10 mmol, 1.5 eq) in DMF (12.5 mL) was added benzyl bromide (1.00 mL, 1.44 g, 8.10 mmol, 1.5 eq). The suspension was stirred for 3 h at 60 °C at which time TLC analysis indicated the reaction complete. After cooling to rt the yellow suspension was diluted with EtOAc (60 mL), washed with 2 M aq. K_2CO_3 (3 × 60 mL), brine (60 mL), dried ($MgSO_4$), filtered, and concentrated in *vacuo*. The yellow oil was purified by silica gel column chromatography eluting with a gradient of 10% to 20% EtOAc in petroleum ether to give a yellow oil **29** (1.37 g, 5.00 mmol, 93%): R_f 0.35 (petroleum ether: EtOAc 6:1); 1H NMR (400 MHz, $CDCl_3$): δ 8.30-8.15 (2H, m, C(1)*H* and C(3)*H*), 7.50-7.34 (6H, m, C(Bn)*H* and C(2)*H*), 5.43 (2H, s, C(4)*H*); ^{19}F NMR (377 MHz, $CDCl_3$): δ -116.2--116.3 (1F, m, *CF*); LRMS *m/z* (ES^+) 298 ($[M+Na]^+$, 100%). These data are in good agreement with the literature.⁵⁶

(R)-Benzyl 2-(1-methoxy-1-oxopropan-2-ylamino)-3-nitrobenzoate ((R)-30)

Benzyl 2-fluoro-3-nitrobenzoate **29** (1.20 g, 4.36 mmol, 1.0 eq) and D-alanine methyl ester hydrochloride (669 mg, 4.80 mmol, 1.1 eq), Cs_2CO_3 (3.13 g, 9.59 mmol, 2.2 eq) in toluene (70 mL) were stirred at 85 °C for 18 h. at which time TLC analysis indicated the reaction complete. After cooling to rt the orange slurry was diluted with EtOAc (150 mL), washed

with 2 M aq. K_2CO_3 (3 × 120 mL), brine (120 mL), dried ($MgSO_4$), filtered, and concentrated *in vacuo*. The orange oil was purified by silica gel chromatography eluting with 10% EtOAc in petroleum ether to give (*R*)-**30** as a yellow oil (1.40 g, 3.91 mmol, 90%): R_f 0.57 (petroleum ether: EtOAc 3:1); $[\alpha]_D^{25} -11.4$ (c 1.0 in $CHCl_3$) [Lit:⁵⁶ $[\alpha]_D = -10.9$ (c 1.0, $CHCl_3$)]; 1H NMR (400 MHz, $CDCl_3$): δ 8.78 (1H, br s, *NH*), 8.14 (1H, dd, J 8.0, 1.7, C(1)*H*), 7.96 (1H, dd, J 8.0 1.7, C(3)*H*), 7.48-7.32 (5H, m, C(Ar)*H*), 6.77 (1H, dd, J 8.0, 8.0, C(2)*H*), 5.37 (2H, s, C(4) H_2), 4.03 (1H, q, J 7.0, C(5)*H*), 3.69 (3H, s, CH_3), 1.43 (3H, d, J 7.0 Hz, C(6) H_3); LRMS m/z (ES^+) 359 ($[M+H]^+$, 100%). These data are in good agreement with the literature.⁵⁶

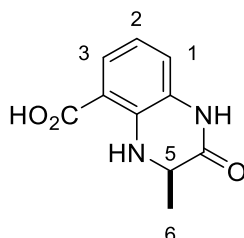
(*R*)-Benzyl 3-methyl-2-oxo-1,2,3,4-tetrahydroquinoxaline-5-carboxylate ((*R*)-31**)**



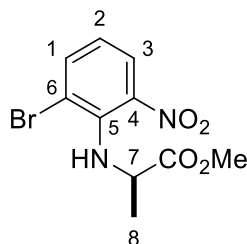
(*R*)-Benzyl 3-methyl-2-oxo-1,2,3,4-tetrahydroquinoxaline-5-carboxylate (*R*)-**30** (1.00 g, 2.79 mmol, 1.0 eq), Zn (4.57 g, 69.8 mmol, 25 eq), NH_4Cl (3.74 g, 69.8 mmol, 25 eq) suspended DMF (56 mL) were stirred for 25 h at ambient temperature. After this time the reaction was judged to be complete by TLC analysis. The suspension was diluted with EtOAc (100 mL) and filtered through Celite®. The filtrate was washed with brine (3 × 100 mL), dried ($MgSO_4$), filtered, and concentrated *in vacuo*. The residue was purified by silica gel chromatography eluting with 70% EtOAc in petroleum ether followed by 10% MeOH in CH_2Cl_2 to afford (*R*)-**31** as a colourless solid (0.68 g, 2.29 mmol, 82%): R_f 0.40 (petroleum ether: EtOAc 1:1); mp 197-200 °C (EtOAc), [Lit:⁵⁶ 199-200 °C (EtOAc)]; $[\alpha]_D^{25} = -50.3$ (c 1.0 in $CHCl_3$), [Lit:⁵⁶ $[\alpha]_D = -48.4$ (c 1.0, $CHCl_3$)]; 1H NMR (400 MHz, $(CD_3)_2CO$): δ 9.46 (1H, br s, *NH*), 7.65 (1H, br s, *NH*) 7.60 (1H, dd, J 8.1, 1.2, C(1)*H*), 7.55-7.51 (2H, m, C(Ar)*H*), 7.47-7.41 (2H, m, C(Ar)*H*), 7.41-7.36 (1H, m, C(Ar)*H*), 7.11-7.04 (1H,

m, C(3)H), 6.70 (1H, dd, J 8.1, 8.1 C(2)H), 5.38 (2H, s, C(4)H₂), 4.16 (1H, dq, J 6.9, 1.5, C(5)H), 1.44 (3H, d, J 6.9, C(6)H₃); LRMS m/z (ES⁺) 297 ([M+H⁺], 100%). These data are in good agreement with the literature.⁵⁶

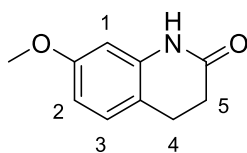
(R)-3-Methyl-2-oxo-1,2,3,4-tetrahydroquinoxaline-5-carboxylic acid ((R)-32)



(R)-Benzyl 3-methyl-2-oxo-1,2,3,4-tetrahydroquinoxaline-5-carboxylate (R)-31 (0.60 g, 2.05 mmol, 1.0 eq), 10% Pd/C (43 mg, 0.041 mmol, 0.02 eq) were suspended in EtOAc (150 mL). The system was purged with N₂, and then H₂ gas added. The suspension was stirred for 17 h under an atmosphere of hydrogen at ambient temperature. After this time the reaction was judged to be complete by TLC analysis. The suspension was diluted with MeOH (50 mL), filtered through Celite® and rinsed with MeOH. The filtrate was concentrated *in vacuo* to give (R)-32 as a yellow solid (0.42 g, 2.04 mmol, 99%), which was used without further purification: R_f 0.45 (EtOAc: AcOH 99:1); mp 230 °C dec. (EtOAc), [Lit:⁵⁶ 230 °C dec (EtOAc)]; [α]_D²⁰ = -121.4 (c 0.5 in MeOH) [Lit:⁵⁶ [α]_D = -124.6 (c 0.5, MeOH)]; ¹H NMR (400 MHz, MeOD): δ 7.58 (1H, dd, J 8.1, 1.1, C(1)H), 6.92 (1H, dd, J 8.1, 1.1, C(3)H), 6.66 (1H, dd, J 8.1, 8.1, C(2)H), 4.07 (1H, q, J 6.7, C(4)H), 1.40 (3H, d, J 6.7, C(5)H); LRMS m/z (ES⁻) 205 ([M-H⁻], 100%). These data are in good agreement with the literature.⁵⁶

Methyl (2-bromo-6-nitrophenyl)-D-alaninate ((R)-34)

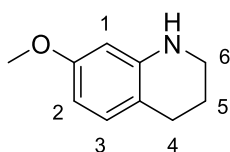
3-Bromo-2-fluoro-3-nitrobenzoate **33** (1.00 g, 4.54 mmol, 1.0 eq) and D-alanine methyl ester hydrochloride (700 mg, 5.02 mmol, 1.1 eq), DIPEA (1.75 g, 13.5 mmol, 3.0 eq) dissolved in DMF (25 mL) was stirred at 70 °C for 23 h. After this time the reaction was judged to be complete by NMR analysis. After cooling to rt the solution was diluted with EtOAc (50 mL), washed with brine (2 × 50 mL), 0.5 M aq. LiCl (2 × 50 mL), brine (50 mL), dried (MgSO₄), filtered, and concentrated *in vacuo* to give (R)-**34** as a yellow oil (1.36 g, 4.49 mmol, 99%), which was used without further purification: *R_f* 0.48 (petroleum ether: EtOAc 4:1); $[\alpha]_D^{25}$ -354.4 (*c* 1.0 in CHCl₃); ν_{\max} (thin film)/cm⁻¹ 3353 (w) (N-H), 2954 (w), 1740 (s) (C=O), 1669 (s) (C=O), 1557 (m), 1480 (s), 1451 (m), 1343 (m), 1135 (m), 743 (m); ¹H NMR (400 MHz, CDCl₃): δ 7.95 (1H, dd, *J* 8.0, 1.5, C(3)*H*), 7.75 (1H, dd, *J* 8.0, 1.5, C(1)*H*), 6.89, (1H, dd, *J* 8.0, 8.0, C(2)*H*), 6.64 (1H, d, *J* 10.5, C(5)*NH*), 4.61 (1H, dq, *J* 10.5, 7.1, C(7)*H*), 3.67 (3H, s, CO₂CH₃), 1.53 (3H, d, *J* 7.1, C(8)*H*₃); ¹³C NMR (126 MHz, CDCl₃): δ 173.9 (CO₂Me), 142.6 (C(5)), 141.7 (C(4)), 139.3 (C(1)), 125.4 C(3), 121.3 (C(2)), 116.8 (C(6)), 54.7 (C(7)), 52.5 (CO₂CH₃), 19.2 (C(8)); GC-HRMS *m/z* (CI⁺) [Found: (M+H)⁺ 302.9972, C₁₀H₁₁⁷⁹BrN₂O₄ requires 302.9972], RP-HPLC: Method A: Retention time 13.32 min, purity 96.0%.

7-Methoxy-3,4-dihydroquinolin-2(1H)-one (38)

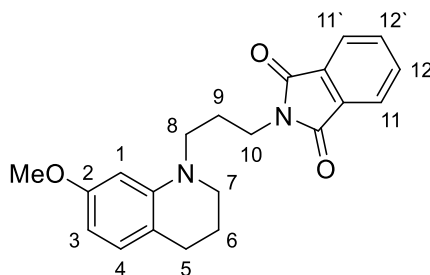
Iodomethane (1.89 mL, 4.31 g, 30.5 mmol, 1.1 eq) was added dropwise to 7-hydroxy-3,4-dihydroquinolin-2(1H)-one **37** (4.50 g, 27.5 mmol, 1.0 eq), K₂CO₃ (7.60 g, 55.0 mmol,

2.0 eq) suspended in DMF (45 mL). The slurry was stirred at 60 °C for 17 h at which time TLC analysis indicated the reaction complete. After cooling to rt the colourless suspension was diluted with EtOAc (500 mL), washed with 2 M aq. K₂CO₃ (3 × 200 mL), brine (200 mL), dried (MgSO₄), filtered, and concentrated *in vacuo*. The crude material was crystallised from EtOH (50 mL) to afford **38** as a colourless solid (2.45 g, 13.8 mmol, 50%): R_f: 0.27 (petroleum ether: EtOAc 1:1); mp 144-145 °C (EtOH) [Lit. 142-147 °C]; ¹H NMR (400 MHz, CDCl₃): δ 8.77 (1H, s, NH), 7.05 (1H, d *J* 8.3 C(3)*H*), 6.52 (1H, dd, *J* 8.3, 2.6, C(2)*H*), 6.37 (1H, d, *J* 2.5, C(1)*H*), 3.78 (3H, s, OCH₃), 2.93-2.86 (2H, m, C(4)*H*), 2.65-2.59 (2H, m, C(5)*H*₂); LRMS *m/z* (ES⁺) 178 ([M+H]⁺, 100%). These data are in accordance with the literature.¹⁷⁷

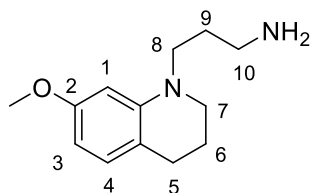
7-Methoxy-1,2,3,4-tetrahydroquinoline (39)



LiAlH₄ in THF (1 M, 15.6 mL, 15.6 mmol, 1.2 eq) was added over 15 min to 7-methoxy-3,4-dihydroquinolin-2(1*H*)-one **38** (2.30 g, 13.0 mmol, 1.0 eq) dissolved in THF (150 mL) at 0 °C. The solution was allowed to warm up to ambient temperature and stirred for 4 h at which time TLC analysis indicated the reaction complete. The green suspension was quenched with EtOAc (18 mL) followed by H₂O (4 mL). The suspension was dried (MgSO₄), filtered through Celite®, and concentrated *in vacuo* to afford **39** as a yellow oil (2.12 g), which was used without further purification: R_f: 0.59 (petroleum ether: EtOAc 2:1); ¹H NMR (400 MHz, CDCl₃): δ 6.85 (1H, d *J* 8.2 Hz, C(3)*H*), 6.20 (1H, dd, *J* 8.2, 2.5, C(2)*H*), 6.04 (1H, d, *J* 2.5, C(1)*H*), 4.00-3.46 (4H, m, OCH₃ and NH), 3.28 (2H, t, *J* 5.5, C(6)*H*₂), 2.70 (2H, t, *J* 6.4, C(4)*H*₂), 1.98-1.86 (2H, m, C(5)*H*₂); LRMS *m/z* (ES⁺) 164 ([M+H]⁺, 100%). These data are in accordance with the literature values.¹⁷⁸

2-(3-(7-Methoxy-3,4-dihydroquinolin-1(2H)-yl)propyl)isoindoline-1,3-dione (40)

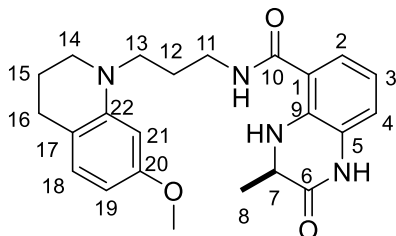
7-Methoxy-1,2,3,4-tetrahydroquinoline **39** (1.50 g, 9.19 mmol, 1.0 eq) was reacted according to general procedure 2B. Purification by silica gel chromatography, eluting with a gradient of 5% to 20% EtOAc in petroleum ether, afforded **40** as a yellow oil (1.93 g, 5.51 mmol, 60%): R_f : 0.49 (petroleum ether: EtOAc 3:1); $^1\text{H NMR}$ (400 MHz, CDCl_3): δ 7.84 (2H, m, C(12) H and C(12') H), 7.72 (2H, m, C(11) H and C(11') H), 6.83 (1H, d, J 8.7, C(4) H), 6.18-6.10 (2H, m, C(1) H and C(3) H), 3.75 (2H, t, J 7.2, C(10) H_2), 3.73 (3H, s, OCH_3), 3.31 (2H, t, J 7.4, C(8) H_2), 3.26 (2H, t, J 5.6, C(7) H_2), 2.67 (2H, t, J 6.3, C(5) H_2), 2.07-1.86 (4H, m, C(6) H_2 and C(9) H_2); LRMS m/z (ES^+) 351 ($[\text{M}+\text{H}]^+$, 100%). These data are in good agreement with the literature.⁵⁷

3-(7-Methoxy-3,4-dihydroquinolin-1(2H)-yl)propan-1-amine (41)

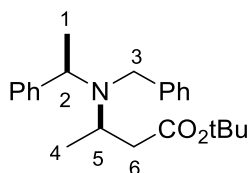
2-(3-(7-Methoxy-3,4-dihydroquinolin-1(2H)-yl)propyl)isoindoline-1,3-dione (**40**) (1.50 g, 4.28 mmol, 1.0 eq), was reacted according to general procedure 3. The crude material was purified *via* an acid base extraction to yield **41** as a yellow oil (850 mg, 4.12 mmol, 96%): R_f : 0.25 (MeOH: CH_2Cl_2 1:5); $^1\text{H NMR}$ (400 MHz, MeOD): δ 6.76 (1H, d, J 8.2, C(4) H), 6.14 (1H, d, J 2.3, C(1) H), 6.09 (1H, d, J 8.2, 2.3, C(3) H), 3.71 (3H, s, OCH_3), 3.30-3.22 (4H, m, C(7) H_2 and C(8) H_2), 2.70 (2H, t, J 7.3, C(5) H_2), 2.64 (2H, t, J 6.4, C(10) H_2) 1.93-1.85 (2H, m,

C(6) H_2), 1.75 (2H, m, C(9) H_2); LRMS m/z (ES⁺) 221 ([M+H]⁺, 100%). These data are in accordance with the literature.⁵⁶

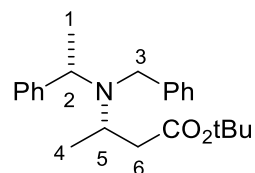
(*R*)-*N*-(3-(7-Methoxy-3,4-dihydroquinolin-1(2*H*)-yl)propyl)-3-methyl-2-oxo-1,2,3,4-tetrahydroquinoxaline-5-carboxamide (*(R)*-12)



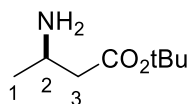
[(*R*)-3-Methyl-2-oxo-1,2,3,4-tetrahydroquinoxaline-5-carboxylic acid] (*(R)*-32 (30 mg, 0.145 mmol, 1.0 eq) and [3-(7-methoxy-3,4-dihydroquinolin-1(2*H*)-yl)propan-1-amine] **41** (38.5 mg, 0.175 mmol, 1.2 eq) were reacted according to general procedure 4 for 15 h. After this time the reaction was judged to be complete by TLC analysis. The crude material was purified by silica gel chromatography, eluting with a gradient of 50% to 80% EtOAc in petroleum ether, to give (*R*)-12 as a pale yellow solid (27 mg, 0.066 mmol, 46%): R_f 0.32 (EtOAc: petroleum ether 1:1); mp 99-101 °C (acetone), [Lit:⁵⁶ 101-103°C (acetone)]; $[\alpha]_D^{25} - 23.3$ (c 0.1 in $(CH_3)_2CO$), [Lit:⁵⁷ $[\alpha]_D - 23.2$ (c 0.5 in $(CH_3)_2CO$)]; ¹H NMR (400 MHz; $(CD_3)_2CO$): δ 9.32 (1H, br s, C(5)NH), 8.00 (1H, br s, C(9)NH), 7.81 (1H, br s, C(1)NH), 7.30 (1H, dd, J 7.9, 1.0, C(2)H), 6.95 (1H, d, J 7.9, 1.0, C(4)H), 6.75 (1H, d, J 8.1, C(18)H), 6.64 (1H, dd, J 7.9, 7.9, C(3)H), 6.16 (1H, d, J 2.5, C(21)H), 6.07 (1H, dd, J 8.1, 2.5, C(19)H), 4.00 (1H, qd, J 6.6, 1.5, C(7)H), 3.65 (3H, s, OCH₃), 3.50-3.43 (2H, m, C(11) H_2), 3.40-3.34 (2H, m, C(13) H_2), 3.31-3.26 (2H, m, C(14) H_2), 2.66-2.60 (2H, m, C(16) H_2), 1.96-1.84 (4H, m, C(12) H_2 and C(15) H_2), 1.37 (3H, d, J 6.6, C(8)CH₃); LRMS m/z (ES⁺) 409 ([M+H]⁺, 100%), RP-HPLC: Method A: Retention time 10.40 min, purity 95.5%. These data are in good agreement with the literature.⁵⁶

(R)-tert-Butyl 3-(benzyl((R)-1-phenylethyl)amino)butanoate ((R/R)-44)

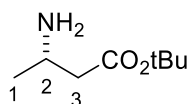
(R)-N-Benzyl-1-phenylethanamine (*R*)-**43** (3.72 g, 16.8 mmol, 1.5 eq) in dry THF (20 mL) was cooled to -78 °C. To the colourless solution *n*-BuLi in hexane (2.5 M, 7.0 mL, 17.5 mmol, 1.6 eq) was added slowly, over a period of 15 min, at -78 °C. After the addition was complete the pink solution was stirred for another 30 min at -78 °C. After this time, *tert*-butyl crotonate **42** (1.56 g, 11.0 mmol, 1.0 eq) in dry THF (15 mL) was added dropwise, over a period of 45 min, at -78 °C and stirred for further 3 h. After this time the reaction was judged to be complete by TLC analysis. The reaction solution was quenched with sat. aq. NH_4Cl (10 mL), and warmed to ambient temperature. The solvent was removed *in vacuo*, and the residue was taken up in 10% *v/v* aq. citric acid (50 mL), and extracted with CH_2Cl_2 (3 \times 50 mL). The combined organic extracts were washed with sat. aq. NaHCO_3 (100 mL), brine (100 mL), dried (MgSO_4), filtered, and concentrated *in vacuo*. The crude material was purified by silica gel chromatography eluting with a gradient from 1% to 10% of Et_2O in petroleum ether to yield (*R/R*)-**44** as a pale yellow oil (3.27 g, 9.25 mmol, 84%): R_f : 0.61 (petroleum ether: EtOAc 10:1); $[\alpha]_D^{25} = -4.9$ (*c* 1.1, CHCl_3) [Lit:⁷⁹ $[\alpha]_D^{25} = -5.2$ (*c* 1.1, CHCl_3)]; $^1\text{H NMR}$ (400 MHz, CDCl_3): δ 7.43-7.16 (10H, m, C(Ar)*H*), 3.88 (1H, q, *J* 6.9, C(2)*H*), 3.75 (1H, d, *J* 15.0, C(3)*H*_A*H*_B), 3.60 (1H, d, *J* 15.0, C(3)*H*_B*H*_A), 3.46-3.36 (1H, m, C(5)*H*), 2.24 (1H, dd, *J* 14.1, 4.7, C(6)*H*_A*H*_B), 2.24 (1H, dd, *J* 14.1, 9.2, C(6)*H*_B*H*_A), 1.38 (9H, s, C(CH_3)₃), 1.32 (3H, d, *J* 6.9, C(1)*H*₃), 1.10 (3H, d, *J* 6.7, C(4)*H*₃); LRMS *m/z* (ES^+) 354 ($[\text{M}+\text{H}]^+$, 100%). These data are in accordance with the literature.⁷⁹

(*S*)-*tert*-Butyl 3-(benzyl(*S*)-1-phenylethylamino)butanoate ((*S/S*)-44)

(*S*)-*tert*-Butyl 3-(benzyl(*S*)-1-phenylethylamino)butanoate (*S/S*)-**44** was synthesised from **42**, in a manner similar to that used for (*R/R*)-**44** yielding a colourless oil (2.67 g, 7.55 mmol, 69%); R_f : 0.68 (petroleum ether: EtOAc 10:1); $[\alpha]_D^{25} = +3.9$ (c 1.1, CHCl_3), [Lit:⁷⁹ $[\alpha]_D^{25} = +5.1$ (c 1.1, CHCl_3)]; other physical and spectroscopic properties are identical to those of (*R/R*)-**44**. These data are in accordance with the literature.⁷⁹

(*R*)-*tert*-Butyl 3-aminobutanoate ((*R*)-45)

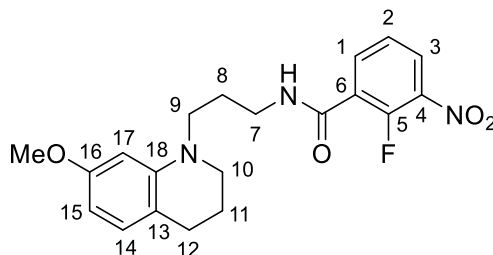
(*R*)-*tert*-Butyl 3-(benzyl(*R*)-1-phenylethylamino)butanoate (*R/R*)-**44** (1.98 g, 5.60 mmol, 1.0 eq) was reacted according to general procedure 1 and (*R*)-**45** was isolated as a yellow oil containing 1.9 eq. acetic acid (1.40 g, 5.12 mmol, 91%): An aliquot was purified for further characterisation: R_f : 0.22 (EtOAc: Et_3N 10:1); $[\alpha]_D^{25} = -18.6$ (c 0.5, CHCl_3), [Lit:⁷⁹ $[\alpha]_D^{25} = -22.2$ (c 0.5, CHCl_3)]; $^1\text{H NMR}$ (400 MHz, CDCl_3) δ 3.38-3.27 (1H, m, C(2)*H*), 2.32 (1H, dd, J 15.4, 4.7, C(3)*H*_A*H*_B), 2.20 (1H, dd, J 15.4, 8.5, C(3)*H*_B*H*_A), 1.45 (9H, s, C(CH_3)₃), 1.10 (3H, d, J 6.5, C(1)*H*₃); LRMS m/z (ES^+) 160 ($[\text{M}+\text{H}]^+$, 100%). These data are in accordance with the literature.⁷⁹

(*S*)-*tert*-Butyl 3-aminobutanoate ((*S*)-45)

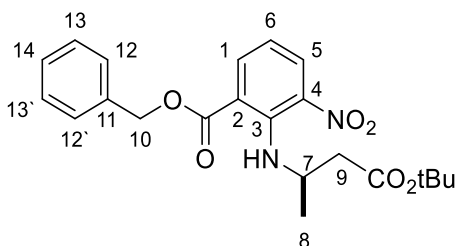
(*S*)-*tert*-Butyl 3-aminobutanoate (*S*)-**45** was synthesised from (*S/S*)-**44**, in a manner similar to that used for (*R*)-**45** yielding a yellow oil (706 mg, 4.43 mmol, 79%); R_f 0.22 (EtOAc: Et_3N 10:1); $[\alpha]_D^{25} = +20.2$ (c 0.5, CHCl_3), [Lit:⁷⁹ $[\alpha]_D^{25} = +21.4$ (c 0.6 CHCl_3)]; other

physical and spectroscopic properties are identical to those as (*R*)-**45**. These data are in accordance with the literature.⁷⁹

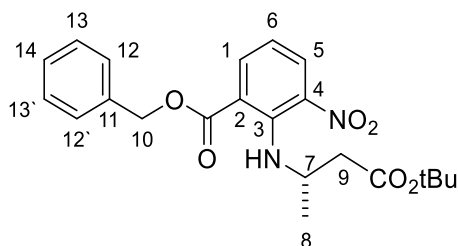
2-Fluoro-*N*-(3-(7-methoxy-3,4-dihydroquinolin-1(2*H*)-yl)propyl)-3-nitrobenzamide (46)



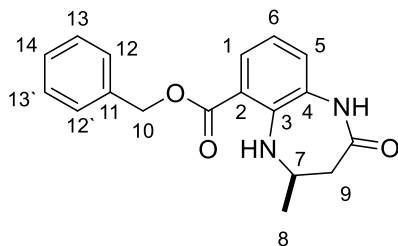
2-Fluoro-3-nitrobenzoic acid **28** (588 mg, 3.18 mmol, 1.0 eq) and 3-(7-methoxy-3,4-dihydroquinolin-1(2*H*)-yl)propan-1-amine **41** (400 mg, 3.18 mmol, 1.0 eq) were reacted according to general procedure 4 for 17 h. After this time the reaction was judged to be complete by TLC analysis. The crude material was purified by silica gel chromatography, eluting with a gradient of 40% to 80% EtOAc in petroleum ether, to afford **46** as a red oil (398 mg, 0.118 mmol, 61%): R_f : 0.45 (petroleum ether: EtOAc 1:1); ν_{\max} (thin film)/ cm^{-1} 3325 (m) (N-H), 2947 (w), 2840 (w), 1642 (s) (C=O), 1611 (s), 1525 (s), 1508 (s), 1345 (m), 1303 (m), 1241 (s), 1171 (s), 817 (s), 743 (s); $^1\text{H NMR}$ (500 MHz; CDCl_3): δ 8.32-8.25 (1H, m, C(1)*H*), 8.15-8.09 (1H, m, C(3)*H*), 7.39 (1H, dd, J 7.9, 7.9, C(2)*H*), 6.83 (1H, d, J 8.0, C(14)*H*), 6.78 (1H, br s, C(7)*NH*), 6.14-6.11 (2H, m, C(15)*H* and C(17)*H*), 3.73 (3H, s, OCH_3), 3.60-3.50 (2H, m, C(7)*H*₂), 3.35 (2H, t, J 7.0, C(9)*H*₂), 3.28-3.24 (2H, m, C(10)*H*₂), 2.67 (2H, t, J 6.4, C(12)*H*), 1.96 (2H, tt, J 7.0, 7.0, C(8)*H*₂), 1.94-1.88 (2H, m, C(11)*H*₂); $^{19}\text{F NMR}$ (471 MHz; CDCl_3): δ -122.0- -122.1 (1F, m, *CF*); $^{13}\text{C NMR}$ (126 MHz; CDCl_3): δ 161.4 (d, J 2.5, (NHCO), 159.1 (C(16)), 153.1 (d, J 264, C(5)), 145.8 (C(18)), 137.9 (d, J 10.4, C(6)), 137.2 (d, J 2.8, C(1)), 129.6 (C(14)), 128.7 (d, J 1.8, C(3)), 124.7 (d, J 4.7, C(2)), 124.3 (d, J 12.1, C(4)), 115.3 (C(13)), 99.9 (C(17)), 97.6 (C(15)), 55.1 (OCH_3), 49.6 (C(10)), 49.2 (C(9)), 38.6 (C(7)), 27.2 (C(12)), 26.3 (C(8)), 22.3 (C(11)); LRMS m/z (ES^+) 388 ($[\text{M}+\text{H}]^+$, 100%); HRMS m/z (ES^+) [Found: ($\text{M}+\text{H}$)⁺ 388.1667, $\text{C}_{20}\text{H}_{23}\text{N}_3\text{O}_4\text{F}^+$ requires 388.1667].

(R)-Benzyl 2-(4-*tert*-butoxy-4-oxobutan-2-ylamino)-3-nitrobenzoate ((R)-48)

Benzyl 2-fluoro-3-nitrobenzoate **29** (1.28 g, 4.66 mmol, 1.0 eq) was added to (*R*)-*tert*-butyl 3-aminobutanoate $\times 1.9$ AcOH (*R*)-**45** (1.40 g, 5.12 mmol, 1.1 eq), Cs₂CO₃ (6.07 g, 18.6 mmol, 4.0 eq) suspended in toluene (80 mL). The yellow suspension was stirred at 85 °C for 14 h at which time TLC analysis indicated the reaction complete. Upon cooling to rt the reaction mixture was diluted with EtOAc (240 mL), washed with 2 M aq. K₂CO₃ (3 \times 150 mL), dried (Na₂SO₄), filtered, and concentrated *in vacuo* to obtain a yellow oil. The crude material was purified by silica gel chromatography, eluting with a gradient of 10% to 20% EtOAc in petroleum ether, to yield (*R*)-**48** as a yellow oil (1.87 g, 4.51 mmol, 97%): R_f 0.34 (petroleum ether: EtOAc 10:1); $[\alpha]_D^{25} = +64.4$ (*c* 1.0, CHCl₃); ν_{\max} (thin film)/cm⁻¹ 3308 (w) (N-H), 2978 (m) (C-H), 1724 (s) (C=O), 1691 (s) (C=O), 1604 (m), 1586 (m), 1530 (m) (N-O), 1499 (m), 1455 (m), 1367 (m) (N-O), 1348 (m), 1248 (s); ¹H NMR (500 MHz, CDCl₃) δ 8.19 (1H, d, *J* 9.6, NH), 8.04 (1H, dd, *J* 8.0, 1.6, C(1)*H*), 7.94 (1H, dd, *J* 8.0, 1.6, C(5)*H*), 7.46-7.33 (5H, m, C(Ar)*H*), 6.70 (1H, dd, *J* 8.0, 8.0, C(6)*H*), 5.35 (2H, s, C(10)*H*₂), 3.63 (1H, m, C(7)*H*), 2.41 (1H, dd, *J* 15.0, 6.2, C(9)*H*_A*H*_B), 2.39 (1H, dd, *J* 15.0, 6.2, C(9)*H*_A*H*_B), 1.33 (9H, s, C(CH₃)₃), 1.25 (3H, d, *J* 6.2, C(8)*H*₃); ¹³C NMR (126 MHz, CDCl₃) δ 170.0 (CO₂*t*Bu), 167.1 (CO₂Bn), 144.6 (C(3)), 138.4 (C(4)), 136.8 (C(1)), 135.4 (C(11)), 131.2 (C(5)), 128.7(C(13) and C(13')), 128.6 (C(14)), 128.4 (C(12) and C(12')), 118.3 (C(2)), 115.5 (C(6)), 80.9 (C(CH₃)₃), 67.2 (C(10)), 50.0 (C(7)), 43.7 (C(9)), 27.9 (C(CH₃)₃), 20.9 (C(8)); LRMS *m/z* (ES⁺) 415 ([M+H]⁺, 100%); HRMS *m/z* (ES⁺) [Found: (M+H)⁺ 415.1851, C₂₂H₂₇O₆N₂⁺, requires 415.1864]. RP-HPLC: Method A: Retention time 15.49 min, purity 97.8%.

(S)-Benzyl 2-(4-*tert*-butoxy-4-oxobutan-2-ylamino)-3-nitrobenzoate ((S)-48)

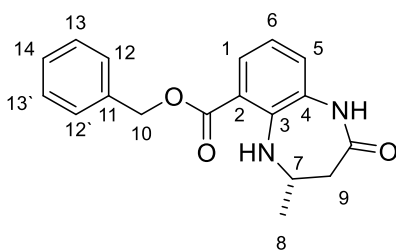
(*S*)-Benzyl 2-(4-*tert*-butoxy-4-oxobutan-2-ylamino)-3-nitrobenzoate was synthesised from **29** and (*S*)-**45**, in a manner similar to that used for (*R*)-**48** yielding (*S*)-**48** as a yellow oil (790 mg, 1.91 mmol, 83%): $[\alpha]_D^{25} = -65.6$ (*c* 0.5, CHCl₃), other physical and spectroscopic properties are identical to those as (*R*)-**48**. RP-HPLC: Method A: Retention time 15.49 min, purity 99.4%.

(R)-Benzyl 4-methyl-2-oxo-2,3,4,5-tetrahydro-1H-benzo[*b*][1,4]diazepine-6-carboxylate ((R)-51)

(*R*)-Benzyl 2-(4-*tert*-butoxy-4-oxobutan-2-ylamino)-3-nitrobenzoate (*R*)-**48** (1.10 g, 2.65 mmol, 1.0 eq) dissolved in trifluoroacetic acid (11 mL) and CH₂Cl₂ (11 mL) was stirred for 2 h at ambient temperature. After this time the reaction was judged to be complete by TLC analysis. The solvent was concentrated *in vacuo*, and the crude material (*R*)-**49** was purified by silica gel chromatography, eluting with 50% ethyl acetate in petroleum ether, to give a brown oil (1.04 g), which still contained some minor impurities. An aliquot of the crude material (*R*)-**49** (660 mg), Zn (2.49 g, 38.1 mmol, 25 eq), NH₄Cl (2.03 g, 38.1 mmol, 25 eq) were suspended in DMF (30 mL), and stirred for 15 h at ambient temperature. After this time the reaction was judged to be complete by TLC analysis. The suspension was filtered through Celite®, and rinsed with DMF (3 mL). The

pH of the filtrate (*R*)-**50** was adjusted to 9 with Et₃N (1.5 mL). PyBOP (791 mg, 1.52 mmol, 1.0 eq) was added, and stirred for 16 h at ambient temperature. The reaction mixture was diluted with EtOAc (250 mL), washed with brine (3 × 200 mL), dried (MgSO₄), filtered, and concentrated *in vacuo*. The crude material was purified by silica gel chromatography, eluting with a gradient of 30% to 50% EtOAc in petroleum ether, to give (*R*)-**51** as a colourless solid (350 mg, 1.13 mmol, 67% over 3 steps): R_f 0.44 (petroleum ether: EtOAc 11:1); mp 133-134 °C (CHCl₃), [α]_D²⁵ = -44.2 (*c* 1.1, CHCl₃); ν_{max} (thin film)/cm⁻¹ 3309 (w) (N-H), 3219 (w) (N-H), 2961 (w) (C-H), 1665 (s) (C=O), 1531 (m), 1497 (m), 1471 (m), 1449 (m), 1265 (s), 1233 (s); ¹H NMR (500 MHz, CDCl₃) δ 8.42 (1H, br s, (CO)NH), 8.00 (1H, br s, (C(3)NH), 7.83 (1H, dd, *J* 7.9, 1.6, (C(5)H), 7.45-7.32 (5H, m, C(12)H, C(12')H, C(13)H, C(13')H and C(14)H), 7.04 (1H, dd, *J* 7.9, 1.6, (C(1)H), 6.70 (1H, t, *J* 7.9, (C(6)H), 5.32 (2H, s, C(10)H₂), 4.11-4.03 (1H, m, C(7)H), 2.68 (1H, dd, *J* 14.1, 2.6, C(9)H_AH_B), 2.58 (1H, dd, *J* 14.1, 8.6, C(9)H_BH_A), 1.39 (3H, d, *J* 6.4, (C(8)H₃); ¹³C NMR (126 MHz, CDCl₃) δ 173.0 (CONH), 168.3 (CO₂), 142.9(C(3)), 135.8 (C(11)), 128.61 (C(13) and C(13')) or C(12) and C(12')), 128.57 (C(5)), 128.3 (C(14)), 128.0 (C(13) and C(13')) or C(12) and C(12')), 127.2 (C(1)), 126.1 (C(4)), 116.9 (C(6)), 114.8 (C(2)), 66.7 (C(10)), 51.4 (C(7)), 42.5 (C(9)), 23.9 (C(8)); LRMS *m/z* (ES⁺) 311 ([M+H]⁺, 100%); HRMS *m/z* (ES⁺) [Found: (M+H)⁺ 311.1387, C₁₈H₁₉O₃N₂⁺ requires 311.1390]. RP-HPLC: Method A: Retention time 12.47 min, purity 99.1%.

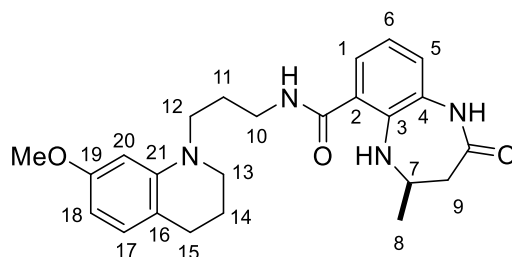
(*S*)-Benzyl 4-methyl-2-oxo-2,3,4,5-tetrahydro-1H-benzo[*b*][1,4]diazepine-6-carboxylate ((*S*)-51**)**



(*S*)-Benzyl 2-(4-*tert*-butoxy-4-oxobutan-2-ylamino)-3-nitrobenzoate (*S*)-**48** (500 mg, 1.21 mmol, 1.0 eq) dissolved in trifluoroacetic acid (5 mL) and dichloromethane (5 mL)

was stirred for 2.5 h at ambient temperature. After this time the reaction was judged to be complete by TLC analysis. The trifluoroacetic acid was removed by azeotropic distillation with cyclohexane to afford a yellow/brown oil (*S*)-**49**, which was used without further purification. The brown oil, Zn (1.98 g, 30.3 mmol, 25 eq), NH₄Cl (1.62 g, 30.3 mmol, 25 eq) suspended in DMF (24 mL) for 16 h at ambient temperature. After this time the reaction was judged to be complete by TLC analysis. The suspension was filtered through Celite®, and rinsed with DMF (3 mL). The pH of the filtrate (*S*)-**50** was adjusted to 9 with Et₃N (1.5 mL). PyBOP (630 mg, 1.21 mmol, 1.0 eq) was added, and stirred for 15 h at ambient temperature. After this time the reaction was judged to be complete by TLC analysis. The reaction mixture was diluted with EtOAc (200 mL), washed with brine (3 × 180 mL), dried (MgSO₄) and concentrated *in vacuo*. The crude material was purified by silica gel chromatography, eluting with a gradient of 30% to 50% EtOAc in petroleum ether, to obtain (*S*)-**51** as a colourless solid (245 mg, 0.789 mmol, 65% over 3 steps): [α]_D²⁵ = +38.2 (*c* 0.5, CHCl₃); other physical and spectroscopic properties are identical to those as (*R*)-**51**. RP-HPLC: Method A: Retention time 12.45 min, purity 99.5%.

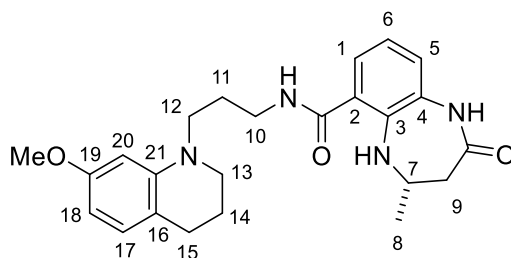
(*R*)-3-(7-Methoxy-3,4-dihydroquinolin-1(2*H*)-yl)propyl 4-methyl-2-oxo-2,3,4,5-tetrahydro-1*H*-benzo[*b*][1,4]diazepine-6-carboxylate ((*R*)-26**)**



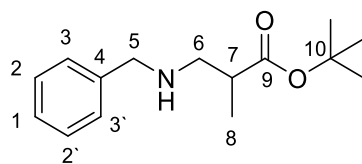
(*R*)-Benzyl 4-methyl-2-oxo-2,3,4,5-tetrahydro-1*H*-benzo[*b*][1,4]-diazepine-6-carboxylate (*R*)-**51** (90 mg, 0.290 mmol, 1.0 eq) in MeOH (10 mL) was added 10% Pd/C (15.4 mg, 0.029 mmol, 0.1 eq). The system was purged with nitrogen, and then hydrogen gas added. The suspension was stirred for 16 h under an atmosphere of hydrogen at ambient temperature. The black suspension was filtered through Celite® and rinsed with MeOH

(2 mL). The filtrate was dried (MgSO_4), filtered, and concentrated *in vacuo* to give a beige solid (63 mg). A solution of crude (*R*)-4-methyl-2-oxo-2,3,4,5-tetrahydro-1*H*-benzo[*b*]-[1,4]diazepine-6-carboxylic acid (*R*)-**52** (63 mg), PyBOP (149 mg, 0.286 mmol, 1.0 eq) and Et_3N (79 μL , 60 mg, 0.572 mmol, 2.0 eq) in DMF (5 mL) was stirred for 15 min at rt. After this time a solution of 3-(7-methoxy-3,4-dihydroquinolin-1(2*H*)-yl)propan-1-amine **41** (69 mg, 0.315 mmol, 1.1 eq) in DMF (0.5 mL) was added and stirred for 5 h at ambient temperature. After this time the reaction was judged to be complete by TLC analysis. The solvent was removed, and the crude material was purified by a silica gel chromatography, eluting with a gradient from 80% to 100% ethyl acetate in petroleum ether, to afford (*R*)-**26** as a colourless solid (82 mg, 0.194 mmol, 68%): R_f 0.41 (EtOAc: petroleum ether 3:1); mp 157-158 °C (CHCl_3), $[\alpha]_D^{25} = -21.0$ (c 0.5, CHCl_3); ν_{max} (thin film)/ cm^{-1} 3310 (w) (N-H), 3213 (w) (N-H), 3069 (w) (N-H), 2941 (m), 1738 (s) (C=O), 1692 (s) (C=O), 1613 (s), 1542 (m), 1508 (s), 1239 (s), 1167 (s); ^1H NMR (500 MHz, CDCl_3) δ 7.77 (1H, br s, C(4)NH), 7.30 (1H, br s, C(3)NH), 7.04 (1H, dd, J 7.8, 1.4, C(1)H), 6.91 (1H, d, J 7.8, (C5)H), 6.86 (1H, d, J 7.8, (C17)H), 6.68 (1H, dd, J 7.8, 7.8, C(6)H), 6.41 (1H, t, J 5.5, C(10)NH), 6.20-6.13 (2H, m, C(18)H and C(20)H), 4.07-3.96 (1H, m, (C(7)H), 3.74 (3H, s, OCH_3), 3.56-3.44 (2H, m, C(10)H₂) 3.36 (2H, t, J 6.9 Hz, C(12)H₂), 3.25 (2H, dd, J 5.6, 5.6, C(13)H), 2.70-2.60 (3H, m, C(15)H and C(9)H_AH_B), 2.48 (1H, dd, J 14.0, 8.0, C(9)H_AH_B), 1.98-1.85 (4H, m, C(11)H₂ and C(14)H₂), 1.33 (3H, d, J 6.3, (C8)H₃); ^{13}C NMR (126 MHz, CDCl_3) δ 172.7 (C9(CONH)), 169.5 (C2(CONH)), 159.2 (C(19)), 145.9 (C(21)), 140.4 (C(3)), 129.7 (C(17)), 128.0 (C(4)), 124.8 C(5)), 124.1 C(1)), 122.3 (C(2)), 118.3 (C(6)), 115.7 (C(16)), 99.9 (C(18)), 97.7 C(20)), 55.2 (OCH_3), 52.5 (C(7)), 49.6 (C(12)), 49.5 (C(13)), 41.8 (C(9)), 38.3 (C(10)), 27.2 (C(15)), 26.4 (C(11)), 23.7 (C(8)), 22.4 (C(14)); LRMS m/z (ES^+) 423 ([$\text{M}+\text{H}$]⁺, 100%); HRMS m/z (ES^+) [Found: ($\text{M}+\text{H}$)⁺ 423.2385. $\text{C}_{24}\text{H}_{31}\text{O}_3\text{N}_4^+$ requires 423.2391]. RP-HPLC: Method A: Retention time 9.88 min, purity 96.0%; Chiral HPLC (AD-H): Retention time 14.47 min, ee > 99%.

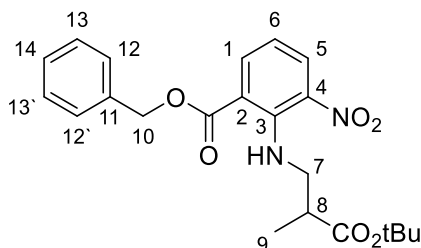
(S)-3-(7-Methoxy-3,4-dihydroquinolin-1(2H)-yl)propyl 4-methyl-2-oxo-2,3,4,5-tetrahydro-1H-benzo[b][1,4]diazepine-6-carboxylate ((S)-26)



(S)-Benzyl 4-methyl-2-oxo-2,3,4,5-tetrahydro-1H-benzo[b][1,4]-diazepine-6-carboxylate (R)-**51** (54 mg, 0.174 mmol, 1.0 eq) in MeOH (10 mL) was added 10% Pd/C (9.3 mg, 0.017 mmol, 0.1 eq). The system was purged with nitrogen, and then hydrogen gas added. The suspension was stirred for 16 h under an atmosphere of hydrogen at ambient temperature. The black suspension was filtered through Celite® and rinsed with MeOH (2 mL). The filtrate was dried (MgSO₄), filtered, and concentrated *in vacuo* to give a beige solid (33 mg). A solution of crude (S)-4-methyl-2-oxo-2,3,4,5-tetrahydro-1H-benzo[b]-[1,4]diazepine-6-carboxylic acid (S)-**52** (33 mg), PyBOP (78 mg, 0.150 mmol, 1.0 eq) and Et₃N (40 μL, 29 mg, 0.290 mmol, 2.0 eq) in DMF (2 mL) was stirred for 15 min at rt. After this time a solution of 3-(7-methoxy-3,4-dihydroquinolin-1(2H)-yl)propan-1-amine (36 mg, 0.165 mmol, 1.1 eq) in DMF (0.5 mL) was added and stirred for 5 h at ambient temperature. After this time the reaction was judged to be complete by TLC analysis. The solvent was removed, and the crude material was purified by a silica gel chromatography, eluting with a gradient from 80% to 100% ethyl acetate in petroleum ether, to afford (S)-**26** a pale yellow solid (19 mg, 0.045 mmol, 26%): R_f 0.41 (EtOAc :petroleum ether 3:1); [α]_D²⁵ = +21.4 (c 0.5, CHCl₃); other physical and spectroscopic properties identical as (R)-**26**, RP-HPLC: Method A: Retention time 9.80 min, purity 97.1%; Chiral HPLC (AD-H): Retention time 11.97 min, ee > 90%.

***tert*-Butyl 3-(benzylamino)-2-methylpropanoate (54)**

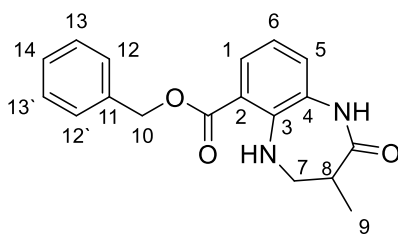
Benzylamine (1.26 mL, 1.23 g, 11.6 mmol, 1.1 eq), *tert*-butylmethacrylate **53** (1.50 g, 10.5 mmol, 1.0 eq) were dissolved in 1,8-diazabicyclo[5.4.0]undec-7-ene (2.41 g, 15.8 mmol, 1.5 eq), and stirred at 90 °C for 16 h, at which time TLC analysis indicated the reaction complete. After cooling to rt the DBU was evaporated at 40 °C and 120 mbar. The crude material was purified by a silica gel chromatography, eluting with a gradient of 10% to 20% EtOAc: petroleum ether, to obtain **54** as a colourless oil (1.34 g, 5.37 mmol, 51%). R_f 0.37 (petroleum ether :EtOAc 5:1); ^1H NMR (500 MHz, CDCl_3): δ 7.35-7.28 (4H, m, C(2)*H*, C(2')*H*, C(3)*H* and C(3')*H*), 7.27-7.21 (1H, m, C(1)*H*), 3.80 (1H, d, J 16.5, C(5)*H*_A*H*_B), 3.77 (1H, d, J 16.5, C(5)*H*_A*H*_B), 2.85 (1H, dd, J 11.5, 7.9, C(6)*H*_A*H*_B) 2.65-2.53 (2H, m, C(6)*H*_A*H*_B and C(7)*H*), 1.44 (9H, s, C(CH₃)₃), 1.13 (3H, d, J 7.0, C(8)*H*₃), ^{13}C NMR (126 MHz, CDCl_3): δ 175.3 (C(9)), 140.4 (C(4)), 128.4 (C(2) and C(2')), 128.1 (C(3) and C(3')), 126.9 (C(1)), 80.3 (C(10)), 53.8 (C(5)), 52.4 (C(6)), 40.9 (C(7)), 28.1 (C(CH₃)₃), 15.4 (C(8)), LRMS m/z (ES⁺) 250 ([M+H]⁺, 100%); HRMS m/z (ES⁺) [Found: (M+H)⁺ 250.1798, C₂₄H₃₁O₃N₄⁺ requires 250.1802]. RP-HPLC: not stable under the conditions using Method A or B.

Benzyl 2-(3-*tert*-butoxy-2-methyl-3-oxopropylamino)-3-nitrobenzoate (56)

tert-Butyl 3-(benzylamino)-2-methylpropanoate **54** (1.47 g, 5.90 mmol, 1.0 eq) was reacted according to general procedure 1 and isolated containing 1.9 eq. acetic acid adducts as a yellow oil (1.46 g), which was used without further purification. *tert*-Butyl 3-amino-2-methylpropanoate × 1.9 AcOH **55** (1.00 g, 3.66 mmol, 1.1 eq) was synthesised in

a manner similar to that used for (*R*)-**48**. The crude material was purified by silica gel chromatography, eluting with a gradient of 10% to 20% EtOAc in petroleum ether, to yield **56** as a yellow oil (1.36 g, 3.28 mmol, 96% over 2 steps). R_f 0.35 (EtOAc :petroleum ether 1:10); ν_{\max} (thin film)/ cm^{-1} 3212 (w) (N-H), 2977 (w), 2936 (w), 1724 (m) (C=O), 1690 (m) (C=O), 1583 (s), 1530 (s), 1500 (s), 1367 (m) (N-O), 1153 (m), 1107 (m); ^1H NMR (500 MHz, CDCl_3) δ 8.55 (1H, t, J 4.7, NH), 8.08 (1H, dd, J 8.0, 1.7, C(1)H), 7.99 (1H, dd, J 8.0, 1.7, C(5)H), 7.45-7.32 (5H, m, C(12)H, C(12')H, C(13)H and C(13')H and C(14)H), 6.67 (1H, dd, J 8.0, 8.0, C(6)H), 5.34 (2H, s, C(10)H₂), 3.11-2.99 (2H, m, C(7)H_AH_B and C(7)H_BH_A), 2.67-2.58 (1H, m, C(8)H), 1.36 (9H, s, C(CH₃)₃), 1.13 (3H, d, J 7.2, C(9)H₃), ^{13}C NMR (126 MHz, CDCl_3) δ 173.5 (CO₂^tBu), 166.9 (CO₂Bn), 145.9 (C(3)), 137.14 (C(4)), 137.05 (C(1)), 135.4 (C(11)), 131.6 (C(5)), 128.7 (C(13) and C(13')), 128.6 (C(14)), 128.4 (C(12) and C(12')), 117.0 (C(2)), 114.6 (C(6)), 81.1 (C(CH₃)₃), 67.1 (C(10)), 50.3 (C(7)), 41.3 (C(5)), 27.9 C(CH₃)₃, 14.9 (C(9)), LRMS m/z (ES⁺) 415 ([M+H]⁺, 100%), 437 ([M+Na]⁺, 93%); HRMS m/z (ES⁺) [Found: (M+Na)⁺ 437.1681, C₂₂H₂₆O₆N₂Na⁺ requires 437.1683]. HPLC: Method: A: Retention time 15.67 min, purity 99.6%.

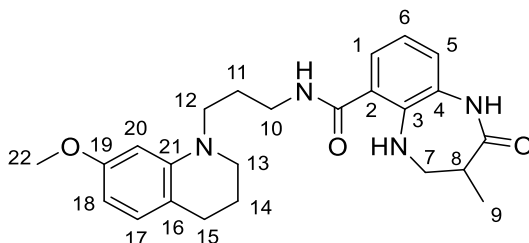
Benzyl 2-(3-*tert*-butoxy-2-methyl-3-oxopropylamino)-3-nitrobenzoate (57)



Benzyl 2-(3-*tert*-butoxy-2-methyl-3-oxopropylamino)-3-nitrobenzoate **56** (1.00 g, 2.41 mmol, 1.0 eq) dissolved in trifluoroacetic acid (10 mL) and dichloromethane (10 mL), was stirred for 2 h, at ambient temperature. The solvent was concentrated *in vacuo* to afford an orange oil. Zn (3.96 g, 60.6 mmol, 25 eq), NH₄Cl (3.24 g, 60.6 mmol, 25 eq) and the residue were suspended in DMF (48 mL), and stirred for 16 h at ambient temperature. After this time the reaction was judged to be complete by TLC analysis. The suspension

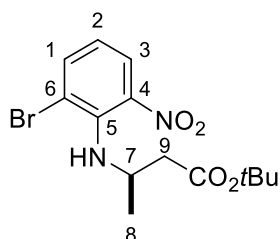
was filtered through Celite® and rinsed with DMF (4 mL). The pH of the filtrate was adjusted to 9 with Et₃N (2.5 mL). To the filtrate, PyBOP (1.25 g, 2.41 mmol, 1.0 eq) was added, and stirred for 20 h at ambient temperature. After this time the reaction was judged to be complete by TLC analysis. The reaction mixture was diluted with EtOAc (150 mL), washed with brine (3 × 200 mL), dried (MgSO₄), filtered, and concentrated *in vacuo*. The crude material was purified by silica gel chromatography, eluting with a gradient of 30% to 50% EtOAc in petroleum ether, to give **57** as a yellow solid. This compound was crystallised in EtOH to give a yellow solid (72 mg, 0.232 mmol, 10% over 3 steps): R_f 0.46 (EtOAc :petroleum ether 1:1); ν_{\max} (thin film)/cm⁻¹ 1673 (s) (C=O), 1538 (w), 1422 (w), 1257 (s), 1234 (s), 1102 (s); ¹H NMR (500 MHz, CDCl₃) δ 8.25 (1H, t, *J* 3.7, C(3)NH), 7.82 (1H, dd, *J* 7.9, 1.5, C(5)H), 7.73 (1H, s br, NHCO), 7.46-7.32 (5H, m, C(12)H, C(12')H, C(13)H and C(13')H and C(14)H), 6.97 (1H, dd, *J* 7.9, 1.5, C(1)H), 6.62 (1H, dd, *J* 7.9, 7.9, C(6)H), 5.32 (2H, s, C(10)H₂), 3.60-3.50 (2H, m, C(7)H_AH_B and C(7)H_BH_A), 2.93-2.83 (1H, m, C(8)H), 1.21 (3H, d, *J* 7.0, C(9)H₃); ¹³C NMR (126 MHz, CDCl₃): δ 176.0 (CONH), 168.4 (CO₂Bn), 143.7 (C(3)), 136.0 (C(11)), 128.7 (C(13 and 13')), 128.5 (C(5)), 128.3 (C(14)), 128.1 (C(12 and 12')), 127.1 (C(1)), 125.5 (C(4)), 116.2 (C(6)), 113.8 (C(2)), 66.6 (C(10)), 50.5 (C(7)), 39.0 (C(8)), 13.7 (C(9)); LRMS *m/z* (ES⁺) 311 ([M+H]⁺, 100%); HRMS *m/z* (ES⁺) [Found: (M+H)⁺ 311.1390, C₁₈H₁₉O₃N₂⁺ requires 311.1390]. RP-HPLC: Method A: Retention time 12.86 min, purity 97.8%.

***N*-(3-(7-Methoxy-3,4-dihydroquinolin-1(2*H*)-yl)propyl)-3-methyl-2-oxo-2,3,4,5-tetrahydro-1*H*-benzo[*b*][1,4]diazepine-6-carboxamide (27)**

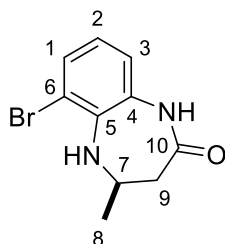


To a solution of benzyl 3-methyl-2-oxo-2,3,4,5-tetrahydro-1*H*-benzo[*b*][1,4]diazepine-6-carboxylate **57** (50 mg, 0.161 mmol, 1.0 eq) in methanol (7 mL) was added 10% Pd/C

(10 mg, 0.009 mmol, 0.06 eq) was added. The system was purged with nitrogen, and then hydrogen gas was added. The suspension was stirred for 20 h under an atmosphere of hydrogen at ambient temperature. The suspension was filtered through Celite®, rinsed with methanol, and the filtrate was concentrated *in vacuo* to afford a colourless solid, which was used without further purification. A solution of the crude residue, PyBOP (83.8 mg, 0.161 mmol, 1.0 eq), 3-(7-methoxy-3,4-dihydroquinolin-1(2*H*)-yl)propan-1-amine **41** (43 mg, 0.193 mmol, 1.2 eq) and Et₃N (50 μL, 36.3 mg, 0.359 mmol, 2.2 eq) in DMF (3 mL) were stirred at ambient temperature for 20 h. After this time the reaction was judged to be complete by TLC analysis. The yellow solution was diluted with EtOAc (20 mL), washed with 2 M aq. K₂CO₃ (2 × 10 mL), brine (10 mL), dried (MgSO₄), filtered, and concentrated *in vacuo*. The crude material was purified by silica gel chromatography, eluting with a gradient of 30% to 100% EtOAc in petroleum ether, to give **27** as a pale yellow solid (23 mg, 0.054 mmol, 34%): R_f 0.37 (EtOAc :petroleum ether 3:1); ν_{\max} (thin film)/cm⁻¹ 3307 (w, br) (N-H), 2934 (m), 1738 (s) (C=O), 1669 (s) (C=O), 1613 (s), 1508 (s), 1282 (s), 1167 (m); ¹H NMR (500 MHz, CDCl₃) δ 7.55 (1H, br s, C(3)NH), 7.38 (1H, s, C(4)NH), 7.03, (1H, dd, *J* 7.8, 1.4, C(1)H), 6.88-6.85 (1H, m, C(17)H), 6.86 (1H, dd, *J* 7.7, 1.4, C(5)H), 6.62 (1H, dd, *J* 7.7, 7.7, C(6)H), 6.45 (1H, t, *J* 4.7, (C10)NH), 6.20-6.15 (2H, m, C(18)H and C(20)H), 3.74 (3H, s, C(22)H₃), 3.55-3.44 (4H, m, C(7)H₂ and C(10)H₂), 3.36 (2H, t, *J* 6.9, C(12)H₂), 3.28-3.24 (2H, m, C(13)H₂), 2.89-2.80 (1H, m, C(8)H), 2.67 (2H, t, *J* 6.4, C(15)H₂), 1.97-1.86 (4H, m, C(11)H₂ and C(14)H₂), 1.18 (3H, d, *J* 5.9, C(9)H₃) ¹³C NMR (126 MHz, CDCl₃) δ 175.9 (C(8)C=O), 169.5 (C(2)C=O), 159.3 (C(19)), 145.9 (C(3)), 141.2 (C(21)), 129.8 (C(17)), 127.0 (C(2)), 125.0(C(5)), 124.0 (C(1)), 120.8 (C(4)), 117.4 (C(6)), 115.8 (C(16)), 100.1 (C(20 or 18)), 97.8 (C(20 or 18)), 55.2 (C(22)), 51.6 (C(10)), 49.6 (C(12) and C(13)), 38.5 (C(7)), 38.3 (C(8)), 27.3 (C(15)), 26.4 (C(11)), 22.4 (C(14)), 13.7 (C(9)), LRMS *m/z* (ES⁺) 423 ([M+H]⁺, 100%); HRMS *m/z* (ES⁺) [Found: (M+H)⁺ 423.2382, C₂₄H₃₁O₃N₄⁺ requires 423.2391]. RP-HPLC: Method A: Retention time 11.74 min, purity 98.3%.

***tert*-Butyl (*R*)-3-((2-bromo-6-nitrophenyl)amino)butanoate (*(R)*-57)**

3-Bromo-2-fluoro-3-nitrobenzoate **33** (3.00 g, 13.6 mmol, 1.0 eq), (*R*)-*tert*-butyl 3-aminobutanoate × 3.0 AcOH (*R*)-**45** (6.21 g, 18.4 mmol, 1.3 eq) and DIPEA (10.2 g, 78.9 mmol, 5.8 eq) dissolved in DMF (50 mL) were stirred at 70 °C for 16 h. After this time the reaction was judged to be complete by TLC analysis. Upon cooling to ambient temperature the solution was diluted with EtOAc (150 mL), washed with 0.5 M aq. LiCl (3 × 100 mL), brine (100 mL), dried (MgSO₄), filtered, and concentrated *in vacuo* to give a (*R*)-**57** yellow oil (4.70 g, 13.1 mmol, 96%), which was used without further purification: *R*_f 0.62 (petroleum ether: EtOAc 4:1); [α]_D²⁵ -74.3 (*c* 1.0 in CHCl₃); ν_{\max} (thin film)/cm⁻¹ 3355 (w) (N-H), 2379 (m), 2932 (w), 1725 (s) (C=O), 1530 (m), 1480 (m), 1367 (m), 1259 (m), 1155 (s); ¹H NMR (400 MHz, CDCl₃) 7.93 (1H, dd, *J* 8.0, 1.5, C(3)*H*), 7.72 (1H, dd, *J* 8.0, 1.5, C(1)*H*), 6.78 (1H, dd, *J* 8.0, 8.0, C(2)*H*), 6.36 (1H, br d, *J* 10.1, C(5)*NH*), 4.24 (1H, dqd, *J* 10.1, 6.8, 6.4, C(7)*H*), 2.45 (2H, d, *J* 6.1, C(9)*H*₂), 1.39 (9H, s, C(CH₃)₃), 1.27 (3H, d, *J* 6.4, C(8)*H*₃); ¹³C NMR (126 MHz, CDCl₃): δ 170.3 (CO₂*t*Bu), 142.5 (C(5)), 141.0 (C(4)), 139.6 (C(1)), 125.7 (C(3)), 120.1 (C(2)), 116.5 (C(6)), 81.1 (C(CH₃)₃), 50.1 C(7)), 43.6 (C(9)), 28.0 (C(CH₃)₃), 21.3 (C(8)); GC-HRMS *m/z* (CI⁺) [Found: (M+H)⁺ 59.0603 C₁₄H₁₉⁷⁹BrN₂O₄ requires 359.0601], RP-HPLC: Method A: Retention time 15.2 min, purity 92.6%.

(R)-6-Bromo-4-methyl-1,3,4,5-tetrahydro-2H-benzo[b][1,4]diazepin-2-one ((R)-58)

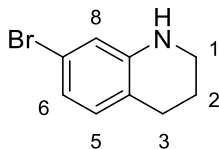
A suspension of *tert*-butyl (*R*)-3-((2-bromo-6-nitrophenyl)amino)butanoate (*R*)-57 (4.70 g, 13.1 mmol, 1.0 eq), activated Fe (3.65 g, 65.3 mmol, 5.0 eq) and trifluoro acetic acid (25 mL) were stirred at 70 °C for 2 h. After cooling to rt the suspension was filtered through Celite®, and concentrated *in vacuo*. The residue was dissolved with EtOAc (200 mL), washed with sat. aq. K₂CO₃ (2 × 200 mL), brine (200 mL), dried (MgSO₄), filtered, and concentrated *in vacuo*. The solid was crystallised using IPA to give (*R*)-58 as a pale yellow solid (1.38 g, 5.41 mmol, 41%): *R*_f 0.63 (petroleum ether: EtOAc 2:1); mp: 164-166 °C (IPA); [α]_D²⁵ -6.3 (*c* 1.0 in CHCl₃); ν_{max} (thin film)/cm⁻¹ 3314 (w) (N-H), 3181 (w) (N-H), 2987 (w), 1661 (s) (C=O), 1435 (m), 1393 (m), 1377 (m), 764 (m), ¹H NMR (500 MHz, CDCl₃): δ 8.59 (1H, s, C(4)NH), 7.31 (1H, dd, *J* 8.0, 1.4, C(1)H), 6.90 (1H, dd, *J* 8.0, 1.4, C(3)H), 6.72 (1H, dd, *J* 8.0, 8.0, C(2)H), 4.19-4.08 (2H, m, C(7)H and C(5)NH), 2.61 (1H, br dd, *J* 13.7, 3.8, C(9)H_AH_B), 2.45 (1H, ddd, *J* 13.7, 8.2, C(9)H_AH_B), 1.38 (3H, d, *J* 6.3, C(8)H₃); ¹³C NMR (126 MHz, CDCl₃): δ 173.1 (C(10)), 136.6 (C(5)), 129.2 (C(4)), 129.0 (C(1)), 121.6 (C(3)), 121.3 (C(2)), 116.0 (C(6)), 54.5 (C(7)), 41.3 (C(9)), 24.0 (C(8)); LRMS *m/z* (ES⁺) 277 ([M⁷⁹Br+Na]⁺, 91%), 279 ([M⁸¹Br+Na]⁺, 100%), HRMS *m/z* (EI⁺) [Found: (M⁷⁹Br +H)⁺ 255.0129 C₁₀H₁₂⁷⁹BrN₂O requires 255.0129], RP-HPLC: Retention time 10.52 min, purity 96.7%, Chiral HPLC (AD-H): Retention time 17.6 min, ee > 99%.

7.4 Chapter 3 Procedures

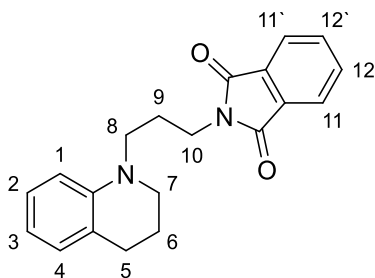
7-Nitro-1,2,3,4-tetrahydroquinoline (**73**)



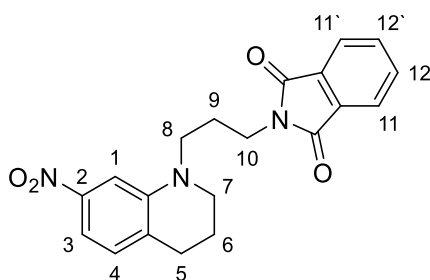
1,2,3,4-Tetrahydroquinoline **71** (2.60 g, 14.6 mmol, 1.0 eq) was added dropwise to conc. H_2SO_4 (9.0 mL) at $-10\text{ }^\circ\text{C}$ and stirred for further 15 min. After this time a precooled mixture of fuming nitric acid (1.0 mL) dissolved in conc. sulfuric acid (4.0 mL) was added dropwise at $-10\text{ }^\circ\text{C}$ over a period of 30 min and subsequently stirred for 1 h at $0\text{ }^\circ\text{C}$. After this time the reaction was judged to be complete by TLC analysis. The solution was poured into ice water (100 g) and the pH was adjusted to 8 using 5 M aq. NaOH. The red suspension was filtered, and rinsed with water. The crude material was purified by silica gel chromatography, eluting with a gradient of 10% to 20% EtOAc in petroleum ether, to give a red solid with a 6:1 mixture of the 5- and 7- regioisomer. The isomers were separated by activated aluminium oxide chromatography, eluting with a gradient of 33% to 100% dichloromethane in petroleum ether, to give **73** as a red solid (1.19 g, 6.68 mmol, 46%): R_f : 0.26 (petroleum ether: EtOAc 10:1); mp $56\text{-}57\text{ }^\circ\text{C}$ (Et_2O), [Lit:¹⁰⁶ $57\text{-}58\text{ }^\circ\text{C}$], $^1\text{H NMR}$ (400 MHz, $(\text{CD}_3)_2\text{SO}$): δ 7.26 (1H, d, J 2.4 Hz, C(1) H), 7.21 (1H, dd, J 8.1, 2.4 Hz, C(3) H), 7.21 (1H, d, J 8.1 Hz, C(4) H), 6.43 (1H, s, NH), 3.25-3.15 (2H, m, C(7) H_2), 2.74 (2H, t, J 6.3 Hz, C(5) H_2) 1.83-1.74 (2H, m, C(6) H_2); LRMS m/z (ES^+) 179 ($[\text{M}+\text{H}]^+$, 100%), 201 ($[\text{M}+\text{Na}]^+$, 53%). These data are in good agreement with the literature.¹⁰⁶

7-Bromo-1,2,3,4-tetrahydroquinoline (74)

A suspension of Ag_2SO_4 (3.83 g, 12.5 mmol, 0.56 eq) in conc. H_2SO_4 (35 mL) was cooled to 0 °C. 1,2,3,4 tetrahydroquinoline **71** (3.01 g, 22.5 mmol, 1.0 eq) was slowly added under vigorous stirring and stirred for further 15 min. Br_2 (4.25 g, 28 mmol, 1.25 eq) was added to the brown solution over 30 min at 0 °C and stirred for further 2 hours at this temperature. After this time the solution was poured onto crushed ice (150 g). The suspension was filtered through Celite® and the filtrate was poured carefully into a mixture of crushed ice (250 g) and KOH (80 g). The resulting suspension was filtered through Celite®. The filtrate was extracted with CH_2Cl_2 (3 × 50 mL). The combined organic extracts were washed with brine (100 mL), dried (MgSO_4), filtered, and concentrated *in vacuo*. The residue was purified by silica gel chromatography, eluting with 25% chloroform in petroleum ether, to give a yellow solid (1.64 g), which is a 3:1 regioisomeric mixture of the 7- and 5- brominated compound. A second silica gel chromatography purification, eluting with 5% EtOAc in petroleum ether, separated the regioisomers to give **74** as a yellow solid (812 mg, 3.83 mmol, 17%): R_f : 0.29 (EtOAc: petroleum ether 1:10); mp 67-69 °C (CHCl_3) [Lit:¹⁰⁵ 68-69 °C]; ν_{max} (thin film)/ cm^{-1} 3397 (m) (N-H), 2949 (w), 2925 (w), 1592 (s), 1476 (s), 1302 (m), 1097 (m), 1004 (m), 839 (s), 785 (s); ^1H NMR (400 MHz, CDCl_3): δ 6.78 (1H, d, J 7.9 Hz, C(5) H), 6.69 (1H, dd, J 7.9, 1.8 Hz, C(6) H), 6.60 (1H, d, J 1.8 Hz, C(8) H), 4.08 (1H, br s, NH), 3.29 (2H, dd, J 5.5, 5.5 Hz, C(1) H_2), 2.69 (2H, dd, J 6.5, 6.5 Hz, C(3) H_2), 1.95-1.87 (2H, m, C(2) H_2); LRMS m/z (ES^+) 212 ($[\text{M}^{79}\text{Br}+\text{H}]^+$, 100%), 214 ($[\text{M}^{81}\text{Br}+\text{H}]^+$, 100%). These data are in good agreement with the literature.¹⁰⁵

2-(3-(3,4-Dihydroquinolin-1(2H)-yl)propyl)isoindoline-1,3-dione (75)

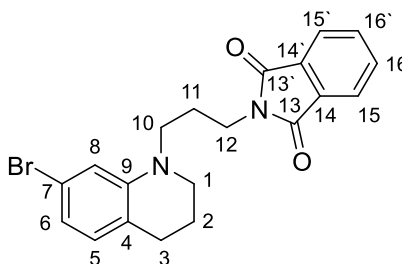
1,2,3,4-Tetrahydroquinoline **71** (2.00 g, 15.0 mmol, 1.0 eq) was reacted according to general procedure 2B for 15 h. The crude material was purified by silica gel chromatography, eluting with a gradient of 10% to 20% ethyl acetate in petroleum ether, afforded **75** as a yellow solid (2.36 g, 7.37 mmol, 49%): R_f : 0.37 (petroleum ether: EtOAc 6:1); mp 78-79 °C (Et₂O); ¹H NMR (400 MHz, CDCl₃): δ 7.88-7.82 (2H, m, C(12)*H* and C(12')*H*), 7.75-7.69 (2H, m, C(11)*H* & C(11')*H*), 7.02 (1H, td, *J* 6.5, 1.3, C(2)*H*), 6.92 (1H, d, *J* 7.2, C(4)*H*), 6.58-6.52 (2H, m, C(1)*H* and C(3)*H*), 3.75 (2H, t, *J* 7.3, C(10)*H*₂), 3.33 (2H, d, *J* 7.3, C(8)*H*₂), 3.26 (2H, t, *J* 5.6, C(7)*H*₂), 2.67 (2H, t, *J* 6.3, C(5)*H*₂), 2.07-1.86 (4H, m, C(6)*H*₂ and C(9)*H*₂); LRMS *m/z* (ES⁺) 321 ([M+H]⁺, 100%). These data are in good agreement with the literature.⁵⁷

2-(3-(7-Nitro-3,4-dihydroquinolin-1(2H)-yl)propyl)isoindoline-1,3-dione (76)

7-Nitro-1,2,3,4-tetrahydroquinoline **73** (650 mg, 3.65 mmol, 1.0 eq), was reacted according to general procedure 2A. Purification by silica gel chromatography, eluting with a gradient of 10% to 40% EtOAc /petroleum ether, afford **76** as a red solid (260 mg, 0.712 mmol, 20%). R_f : 0.40 (EtOAc: petroleum ether 40/60 1:2); mp 148-150 °C (CH₂Cl₂); ¹H NMR (400 MHz, CDCl₃): δ 7.88-7.83 (2H, m, C(11)*H* and C(11')*H*), 7.76-7.71 (2H, m, C(12)*H* and

C(12`H), 7.39 (1H, dd, *J* 8.2, 2.0 Hz, C(3)H), 7.32 (1H, d, *J* 2.0 Hz, C(1)H), 7.01 (1H, d, *J* 8.2 Hz, C(4)H), 3.79 (2H, t, *J* 7.2 Hz, C(10)H₂), 3.40 (2H, t, *J* 7.3 Hz, C(8)H₂), 3.34 (2H, t, *J* 5.9 Hz, C(7)H₂), 2.79 (2H, t, *J* 6.4 Hz, C(5)H₂), 2.09-1.93 (4H, m, C(6)H₂ and C(8)H₂); LRMS *m/z* (ES⁺) 366 ([M+H]⁺, 100%). These data are in good agreement with the literature.⁵⁷

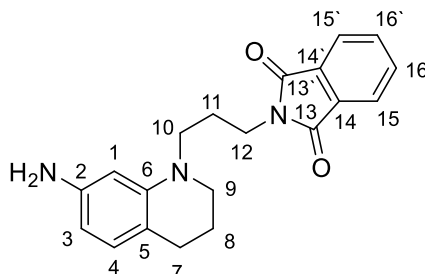
2-(3-(7-Bromo-3,4-dihydroquinolin-1(2H)-yl)propyl)isoindoline-1,3-dione (77)



7-Bromo-1,2,3,4-tetrahydroquinoline **74** (500 mg, 2.36 mmol, 1.0 eq) was reacted according to general procedure 2A for 15 h. The crude material was purified by silica gel chromatography, eluting with a gradient of 10% to 20% EtOAc in petroleum ether, to give **77** as a yellow oil (226 mg, 0.566 mmol, 24%): *R_f*: 0.28 (petroleum ether: EtOAc 4:1); *v*_{max} (thin film)/cm⁻¹ 2934 (m), 1705 (s) (C=O), 1593 (m), 1496 (m), 1394 (s), 1004 (m), 716 (s); ¹H NMR (500 MHz, CDCl₃): δ 7.88-7.83 (2H, m, C(15)H and C(15`H)), 7.75-7.69 (2H, m, C(16)H and C(16`H)), 6.76-6.73 (1H, m, C(5)H), 6.63 (1H, dd, *J* 7.8, 1.9 Hz, C(6)H), 6.60 (1H, d, *J* 1.9 Hz, C(8)H), 3.76 (2H, t, *J* 7.2 Hz, C(12)H₂), 3.32-3.24 (4H, m, C(1)H₂ and C(10)H₂), 2.66 (2H, t, *J* 6.3 Hz C(3)H₂), 2.03-1.95 (2H, m, C(2)H₂) 1.94-1.87 (2H, m, C(11)H₂); ¹³C NMR (126 MHz, CDCl₃): δ 168.4 (C(13) and C(13`)), 146.2 (C(9)), 134.0(C(16) and C(16`)), 132.0 (C(14) and C(14`)), 130.2 (C(5)), 123.3 (C(15) and C(15`)), 121.3 (C(4)), 120.6 (C(7)), 118.3 (C(6)), 112.9 (C(8)), 49.0 (C(1)), 48.7 (C(10)), 35.9 (C(12)), 27.6 (C(3)), 25.4 (C(11)), 21.8 (C(2)); 147.9 (C(4)), 134.1 (C(10) and C(10`)), 132.1 (C(8) and C(8`)), 129.3 (C(2) and C(2`)), 123.3 (C(9) and C(9`)), 117.3 (C(1)), 112.9 (C(3) and C(3`)), 40.7 (C(5)), 35.4 (C(7)), 27.9 (C(6)); LRMS *m/z* (ES⁺) 401 ([M⁷⁹Br+H]⁺, 100%), 403 ([M⁸¹Br+H]⁺, 100%); HRMS *m/z*

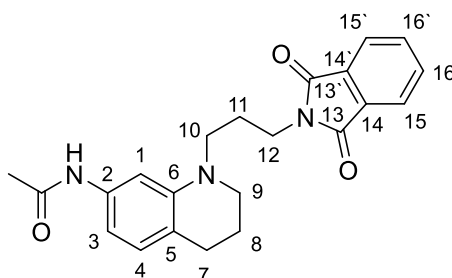
(ES⁺) [Found: (M⁷⁹Br +H)⁺ 399.0702, C₂₀H₂₀O₂N₂⁷⁹Br⁺ requires 399.0703 and (M⁸¹Br +H)⁺ 401.0682 C₂₀H₂₀O₂N₂⁸¹Br⁺ requires 401.0682].

2-(3-(7-Amino-3,4-dihydroquinolin-1(2H)-yl)propyl)isoindoline-1,3-dione (78)

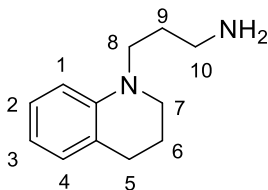


To a solution of 2-(3-(7-nitro-3,4-dihydroquinolin-1(2H)-yl)propyl)isoindoline-1,3-dione **76** (200 mg, 0.547 mmol, 1.0 eq) in MeOH (5 mL) and CH₂Cl₂ (5 mL), was added 20% Pd/C (667 mg, 0.025 mmol, 0.05 eq). The system was purged with nitrogen, and then hydrogen gas added. The suspension was stirred under an atmosphere of hydrogen for 3 h at which time TLC analysis indicated the reaction complete. The suspension was filtered through Celite®, and concentrated *in vacuo*. The residue was purified by silica gel chromatography, eluting with a gradient of 20% to 50% EtOAc in petroleum ether, to give **78** as a yellow oil (127 mg, 0.379 mmol, 69%). R_f: 0.25 (petroleum ether: EtOAc 1:1); ν_{max} (thin film)/cm⁻¹ 3453 (w) (N-H), 3363 (w) (N-H), 2935 (m), 1704 (s) (C-O), 1615 (m); 1510 (m), 1396 (m), 720 (s); ¹H NMR (400 MHz, CDCl₃): δ 7.87-7.80 (2H, m, C(15)H and C(15')H), 7.74-7.68 (2H, m, C(16)H and C(16')H), 6.71 (1H, d, *J* 7.9, C(4)H), 5.99-5.95 (2H, m, C(1)H and C(3)H), 3.75 (2H, t, *J* 7.3, C(12)H₂), 3.50 (2H, br s, NH₂), 3.30-3.23 (2H, m, C(10)H₂), 3.23-3.19 (2H, m, C(9)H₂), 2.62 (2H, t, *J* 6.5, C(7)H₂), 2.04-1.94 (2H, m, C(11)H₂), 1.93-1.85 (2H, m, C(8)H₂); ¹³C NMR (126 MHz, CDCl₃): δ 168.3 (C(13) and C(13')), 145.7 (C(6)), 145.0(C(2)), 133.9 (C(16)) and (C(16')), 132.0 (C(14) and C(14')), 129.8 (C(4)), 123.2 (C(15)) and (C(15')), 113.7 (C(5)), 103.5 (C(3)), 98.2 (C(1)), 49.3 (C(9)), 48.9 (C(10)), 36.1 (C(12)), 27.3 (C(7)), 25.5 (C(11)), 22.5 (C(8)); LRMS *m/z* (ES⁺) 336 ([M+H]⁺, 100%); HRMS *m/z* (ES⁺) [Found: (M+H)⁺ 336.1706, C₂₀H₂₂ON₄⁺ requires 336.1707].

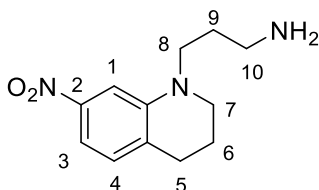
***N*-(1-(3-(1,3-dioxoisindolin-2-yl)propyl)-1,2,3,4-tetrahydroquinolin-7-yl)acetamide (79)**



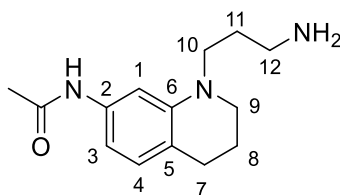
A solution of 2-(3-(7-amino-3,4-dihydroquinolin-1(2*H*)-yl)propyl)isoindoline-1,3-dione **78** (70 mg, 0.209 mmol, 1.0 eq) and Et₃N (44 μL, 31.9 mg, 0.313 mmol, 1.5 eq) dissolved in CH₂Cl₂ (2 mL) was cooled to 0 °C. Acetyl chloride (15 μL, 16.5 mg, 0.209 mmol, 1.0 eq) was added, and the reaction solution was warmed to ambient temperature. After 1 hour the TLC indicate completion and the reaction mixture was absorbed onto Celite®. The residue was purified by a silica gel chromatography, eluting with a gradient elution of 40% to 80% EtOAc in petroleum ether, to afford **79** as a yellow oil (58 mg, 0.154 mmol, 74%): R_f: 0.32 (petroleum ether: EtOAc 1:3); ν_{max} (thin film)/cm⁻¹ 3304 (w) (N-H), 2934 (w), 2839 (w), 1704 (s) (C=O), 1662 (m) (C=O), 1612 (m), 1394 (m), 718 (s); ¹H NMR (400 MHz, CDCl₃): δ 7.85-7.78 (2H, m, C(15)*H* and C(15')*H*), 7.73-7.67 (2H, m, C(16)*H* and C(16')*H*), 7.39 (1H, s br, NH), 6.82 (1H, d, *J* 7.9, C(4)*H*), 6.72 (1H, d, *J* 1.8, C(1)*H*), 6.70 (1H, d, *J* 7.9, 1.8, C(3)*H*), 3.73 (2H, t, *J* 7.4, C(12)*H*₂), 3.29 (2H, t, *J* 7.5, C(10)*H*₂), 3.25-3.21 (2H, m, C(9)*H*₂), 2.66 (2H, t, *J* 6.5, C(7)*H*₂), 2.13 (3H, s, CH₃), 2.03-1.95 (2H, m, C(11)*H*₂), 1.94-1.86 (2H, m, C(8)*H*₂); ¹³C NMR (101 MHz, CDCl₃): δ 168.4 (C(13) and C(13')), 168.3 (NHCO), 145.3 (C(6)), 137.1 (C(2)), 134.0 (C(16)) and (C(16')), 132.0 (C(14) and C(14')), 129.3 (C(4)), 123.1 (C(15)) and (C(15')), 118.1 (C(5)), 107.6 (C(3)), 102.5 (C(1)), 49.3 (C(9)), 48.9 (C(10)), 36.1 (C(12)), 27.6 (C(7)), 25.5 (C(11)), 24.7 (CH₃CO), 22.5 (C(8)); LRMS *m/z* (ES⁺) 378 ([M+H]⁺, 100%); HRMS *m/z* (ES⁺) [Found: (M+H)⁺ 378.1806, C₂₂H₂₄O₃N₃⁺ requires 378.1812].

3-(3,4-Dihydroquinolin-1(2H)-yl)propan-1-amine (83)

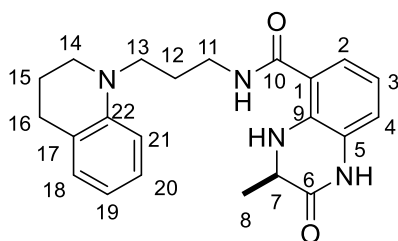
3,4-Dihydroquinolin-1(2H)-yl)propyl)isoindoline-1,3-dione **75** (961 mg, 3.00 mmol, 1.0 eq), was reacted according to general procedure 3. The crude material was purified by silica gel chromatography, eluting with CH₂Cl₂/MeOH/Et₃N (100:10:1), to afford **83** as a yellow oil (350 mg, 1.84 mmol, 61%): R_f: 0.29 (MeOH: CH₂Cl₂ 1:5); ¹H NMR (400 MHz, CDCl₃): δ 7.00-6.92 (1H, m, C(2)H), 6.89-6.83 (1H, m, C(4)H), 6.54-6.43 (2H, m, C(1)H and C(3)H), 3.29-3.16 (4H, m, C(7)H₂ and C(8)H₂), 2.76 (2H, t, *J* 7.2, C(5)H₂), 2.64 (2H, t, *J* 6.6, C(10)H₂) 1.91-1.83 (2H, m, C(6)H₂), 1.78-1.69 (2H, m, C(9)H₂); LRMS *m/z* (ES⁺) 191 ([M+H]⁺, 100%). These data are in accordance with the literature.⁵⁶

3-(7-Nitro-3,4-dihydroquinolin-1(2H)-yl)propan-1-amine (84)

[2-[3-(7-Nitro-3,4-dihydroquinolin-1(2H)-yl)propyl]-1H-isoindole-1,3(2H)-dione] **76** (230 mg, 0.629 mmol, 1.0 eq), was reacted according to general procedure 3. The crude material was purified *via* an acid base extraction, to yield **84** as an orange oil (47 mg, 0.200 mmol, 32%): R_f: 0.19 (MeOH: CH₂Cl₂:Et₃N 10:100:1); ¹H NMR (400 MHz; CDCl₃): δ 7.38 (1H, d, *J* 2.3 Hz, C(1)H), 7.36 (1H, dd, *J* 7.6 2.3 Hz, C(2)H), 7.00 (1H, d, *J* 7.6 Hz, C(3)H), 3.44 (2H, t, *J* 7.4 Hz, C(7)H₂), 3.34 (2H, t, *J* 5.7 Hz, C(6)H₂), 2.94 (2H, t, *J* 7.4 Hz, C(9)H₂), 2.79 (2H, t, *J* 6.6 Hz, C(4)H₂), 2.03-1.83 (4H, m, C(5)H₂ and C(8)H₂); LRMS *m/z* (ES⁺) 236 ([M+H]⁺, 100%). These data are in good agreement with the literature.⁵⁷

***N*-(1-(3-aminopropyl)-1,2,3,4-tetrahydroquinolin-7-yl)acetamide (85)**

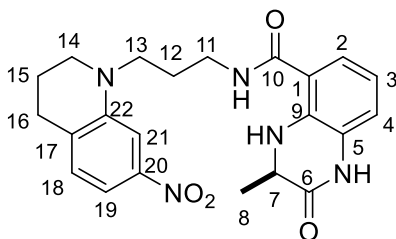
N-(1-(3-(1,3-Dioxoisindolin-2-yl)propyl)-1,2,3,4-tetrahydroquinolin-7-yl)-acetamide **79** (128 mg, 0.339 mmol, 1.0 eq) was reacted according to general procedure 3. Purification *via* acid base extraction, yielded **85** as a yellow oil (55 mg, 0.222 mmol, 66%), which was used without further purification: R_f : 0.05 (EtOH); ν_{\max} (thin film)/ cm^{-1} 3291 (w) (N-H), 2929 (w), 2839 (w), 1660 (m) (C-O), 1612 (s), 1590 (s), 1509 (s), 1427 (m), 1316 (m), 732 (s); ^1H NMR (400 MHz, CDCl_3): δ 8.00 (1H, br s, NH), 6.88 (1H, d, J 1.8, C(1)*H*), 6.74 (1H, d, J 8.0, C(4)*H*), 6.51 (1H, dd, J 8.0, 1.8, C(3)*H*), 3.22-3.11 (4H, m, C(9)*H*₂ and C(10)*H*₂), 2.67 (2H, t, J 6.9, C(12)*H*₂), 2.66 (2H, t, J 6.5, C(7)*H*₂), 2.03 (3H, s, CH₃), 1.87-1.77 (2H, m, C(8)*H*₂), 1.70-1.61 (2H, m, C(11)*H*₂); ^{13}C NMR (101 MHz, CDCl_3): δ 168.6 (NHCO), 145.5 (C(6)), 137.4 (C(2)), 129.1 (C(3)), 118.4 (C(5)), 107.1 (C(4)), 102.6 (C(1)), 49.4 (C(9) or C(10)), 49.0 (C(9) or C(10)), 40.2 (C(12)), 30.3 (C(11)), 27.7 (C(7)), 24.5 (CH₃), 22.3 (C(8)); LRMS m/z (ES⁺) 248 ([M+H]⁺, 100%); HRMS m/z (ES⁺) [Found: (M+H)⁺ 248.1758 C₁₄H₂₂ON₃⁺ requires 248.1757].

***(R)*-N-(3-(3,4-Dihydroquinolin-1(2*H*)-yl)propyl)-3-methyl-2-oxo-1,2,3,4-tetrahydroquinoxaline-5-carboxamide (86)**

[(*R*)-3-methyl-2-oxo-1,2,3,4-tetrahydroquinoxaline-5-carboxylic acid] (*R*)-**32** (30 mg, 0.145 mmol, 1.0 eq) and [3,4-dihydroquinolin-1(2*H*)-yl]propan-1-amine] **83** (33 mg, 0.174 mmol, 1.2 eq) were reacted according to general procedure 4 for 16 h. The crude

material was purified by silica gel chromatography, eluting with 66% EtOAc in petroleum ether, to give **86** as a yellow oil (25 mg, 0.066 mmol, 46%): R_f 0.47 (2:1 EtOAc: petroleum ether); $[[\alpha]_D^{25} = -23.0$ (c 0.2 in CHCl_3), [Lit:⁵⁶ $[\alpha]_D = -23.8$ (c 1.0 in CHCl_3)]; ^1H NMR (400 MHz; $(\text{CD}_3)_2\text{CO}$): 9.33 (1H, br s, C(5)NH), 8.01 (1H, br s, C(9)NH), 7.80 (1H, br s, C(1)NH), 7.30 (1H, d, J 7.9, C(2)H), 6.97-6.90 (2H, m, C(4)H and C(20)H), 6.87-6.83 (1H, m, C(18)H), 6.67-6.57 (2H, m, C(3)H and C(21)H), 6.45 (1H, m, C(19)H), 4.00 (1H, qd, J 6.6, 1.5, C(7)H), 3.49-3.42 (2H, m, C(11)H₂), 3.41-3.35 (2H, m, C(13)H₂), 3.33-3.27 (2H, m, C(14)H₂), 2.72-2.67 (2H, m, C(16)H₂), 1.95-1.85 (4H, m, C(12)H₂ and C(15)H₂), 1.37 (3H, d, J 6.6, C(8)CH₃); LRMS m/z (ES⁺) 379 ($[\text{M}+\text{H}]^+$, 100%), RP-HPLC: Method A: Retention time 9.71 min, purity 97.0%. These data are in good agreement with the literature.⁵⁶

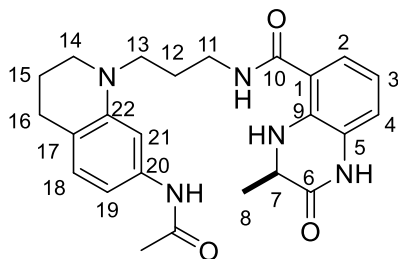
(3R)-N-[3-(7-Nitro-3,4-dihydroquinolin-1(2H)-yl)propyl]-3-methyl-2-oxo-1,2,3,4-tetrahydroquinoxaline-5-carboxamide (87)



[(*R*)-3-methyl-2-oxo-1,2,3,4-tetrahydroquinoxaline-5-carboxylic acid] (*R*)-**32** (40 mg, 0.194 mmol, 1.0 eq) and [3-(7-nitro-3,4-dihydroquinolin-1(2H)-yl)propan-1-amine] **84** (47 mg, 0.200 mmol, 1.0 eq) were reacted according to general procedure 4 for 18 h. The crude material was purified by silica gel chromatography, eluting with a gradient of 30% to 80% EtOAc in petroleum ether, to yield **87** as an orange oil (63 mg, 0.149 mmol, 77%): R_f 0.27 (3:1 EtOAc: petroleum ether); $[[\alpha]_D^{25} = -59.5$ (c 1.0 in MeOH), Lit: $[\alpha]_D = -39.5$ (c 1.0 in $(\text{CH}_3)_2\text{CO}$); ^1H NMR (400 MHz; $(\text{CD}_3)_2\text{CO}$): δ 9.32 (1H, br s, C(5)NH), 8.00 (1H, br s, C(9)NH), 7.83 (1H, t, J 4.7, C(11)NH), 7.38 (1H, d, J 2.2, C(21)H), 7.35-7.29 (2H, m, C(2)H and C(19)H), 7.10 (1H, d, J 8.1, C(18)H), 6.97-6.94 (1H, m, C(4)H), 6.65 (1H, dd, J 8.0, 8.0, C(3)H), 4.01 (1H, qd, J 6.7, 1.5, C(7)H), 3.54-3.47 (4H, m, C(11)H₂ and C(13)H₂), 3.41 (2H, t, J 5.8, C(14)H₂), 2.82 (2H, t, J 6.3, C(16)H₂), 2.03-1.91 (4H, m, C(12)H₂ and C(15)H₂), 1.38

(3H, d, J 6.7, C(8)CH₃); LRMS m/z (ES⁺) 424 ([M+H]⁺, 22%), 446 ([M+Na]⁺, 33%), 869 ([2M+Na]⁺, 100%), These data are in good agreement with the literature.⁵⁷

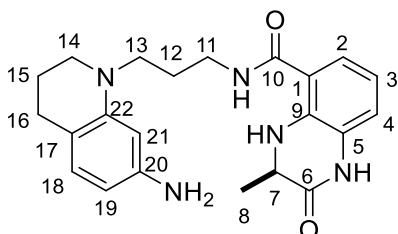
(*R*)-*N*-(3-(7-Acetamido-3,4-dihydroquinolin-1(2*H*)-yl)propyl)-3-methyl-2-oxo-1,2,3,4-tetrahydroquinoxaline-5-carboxamide (88**)**



[(*R*)-3-methyl-2-oxo-1,2,3,4-tetrahydroquinoxaline-5-carboxylic acid] (*R*)-**32** (40 mg, 0.194 mmol, 1.0 eq) and 3-(6-methoxy-1*H*-indol-1-yl)propan-1-amine **85** (55 mg, 0.222 mmol, 1.15 eq) were reacted according to general procedure 4 for 17 h. The crude material was purified by silica gel chromatography, eluting with a gradient of 75% to 100% EtOAc in petroleum ether, to give **88** as a colourless solid (52 mg, 0.119 mmol, 62%): R_f : 0.18 (EtOAc); mp 191-193 °C (acetone); $[\alpha]_D^{25}$ -33.3 (c 0.25 in MeOH), ν_{\max} (thin film) /cm⁻¹ 3313 (br w) (N-H), 2938 (w), 1680 (s) (C-O), 1631 (m) (C-O), 1591 (s), 1531 (s), 1265 (s), 730 (s); ¹H NMR (400 MHz, (CD₃)₂SO): δ 10.34 (1H, s, C(5)NH), 9.57 (1H, s, C(20)NH), 8.38 (1H, t, J 5.2, C(10)NH), 7.80 (1H, br s, C(7)NH), 7.29 (1H, d, J 8.0, C(4)H), 6.90-6.83 (2H, m, C(2)H and C(18)H), 6.77-6.69 (2H, m, C(19)H and C(21)H), 6.63 (1H, dd, J 8.0, 8.0, C(3)H), 3.94 (1H, q, J 6.7, C(7)H), 3.34-3.19 (6H, m, C(11)H, C(13)H and C(14)H), 2.61 (2H, t, J 6.2, C(16)H), 1.98 (3H, s, COCH₃), 1.87-1.75 (4H, m, C(12)H₂ and C(15)H₂), 1.26 (3H, d, J 6.7, C(8)H₃); ¹³C NMR (101 MHz, (CD₃)₂SO): δ 168.6 (C(10)), 168.3 (C(6) or COCH₃), 168.2 (C(6) or COCH₃), 145.4 (C(22)), 138.8 (C(20)), 136.1 (C(9)), 129.1 (C(18)), 127.9 (C(5)), 122.2 (C(4)), 117.4 (C(17)), 117.3 (C(21)), 116.8 (C(3)), 116.1 (C(1)), 106.9 (C(21)), 102.1 (C(19)), 50.6 (C(7)), 49.4 (C(13)), 49.1 (C(14)), 37.6 (C(11)), 27.5 (C(15)), 26.5 (C(12)), 24.5 (CH₃CO), 22.4 (C(15)), 18.6 (C(8)); LRMS m/z (ES⁺) 436 ([M+H]⁺, 100%), HRMS m/z (ES⁺) [Found: (M+H)⁺ 436.2345 C₂₄H₃₀O₃N₅⁺ requires 436.2343];

RP-HPLC: Method A: Retention time 10.18 min, purity 95.5%. Chiral HPLC (AD-H): Retention time 12.28 min, ee > 99%.

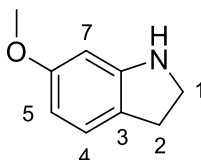
(R)-N-(3-(7-Amino-3,4-dihydroquinolin-1(2H)-yl)propyl)-3-methyl-2-oxo-1,2,3,4-tetrahydroquinoxaline-5-carboxamide (89)



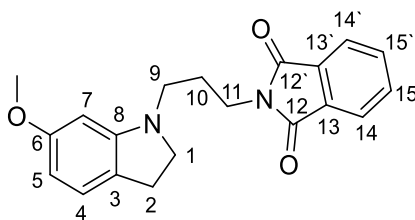
A suspension of (R)-3-methyl-N-(3-(7-nitro-3,4-dihydroquinolin-1(2H)-yl)propyl)-2-oxo-1,2,3,4-tetrahydroquinoxaline-5-carboxamide **88** (50 mg, 0.118 mmol, 1.0 eq), Zn (193 mg, 2.95 mmol, 25 eq), NH₄Cl (158 mg, 2.95 mmol, 25 eq) in DMF (2.5 mL) were stirred at ambient temperature for 60 min. After this time the reaction was judged to be complete by TLC analysis. The suspension was filtered through Celite® and rinsed with EtOAc (10 mL). The filtrate was washed with sat. aq. NaHCO₃ (3 × 15 mL), dried (Na₂SO₄), filtered, and concentrated *in vacuo*. The crude material was purified by silica gel chromatography, eluting with a gradient of 50% to 100% EtOAc in petroleum ether, to afford **89** as a yellow oil (28 mg, 0.071 mmol, 60 %): R_f: 0.39 (EtOAc); [α]_D²⁵ -35.3 (c 0.15 in CHCl₃), ν_{\max} (thin film)/cm⁻¹ 3344 (m) (N-H), 3175 (w br), 1688 (s) (C-O), 1626 (s) (C-O), 1509 (s), 1375 (s), 1505 (s), 1481 (m), 1373 (m), 1297 (s), 807 (s); ¹H NMR (500 MHz, CDCl₃): δ 8.00 (1H, br s, C(5)NH), 7.78 (1H, br s, C(7)NH), 6.86 (1H, dd, *J* 7.7, 1.1, C(2)H), 6.76-6.71 (4H, m, C(4)H and C(18)H), 6.58 (1H, dd, *J* 7.8, 7.8, C(3)H), 6.45 (1H, br t, *J* 5.5, C(10)NH), 6.01-5.98 (2H, m, C(19)H and C(21)H), 4.10 (1H, dq, *J* 6.6, 1.5, C(7)H), 3.53-3.48 (2H, m, C(11)H₂), 3.46 (2H, br s, NH₂), 3.34 (2H, t, *J* 6.8, C(13)H₂), 3.25-3.21 (2H, m, C(14)H₂), 2.63 (2H, t, *J* 6.3 Hz, C(16)H₂), 1.93 (2H, tt, *J* 6.8, 6.8 Hz, C(12)H₂), 1.91-1.85 (2H, m, C(15)H₂), 1.49 (3H, d, *J* 6.6 Hz, C(8)H₃); ¹³C NMR (126 MHz, CDCl₃): δ 168.7 (C(6)), 168.5 (C(10)), 145.8 (C(22)), 145.7 (C(20)), 136.5 (C(9)), 130.1 (C(18)), 126.8 (C(5)), 121.4 (C(4)), 117.4 (C(2)), 116.9 (C(3)), 115.5 (C(1)), 113.6 (C(17)), 103.7 (C(19)), 98.0

(C(21)), 51.1 (C(7)), 49.8 (C(14)), 49.7 (C(13)), 38.3 (C(11)), 27.3 (C(16)), 26.5 (C(12)), 22.6 (C(15)), 18.5 (C(8)); LRMS m/z (ES⁺) 394 ([M+H]⁺, 100%), HRMS m/z (ES⁺) [Found: (M+H)⁺ 394.2239 C₂₂H₂₈O₂N₅ requires 394.2238]; RP-HPLC: Compound unstable using Method A or B.

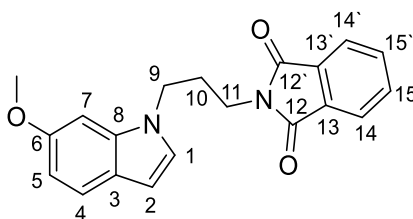
6-Methoxyindoline (91)



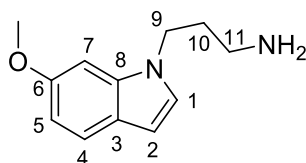
A solution of 6-methoxyindole **90** (800 mg, 5.44 mmol, 1.0 eq) in dry THF (5 mL) was cooled to 0 °C. BH₃ in THF (1 M, 5.44 mL, 5.44 mmol, 1.0 eq) was added over 10 minutes. After 30 min at 0 °C, trifluoro acetic acid (5.44 mL) was added dropwise and stirred for another 45 min. The brown solution was basified with 2 M aq. NaOH (40 mL) and stirred for 15 min at ambient temperature. The organic solvent was removed *in vacuo*. To the residue EtOAc (50 mL) was added and the organic extracts were washed with brine (50 mL), dried (Na₂SO₄), filtered, and concentrated *in vacuo*. The residue was purified by silica gel chromatography, eluting with a gradient of 10 to 20% EtOAc in petroleum ether, to afford **91** as a pale yellow oil (666 mg, 4.46 mmol, 82%): R_f: 0.30 (EtOAc: petroleum ether 1:5); ¹H NMR (400 MHz, CDCl₃): δ 7.02-6.96 (1H, m, C(4)H), 6.28-6.22 (2H, m, C(5)H and C(7)H), 3.77 (1H, br s, NH), 3.75 (3H, s, OCH₃), 3.56 (2H, t, *J* 8.3, C(1)H₂), 2.69 (2H, t, *J* 8.3, 8.3, C(2)H₂); LRMS m/z (ES⁺) 150 ([M+H]⁺, 100%). These data are in accordance with the literature.¹⁷⁹

2-(3-(6-Methoxyindolin-1-yl)propyl)isoindoline-1,3-dione (93)

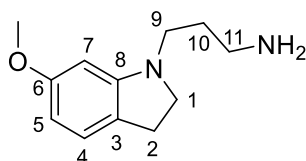
6-Methoxyindole **91** (600 mg, 4.02 mmol, 1.0 eq) was reacted according to general procedure 2B. Purification by silica gel chromatography, eluting with a gradient of 10% to 30% EtOAc in petroleum ether, yielded **93** as a yellow oil (933 mg, 2.77 mmol, 69%): R_f 0.38 (petroleum ether: EtOAc 1:3); ν_{\max} (thin film)/ cm^{-1} 2942 (w), 2833 (w), 1706 (s) (C=O), 1619 (m); 1496 (m), 1394 (m), 1212(m), 718 (s); $^1\text{H NMR}$ (500 MHz, CDCl_3): δ 7.86-7.81 (2H, m, C(14)*H* and C(14')*H*), 7.73-7.68 (2H, m, C(15)*H* and C(15')*H*), 6.92 (1H, d, J 7.9, C(4)*H*), 6.22-6.13 (1H, m, C(5)*H*), 6.10-6.05 (1H, m, C(7)*H*), 3.84-3.79 (2H, m, C(11)*H*₂), 3.76 (3H, s, OCH_3), 3.38 (2H, t, J 8.3, C(1)*H*₂), 3.12 (2H, t, J 7.0, C(9)*H*₂), 2.86 (2H, t, J 8.3, C(2)*H*₂), 2.00 (2H, tt, J 7.0, 7.0, C(10)*H*₂); $^{13}\text{C NMR}$ (126 MHz, CDCl_3): δ 168.4 (C(12) and C(12')), 160.1 (C(6)), 153.5 (C(8)), 134.0 (C(15) and C(15')), 132.1 (C(3)), 124.4 (C(4)), 123.2 (C(14) and C(14')), 122.5, 101.9 (C(7)), 94.9 (C(5)), 55.4 (OCH_3), 53.7 (C(1)), 47.0 (C(9)), 36.1 (C(11)), 27.8 (C(2)), 26.4 (C(10)); 147.9 (C(4)), 134.1 (C(10) and C(10')), 132.1 (C(8) and C(8')), 129.3 (C(2) and C(2')), 123.3 (C(9) and C(9')), 117.3 (C(1)), 112.9 (C(3) and C(3')), 40.7 (C(5)), 35.4 (C(7)), 27.9 (C(6)); LRMS m/z (ES^+) 337 ($[\text{M}+\text{H}]^+$, 100%), HRMS m/z (ES^+) [Found: $(\text{M}+\text{Na})^+$ 359.1367, $\text{C}_{20}\text{H}_{20}\text{O}_3\text{N}_2\text{Na}^+$ requires 359.1366]; RP-HPLC: Retention time 11.66 min, purity 96.2%.

2-(3-(6-Methoxy-1*H*-indol-1-yl)propyl)isoindoline-1,3-dione (92)

A suspension of 2-(3-(6-methoxyindolin-1-yl)propyl)isoindoline-1,3-dione **93** (450 mg, 1.34 mmol, 1.0 eq), MnO₂ (580 mg, 6.69 mmol, 5.0 eq) in CH₂Cl₂ (20 mL) were stirred under reflux for 16 h. After this time the reaction was judged to be complete by TLC analysis. After cooling to ambient temperature the suspension was filtered through Celite®, rinsed with CH₂Cl₂, and the filtrate was concentrated *in vacuo*. The residue was purified by silica gel chromatography, eluting with a gradient of 10% to 30% EtOAc in petroleum ether, to afford **92** as a yellow oil (347 mg, 1.04 mmol, 78%). R_f: 0.38 (petroleum ether: EtOAc 1:3); ν_{\max} (thin film)/cm⁻¹ 2954 (w), 1769 (m) (C=O), 1702 (s), 1398 (m), 1210 (s), 708 (s); ¹H NMR (500 MHz, CDCl₃): δ 7.86-7.81 (2H, m, C(15)*H* and C(15')*H*), 7.74-7.69 (2H, m, C(14)*H* and C(14')*H*), 7.46 (1H, d, *J* 8.5, C(4)*H*), 7.11 (1H, d, *J* 3.2, C(1)*H*), 6.79-6.77 (1H, m, C(7)*H*), 6.76 (1H, dd, *J* 8.5, 2.2, C(5)*H*), 6.41 (1H, dd, *J* 3.2, 0.7, C(2)*H*), 4.14 (2H, t, *J* 7.0, C(9)*H*₂), 3.86 (3H, s, OCH₃), 3.76 (2H, t, *J* 7.0, C(11)*H*₂), 2.25 (2H, tt, *J* 7.0, 7.0, C(10)*H*₂); ¹³C NMR (126 MHz, CDCl₃): δ 168.3 (C(12)*H* and C(12')*H*), 156.2 (C(6)), 136.5 (C(8)), 134.0 (C(14)*H* and C(14')*H*), 131.9 (C(13)*H* and C(13')*H*), 126.7 (C(1)), 123.3 (C(15)*H* and C(15')*H*), 122.9 (C(3)), 121.5 (C(4)), 109.3 (C(5)), 101.3 (C(2)), 92.9 (C(7)), 55.7 (C(OCH₃)), 43.8 (C(9)), 35.7 (C(11)), 28.9 (C(10)); LRMS *m/z* (ES⁺) 335 ([M+H]⁺, 100%), HRMS *m/z* (ES⁺) [Found: (M+Na)⁺ 357.1209 C₂₀H₁₈O₃N₂Na⁺ requires 357.1210]; RP-HPLC: Retention time 13.36 min, purity 98.3%.

3-(6-Methoxy-1H-indol-1-yl)propan-1-amine (94)

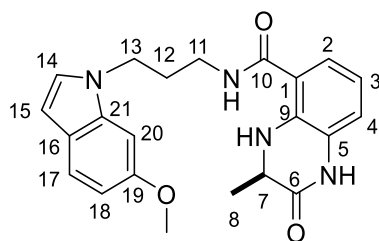
2-(3-(6-methoxy-1H-indol-1-yl)propyl)isoindoline-1,3-dione **92** (290 mg, 0.867 mmol, 1.0 eq) was reacted according to general procedure 3. The crude material was purified by silica gel chromatography, eluting with CH₂Cl₂/MeOH/Et₃N (100:10:1), to yield **94** as a colourless oil (93 mg, 0.455 mmol, 53%): R_f: 0.17 (CH₂Cl₂: MeOH: Et₃N 100:10:1); ν_{\max} (thin film)/cm⁻¹ 3218 (br w) (N-H), 2937 (m), 2833 (w), 1620 (s), 1490 (m), 1465 (m), 1325 (m) 1214 (s), 1030 (s), 807 (s); ¹H NMR (400 MHz, CDCl₃): δ 7.52-7.45 (1H, m, C(4)H), 7.02-6.98 (1H, m, C(1)H), 6.85-6.81 (1H, m, C(7)H), 6.80-6.75 (1H, m, C(5)H), 6.42 (1H, d, *J* 3.0, C(2)H), 4.18 (2H, d, *J* 6.9, C(9)H₂), 3.87 (3H, s, OCH₃), 2.76 (2H, d, *J* 6.9, C(11)H₂), 2.03 (2H, tt, *J* 6.9, 6.9, C(10)H₂); ¹³C NMR (101 MHz, CDCl₃): δ 156.1 (C(6)), 136.6 (C(8)), 126.7 (C(1)), 122.8 (C(3)), 121.5 (C(4)), 109.1 (C(5)), 101.1 (C(2)), 93.2 (C(7)), 55.8 (OCH₃), 43.5 (C(9)), 38.8 (C(11)), 32.0 (C(10)); LRMS *m/z* (ES⁺) 205 ([M+H]⁺, 100%); HRMS *m/z* (ES⁺) [Found: (M+H)⁺ 205.1337, C₁₂H₁₇ON₂⁺ requires 205.1335].

3-(6-Methoxyindolin-1-yl)propan-1-amine (95)

2-(3-(6-Methoxyindolin-1-yl)propyl)isoindoline-1,3-dione **93** (200 mg, 0.595 mmol, 1.0 eq) was reacted according to general procedure 3. The crude material was purified *via* an acid base extraction, to yield **95** as a colourless oil (82 mg, 0.397 mmol, 67%): R_f: 0.38 (petroleum ether: EtOAc 1:3); ν_{\max} (thin film)/cm⁻¹ 3457 (br w) (N-H), 3016 (m), 2970 (m), 2945 (m), 1448 (m), 1377 (s), 1217 (s); ¹H NMR (400 MHz, CDCl₃): δ 6.94 (1H, d, *J* 7.9, C(4)H), 6.16 (1H, dd, *J* 7.9, 2.2, C(5)H), 6.07 (1H, d, *J* 2.2, C(7)H), 3.77 (3H, s, OCH₃), 3.36 (2H, t, *J* 8.2, C(1)H₂), 3.10 (2H, t, *J* 7.1, C(9)H₂), 2.89 (2H, t, *J* 8.2, C(2)H₂), 2.82 (2H, t, *J* 7.1,

C(11) H_2), 1.75 (2H, tt, J 7.1, 7.1, C(10) H_2); ^{13}C NMR (126 MHz, CDCl_3): δ 160.1 (C(6)), 154.0 (C(8)), 124.4 (C(4)), 122.4 (C(3)), 101.2 (C(5)), 94.6 (C(7)), 55.4 (OCH₃), 53.8 (C(1)), 46.8 (C(9)), 40.2 (C(11)), 31.1 (C(2)), 27.8 (C(10)); LRMS m/z (ES⁺) 207 ([M+H]⁺, 100%), 239 ([M+Na]⁺, 79%); HRMS m/z (ES⁺) [Found: (M+H)⁺ 207.1493, C₁₂H₁₉ON₂⁺ requires 207.1492].

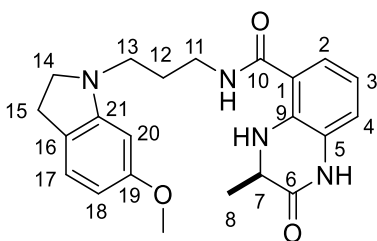
(*R*)-*N*-(3-(6-Methoxy-1*H*-indol-1-yl)propyl)-3-methyl-2-oxo-1,2,3,4-tetrahydroquinoxaline-5-carboxamide (96**)**



(*R*)-3-Methyl-2-oxo-1,2,3,4-tetrahydroquinoxaline-5-carboxylic acid] (*R*)-**32** (40 mg, 0.194 mmol, 1.0 eq) and 3-(6-methoxy-1*H*-indol-1-yl)propan-1-amine **94** (60 mg, 0.291 mmol, 1.5 eq) were reacted according to general procedure 4 for 15 h. The crude material was purified by silica gel chromatography, eluting with a gradient of 30% to 70% EtOAc in petroleum ether, to give **96** as a colourless solid (68 mg, 0.173 mmol, 89%): R_f : 0.32 (petroleum ether: EtOAc 1:3); mp 182-185 °C (acetone); $[\alpha]_D^{25}$ -46.7 (c 0.2 in MeOH), ν_{max} (thin film)/ cm^{-1} 3344 (m) (N-H), 3175 (w br), 1688 (s) (C-O), 1626 (s) (C-O), 1509 (s), 1375 (s), 1505 (s), 1481 (m), 1373 (m), 1297 (s), 807 (s); ^1H NMR (500 MHz, $(\text{CD}_3)_2\text{SO}$): δ 9.31 (1H, s, C(5)NH), 8.00 (1H, s, C(7)NH), 7.78 (1H, t, J 5.7, C(11)NH), 7.42 (1H, d, J 8.6, C(17)H), 7.26 (1H, dd, J 7.8, 1.2, C(4)H), 7.22 (1H, d, J 3.2, C(14)H), 6.99 (1H, d, J 2.1, C(20)H), 6.97-6.94 (1H, m, C(15)H), 6.87 (1H, dd, J 7.8, 1.2, C(2)H), 6.69 (1H, dd, J 8.6, 2.1, C(18)H), 6.64 (1H, dd, J 7.8, 7.8, C(3)H), 6.35 (1H, dd, J 3.1, 0.5, C(15)H), 4.19 (2H, t, J , C(13) H_2), 3.93 (1H, q, J 6.6, C(7)H), 3.76 (3H, s, OCH₃), 3.27-3.20 (2H, m, C(11) H_2), 2.04-1.97 (2H, m, C(12) H_2), 1.26 (3H, d, J 6.6, C(8) H_3); ^{13}C NMR (126 MHz, $(\text{CD}_3)_2\text{SO}$): δ 168.7 (C(10)), 168.2 (C(6)), 156.0 (C(19)), 136.8 (C(21)), 136.2 (C(9)), 127.92 (C(14)), 127.86 (C(5)), 122.7 (C(17)), 122.2 (C(4)), 121.4 (C(16)), 117.4 (C(2)), 116.8 (C(3)), 116.0 (C(1)),

109.5 (C(18)), 100.9 (C(15)), 93.6 (C(20)), 55.7 (C(OCH₃)), 50.6 (C(7)), 43.7 (C(13)), 37.2 (C(11)), 30.0 (C(12)), 18.6 (C(8)); LRMS *m/z* (ES⁺) 393 ([M+H]⁺, 100%); HRMS *m/z* (ES⁺) [Found: (M+Na)⁺ 415.1742, C₂₂H₂₅O₃N₄Na⁺ requires 415.1741]; RP-HPLC: Method A: Retention time 11.89 min, purity 95.8%; Chiral HPLC (AD-H): Retention time 10.36 min, ee > 99%.

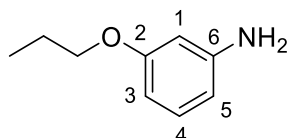
(R)-N-(3-(6-Methoxyindolin-1-yl)propyl)-3-methyl-2-oxo-1,2,3,4-tetrahydroquinoxaline-5-carboxamide (97)



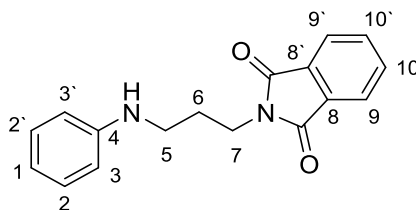
[(R)-3-Methyl-2-oxo-1,2,3,4-tetrahydroquinoxaline-5-carboxylic acid] (R)-**32** (40 mg, 0.194 mmol, 1.0 eq) and 3-(6-methoxyindolin-1-yl)propan-1-amine **95** (60 mg, 0.291 mmol, 1.5 eq) were reacted according to general procedure 4 for 16 h. The crude material was purified by silica gel chromatography, eluting with a gradient of 30% to 60% EtOAc in petroleum ether, to afford **97** as a colourless solid (56 mg, 0.142 mmol, 73%): R_f: 0.44 (petroleum ether: EtOAc 1:3); mp 65-67 °C (EtOAc); [α]_D²⁵ -32.6 (c 0.3 in CHCl₃), ν_{max} (thin film)/cm⁻¹ 3340 (w br) (N-H), 2937 (w), 2833 (w), 1680 (s) (C-O), 1632 (m), 1620 (m), 1495 (s), 1481 (s), 1283 (s), 1258 (s), 1201 (s), 843 (s); ¹H NMR (500 MHz, (CD₃)₂SO): δ 10.37 (1H, s, C(5)NH), 8.44 (1H, t, *J* 5.5, C(11)NH), 7.82 (1H, br s, C(7)NH), 7.30 (1H, dd, *J* 7.8, 1.0, C(4)H), 6.89 (1H, d, *J* 8.2, C(17)H), 6.86 (1H, dd, *J* 7.8, 1.0, C(2)H), 6.64 (1H, dd, *J* 7.8, 7.8, C(3)H), 6.10 (1H, dd, *J* 8.2, 2.2, C(18)H), 6.07 (1H, d, *J* 2.3, C(20)H), 3.94 (1H, dq, *J* 6.6, 1.2, C(7)H), 3.65 (3H, s, OCH₃), 3.35-3.29 (4H, m, C(14)H₂ and C(11)H₂), 3.08 (2H, t, *J* 7.2, C(13)H₂), 2.80 (2H, t, *J* 8.3, C(15)H₂), 1.80 (2H, tt, *J* 7.2, 7.2, C(12)H₂), 1.27 (3H, d, *J* 6.6, C(8)H₃); ¹³C NMR (126 MHz, (CD₃)₂SO): δ 168.6 (C(10)), 168.3 (C(6)), 160.1 (C(19)), 154.2 (C(21)), 136.2 (C(9)), 127.9 (C(5)), 124.6 (C(17)), 122.22 (C(16)), 122.18 (C(4)), 117.4 (C(2)), 116.8 (C(3)), 116.1 (C(1)), 101.8 (C(18)), 94.7 (C(20)), 55.4 (OCH₃), 53.5 (C(14)),

50.6 (C(7)), 46.7 (C(13)), 37.5 (C(11)), 27.7 (C(15)), 27.1 (C(12)), 18.6 (C(8)); LRMS m/z (ES⁺) 395 ([M+H]⁺, 100%), HRMS m/z (ES⁺) [Found: (M+H)⁺ 395.2078 C₂₂H₂₇O₃N₄⁺ requires 395.2078]; RP-HPLC: Method A: Retention time 11.98 min, purity 96.7 %; Chiral HPLC (AD-H): Retention time 12.23 min, ee > 99%.

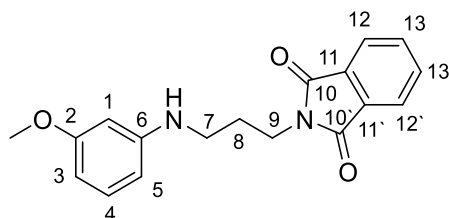
3-Propoxyaniline (110)



3-Nitrophenol (2.00 g, 14.3 mmol, 1.0 eq), K₂CO₃ (2.00 g, 14.4 mmol, 1.0 eq) and 1-bromopropane (1.94 g, 15.8 mmol, 1.1 eq) were suspended in DMF (20 mL), and stirred at 60 °C for 3 h. After this time the reaction was judged to be complete by TLC analysis. After cooling to rt the reaction mixture was dissolved in EtOAc (100 mL) and water (50 mL). The organic extracts were washed with sat. aq. K₂CO₃ (3 × 70 mL), dried (MgSO₄), filtered and concentrated *in vacuo*. The residue was dissolved in EtOH (60 mL) and acetic acid (2.7 mL) and the solution was heated under reflux for 20 min. To the yellow solution activated Fe (5.80 g, 100 mmol, 7.0 eq) and FeCl₃ hexahydrate (648 mg, 2.32 mmol, 0.15 eq) were added and the suspension stirred for 15 h at 60 °C. After this time the reaction was judged to be complete by TLC analysis. After cooling to rt the suspension was filtered through Celite® and concentrated *in vacuo*. The residue was purified by silica gel chromatography, eluting with a gradient of 10% to 30% EtOAc in petroleum ether, to give **110** as a yellow oil (930 mg, 6.15 mmol, 43%): R_f: 0.37 (petroleum ether: EtOAc 2:1); ¹H NMR (400 MHz, CDCl₃): δ 7.05 (1H, dd, *J* 8.0, 8.0 C(4)*H*), 6.33 (1H, dd, *J* 8.0, 1.9, C(3)*H*), 6.28 (1H, dd, *J* 8.0, 1.9, C(5)*H*), 6.25 (1H, dd, *J* 1.9, 1.9 C(3)*H*) 3.88 (2H, t, *J* 6.8, OCH₂), 3.64 (2H, s br, NH₂), 1.79 (2H, qt, *J* 6.8, 6.8, CH₂CH₃), 1.02 (3H, t, *J*, 6.8, CH₃), LRMS m/z (ES⁺) 125 ([M+H]⁺, 100%). These data are in good agreement with the literature.¹⁸⁰

2-(3-(Phenylamino)propyl)isoindoline-1,3-dione (113)

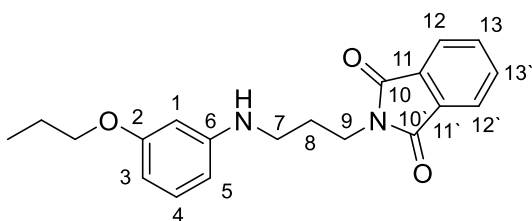
Aniline **108** (931 mg, 10.0 mmol, 1.0 eq), was reacted according to general procedure 2B. Purification by silica gel chromatography, eluting with a gradient of 10% to 30% EtOAc in petroleum ether, afforded **113** as a yellow solid (1.31 g, 4.67 mmol, 47%): R_f : 0.33 (petroleum ether: EtOAc 5:2); mp 96-98 °C (EtOAc); ν_{\max} (thin film)/ cm^{-1} 3388 (m) (N-H), 1705 (s) (C=O), 1602 (m); 1465 (m), 1045 (m), 796 (s), 723 (s); ^1H NMR (400 MHz, CDCl_3): δ 7.89-7.82 (2H, m, C(9)H and C(9')H), 7.75-7.70 (2H, m, C(10)H and C(10')H), 7.20-7.12 (2H, m, C(2)H and C(2')H), 6.69 (1H, tt, J 7.3, 1.1, C(1)H), 6.65-6.60 (2H, m, C(3)H and C(3')H), 4.05 (1H, s br, NH), 3.81 (2H, t, J 6.6, C(7)H₂), 3.19 (2H, d, J 6.6, C(5)H₂), 1.98 (2H, tt, J 6.6, 6.6, C(6)H₂); ^{13}C NMR (101 MHz, CDCl_3): δ 168.6 (C=O), 147.9 (C(4)), 134.1 (C(10) and C(10')), 132.1 (C(8) and C(8')), 129.3 (C(2) and C(2')), 123.3 (C(9) and C(9')), 117.3 (C(1)), 112.9 (C(3) and C(3')), 40.7 (C(5)), 35.4 (C(7)), 27.9 (C(6)); LRMS m/z (ES⁺) 281 ([M+H]⁺, 100%);, HRMS m/z (ES⁺) [Found: (M+H)⁺ 281.1283, C₁₇H₁₇O₂N₂⁺ requires 281.1283]; RP-HPLC: compound unstable using Method A or B.

2-(3-((3-Methoxyphenyl)amino)propyl)isoindoline-1,3-dione (114)

3-Anisidine **109** (750 mg, 6.09 mmol, 1.0 eq) was reacted according to general procedure 2B for 16 h. Purification by silica gel chromatography, eluting with a gradient of 10% to 30% EtOAc in petroleum ether, afforded **114** as a yellow solid (910 mg, 2.93 mmol, 48%): R_f : 0.38 (petroleum ether: EtOAc 2:1); mp 92-94 °C (CHCl_3); ν_{\max} (thin film)/ cm^{-1} 3399 (w)

(N-H), 2940 (w), 1703 (s) (C-O), 1613 (m), 1395 (m), 1161 (m), 1039 (m), 718 (s); ^1H NMR (400 MHz, CDCl_3): δ 7.86-7.79 (2H, m, C(12)*H* and C(12')*H*), 7.72-7.66 (2H, m, C(13)*H* and C(13')*H*), 7.05 (1H, dd, *J* 8.0, 8.0, C(4)*H*), 6.25-6.20 (2H, C(3)*H* and C(5)*H*), 6.16 (1H, dd, *J* 2.2, 2.2, C(1)*H*), 4.13 (1H, s, NH), 3.78 (2H, t, *J* 6.7, C(9)*H*₂), 3.74 (3H, s, OCH₃), 3.15 (2H, t, *J* 6.7, C(7)*H*₂), 1.95 (2H, tt, *J* 6.7, 6.7, C(8)*H*₂); ^{13}C NMR (101 MHz, CDCl_3): δ 168.6 (C(10) and C(10')), 160.9 (C(2)), 149.4 (C(6)), 134.1 (C(13) and C(13')), 132.0 (C(11) and C(11')), 130.0 (C(4)), 123.3 (C(12) and C(12')), 106.0 (C(3) or C(5)), 102.4 (C(3) or C(5)), 98.8 (C(1)), 55.1 (OCH₃) 40.7 (C(9)), 35.4 (C(7)), 27.9 (C(8)); LRMS *m/z* (ES⁺) 311 ([M+H]⁺, 100%); HRMS *m/z* (ES⁺) [Found: (M+H)⁺ 311.1389, C₁₈H₁₉O₃N₂⁺ requires 311.1390]; RP-HPLC: Method A: Retention time 11.57 min, purity 95.6%.

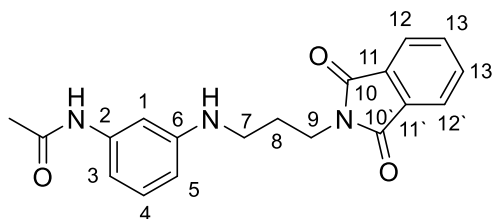
2-(3-((3-Propoxyphenyl)amino)propyl)isoindoline-1,3-dione (**115**)



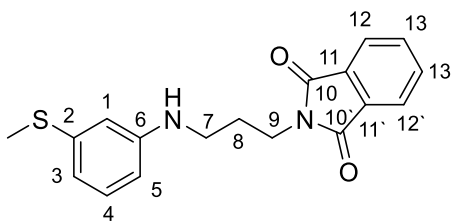
3-Propoxyaniline **110** (930 mg, 6.15 mmol, 1.0 eq) was reacted according to general procedure 2B for 20 h. Purification by silica gel chromatography, eluting with a gradient of 10% to 40% EtOAc in petroleum ether, afforded **115** as a yellow oil (1090 mg, 3.22 mmol, 52%), containing minor impurities: *R_f*: 0.48 (petroleum ether: EtOAc 2:1); ν_{max} (thin film)/ cm^{-1} 3400 (w) (N-H), 2937 (w), 1703 (s) (C-O), 1613 (m), 1394 (m), 1189 (m), 1162 (m), 718 (s); ^1H NMR (400 MHz, CDCl_3): δ 7.89-7.81 (2H, m, C(12)*H* and C(12')*H*), 7.75-7.67 (2H, m, C(13)*H* and C(13')*H*), 7.04 (1H, dd, *J* 8.0, 8.0, C(4)*H*), 6.27-6.20 (2H, C(3)*H* and C(5)*H*), 6.17 (1H, dd, *J* 2.0, 2.0, C(1)*H*), 4.06 (1H, s, NH), 3.87 (2H, t, *J* 6.9, OCH₂) 3.80 (2H, t, *J* 6.6, C(9)*H*₂), 3.74 (3H, s, OCH₃), 3.16 (2H, m, C(7)*H*₂), 1.97 (2H, tt, *J* 6.6, 6.6, C(8)*H*₂), 1.77 (2H, tq, *J* 6.9, 6.9, CH₂CH₃), 1.02 (3H, t, *J* 6.9, 6.9, CH₃); ^{13}C NMR (101 MHz, CDCl_3): δ 168.6 (C(10) and C(10')), 160.4 (C(2)), 149.3 (C(6)), 134.0 (C(13) and C(13')), 132.1 (C(11) and C(11')), 129.9 (C(4)), 123.3 (C(12) and C(12')), 105.9 (C(3) or C(5)), 103.2 (C(3) or C(5)),

99.4 (C(1)), 69.3 (OCH₂) 40.7 (C(9)), 35.4 (C(7)) , 27.9 (C(8)) 22.7 (CH₂CH₃), 10.6 (CH₂CH₃); LRMS *m/z* (ES⁺) 339 [(M+H)⁺, 100%]; HRMS *m/z* (ES⁺) [Found: (M+H)⁺ 339.1703, C₂₀H₂₃O₃N₂⁺ requires 339.1703]; RP-HPLC: Method A: Retention time 11.11 min, purity 94.7%.

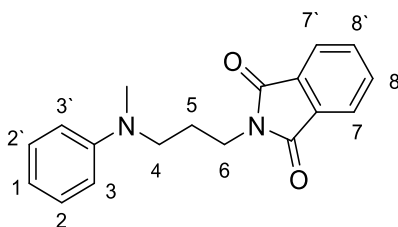
***N*-(3-((3-(1,3-Dioxoisindolin-2-yl)propyl)amino)phenyl)acetamide (116)**



3'-Aminoacetanilide **111** (2.00 g, 13.3 mmol, 1.0 eq) was reacted according to general procedure 2A for 16 h. Purification by silica gel chromatography, eluting with a gradient of 50% to 80% EtOAc in petroleum ether, afforded (3.31 g) of **116** as an impure yellow oil, which was used without further purification: An aliquot was purified for characterisation. *R_f*: 0.22 (petroleum ether: EtOAc 1:2); *v*_{max} (thin film)/cm⁻¹ 3370 (w) (N-H), 2980 (w), 1704 (s) (C=O), 1612 (m), 1396 (s), 1370 (m), 1040 (w), 907 (m), 718 (s); ¹H NMR (400 MHz, CDCl₃): δ 7.84-7.78 (2H, m, C(12)*H* and C(12')*H*), 7.72-7.68 (2H, m, C(13)*H* and C(13')*H*), 7.65 (1H, s, *NHAc*), 7.04 (1H, dd, *J* 8.0, 8.0 C(4)*H*), 6.94(1H, dd, *J* 1.6, 1.6 C(1)*H*), 6.71 (1H, ddd, *J* 8.0, 1.6, 1.6 C(3)*H*), 6.33 (1H, ddd, *J* 8.0, 1.6, 1.6 C(5)*H*), 4.09 (1H, s, *NH*), 3.76 (2H, t, *J* 6.7, C(9)*H*₂), 3.12 (2H, t, *J* 6.7, C(7)*H*₂), 2.12 (3H, s, COCH₃), 1.92 (2H, tt, *J* 6.7, 6.7, C(8)*H*₂); ¹³C NMR (101 MHz, CDCl₃): δ 168.50 (C(10) and C(10')), 168.47 (CONH), 148.5 (C(6)), 139.0 (C(2)), 134.0 (C(13) and C(13')), 131.9 (C(11) and C(11')), 129.5 (C(4)), 123.2 (C(12) and C(12')), 108.69 (C(3) or C(5)), 108.68 (C(3) or C(5)), 104.3 (C(1)), 40.6 (C(9)), 35.3 (C(7)) , 27.8 (C(8)), 24.6 (CH₃CO); LRMS *m/z* (ES⁺) 338 [(M+H)⁺, 100%]; HRMS *m/z* (ES⁺) [Found: (M+H)⁺ 338.1498, C₁₉H₂₀O₃N₂⁺ requires 338.1499].

2-(3-((3-(Methylthio)phenyl)amino)propyl)isoindoline-1,3-dione (117)

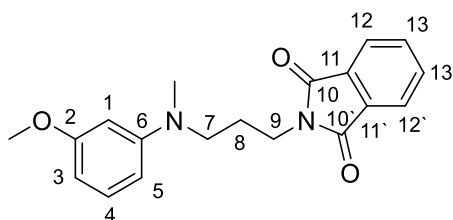
3-Methylthio(aniline) **112** (2.00 g, 14.4 mmol, 1.0 eq) was reacted according to general procedure 2B for 17 h. Purification by silica gel chromatography, eluting with a gradient of 10% to 30% EtOAc in petroleum ether, afforded **117** as a yellow oil (2.73 g, 8.37 mmol, 58%): R_f : 0.24 (petroleum ether: EtOAc 3:1); ν_{\max} (thin film)/ cm^{-1} 3392 (w) (N-H), 2922 (w), 1702 (s) (C-O), 1570 (m), 1395 (m), 1040 (w), 717 (s); $^1\text{H NMR}$ (400 MHz, CDCl_3): δ 7.88-7.82 (2H, m, C(12)*H* and C(12')*H*), 7.75-7.70 (2H, m, C(13)*H* and C(13')*H*), 7.08 (1H, dd, J 7.9, 7.9, C(4)*H*), 6.58 (1H, ddd, J 7.9, 1.9, 1.6 C(3)*H*), 6.51 (1H, dd, J 1.9, 1.9 C(1)*H*), 6.32 (1H, ddd, J 7.9, 1.9, 1.6 C(5)*H*), 4.11 (1H, s, NH), 3.81 (2H, t, J 6.6, C(9)*H*₂), 3.16 (2H, t, J 6.6, C(7)*H*₂), 2.45 (3H, s, SCH_3), 1.97 (2H, tt, J 6.6, 6.6, C(8)*H*₂); $^{13}\text{C NMR}$ (101 MHz, CDCl_3): δ 168.6 (C(10) and C(10')), 148.2 (C(6)), 139.3 (C(2)), 134.1 (C(13) and C(13')), 132.0 (C(11) and C(11')), 129.6 (C(4)), 123.3 (C(12) and C(12')), 115.4 (C(3)), 110.7 (C(1)), 110.0 (C(5)), 40.5 (C(9)), 35.3 (C(7)), 27.8 (C(8)), 15.8 (SCH_3); LRMS m/z (ES^+) 327 ($[\text{M}+\text{H}]^+$, 100%); HRMS m/z (ES^+) [Found: $[\text{M}+\text{H}]^+$ 327.1160, $\text{C}_{18}\text{H}_{19}\text{O}_2\text{N}_2\text{S}^+$ requires 327.1162]; RP-HPLC: Method A: Retention time 11.10 min, purity 94.7%.

2-(3-(Methyl(phenyl)amino)propyl)isoindoline-1,3-dione (118)

A suspension of 2-(3-(phenylamino)propyl)isoindoline-1,3-dione **113** (400 mg, 1.43 mmol, 1.0 eq), iodomethane (100 μL , 228 mg, 1.61 mmol, 1.1 eq), K_2CO_3 (225 mg, 1.63 mmol, 1.1 eq) in DMF (3 mL) were stirred at 90 $^\circ\text{C}$ for 15 hours. After this time the

reaction was judged to be complete by TLC analysis. After cooling to rt the suspension was diluted with EtOAc (50 mL), washed with brine (3 × 50 mL), dried (Na₂SO₄), filtered, and concentrated *in vacuo*. The crude material was purified by silica gel chromatography, eluting with a gradient of 10 to 20% EtOAc in petroleum ether, to afford **118** as a yellow oil (310 mg, 1.05 mmol, 74%): R_f: 0.33 (petroleum ether: EtOAc 5:1); ¹H NMR (400 MHz, CDCl₃): δ 7.88-7.82 (2H, m, C(7)H and C(7')H), 7.75-7.69 (2H, m, C(8)H and C(8')H), 7.23-7.17 (2H, m, C(2)H and C(2')H), 6.75-6.65 (3H, m, C(3)H, C(3')H and C(1)H), 4.05 (1H, br s, NH), 3.74 (2H, t, *J* 7.3, C(6)H₂), 3.39 (2H, d, *J* 7.3, C(4)H₂), 2.93 (3H, s, NCH₃), 1.98 (2H, tt, *J* 7.3, 7.3, C(5)H₂); LRMS *m/z* (ES⁺) 295 ([M+H]⁺, 100%). These data are in accordance with the literature.¹⁸¹

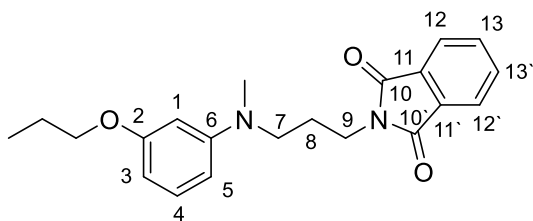
2-(3-((3-Methoxyphenyl)(methyl)amino)propyl)isoindoline-1,3-dione (**119**)



A suspension of 2-(3-((3-methoxyphenyl)amino)propyl)isoindoline-1,3-dione **114** (300 mg, 0.967 mmol, 1.0 eq), iodomethane (67 μL, 151 mg, 1.06 mmol, 1.1 eq), K₂CO₃ (147 mg, 1.06 mmol, 1.1 eq) in DMF (3 mL) were stirred at 85 °C for 2 h. After this time the reaction was judged to be complete by TLC analysis. After cooling to ambient temperature the suspension was diluted with EtOAc (20 mL), washed with brine (3 × 20 mL), dried (MgSO₄), filtered, and concentrated *in vacuo*. The crude material was purified by silica gel chromatography, eluting with a gradient of 10% to 30% of EtOAc in petroleum ether, to afford **119** as a yellow oil (152 mg, 0.469 mmol, 48%): R_f: 0.42 (petroleum ether: EtOAc 2:1); *v*_{max} (thin film)/cm⁻¹ 2940 (w), 1704 (s) (C-O), 1608 (m), 1037 (m), 718 (s); ¹H NMR (400 MHz, CDCl₃): δ 7.88-7.83 (2H, m, C(12)H and C(12')H), 7.75-7.70 (2H, m, C(13)H and C(13')H), 7.12 (1H, dd, *J* 8.2, 8.2, C(4)H), 6.34 (1H, dd, *J* 8.2, 2.4, C(5)H), 6.27 (1H, dd, *J* 8.2, 2.4, C(3)H), 6.25 (1H, dd, *J* 2.4, 2.4, C(1)H), 3.78 (3H, s, OCH₃), 3.75 (2H, t, *J* 7.2, C(9)H₂),

3.40 (2H, t, J 7.2, C(7)H₂), 2.94 (3H, s, NCH₃) 2.00 (2H, tt, J 7.2, 7.2, C(8)H₂); ¹³C NMR (101 MHz, CDCl₃): δ 168.3 (C(10) and C(10')), 160.8 (C(2)), 150.6 (C(6)), 134.0 (C(13) and C(13')), 132.1 (C(11) and C(11')), 129.9 (C(4)), 123.3 (C(12) and C(12')), 105.6 (C(5)), 101.4 (C(3)), 99.0 (C(1)), 55.1 (OCH₃), 50.3 (C(7)), 38.3 (NCH₃), 36.0 (C(9)), 26.0 (C(8)); LRMS m/z (ES⁺) 325 ([M+H]⁺, 100%), HRMS m/z (ES⁺) [Found: (M+H)⁺ 325.1549, C₁₉H₂₁O₃N₂⁺ requires 325.1549]; RP-HPLC: Method A: Retention time 10.05 min, purity 98.9%.

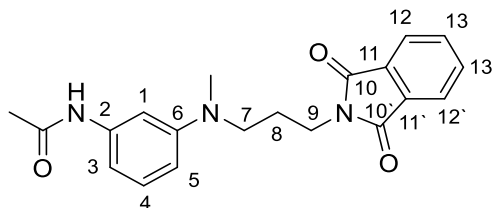
2-(3-((3-Propoxyphenyl)(methyl)amino)propyl)isoindoline-1,3-dione (**120**)



A suspension of 2-(3-((3-propoxyphenyl)amino)propyl)isoindoline-1,3-dione **115** (350 mg, 1.03 mmol, 1.0 eq), iodomethane (67 μ L, 151 mg, 1.06 mmol, 1.1 eq), K₂CO₃ (147 mg, 1.06 mmol, 1.1 eq) in DMF (3 mL) were stirred at 85 °C for 2 h. After this time the reaction was judged to be complete by TLC analysis. After cooling to ambient temperature the suspension was diluted with EtOAc (20 mL), washed with brine (3 \times 20 mL), dried (MgSO₄), filtered and concentrated *in vacuo*. The crude material was purified by silica gel chromatography, eluting with a gradient of 10% to 30% of EtOAc in petroleum ether, to afford **120** as a yellow oil (179 mg, 0.507 mmol, 49%): R_f: 0.53 (petroleum ether: EtOAc 2:1); ν_{\max} (thin film)/cm⁻¹ 2936 (w), 1707 (s) (C=O), 1610 (m), 1395 (m), 719 (s); ¹H NMR (400 MHz, CDCl₃): δ 7.87-7.80 (2H, m, C(12)H and C(12')H), 7.74-7.68 (2H, m, C(13)H and C(13')H), 7.09 (1H, dd, J 8.0, 8.0, C(4)H), 6.31 (1H, dd, J 8.0, 2.4 C(3)H or C(5)H), 6.25 (1H, dd, J 8.0, 2.4 C(3)H or C(5)H), 6.24 (1H, dd, J 2.4, 2.4, C(1)H), 3.88 (2H, t, J 6.9, OCH₂) 3.73 (2H, t, J 7.2, C(9)H₂), 3.37 (2H, t, J 7.2, C(7)H₂), 2.92 (3H, s, NCH₃), 1.98 (2H, tt, J 7.2, 7.2, C(8)H₂), 1.78 (2H, tq, J 6.6, 6.6, CH₂CH₃), 1.02 (3H, t, J 6.6, CH₃); ¹³C NMR (101 MHz, CDCl₃): δ 168.3 (C(10) and C(10')), 160.4 (C(2)), 150.7 (C(6)), 134.0 (C(13) and C(13')), 132.1 (C(11) and C(11')), 129.8 (C(4)), 123.2 (C(12) and C(12')), 105.5 (C(3) or C(5)), 102.0

(C(3) or C(5)), 99.7 (C(1)), 69.3 (OCH₂) 50.3 (C(9)), 38.3 (NCH₃), 36.0 (C(7)) 26.0 (C(8)) 22.7 (CH₂CH₃), 10.6 (CH₂CH₃); LRMS *m/z* (ES⁺) 353 ([M+H]⁺, 100%), HRMS *m/z* (ES⁺) [Found: (M+H)⁺ 353.1859, C₂₁H₂₅O₃N₂⁺ requires 353.1860]; RP-HPLC: Method A: Retention time 11.12 min, purity 99.7%.

***N*-[3-((3-(1,3-Dioxoisindolin-2-yl)propyl)(methyl)amino)phenyl]acetamide (121)**

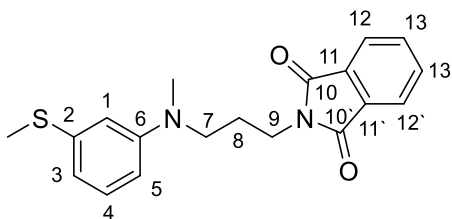


A suspension of *N*-[3-((3-(1,3-Dioxoisindolin-2-yl)propyl)amino)phenyl]acetamide **116** (1.00 g, 2.96 mmol, 1.0 eq), iodomethane (203 μ L, 463 mg, 3.26 mmol, 1.1 eq), K₂CO₃ (491 mg, 3.55 mmol, 1.2 eq) in DMF (10 mL) was stirred at 85 °C for 2 h. After this time the reaction was judged to be complete by TLC analysis. After cooling to ambient temperature the suspension was diluted with EtOAc (50 mL) and H₂O (50 mL). The organic extracts were washed with brine (3 \times 100 mL), dried (MgSO₄), filtered, and concentrated *in vacuo*. The crude material was purified by silica gel chromatography, eluting with a gradient of 50% to 80% of EtOAc in petroleum ether, to afford **121** as a yellow oil (410 mg, 1.17 mmol, 29% over 2 steps): R_f: 0.36 (petroleum ether: EtOAc 1:2); ν_{max} (thin film)/cm⁻¹ 3371 (w) (N-H), 2982 (w), 1704 (s) (C-O), 1608 (m), 1496 (m), 1396 (m), 1369 (m), 909 (m), 717 (s); ¹H NMR (500 MHz, CDCl₃): δ 7.86-7.82 (2H, m, C(12)*H* and C(12')*H*), 7.74-7.69 (2H, m, C(13)*H* and C(13')*H*), 7.17-7.10 (2H, m, NHAc & C(4)*H*), 6.98-6.93 (1H, m, C(1)*H*), 6.79-6.74 (1H, m, C(3)*H*), 6.47-6.42 (1H, m, C(5)*H*), 3.73 (2H, t, *J* 7.4, C(9)*H*₂), 3.38 (2H, t, *J* 7.4, C(7)*H*₂), 2.93 (3H, s, NCH₃), 2.15 (3H, s, COCH₃), 1.92 (2H, tt, *J* 7.3, 7.3 C(8)*H*₂); ¹³C NMR (126 MHz, CDCl₃): δ 168.40 (C(10) and C(10')), 168.2 (CONH), 149.8 (C(6)), 139.0 (C(2)), 134.0 (C(13) and C(13')), 132.1 (C(11) and C(11')), 129.6 (C(4)), 123.3 (C(12) and C(12')), 108.6 (C(5)), 108.0 (C(3)), 104.0 (C(1)), 50.3 (C(9)), 38.4 (NCH₃), 36.0 (C(7)), 26.0 (C(8)), 24.8 (CH₃CO); LRMS *m/z* (ES⁺) 352 ([M+H]⁺, 100%);

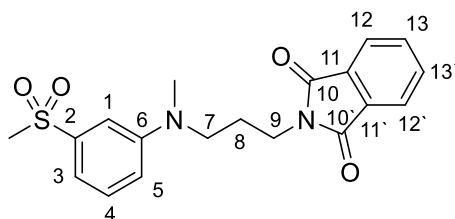
HRMS m/z (ES^+) [Found: $(M+H)^+$ 352.1657 $C_{20}H_{22}O_3N_3^+$ requires 352.1656], RP-HPLC:

Method A: Retention time 8.84 min, purity 97.8%.

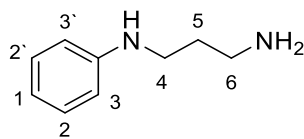
2-(3-(Methyl(3-(methylthio)phenyl)amino)propyl)isoindoline-1,3-dione (**122**)



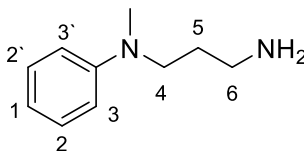
A suspension of 2-(3-((3-(Methylthio)phenyl)amino)propyl)isoindoline-1,3-dione **117** (800 mg, 2.45 mmol, 1.0 eq), iodomethane (183 μ L, 417 mg, 2.94 mmol, 1.2 eq), K_2CO_3 (225 mg, 1.63 mmol, 1.2 eq) in DMF (6 mL) was stirred at 85 $^\circ$ C for 5 h. After this time the reaction was judged to be complete by TLC analysis. After cooling to ambient temperature the suspension was dissolved with EtOAc (100 mL) and H_2O (50 mL). The organic extracts were washed with brine (3 \times 50 mL), dried ($MgSO_4$), filtered, and concentrated *in vacuo*. The crude material was purified by silica gel chromatography eluting with a gradient of 10% to 25% of EtOAc in petroleum ether to afford **121** as a yellow oil (590 mg, 1.73 mmol, 71%): R_f : 0.35 (petroleum ether: EtOAc 3:1); ν_{max} (thin film)/ cm^{-1} 2922 (w), 1704 (s) (C-O), 1585 (m), 753 (m), 717 (s); 1H NMR (400 MHz, $CDCl_3$): δ 7.86-7.80 (2H, m, C(12)*H* and C(12')*H*), 7.73-7.68 (2H, m, C(13)*H* and C(13')*H*), 7.11 (1H, dd, J 8.0, 8.0 C(4)*H*), 6.60-6.54 (2H, m, C(3)*H* and C(1)*H*), 6.50-6.48 (1H, m, C(5)*H*), 3.72 (2H, t, J 7.3, C(9)*H*₂), 3.37 (2H, t, J 7.3, C(7)*H*₂), 2.92 (3H, s, NCH_3), 2.43 (3H, s, SCH_3), 1.97 (2H, tt, J 7.3, 7.3 C(8)*H*₂); ^{13}C NMR (101 MHz, $CDCl_3$): δ 168.3 (C(10) and C(10')), 149.5 (C(6)), 139.2 (C(2)), 134.0 (C(13) and C(13')), 132.1 (C(11) and C(11')), 129.5 (C(4)), 123.2 (C(12) and C(12')), 114.7 (C(3)), 110.6 (C(1)), 109.7 (C(5)), 50.2 (C(7)), 38.3 (NCH_3), 36.0 (C(9)), 26.0 (C(8)), 15.9 (SCH_3); LRMS m/z (ES^+) 341 ($[M+H]^+$, 100%), HRMS m/z (ES^+) [Found: $(M+H)^+$ 341.1318, $C_{19}H_{21}O_2N_2S^+$ requires 341.1318]; RP-HPLC: Method A: Retention time 11.07 min, purity 97.3%.

2-(3-(Methyl(3-(methylsulfonyl)phenyl)amino)propyl)isoindoline-1,3-dione (123)

2-(3-(Methyl(3-(methylthio)phenyl)amino)propyl)isoindoline-1,3-dione **122** (250 mg, 0.734 mmol, 1.0 eq) was dissolved in CH_2Cl_2 (25 mL) and cooled to 0 °C. *m*CPBA (525 mg, 2.13 mmol, 3.0 eq) was added in 4 portions over 10 minutes. The solution was stirred for 2 h at 0 °C until TLC and MS indicated complete oxidation of the starting material. $\text{B}_2(\text{OH})_4$ (75 mg, 0.734 mmol, 1.0 eq) and MeOH (1 mL) was added and the colourless reaction mixture was stirred overnight. After this time the solution was adsorbed onto Celite® and purified by silica gel chromatography, eluting with a gradient of 10% to 100% of EtOAc in petroleum ether, to afford **123** as a pale yellow oil (204 mg, 0.548 mmol, 75%): R_f : 0.30 (petroleum ether: EtOAc 1:1); ν_{max} (thin film)/ cm^{-1} 2929 (w), 1704 (s) (C-O), 1597 (m), 1497 (m), 1373 (m), 1299 (s) (S=O), 1143 (s) (S=O), 719 (s); ^1H NMR (500 MHz, CDCl_3): δ 7.86-7.81 (2H, m, C(12)*H* and C(12')*H*), 7.74-7.70 (2H, m, C(13)*H* and C(13')*H*), 7.34 (1H, dd, J 8.0, 8.0 C(4)*H*), 7.20-7.16 (1H, m, C(5)*H*), 7.15-7.12 (1H, m, C(1)*H*), 6.90-6.86 (1H, m, C(3)*H*), 3.74 (2H, t, J 7.3, C(9)*H*₂), 3.45 (2H, t, J 7.3, C(7)*H*₂), 3.03 (3H, s, SO_2CH_3), 3.00 (3H, s, NCH_3), 1.99 (2H, tt, J 7.3, 7.3 C(8)*H*₂); ^{13}C NMR (126 MHz, CDCl_3): δ 168.3 (C(10) and C(10')), 149.4 (C(6)), 141.3 (C(2)), 134.1 (C(13) and C(13')), 131.9 (C(11) and C(11')), 130.1 (C(4)), 123.3 (C(12) and C(12')), 116.6 (C(3)), 114.3 (C(5)), 109.8 (C(1)), 50.0 (C(7)), 44.4 (C(SO_2CH_3)), 38.4 (NCH_3), 35.7 (C(9)), 25.7 (C(8)); LRMS m/z (ES^+) 373 ($[\text{M}+\text{H}]^+$, 100%), HRMS m/z (ES^+) [Found: $(\text{M}+\text{H})^+$ 373.1216, $\text{C}_{19}\text{H}_{21}\text{O}_4\text{N}_2\text{S}^+$ requires 373.1216]; RP-HPLC: Method A: Retention time 11.71 min, purity 98.0%.

N¹-Phenylpropane-1,3-diamine (125)

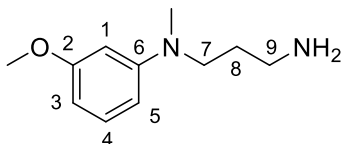
2-(3-(Phenylamino)propyl)isoindoline-1,3-dione **113** (300 mg, 1.07 mmol, 1.0 eq) was reacted according to general procedure 3. The crude material was purified by silica gel chromatography, eluting with CH₂Cl₂/MeOH/Et₃N (100:10:1), to yield **125** as a colourless oil (155 mg, 0.907 mmol, 96%): R_f: 0.17 (CH₂Cl₂: MeOH: Et₃N 100:10:1); ν_{\max} (thin film)/cm⁻¹ 3285 (w) (N-H), 3050 (w) (N-H); 2929 (m), 2859 (m), 1601 (s), 1501 (m), 1319 (m), 1259 (m), 746 (s), 692 (s); ¹H NMR (400 MHz, CDCl₃): δ 7.21-7.14 (2H, m, C(2)H and C(2')H), 6.69 (1H, tt, *J* 7.2, 1.1, C(1)H), 6.64-6.59 (2H, m, C(3)H and C(3')H), 3.20 (2H, d, *J* 6.7, C(4)H₂), 2.86 (2H, d, *J* 6.7, C(3)H₂), 1.75 (2H, tt, *J* 6.7, 6.7, C(6)H₂); LRMS *m/z* (ES⁺) 295 ([M+H]⁺, 100%). These data are in accordance with the literature.¹⁸²

N¹-Methyl-N¹-phenylpropane-1,3-diamine (126)

2-(3-(Methyl(phenyl)amino)propyl)isoindoline-1,3-dione **118** (300 mg, 1.02 mmol, 1.0 eq) was reacted according to general procedure 3. The crude material was purified by silica gel chromatography, eluting with CH₂Cl₂/MeOH/Et₃N (100:10:1), to afford **126** as a colourless oil (105 mg, 0.640 mmol, 64%): R_f: 0.33 (petroleum ether: EtOAc 5:2); ν_{\max} (thin film)/cm⁻¹ 2927 (m), 2863 (m), 1597 (s), 1504 (s), 1368 (m), 745 (s), 691 (s); ¹H NMR (500 MHz, CDCl₃): δ 7.25-7.19 (2H, m, C(2)H and C(2')H), 6.74-6.70 (2H, m, C(3)H and C(3')H), 6.69 (1H, tt, *J* 7.3, 1.0, C(1)H), 3.39 (2H, t, *J* 7.2, C(4)H₂), 2.93 (3H, s, NCH₃), 3.39 (2H, t, *J* 7.2, C(6)H₂), 1.98 (2H, tt, *J* 7.2, 7.2, C(5)H₂); ¹³C NMR (126 MHz, CDCl₃): δ 149.4 (C_{Ar}N), 129.2 (C(2) and C(2')), 116.2 (C(3) and C(3')), 112.3 (C(1)), 50.4 (C(4)), 40.0

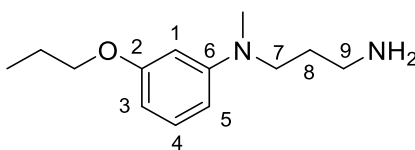
(C(6)), 38.4 (CH₃N), 30.5 (C(5)); LRMS m/z (ES⁺) 281 ([M+H]⁺, 100%), HRMS m/z (ES⁺) [Found: (M+H)⁺ 281.1283, C₁₇H₁₇O₂N₂⁺ requires 281.1283].

***N*¹-(3-Methoxyphenyl)-*N*¹-methylpropane-1,3-diamine (127)**



2-(3-((3-Methoxyphenyl)(methyl)amino)propyl)isoindoline-1,3-dione **119** (159 mg, 0.490 mmol, 1.0 eq) was reacted according to general procedure 3 for 1.5 h. The crude material was purified *via* an acid base extraction, to yield **127** as a yellow oil (81 mg, 0.384 mmol, 85%): R_f: 0.00 (EtOAc), ν_{\max} (thin film)/cm⁻¹ 2936 (m), 1610 (s), 1573 (s), 1500 (s), 1239 (m); ¹H NMR (400 MHz, CDCl₃): δ 7.12 (1H, dd, *J* 8.4, 8.4, C(4)*H*), 6.34 (1H, ddd, *J* 8.4, 2.3, 1.0, C(5)*H*), 6.27-6.22 (2H, m, C(3)*H*) and C(1)*H*), 3.77 (3H, s, OCH₃), 3.35 (2H, t, *J* 7.3, C(7)*H*₂), 2.90 (3H, s, NCH₃), 2.72 (2H, t, *J* 7.3, C(9)*H*₂), 1.70 (2H, tt, *J* 7.3, 7.3, C(8)*H*₂); ¹³C NMR (101 MHz, CDCl₃): δ 160.6 (C(2)), 150.5 (C(6)), 129.6 (C(4)), 105.2 (C(5)), 100.5 (C(3)), 98.6 (C(1)), 54.9 (OCH₃), 50.1 (C(7)), 39.8 (C(9)), 38.2 (NCH₃), 30.6 (C(8)); LRMS m/z (ES⁺) 195 ([M+H]⁺, 100%), HRMS m/z (ES⁺) [Found: (M+H)⁺ 195.1491 C₁₁H₁₉O₁N₂⁺ requires 195.1492].

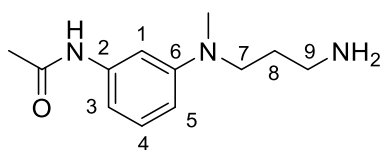
***N*¹-(3-Propoxyphenyl)-*N*¹-methylpropane-1,3-diamine (128)**



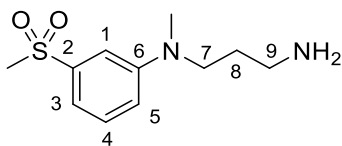
2-(3-((3-Propoxyphenyl)(methyl)amino)propyl)isoindoline-1,3-dione **120** (179 mg, 0.507 mmol, 1.0 eq) was reacted according to general procedure 3. The crude material was purified *via* an acid base extraction, to yield **128** as a yellow oil (100 mg, 0.450 mmol, 89%): R_f: 0.00 (EtOAc), ν_{\max} (thin film)/cm⁻¹ 2933 (m), 1610 (s), 1572 (s), 1499 (s), 1236 (m), 1169 (m); ¹H NMR (400 MHz, CDCl₃): δ 7.11 (1H, dd, *J* 8.1, 8.1, C(4)*H*), 6.31 (1H, dd, *J* 8.1, 2.5 C(3)*H*), 6.28-6.23 (2H, m, C(5)*H* and C(1)*H*), 3.91 (2H, t, *J* 6.7, OCH₂) 3.35 (2H, t,

J 7.3, C(7) H_2), 2.91 (3H, s, NCH₃), 2.75 (2H, t, J 7.3, C(9) H_2), 1.79 (2H, qt, J 6.7, 6.7, C(8) H_2), 1.72 (2H, tt, J 7.3, 7.3, CH₂CH₃), 1.03 (3H, t, J 6.7, CH₃); ¹³C NMR (101 MHz, CDCl₃) 160.4 (C(2)), 150.8 (C(6)), 129.8 (C(4)), 105.4 (C(3)), 101.6 (C(5)), 99.5 (C(1)), 69.3 (OCH₂) 50.4 (C(9)), 40.1 (C(7)), 38.3 (NCH₃), 30.9 (C(8)), 22.7 (CH₂CH₃), 10.6 (CH₂CH₃); LRMS m/z (ES⁺) 223 ([M+H]⁺, 100%); HRMS m/z (ES⁺) [Found: (M+H)⁺ 223.1805, C₁₃H₂₃O₁N₂⁺ requires 223.1805].

***N*-((3-((3-Aminopropyl)(methyl)amino)phenyl)acetamide (129)**

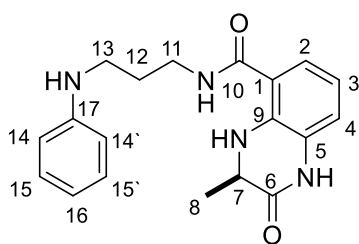


N-((3-((3-(1,3-Dioxoisindolin-2-yl)propyl)(methyl)amino)phenyl)acetamide **121**
(250 mg, 0.710 mmol, 1.0 eq) was reacted according to general procedure 3. The crude material was purified *via* an acid base extraction, to yield **129** as a colourless oil (78 mg, 0.352 mmol, 50%): R_f: 0.00 (petroleum ether: EtOAc 1:1); ν_{\max} (thin film)/cm⁻¹ 3289 (br, m) (N-H), 2931 (w), 1609 (s) (C-O), 1581 (s), 1554 (s), 1497 (s), 1274 (m); ¹H NMR (400 MHz, CDCl₃): δ 7.80 (1H, s, NHAc), 7.14-7.05 (2H, m, C(1) H & C(4) H), 6.71-6.65 (1H, m, C(3) H), 6.45-6.39 (1H, m, C(5) H), 3.73 (2H, t, J 7.4, C(9) H_2), 3.33 (2H, t, J 7.2, C(7) H_2), 2.88 (3H, s, NCH₃), 2.72 (2H, t, J 7.2, C(9) H_2), 2.11 (3H, s, COCH₃), 1.70 (2H, tt, J 7.2, 7.2 C(8) H_2); ¹³C NMR (101 MHz, CDCl₃): δ 168.5 (CONH), 149.9 (C(6)), 139.1 (C(2)), 129.4 (C(4)), 108.2 (C(5)), 107.6 (C(3)), 103.9 (C(1)), 50.2 (C(7)), 39.8 (C(7)), 38.2 (NCH₃), 30.4 (C(8)), 24.5 (CH₃CO); LRMS m/z (ES⁺) 222 ([M+H]⁺, 100%); HRMS m/z (ES⁺) [Found: (M+H)⁺ 222.1601 C₁₂H₂₀ON₃⁺ requires 222.1601].

***N*¹-Methyl-*N*¹-(3-(methylsulfonyl)phenyl)propane-1,3-diamine (130)**

2-(3-(Methyl(3-(methylsulfonyl)phenyl)amino)propyl)isoindoline-1,3-dione **123**

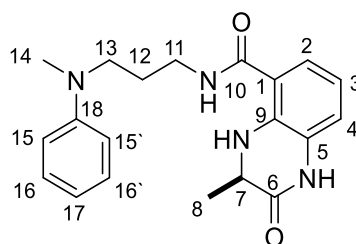
(200 mg, 0.537 mmol, 1.0 eq) was reacted according to general procedure 3. The crude material was purified *via* an acid base extraction, to yield **130** as a colourless oil (93 mg, 0.384 mmol, 71%): *R*_f: 0.00 (petroleum ether: EtOAc 1:1); ν_{max} (thin film)/cm⁻¹ 3363 (br, m) (N-H), 2926 (w), 1597 (s), 1498 (s), 1373 (m), 1292 (s) (S=O), 1097 (s) (S=O); ¹H NMR (400 MHz, CDCl₃): δ 7.33 (1H, dd, *J* 8.0, 8.0 C(4)*H*), 7.18-7.11 (2H, m, C(5)*H* & C(1)*H*), 6.91-6.86 (1H, m, C(3)*H*), 3.43 (2H, t, *J* 7.2 C(7)*H*₂), 3.01 (3H, s, SO₂CH₃), 2.97 (3H, s, NCH₃), 2.73 (2H, t, *J* 7.2, C(9)*H*₂), 1.70 (2H, tt, *J* 7.2, 7.2 C(8)*H*₂); ¹³C NMR (101 MHz, CDCl₃): δ 149.6 (C(6)), 141.3 (C(2)), 130.1 (C(4)), 116.3 (C(3)), 113.7 (C(5)), 109.5 (C(1)), 49.9 (C(7)), 44.3 (C(SO₂CH₃)), 39.6 (C(9)), 38.3 (NCH₃), 30.4(C(8)); LRMS *m/z* (ES⁺) 243 ([M+H]⁺, 100%); HRMS *m/z* (ES⁺) [Found: (M+H)⁺ 243.1162, C₁₁H₁₉O₂N₂S⁺ requires 243.1162].

(*R*)-3-Methyl-2-oxo-*N*-(3-(phenylamino)propyl)-1,2,3,4-tetrahydroquinoxaline-5-carboxamide (98)

[(*R*)-3-methyl-2-oxo-1,2,3,4-tetrahydroquinoxaline-5-carboxylic acid] (*R*)-**32** (40 mg, 0.194 mmol, 1.0 eq) and *N*¹-phenylpropane-1,3-diamine **125** (44 mg, 0.291 mmol, 1.5 eq) were reacted according to general procedure 4 for 15 h. The crude material was purified by silica gel chromatography, eluting with a gradient of 30% to 80% EtOAc in petroleum ether, to yield **98** as a colourless solid (28 mg, 0.083 mmol, 43%). *R*_f: 0.19 (petroleum ether: EtOAc 1:3); mp 163-165 °C (EtOAc); ν_{max} (thin film)/cm⁻¹ 3293 (m) (N-H), 3058 (w)

(N-H), 2948 (w), 1679 (s) (C-O), 1632 (m) (C-O), 1600 (m), 1542 (m), 1494 (m), 1294 (m), 1249 (m), 765 (s), 696 (m); ^1H NMR (500 MHz, $(\text{CD}_3)_2\text{SO}$): δ 10.36 (1H, s, C(5)NH), 8.42 (1H, t, J 5.7, C(11)NH), 7.81 (1H, s, C(7)NH), 7.28 (1H, dd, J 8.1, 1.1, C(4)H), 7.08-7.22 (2H, m, C(15)H and C(15')H), 6.85 (1H, dd, J 7.7, 0.9, C(2)H), 6.63 (1H, dd, J 7.9, 7.9, C(3)H), 6.57-6.53 (2H, m, C(14)H and C(14')H), 6.50 (1H, tt, J 7.3, 0.9, C(16)H), 5.54 (1H, t, J 5.5, C(13)NH), 3.93 (1H, qd, J 7.3, 1.6 C(7)H), 3.35-3.28 (2H, m, C(11)H₂), 3.07- 3.01 (2H, m, C(13)H₂), 1.78 (2H, tt, J 6.9, 6.9, C(12)H₂) 1.26 (3H, d, J 7.3, C(8)H₃); ^{13}C NMR (126 MHz, $(\text{CD}_3)_2\text{SO}$): δ 168.6 (C(10)), 168.3 (C(6)), 149.4(C(17)), 136.2 (C(9)), 129.3 (C(15) and C(15')), 127.9 (C(5)), 122.2 (C(4)), 117.4 (C(2)), 116.8 (C(3)), 116.1 (C(1)), 115.9 (C(16)), 112.4 (C(14) and C(14')), 50.6 (C(7)), 41.0 (C(11)), 37.5 (C(13)), 29.1 (C(12)), 18.6 (C(8)); LRMS m/z (ES⁺) 339 ([M+H]⁺, 100%), HRMS m/z (ES⁺) [Found: (M+H)⁺ 339.1817, C₁₉H₂₃O₂N₄⁺ requires 339.1816]; RP-HPLC: Method A: Retention time 8.16 min, purity 99.4%. Chiral HPLC (AD-H): Retention time 10.36 min, ee > 99%.

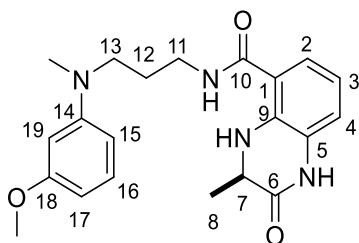
(R)-3-Methyl-N-(3-(methyl(phenyl)amino)propyl)-2-oxo-1,2,3,4-tetrahydroquinoxaline-5-carboxamide (99)



(R)-3-methyl-2-oxo-1,2,3,4-tetrahydroquinoxaline-5-carboxylic acid] (**R**)-**32** (40 mg, 0.194 mmol, 1.0 eq) and *N*¹-methyl-*N*¹-phenylpropane-1,3-diamine **126** (48 mg, 0.291 mmol, 1.5 eq) were reacted according to general procedure 4 for 15 h. The crude was purified by silica gel chromatography, eluting with a gradient of 30% to 80% EtOAc in petroleum ether, to yield **99** as a yellow solid (32 mg, 0.091 mmol, 47%): R_f : 0.44 (petroleum ether: EtOAc 1:3); mp 61-62 °C (EtOAc); $[\alpha]_D^{25}$ -29.2 (c 0.5 in CHCl₃), ν_{max} (thin film)/cm⁻¹ 3321 (w br) (N-H), 1680 (s) (C-O), 1632 (m); 1598 (s), 1529 (m), 1505 (s), 1481 (m), 1373 (m), 1284 (s), 846 (s), 745 (s); ^1H NMR (500 MHz, $(\text{CD}_3)_2\text{SO}$): δ 10.37 (1H,

s, C(5)NH), 8.43 (1H, t, J 5.5, C(11)NH), 7.81 (1H, s, C(7)NH), 7.29 (1H, dd, J 7.8, 1.1, C(4)H), 7.17-7.11 (2H, m, C(16)H and C(16')H), 6.86 (1H, dd, J 7.8, 0.9, C(2)H), 6.71-6.67 (2H, m, C(15)H and C(15')H), 6.65 (1H, dd, J 7.8, 7.8, C(3)H), 6.59 (1H, tt, J 7.2, 0.9, C(17)H), 3.94 (1H, dd, J 6.6, 1.6, C(7)H), 3.40-3.35 (2H, m, C(11)H₂), 3.30- 3.24 (2H, m, C(13)H₂), 2.88 (3H, s, C(14)H₃) 1.76 (2H, tt, J 7.1, 7.1, C(12)H₂), 1.26 (3H, d, J 6.6, C(8)H₃); ¹³C NMR (126 MHz, (CD₃)₂SO): δ 168.6 (C(10)), 168.3 (C(6)), 149.4(C(18)), 136.2 (C(9)), 129.5 (C(16) and C(16')), 127.9 (C(5)), 122.2 (C(4)), 117.4 (C(2)), 116.8 (C(3)), 116.1 (C(1)), 116.0 (C(17)), 112.4 (C(15) and C(15')), 50.6 (C(7)), 50.0 (C(13)), 38.4 (C(14)), 37.4 (C(11)), 29.6 (C(12)), 18.6 (C(8)); LRMS m/z (ES⁺) 353 ([M+H]⁺, 100%), HRMS m/z (ES⁺) [Found: (M+H)⁺ 353.1971 C₂₀H₂₅O₂N₄⁺ requires 353.1972]; RP-HPLC: Method A: Retention time 11.96 min, purity 94.8%; Chiral HPLC (AD-H): Retention time 9.79 min, ee > 99%.

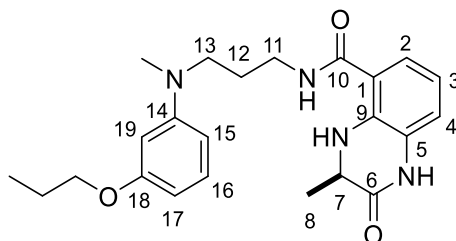
(*R*)-*N*-(3-((3-Methoxyphenyl)(methyl)amino)propyl)-3-methyl-2-oxo-1,2,3,4-tetrahydroquinoxaline-5-carboxamide (100)



[(*R*)-3-methyl-2-oxo-1,2,3,4-tetrahydroquinoxaline-5-carboxylic acid] (*R*)-**32** (40 mg, 0.194 mmol, 1.0 eq) and *N*¹-(3-methoxyphenyl)-*N*¹-methylpropane-1,3-diamine **127** (41 mg, 0.211 mmol, 1.1 eq) were reacted according to general procedure 4 for 20 h. The crude material was purified by silica gel chromatography, eluting with a gradient of 50% to 80% EtOAc in petroleum ether, to yield **100** as a yellow oil (36 mg, 0.094 mmol, 49%): R_f : 0.48 (petroleum ether: EtOAc 1:3); $[\alpha]_D^{25}$ -35.5 (c 0.4 in MeOH), ν_{\max} (thin film)/cm⁻¹ 3656 (w), 3219 (w) 2981 (s) (C-H), 2886 (m) (C-H), 1680 (s) (C=O), 1632 (s) (C=O), 1602 (s), 1379 (s), 1244 (s), 1169 (s); ¹H NMR (500 MHz; (CD₃)₂CO): δ 9.34 (1H, br s, C(5)NH), 8.06 (1H, br s, C(7)NH), 7.80 (1H, br t, J 5.4 C(10)NH), 7.33 (1H, dd, J 8.0, 1.3, C(4)H), 7.09 (1H, dd, J 8.2, 8.2, C(16)H), 7.01-6.97 (1H, m, C(2)H), 6.68 (1H, dd, J 8.0, 8.0 C(3)H), 6.38

(1H, ddd, J 8.2, 2.4, 0.5, C(15) H), 6.30 (1H, dd, J 2.4, 2.4, C(19) H), 6.26 (1H, ddd, J 8.2, 2.4, 0.5, C(17) H), 4.05 (1H, qd, J 6.7, 1.5 Hz, C(7) H), 3.75 (3H, s, OCH₃), 3.51-3.46 (4H, m, C(13) H_2 and C(11) H_2), 2.98 (3H, s, NCH₃), 1.94 (2H, tt, J 7.3, 7.3 C(12) H_2) 1.42 (3H, d, J 6.7 Hz, C(8) H_3), ¹³C NMR (126 MHz; (CD₃)₂CO): δ 168.5 (C(10)), 167.7 (C(6)), 161.0 (C(18)), 150.8 (C(14)), 136.5 (C(9)), 129.6 (C(16)), 127.9 (C(5)), 121.3 (C(4)), 116.9 (C(2)), 116.6 (C(3)), 116.0 (C(1)), 105.2 (C(15)), 101.2 (C(17)), 98.5 (C(19)), 54.2 (OCH₃), 50.7 (C(7)), 50.1 (C(13)), 37.7 (NCH₃), 37.2 (C(11)), 26.7 (C(12)), 17.8 (C(8)); LRMS m/z (ES⁺) 383 ([M+H]⁺, 100%); HRMS m/z (ES⁺) [Found: (M+H)⁺ 383.2079 C₂₁H₂₇N₄O₃ requires 383.2079]; RP-HPLC: Method A: Retention time 8.60 min, purity 99.5%. Chiral HPLC (AD-H): Retention time 9.27 min, ee > 99.

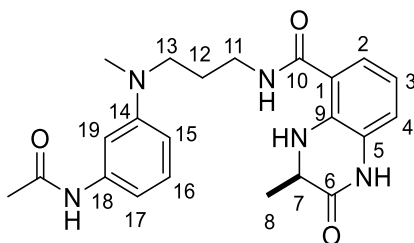
(*R*)-*N*-(3-((3-Propoxyphenyl)(methyl)amino)propyl)-3-methyl-2-oxo-1,2,3,4-tetrahydroquinoxaline-5-carboxamide (101)



[(*R*)-3-methyl-2-oxo-1,2,3,4-tetrahydroquinoxaline-5-carboxylic acid] (**R**-**32** (40 mg, 0.194 mmol, 1.0 eq) and *N*¹-(3-propoxyphenyl)-*N*¹-methylpropane-1,3-diamine **128** (47 mg, 0.211 mmol, 1.1 eq) were reacted according to general procedure 4 for 20 h. The crude material was purified by silica gel chromatography, eluting with a gradient of 50% to 70% EtOAc in petroleum ether, to yield **101** as a pale yellow solid (52 mg, 0.127 mmol, 60%): R_f : 0.59 (petroleum ether: EtOAc 1:3); mp 108-109 °C (acetone), $[\alpha]_D^{25}$ -55.5 (c 0.2 in MeOH), ν_{\max} (thin film)/cm⁻¹ 3657 (w) (N-H), 3308 (w br) (N-H), 3219 (w) (N-H), 2980 (m) (C-H), 2931 (s) (C-H); 1681 (s) (C=O), 1628 (m), 1612 (s) (C=O), 1528 (s), 1499 (s), 1379 (s), 1285 (s), 1243 (s), 1172 (s), 740 (s); ¹H NMR (500 MHz; (CD₃)₂CO): δ 9.37 (1H, br s, C(5) NH), 8.06 (1H, br s, C(7) NH), 7.81 (1H, br t, J 5.3 C(10) NH), 7.34 (1H, dd, J 8.1, 1.2, C(4) H), 7.07 (1H, dd, J 8.2, 8.2, C(16) H), 7.01-6.98 (1H, m, C(2) H), 6.68 (1H, dd, J 8.1, 8.1

C(3)*H*), 6.37 (1*H*, dd, *J* 8.1, 2.5, C(15)*H*), 6.30 (1*H*, dd, *J* 2.5, 2.5, C(19)*H*), 6.25 (1*H*, dd, *J* 8.1, 2.5, C(17)*H*), 4.05 (1*H*, qd, *J* 6.8, 1.4 Hz, C(7)*H*), 3.91 (2*H*, t, *J* 7.2, OCH₂), 3.51-3.46 (4*H*, m, C(13)*H*₂ and C(11)*H*₂), 2.97 (3*H*, s, NCH₃), 1.94 (2*H*, tt, *J* 7.2, 7.2 C(12)*H*₂), 1.76 (2*H*, qt, *J* 7.2, 7.2 CH₂CH₃), 1.42 (3*H*, d, *J* 6.7 Hz, C(8)*H*₃), 1.02 (3*H*, d, *J* 7.2 Hz, C(8)*H*₃), ¹³C NMR (126 MHz; (CD₃)₂CO): δ 168.5 (C(10)), 167.8 (C(6)), 160.5 (C(18)), 150.8 (C(14)), 136.5 (C(9)), 129.6 (C(16)), 127.9 (C(5)), 121.3 (C(4)), 116.9 (C(2)), 116.6 (C(3)), 116.0 (C(1)), 105.1 (C(15)), 101.9 (C(17)), 99.0 (C(19)), 68.7 (OCH₂), 50.7 (C(7)), 50.1 (C(13)), 37.7 (NCH₃), 37.2 (C(11)), 26.7 (C(12)), 22.5 (CH₂CH₃), 17.8 (C(8)), 10.0 (CH₂CH₃), LRMS *m/z* (ES⁺) 411 ([M+H]⁺, 100%); HRMS *m/z* (ES⁺) [Found: (M+H)⁺ 411.2376, C₂₃H₃₁N₄O₃ requires 411.2391]; RP-HPLC: Method A: Retention time 9.80 min, purity 98.0%. Chiral HPLC (AD-H): Retention time 8.60 min, ee > 99%.

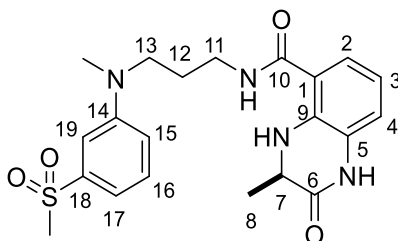
(*R*)-*N*-(3-((3-Acetamidophenyl)(methyl)amino)propyl)-3-methyl-2-oxo-1,2,3,4-tetrahydroquinoxaline-5-carboxamide (102)



[(*R*)-3-methyl-2-oxo-1,2,3,4-tetrahydroquinoxaline-5-carboxylic acid] (*R*)-**32** (40 mg, 0.194 mmol, 1.0 eq) and *N*-(3-((3-aminopropyl)(methyl)amino)phenyl)acetamide **129** (78 mg, 0.332 mmol, 1.7 eq) were reacted according to general procedure 4 for 17 h. The crude material was purified by silica gel chromatography, eluting with a gradient of 70% to 100% EtOAc in petroleum ether, to afford **102** (60 mg, 0.147 mmol, 76%) as a colourless solid. *R*_f: 0.32 (EtOAc); [α]_D²⁵ -46.3 (*c* 0.3 in MeOH), *v*_{max} (thin film)/cm⁻¹ 3656 (w) (N-H), 3309 (br, w) (N-H), 2981 (m), 1679 (s) (C=O), 1609 (s), 1378 (s); ¹H NMR (500 MHz; (CD₃)₂CO): δ 9.37 (1*H*, br s, C(5)*NH*), 8.98 (1*H*, s, *NHAc*), 8.03 (1*H*, br s, C(7)*NH*), 7.79 (1*H*, br t, *J* 5.3 C(10)*NH*), 7.33 (1*H*, dd, *J* 8.1, 1.2, C(4)*H*), 7.23 (1*H*, dd, *J* 2.1, 2.1, C(19)*H*), 7.07 (1*H*, dd, *J* 8.1, 8.1, C(16)*H*), 6.99-6.95 (1*H*, m, C(2)*H*), 6.90-6.85 (1*H*, m,

C(17)*H*), 6.66 (1H, dd, *J* 8.1, 8.1 C(3)*H*), 6.46 (1H, dd, *J* 8.5, 2.5, C(15)*H*), 4.02 (1H, qd, *J* 6.8, 1.4 Hz, C(7)*H*), 3.48-3.43 (4H, m, C(13)*H*₂ and C(11)*H*₂), 2.93 (3H, s, NCH₃), 2.07 (3H, s, CH₃CO), 1.93 (2H, tt, *J* 7.2, 7.2 C(12)*H*₂), 1.39 (3H, d, *J* 6.7 Hz, C(8)*H*₃); ¹³C NMR (126 MHz; (CD₃)₂CO): δ 168.6 (C(10)), 167.9 (COCH₃), 167.8 (C(6)), 149.9 (C(14)), 140.5 (C(18)), 136.5 (C(9)), 129.1 (C(16)), 127.9 (C(5)), 121.5 (C(4)), 117.0 (C(2)), 116.6 (C(3)), 116.0 (C(1)), 107.5 (C(15)), 107.2 (C(17)), 103.4 (C(19)), 50.8 (C(7)), 50.1 (C(13)), 37.7 (NCH₃), 37.3 (C(11)), 26.7 (C(12)), 23.5, 17.8 (C(8)); LRMS *m/z* (ES⁺) 410 ([M+H]⁺, 100%); HRMS *m/z* (ES⁺) [Found: (M+H)⁺ 410.2186, C₂₂H₂₈N₅O₃ requires 410.2187]; RP-HPLC: Method A: Retention time 8.09 min, purity 95.2%. Chiral HPLC (AD-H): Retention time 7.94 min, ee 90%.

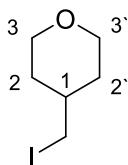
(*R*)-3-Methyl-*N*-(3-(methyl(3-(methylsulfonyl)phenyl)amino)propyl)-2-oxo-1,2,3,4-tetrahydroquinoxaline-5-carboxamide (103)



[(*R*)-3-methyl-2-oxo-1,2,3,4-tetrahydroquinoxaline-5-carboxylic acid] (*R*)-**32** (40 mg, 0.194 mmol, 1.0 eq) and *N*¹-methyl-*N*¹-(3-(methylsulfonyl)phenyl)propane-1,3-diamine **130** (93 mg, 0.384 mmol, 2.0 eq) were reacted according to general procedure 4 for 15 h. The crude material was purified by silica gel chromatography, eluting with a gradient of 50% to 100% EtOAc in petroleum ether, to yield **103** as a colourless solid (51 mg, 0.118 mmol, 61%): *R*_f: 0.15 (petroleum ether: EtOAc 1:2); [α]_D²⁵ -51.6 (*c* 0.3 in MeOH), mp 82-84 (acetone), ν_{max} (thin film)/cm⁻¹ 2927 (w), 1683 (s) (C=O), 1667 (s) (C=O), 1599 (s), 1539 (m), 1292 (s) (S=O), 1148 (s); ¹H NMR (500 MHz; (CD₃)₂CO): δ 9.42 (1H, br s, C(5)NH), 8.12 (1H, br s, C(7)NH), 7.91 (1H, br t, *J* 6.3 C(10)NH), 7.51 (1H, dd, *J* 8.0, 8.0 C(16)*H*), 7.43 (1H, dd, *J* 8.0, 1.1 C(4)*H*), 7.35-7.31 (1H, m, C(19)*H*), 7.28-7.24 (1H, m,

C(15)H or C(17)H), 7.16 (1H, dd, J 8.4, 2.4 C(15)H or C(17)H), 7.09-7.06 (1H, m, C(2)H), 6.77 (1H, dd, J 7.9, 7.9 C(3)H), 4.13 (1H, qd, J 6.7 1.4 Hz, C(7)H), 3.69 (2H, t, J 7.4 Hz, C(13)H₂), 3.59 (2H, td, J 7.4, 6.3, C(11)H₂), 3.174 (3H, s, NCH₃), 3.167 (3H, s, SO₂CH₃), 2.07 (2H, tt, J 7.3, 7.3 C(12)H₂) 1.50 (3H, d, J 6.7 Hz, C(8)H₃); ¹³C NMR (126 MHz; (CD₃)₂CO): δ 168.6 (C(10)), 167.7 (C(6)), 149.7 (C(14)), 142.3 (C(18)), 136.5 (C(9)), 129.9 (C(16)), 127.9 (C(5)), 121.4 (C(4)), 117.0 (C(2)), 116.6 (C(3)), 116.3 (C(15) or C(17)), 115.9 (C(9)), 113.6 (C(15) or C(17)), 109.5 (C(19)), 50.7 (C(7)), 49.8 (C(13)), 43.4 (SO₂CH₃), 37.7 (NCH₃), 37.1 (C(11)), 26.6 (C(12)), 17.8 (C(8)); LRMS m/z (ES⁺) 431 ([M+H]⁺, 100%); HRMS m/z (ES⁺) [Found: (M+H)⁺ 431.1745. C₂₁H₂₇N₄O₄S⁺ requires 431.1748]; RP-HPLC: Method A: Retention time 10.15 min, purity 97.6%. Chiral HPLC (AD-H): Retention time 11.6 min, ee > 99%.

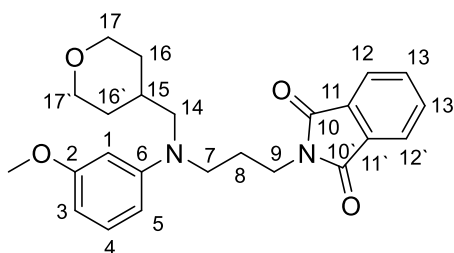
4-(Iodomethyl)tetrahydro-2H-pyran (**132**)



A solution of 2-tetrahydro-2H-pyran-4-yl **131** (3.50 g, 30.1 mmol, 1.0 eq), Et₃N (3.51 g, 34.7 mmol, 1.15 eq), and toluene (24 mL) was cooled to 0 °C. Methanesulfonyl chloride (2.57 mL, 3.80 g, 33.2 mmol, 1.1 eq) was added dropwise at 0 °C. The reaction mixture was warmed to ambient temperature and stirred for 2 hours. After this time the suspension was quenched with H₂O (50 mL). The organic components of the aqueous phase were extracted with toluene (25 mL). The combined organic extracts were dried (MgSO₄), filtered, and concentrated *in vacuo*. The residue was dissolved in acetone (28 mL), NaI (11.3 g, 75.3 mmol, 2.5 eq) added and stirred at 60 °C for 4 h. After this time the reaction was judged to be complete by TLC analysis. The black suspension was concentrated *in vacuo*. The black residue was dissolved in EtOAc (200 mL) and H₂O (100 mL). The organic layer was washed with 10% aq. Na₂S₂O₃ (100 mL), brine (2 × 100 mL), dried (MgSO₄), filtered, and concentrated *in vacuo* to afford **132** as a pale yellow oil (2.90 g, 12.9 mmol,

43%), which did not require further purification. R_f : 0.29 (petroleum ether:EtOAc 10:1); $^1\text{H NMR}$ (400 MHz, CDCl_3): δ 4.01-3.90 (2H, m, C(3) H_{AB}), 3.43-3.30 (2H, m, C(3) H_{AB}), 3.10 (2H, d, J 6.5, CH_2), 1.83-1.63 (3H, m, C(2) H and C(3) H_{AB}), 1.34-1.20 (2H, m, C(3) H_{AB}), LRMS m/z (ES^+) 227 ($[\text{M}+\text{H}]^+$, 100%). The data are in good agreement with the literature.¹⁸³

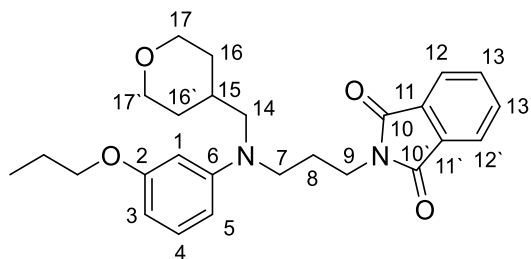
2-(3-((3-Methoxyphenyl)((tetrahydro-2H-pyran-4-yl)methyl)amino)propyl)-isoindoline-1,3-dione (133)



A suspension of 2-(3-((3-methoxyphenyl)amino)propyl)isoindoline-1,3-dione **105** (500 mg, 1.61 mmol, 1.0 eq), 4-(iodomethyl)tetrahydro-2H-pyran **132** (728 mg, 3.22 mmol, 2.0 eq), K_2CO_3 (334 mg, 2.42 mmol, 1.5 eq) in DMF (5 mL) were stirred at 85 °C for 20 h. After this time the reaction was judged to be complete by TLC analysis. After cooling to ambient temperature the suspension was diluted with EtOAc (100 mL), washed with brine (3 × 50 mL), dried (MgSO_4), filtered, and concentrated *in vacuo*. The crude material was purified by silica gel chromatography, eluting with a gradient of 10% to 40% of EtOAc in petroleum ether to give **133** as a yellow oil (283 mg, 0.693 mmol, 43%): R_f : 0.29 (petroleum ether: EtOAc 2:1); ν_{max} (thin film)/ cm^{-1} 2933 (w), 1707 (s) (C-O), 1609 (m), 1498 (m), 1395 (m), 718 (s); $^1\text{H NMR}$ (400 MHz, CDCl_3): δ 7.90-7.85 (2H, m, C(12) H and C(12') H), 7.78-7.74 (2H, m, C(13) H and C(13') H), 7.13 (1H, dd, J 8.0, 8.0, C(4) H), 6.31 (1H, dd, J 8.2, 2.5, C(3) H or C(5) H), 6.31 (1H, dd, J 8.2, 2.5, C(3) H or C(5) H), 6.21 (1H, dd, J 2.4, 2.4, C(1) H), 4.01-3.95 (2H, m, C(17) H_{AHB} and C(17') H_{AHB}), 3.79 (3H, s, OCH_3), 3.75 (2H, t, J 7.1, C(7) H_2), 3.43-3.29 (4H, m, C(9) H_2 , C(17) H_{AHB} and C(17') H_{AHB}), 3.18 (2H, d, J 7.2, C(14) H_2), 2.06-1.92 (3H, m, C(8) H_2 and C(15) H), 1.67-1.60 (2H, m, C(16) H_{AHB} and C(16') H_{AHB}), 1.39-1.25 (2H, m, C(16) H_{AHB} and C(16') H_{AHB}),

^{13}C NMR (101 MHz, CDCl_3): δ 168.4 (C(10) and C(10')), 160.8 (C(2)), 149.3 (C(6)), 134.1 (C(13) and C(13')), 132.0 (C(11) and C(11')), 130.0 (C(4)), 123.3 (C(12) and C(12')), 105.7 (C(5)), 100.8 (C(3)), 99.2 (C(1)), 67.8 (C(17) and C(17')), 57.4 (C(14)), 55.1 (OCH_3), 49.9 (C(7)), 35.9 (C(9)), 33.9 (C(15)), 31.1 (C(16) and C(16')), 26.0 (C(8)); LRMS m/z (ES^+) 409 [(M+H) $^+$, 100%], HRMS m/z (ES^+) [Found: (M+H) $^+$ 409.2123 $\text{C}_{24}\text{H}_{29}\text{O}_4\text{N}_2^+$ requires 409.2122], RP-HPLC: Method A: Retention time 10.80 min, purity 90.8%.

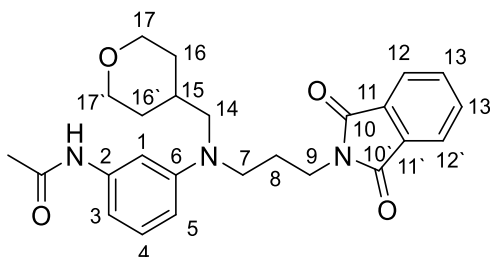
2-(3-((3-Propoxyphenyl)((tetrahydro-2H-pyran-4-yl)methyl)amino)propyl)-isoindoline-1,3-dione (134)



A suspension of 2-(3-((3-propoxyphenyl)amino)propyl)isoindoline-1,3-dione **106** (600 mg, 1.77 mmol, 1.0 eq), 4-(iodomethyl)tetrahydro-2H-pyran **132** (728 mg, 3.22 mmol, 1.8 eq), K_2CO_3 (334 mg, 2.42 mmol, 1.35 eq) in DMF (5 mL) was stirred at 85 °C for 15 h. After this time the reaction was judged to be complete by TLC analysis. After cooling to ambient temperature the suspension was diluted with EtOAc (50 mL), washed with brine (3 \times 50 mL), dried (MgSO_4), filtered and concentrated *in vacuo*. The crude material was purified by silica gel chromatography eluting with a gradient of 10% to 30% of EtOAc in petroleum ether to give **134** as a yellow oil (450 mg, 1.03 mmol, 58%): R_f : 0.43 (petroleum ether: EtOAc 2:1); ν_{max} (thin film)/ cm^{-1} 2932 (w), 1708 (s) (C-O), 1610 (m), 1499 (m), 1395 (m), 1366 (m), 720 (s); ^1H NMR (400 MHz, CDCl_3): δ 7.89-7.84 (2H, m, C(12) H and C(12') H), 7.76-7.73 (2H, m, C(13) H and C(13') H), 7.10 (1H, dd, J 8.2, 8.2, C(4) H), 6.28 (1H, dd, J 8.2, 2.5, C(3) H or C(5) H), 6.25 (1H, dd, J 8.2, 2.5, C(3) H or C(5) H), 6.21 (1H, dd, J 2.5, 2.5, C(1) H), 4.01-3.94 (2H, m, C(17) $H_{\text{A}}H_{\text{B}}$ and C(17') $H_{\text{A}}H_{\text{B}}$), 3.90 (2H, t, J 6.6, OCH_2), 3.74 (2H, t, J 7.2, C(7) H_2), 3.42-3.29 (4H, m, C(9) H_2 , C(17) $H_{\text{A}}H_{\text{B}}$ and C(17') $H_{\text{A}}H_{\text{B}}$), 3.17 (2H, d, J 7.3, C(14) H_2), 2.05-1.92 (3H, m, C(8) H_2 and C(15) H), 1.80 (2H,

qt, J 6.6, 6.6, CH_2CH_3), 1.67-1.60 (2H, m, C(16) H_AH_B and C(16') H_AH_B), 1.38-1.26 (2H, m, C(16) H_AH_B and C(16') H_AH_B), 1.04 (3H, t, J 6.6, CH_3CH_2), ^{13}C NMR (101 MHz, CDCl_3): δ 168.3 (C(10) and C(10')), 160.4 (C(2)), 149.4 (C(6)), 134.0 (C(13) and C(13')), 132.1 (C(11) and C(11')), 129.9 (C(4)), 123.3 (C(12) and C(12')), 105.7 (C(5)), 101.7 (C(3)), 99.9 (C(1)), 69.3 (OCH_2), 67.8 (C(17) and C(17')), 57.4 (C(14)), 49.8 (C(7)), 36.0 (C(9)), 33.9 (C(15) and C(15')), 31.1 (C(16) and C(16')), 26.1 (C(8)), 22.7 (CH_2CH_3), 10.6 (CH_3CH_2); LRMS m/z (ES^+) 437 ($[\text{M}+\text{H}]^+$, 100%), HRMS m/z (ES^+) [Found: ($\text{M}+\text{H})^+$ 437.2435, $\text{C}_{26}\text{H}_{33}\text{O}_4\text{N}_2^+$ requires 437.2435], RP-HPLC: Method A: Retention time 11.57 min, purity 98.4%.

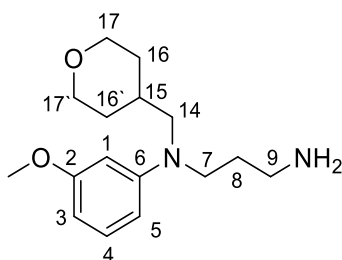
***N*-(3-((3-(1,3-Dioxoisindolin-2-yl)propyl)((tetrahydro-2*H*-pyran-4-yl)methyl)-amino)phenyl)acetamide (135)**



A suspension of *N*-(3-((3-(1,3-Dioxoisindolin-2-yl)propyl)amino)phenyl)acetamide **107** (1.00 g, 2.96 mmol, 1.0 eq), 4-(iodomethyl)tetrahydro-2*H*-pyran **132** (1.34 g, 5.93 mmol, 2.0 eq), K_2CO_3 (450 mg, 3.26 mmol, 1.1 eq) in DMF (10 mL) was stirred at 85 °C for 17 h. After this time the reaction was judged to be complete by TLC analysis. After cooling to rt the suspension was diluted with EtOAc (100 mL), washed with brine (3 × 50 mL), dried (MgSO_4), filtered and concentrated *in vacuo*. The crude material was purified by silica gel chromatography, eluting with a gradient of 80% to 90% of EtOAc in petroleum ether, to afford **135** as a yellow oil (144 mg, 0.321 mmol, 11%): R_f : 0.08 (petroleum ether: EtOAc 2:1); ν_{max} (thin film)/ cm^{-1} 3306 (w) (N-H), 2932 (w), 1706 (s) (C=O), 1609 (m), 1496 (m), 1396 (m), 1367 (m), 720 (s); ^1H NMR (400 MHz, CDCl_3): δ 7.86-7.80 (2H, m, C(12) H and C(12') H), 7.74-7.69 (2H, m, C(13) H and C(13') H), 7.35 (1H, br s, NH), 7.08 (1H, dd, J 8.3, 8.3, C(4) H), 7.06-7.01 (1H, m, C(1) H) 6.72-6.63 (1H, m, C(3) H), 6.39 (1H, dd, J 8.2, 1.9, C(5) H), 3.93 (2H, dd, J 11.6, 3.6, C(17) H_AH_B and C(17') H_AH_B), 3.72 (2H, t, J 7.2, C(7) H_2),

3.39-3.26 (4H, m, C(9) H_2 , C(17) H_AH_B and C(17') H_AH_B), 3.15 (2H, d, J 7.1, C(14) H_2), 2.13 (3H, s, CH_3CONH) 2.01-1.89 (3H, m, C(8) H_2 and C(15) H), 1.80 (2H, qt, J 6.6, 6.6, CH_2CH_3), 1.64-1.57 (2H, m, C(16) H_AH_B and C(16') H_AH_B), 1.29 (2H, ddd, J 12.3, 7.3, 4.2, C(16) H_AH_B and C(16') H_AH_B), ^{13}C NMR (101 MHz, $CDCl_3$): δ 168.4 (C(10) and C(10')), 168.3 (CONH), 148.6 (C(6)), 139.2 (C(2)), 134.0 (C(13) and C(13')), 132.1 (C(11) and C(11')), 129.6 (C(4)), 123.3 (C(12) and C(12')), 108.6 (C(5)), 107.7 (C(3)), 104.2 (C(1)), 67.7 (C(17) and C(17')), 57.5 (C(14)), 49.9 (C(7)), 36.0 (C(9)), 33.9 (C(15) and C(15')), 31.1 (C(16) and C(16')), 26.0 (C(8)), 24.7 (CH_3CONH), LRMS m/z (ES^+) 436 ($[M+H]^+$, 100%), HRMS m/z (ES^+) [Found: $(M+H)^+$ 436.2223, $C_{25}H_{30}O_4N_3^+$ requires 436.2231]; RP-HPLC: Method A: Retention time 9.41 min, purity 96.1%.

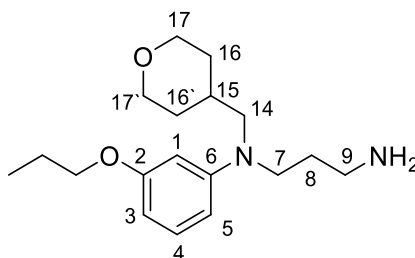
***N*¹-(3-Methoxyphenyl)-*N*¹-((tetrahydro-2*H*-pyran-4-yl)methyl)propane-1,3-diamine (136)**



2-(3-((3-Methoxyphenyl)((tetrahydro-2*H*-pyran-4-yl)methyl)amino)propyl)-isoindoline-1,3-dione **133** (280 mg, 0.685 mmol, 1.0 eq) was reacted according to general procedure 3. The crude material was purified *via* an acid base extraction, to yield **136** as a yellow oil (141 mg, 0.506 mmol, 74%): R_f : 0.00 (EtOAc), ν_{max} (thin film)/ cm^{-1} 2930 (m), 1608 (s), 1572 (s), 1498 (s), 1366 (m), 1140 (s), 1091 (s); 1H NMR (400 MHz, $CDCl_3$): δ 7.10 (1H, dd, J 8.0, 8.0, C(4) H), 6.28 (1H, dd, J 8.0, 2.4, C(5) H), 6.23-6.17 (2H, m, C(1) H and C(3) H), 3.97-3.88 (2H, m, C(17) H_AH_B and C(17') H_AH_B), 3.76 (3H, s, OCH_3), 3.37-3.26 (4H, m, C(7) H_2 , C(17) H_AH_B and C(17') H_AH_B), 3.12 (2H, d, J 7.3, C(14) H_2), 2.72 (2H, t, J 7.1, C(9) H_2), 2.13-1.90 (3H, m, NH_2 and C(15) H), 1.71 (2H, tt, J 7.1, 7.1, C(8) H_2), 1.63-1.57 (2H, m, C(16) H_AH_B and C(16') H_AH_B), 1.30 (2H, ddd, J 12.2, 12.2, 4.5, C(16) H_AH_B and C(16') H_AH_B), ^{13}C NMR

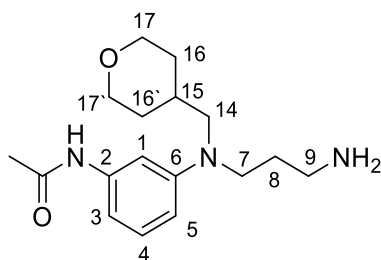
(101 MHz, CDCl₃): δ 160.8 (C(2)), 149.4 (C(6)), 129.9 (C(4)), 105.6 (C(5)), 100.1 (C(3)), 99.1 (C(1)), 67.8 (C(17) and C(17')), 57.5 (C(14)), 55.1 (OCH₃), 49.9 (C(7)), 39.8 (C(9)), 33.9 (C(15)), 31.2 (C(16) and C(16')), 30.4 (C(8)); LRMS m/z (ES⁺) 279 ([M+H]⁺, 100%), HRMS m/z (ES⁺) [Found: (M+H)⁺ 279.2063 C₁₆H₂₇O₂N₂⁺ requires 279.2067].

2-(3-((3-Propoxyphenyl)((tetrahydro-2H-pyran-4-yl)methyl)amino)propyl)-isoindoline-1,3-dione (137)



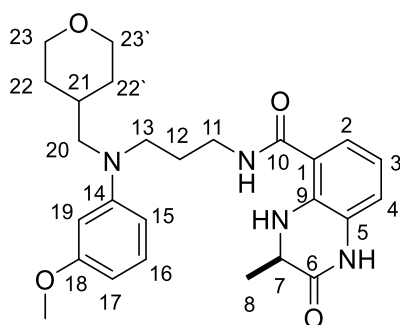
2-(3-((3-Propoxyphenyl)((tetrahydro-2H-pyran-4-yl)methyl)amino)propyl)-isoindoline-1,3-dione **134** (450 mg, 1.03 mmol, 1.0 eq) was reacted according to general procedure 3. The crude material was purified *via* an acid base extraction, to yield **137** as a pale yellow oil (162 mg, 0.529 mmol, 51%), which was used without further purification; R_f: 0.00 (EtOAc), ν_{\max} (thin film)/cm⁻¹ 2931 (m), 2844 (m), 1610 (s), 1571 (m), 1499 (s), 1140 (m); ¹H NMR (400 MHz, CDCl₃): δ 7.12-7.06 (1H, m, C(4)H), 6.28 (1H, dd, *J* 7.8, 2.1, C(5)H), 6.25-6.19 (2H, m, C(1)H and C(3)H), 3.96 (2H, dd, *J* 11.4, 3.7, C(17)_AH_B and C(17')_AH_B), 3.90 (3H, t, *J* 6.7, OCH₂), 3.42-3.28 (4H, m, C(7)H₂, C(17)_AH_B and C(17')_AH_B), 3.14 (2H, d, *J* 7.3, C(14)H₂), 2.74 (2H, t, *J* 7.1, C(9)H₂), 2.03-1.93 (1H, m, C(15)H), 1.80 (2H, qt, *J* 6.7, 6.7, CH₂CH₂O), 1.71 (2H, tt, *J* 7.1, 7.1, C(8)H₂), 1.67-1.59 (2H, m, C(16)_AH_B and C(16')_AH_B), 1.30 (2H, ddd, *J* 12.5, 12.5, 4.3, C(16)_AH_B and C(16')_AH_B), 1.03 (3H, t, *J* 6.7, CH₃CH₂) ¹³C NMR (101 MHz, CDCl₃): δ 160.4 (C(2)), 149.5 (C(6)), 129.8 (C(4)), 105.4 (C(5)), 100.9 (C(3)), 99.5 (C(1)), 69.3 (OCH₂), 67.8 (C(17) and C(17')), 57.5 (C(14)), 49.9 (C(7)), 40.0 (C(9)), 33.9 (C(15)), 31.2 (C(16) and C(16')), 30.8 (C(8)), 22.7 (CH₂CH₃), 10.6 (CH₂CH₃); LRMS m/z (ES⁺) 307 ([M+H]⁺, 100%), HRMS m/z (ES⁺) [Found: (M+H)⁺ 307.2380, C₁₈H₃₁O₂N₂⁺ requires 307.2380].

***N*-(3-((3-Aminopropyl)((tetrahydro-2*H*-pyran-4-yl)methyl)amino)phenyl)-acetamide (138)**



N-(3-((3-(1,3-Dioxoisindolin-2-yl)propyl)((tetrahydro-2*H*-pyran-4-yl)methyl)-amino)-phenyl)acetamide **135** (144 mg, 0.331 mmol, 1.0 eq) was reacted according to general procedure 3 for 1.5 h. Purification *via* acid base extraction yielded **138** as a yellow oil (98 mg, 0.321 mmol, 97%): *R*_f: 0.00 (EtOAc), ν_{max} (thin film)/cm⁻¹ 3291 (w) (N-H), 2930 (m), 2846 (m), 1665 (m) (C-O), 1610 (s), 1582 (m), 1553 (m), 1497 (s), 1368 (m), 729 (s); ¹H NMR (400 MHz, CDCl₃): δ 7.66 (1H, br s, NH), 7.18 (1H m, C(1)H), 7.08 (1H, dd, *J* 8.3, 8.3, C(4)H), 7.06-7.01 (1H, m, C(1)H) 6.59-6.52 (1H, m, C(3)H), 6.39 (1H, dd, *J* 8.3, 1.9, C(5)H), 3.94 (2H, dd, *J* 11.6, 3.4, C(17)*H*_A*H*_B and C(17')*H*_A*H*_B), 3.38-3.27 (4H, m, C(7)*H*₂, C(17)*H*_A*H*_B and C(17')*H*_A*H*_B), 3.13 (2H, d, *J* 7.1, C(14)*H*₂), 2.72 (2H, t, *J* 6.9, C(9)*H*₂), 2.13 (3H, s, CH₃CONH), 2.03-1.91 (1H, m, C(15)H), 1.70 (2H, tt, *J* 6.9, 6.9, C(8)*H*₂), 1.65-1.57 (2H, m, C(16)*H*_A*H*_B and C(16')*H*_A*H*_B), 1.30 (2H, ddd, *J* 12.9, 12.7, 4.0, C(16)*H*_A*H*_B and C(16')*H*_A*H*_B), ¹³C NMR (101 MHz, CDCl₃): δ 168.5 (CONH), 148.7 (C(6)), 139.2 (C(2)), 129.4 (C(4)), 108.2 (C(5)), 107.1 (C(3)), 104.0 (C(1)), 67.8 (C(17) and C(17')), 57.5 (C(14)), 49.9 (C(7)), 40.0 (C(9)), 33.9 (C(15)), 31.1 (C(16) and C(16')), 30.5 (C(8)), 24.7 (CH₃CONH); LRMS *m/z* (ES⁺) 306 ([M+H]⁺, 100%); HRMS *m/z* (ES⁺) [Found: (M+H)⁺ 306.2176 C₁₇H₂₈O₂N₃⁺ requires 306.2176].

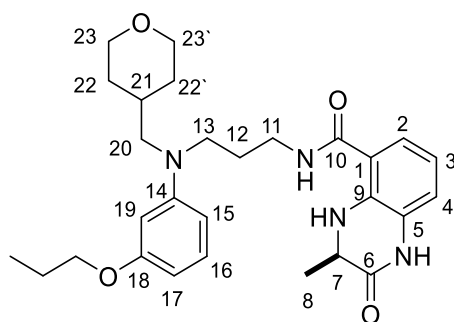
(*R*)-*N*-3-((3-Methoxyphenyl)((tetrahydro-2*H*-pyran-4-yl)methyl)amino)propyl)-3-methyl-2-oxo-1,2,3,4-tetrahydroquinoxaline-5-carboxamide (105**)**



[(*R*)-3-Methyl-2-oxo-1,2,3,4-tetrahydroquinoxaline-5-carboxylic acid] (*R*)-**32** (40 mg, 0.194 mmol, 1.0 eq) and *N*¹-(3-methoxyphenyl)-*N*¹-((tetrahydro-2*H*-pyran-4-yl)methyl)propane-1,3-diamine **136** (59 mg, 0.212 mmol, 1.1 eq) were reacted according to general procedure 4 for 20 h. The crude material was purified by silica gel chromatography, eluting with a gradient of 60% to 80% EtOAc in petroleum ether, to yield **105** as a colourless solid (47 mg, 0.101 mmol, 52%): *R*_f: 0.37 (petroleum ether: EtOAc 1:3); mp 68-71 °C (acetone); $[\alpha]_D^{25}$ -44.8 (*c* 0.3 in MeOH), ν_{\max} (thin film)/cm⁻¹ 3307 (w br), 2932 (m) (C-H), 2840 (m) (C-H); 1682 (s) (C=O), 1635 (m) (C=O), 1607 (s), 1498 (s), 1284 (s), 1250 (s), 746 (s); ¹H NMR (500 MHz; (CD₃)₂CO): δ 9.36 (1H, br s, C(5)NH), 8.06 (1H, br s, C(7)NH), 7.82 (1H, br t, *J* 5.4 C(10)NH), 7.34 (1H, dd, *J* 8.0, 1.1, C(4)H), 7.07 (1H, dd, *J* 8.2, 8.2, C(16)H), 7.00 (1H, dd, *J* 8.0, 1.1, C(2)H), 6.68 (1H, dd, *J* 8.0, 8.0 C(3)H), 6.39 (1H, dd, *J* 8.2, 2.4, C(15)H), 6.29 (1H, dd, *J* 2.4, 2.4, C(19)H), 6.23 (1H, ddd, *J* 8.2, 2.4, C(17)H), 4.05 (1H, qd, *J* 6.7, 1.5 Hz, C(7)H), 3.93-3.87 (2H, m, C(23)*H*_A*H*_B and C(23')*H*_A*H*_B), 3.75 (3H, s, OCH₃), 3.53-3.45 (4H, m, C(13)*H*₂ and C(11)*H*₂), 3.32 (2H, td, *J* 12.2, 1.7, C(23)*H*_A*H*_B and C(23')*H*_A*H*_B), 3.27 (2H, d, *J* 7.2, C(20)*H*₂), 2.07-1.98 (1H, m, C(21)H), 1.94 (2H, tt, *J* 7.4, 7.4 C(12)*H*₂), 1.68-1.62 (2H, m, C(22)*H*_A*H*_B and C(22')*H*_A*H*_B), 1.42 (3H, d, *J* 6.7 Hz, C(8)*H*₃), 1.30 (2H, ddd, *J* 12.2, 12.2, 4.1, C(22)*H*_A*H*_B and C(22')*H*_A*H*_B), ¹³C NMR (126 MHz; (CD₃)₂CO): δ 168.6 (C(10)), 167.7 (C(6)), 161.0 (C(18)), 149.7 (C(14)), 136.5 (C(9)), 129.7 (C(16)), 127.9 (C(5)), 121.4 (C(4)), 117.0 (C(2)), 116.6 (C(3)), 116.0 (C(1)), 105.5 (C(15)), 100.7 (C(17)), 98.7 (C(19)), 67.2 (C(23) and C(23')), 57.1 (C(20)), 54.2 (OCH₃), 50.7 (C(7)), 49.5

(C13), 37.1 (C11), 34.1 (C(21)), 31.1 (C(22) and C(22')), 26.8 (C(12)), 17.8 (C(8)), LRMS m/z (ES⁺) 467 ([M+H]⁺, 100%); HRMS m/z (ES⁺) [Found: (M+H)⁺ 467.2650, C₂₆H₃₅N₄O₄ requires 467.2653]; RP-HPLC: Method A: Retention time 9.32 min, purity 99.7%. Chiral HPLC (AD-H): Retention time 11.7 min, ee > 99%.

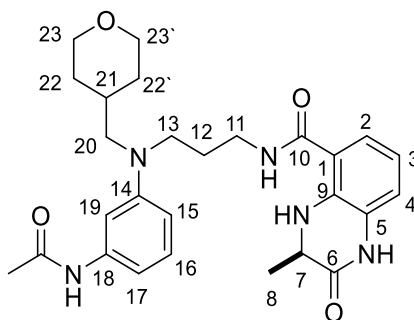
(*R*)-3-Methyl-2-oxo-*N*-(3-((3-propoxyphenyl)((tetrahydro-2*H*-pyran-4-yl)methyl)amino)propyl)-1,2,3,4-tetrahydroquinoxaline-5-carboxamide (106)



[(*R*)-3-Methyl-2-oxo-1,2,3,4-tetrahydroquinoxaline-5-carboxylic acid] (*R*)-**32** (40 mg, 0.194 mmol, 1.0 eq) and 2-(3-((3-propoxyphenyl)((tetrahydro-2*H*-pyran-4-yl)methyl)amino)propyl)-isoindoline-1,3-dione **137** (65 mg, 0.212 mmol, 1.1 eq) were reacted according to general procedure 4 for 40 h. The crude material was purified by silica gel chromatography, eluting with a gradient of 60% to 80% EtOAc in petroleum ether, to afford **106** as a yellow solid (36 mg, 0.073 mmol, 38%; R_f: 0.40 (petroleum ether: EtOAc 1:3); mp 68-70 °C (acetone); [α]_D²⁵ -14.4 (c 0.5 in MeOH); ν_{max} (thin film)/cm⁻¹ 3308 (w br), 2931 (w) (C-H), 2874 (w) (C-H), 1681 (s) (C=O), 1634 (m), 1606 (s) (C=O), 1532 (m), 1284 (s), 1248 (m), 744 (s); ¹H NMR (500 MHz; (CD₃)₂CO): δ 9.33 (1H, br s, C(5)NH), 8.02 (1H, br s, C(7)NH), 7.78 (1H, m, C(10)NH), 7.30 (1H, d, *J* 8.1, C(4)H), 7.02 (1H, dd, *J* 8.1, 8.1, C(16)H), 6.98-6.94 (1H, m, C(2)H), 6.65 (1H, dd, *J* 8.1, 8.1, C(3)H), 6.33 (1H, dd, *J* 8.1, 2.0, C(15)H), 6.26 (1H, dd, *J* 2.0, 2.0, C(19)H), 6.19 (1H, dd, *J* 8.1, 1.8, C(17)H), 4.01 (1H, qd, *J* 6.7, 1.2, C(7)H), 3.89-3.94 (4H, m, OCH₂C(23)H_AH_B and C(23')H_AH_B), 3.50-3.40 (4H, m, C(13)H₂ and C(11)H₂), 3.30-3.21 (4H, m, C(23)H_AH_B, C(23')H_AH_B and C(20)H₂), 2.03-1.95 (1H, m, C(21)H), 1.90 (2H, tt, *J* 7.3, 7.3, C(12)H₂), 1.71 (2H, qt, *J* 7.1, 7.1, CH₂CH₃), 1.64-1.57 (2H, m, C(22)H_AH_B and C(22')H_AH_B), 1.38 (3H, d, *J* 6.7, C(8)H₃), 1.28 (2H, ddd, *J* 12.2, 12.2,

4.1, C(22) H_AH_B and C(22') H_AH_B), 0.98 (3H, t, J 7.2, C(8) H_3), ^{13}C NMR (126 MHz; $(CD_3)_2CO$): δ 168.6 (C(10)), 167.7 (C(6)), 160.5 (C(18)), 149.7 (C(14)), 136.5 (C(9)), 129.6 (C(16)), 127.9 (C(5)), 121.3 (C(4)), 117.0 (C(2)), 116.6 (C(3)), 116.0 (C(1)), 105.4 (C(15)), 101.5 (C(17)), 99.2 (C(19)), 68.7 (OCH₂), 67.2 (C(23) and C(23')), 57.1 (C(20)), 50.7 (C(7)), 49.5 (C(13)), 37.1 (C(11)), 34.1 (C(21)), 31.1 (C(22) and C(22')), 26.8 (C(12)), 22.5 (CH₂CH₃), 17.8 (C(8)), 10.0 (CH₂CH₃), LRMS m/z (ES⁺) 495 ([M+H]⁺, 100%), HRMS m/z (ES⁺) [Found: (M+H)⁺ 495.2963, C₂₈H₃₉N₄O₄ requires 495.2966]; RP-HPLC: Method A: Retention time 10.28 min, purity 96.6%. Chiral HPLC (AD-H): Retention time 10.7 min, ee 92%.

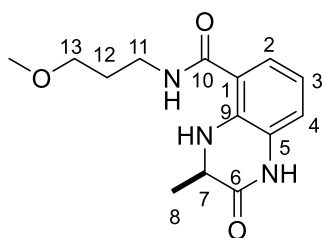
(*R*)-*N*-(3-((3-Acetamidophenyl)((tetrahydro-2*H*-pyran-4-yl)methyl)amino)propyl)-3-methyl-2-oxo-1,2,3,4-tetrahydroquinoxaline-5-carboxamide (107)



[(*R*)-3-Methyl-2-oxo-1,2,3,4-tetrahydroquinoxaline-5-carboxylic acid] (*R*)-**32** (40 mg, 0.194 mmol, 1.0 eq) and *N*-(3-((3-aminopropyl)((tetrahydro-2*H*-pyran-4-yl)methyl)amino)phenyl)-acetamide **138** (98 mg, 0.321 mmol, 1.7 eq) were reacted according to general procedure 4 for 18 h. The crude material was purified by silica gel chromatography, eluting with EtOAc, to afford **107** as a pale yellow solid (41 mg, 0.083 mmol, 43%): R_f : 0.11 (EtOAc); $[\alpha]_D^{25}$ -13.9 (c 0.5 in MeOH), ν_{max} (thin film)/cm⁻¹ 3307 (w br), 2980 (w), 1674 (s) (C=O), 1631 (s) (C=O), 1605 (s) (C=O), 1581 (s), 1484 (s), 1369 (s), 1283 (s), 1263 (s), 1133 (m); 1H NMR (500 MHz; $(CD_3)_2CO$): δ 9.35 (1H, br s, C(5)NH), 8.98 (1H, br s, C(18)NH), 8.02 (1H, br s, C(7)NH), 7.78 (1H, m, C(10)NH), 7.34 (1H, dd, J 8.0, 0.9, C(4)H), 7.29 (1H, m, C(19)H), 7.05 (1H, dd, J 8.2, 8.2, C(16)H), 6.99-6.95 (1H, m, C(2)H), 6.83-6.79 (1H, m, C(17)H), 6.66 (1H, dd, J 8.0, 8.0 C(3)H), 6.47 (1H, dd, J 8.2, 2.0, C(15)H), 4.03 (1H, qd, J 6.7, 1.4 Hz, C(7)H), 3.90-3.84 (2H, m, C(23) H_AH_B and

C(23') H_AH_B), 3.50-3.43 (4H, m, C(13) H_2 and C(11) H_2), 3.27 (2H, dt, J 10.3, 1.1, C(23) H_AH_B , and C(23'') H_AH_B), 3.23 (2H, d, J 7.0, C(20) H_2), 2.06 (3H, s, $NHCOCH_3$), 2.04-1.97 (1H, m, C(21) H), 1.93 (2H, tt, J 7.1, 7.1 C(12) H_2), 1.65-1.59 (2H, m, C(22) H_AH_B and C(22'') H_AH_B), 1.40 (3H, d, J 6.7 Hz, C(8) H_3), 1.29 (2H, ddd, J 12.2, 12.2, 4.1, C(22) H_AH_B and C(22'') H_AH_B), ^{13}C NMR (126 MHz; $(CD_3)_2CO$): δ 168.6 (C(10)), 167.9 ($NHCOCH_3$), 167.8 (C(6)), 148.8 (C(14)), 140.5 (C(18)), 136.5 (C(9)), 129.1 (C(16)), 127.9 (C(5)), 121.5 (C(4)), 117.0 (C(2)), 116.6 (C(3)), 116.0 (C(1)), 107.6 (C(15)), 106.7 (C(17)), 103.6 (C(19)), 67.2 (C(23) and C(23'')), 57.2 (C(20)), 50.8 (C(7)), 49.5 (C(13)), 37.2 (C(11)), 34.0 (C(21)), 31.1 (C(22) and C(22'')), 26.7 (C(12)), 23.6 (CH_3CONH), 17.8 (C(8)), LRMS m/z (ES^+) 494 ($[M+H]^+$, 100%), 516 ($[M+Na]^+$, 43%), HRMS m/z (ES^+) [Found: $(M+H)^+$ 494.2760 $C_{27}H_{36}N_5O_4$ requires 494.2762]; RP-HPLC: Method A: Retention time 8.36 min, purity 99.2%. Chiral HPLC (AD-H): Retention time 10.5 min, ee 97%.

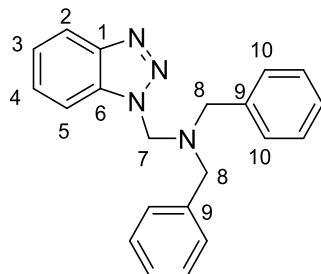
(R)-N-(3-Methoxypropyl)-3-methyl-2-oxo-1,2,3,4-tetrahydroquinoxaline-5-carboxamide (104)



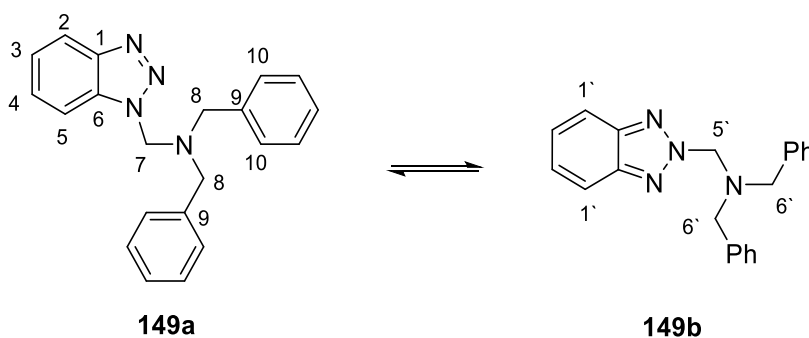
[(R)-3-Methyl-2-oxo-1,2,3,4-tetrahydroquinoxaline-5-carboxylic acid] (R)-**32** (40 mg, 0.194 mmol, 1.0 eq) and 3-methoxypropylamine **139** (30 μ L, 26 mg, 0.291 mmol, 1.5 eq) were reacted according to general procedure 4 for 17 h. . The crude material was purified by silica gel chromatography, eluting with a gradient of 50% to 80% EtOAc in petroleum ether, to afford **104** as a colourless solid (44 mg, 0.159 mmol, 82%): R_f : 0.24 (EtOAc: petroleum ether 3:1); mp 125-127 $^{\circ}C$ ($CHCl_3$); $[\alpha]_D^{25}$ -18.3 (c 0.5 in MeOH), ν_{max} (thin film) / cm^{-1} 3409 (w), (N-H), 3309 (w) (N-H), 2941 (w), 1691 (s) (C-O), 1632 (m) (C-O), 1531 (s), 1275 (s), 1090 (s), 730 (s); 1H NMR (500 MHz, $(CD_3)_2CO$): δ 9.36 (1H, s, C(5) NH), 8.04 (1H, br s, C(4) NH), 7.74 (1H, br s, C(7) NH), 7.28 (1H, dd, J 8.0, 1.0, C(4) H), 6.96 (1H, dd, J

8.0, 1.0, C(2)*H*), 6.66 (1H, dd, *J* 8.0, 8.0, C(3)*H*), 4.02 (1H, qd, *J* 6.7, 1.5, C(7)*H*), 3.49-3.43 (4H, m, C(11)*H* and C(13)*H*), 3.31 (3H, s, OCH₃), 1.86 (2H, tt, *J* 6.3, 6.3, C(12)*H*₂), 1.39 (3H, d, *J* 6.7, C(8)*H*₃); ¹³C NMR (126 MHz, (CD₃)₂CO): δ 168.4 (C(10)), 167.8 (C(6)), 136.5 (C(9)), 127.9 (C(5)), 121.3 (C(4)), 116.9 (C(2)), 116.6 (C(3)), 116.0 (C(1)), 70.5 (C(13)), 57.8 (OCH₃), 50.7 (C(7)), 37.0 (C(11)), 29.4 (C(12) by HSQC) 17.8 (C(8)), LRMS *m/z* (ES⁺) 300 ([M+Na]⁺, 100%), HRMS *m/z* (ES⁺) [Found: (M+Na)⁺ 300.1319, C₁₄H₁₉O₃N₃Na⁺ requires 436.2343]; RP-HPLC: Retention time 8.37 min, purity 98.5%. Chiral HPLC (AD-H): Retention time 10.8 min, ee > 99%.

7.5 Chapter 4 Procedures

***N*-((1*H*-Benzo[*d*]-[1,2,3]triazol-1-yl)methyl)-*N*-benzyl-1-phenylmethanamine (149a)**

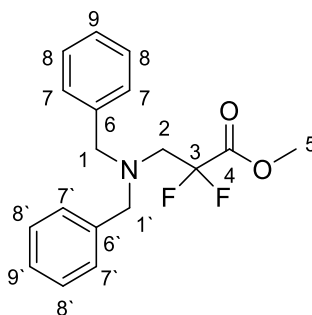
To a solution of 1*H*-benzotriazole **148** (2.18 g, 18.3 mmol, 1.0 eq), dibenzylamine (3.84 mL, 3.94 g, 20.0 mmol, 1.1 eq) in methanol (8 mL) was added slowly aq. formaldehyde (37% v/v, 1.76 mL, 23.6 mmol, 1.3 eq). Diethyl ether (10 mL) was added to dissolve the precipitate and the resulting solution was heated under reflux for 16 h, at which time TLC analysis indicated the reaction complete. After cooling to rt the reaction mixture was filtered, rinsed with cold diethyl ether (3 × 25 mL), and dried *in vacuo* to give a colourless solid (4.36 g, 13.3 mmol, 73%): R_f 0.30 (petroleum ether: EtOAc 10:1); mp 120-122 °C (EtOAc) [Lit.¹¹⁸ 121-122 °C]; In solution it is a mixture of the 1*H*- and the 2*H*- substituted benzotriazole.



¹H NMR (400 MHz, CDCl₃): **149a**: δ 8.13 (d, *J* 8.0, 1H, C(1)*H*), 7.55-7.20 (m, 13H, aromatic), 5.52 (s, 2H, C(5)*H*), 3.83 (s, 4H, C(6)*H*). **149b**: δ 9.04-7.98 (m, 2H, C(1')*H*), 7.55-7.20 (m, 12H, aromatic), 5.59 (s, 2H, C(5')*H*), 3.86 (s, 4H, C(6')*H*). Ratio between **149a** and **149b** 83:17; (400 MHz, C₆D₆): Isomer A: δ 8.00 (1H, d, *J* 8.0, C(1)*H*), 7.46-6.78 (13H, m, aromatic), 4.95 (2H, s, C(5)*H*), 3.49 (4H, s, C(6)*H*). Isomer B: δ 7.94-7.89 (2H, m,

C(1`H)), 7.46-6.78 (12H, m, (C(Ar)H), 5.27 (2H, s, C(5`H)), 3.49 (4H, s, C(6`H)). Ratio between **149a** and **149b** isomer 73:27; LRMS m/z (ES⁺) 328 ([M+H]⁺, 100%). These data are in accordance with the literature.¹¹⁸

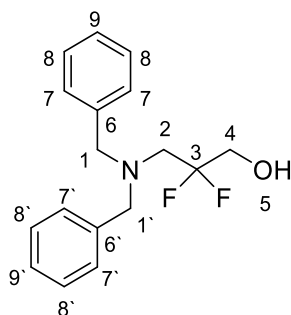
Methyl 3-(dibenzylamino)-2,2-difluoropropanoate (**144**)



To a suspension of Zn (1.16 g, 17.7 mmol, 3.0 eq) in THF (20 mL) was added trimethylsilyl chloride (1.16 mL, 0.99 g, 9.14 mmol, 1.6 eq), and stirred for 10 min, at ambient temperature. After this time methyl bromodifluoroacetate (1.11 g, 5.87 mmol, 1.0 eq) was added slowly, and stirred for 10 min, at ambient temperature. Then, *N*-(dibenzylaminomethyl) benzotriazole **149** (3.00 g, 9.13 mmol, 1.6 eq) dissolved in THF (30 mL) were added over 15 min at ambient temperature. After 4.5 h at rt the reaction was judged to be complete by TLC analysis. The suspension was quenched with 1 M aq. K₂CO₃ (25 mL), and diluted with EtOAc (35 mL). The suspension was filtered through Celite®, and rinsed with EtOAc (50 mL). The organic components of the aqueous layer were extracted with EtOAc (100 mL). The combined organic extracts were washed with brine (100 mL), dried (MgSO₄), filtered, and concentrated *in vacuo*. The crude material was purified by silica gel chromatography, eluting with 5% ethyl acetate in petroleum ether. A second silica gel purification, eluting with 10% diethyl ether in petroleum ether, yielded **144** as a colourless oil (620 mg, 1.94 mmol, 33%): R_f 0.51 (petroleum ether: EtOAc 10:1); ν_{\max} (thin film)/cm⁻¹ 3087 (w), 3064 (w), 3029 (m), 2956 (m), 2834 (w), 2812 (w), 1772 (s), 1495 (m); 1453 (m), 1442 (m), 1193 (s), 1059 (s); ¹H NMR (400 MHz, CDCl₃): δ 7.34-7.14 (10H, m, C(Ar)H), 3.60 (3H, s, C(5)H), 3.59 (4H, s, C(1)H C(1`H)), 3.06 (2H, t,

J 12.9, C(2) H); ^{19}F NMR (376 MHz, CDCl_3): δ -106.4 (2F, t, J 13.0, C(3) F_2); ^{13}C NMR (126 MHz, CDCl_3): δ 164.2 (t, J 32, C(4)), 138.2 (C(6) and C(6')), 129.2 (C(7) and C(7')), 128.3 (C(8) and C(8')), 127.3 (C(9) and C(9')), 116.3 (t, J 253, C(3)), 58.6 (C(1) and C(1')), 55.1 (t, J 26 C(2)), 53.1 (C(5)); LRMS m/z (ES^+) 320 ($[\text{M}+\text{H}]^+$, 100%); HRMS m/z (ES^+) [Found: $(\text{M}+\text{Na})^+$ 342.1273, $\text{C}_{18}\text{H}_{19}\text{F}_2\text{NNaO}_2^+$ requires 342.1276].

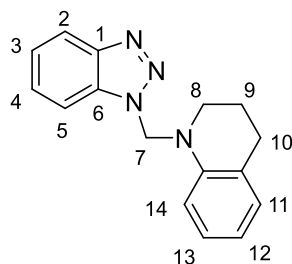
3-(Dibenzylamino)-2,2-difluoropropan-1-ol (**150**)



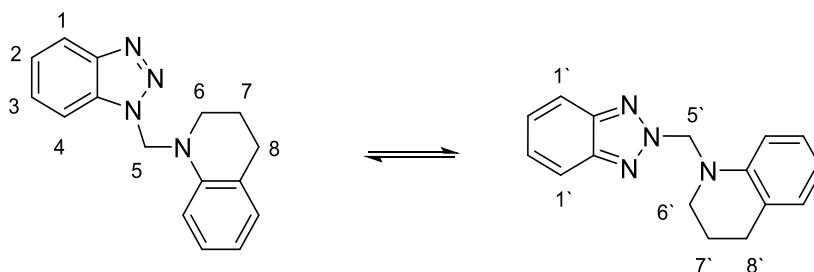
To a solution of methyl 3-(dibenzylamino)-2,2-difluoropropanoate **144** (420 mg, 1.32 mmol, 1.0 eq) in THF (25 mL) was added LiAlH_4 in THF (1 M, 2.64 mL, 2.64 mmol, 2.0 eq) over a period of 15 min at 0 °C. After the completed addition the reaction mixture warmed to ambient temperature and stirred for 2 h. After this time the reaction was judged to be complete by TLC analysis. The reaction mixture was sequentially quenched with H_2O (5 mL), followed by 2 M aq. NaOH (5 mL). The suspension was filtered through Celite[®], and rinsed with diethyl ether. The organic components of the aqueous layer were extracted with diethyl ether (2 × 100 mL). The combined organic extracts were washed with brine (100 mL), dried (MgSO_4), filtered, and concentrated *in vacuo*. The crude material was purified by silica gel chromatography, eluting with a gradient of 5% to 10% EtOAc in petroleum ether, to afford **150** as a colourless oil (320 mg, 1.10 mmol, 83%): R_f 0.27 (petroleum ether: EtOAc 10:1); ν_{max} (thin film)/ cm^{-1} 3341 (br) (O-H), 3063 (w), 3029 (m), 2834 (w), 1601 (m), 1495 (m); 1453 (s), 1371 (m), 1078 (m), 1061 (s); ^1H NMR (400 MHz, CDCl_3): δ 7.33 - 7.18 (10H, m, aromatic), 3.61 (4H, s, C(1) H), 3.59 (2H, t, J 12.3, C(4) H_2), 2.88 (2H, t, J 12.8, C(2) H_2), 2.60 (1H, s, OH); ^{19}F NMR (376 MHz, CDCl_3): δ -107.5 (2F, tt, J 12.3, 12.3, C(3) F_2); ^{13}C NMR (126 MHz, CDCl_3): δ 138.0 (C(6) and C(6')), 129.3

(C(7) and C(7')), 128.8 (C(8) and C(8')), 127.7 (C(9) and C(9')), 121.9 (t, *J* 245, C(3)), 63.6 (t, *J* 31, C(4)), 59.5 (C(1) and C(1')), 54.5 (t, *J* 29, C(2)); LRMS *m/z* (ES⁺) 292 ([M+H]⁺, 100%); HRMS *m/z* (ES⁺) [Found: (M+H)⁺ 292.1501, C₁₇H₂₀F₂NO⁺ requires 292.1507].

1-((1*H*-Benzo[d][1,2,3]triazol-1-yl)methyl)-1,2,3,4-tetrahydroquinoline (**146**)



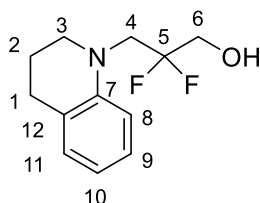
To a solution of 1*H*-benzotriazole **148** (2.18 g, 18.3 mmol, 1.0 eq) and 1,2,3,4-tetrahydroquinoline **71** (2.52 mL, 20.0 mmol, 1.1 eq) in methanol (8 mL) was added slowly aq. formaldehyde (37% v/v, 1.76 mL, 23.6 mmol, 1.3 eq). Diethyl ether (15 mL) was added to dilute the precipitate and the resulting solution was heated under reflux for 4 h, at which time TLC analysis indicated the reaction complete. After cooling to rt the reaction mixture was filtered, rinsed with cold diethyl ether (3 × 25 mL), and dried *in vacuo* to give **146** as a colourless solid (4.44 g, 16.8 mmol, 92%). R_f: 0.44 (petroleum ether: EtOAc 3:1); mp 130-131 °C (Et₂O), in solution it is a mixture of the 1*H* and the 2*H* substituted benzotriazole.



¹H NMR (400 MHz, CDCl₃): δ 8.06 (0.7H d, *J* 8.3 Hz, C(1)*H*), 7.90-7.83 (0.5H, m, C(1')*H*), 7.52-7.30 (2.8H, m, C(Ar)*H*), 7.25-7.05 (2.0H, m, C(Ar)*H*), 7.03-6.95 (1.0H, m, C(Ar)*H*) 6.14 (2H, s, C(5)*H*), 3.80-3.74 (0.5H, m, C(6')*H*), 3.55-3.48 (1.6 H, m, C(6)*H*), 2.78 (0.5H, t, *J* 6.4,

C(8')H), 2.72 (1.6 H, t, J 6.4, C(8)H) 2.07-1.98 (0.5 H, m, C(7')H), 1.95-1.85 (1.6 H, m, C(7)H); ^{13}C NMR (101 MHz, CDCl_3): δ 146.1, 144.1, 143.0, 142.7, 132.5, 129.7, 129.3, 127.4, 127.1, 127.0, 126.3, 123.8, 123.5, 119.8, 118.6, 118.4, 118.2, 112.6, 112.2, 110.0, 71.4, 65.1, 50.2, 49.3, 27.6, 22.1, 21.7; ν_{max} (thin film)/ cm^{-1} 3016 (w) (C-H), 2970 (w) (C-H), 2947 (w), 1739 (s), 1438 (m), 1296 (s) (C-N); 1229 (s) (C-N), 1217 (s) (C-N); LRMS m/z (ES $^+$) 287 [(M+Na) $^+$, 100%]; HRMS m/z (ES $^+$) [Found: (M+Na) $^+$ 287.1266, $\text{C}_{16}\text{H}_{16}\text{N}_4\text{Na}^+$ requires 287.1267]. The compound hydrolysed on the HPLC and no purity data could be obtained.

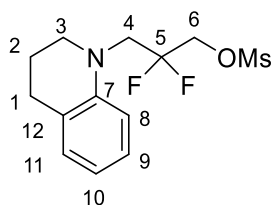
3-(3,4-Dihydroquinolin-1(2H)-yl)-2,2-difluoropropan-1-ol (149)



To a suspension of Zn (1.54 g, 23.8 mmol, 3.0 eq) in THF (4 mL) was added trimethylsilyl chloride (1.52 mL, 1.78 g, 12.3 mmol, 1.6 eq), and stirred for 10 min, at ambient temperature. After this time ethyl bromodifluoroacetate (1.61 g, 7.94 mmol, 1.0 eq) was added slowly, and stirred for 10 min, at ambient temperature. Then, 1-((1H-benzo[d][1,2,3]triazol-1-yl)methyl)-1,2,3,4-tetrahydroquinoline **146** (3.25 g, 12.3 mmol, 1.6 eq) suspended in THF (40 mL) was added over 15 min at ambient temperature. The suspension was stirred for 75 min, at 60 °C, at which time TLC analysis indicated the reaction complete. After cooling to ambient temperature the suspension was filtered through Celite[®], and rinsed with EtOAc (100 mL). The filtrate was adsorbed on Celite[®], and purified by silica gel chromatography, eluting with 5% EtOAc in petroleum ether, to afford a colourless oil (1.05 g), which still contained some minor impurities. An aliquot of ethyl 3-(3,4-dihydroquinolin-1(2H)-yl)-2,2-difluoropropanoate (800 mg, 2.97 mmol, 1.0 eq) was dissolved in THF (50 mL) and a solution of LiAlH_4 in THF (1 M, 5.94 mL, 5.94 mmol, 2.0 eq) was added over a period of 15 min at 0 °C. Subsequently, the reaction mixture was warmed to ambient temperature and stirred for 1 h. The reaction mixture

was quenched with H₂O (8 mL), followed by 2 M aq. NaOH (8 mL) and H₂O (8 mL). The suspension was filtered through Celite®, and rinsed with diethyl ether. The filtrate was washed with brine (30 mL), dried (MgSO₄), filtered, and concentrated *in vacuo*. The crude material was purified by silica gel chromatography, eluting with a gradient of 10% to 20% ethyl acetate in petroleum ether, to afford **149** as a colourless oil (370 mg, 1.63 mmol, 27% over 2 steps): R_f: 0.41 (petroleum ether: EtOAc 3:1); ν_{\max} (thin film)/cm⁻¹ 3383 (br) (O-H), 2933 (w) (C-H), 2845 (w), 1602 (m), 1576 (w), 1498 (s); 1458 (m), 1091 (m), 1058 (s) (C-F); ¹H NMR (400 MHz, CDCl₃): δ 7.11-7.02 (1H, m, C(11)H), 7.01-6.93 (1H, m, C(9)H), 6.84-6.76 (1H, m, C(10)H), 6.72-6.52 (1H, m, C(8)H), 3.83 (2H, t, *J* 13.2, C(6)H₂), 3.71 (2H, t, *J* 13.2, C(4)H₂), 3.42-3.36 (2H, m, C(3)H₂), 2.79 (2H, t, *J* 6.3, C(1)H₂), 2.02 (1H, br s, OH), 1.99-1.91 (2H, m, C(2)H₂); ¹⁹F NMR (376 MHz, CDCl₃): δ -110.3 (2F, tt, *J* 13.2, 13.2, C(5)F₂); ¹³C NMR (101 MHz, CDCl₃): δ 145.3 (C(7)), 129.6 (C(11)), 127.2 (C(9)), 122.9 (C(12)), 122.7 (t, *J* 244, C(5)), 117.3 (C(10)), 111.9 (C(8)), 62.3 (t, *J* 32, C(6)), 53.7 (t, *J* 29, C(4)), 51.4 (C(3)), 28.1 (C(1)), 22.0 (C(2)); LRMS *m/z* (ES⁺) 228 ([M+H]⁺, 100%); HRMS *m/z* (ES⁺) [Found: (M+Na)⁺ 250.1021. C₁₂H₁₅F₂NONa⁺ requires 250.1014]. RP-HPLC: Method A: Retention time 12.47 min, purity 98.8%.

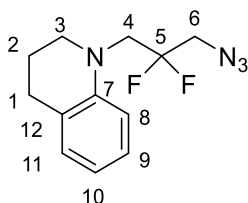
3-(3,4-Dihydroquinolin-1(2H)-yl)-2,2-difluoropropyl methanesulfonate (150)



3-(3,4-Dihydroquinolin-1(2H)-yl)-2,2-difluoropropan-1-ol **149** (170 mg, 0.748 mmol, 1.0 eq), methane sulfonylchloride (69 μ L, 47 mg, 0.898 mmol, 1.2 eq), Et₃N (146 μ L, 106 mg, 1.05 mmol, 1.4 eq) in CH₂Cl₂ (5 mL) were stirred at ambient temperature for 3 h. After this time the reaction was judged to be complete by TLC analysis. The solution was diluted with CH₂Cl₂ (10 mL), washed with brine (5 mL), dried (MgSO₄), filtered through a silica plug and concentrated *in vacuo*. The colourless oil was further purified by silica gel

chromatography, eluting with a gradient of 10% to 20% EtOAc in petroleum ether, to give **150** as a colourless oil (220 mg, 0.721 mmol, 97%): R_f : 0.32 (petroleum ether: EtOAc 3:1); ν_{\max} (thin film)/ cm^{-1} 3024 (w) (C-H), 2937 (m) (C-H), 2846 (w), 1603 (m), 1576 (w); 1499 (s), 1459 (m), 1351 (s) (C-N), 1175 (s) (C-O), 1014 (s) (C-F); ^1H NMR (400 MHz, CDCl_3): δ 7.12–7.04 (1H, m, C(11)H), 6.99 (1H, d J 7.4, C(9)H), 6.74–6.68 (2H, m, C(10)H and C(8)H), 4.42 (2H, t, J 12.0, C(6)H₂), 3.74 (2H, t, J 13.5, C(4)H₂), 3.42–3.35 (2H, m, C(3)H₂), 3.08 (3H, s, OSO_2CH_3), 2.80 (2H, t, J 5.9, C(1)H₂), 1.97 (2H, tt, J 5.9, 5.9, C(2)H₂); ^{19}F NMR (376 MHz, CDCl_3): δ -107.8 (2F, m, C(5)F₂); ^{13}C NMR (101 MHz, CDCl_3): δ 145.1 (C(7)), 129.9 (C(11)), 127.3 (C(9)), 123.3 (C(12)), 120.7 (t, J 248, C(5)), 117.9 (C(10)), 111.8 (C(8)), 66.6 (t, J 33, C(6)), 54.2 (t, J 28, C(4)), 51.7 ($\text{H}_3\text{C}(\text{SO}_3\text{R})$), 38.0 (C(3)), 28.1 (C(1)), 22.1 (C(2)); LRMS m/z (ES⁺) 306 ([M+H]⁺, 100%), 328 ([M+Na]⁺); HRMS m/z (ES⁺) [Found: (M+Na)⁺ 328.0797, C₁₃H₁₇F₂NO₃SNa⁺ requires 328.0789]; RP-HPLC (Method B): Retention time 13.24 min, purity 99.0%.

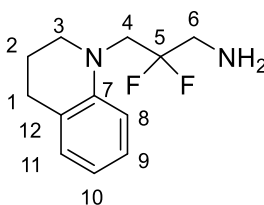
1-(3-Azido-2,2-difluoropropyl)-1,2,3,4-tetrahydroquinoline (151)



A suspension of 3-(3,4-dihydroquinolin-1(2H)-yl)-2,2-difluoropropyl methanesulfonate **150** (225 mg, 0.737 mmol, 1.0 eq), sodium azide (191 mg; 2.94 mmol, 4.0 eq) in DMF (6.5 mL) was stirred for 16 h at 110 °C. After this time the reaction was judged to be complete by TLC analysis. After cooling to ambient temperature the suspension was dissolved in EtOAc (30 mL) and H₂O (15 mL). The organic extracts, were washed with H₂O (15 mL), brine (15 mL), dried (MgSO_4), filtered, and concentrated *in vacuo*. The yellow oil was purified by a silica gel chromatography, eluting with 5% EtOAc in petroleum ether, to give **151** as a colourless oil (160 mg, 0.634 mmol, 86%): R_f : 0.55 (petroleum ether: EtOAc 10:1); ν_{\max} (thin film)/ cm^{-1} 2931 (m), 2847 (w), 2104 (s), 1677 (w), 1603 (m), 1577 (w)

1498 (s); 1253 (s), 1060 (s); ^1H NMR (400 MHz, CDCl_3): δ 7.10–7.05 (1H, m, C(11)H), 7.00–6.95 (1H, m, C(9)H), 6.78–6.72 (1H, m, C(8)H), 6.70–6.64 (1H, m, C(10)H), 3.68 (2H, t, J 13.0, C(4)H₂), 3.57 (2H, t, J 13.0, C(6)H₂), 3.39–3.34 (2H, m, C(3)H₂), 2.78 (2H, t, J 6.3, C(1)H₂), 1.94 (2H, tt, J 6.3, 6.3, C(2)H₂); ^{19}F NMR (376 MHz, CDCl_3): δ -104.8 (2F, qn, J 13.0, C(5)F₂); ^{13}C NMR (101 MHz, CDCl_3): δ 145.2 (C(7)), 129.7 (C(11)), 127.2 (C(9)), 123.0 (C(12)), 122.6 (t, J 248, C(5)), 117.5 (C(10)), 111.8 (C(8)), 54.2 (t, J 28, C(6)), 52.1 (t, J 30, C(4)), 51.5 (C(3)), 28.1 (C(1)), 22.0 (C(2)); LRMS m/z (ES⁺) 253 ([M+H]⁺, 100%); HRMS m/z (ES⁺) [Found: (M+Na)⁺ 275.1080, C₁₂H₁₄F₂N₄Na⁺ requires 275.1079]; RP-HPLC: Method A: Retention time 14.35 min, purity 96.7%.

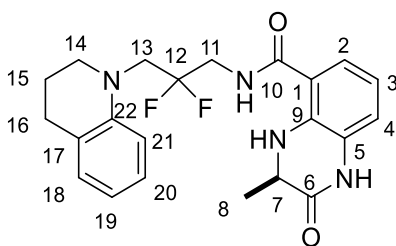
3-(3,4-Dihydroquinolin-1(2H)-yl)-2,2-difluoropropan-1-amine (142)



To a solution of 1-(3-azido-2,2-difluoropropyl)-1,2,3,4-tetrahydroquinoline **151** (70 mg, 0.277 mmol, 1.0 eq) in EtOAc (15 mL) was added 10% Pd/C (14.7 mg, 0.014 mmol, 0.05 eq). The system was purged with nitrogen, and then hydrogen gas was added. The suspension was stirred for 16 h under an atmosphere of hydrogen at ambient temperature. After this time the reaction was judged to be complete by TLC analysis. The suspension was filtered through Celite®, and concentrated *in vacuo*, to afford **142** as a yellow oil (58 mg, 0.256 mmol, 93%), which was used without further purification: R_f: 0.26 (EtOAc); ν_{max} (thin film)/cm⁻¹ 3402 (br) (N-H), 2932 (m) (C-H), 2863 (w), 2511 (br), 2209 (w), 2067 (m), 1660 (s), 1603 (m), 1576 (w) 1500 (m); 1256 (w) (C-N), 1096 (m) (C-F), 1014 (m); ^1H NMR (400 MHz, MeOD): δ 7.00–6.92 (1H, m, C(11)H), 6.92–6.85 (1H, m, C(9)H), 6.74–6.69 (1H, m, C(8)H), 6.59–6.52 (1H, m, C(10)H), 3.68 (2H, t, J 14.6, C(4)H), 3.42–3.34 (2H, m, C(3)H), 3.00 (2H, t, J 14.6, C(6)H), 2.74 (2H, t, J 6.4, C(1)H), 1.91 (2H, qn, J 6.4, C(2)H); ^{19}F NMR (376 MHz, MeOD): δ -106.07 (2F, qn, J 14.6, C(5)F₂);

^{13}C NMR (101 MHz, MeOD): δ 147.7 (C(7)), 131.1 (C(11)), 128.8 (C(9)), 125.9 (t, J 244, C(5)), 124.7 (C(12)), 118.8 (C(10)), 113.8 (C(8)), 56.1 (t, J 28, C(4)), 53.4 (C(3)) 46.5 (t, J 27, C(6)), 30.1 (C(1)), 24.1 (C(2)); LRMS m/z (ES $^+$) 227 ([M+H] $^+$, 100%), HRMS m/z (ES $^+$) [Found: (M+H) $^+$ 227.1359. C₁₂H₁₇F₂N₂ $^+$ requires 227.1354]. RP-HPLC: Method A: Retention time 9.73 min, purity 93.7%.

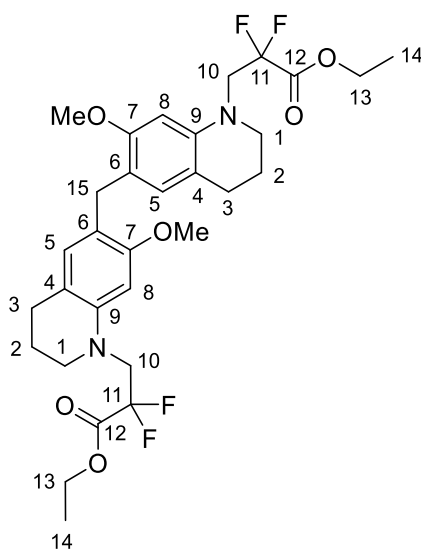
(R)-N-(3-(3,4-Dihydroquinolin-1(2H)-yl)-2,2-difluoropropyl)-3-methyl-2-oxo-1,2,3,4-tetrahydroquinoxaline-5-carboxamide (141)



(R)-3-Methyl-2-oxo-1,2,3,4-tetrahydroquinoxaline-5-carboxylic acid (**R**)-**32** (53 mg, 0.256 mmol, 1.0 eq) and 3-(3,4-dihydroquinolin-1(2H)-yl)-2,2-difluoropropan-1-amine **142** (58 mg, 0.256 mmol, 1.0 eq) were reacted according to general procedure 4 for 17 h. Purification by silica gel chromatography, eluting with a gradient of 30% to 50% ethyl acetate in petroleum ether, afforded **141** as a colourless solid (79 mg, 174 μmol , 68%): R_f: 0.32 (petroleum ether: EtOAc 1:1); mp 193-195 °C ((CH₃)₂CO); ν_{max} (thin film)/cm⁻¹ 3386 (w) (N-H), 3310 (w) (N-H), 3232 (w) (N-H), 2932 (w) (C-H), 1666 (s) (C=O), 1636 (m), 1554 (m), 1303 (m); 742 (s); ^1H NMR (500 MHz, (CD₃)₂CO): δ 9.38 (1H, br s, NH(C(6)O), 8.01 (1H, d, J 6.2, NH(C(9))), 7.90 (1H, br s, NH(C(10)O)), 7.40 (1H, dd J 8.0, 1.2, C(4)H), 7.03-6.99 (1H, m, C(2)H), 6.99-6.94 (1H, m, C(20)H), 6.94-6.89 (1H, m, C(21)H), 6.77-6.72 (1H, m, C(18)H), 6.72-6.68 (1H, m, C(3)H), 6.56 (1H, ddd J 7.3, 7.3, 0.9, C(19)H), 4.08-4.02 (1H, m, C(7)H), 4.02-3.92 (2H, m, C(13)H₂), 3.83 (2H, t J 15.1, C(11) H₂), 3.48-3.43 (2H, m, C(14) H₂), 2.77 (2H, t J 6.4, C(16) H₂), 1.98-1.91 (2H, m, C(15) H₂), 1.39 (3H, d J 6.7, C(8) H₃); ^{19}F NMR (376 MHz, CDCl₃): δ -105.1 (2F, tt, J 13.4, 13.4, C(5)F₂); ^{13}C NMR (126 MHz, CDCl₃): δ 169.8 (C(10)), 168.5 (C(6)), 146.4 (C(22)), 137.5 (C(9)), 130.0 (C(21)), 128.8 (C(1)), 127.7 (C(20)), 124.2 (t J 245 Hz, C(12)), 123.3 (C(17)), 122.5 (C(4)),

118.3 (C(2)), 117.5 (C(19)), 117.5 (C(9)), 115.9 (C(5)), 112.5 (C(18)), 55.2 (t, J 25, C(11)), 52.1 (C(14)), 51.6 (C(7)), 42.8 (t J 28, C(13)), 28.8 (C(16)), 22.8 (C(15)), 18.7 (C(8)); LRMS m/z (ES⁺) 415 ([M+H]⁺, 100%), 437 ([M+Na]⁺, 48%); HRMS m/z (ES⁺) [Found: (M+Na)⁺ 437.1765. C₂₂H₂₄F₂N₄O₂Na⁺ requires 437.1760]; RP-HPLC: Method A: Retention time 12.72 min, purity 96.9%; Chiral HPLC (AD-H): Retention time 10.84 min, ee 95%.

Diethyl 3,3'-(methylenebis(7-methoxy-3,4-dihydroquinoline-6,1(2H)-diyl))bis(2,2-difluoropropanoate) (152)

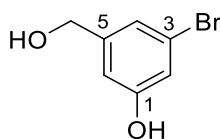


To a solution of 1H-benzotriazole **148** (1.33 g, 11.2 mmol, 1.0 eq), 7-methoxy-1,2,3,4-tetrahydroquinoline **39** (2.00 g, 12.3 mmol, 1.1 eq) in MeOH (5 mL) was added slowly aq. formaldehyde (37% v/v, 1.08 mL, 23.6 mmol, 1.3 eq). Diethyl ether (10 mL) was added to dilute the precipitate and the resulting solution was heated under reflux for 4 h, at which time TLC analysis indicated the reaction complete. After cooling to rt the reaction mixture was concentrated *in vacuo*. The residue was suspended in diethyl ether (20 mL), filtrated, rinsed with cold Et₂O (2 × 20 mL), and dried *in vacuo* to give a beige solid (2.13 g), which was used without further purification. To a suspension of Zn (216 mg, 3.30 mmol, 3.0 eq) in THF (4 mL) was added (216 μL, 185 mg, 1.70 mmol, 1.6 eq), and stirred for 10 min, at ambient temperature. After this time ethyl bromodifluoroacetate ethyl bromodifluoroacetate (208 mg, 1.10 mmol, 1.0 eq) was added slowly, and stirred for

10 min, at ambient temperature. Then, 1-((1*H*-benzo[*d*][1,2,3]triazol-1-yl)methyl)-1,2,3,4-7-methoxy-tetrahydroquinoline (500 mg, 1.70 mmol, 1.6 eq) suspended in THF (5 mL) was added over 15 min at ambient temperature. The suspension was stirred for 3 h, at ambient temperature, at which time TLC analysis indicated the reaction complete. After cooling to ambient temperature the suspension was filtered through Celite®, rinsed with EtOAc (15 mL), and concentrated *in vacuo*. The crude material was purified by silica gel chromatography, eluting with ethyl acetate in petroleum ether, to give **152** as a colourless oil (56 mg, 0.189 mmol, 22%). *R*_f: 0.58 (EtOAc: petroleum ether 3:1), *v*_{max} (thin film)/cm⁻¹ 2935 (w), 2841 (w), 1757 (m) (C=O), 1618 (m), 1575 (w), 1514 (s), 1454 (m), 1378 (w) 1316 (m); 1194 (m), 1089 (s), 1052 (m), ¹H-NMR (500 MHz, CDCl₃): δ 6.58 (2H, s, C(5)*H*), 6.28 (2H, s, C(8)*H*), 4.23 (4H, q, *J* 7.1 C(13)*H*₂), 3.85 (4H, t, *J* 13.4, C(10)*H*₂), 3.78 (6H, s, OCH₃), 3.68 (2H, s, C(15)*H*₂), 3.33-3.26 (4H, m, C(1)*H*₂), 2.61 (4H, t, *J* 6.1, C(3)*H*₂), 1.90-1.83 (4H, m, C(2)*H*₂), 1.25 (6H, t, *J* 7.1, C(14)*H*₃), ¹⁹F-NMR (376 MHz, CDCl₃): -107.8 (4F, t, *J* 13.0 C(11)*F*₂), ¹³C-NMR (126 MHz, CDCl₃): δ 164.3 (t, *J* 32, C(11)), 156.7 (C(7)), 143.8 (C(9)), 131.1 (C(5)), 119.4 (C(4)), 115.4 (t, *J* 253, C(11)), 115.1 (C(6)), 96.5 (C(8)), 63.3 (C(13)), 56.0 (t, *J* 27, C(10)), 51.3 (C(1)), 27.6 (C(15)), 27.3 (C(3)), 22.3 (C(2)), 14.0 (C(14)), LRMS *m/z* (ES⁺) 611 ([M+H]⁺, 23%), 633 ([M+Na]⁺, 100%).

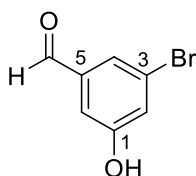
7.6 Chapter 5 Procedures

3-Bromo-5-(hydroxymethyl)phenol (**175**)



A solution of 3-bromo-5-hydroxybenzoic acid **171** (3.00 g, 13.8 mmol, 1.0 eq) in dry THF (120 mL) was cooled to 0 °C. BH_3 in THF (1 M, 40 mL, 40 mmol, 3.0 eq) was added slowly over a period of 45 minutes. After the addition was complete the reaction solution was warmed to ambient temperature and stirred for 20 h after which time TLC analysis indicated complete consumption of the starting material. The solution was cooled to 0 °C, quenched with conc. aq. HCl (6 mL), and the solvent was removed *in vacuo*. The residue was suspended in H_2O (90 mL) and extracted with EtOAc (3 × 80 mL). The combined organic extracts were washed with sat. aq. NaHCO_3 (3 × 200 mL), brine (200 mL), dried (MgSO_4), filtered and concentrated *in vacuo*. The residue was purified by silica gel chromatography, eluting with a gradient of 40% to 75% EtOAc in petroleum ether, to afford **175** as a colourless solid (2.67 g, 13.1 mmol, 95%): R_f : 0.48 (petroleum ether: EtOAc 1:1); mp 87–89 °C (EtOAc); $^1\text{H NMR}$ (400 MHz, CDCl_3): δ 7.12–7.09 (1H, m, C(6)H), 6.96 (1H, dd, J 1.9, 1.9, C(2)H), 6.84–6.80 (1H, m, C(4)H), 5.11 (1H, s, C(1)OH), 4.66 (2H, d, J 5.7 CH_2OH), 1.76 (1H, t, J 5.7, CH_2OH); LRMS m/z (ES^-) 201 ($[\text{M}^{79}\text{Br}-\text{H}]^-$, 100%), 203 ($[\text{M}^{81}\text{Br}-\text{H}]^-$, 100%). These data are in good agreement with the literature.⁵⁹

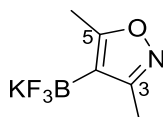
3-Bromo-5-hydroxybenzaldehyde (**172**)



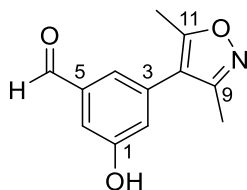
3-Bromo-5-(hydroxymethyl)phenol **175** (2.20 g, 11.3 mmol, 1.0 eq) was dissolved in CHCl_3 (60 mL) and acetone (2 mL). Activated MnO_2 (6.40 g, 80.5 mmol, 6.8 eq) was added and stirred at reflux for 3 h after which time TLC analysis indicated complete consumption

of the starting material. After cooling to ambient temperature the suspension was filtered through Celite®, and concentrated *in vacuo*. The residue was purified by silica gel chromatography, eluting with a gradient of 30% to 60% Et₂O in petroleum ether, to afford **172** as a yellow solid (1.68 g, 8.36 mmol, 74%): R_f: 0.36 (petroleum ether: Et₂O 1:1); mp 136-138 °C (CHCl₃) [Lit:⁵⁹ 137-140 °C]; ¹H NMR (400 MHz, (CD₃)₂SO) 10.46 (1H, s, CHO), 9.88 (1H, s, C(1)OH), 7.52 (1H, dd, *J* 1.4, 1.4, C(2')H), 7.29-7.24 (2H, m, C(4')H and C(6')H₂); LRMS *m/z* (ES⁻) 199 ([M⁷⁹Br-H]⁻, 100%), 201 ([M⁸¹Br-H]⁻, 100%). These data are in accordance with the literature.⁵⁹

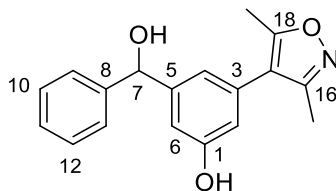
Potassium (3,5-dimethylisoxazol-4-yl)trifluoroborate (176)



A suspension of 3,5-dimethylisoxazole-4-yl-boronic acid **170** (920 mg, 7.35 mmol, 1.0 eq) in MeOH (2 mL) was cooled to 0 °C. KHF₂ (1.71 g, 21.9 mmol, 3.0 eq) was added, followed by a dropwise addition of water (4.8 mL). The reaction mixture was warmed to ambient temperature and stirred for another 10 min. After this time the solution was concentrated *in vacuo*. The residue was extracted with acetone in a Soxhlet apparatus for 20 hours. After this time the extract was concentrated *in vacuo*, and the residue was redissolved in acetone (140 mL). The solution was precipitated by the addition of diethyl ether (300 mL). Then the precipitate was cooled to 0 °C, filtered, rinsed with cold diethyl ether (2 × 10 mL), and dried *in vacuo* to afford **176** as a colourless solid (1.24 g, 6.11 mmol, 83%). R_f: 0.10 (petroleum ether: Et₂O 1:1); mp >300 °C (acetone) [Lit:⁵⁹ > 200 °C]; ¹H NMR (400 MHz, (CD₃)₂SO): δ 2.20 (3H, s, C(3)CH₃), 2.05 (3H, s, C(5)CH₃); ¹⁹F NMR (376 MHz, (CD₃)₂SO): δ -134.1 - -134.8 (3F, m); ¹¹B NMR (128 MHz, (CD₃)₂SO): δ 2.33 (1B, q, *J* 49), LRMS *m/z* (ES⁻) 164 ([M-K]⁻, 100%), 186 ([M-K-H+Na]⁻, 62%). These data are in accordance with the literature.⁵⁹

3-(3,5-Dimethylisoxazol-4-yl)-5-hydroxybenzaldehyde (173)

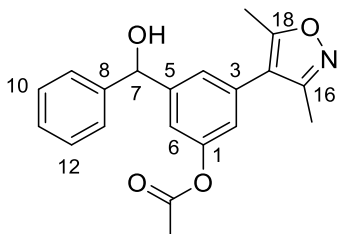
In a flame dried microwave vial, 3-bromo-5-hydroxybenzaldehyde **172** (709 mg, 3.49 mmol, 1.0 eq), potassium (3,5-dimethylisoxazol-4-yl)trifluoroborate (780 mg, 3.84 mmol, 1.1 eq), Pd(OAc)₂ (46 mg, 0.210 mmol, 0.06 eq), RuPhos (191 mg, 0.419 mmol, 0.12 eq), Na₂CO₃ (718 mg, 6.78 mmol, 2.0 eq) and degassed EtOH (30 mL) were stirred at 70 °C, for 2.5 h. After this time the reaction was judged to be complete by TLC analysis. After cooling to rt the suspension was filtered through Celite®, and concentrated *in vacuo*. The residue was suspended in CH₂Cl₂ (15 mL), filtered, and dried *in vacuo* to afford a pale yellow solid (395 mg). The filtrate was concentrated *in vacuo* and purified by silica gel chromatography, eluting with a gradient of 20% to 40% EtOAc in petroleum ether, to afford a yellow solid (190 mg). The combined yield of **173** (585 mg, 2.69 mmol) is 76%: R_f: 0.11 (petroleum ether: Et₂O 1:1); mp 189-191 °C (CHCl₃) [Lit⁵⁹ 184-187 °C]; ¹H NMR (400 MHz, (CD₃)₂SO): δ 10.18 (1H, s, CHO), 9.97 (1H, s, OH), 7.39-7.36 (1H, m, C(4)H), 7.27-7.24 (1H, m, C(2)H), 7.11-7.07 (1H, m, C(6)H), 2.43 (3H, s, C(9)CH₃), 2.25 (3H, s, C(11)CH₃); LRMS *m/z* (ES⁻) 216 ([M-H]⁻, 61%), 433 ([2M-H]⁻, 100%). These data are in accordance with the literature.⁵⁹

3-(3,5-Dimethylisoxazol-4-yl)-5-(hydroxy(phenyl)methyl)phenol (2)

A solution of 3-(3,5-dimethylisoxazol-4-yl)-5-hydroxybenzaldehyde **173** (390 mg, 1.79 mmol, 1.0 eq) in dry THF (25 mL) was cooled to 0 °C. A 1 M phenylmagnesium bromide solution in THF (5.38 mL, 5.38 mmol, 3.0 eq) was added dropwise over 15 min.

The suspension was allowed to warm up to ambient temperature and stirred for 1 h. The suspension was quenched at 0 °C with 1 M aq. HCl (10 mL) and concentrated *in vacuo*. The residue was suspended in H₂O (20 mL) and extracted with Et₂O (3 × 30 mL). The combined organic extracts were washed with brine (50 mL), dried (MgSO₄), filtered and concentrated *in vacuo*. The crude material was purified by silica gel chromatography eluting with a gradient of 20% to 50% EtOAc in petroleum ether to afford **2** as a colourless solid (429 mg, 1.45 mmol, 81%). R_f: 0.35 (petroleum ether: EtOAc 1:1); mp 199-202 °C (CHCl₃) [Lit:⁵⁹ 187-188 °C]; ¹H NMR (400 MHz, (CD₃)₂CO): δ 8.45 (1H, s, OH), 7.50-7.45 (2H, m, C(9)H and C(13)H), 7.36-7.30 (2H, m, C(10)H and C(12)H), 7.23 (1H, dddd, J 7.3, 7.3, 1.3, 1.3, C(11)H), 6.96-6.93 (1H, m, C(6)H), 6.93-6.90 (1H, m, C(4)H), 6.69 (1H, dd, J 1.8, 1.8, C(2)H), 5.83 (1H, d, J 4.2, C(7)H), 4.91 (1H, d, J 4.2, CHOH), 2.38 (3H, s, C(16)CH₃), 2.20 (3H, s, C(18)CH₃); LRMS *m/z* (ES⁻) 294 ([M-H]⁻, 100%). RP-HPLC: Method A: Retention time: 10.91 min, purity 99.2%. These data are in accordance with the literature except the reported melting point is 10 °C lower.⁵⁹

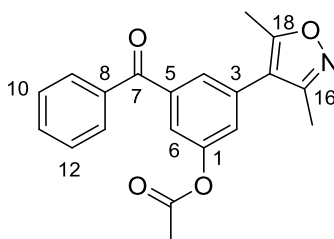
3-(3,5-Dimethylisoxazol-4-yl)-5-(hydroxy(phenyl)methyl)phenyl acetate (**167**)



To a solution of 3-(3,5-dimethylisoxazol-4-yl)-5-(hydroxy(phenyl)methyl)phenol **2** (400 mg, 1.35 mmol, 1.0 eq) in *i*PrOH (20 mL) was added a solution of NaOH (148 mg, 3.66 mmol, 2.7 eq) in water (0.2 mL). After the completed addition, Ac₂O (344 μL, 3.66 mmol, 2.7 eq) was added over 5 min, and the suspension was stirred for 60 min, at ambient temperature. After this time the reaction was judged to be complete by TLC analysis. The suspension was adsorbed onto Celite®, and concentrated *in vacuo*. The residue was purified by silica gel chromatography, eluting with a gradient of 10% to 50% EtOAc in petroleum ether, to afford **167** as a colourless oil (390 mg, 1.16 mmol, 85%). R_f: 0.10

(petroleum ether: EtOAc 3:1); ^1H NMR (400 MHz, CDCl_3): δ 7.41-7.33 (4H, m, C(9)H, C(10)H, C(12')H and C(13)H), 7.32-7.27 (1H, m, C(11)H), 7.16-7.13 (1H, m, C(6)H), 7.12-7.09 (1H, m, C(4)H), 6.89 (1H, dd, J 1.8, 1.8, C(2)H), 5.86 (1H, s, C(7)H), 2.37 (3H, s, C(18)CH₃), 2.30 (3H, s, COCH₃), 2.22 (3H, s, C(16)CH₃); LRMS m/z (ES⁺) 338 ([M+H]⁺, 51%), 360 ([M+Na]⁺, 100%). These data are in accordance with the literature.⁵⁹

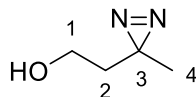
3-Benzoyl-5-(3,5-dimethylisoxazol-4-yl)phenyl acetate (168)



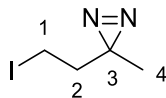
To a solution of 3-(3,5-dimethylisoxazol-4-yl)-5-(hydroxy(phenyl)methyl)phenyl acetate **167** (120 mg, 0.356 mmol, 1.0 eq) in CH_2Cl_2 was added PCC (85 mg, 0.391 mmol, 1.1 eq). The orange/brown suspension was stirred for 3 h, at ambient temperature, until TLC analysis indicated complete consumption of the starting material. The suspension was filtered through Celite®, and concentrated *in vacuo*. The crude material was purified by silica gel chromatography, eluting with a gradient of 20% to 50% EtOAc in petroleum ether, to afford **168** as a colourless solid (43 mg, 0.128 mmol, 36%). R_f: 0.58 (petroleum ether: EtOAc 1:1); mp 136-138 °C (acetone); ν_{max} (thin film)/cm⁻¹ 1764 (m) (C=O), 1655 (m) (C=O), 1322 (m), 1197 (s); ^1H NMR (500 MHz, $(\text{CD}_3)_2\text{CO}$): δ 7.89-7.85 (2H, m, C(9)H and C(13)H), 7.71 (1H, dddd, J 7.4, 7.4, 1.4, 1.4, C(11)H), 7.63 (1H, dd, J 1.6, 1.6, C(6)H), 7.62-7.58 (2H, m, C(10)H and C(12)H), 7.55 (1H, dd, J 2.3, 1.6, C(4)H), 7.49 (1H, dd, J 2.3, 1.6, C(2)H), 2.47 (3H, s, C(16)CH₃), 2.33 (3H, s, COCH₃), 2.29 (3H, s, C(18)CH₃); ^{13}C NMR (126 MHz; $(\text{CD}_3)_2\text{CO}$): δ 194.4 (C(7)), 168.8 (C=OCH₃), 165.9 (C(16)), 157.9 (C(18)), 151.2 (C(1)), 139.4 (C(5)), 137.1 (C(8)), 132.8 (C(11)), 132.2 (C(3')), 129.8 (C(9) and C(13)), 128.5 (C(10) and C(12)), 127.4 (C(6)), 126.2 (C(2)), 121.9 (C(4)), 114.9 (C(17)), 20.1 (COCH₃), 10.8 (C(16)CH₃), 9.9 (C(18)CH₃), LRMS m/z (ES⁺) 336 ([M+H]⁺, 56%), 358

[[M+Na]⁺, 100%]; HRMS *m/z* (ES⁺) [Found: (M+H)⁺ 336.1230. C₂₀H₁₈N₁O₄⁺ requires 336.1230]; RP-HPLC: Method A: Retention time 13.11 min, purity 99.3%.

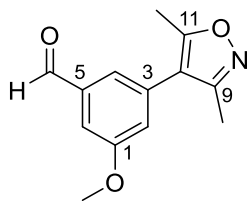
2-(3-Methyl-3*H*-diazirin-3-yl)ethan-1-ol (**177**)



4-Hydroxy-2-one **173** (5.00 g, 56.7 mmol, 1.0 eq) was added dropwise to liquid NH₃ (40 mL) at -78 °C. The solution was warmed to -40 °C and stirred for 5 h. After this time the colourless solution was cooled to -78 °C. A solution of hydroxylamine-*O*-sulfonic acid (7.10 g, 62.8 mmol, 1.1 eq) in MeOH (45 mL) was added dropwise over 30 min. The suspension warmed to -40 °C, and stirred for 1.5 h. After this time the suspension was slowly warmed to ambient temperature overnight. The colourless suspension was filtered, rinsed (MeOH), and the filtrate was concentrated *in vacuo*. The residue was dissolved in Et₃N (8.0 mL) and Et₂O (50 mL), and cooled to 0 °C. I₂ (7.68 g, 60.5 mmol, 1.05 eq) was added portionwise until the red color persist. After 30 min the mixture was diluted with H₂O (50 mL). The organic components of the aqueous layer were extracted with Et₂O (3 × 50 mL). The combined organic extracts were dried (Na₂SO₄), filtered, and concentrated *in vacuo*. The oil was purified by Kugelrohr distillation (120 °C, 20 mbar), to afford **177** as a colourless oil (1.50 g, 15.0 mmol, 26%). R_f: 0.23 (petroleum ether :EtOAc 5:1); ¹H NMR (400 MHz; CDCl₃): δ 3.53 (2H, br t, *J* 6.3, C(1)H₂), 1.63 (2H, t, *J* 6.3, C(2)H₂), 1.07 (3H, s, C(4)H₃), ¹³C NMR (101 MHz; CDCl₃): δ 57.7 (C(1)), 37.0 (C(2)), 24.2 (C(3)), 20.2 (C(4)), , Compound mass was not observed by LRMS and HRMS. These data are in good agreement with the literature.¹⁸⁴

3-(2-Iodoethyl)-3-methyl-3H-diazirine (174)

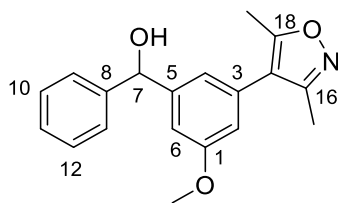
A solution of 1H-imidazole (410 mg, 6.02 mmol, 3.0 eq), triphenyl phosphine (580 mg, 2.08 mmol, 1.05 eq) and I₂ (610 mg, 2.40 mmol, 1.2 eq) in CH₂Cl₂ (12 mL) was cooled to 0 °C. To this solution was added 2-(3-methyl-3H-diazirin-3-yl)ethan-1-ol **177** (200 mg, 2.00 mmol, 1.0 eq) in CH₂Cl₂ (1 mL) was added over a period of 5 min, and the mixture was warmed to ambient temperature. After 3 h the the reaction was judged to be complete by ¹H NMR analysis. The reaction mixture was adsorbed onto Celite®, and purified by silica gel chromatography, eluting with 10% Et₂O in pentane, to afford **174** as a volatile, colourless oil (210 mg, 1.00 mmol, 50%). R_f: 0.09 (petroleum ether); ¹H NMR (400 MHz; CDCl₃): δ 2.88 (2H, t, *J* 7.6, C(1)H₂), 1.96 (2H, t, *J* 7.6, C(2)H₂), 1.01 (3H, s, C(4)H₃), ¹³C NMR (101 MHz; CDCl₃): δ 38.9 (C(2)), 26.2 (C(3)), 19.4 (C(4)), -3.7 (C(1)). Compound mass could not be observed by LRMS and HRMS. These data are in good agreement with the literature.¹⁵⁴

3-(3,5-Dimethylisoxazol-4-yl)-5-methoxybenzaldehyde (179)

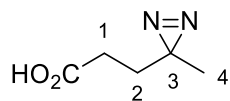
To a suspension of 3-(3,5-dimethylisoxazol-4-yl)-5-hydroxybenzaldehyde **173** (310 mg, 1.43 mmol, 1.0 eq), Cs₂CO₃ (697 mg, 2.14 mmol, 1.5 eq) in dry DMF (5 mL) was added iodomethane (178 μL, 406 mg, 2.86 mmol, 1.5 eq), and stirred for 2.5 h, at ambient temperature. After this time TLC analysis indicated some starting, so morer iodomethane (178 μL, 406 mg, 2.86 mmol, 1.5 eq) was added. After 5 h at ambient temperature the reaction was judged to be complete by TLC analysis. The yellow suspension was quenched with water (10 mL), and diluted with EtOAc (30 mL). The mixture was washed with brine

(3 × 30 mL), dried (MgSO₄), filtered, and concentrated *in vacuo*. The residue was purified by silica gel chromatography, eluting with a gradient of 10% to 40% EtOAc in petroleum ether to afford **179** as a brown solid (245 mg, 1.06 mmol, 74%). R_f: 0.10 (petroleum ether: EtOAc 3:1); mp 92-95 °C (CHCl₃) [Lit⁵⁹ 90-92 °C]; ¹H NMR (400 MHz, CDCl₃) 10.04 (1H, s, CHO), 7.44-7.40 (1H, m, C(4)H), 7.39-7.35 (1H, m, C(2)H), 7.10-7.06 (1H, m, C(6)H), 3.94 (3H, s, OCH₃), 2.46 (3H, s, C(9)H₃), 2.32 (3H, s, C(11)H₃); LRMS *m/z* (ES⁺) 232 ([M+H]⁺, 100%). These data are in accordance with the literature.⁵⁹

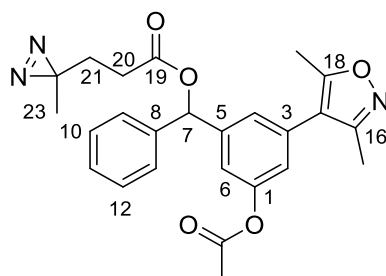
(3-(3,5-Dimethylisoxazol-4-yl)-5-methoxyphenyl)(phenyl)methanol (**180**)



A solution of 3-(3,5-dimethylisoxazol-4-yl)-5-methoxybenzaldehyde **179** (240 mg, 1.04 mmol, 1.0 eq) in dry THF (15 mL) was cooled to 0 °C. Phenylmagnesium bromide in THF (1 M, 2.07 mL, 2.07 mmol, 2.0 eq) was added dropwise over 10 min. After the complete addition the suspension was warmed to ambient temperature and stirred for 1.5 h. After this time the reaction was judged to be complete by TLC analysis. The suspension was quenched at 0 °C with 1 M aq. HCl (15 mL) and concentrated *in vacuo*. The residue was suspended in EtOAc (40 mL), washed with brine (3 × 30 mL), dried (MgSO₄), filtered, and concentrated *in vacuo*. The crude material was purified by silica gel chromatography, eluting with a gradient of 10% to 50% EtOAc in petroleum ether, to afford **180** as a colourless oil (318 mg, 1.03 mmol, 99%). R_f: 0.17 (petroleum ether: EtOAc 1:1); ¹H NMR (400 MHz, CDCl₃): δ 8.45 (1H, s, OH), 7.46-7.36 (4H, m, C(9)H, C(10)H, C(12)H and C(13)H), 7.34-7.30 (1H, m, C(11)H), 7.01-6.98 (1H, m, C(6)H), 6.86-6.83 (1H, m, C(4)H), 6.71-6.68 (1H, m, C(2)H), 5.88 (1H, s, C(7)H), 3.84 (3H, s, OCH₃), 2.39 (3H, s, C(16)CH₃), 2.25 (3H, s, C(18)CH₃); LRMS *m/z* (ES⁺) 310 ([M+H]⁺, 100%), 332 ([M+Na]⁺, 41%). These data are in accordance with the literature.⁵⁹

3-(3-Methyl-3H-diazirin-3-yl)propanoic acid (183)

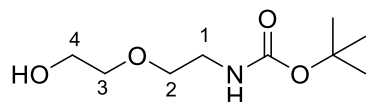
A solution of leuvenic acid **182** (1.00 g, 8.60 mmol, 1.0 eq) in MeOH (2 mL) was cooled to 0 °C. Ammonia solution in MeOH (7 M, 10 mL) was added and stirred for 3 h. After this time a solution of hydroxylamine-*O*-sulfonic acid (1.02 g, 9.90 mmol, 1.15 eq) in MeOH (6 mL) was added dropwise over 10 min and the reaction was warmed to ambient temperature overnight. The suspension was filtered, and concentrated *in vacuo*. The residue was dissolved in MeOH (4 mL) and triethylamine (1.8 mL), and cooled to 0 °C. Iodine (2.0 g) was added portionwise until the brown colour persisted. After 30 min the brown solution was dissolved in EtOAc (20 mL), washed with 1 M aq. HCl (2 × 15 mL), 10% aq. Na₂S₂O₄ (2 × 10 mL), brine (10 mL), dried (MgSO₄), filtered and concentrated *in vacuo* to afford **183** as a yellow oil (490 mg, 3.82 mmol, 44%): R_f: 0.53 (petroleum ether :EtOAc 1:1); ¹H NMR (400 MHz; CDCl₃): δ 10.23 (1H, br s, CO₂H), 2.19 (2H, t, *J* 7.8, C(1)H₂), 1.67 (2H, t, *J* 7.8, C(2)H₂), 1.00 (3H, s, C(4)H₃), ¹³C NMR (101 MHz; CDCl₃): δ 178.5 (CO₂H), 29.3 (C(2)), 28.5 (C(1)), 25.0 (C(3)), 19.6 (C(4)); LRMS *m/z* (ES⁻) 127 ([M-H]⁻, 100%). These data are in good agreement with the literature.^{160,184}

(3-Acetoxy-5-(3,5-dimethylisoxazol-4-yl)phenyl)(phenyl)methyl 3-(3-methyl-3H-diazirin-3-yl)propanoate (184)

A solution of 3-(3-methyl-3H-diazirin-3-yl)propanoic acid (**183**) (100 mg, 0.780 mmol, 5.3 eq) in SOCl₂ (1 mL) was stirred at 40 °C for 20 min. After this time the solution was concentrated *in vacuo*. The acid chloride was dissolved in dry CH₂Cl₂ (0.5 mL) and added

dropwise to a solution of 3-(3,5-dimethylisoxazol-4-yl)-5-(hydroxyl(phenyl)methyl)phenyl acetate **167** (50 mg, 0.148 mmol, 1.0 eq) in dry CH₂Cl₂ (0.7 mL). After the completed addition DIPEA (50 μL, 67.4 mg, 0.521 mmol, 3.5 eq) was added and stirred for 20 min at ambient temperature, after which time TLC showed complete consumption of the starting material. The solution was quenched with isopropanol (50 μL), and concentrated *in vacuo*. The residue was purified by silica gel chromatography, eluting with 33% ethyl acetate in petroleum ether, to afford **184** as a yellow oil (30 mg, 0.067 mmol, 45%). R_f: 0.62 (petroleum ether: EtOAc 1:1); ν_{max} (thin film)/cm⁻¹ 2928 (w), 1767 (s) (C=O), 1738 (s) (C=O), 1551 (m), 1415(m), 1368 (m), 1199 (s); ¹H NMR (400 MHz, D₆-acetone) 7.55-7.50 (2H, m, C(9)H and C(13)H), 7.45-7.39 (2H, m, C(10)H and C(12)H), 7.38-7.32 (2H, m, C(11)H and C(2)H), 7.25-7.22 (1H, m, C(4)H), 7.15 (1H, dd, *J* 1.9, 1.9 C(6)H), 6.98 (1H, s, C(7)H), 2.47 (2H, t, *J* 7.3, C(22)H₂), 2.43 (3H, s, C(16)CH₃), 2.30 (3H, s, COCH₃), 2.25 (3H, s, C(18)CH₃), 1.77 (2H, t, *J* 7.3, C(21)H₂), 1.04 (3H, s, C(23)H₃), ¹³C NMR (101 MHz, D₆-acetone): 170.8 (C(19)), 168.6 (COCH₃), 165.5 (C(16)), 157.9 (C(18)), 151.4 (C(1)), 143.0 (C(5)), 140.3 (C(8)), 131.9 (C(3)), 128.6 (C(10) and C(12)), 128.0 (C(11)), 126.9 (C(9) and C(13)), 124.6 (C(2)), 121.7 (C(6)), 119.0 (C(4)), 115.3 (C(17)), 76.2 (C(7)), 29.3 (C(21)) by HSQC, 28.4 (C(20)), 25.0 (C(22)), 20.1 (COCH₃), 18.7 (C(23)), 10.7 (C(16)CH₃), 9.9 (C(18)CH₃); GC-HRMS *m/z* (CI⁺) [Found: (M+H)⁺ 448.1872 C₂₅H₂₅N₃O₅ requires 448.1867]; RP-HPLC: Method B: Retention time 13.86 min, purity 93.7%.

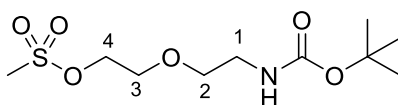
***tert*-Butyl 2-(2-hydroxyethoxy)ethylcarbamate (188)**



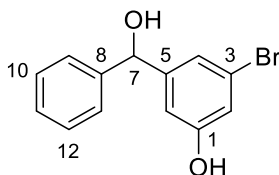
To a solution of 2-(2-aminoethoxy)ethanol **187** (2.00 g, 19.0 mmol, 1.0 eq) in THF (20 mL) was added a solution of Boc₂O (4.36 g, 20.0 mmol, 1.1 eq) in THF over 10 minutes. After 3 h the reaction was judged to be complete by TLC analysis. The colourless solution was concentrated *in vacuo*. The resulting oil was diluted with EtOAc (50 mL), washed with sat. aq. NH₄Cl (3 × 30 mL), dried (MgSO₄), filtered and concentrated *in vacuo* to afford **188** as a

colourless oil (3.76 g, 18.3 mmol, 96%), which was used without further purification. R_f : 0.52 (EtOAc); ν_{\max} (thin film)/ cm^{-1} 3343 (br m), 2976 (m), 2932 (m), 2871 (m), 1688 (s) (C-O), 1522 (m), 1366 (m), 1277 (m), 1250 (m), 1168 (s), 1123 (s), 1064 (s), ^1H NMR (400 MHz, CDCl_3): δ 5.38 (1H, s, NH), 3.68-3.62 (2H, m, C(2) H_2), 3.52-3.44 (4H, m, C(3) H_2 and C(4) H_2), 3.40-3.35 (1H, m, OH), 3.24 (2H, dt, J 5.1, 5.1, C(1) H_2), 1.36 (9H, s, C(CH_3) $_3$); LRMS m/z (ES^+) 228 ($[\text{M}+\text{Na}]^+$, 100%). These data are in accordance with the literature.¹⁸⁵

2-(2-(*tert*-Butoxycarbonylamino)ethoxy)ethyl methanesulfonate (**189**)

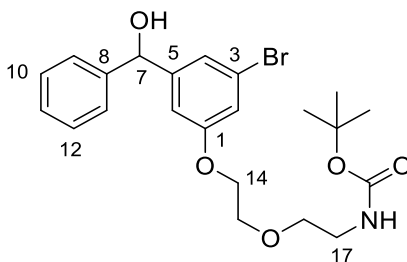


A solution of *tert*-butyl 2-(2-hydroxyethoxy)ethylcarbamate **188** (2.00 g, 9.74 mmol, 1.0 eq), Et_3N (2.66 mL, 2.00 g, 19.5 mmol, 2.0 eq) in THF (125 mL) was cooled to 0 °C. Methanesulphonyl chloride (2.24 g, 19.5 mmol, 2.0 eq) was added over 15 minutes. After the completed addition the solution was warmed to ambient temperature. After 15 minutes the TLC analysis indicated completion and the solvent was removed *in vacuo*. The residue was dissolved in EtOAc (150 mL), washed with brine (100 mL), dried (MgSO_4), filtered and concentrated *in vacuo*. The crude material was purified by silica gel chromatography, eluting with a gradient of 10% to 100% EtOAc in petroleum ether, to afford **189** as a colourless oil (2.05 g, 7.24 mmol, 74%). R_f : 0.71 (EtOAc); ν_{\max} (thin film)/ cm^{-1} 3420 (br w) (N-H), 2979 (w), 2937 (w), 1737 (s) (C=O), 1511 (m), 1351 (s), 1245 (s), 1172 (s), 1128 (s); ^1H NMR (400 MHz, CDCl_3) 4.97 (1H, s, NH), 4.38-4.33 (2H, m, C(4) H_2), 3.74-3.69 (2H, m, C(3) H_2), 3.55 (2H, t, J 5.3, C(2) H_2), 3.35-3.26 (2H, m, C(1) H_2), 3.05 (3H, s, CH_3SO_2), 1.43 (9H, s, C(CH_3) $_3$); ^{13}C NMR (101 MHz, CDCl_3) 155.9 (C=O), 79.4 (C(CH_3) $_3$), 70.4 (C(2)), 68.9 (C(3)), 68.7 (C(4)), 40.2 (C(1)), 37.7 (CH_3SO_3), 28.4 (C(CH_3) $_3$); LRMS m/z (ES^+) 306 ($[\text{M}+\text{Na}]^+$, 100%).

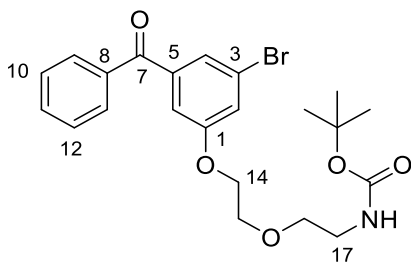
3-Bromo-5-(hydroxy(phenyl)methyl)phenol (190)

A solution of 3-bromo-5-hydroxybenzaldehyde **172** (800 mg, 3.95 mmol, 1.0 eq) in dry THF (50 mL) was cooled to 0 °C. Phenyl magnesium bromide in THF (1 M, 12 mL, 12.0 mmol, 3.0 eq) was added dropwise over 15 minutes. The suspension was warmed to ambient temperature and stirred for 17 hours. After this time the reaction was judged to be complete by TLC analysis. After cooling to 0 °C the suspension was quenched with 1 M aq. HCl (10 mL), and concentrated *in vacuo*. The residue was dissolved in EtOAc (50 mL), washed with brine (3 × 50 mL), dried (Na₂SO₄), filtered, and concentrated *in vacuo*. The crude material was purified by silica gel chromatography, eluting with a gradient of 5% to 30% EtOAc in petroleum ether, to give **190** as a pale yellow solid (1049 mg, 3.76 mmol, 100%). R_f: 0.18 (petroleum ether: EtOAc 4:1); mp 110-111 °C (acetone), ν_{\max} (thin film)/cm⁻¹ 3394 (br m) (OH), 3088 (br m) (OH), 1596 (s), 1474 (s), 1275 (s), 1021 (s); ¹H NMR (400 MHz, (CD₃)₂CO): δ 8.72 (1H, s, C(1)OH), 7.45-7.40 (2H, m, C(10)H and C(12)H), 7.36 (2H, tt, *J* 7.4, 1.7, C(9)H and C(13)H), 7.25 (1H, tt, *J* 7.3, 2.2, C(11)H), 7.12-7.09 (1H, m, C(2)H), 6.92-6.87 (2H, m, C(4)H and C(6)H), 5.77 (1H, d, *J* 3.9, C(7)OH), 4.99 (1H, d, *J* 3.9, C(7)H); ¹³C NMR (101 MHz, (CD₃)₂CO): δ 158.3 (C(1)), 149.3 (C(5)), 144.9 (C(8)), 128.2 (C(9) and C(13)), 127.1 (C(11)), 126.4 (C(10) and C(12)), 121.9 (C(3)), 120.5 (C(2)), 116.8 (C(6)), 112.6 (C(4)), 74.5 (C(7)); LRMS *m/z* (ES⁻) 277 ([M⁷⁹Br-H]⁻, 100%), 279 ([M⁸¹Br-H]⁻, 100%), HRMS *m/z* (ES⁻) [Found: (M⁷⁹Br-H)⁻ 276.9866 C₁₃H₁₀O₂⁷⁹Br⁻ requires 276.9870]; RP-HPLC: Method A: Retention time 11.58 min, purity 99.3%.

***tert*-Butyl 2-(2-(3-bromo-5-(hydroxy(phenyl)methyl)phenoxy)ethoxy)ethylmethanesulfonate (191)**

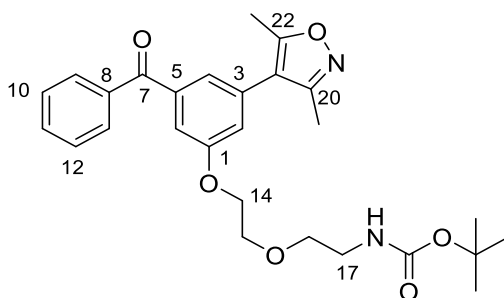


A suspension of 3-bromo-5-(hydroxy(phenyl)methyl)phenol **190** (420 mg, 1.50 mmol, 1.0 eq), 2-(2-(*tert*-butoxycarbonylamino)ethoxy)ethyl methanesulfonate (760 mg, 2.68 mmol, 1.8 eq) and Cs₂CO₃ (876 mg, 2.69 mmol, 1.8 eq) in DMF (15 mL) was stirred for 16 hours at ambient temperature. After this time the reaction was judged to be incomplete by TLC analysis. The suspension was heated at 60 °C for 1 hour and the starting material disappeared by TLC. After cooling to ambient temperature the suspension was diluted with EtOAc (50 mL), washed with water (2 × 40 mL), brine (50 mL), dried (MgSO₄), filtered, and concentrated *in vacuo*. The residue was purified by silica gel chromatography, eluting with a gradient of 10% to 50% EtOAc in petroleum ether, to afford **191** as a colourless oil (370 mg, 0.793 mmol, 53%). R_f: 0.48 (petroleum ether:EtOAc 1:1); ν_{max} (thin film)/cm⁻¹ 3368 (br w) (O-H and N-H), 2976 (w), 1688 (s) (C=O), 1439 (s), 1265 (s), 1156 (s), 1125 (s), 993 (s), 703 (s); ¹H NMR (400 MHz, (CD₃)₂CO): δ 7.46-7.41 (2H, m, C(9)*H* and C(13)*H*), 7.35-7.29 (2H, m, C(10)*H* and C(12)*H*), 7.23 (1H, tt, *J* 7.4, 2.0, C(11)*H*), 7.20-7.18 (1H, m, C(2)*H*), 7.05-7.02 (1H, m, C(4)*H*), 6.98 (1H, dd, *J* 2.0, 2.0 C(6)*H*), 5.90 (1H, br s, *NH*), 5.80 (1H, d, 4.2, C(7)*H*), 5.05 (1H, d, 4.2, *OH*), 4.16-4.14 (2H, m, C(14)*H*₂), 3.82-3.79 (2H, m, C(15)*H*₂), 3.55 (2H, t, 5.8, C(16)*H*₂), 3.23 (2H, dt, 5.8, 5.8, C(17)*H*₂), 1.39 (9H, s, C(CH₃)₃); ¹³C NMR (101 MHz, (CD₃)₂CO): δ 160.3 (C(1)), 155.8 (NHC*o*tBu), 149.3 (C(8)), 144.8 (C(5)), 128.2 (C(10) and C(12)), 127.2 (C(11)), 126.4 (C(9) and C(13)), 122.0 (C(3)), 121.6 (C(4)), 115.7 (C(2)), 112.1 (C(6)), 77.8 (C(CH₃)₃), 74.5 (C(7)), 69.9 (C(16)), 69.0 (C(15)), 67.8 (C(14)), 40.1 (C(17)), 27.8 (C(CH₃)₃). Compound mass could not be detected by LRMS and HRMS.

***tert*-Butyl (2-(2-(3-benzoyl-5-bromophenoxy)ethoxy)ethyl)carbamate (192)**

tert-Butyl 2-(2-(3-bromo-5-(hydroxy(phenyl)methyl)phenoxy)ethoxy)ethylcarbamate **191** (300 mg, 0.643 mmol, 1.0 eq), pyridinium dichromate (266 mg, 0.708 mmol, 1.1 eq) and Celite® (200 mg) were stirred in CH₂Cl₂ (10 mL) at ambient temperature for 6 h. After this time the reaction was judged to be complete by TLC analysis. The suspension was filtered through Celite®, and concentrated *in vacuo*. The compound was purified by silica gel chromatography, eluting with a gradient of 10% to 50% EtOAc in petroleum ether, to afford **192** as a colourless oil (130 mg, 0.280 mmol, 44%); R_f: 0.14 (petroleum ether:EtOAc 4:1); ν_{\max} (thin film)/cm⁻¹ 3371 (br w) (N-H), 2975 (w), 2930 (w), 1709 (s) (C=O), 1660 (s) (C=O), 1564 (m), 1279 (s), 1170 (s), 1125 (s), 696 (s); ¹H NMR (400 MHz, (CD₃)₂CO): δ 7.83-7.78 (2H, m, C(9)H and C(13)H), 7.68 (1H, tt, *J* 7.5, 1.9, C(11)H) 7.60-7.54 (2H, m, C(10)H and C(12)H), 7.45-7.41 (2H, m, C(2)H), 7.29 (1H, dd, *J* 2.4, 1.4, C(6)H), 5.85 (1H, br s, NH), 4.27-4.22 (2H, m, C(14)H₂), 3.85-3.81 (2H, m, C(15)H₂), 3.57 (2H, t, *J* 5.8, C(16)H₂), 3.25 (2H, dt, *J* 5.8, 5.8, C(17)H₂), 1.39 (9H, s, C(CH₃)₃); ¹³C NMR (101 MHz, (CD₃)₂CO): δ 194.0 (C(7)), 159.8 (C(1)), 155.7 (NHCO), 140.5 (C(5)), 137.0 (C(8)), 132.8 (C(11)), 129.7 (C(9) and C(13)), 128.5 (C(10) and C(12)), 124.5 (C(4)), 122.3 (C(3)), 121.4 (C(2)), 114.8 (C(6)), 77.6 (OC(CH₃)₃) 69.9 (C(16)), 68.9 (C(15)), 68.3 (C(14)), 40.1 (C(17)), 27.7 (C(CH₃)₃). GC-HRMS *m/z* (CI⁺) [Found: (M+H)⁺ 464.1073 C₂₂H₂₆⁷⁹BrN₁O₅ requires 464.1067].

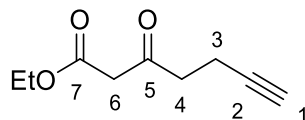
***tert*-Butyl (2-(2-(3-benzoyl-5-(3,5-dimethylisoxazol-4-yl)phenoxy)ethoxy)ethyl)carbamate (185)**



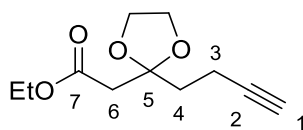
A solution of *tert*-Butyl (2-(2-(3-benzoyl-5-bromophenoxy)ethoxy)ethyl)carbamate **192** (120 mg, 0.259 mmol, 1.0 eq) in degassed EtOH (2.5 mL) was added to potassium (3,5-dimethylisoxazol-4-yl)trifluoroborate **176** (58 mg, 0.285 mmol, 1.1 eq), RuPhos (14.5 mg, 0.031 mmol 0.12 eq), Pd(OAc)₂ (4.0 mg, 0.016 mmol, 0.06 eq) and Na₂CO₃ (55 mg, 0.518 mmol, 2.0 eq). The suspension was purged with Ar and stirred at 75 °C for 3 h. After this time the reaction was judged to be complete by TLC analysis. After cooling to rt the suspension was filtered through Celite®, rinsed with EtOH, and concentrated *in vacuo*. The residue was purified by silica gel chromatography, eluting with a gradient of 20% to 40% EtOAc in petroleum ether, to afford **185** as a pale yellow oil (84 mg, 0.175 mmol, 67%): R_f: 0.33 (petroleum ether:EtOAc 3:2); ν_{\max} (thin film)/cm⁻¹ 3347 (br w) (N-H), 2975 (w), 2931 (w), 1709 (s) (C=O), 1660 (m) (C=O), 1331 (s), 1266 (s), 1239 726 (m); ¹H NMR (500 MHz, (CD₃)₂CO): δ 7.87-7.82 (2H, m, C(9)H and C(13)H), 7.68 (1H, tt, *J* 7.4, 1.1, C(11)H) 7.60-7.54 (2H, m, C(10)H and C(12)H), 7.36-7.33 (1H, m, C(4)H), 7.28-7.26 (1H, m, C(6)H), 7.25-7.22 (1H, m, C(2)H), 5.88 (1H, br s, NH), 4.31-4.25 (2H, m, C(14)H₂), 3.86-3.82 (2H, m, C(15)H₂), 3.59 (2H, t, 5.7, C(16)H₂), 3.25 (2H, dt, 5.7, 5.7, C(17)H₂), 2.44 (3H, s, C(20)CH₃), 2.26 (3H, s, C(22)CH₃), 1.37 (9H, s, C(CH₃)₃); ¹³C NMR (126 MHz, (CD₃)₂CO): δ 195.1 (C(7)), 165.6 (C(20)), 159.4 (C(1)), 158.0 (C(22)), 155.7 (NHCO), 139.6 (C(5)), 137.5 (C(8)), 132.7 (C(11)), 132.1 (C(21)), 129.8 (C(9) and C(13)), 128.5 (C(10) and C(12)), 122.8 (C(6)), 119.2 (C(2)), 115.6 (C(3)), 114.2 (C(4)), 77.7 (OC(CH₃)₃), 69.9 (C(16)), 69.0 (C(15)), 68.0 (C(14)), 40.1 (C(17)), 27.7 (C(CH₃)₃), 10.8 (C(20)CH₃), 10.0

(C(22)CH₃); LRMS m/z (ES⁺) 381 ([M+H-Boc]⁺, 100%); HRMS m/z (ES⁺) [Found: (M+H-Boc)⁺ 381.1803; C₂₂H₂₅O₄N₂ requires 381.1803].

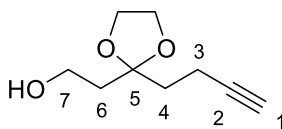
Ethyl 3-oxohept-6-ynoate (194)



A solution of diisopropyl amine (10.2 g, 101 mmol, 2.0 eq) in distilled THF (100 mL) was cooled to -78 °C. *n*-BuLi in hexanes (2.5 M, 40.5 mL, 101 mmol, 2.0 eq) was added over 5 minutes. After the completed addition the solution was warmed to 0 °C and stirred for 30 minutes. After this time the solution was cooled to -78 °C. Ethyl acetoacetate **193** (6.60 g, 50.7 mmol, 1.0 eq) in distilled THF (20 mL) was added over 5 minutes. After the completed addition the solution was warmed to 0 °C and stirred for 1 h. Propargyl bromide (80% in toluene, 7.52 g, 50.7 mmol, 1.0 eq) was added, and stirred for 1 h, at 0 °C. After this time the solution was quenched by slow addition of glacial acetic acid (5.8 mL). The suspension was concentrated *in vacuo*, and the residue was redissolved in EtOAc (250 mL) and H₂O (200 mL). The organic extracts were washed with brine (2 × 150 mL), dried (MgSO₄), filtered, and concentrated *in vacuo*. The residual oil was purified by vacuum distillation (110 °C, 15 mbar), to afford **195** as a pale yellow oil (4.81 g, 28.6 mmol, 56%). R_f : 0.42 (petroleum ether: EtOAc 4:1); ¹H NMR (400 MHz, CDCl₃) 4.19 (2H, q, J 7.3, OCH₂), 3.46 (2H, s, C(6)H₂), 2.81 (2H, t, J 7.2, C(4)H₂), 2.46 (2H, td, J 7.2, 2.5, C(3)H₂), 1.96 (1H, t, J 2.5, C(1)CH), 1.27 (3H, t, J 7.3, CH₃CH₂O), ¹³C NMR (101 MHz, CDCl₃): 200.6 (C(5)), 166.9 (C(7)), 82.5 (C(2)), 69.0 (C(1)), 61.5 (OCH₂), 49.1 (C(5)), 41.6 (C(4)), 14.1 (CH₃CH₂), 12.8 (C(3)); GC-HRMS m/z (CI⁺) [Found: (M+H)⁺ 169.0862 C₉H₁₂O₃ requires 169.0859]. These data are in good agreement with the literature.¹⁸⁶

Ethyl 2-(2-(but-3-yn-1-yl)-1,3-dioxolan-2-yl)acetate (195)

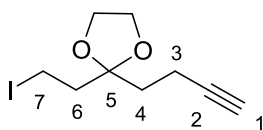
A solution of ethyl 3-oxohept-6-ynoate **194** (4.81 g, 28.6 mmol, 1.0 eq), ethylene glycol (1.90 g, 30.6 mmol, 1.1 eq), 4-toluenesulfonic acid monohydrate (250 mg, 1.31 mmol, 0.05 eq) in toluene (200 mL) was stirred at reflux, for 19 h in a Dean-Stark apparatus. After cooling to ambient temperature the organic layer was washed with 1 M aq. Na_2CO_3 (3×100 mL), brine (100 mL), dried (MgSO_4), filtered and concentrated *in vacuo* to afford **195** as a pale yellow oil (4.41 g), which was used without further purification. R_f : 0.56 (petroleum ether: EtOAc 4:1); ^1H NMR (400 MHz, CDCl_3): δ 4.17 (2H, q, J 7.5, OCH_2), 4.05-3.97 (4H, m, $\text{O}(\text{CH}_2)_2\text{O}$), 2.67 (2H, s, $\text{C}(6)\text{H}_2$), 2.32 (2H, td, J 7.2, 2.6, $\text{C}(3)\text{H}_2$), 2.17-2.11 (2H, m, $\text{C}(4)\text{H}_2$), 1.95 (1H, t, J 2.6, $\text{C}(1)\text{CH}$), 1.28 (3H, t, J 7.5, $\text{CH}_3\text{CH}_2\text{O}$), ^{13}C NMR (101 MHz, CDCl_3): δ 169.2 ($\text{C}(7)$), 108.3 ($\text{C}(5)$), 84.0 ($\text{C}(2)$), 68.1 ($\text{C}(1)$), 65.2 ($\text{O}(\text{CH}_2)_2\text{O}$), 60.6 (OCH_2), 42.7 ($\text{C}(6)$), 36.4 ($\text{C}(4)$), 14.2 (CH_3CH_2), 12.8 ($\text{C}(3)$); LRMS m/z (ES^+) 235 ($[\text{M}+\text{Na}]^+$, 100%). These data are in good agreement with the literature.¹⁸⁶

2-(2-(But-3-yn-1-yl)-1,3-dioxolan-2-yl)ethan-1-ol (196)

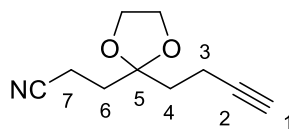
To a solution ethyl 2-(2-(but-3-yn-1-yl)-1,3-dioxolan-2-yl)acetate **195** (4.41 g, 20.8 mmol, 1.0 eq) in Et_2O (100 mL) was added LiAlH_4 (1 M in THF, 15 mL, 15 mmol, 0.75 eq) dropwise at 0°C . After 1 h the reaction was judged to be complete by TLC analysis. The solution was quenched with EtOAc (10 mL) followed by addition of H_2O (2 mL). To the suspension sat. aq. Rochelle salt (50 mL) was added and stirred until the suspension cleared up. The organic extracts were washed with brine (100 mL), dried (MgSO_4), filtered, and concentrated *in vacuo* to afford **196** as a pale yellow oil (2.90 g, 17.0 mmol, 60% over 2 steps). R_f : 0.12 (petroleum ether: EtOAc 4:1); ^1H NMR (400 MHz, CDCl_3) 4.07-

3.98 (4H, m, O(CH₂)₂O), 3.79 (2H, dt, *J* 5.6, 5.6, C(7)H₂), 2.66 (1H, t, *J* 5.6, OH), 2.29 (2H, td, *J* 7.4, 2.6, C(3)H₂), 1.99-1.92 (5H, m, C(1)H, C(4)H₂ and C(6)H₂), ¹³C NMR (101 MHz, CDCl₃): (C(7)), 111.1 (C(5)), 83.9 (C(2)), 68.3 (C(1)), 65.0 (O(CH₂)₂O), 58.7 (C(7)), 38.2 (C(6)), 35.9 (C(4)), 13.1 (C(3)). GC-HRMS *m/z* (CI⁺) [Found: (M+H)⁺ 171.1016 C₉H₁₄O₃ requires 171.1016]. These data are in good agreement with the literature.¹⁸⁶

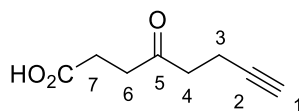
2-(But-3-yn-1-yl)-2-(2-iodoethyl)-1,3-dioxolane (**197**)



To a solution of PPh₃ (2.60 g, 9.91 mmol, 1.1 eq) and 1*H*-imidazole (1.80 g, 26.4 mmol, 3.0 eq) in CH₂Cl₂ (60 mL) was added iodine (2.70 g, 10.6 mmol, 1.2 eq) and stirred for 15 min. 2-(2-(but-3-yn-1-yl)-1,3-dioxolan-2-yl)ethan-1-ol **196** (1.50 g, 8.81 mmol, 1.0 eq) in CH₂Cl₂ (15 mL) was added over 15 minutes. After the completed addition the reaction mixture was stirred under reflux for 1 h where TLC and ¹H NMR indicated complete conversion of the alcohol. After cooling to ambient temperature the brown solution was quenched with 10% *w/v* aq. Na₂S₂O₃ (50 mL). The organic layer was washed with brine (2 × 50 mL), dried (MgSO₄), filtered and concentrated *in vacuo*. The residual solid was stirred in petroleum ether (44 mL) and Et₂O (6 mL) for 5 min, filtered and concentrated *in vacuo* to afford **197** as a yellow oil (2.30 g) which was used without further purification. R_f: 0.90 (petroleum ether: EtOAc 4:1); ν_{max} (thin film)/cm⁻¹ 3293 (w) (C≡C-H), 2958 (w), 2885 (w), 1120 (s), 1042 (s), 635 (s), ¹H NMR (400 MHz, CDCl₃) 3.88 (4H, s, O(CH₂)₂O), 3.11-3.04 (2H, m, C(7)H₂), 2.25-2.15 (4H, m, C(4)H₂ and C(6)H₂), 1.89 (1H, t, *J* 2.6, C(1)H), 1.83-1.77 (2H, m, C(3)H₂), ¹³C NMR (101 MHz, CDCl₃): 110.5 (C(5)), 83.8 (C(2)), 68.3 (C(1)), 65.3 (O(CH₂)₂O), 42.5 (C(6)), 35.8 (C(4)), 13.0 (C(3)), -2.7 (C(7)); GC-HRMS *m/z* (CI⁺) [Found: (M+NH₄)⁺ 298.0309 C₉H₁₇O₂NI requires 298.0298].

3-(2-(But-3-yn-1-yl)-1,3-dioxolan-2-yl)propanenitrile (198)

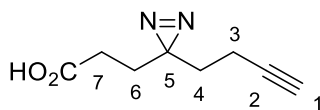
A solution of 2-(but-3-yn-1-yl)-2-(2-iodoethyl)-1,3-dioxolane **197** (2.30 g, 8.81 mmol, 1.0 eq), potassium cyanide (602 mg, 9.25 mmol, 1.05 eq) in DMF (15 mL) was stirred at 70 °C for 3 hours. After this time the reaction was judged to be complete by TLC analysis. After cooling to rt the suspension was diluted with sat. aq. NaHCO₃ (30 mL) and EtOAc (100 mL). The organic layer was washed with LiCl (0.5 M, 2 × 60 mL), brine (50 mL), dried (MgSO₄), filtered, and concentrated *in vacuo*. The residue was purified by silica gel chromatography, eluting with a gradient of 0% to 30% EtOAc in petroleum ether, to afford **198** as a colourless oil (1110 mg, 6.20 mmol, 70% over 2 steps). R_f: 0.33 (petroleum ether: EtOAc 4:1); ν_{\max} (thin film)/cm⁻¹ 3289 (w) (C≡C-H), 2963 (w), 2892 (w), 2249 (w, C≡N), 1144 (m), 1047 (s), ¹H NMR (500 MHz, CDCl₃) 3.98 (4H, s, O(CH₂)₂O), 2.41 (2H, t, *J* 7.6, C(7)H₂), 2.26 (2H, td, *J* 7.8, 2.6 C(3)H₂), 2.04 (2H, t, *J* 7.6, C(6)H₂), 1.96 (1H, t, *J* 2.6, C(1)H), 1.86 (2H, t, *J* 7.8 C(4)H₂), ¹³C NMR (126 MHz, CDCl₃): 119.7 (CN), 108.9 (C(5)), 83.6 (C(2)), 68.6 (C(1)), 65.3 (O(CH₂)₂O), 35.9 (C(4)), 32.5 (C(6)), 13.2 (C(3)), 11.6 (C(7)), LRMS *m/z* (ES⁺) 202 ([M+Na]⁺, 100%); HRMS *m/z* (ES⁺) [Found: (M+Na)⁺ 202.0841 C₁₀H₁₃NO₂Na requires 202.0839].

4-Oxo-oct-7-ynoic acid (199)

A solution of 3-(2-(but-3-yn-1-yl)-1,3-dioxolan-2-yl)propanenitrile **198** (1110 mg, 6.20 mmol, 1.0 eq) in 10% NaOH (10 mL) was stirred at reflux. After 3 h the reaction was judged to be complete by TLC analysis. After cooling, the aqueous layer was washed with Et₂O (5 mL). The pH of the aqueous layer was adjusted with 5 M aq. HCl to 1, and stirred vigorously for 3 h, at ambient temperature. The organic extracts of the aqueous layer were

extracted with CH_2Cl_2 (4×50 mL). The combined organic layers were dried (MgSO_4), filtered, and concentrated *in vacuo* to afford a yellow oil. The crude material was purified by silica gel chromatography, eluting with a gradient of 50% to 100% petroleum ether in EtOAc: AcOH (20:1), to afford **199** as a colourless oil (630 mg, 4.09 mmol, 66%). R_f : 0.22 (petroleum ether: EtOAc 6:4 + 1% AcOH); mp 54-56 °C (CHCl_3); ν_{max} (thin film)/ cm^{-1} 3500-2500 (br w) (CO_2H), 3290 (w) ($\text{C}\equiv\text{C-H}$), 2923 (w), 1710 (s) (C=O), ^1H NMR (500 MHz, CDCl_3) 10.70 (1H, br s, CO_2H), 2.79-2.71 (4H, m, C(4)H_2 and C(6)H_2), 2.68 (2H, t, J 6.2 C(7)H_2), 2.49 (2H, td, J 7.6, 2.5, C(3)H_2), 1.97 (1H, t, J 2.5, C(1)H), ^{13}C NMR (126 MHz, CDCl_3): 206.3 (C(5)), 178.1 (CO_2H), 82.9 (C(2)), 68.9 (C(1)), 41.3 (C(4)), 36.8 (C(6)), 27.6 (C(7)), 12.9 (C(3)), LRMS m/z (ES^-) 153 ($[\text{M-H}]^-$, 100%); HRMS m/z (ES^-) [Found: (M-H) 153.0556 $\text{C}_8\text{H}_9\text{O}_3$ requires 153.0557].

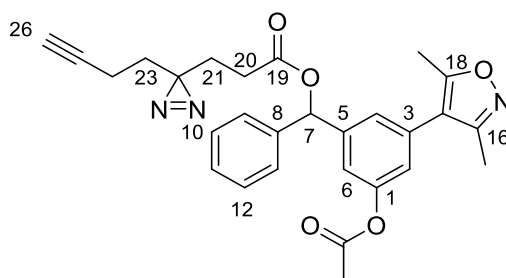
3-(3-(But-3-yn-1-yl)-3H-diazirin-3-yl)propanoic acid (**200**)



4-Oxooc-7-ynoic acid **199** (200 mg, 1.30 mmol, 1.0 eq) in liquid NH_3 (5 mL) was stirred at -40 °C for 5 h. After this time a solution of $\text{H}_2\text{N-OSO}_3\text{H}$ (241 mg, 2.13 mmol, 1.6 eq) in dry MeOH (2 mL) was added dropwise. After one hour at -40 °C the suspension was warmed to ambient temperature overnight. The suspension was diluted with MeOH (5 mL), filtered, rinsed (MeOH), and concentrated *in vacuo*. The residue was dissolved in Et_2O (2 mL) and triethylamine (450 μL), and cooled to 0 °C. I_2 (500 mg) was added in 5 portions until the brown colour persist. After 30 minutes the solution was diluted with EtOAc (10 mL), washed with 1 M aq. HCl (10 mL), 10% w/v aq. $\text{Na}_2\text{S}_2\text{O}_3$ (10 mL), 1 M aq. HCl (10 mL), dried (MgSO_4), filtered and concentrated *in vacuo*. The crude material was purified by silica gel chromatography, eluting with 40% petroleum ether in EtOAc and 1% AcOH, to afford **200** as a yellow oil (83 mg, 0.500 mmol, 38%). R_f : 0.32 (petroleum ether: EtOAc 6:4); ν_{max} (thin film)/ cm^{-1} 3500-2500 (br w) (CO_2H), 3297 (w) ($\text{C}\equiv\text{C-H}$), 2924 (w), 1710 (s) (C=O), 1434 (w) (diazarine), 1290 (w), 1224 (w), 924 (w); ^1H NMR (500 MHz,

CDCl₃) 10.62 (1H, br s, CO₂H), 2.17 (2H, t, *J* 7.8, C(7)H₂), 2.03-1.97 (3H, m, C(1)H and C(6)H₂), 1.80 (2H, t, *J* 7.6, C(4)H₂), 1.67-1.61 (2H, m, C(3)H₂), LRMS *m/z* (ES⁻) 165 ([M-H]⁻, 100%), 331 ([2M-H]⁻, 89%); HRMS *m/z* (ES⁻) [Found: (M-H)⁻ 165.0666 C₈H₉O₂N₂ requires 165.0659]. These data are in good agreement with the literature.¹⁵⁸

(3-Acetoxy-5-(3,5-dimethylisoxazol-4-yl)phenyl)(phenyl)methyl 3-(3-(but-3-yn-1-yl)-3H-diazirin-3-yl)propanoate (186)



3-(3-(but-3-yn-1-yl)-3H-diazirin-3-yl)propanoic acid **200** (80 mg, 0.481 mmol, 3.3 eq) in SOCl₂ (2 mL) was stirred at 40 °C for 15 min. After this time the solution was concentrated *in vacuo* and the residue was dissolved in dry CH₂Cl₂ (1 mL). To this, a solution of 3-(3,5-dimethylisoxazol-4-yl)-5-(hydroxyl(phenyl)methyl)phenyl acetate **167** (50 mg, 0.148 mmol, 1.0 eq) in dry CH₂Cl₂ (1.5 mL) was added dropwise over a period of 5 min. After the completed addition, pyridine (50 μL, 49.1 mg, 0.621 mmol, 4.2 eq) was added, and the resulting solution was stirred for 20 min at ambient temperature. After this time the reaction was judged to be complete by TLC analysis. The solution was quenched with H₂O (0.5 mL), and diluted with CH₂Cl₂ (10 mL). The organic layer was washed with 10% *w/v* aq. Na₂CO₃ (10 mL), 1 M aq. HCl (10 mL), brine (10 mL), dried (MgSO₄), filtered and concentrated *in vacuo*. The residue was purified by silica gel chromatography, eluting with 25% petroleum ether in ethyl acetate, to afford **186** as a colourless oil (11 mg, 0.023 mmol, 15%). R_f: 0.20 (petroleum ether: EtOAc 4:1); *v*_{max} (thin film)/cm⁻¹ 3295 (w) (C≡C-H), 2927 (w) (C-H), 1768 (m) (C=O), 1740 (m) (C=O), 1702 (m), 1247 (m), 1204 (s); ¹H NMR (500 MHz, D₆-acetone) 7.51-7.47 (2H, m, C(9)H and C(13)H), 7.41-7.36 (2H, m, C(10)H and C(12)H), 7.34-7.29 (2H, m, C(11)H and C(2)H), 7.19 (1H, dd, *J* 1.6, 1.6 C(4)H),

7.11 (1H, dd, *J* 1.6, 1.6 C(6)*H*), 6.93 (1H, s, C(7)*H*), 2.41-2.35 (6H, m, C(16)CH₃, C(20)*H*₂ and C(26)*H*), 2.26 (3H, s, COCH₃), 2.22 (3H, s, C(18)CH₃), 2.01 (2H, td, *J* 7.5, 2.6 C(24)*H*₂), 1.83 (2H, t, *J* 7.5, C(23)*H*₂), 1.63 (2H, t, *J* 7.6, C(21)*H*₂), ¹³C NMR (126 MHz, (CD₃)₂CO): δ 170.8 (C(19)), 168.7 (COCH₃), 165.5 (C(16)), 157.9 (C(18)), 151.4 (C(1)), 143.0 (C(5)), 140.3 (C(8)), 131.9 (C(3)), 128.6 (C(10) and C(12)), 128.0 (C(11)), 126.9 (C(9) and C(13)), 124.6 (C(2)), 121.7 (C(6)), 119.0 (C(4)), 115.3 (C(17)), 82.6 (C(25)), 76.2 (C(7)), 69.7 (C(26)), 32.0 (C(21)), 28.1 (C(20)), 27.7 (C(23)), 27.6 (C(22)), 20.1 (COCH₃), 12.7 (C(24)), 10.7 (C(16)CH₃), 9.9 (C(18)CH₃); LRMS *m/z* (ES⁺) 486 ([M+H]⁺, 53%), 508 ([M+Na]⁺, 100%); HRMS *m/z* (ES⁺) [Found: (M+Na)⁺ 508.1847 C₂₈H₂₇O₅N₃Na requires 508.1843]; RP-HPLC: Method A: Retention time 14.10 min, purity 94.0%.

Bibliography

- (1) Berger, S. L.; Kouzarides, T.; Shiekhattar, R.; Shilatifard, A. An Operational Definition of Epigenetics. *Genes Dev.* **2009**, *23* (7), 781–783.
- (2) Portela, A.; Esteller, M. Epigenetic Modifications and Human Disease. *Nat. Biotechnol.* **2010**, *28* (10), 1057–1068.
- (3) Filippakopoulos, P.; Knapp, S. Targeting Bromodomains: Epigenetic Readers of Lysine Acetylation. *Nat. Rev. Drug Discov.* **2014**, *13* (5), 337–356.
- (4) Hewings, D. S.; Rooney, T. P. C.; Jennings, L. E.; Hay, D.; Schofield, C. J.; Brennan, P. E.; Knapp, S.; Conway, S. J. Progress in the Development and Application of Small Molecule Inhibitors of Bromodomain-Acetyl-Lysine Interactions. *J. Med. Chem.* **2012**, *55* (22), 9393–9413.
- (5) Jennings, L. E.; Measures, A. R.; Wilson, B. G.; Conway, S. J. Phenotypic Screening and Fragment-Based Approaches to the Discovery of Small-Molecule Bromodomain Ligands. *Future Med. Chem.* **2014**, *6* (2), 179–204.
- (6) Cohen, I.; Poręba, E.; Kamieniarz, K.; Schneider, R. Histone Modifiers in Cancer: Friends or Foes? *Genes Cancer* **2011**, *2* (6), 631–647.
- (7) Dancy, B. M.; Cole, P. A. Protein Lysine Acetylation by p300/CBP. *Chem. Rev.* **2015**, *115* (6), 2419–2452.
- (8) Richmond, R. K.; Sargent, D. F.; Richmond, T. J.; Luger, K.; Ma, A. W. Crystal Structure of the Nucleosome Core Particle at 2.8 Å Resolution. *Nature* **1997**, *389* (6648), 251–260.
- (9) Bannister, A. J.; Kouzarides, T. Regulation of Chromatin by Histone Modifications. *Cell Res.* **2011**, *21* (3), 381–395.
- (10) Jenuwein, T.; Allis, C. D. Translating the Histone Code. *Science* **2001**, *293* (5532), 1074–1080.
- (11) Dawson, M. A.; Kouzarides, T. Cancer Epigenetics: From Mechanism to Therapy. *Cell* **2012**, *150* (1), 12–27.
- (12) Kouzarides, T. Chromatin Modifications and Their Function. *Cell* **2007**, *128* (4), 693–705.
- (13) Qiu, J. Epigenetics: Unfinished Symphony. *Nature* **2006**, *441* (7090), 143–145.
- (14) Allfrey, V. G.; Faulkner, R.; Mirsky, A. E. Acetylation and Methylation of Histones and Their Possible Role in the Regulation of RNA Synthesis. *Proc. Natl. Acad. Sci. USA* **1964**, *51* (5), 786–794.
- (15) Gershey, E. L.; Vidali, G.; Allfrey, V. G. Chemical Studies of Histone Acetylation. *J. Biol. Chem.* **1968**, *243* (19), 5018–5022.
- (16) Allfrey, G.; Faulkner, R.; Mirsky, A. E. Possible Role in the Regulation of RNA Synthesis. *Proc. Natl. Acad. Sci. U.S.A.* **1964**, *315* (1938), 786–794.
- (17) Kouzarides, T. Acetylation: A Regulatory Modification to Rival Phosphorylation? *EMBO J.* **2000**, *19* (6), 1176–1179.
- (18) Kaminskas, E.; Farrell, A. T.; Wang, Y.-C.; Sridhara, R.; Pazdur, R. FDA Drug Approval Summary: Azacitidine (5-Azacytidine, Vidaza) for Injectable Suspension. *Oncologist* **2005**, *10* (3), 176–182.

Bibliography

- (19) Heerboth, S.; Lapinska, K.; Snyder, N.; Leary, M.; Rollinson, S.; Sarkar, S. Use of Epigenetic Drugs in Disease: An Overview. *Genet. Epigenet.* **2014**, *6*, 9–19.
- (20) Mottamal, M.; Zheng, S.; Huang, T.; Wang, G. Histone Deacetylase Inhibitors in Clinical Studies as Templates for New Anticancer Agents. *Mol. 2015* **2015**, *20* (3), 3898–3941.
- (21) Haynes, S. R.; Dollard, C.; Winston, F.; Beck, S.; Trowsdale, J.; Dawid, I. B. The Bromodomain: A Conserved Sequence Found in Human, Drosophila and Yeast Proteins. *Nucleic Acids Res.* **1992**, *20* (10), 2603.
- (22) Tamkun, J. W.; Deuring, R.; Scott, M. P.; Kissinger, M.; Pattatucci, A. M.; Kaufman, T. C.; Kennison, J. A. Brahma: A Regulator of Drosophila Homeotic Genes Structurally Related to the Yeast Transcriptional Activator SNF2SWI2. *Cell* **1992**, *68* (3), 561–572.
- (23) Filippakopoulos, P.; Picaud, S.; Mangos, M.; Keates, T.; Lambert, J.-P.; Barsyte-Lovejoy, D.; Felletar, I.; Volkmer, R.; Müller, S.; Pawson, T.; Gingras, A.-C.; Arrowsmith, C. H.; Knapp, S. Histone Recognition and Large-Scale Structural Analysis of the Human Bromodomain Family. *Cell* **2012**, *149* (1), 214–231.
- (24) Brand, M.; Measures, A. M.; Wilson, B. G.; Cortopassi, W. A.; Alexander, R.; Ho, M.; Hewings, D. S.; Rooney, T. P. C.; Paton, R. S.; Conway, S. J. Small Molecule Inhibitors of Bromodomain - Acetyl-Lysine Interactions. *ACS Chem. Biol.* **2015**, *10* (1), 22–39.
- (25) Dhalluin, C.; Carlson, J. E.; Zeng, L.; He, C.; Aggarwal, A. K.; Zhou, M.-M. Structure and Ligand of a Histone Acetyltransferase Bromodomain. *Nature* **1999**, *399* (6735), 491–496.
- (26) Smith, S. G.; Zhou, M.-M. The Bromodomain: A New Target in Emerging Epigenetic Medicine. *ACS Chem. Biol.* **2016**, *11* (3), 598–608.
- (27) Wilson, A. J. Inhibition of Protein-Protein Interactions Using Designed Molecules. *Chem. Soc. Rev.* **2009**, *38* (12), 3289–3300.
- (28) Vidler, L. R.; Brown, N.; Knapp, S.; Hoelder, S. Druggability Analysis and Structural Classification of Bromodomain Acetyl-Lysine Binding Sites. *J. Med. Chem.* **2012**, *55* (17), 7346–7359.
- (29) Filippakopoulos, P.; Qi, J.; Picaud, S.; Shen, Y.; Smith, W. B.; Fedorov, O.; Morse, E. M.; Keates, T.; Hickman, T. T.; Felletar, I.; Philpott, M.; Munro, S.; McKeown, M. R.; Wang, Y.; Christie, A. L.; West, N.; Cameron, M. J.; Schwartz, B.; Heightman, T. D.; La Thangue, N.; French, C. a; Wiest, O.; Kung, A. L.; Knapp, S.; Bradner, J. E. Selective Inhibition of BET Bromodomains. *Nature* **2010**, *468* (7327), 1067–1073.
- (30) Nicodeme, E.; Jeffrey, K. L.; Schaefer, U.; Beinke, S.; Dewell, S.; Chung, C.-W.; Chandwani, R.; Marazzi, I.; Wilson, P.; Coste, H.; White, J.; Kirilovsky, J.; Rice, C. M.; Lora, J. M.; Prinjha, R. K.; Lee, K.; Tarakhovskiy, A. Suppression of Inflammation by a Synthetic Histone Mimic. *Nature* **2010**, *468* (7327), 1119–1123.
- (31) Romero, F. A.; Taylor, A. M.; Crawford, T. D.; Tsui, V.; Co, A.; Magnuson, S. Disrupting Acetyl-Lysine Recognition: Progress in the Development of Bromodomain Inhibitors. *J. Med. Chem.* **2016**, *59*, 1271–1298.
- (32) Theodoulou, N. H.; Tomkinson, N. C.; Prinjha, R. K.; Humphreys, P. G. Clinical Progress and Pharmacology of Small Molecule Bromodomain Inhibitors. *Curr. Opin. Chem. Biol.* **2016**, *33*, 58–66.
- (33) RVX-208 clinical trial: NCT02586155, <https://clinicaltrials.gov/ct2/show/NCT02586155> Date accessed: 23.08.2016.

-
- (34) Bedford, D. C.; Kasper, L. H.; Fukuyama, T.; Brindle, P. K. Target Gene Context Influences the Transcriptional Requirement for the KAT3 Family of CBP and p300 Histone Acetyltransferases. *Epigenetics* **2010**, *5* (1), 9–15.
- (35) Jang, S. Y.; Kim, S. Y.; Bae, Y.-S. p53 Deacetylation by SIRT1 Decreases during Protein Kinase CKII Downregulation-Mediated Cellular Senescence. *FEBS Lett.* **2011**, *585* (21), 3360–3366.
- (36) Sakaguchi, K.; Herrera, J. E.; Saito, S.; Miki, T.; Bustin, M.; Vassilev, A.; Anderson, C. W.; Appella, E. DNA Damage Activates p53 through a Phosphorylation-Acetylation Cascade. *Genes Dev.* **1998**, *12* (18), 2831–2841.
- (37) Tanaka, Y.; Naruse, I.; Maekawa, T.; Masuya, H.; Shiroishi, T.; Ishii, S. Abnormal Skeletal Patterning in Embryos Lacking a Single Cbp Allele: A Partial Similarity with Rubinstein-Taybi Syndrome. *Proc. Natl. Acad. Sci. U. S. A.* **1997**, *94* (19), 10215–10220.
- (38) Yao, T. P.; Oh, S. P.; Fuchs, M.; Zhou, N. D.; Ch'ng, L. E.; Newsome, D.; Bronson, R. T.; Li, E.; Livingston, D. M.; Eckner, R. Gene Dosage-Dependent Embryonic Development and Proliferation Defects in Mice Lacking the Transcriptional Integrator p300. *Cell* **1998**, *93* (3), 361–372.
- (39) Finn, R. D.; Coggill, P.; Eberhardt, R. Y.; Eddy, S. R.; Mistry, J.; Mitchell, A. L.; Potter, S. C.; Punta, M.; Qureshi, M.; Sangrador-Vegas, A.; Salazar, G. A.; Tate, J.; Bateman, A. The Pfam Protein Families Database: Towards a More Sustainable Future. *Nucleic Acids Res.* **2016**, *44* (D1), D279–D285.
- (40) Iyer, N. G.; Özdag, H.; Caldas, C. p300/CBP and Cancer. *Oncogene* **2004**, *23* (24), 4225–4231.
- (41) Tillinghast, G. W.; Partee, J.; Albert, P.; Kelley, J. M.; Burtow, K. H.; Kelly, K. Analysis of Genetic Stability at the EP300 and CREBBP Loci in a Panel of Cancer Cell Lines. *Genes, Chromosom. Cancer* **2003**, *37* (2), 121–131.
- (42) Pasqualucci, L.; Dominguez-Sola, D.; Chiarenza, A.; Fabbri, G.; Grunn, A.; Trifonov, V.; Kasper, L. H.; Lerach, S.; Tang, H.; Ma, J.; Rossi, D.; Chadburn, A.; Murty, V. V.; Mullighan, C. G.; Gaidano, G.; Rabadan, R.; Brindle, P. K.; Dalla-Favera, R. Inactivating Mutations of Acetyltransferase Genes in B-Cell Lymphoma. *Nature* **2011**, *471* (7337), 189–195.
- (43) Matt, T. Transcriptional Control of the Inflammatory Response: A Role for the CREB-Binding Protein (CBP). *Acta Med. Austriaca* **2002**, *29* (3), 77–79.
- (44) Wen, A. Y.; Sakamoto, K. M.; Miller, L. S. The Role of the Transcription Factor CREB in Immune Function. *J. Immunol.* **2010**, *185* (11), 6413–6419.
- (45) Roelfsema, J. H.; Peters, D. J. M. Rubinstein-Taybi Syndrome: Clinical and Molecular Overview. *Expert Rev. Mol. Med.* **2007**, *9* (23), 1–16.
- (46) Bartsch, O.; Schmidt, S.; Richter, M.; Morlot, S.; Seemanová, E.; Wiebe, G.; Rasi, S. DNA Sequencing of CREBBP Demonstrates Mutations in 56% of Patients with Rubinstein-Taybi Syndrome (RSTS) and in Another Patient with Incomplete RSTS. *Hum. Genet.* **2005**, *117* (5), 485–493.
- (47) Lopez-Atalaya, J. P.; Gervasini, C.; Mottadelli, F.; Spina, S.; Piccione, M.; Scarano, G.; Selicorni, A.; Barco, A.; Larizza, L. Histone Acetylation Deficits in Lymphoblastoid Cell Lines from Patients with Rubinstein-Taybi Syndrome. *J. Med. Genet.* **2012**, *49* (1), 66–74.

- (48) Alarcón, J. M.; Malleret, G.; Touzani, K.; Vronskaya, S.; Ishii, S.; Kandel, E. R.; Barco, A. Chromatin Acetylation, Memory, and LTP Are Impaired in CBP+/- Mice: A Model for the Cognitive Deficit in Rubinstein-Taybi Syndrome and Its Amelioration. *Neuron* **2004**, *42* (6), 947–959.
- (49) Bourtchouladze, R.; Lidge, R.; Catapano, R.; Stanley, J.; Gossweiler, S.; Romashko, D.; Scott, R.; Tully, T. A Mouse Model of Rubinstein-Taybi Syndrome: Defective Long-Term Memory Is Ameliorated by Inhibitors of Phosphodiesterase 4. *Proc. Natl. Acad. Sci. U. S. A.* **2003**, *100* (18), 10518–10522.
- (50) Mujtaba, S.; He, Y.; Zeng, L.; Yan, S.; Plotnikova, O.; Sachchidanand; Sanchez, R.; Zeleznik-Le, N. J.; Ronai, Z.; Zhou, M.-M. Structural Mechanism of the Bromodomain of the Coactivator CBP in p53 Transcriptional Activation. *Mol. Cell* **2004**, *13* (2), 251–263.
- (51) Sachchidanand; Resnick-Silverman, L.; Yan, S.; Mutjaba, S.; Liu, W.-J.; Zeng, L.; Manfredi, J. J.; Zhou, M.-M. Target Structure-Based Discovery of Small Molecules That Block Human p53 and CREB Binding Protein Association. *Chem. Biol.* **2006**, *13* (1), 81–90.
- (52) Borah, J. C.; Mujtaba, S.; Karakikes, I.; Zeng, L.; Muller, M.; Patel, J.; Moshkina, N.; Morohashi, K.; Zhang, W.; Gerona-Navarro, G.; Hajjar, R. J.; Zhou, M.-M. A Small Molecule Binding to the Coactivator CREB-Binding Protein Blocks Apoptosis in Cardiomyocytes. *Chem. Biol.* **2011**, *18* (4), 531–541.
- (53) Gerona-Navarro, G.; Rodríguez-fernández, Y.; Mujtaba, S.; Patel, J.; Zeng, L.; Plotnikov, A. N.; Osman, R.; Zhou, M. Rational Design of Cyclic Peptide Modulators of the Transcriptional Co-Activator CBP: A New Class of p53 Inhibitors. *J. Am. Chem. Soc.* **2011**, *133* (7), 2040–2043.
- (54) Berman, H. M.; Westbrook, J.; Feng, Z.; Gilliland, G.; Bhat, T. N.; Weissig, H.; Shindyalov, I. N.; Bourne, P. E. The Protein Data Bank. *Nucleic Acids Res.* **2000**, *28* (1), 235–242.
- (55) Hewings, D. S.; Wang, M.; Philpott, M.; Fedorov, O.; Uttarkar, S.; Filippakopoulos, P.; Picaud, S.; Vuppasetty, C.; Marsden, B.; Knapp, S.; Conway, S. J.; Heightman, T. D. 3,5-Dimethylisoxazoles Act as Acetyl-Lysine-Mimetic Bromodomain Ligands. *J. Med. Chem.* **2011**, *54* (19), 6761–6770.
- (56) Rooney, T. P. C.; Filippakopoulos, P.; Fedorov, O.; Picaud, S.; Cortopassi, W.; Hay, D.; Martin, S.; Tumber, A.; Rogers, C. M.; Philpott, M.; Wang, M.; Thompson, A. L.; Heightman, T. D.; Pryde, D. C.; Cook, A.; Paton, R. S.; Müller, S.; Knapp, S.; Brennan, P. E.; Conway, S. J. A Series of Potent CREBBP Bromodomain Ligands Reveals an Induced-Fit Pocket Stabilized by a Cation- π Interaction. *Angew. Chem. Int. Ed. Engl.* **2014**, *53* (24), 6126–6130.
- (57) Rooney, T. P. C. Development of Small Molecule Inhibitors of the Bromodomain-Histone Interaction, Department of Organic Chemistry, University of Oxford, 2015.
- (58) Philpott, M.; Yang, J.; Tumber, T.; Fedorov, O.; Uttarkar, S.; Filippakopoulos, P.; Picaud, S.; Keates, T.; Felletar, I.; Ciulli, A.; Knapp, S.; Heightman, T. D. Bromodomain-Peptide Displacement Assays for Interactome Mapping and Inhibitor Discovery. *Mol. Biosyst.* **2011**, *7* (10), 2899–2908.
- (59) Hewings, D. S.; Fedorov, O.; Filippakopoulos, P.; Martin, S.; Picaud, S.; Tumber, A.; Wells, C.; Olcina, M. M.; Freeman, K.; Gill, A.; Ritchie, A. J.; Sheppard, D. W.; Russell, A. J.; Hammond, E. M.; Knapp, S.; Brennan, P. E.; Conway, S. J. Optimization of 3,5-Dimethylisoxazole Derivatives as Potent Bromodomain Ligands. *J. Med. Chem.* **2013**, *56* (8), 3217–3227.

- (60) Seal, J.; Lamotte, Y.; Donche, F.; Bouillot, A.; Mirguet, O.; Gellibert, F.; Nicodeme, E.; Krysa, G.; Kirilovsky, J.; Beinke, S.; McCleary, S.; Rioja, I.; Bamborough, P.; Chung, C.-W.; Gordon, L.; Lewis, T.; Walker, A. L.; Cutler, L.; Lugo, D.; Wilson, D. M.; Witherington, J.; Lee, K.; Prinjha, R. K. Identification of a Novel Series of BET Family Bromodomain Inhibitors: Binding Mode and Profile of I-BET151 (GSK1210151A). *Bioorg. Med. Chem. Lett.* **2012**, *22* (8), 2968–2972.
- (61) Mirguet, O.; Lamotte, Y.; Donche, F.; Toum, J.; Gellibert, F.; Bouillot, A.; Gosmini, R.; Nguyen, V.-L.; Delannée, D.; Seal, J.; Blandel, F.; Boullay, A.-B.; Boursier, E.; Martin, S.; Brusq, J.-M.; Krysa, G.; Riou, A.; Tellier, R.; Costaz, A.; Huet, P.; Dudit, Y.; Trottet, L.; Kirilovsky, J.; Nicodeme, E. From ApoA1 Upregulation to BET Family Bromodomain Inhibition: Discovery of I-BET151. *Bioorg. Med. Chem. Lett.* **2012**, *22* (8), 2963–2967.
- (62) Hay, D.; Fedorov, O.; Filippakopoulos, P.; Martin, S.; Philpott, M.; Picaud, S.; Hewings, D. S.; Uttakar, S.; Heightman, T. D.; Conway, S. J.; Knapp, S.; Brennan, P. E. The Design and Synthesis of 5-and 6-Isoxazolylbenzimidazoles as Selective Inhibitors of the BET Bromodomains. *Medchemcomm* **2013**, *4* (1), 140–144.
- (63) Hay, D.; Fedorov, O.; Martin, S.; Singleton, D. C.; Tallant, C.; Wells, C.; Picaud, S.; Philpott, M.; Monteiro, O. P.; Rogers, C. M.; Conway, S. J.; Rooney, T. P. C.; Tumber, A.; Yapp, C.; Filippakopoulos, P.; Bunnage, M. E.; Müller, S.; Knapp, S.; Schofield, C. J.; Brennan, P. E. Discovery and Optimization of Small-Molecule Ligands for the CBP/p300 Bromodomains. *J. Am. Chem. Soc.* **2014**, *136* (26), 9308–9319.
- (64) Hammitzsch, A.; Tallant, C.; Fedorov, O.; O'Mahony, A.; Brennan, P. E.; Hay, D. A.; Martinez, F. O.; Al-Mossawi, M. H.; de Wit, J.; Vecellio, M.; Wells, C.; Wordsworth, P.; Müller, S.; Knapp, S.; Bowness, P. CBP30, a Selective CBP/p300 Bromodomain Inhibitor, Suppresses Human Th17 Responses. *Proc. Natl. Acad. Sci.* **2015**, *112* (34), 10768–10773.
- (65) Chekler, E. L. P.; Pellegrino, J. A.; Lanz, T. A.; Lee, K.; Pletcher, M. T.; Jones, L. H. Transcriptional Profiling of a Selective CREB Binding Protein Bromodomain Inhibitor Highlights Article Transcriptional Profiling of a Selective CREB Binding Protein Bromodomain Inhibitor Highlights Therapeutic Opportunities. *Chem. Biol.* **2015**, *22* (12), 1588–1596.
- (66) Picaud, S.; Fedorov, O.; Thanasopoulou, A.; Leonards, K.; Jones, K.; Meier, J.; Olzscha, H.; Monteiro, O.; Martin, S.; Philpott, M.; Tumber, A.; Filippakopoulos, P.; Yapp, C.; Wells, C.; Che, K. H.; Bannister, A.; Robson, S.; Kumar, U.; Parr, N.; Lee, K.; Lugo, D.; Jeffrey, P.; Taylor, S.; Vecellio, M. L.; Bountra, C.; Brennan, P. E.; O'mahony, A.; Velichko, S.; Muller, S.; Hay, D.; Daniels, D. L.; Urh, M.; Thangue, N. B. La; Kouzarides, T.; Prinjha, R.; Urg Schwaller, J.; Knapp, S. Generation of a Selective Small Molecule Inhibitor of the CBP/p300 Bromodomain for Leukemia Therapy. *Cancer Res.* **2015**, *75* (23), 5106–5119.
- (67) SGC. I-CBP112 - a CREBBP/EP300-selective chemical probe. <http://www.thesgc.org/chemical-probes/ICBP112> Date accessed: 18.08.2016.
- (68) Popp, T. A. Benzoxazepine-Type Inhibitors for the CBP/p300 Bromodomains, Fakultät für Chemie und Pharmazie, Ludwig-Maximilians-Universität München, 2016.
- (69) Popp, T. A.; Tallant, C.; Rogers, C.; Fedorov, O.; Brennan, P. E.; Müller, S.; Knapp, S.; Bracher, F. Development of Selective CBP/P300 Benzoxazepine Bromodomain Inhibitors. *J. Med. Chem.* **2016**, *59* (19), 8889–8912.

- (70) Xu, M.; Unzue, A.; Dong, J.; Spiliotopoulos, D.; Nevado, C.; Amedeo Cafilisch. Discovery of CREBBP Bromodomain Inhibitors by High-Throughput Docking and Hit Optimization Guided by Molecular Dynamics. *J. Med. Chem.* **2016**, *59* (1), 1340–1349.
- (71) Unzue, A.; Xu, M.; Dong, J.; Wiedmer, L.; Spiliotopoulos, D.; Ca, A.; Nevado, C. Fragment-Based Design of Selective Nanomolar Ligands of the CREBBP Bromodomain. *J. Med. Chem.* **2016**, *59* (1), 1350–1356.
- (72) Crawford, T. D.; Romero, F. A.; Lai, K. W.; Tsui, V.; Taylor, A. M.; de Leon Boenig, G.; Noland, C. L.; Murray, J.; Ly, J.; Choo, E. F.; Hunsaker, T. L.; Chan, E. W.; Merchant, M.; Kharbanda, S.; Gascoigne, K. E.; Kaufman, S.; Beresini, M. H.; Liao, J.; Liu, W.; Chen, K. X.; Chen, Z.; Conery, A. R.; Côté, A.; Jayaram, H.; Jiang, Y.; Kiefer, J. R.; Kleinheinz, T.; Li, Y.; Maher, J.; Pardo, E.; Poy, F.; Spillane, K. L.; Wang, F.; Wang, J.; Wei, X.; Xu, Z.; Xu, Z.; Yen, I.; Zawadzke, L.; Zhu, X.; Bellon, S.; Cummings, R.; Cochran, A. G.; Albrecht, B. K.; Magnuson, S. Discovery of a Potent and Selective in Vivo Probe (GNE-272) for the Bromodomains of CBP/EP300. *J. Med. Chem.* **2016**, *59* (23), 10549–10563.
- (73) Morris, G. M.; Goodsell, D. S.; Halliday, R. S.; Huey, R.; Hart, W. E.; Belew, R. K.; Olson, A. J.; Al, M. E. T. Automated Docking Using a Lamarckian Genetic Algorithm and an Empirical Binding Free Energy Function. *J. Comput. Chem.* **1998**, *19* (14), 1639–1662.
- (74) Müller, A.; Vogt, C.; Sewald, N. Synthesis of Fmoc- β -Homoamino Acids by Ultrasound-Promoted Wolff Rearrangement. *Synthesis (Stuttg.)* **1998**, *1998* (6), 837–841.
- (75) Ikemoto, N.; Tellers, D. M.; Dreher, S. D.; Liu, J.; Huang, A.; Rivera, N. R.; Njolito, E.; Hsiao, Y.; McWilliams, J. C.; Williams, J. M.; Armstrong, J. D.; Sun, Y.; Mathre, D. J.; Grabowski, E. J. J.; Tillyer, R. D. Highly Diastereoselective Heterogeneously Catalyzed Hydrogenation of Enamines for the Synthesis of Chiral α -Amino Acid Derivatives. *J. Am. Chem. Soc.* **2004**, *126* (10), 3048–3049.
- (76) Davies, S. G.; Fletcher, A. M.; Roberts, P. M.; Thomson, J. E. The Conjugate Addition of Enantiomerically Pure Lithium Amides as Chiral Ammonia Equivalents Part II: 2005 - 2011. *Tetrahedron: Asymmetry* **2012**, *23* (15–16), 1111–1153.
- (77) Davies, S. G.; Smith, A. D.; Price, P. D. The Conjugate Addition of Enantiomerically Pure Lithium Amides as Homochiral Ammonia Equivalents: Scope, Limitations and Synthetic Applications. *Tetrahedron: Asymmetry* **2005**, *16* (84), 2833–2891.
- (78) Costello, J. F.; Davies, S. G.; Ichihara, O. Origins of the High Stereoselectivity in the Conjugate Addition of Lithium(α -Methylbenzyl)benzylamide to T-Butyl Cinnamate. *Tetrahedron: Asymmetry* **1994**, *5* (10), 1999–2008.
- (79) Davies, S. G.; Mulvaney, A. W.; Russell, A. J.; Smith, A. D. Parallel Synthesis of Homochiral β -Amino Acids. *Tetrahedron: Asymmetry* **2007**, *18* (13), 1554–1566.
- (80) Niesen, F. H.; Berglund, H.; Vedadi, M. The Use of Differential Scanning Fluorimetry to Detect Ligand Interactions That Promote Protein Stability. *Nat. Protoc.* **2007**, *2* (9), 2212–2221.
- (81) Hammonds, T.; Simpson, P. B. *The Handbook of Medicinal Chemistry: Principles and Practice*; Davis, A., Ward, S. E., Eds.; The Royal Society of Chemistry, 2015.
- (82) Claudio Dalvit. Theoretical Analysis of the Competition Ligand-Based NMR Experiments and Selected Applications to Fragment Screening and Binding Constant Measurements. *Concepts Magn. Reson. Part A* **2008**, *88A* (12), 341–372.

Bibliography

- (83) Arntson, K. E.; Pomerantz, W. C. K. Protein-Observed Fluorine NMR: A Bioorthogonal Approach for Small Molecule Discovery. *J. Med. Chem.* **2016**, *59* (11), 5158–5171.
- (84) Gerig, J. T. Fluorine NMR of Proteins. *Prog. Nucl. Magn. Reson. Spectrosc.* **1994**, *26* (4), 293–370.
- (85) Mishra, N. K.; Urick, A. K.; Ember, S. W. J.; Schoenbrunn, E.; Pomerantz, W. C. Fluorinated Aromatic Amino Acids Are Sensitive ^{19}F NMR Probes for Bromodomain-Ligand Interactions. *ACS Chem. Biol.* **2014**, *9* (12), 2755–2760.
- (86) Urick, A. K.; Hawk, L. M. L.; Cassel, M. K.; Mishra, N. K.; Liu, S.; Adhikari, N.; Zhang, W.; Dos Santos, C. O.; Hall, J. L.; Pomerantz, W. C. K. Dual Screening of BPTF and Brd4 Using Protein-Observed Fluorine NMR Uncovers New Bromodomain Probe Molecules. *ACS Chem. Biol.* **2015**, *10* (10), 2246–2256.
- (87) Plotnikov, A. N.; Yang, S.; Zhou, T. J.; Rusinova, E.; Frasca, A.; Zhou, M. M. Structural Insights into Acetylated-Histone H4 Recognition by the Bromodomain-PHD Finger Module of Human Transcriptional Coactivator CBP. *Structure* **2014**, *22* (2), 353–360.
- (88) Taylor, A. M.; Côté, A.; Hewitt, M. C.; Pastor, R.; Leblanc, Y.; Nasveschuk, C. G.; Romero, F. A.; Crawford, T. D.; Cantone, N.; Jayaram, H.; Setser, J.; Murray, J.; Beresini, M. H.; de Leon Boenig, G.; Chen, Z.; Conery, A. R.; Cummings, R. T.; Dakin, L. A.; Flynn, E. M.; Huang, O. W.; Kaufman, S.; Keller, P. J.; Kiefer, J. R.; Lai, T.; Li, Y.; Liao, J.; Liu, W.; Lu, H.; Pardo, E.; Tsui, V.; Wang, J.; Wang, Y.; Xu, Z.; Yan, F.; Yu, D.; Zawadzke, L.; Zhu, X.; Zhu, X.; Sims, R. J.; Cochran, A. G.; Bellon, S.; Audia, J. E.; Magnuson, S.; Albrecht, B. K. Fragment-Based Discovery of a Selective and Cell-Active Benzodiazepinone CBP/EP300 Bromodomain Inhibitor (CPI-637). *ACS Med. Chem. Lett.* **2016**, *7* (5), 531–536.
- (89) Ghosh, S.; Taylor, A.; Chin, M.; Huang, H.-R.; Conery, A. R.; Mertz, J. A.; Salmeron, A.; Dakle, P. J.; Mele, D.; Cote, A.; Jayaram, H.; Setser, J. W.; Poy, F.; Hatzivassiliou, G.; DeAlmeida-Nagata, D.; Sandy, P.; Hatton, C.; Romero, F. A.; Chiang, E.; Reimer, T.; Crawford, T.; Pardo, E.; Watson, V. G.; Tsui, V.; Cochran, A. G.; Zawadzke, L.; Harmange, J.-C.; Audia, J. E.; Bryant, B. M.; Cummings, R. T.; Magnuson, S. R.; Grogan, J. L.; Bellon, S. F.; Albrecht, B. K.; Sims, R. J.; Lora, J. M. Regulatory T Cell Modulation by CBP/EP300 Bromodomain Inhibition. *J. Biol. Chem.* **2016**, *291* (25), 13014–13027.
- (90) Ma, J. C.; Dougherty, D. A. The Cation- π Interaction. *Chem Rev* **1997**, *97* (5), 1303–1324.
- (91) Sussman, J. L.; Harel, M.; Frolow, F.; Oefner, C.; Goldman, A.; Toker, L.; Silman, I. Atomic Structure of Acetylcholinesterase from Torpedo Californica: A Prototypic Acetylcholine-Binding Protein. *Science* **1991**, *253* (5022), 872–879.
- (92) Shafferman, A.; Velan, B.; Ordentlich, A.; Kronman, C.; Grosfeld, H.; Leitner, M.; Flashner, Y.; Cohen, S.; Barak, D.; Ariel, N. Substrate Inhibition of Acetylcholinesterase: Residues Affecting Signal Transduction from the Surface to the Catalytic Center. *EMBO J.* **1992**, *11* (10), 3561–3568.
- (93) Beene, D. L.; Brandt, G. S.; Zhong, W.; Zacharias, N. M.; Lester, H. A.; Dougherty, D. A. Cation- π Interactions in Ligand Recognition by Serotonergic (5-HT_{3A}) and Nicotinic Acetylcholine Receptors: The Anomalous Binding Properties of Nicotine†. *Biochemistry* **2002**, *41* (32), 10262–10269.
- (94) Dougherty, D. A.; Stauffer, D. A. Acetylcholine Binding by a Synthetic Receptor: Implications for Biological Recognition. *Science* **1990**, *250* (4987), 1558–1560.

- (95) Kumpf, R. A.; Dougherty, D. A. A Mechanism for Ion Selectivity in Potassium Channels: Computational Studies of Cation- π Interactions. *Science* **1993**, *261* (5129), 1708–1710.
- (96) Dougherty, D. A. Cation- π Interactions in Chemistry and Biology: A New View of Benzene, Phe, Tyr, and Trp. *Science* **1996**, *271* (5246), 163–168.
- (97) Gallivan, J. P.; Dougherty, D. Cation- π Interactions in Structural Biology. *Proc. Natl. Acad. Sci. USA* **1999**, *96* (17), 9459–9464.
- (98) Sandro Mecozzi; Anthony P. West, Jr., A.; Dougherty, D. A. Cation- π Interactions in Simple Aromatics: Electrostatics Provide a Predictive Tool. *J. Am. Chem. Soc.* **1996**, *118* (9), 2307–2308.
- (99) Mecozzi, S.; West, A. P.; Dougherty, D. A. Cation- π Interactions in Aromatics of Biological and Medicinal Interest: Electrostatic Potential Surfaces as a Useful Qualitative Guide. *Proc. Natl. Acad. Sci. U. S. A.* **1996**, *93* (20), 10566–10571.
- (100) Sörme, P.; Qian, Y.; Nyholm, P. G.; Leffler, H.; Nilsson, U. J. Low Micromolar Inhibitors of Galectin-3 Based on 3'-Derivatization of N-Acetyllactosamine. *ChemBioChem* **2002**, *3* (2), 183–189.
- (101) Sörme, P.; Arnoux, P.; Kahl-Knutsson, B.; Leffler, H.; Rini, J. M.; Nilsson, U. J. Structural and Thermodynamic Studies on Cation- π Interactions in Lectin-Ligand Complexes: High-Affinity Galectin-3 Inhibitors through Fine-Tuning of an Arginine-Arene Interaction. *J. Am. Chem. Soc.* **2005**, *127* (6), 1737–1743.
- (102) Jiang, Z.-Y.; Lu, M.-C.; You, Q.-D. Discovery and Development of Kelch-like ECH-Associated Protein 1. Nuclear Factor Erythroid 2-Related Factor 2 (KEAP1:NRF2) Protein-Protein Interaction Inhibitors: Achievements, Challenges, and Future Directions. *J. Med. Chem.* **2016**, acs.jmedchem.6b00586.
- (103) Winkel, A. F.; Engel, C. K.; Margerie, D.; Kannt, A.; Szillat, H.; Glombik, H.; Kallus, C.; Ruf, S.; Güssregen, S.; Riedel, J.; Herling, A. W.; von Knethen, A.; Weigert, A.; Brüne, B.; Schmoll, D. Characterization of RA839, a Noncovalent Small Molecule Binder to Keap1 and Selective Activator of Nrf2 Signaling. *J. Biol. Chem.* **2015**, *290* (47), 28446–28455.
- (104) Cortopassi, W. A.; Kumar, K.; Paton, R. S. Cation- π Interactions in CREBBP Bromodomain Inhibition: An Electrostatic Model for Small-Molecule Binding Affinity and Selectivity. *Org. Biomol. Chem.* **2016**, *14* (46), 10926–10938.
- (105) Kolmakov, K.; Belov, V. N.; Wurm, C. a.; Harke, B.; Leutenegger, M.; Eggeling, C.; Hell, S. W. A Versatile Route to Red-Emitting Carbopyronine Dyes for Optical Microscopy and Nanoscopy. *European J. Org. Chem.* **2010**, *2010* (19), 3593–3610.
- (106) Cordeiro, A.; Shaw, J.; O'Brien, J.; Blanco, F.; Rozas, I. Synthesis of 6-Nitro-1,2,3,4-Tetrahydroquinoline: An Experimental and Theoretical Study of Regioselective Nitration. *European J. Org. Chem.* **2011**, *2011* (8), 1504–1513.
- (107) Zhu, W.; Ma, D. Synthesis of Aryl Sulfones via L-Proline-Promoted CuI-Catalyzed Coupling Reaction of Aryl Halides with Sulfinic Acid Salts. *J. Org. Chem.* **2005**, *70* (7), 2696–2700.
- (108) Kokatla, H. P.; Thomson, P. F.; Bae, S.; Doddi, V. R.; Lakshman, M. K. Reduction of Amine N -Oxides by Diboron Reagents. *J. Org. Chem.* **2011**, *76* (19), 7842–7848.
- (109) Kim, J.; Bertozzi, C. R. A Bioorthogonal Reaction of N -Oxide and Boron Reagents. *Angew. Chemie Int. Ed.* **2015**, *54* (52), 15777–15781.
- (110) Verdonk, M. L.; Rees, D. C. Group Efficiency: A Guideline for Hits-to-Leads Chemistry. *ChemMedChem* **2008**, *3* (8), 1179–1180.

- (111) Zhou, Y.; Wang, J.; Gu, Z.; Wang, S.; Zhu, W.; Aceña, J. L.; Soloshonok, V. A.; Izawa, K.; Liu, H. Next Generation of Fluorine-Containing Pharmaceuticals, Compounds Currently in Phase II–III Clinical Trials of Major Pharmaceutical Companies: New Structural Trends and Therapeutic Areas. *Chem Rev* **2016**, *116* (2), 422–518.
- (112) Ilardi, E. A.; Vitaku, E.; Njardarson, J. T. Data-Mining for Sulfur and Fluorine: An Evaluation of Pharmaceuticals To Reveal Opportunities for Drug Design and Discovery. *J. Med. Chem.* **2014**, *57* (7), 2832–2842.
- (113) O'Hagan, D. Understanding Organofluorine Chemistry . An Introduction to the C - F Bond. *Chem. Soc. Rev.* **2008**, *37*, 308–319.
- (114) Hunter, L. The C - F Bond as a Conformational Tool in Organic and Biological Chemistry. *Beilstein J. Org. Chem.* **2010**, *6* (38), 1–14.
- (115) O'Hagan, D.; Bilton, C.; Howard, J. a. K.; Knight, L.; Tozer, D. J. The Preferred Conformation of N- β -Fluoroethylamides. Observation of the Fluorine Amide Gauche Effect. *J. Chem. Soc. Perkin Trans. 2* **2000**, *4*, 605–607.
- (116) Briggs, C. R. S.; Hagan, D. O.; Howard, J. A. K.; Yu, D. S. The C \pm F Bond as a Tool in the Conformational Control of Amides. *J. Fluor. Chem.* **2003**, *119* (1), 9–13.
- (117) Cheguillaume, A.; Lacroix, S.; Marchand-Brynaert, J. A Practical Synthesis of 2,2-Difluoro-3-Amino-Propanoic Acid (A, α -Difluoro- β -Alanine). *Tetrahedron Lett.* **2003**, *44* (11), 2375–2377.
- (118) Smith, J. R. L.; Sadd, J. S. Isomerism of 1- and 2-(N,N-Disubstituted Aminomethyl)benzotriazoles; an Investigation by Nuclear Magnetic Resonance Spectroscopy. *J. Chem. Soc., Perkin Trans. 1* **1975**, 1181–1184.
- (119) Haniti, M.; Hamid, S. A.; Allen, C. L.; Lamb, G. W.; Maxwell, A. C.; Maytum, H. C.; Watson, A. J. A.; Williams, J. M. J. Ruthenium-Catalyzed N-Alkylation of Amines and Sulfonamides Using Borrowing Hydrogen Methodology. *J. Am. Chem. Soc.* **2009**, *131* (5), 1766–1774.
- (120) Katritzky, A. R.; Lan, X.; Lam, J. N. N-[α -(O- and P-Methoxyaryl)alkyl]benzotriazoles: Preparation and Use in Synthesis. *Chem. Ber.* **1991**, *124* (8), 1819–1826.
- (121) Heal, W. P.; Dang, T. H. T.; Tate, E. W. Activity-Based Probes: Discovering New Biology and New Drug Targets. *Chem. Soc. Rev.* **2011**, *40* (1), 246–257.
- (122) Willems, L. I.; Overkleeft, H. S.; van Kasteren, S. I. Current Developments in Activity-Based Protein Profiling. *Bioconjug. Chem.* **2014**, *25* (7), 1181–1191.
- (123) Smith, E.; Collins, I. Photoaffinity Labeling in Target- and Binding-Site Identification. *Futur. Med Chem* **2015**, *7* (2), 159–183.
- (124) Dubinsky, L.; Krom, B. P.; Meijler, M. M. Diazirine Based Photoaffinity Labeling. *Bioorg. Med. Chem.* **2012**, *20* (2), 554–570.
- (125) Lapinsky, D. J. Tandem Photoaffinity Labeling–bioorthogonal Conjugation in Medicinal Chemistry. *Bioorg. Med. Chem.* **2012**, *20* (21), 6237–6247.
- (126) Sakurai, K.; Ozawa, S.; Yamada, R.; Yasui, T.; Mizuno, S. Comparison of the Reactivity of Carbohydrate Photoaffinity Probes with Different Photoreactive Groups. *ChemBioChem* **2014**, *15* (10), 1399–1403.
- (127) Hashimoto, M.; Hatanaka, Y. Recent Progress in Diazirine-Based Photoaffinity Labeling. *European J. Org. Chem.* **2008**, *2008* (15), 2513–2523.
- (128) Kolb, H. C.; Finn, M. G.; Sharpless, K. B. Click Chemistry: Diverse Chemical Function from a Few Good Reactions. *Angew. Chem. Int. Ed. Engl.* **2001**, *40* (11), 2004–2021.

Bibliography

- (129) Himo, F.; Lovell, T.; Hilgraf, R.; Rostovtsev, V. V.; Noodleman, L.; Sharpless, K. B.; Fokin, V. V. Copper(I)-Catalyzed Synthesis of Azoles. DFT Study Predicts Unprecedented Reactivity and Intermediates. *J. Am. Chem. Soc.* **2005**, *127* (1), 210–216.
- (130) Christian W. Tornøe; Christensen, C.; Meldal, M. Peptidotriazoles on Solid Phase: [1,2,3]-Triazoles by Regiospecific Copper(I)-Catalyzed 1,3-Dipolar Cycloadditions of Terminal Alkynes to Azides. *J. Org. Chem.* **2002**, *67* (9), 3057–3064.
- (131) Rostovtsev, V. V.; Green, L. G.; Fokin, V. V.; Sharpless, K. B. A Stepwise Huisgen Cycloaddition Process: Copper(I)-Catalyzed Regioselective “Ligation” of Azides and Terminal Alkynes. *Angew. Chemie Int. Ed.* **2002**, *41* (14), 2596–2599.
- (132) Kennedy, D. C.; McKay, C. S.; Legault, M. C. B.; Danielson, D. C.; Blake, J. A.; Pegoraro, A. F.; Stolow, A.; Mester, Z.; Pezacki, J. P. Cellular Consequences of Copper Complexes Used To Catalyze Bioorthogonal Click Reactions. *J. Am. Chem. Soc.* **2011**, *133* (44), 17993–18001.
- (133) Baskin, J. M.; Prescher, J. A.; Laughlin, S. T.; Agard, N. J.; Chang, P. V.; Miller, I. A.; Lo, A.; Codelli, J. A.; Bertozzi, C. R. Copper-Free Click Chemistry for Dynamic in Vivo Imaging. *Proc. Natl. Acad. Sci. U. S. A.* **2007**, *104* (43), 16793–16797.
- (134) Debets, M. F.; van der Doelen, C. W. J.; Rutjes, F. P. J. T.; van Delft, F. L. Azide: A Unique Dipole for Metal-Free Bioorthogonal Ligations. *Chembiochem* **2010**, *11* (9), 1168–1184.
- (135) Laughlin, S. T.; Baskin, J. M.; Amacher, S. L.; Bertozzi, C. R. In Vivo Imaging of Membrane-Associated Glycans in Developing Zebrafish. *Science* **2008**, *320* (5876), 664–667.
- (136) Köhn, M.; Breinbauer, R. The Staudinger Ligation-A Gift to Chemical Biology. *Angew. Chem. Int. Ed. Engl.* **2004**, *43* (24), 3106–3116.
- (137) Dantas de Araújo, A.; Palomo, J. M.; Cramer, J.; Köhn, M.; Schröder, H.; Wacker, R.; Niemeyer, C.; Alexandrov, K.; Waldmann, H. Diels-Alder Ligation and Surface Immobilization of Proteins. *Angew. Chemie Int. Ed.* **2006**, *45* (2), 296–301.
- (138) Blackman, M. L.; Royzen, M.; Fox, J. M. Tetrazine Ligation: Fast Bioconjugation Based on Inverse-Electron-Demand Diels-Alder Reactivity. *J. Am. Chem. Soc.* **2008**, *130* (41), 13518–13519.
- (139) Kodama, K.; Fukuzawa, S.; Nakayama, H.; Sakamoto, K.; Kigawa, T.; Yabuki, T.; Matsuda, N.; Shirouzu, M.; Takio, K.; Yokoyama, S.; Tachibana, K. Site-Specific Functionalization of Proteins by Organopalladium Reactions. *ChemBioChem* **2007**, *8* (2), 232–238.
- (140) Vlahos, C. J.; Matter, W. F.; Hui, K. Y.; Brown, R. F. A Specific Inhibitor of Phosphatidylinositol 3-Kinase, 2-(4-Morpholinyl)-8-Phenyl-4H-1-Benzopyran-4-One (LY294002). *J. Biol. Chem.* **1994**, *269* (7), 5241–5248.
- (141) Dittmann, A.; Werner, T.; Chung, C.; Savitski, M. M.; Fa, M.; Grandi, P.; Hopf, C.; Lindon, M.; Neubauer, G.; Prinjha, R. K.; Bantsche, M.; Drewes, G. The Commonly Used PI3-Kinase Probe LY294002 Is an Inhibitor of BET Bromodomains. *ACS Chem. Biol.* **2014**, *9*, 495–502.
- (142) Gharbi, S. I.; Zvelebil, M. J.; Shuttleworth, S. J.; Hancox, T.; Saghir, N.; Timms, J. F.; Waterfield, M. D. Exploring the Specificity of the PI3K Family Inhibitor LY294002. *Biochem. J.* **2007**, *404* (1), 15–21.

- (143) Hett, E. C.; Chekler, E. L. P.; Basak, A.; Bonin, P. D.; Denny, R. A.; Flick, A. C.; Geoghegan, K. F.; Liu, S.; Pletcher, M. T.; Sahasrabudhe, P.; Salter, S. C.; Stock, I. A.; Taylor, A. P.; Jones, L. H. Direct Photocapture of Bromodomains Using Tropolone Chemical Probes. *Medchemcomm* **2015**, *6* (6), 1018–1023.
- (144) Li, Z.; Wang, D.; Li, L.; Pan, S.; Na, Z.; Tan, C. Y. J.; Yao, S. Q. “Minimalist” Cyclopropene-Containing Photo-Cross-Linkers Suitable for Live-Cell Imaging and Affinity-Based Protein Labeling. *J. Am. Chem. Soc.* **2014**, *136* (28), 9990–9998.
- (145) Yang, T.; Liu, Z.; Li, X. D. Developing Diazirine-Based Chemical Probes to Identify Histone Modification “readers” and “erasers.” *Chem. Sci.* **2015**, *6* (2), 1011–1017.
- (146) Yang, T.; Li, X.-M.; Bao, X.; Fung, Y. M. E.; Li, X. D. Photo-Lysine Captures Proteins That Bind Lysine Post-Translational Modifications. *Nat. Chem. Biol.* **2016**, *12* (2), 70–72.
- (147) Li, X.; Kapoor, T. M. Approach to Profile Proteins That Recognize Post-Translationally Modified Histone “Tails.” *J. Am. Chem. Soc.* **2010**, *132* (8), 2504–2505.
- (148) Anelli, P. L.; Montanari, F.; Quici, S. A General Synthetic Method for the Oxidation of Primary Alcohols to Aldehydes: (S)-(+)-2-Methylbutanal. *Org. Synth.* **1990**, *69*, 212.
- (149) Meyer, S. D.; Schreiber, S. L. Acceleration of the Dess-Martin Oxidation by Water. *J. Org. Chem.* **1994**, *59* (24), 7549–7552.
- (150) Lennox, A. J. J.; Lloyd-Jones, G. C. Organotrifluoroborate Hydrolysis: Boronic Acid Release Mechanism and an Acid-Base Paradox in Cross-Coupling. *J. Am. Chem. Soc.* **2012**, *134* (17), 7431–7441.
- (151) Molander, G. A.; Canturk, B.; Kennedy, L. E. Scope of the Suzuki–Miyaura Cross-Coupling Reactions of Potassium Heteroaryltrifluoroborates. *J. Org. Chem.* **2009**, *74* (3), 973–980.
- (152) Srivastava, V.; Tandon, A.; Ray, S. Convenient and Selective Acetylation of Phenols, Amines and Alcohols. *Synth. Commun.* **1992**, *22* (18), 2703–2706.
- (153) Shigdel, U. K.; Zhang, J.; He, C. Diazirine-Based DNA Photo-Cross-Linking Probes for the Study of Protein – DNA Interactions. *Angew. Chemie Int. Ed.* **2008**, *47* (1), 90–93.
- (154) Durek, T.; Zhang, J.; He, C.; Kent, S. B. H. Synthesis of Photoactive Analogues of a Cystine Knot Trypsin Inhibitor Protein. *Org. Lett.* **2007**, *9* (26), 5547–5500.
- (155) Liu, M. T. H.; Tencer, M.; Stevens, I. D. R. On the Thermal Decomposition of Diazirines. *J. Chem. Soc., Perkin Trans. 2* **1986**, 211–214.
- (156) Stevens, I. D. R.; Liu, M. T. H.; Soundararajan, N.; Paike, N. The Thermal Decomposition of Diazirines: 3-(3-Methyldiazirin-3-Yl)propan-1-ol and 3-(3-Methyldiazirin-3-Yl)propanoic Acid. *J. Chem. Soc. Perkin Trans. 2* **1990**, *11* (5), 661–667.
- (157) Kambe, T.; Correia, B. E.; Niphakis, M. J.; Cravatt, B. F. Mapping the Protein Interaction Landscape for Fully Functionalized Small-Molecule Probes in Human Cells. *J. Am. Chem. Soc.* **2014**, *136* (30), 10777–10782.
- (158) Li, Z.; Hao, P.; Li, L.; Tan, C. Y. J.; Cheng, X.; Chen, G. Y. J.; Sze, S. K.; Shen, H.; Yao, S. Q. Design and Synthesis of Minimalist Terminal Alkyne-Containing Diazirine Photo-Crosslinkers and Their Incorporation into Kinase Inhibitors for Cell- and Tissue-Based Proteome Profiling. *Angew. Chemie Int. Ed.* **2013**, *52*, 8551–8556.
- (159) Graffy, M. Photoaffinity Probes for BET Bromodomain Inhibitors, University of Oxford, 2014.

Bibliography

- (160) Ikeda, Y.; Behrman, E. J. Improved Synthesis of Photo-Leucine. *Synth. Commun.* **2008**, *38*, 2276–2284.
- (161) Brunner, J.; Senn, H.; Richards, F. M. 3-Trifluoromethyl-3-Phenyldiazirine. A New Carbene Generating Group for Photolabeling Reagents. *J. Biol. Chem.* **1980**, *255* (8), 3313–3318.
- (162) Qian Wang; Timothy R. Chan; Robert Hilgraf; Fokin, V. V.; Sharpless, K. B.; Finn, M. G. Bioconjugation by Copper(I)-Catalyzed Azide-Alkyne [3 + 2] Cycloaddition. *J. Am. Chem. Soc.* **2003**, *125* (11), 3192–3193.
- (163) Cox, O. B.; Krojer, T.; Collins, P.; Monteiro, O.; Talon, R.; Bradley, A.; Fedorov, O.; Amin, J.; Marsden, B. D.; Spencer, J.; von Delft, F.; Brennan, P. E. A Poised Fragment Library Enables Rapid Synthetic Expansion Yielding the First Reported Inhibitors of PHIP(2), an Atypical Bromodomain. *Chem. Sci.* **2016**, *7* (3), 2322–2330.
- (164) Alonso, V. L.; Ritagliati, C.; Cribb, P.; Cricco, J. A.; Serra, E. C. Overexpression of Bromodomain Factor 3 in Trypanosoma Cruzi (TcBDF3) Affects Differentiation of the Parasite and Protects It against Bromodomain Inhibitors. *FEBS J.* **2016**, *283* (11), 2051–2066.
- (165) McClelland, M. L.; Mesh, K.; Lorenzana, E.; Chopra, V. S.; Segal, E.; Watanabe, C.; Haley, B.; Mayba, O.; Yaylaoglu, M.; Gnad, F.; Firestein, R. CCAT1 Is an Enhancer-Templated RNA That Predicts BET Sensitivity in Colorectal Cancer. *J. Clin. Invest.* **2016**, *126* (2), 639–652.
- (166) Mackinnon, A. L.; Taunton, J. Target Identification by Diazirine Photo-Cross-Linking and Click Chemistry. *Curr. Protoc. Chem. Biol.* **2009**, *1*, 55–73.
- (167) Cosier, J.; Glazer, A. M.; IUCr. A Nitrogen-Gas-Stream Cryostat for General X-Ray Diffraction Studies. *J. Appl. Crystallogr.* **1986**, *19* (2), 105–107.
- (168) Gasteiger, E.; Hoogland, C.; Gattiker, A.; Duvaud, S.; Wilkins, M. R.; Appel, R. D.; Bairoch, A. Protein Identification and Analysis Tools on the ExPASy Server. In *The Proteomics Protocols Handbook*; Humana Press: Totowa, NJ, 2005; pp 571–607.
- (169) Aguilar, J. A.; Nilsson, M.; Bodenhausen, G.; Morris, G. A. Spin Echo NMR Spectra without J Modulation. *Chem. Commun.* **2012**, *48* (6), 811–813.
- (170) Kabsch, W. Automatic Indexing of Rotation Diffraction Patterns. *J. Appl. Crystallogr.* **1988**, *21* (1), 67–72.
- (171) McCoy, A. J.; Grosse-Kunstleve, R. W.; Storoni, L. C.; Read, R. J. Likelihood-Enhanced Fast Translation Functions. *Acta Crystallogr. Sect. D Biol. Crystallogr.* **2005**, *61* (4), 458–464.
- (172) Perrakis, A.; Morris, R.; Lamzin, V. S. Automated Protein Model Building Combined with Iterative Structure Refinement. *Nat. Struct. Biol.* **1999**, *6* (5), 458–463.
- (173) Emsley, P.; Cowtan, K. Coot: Model-Building Tools for Molecular Graphics. *Acta Crystallogr. D. Biol. Crystallogr.* **2004**, *60* (Pt 12), 2126–2132.
- (174) Murshudov, G. N.; Vagin, A. A.; Dodson, E. J. Refinement of Macromolecular Structures by the Maximum-Likelihood Method. *Acta Crystallogr. Sect. D Biol. Crystallogr.* **1997**, *53* (3), 240–255.
- (175) Painter, J.; Merritt, E. A. Optimal Description of a Protein Structure in Terms of Multiple Groups Undergoing TLS Motion. *Acta Crystallogr. D. Biol. Crystallogr.* **2006**, *62* (Pt 4), 439–450.

- (176) Fulmer, G. R.; Miller, A. J. M.; Sherden, N. H.; Gottlieb, H. E.; Nudelman, A.; Stoltz, B. M.; Bercaw, J. E.; Goldberg, K. I. NMR Chemical Shifts of Trace Impurities: Common Laboratory Solvents, Organics, and Gases in Deuterated Solvents Relevant to the Organometallic Chemist. *Organometallics* **2010**, *29* (9), 2176–2179.
- (177) Zhang, L.; Sonaglia, L.; Stacey, J.; Lautens, M. Multicomponent Multicatalyst Reactions (MC)2R: One-Pot Synthesis of 3,4-Dihydroquinolinones. *Org. Lett.* **2013**, *15* (9), 2128–2131.
- (178) Pauff, S. M.; Miller, S. C. Synthesis of near-IR Fluorescent Oxazine Dyes with Esterase-Labile Sulfonate Esters. *Org. Lett.* **2011**, *13* (23), 6196–6199.
- (179) Vermeulen, E. S.; Marjan, van S.; Anne W., S.; Jeffrey S, S.; Wikström, H. V.; Grol, C. J. Novel 5-HT7 Receptor Inverse Agonists. Synthesis and Molecular Modeling of Arylpiperazine- and 1,2,3,4-Tetrahydroisoquinoline-Based Arylsulfonamides. *J. Med. Chem.* **2004**, *47* (22), 5451–5466.
- (180) Kumaran, E.; Leong, W. K. [Cp*RhCl₂]₂-Catalyzed Alkyne Hydroamination to 1,2-Dihydroquinolines. *Organometallics* **2015**, *34* (9), 1779–1782.
- (181) Cavazzini, M.; Quici, S.; Orlandi, S.; Sissa, C.; Terenziani, F.; Painelli, A. Intimately Bound Coumarin and Bis(alkylaminostyryl)benzene Fragments: Synthesis and Energy Transfer. *Tetrahedron* **2013**, *69* (13), 2827–2833.
- (182) Beletskaya, I. P.; Bessmertnykh, A. G.; Averin, A. D.; Denat, F.; Guilard, R. Palladium-Catalyzed Arylation of Linear and Cyclic Polyamines. *European J. Org. Chem.* **2005**, *2005* (2), 261–280.
- (183) Yamagami, T.; Hatsuda, M.; Utsugi, M.; Kobayashi, R.; Moritani, Y. Highly Diastereoselective Esterification of Ketenes Generated In Situ from Acyl Chlorides with (R) -Pantolactone Derivatives. *European J. Org. Chem.* **2013**, *2013* (33), 7467–7470.
- (184) Henze, M.; Kreye, O.; Brauch, S.; Nitsche, C.; Naumann, K.; Wessjohann, L. A.; Westermann, B. Photoaffinity-Labeled Peptoids and Depsipeptides by Multicomponent Reactions. *Synthesis (Stuttg.)* **2010**, *17*, 2997–3003.
- (185) Singh, V.; Wang, S.; Kool, E. T. Genetically Encoded Multispectral Labeling of Proteins with Polyfluorophores on a DNA Backbone. *J. Am. Chem. Soc.* **2013**, *135* (16), 6184–6191.
- (186) Hayakawa, K.; Yodo, M.; Ohsuki, S.; Kanematsu, K. Novel Bicycloannulation via Tandem Vinylation and Intramolecular Diels-Alder Reaction of Five-Membered Heterocycles: A New Approach to Construction of Psoralen and Azapsoralen. *J. Am. Chem. Soc.* **1984**, *22* (106), 6735–6740.

Appendix

A Brief description and optimisation of the biophysical assays

A1 Differential scanning fluorimetry

Differential scanning fluorimetry (DSF) is a widely used technique for high throughput screening of compound libraries.^{1,2} This technique has been successfully applied in the discovery of bromodomain ligands for the BET bromodomain^{3,4} as well as for the discovery of CREBBP fragments, which were further optimised to potent ligands.⁵⁻⁷ This method uses the difference in melting temperatures of proteins (ΔT_M) in complex with a small molecule ligand as

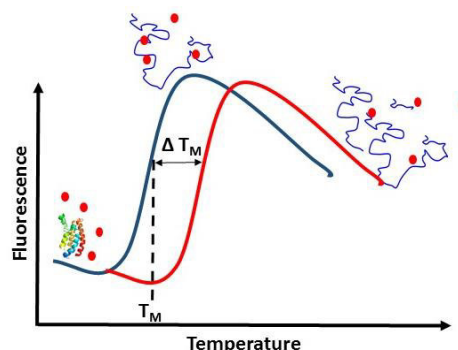


Figure A1 Schematic overview of a thermal shift curve (T_M). The blue line represents the melting curve of the protein and the red line the melting curve of the protein in presence of the ligand. ΔT_M is the melting difference

a measure of ligand affinity (Figure A1). A higher protein melting point in the presence of ligand indicates protein stabilisation due ligand binding.

The assay was performed in a PCR machine using purified bromodomain protein, small molecule ligands and SYPRO® orange, which is a solvatochromic fluorescent dye that fluoresces when in a hydrophobic environment. However, the fluorescence is quenched in polar solvents, such as the aqueous buffer. As a result, the fluorescence signal is only observed upon protein melting as the hydrophobic patches of the protein are exposed and interact with the dye.

The key parameters for the optimisation of the assay conditions were having a good fluorescent signal and low DMSO concentrations, because DMSO is known to bind to bromodomains (IC_{50} of 40 mM for the CREBBP bromodomain and 290 mM for BRD4(1)).⁸ However, it is important to have a small amount of DMSO in the assay to aid compound solubility by preventing the precipitation of the hydrophobic compounds. It was observed that the presence of 1% DMSO increases the protein melting temperature by 2 °C. For this

reason, the assay was performed in 0.2% DMSO. We also observed that increasing the concentrations of the fluorescent dye decreases protein stability, resulting in a lower protein melting temperature. The fluorescence intensity was found to be satisfactory by using $5 \times$ SYPRO® orange. The optimal experimental conditions for the assay was using $2 \mu\text{M}$ of bromodomain, $10 \mu\text{M}$ ligand and $5 \times$ SYPRO® orange with a final concentration of 0.2% DMSO.

A2 AlphaScreen™

AlphaScreen™ is an amplified luminescent proximity homogeneous peptide displacement assay⁹ that assesses ligand affinities. This technique has been used in plethora of small molecule bromodomain ligands assessing their binding affinities.^{3,5,10-12}

This method labels the biotinylated tail of a truncated acetylated histone peptide, which is a known binder to bromodomains, with a streptavidine-coated donor bead. The bromodomain

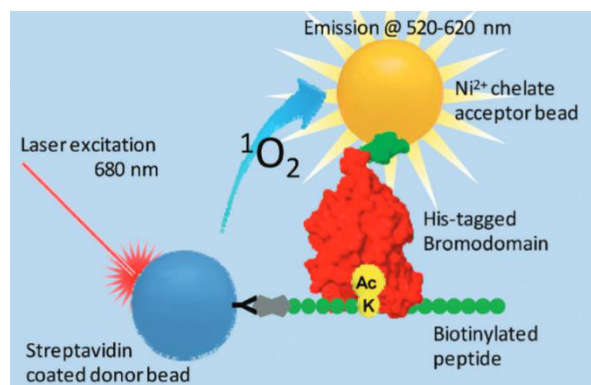


Figure A2 Principle of the AlphaScreen™ assay.

Reproduced from the literature⁸ with permission of The Royal Society of Chemistry.

His-tag is linked with a Ni^{2+} chelate acceptor bead (Figure A2). Upon laser excitation (680 nm), the donor bead generates $^1\text{O}_2$, which is a short lived, high-energy oxygen species that can diffuse up to 200 nm. The $^1\text{O}_2$ transfers energy by making contact with the acceptor bead resulting in fluorescence emission in the range of 520 to 620 nm. Upon ligand binding, the peptide-bromodomain interaction will be outcompeted and results in a loss of a fluorescence signal. An IC_{50} value can get obtained by performing a dose-response experiment.

A3 Isothermal titration calorimetry

Isothermal titration calorimetry (ITC) is a technique used to measure heat exchange associated in molecular interactions.^{13,14} It is an extremely powerful biophysical technique and regarded as a “gold standard” in obtaining binding affinities between biomolecules and small molecules.^{13,14}

In our case, the ITC setup consists of a reference cell (filled with water) and the sample cell (filled with the small molecule ligand), surrounded by an adiabatic jacket (Figure 3). Through the syringe, small injections (2 μL every 3 min) of the purified bromodomain were added, and the heat exchange between the reference and the sample cell was constantly recorded (Figure 3). The power was plotted against time and this data can be used to determine the dissociation constant (K_D) as well as the thermodynamic parameter.

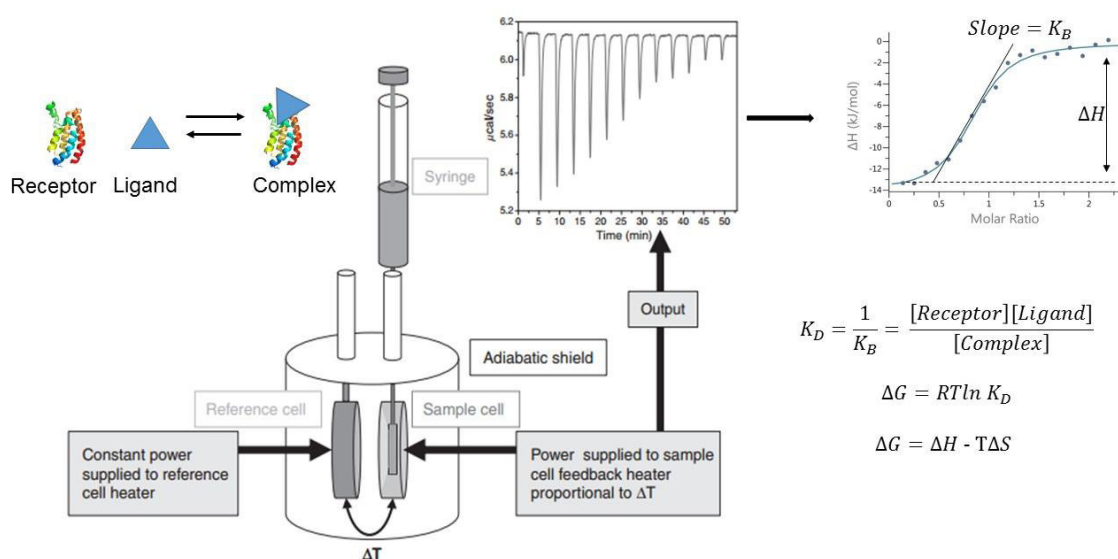


Figure A3 Schematic overview of the ITC. The ITC consists of a reference cell and a sample cell, and the temperature change is measured. Titrant is added *via* the syringe and the heat capacity difference is recorded to obtain the raw data. This data can be used to calculate the K_D from the measured heat capacity. Figure adapted with permission from the literature.¹⁴

It is important to have the same buffer composition in the syringe and the sample cell as otherwise the heat capacity of the buffer may cover the binding signal. Therefore, the proteins were dialysed to match the composition of the solution containing the small molecule. Furthermore, the DMSO concentration was kept to a minimum as it is a known

Appendix A

binder to the CREBBP bromodomain.⁷ The first experiments were performed at 25 °C in HEPES buffer, but the titration of protein into buffer in the absence of ligand resulted in a noisy signal (Figure A4a). This noisy signal can be attributed to either protein degradation, aggregation and/or a change in viscosity inside the cell. To overcome this artefact the bromodomain concentration in the syringe was lowered from 500 to 250 μM , but the noisy signal did not vanish. However, decreasing the cell temperature to 15 °C seemed to stabilise the protein and an acceptable heated dilution could be observed (Figure 4b). This optimised conditions were satisfactory to measure the dissociation constants of the small molecules.

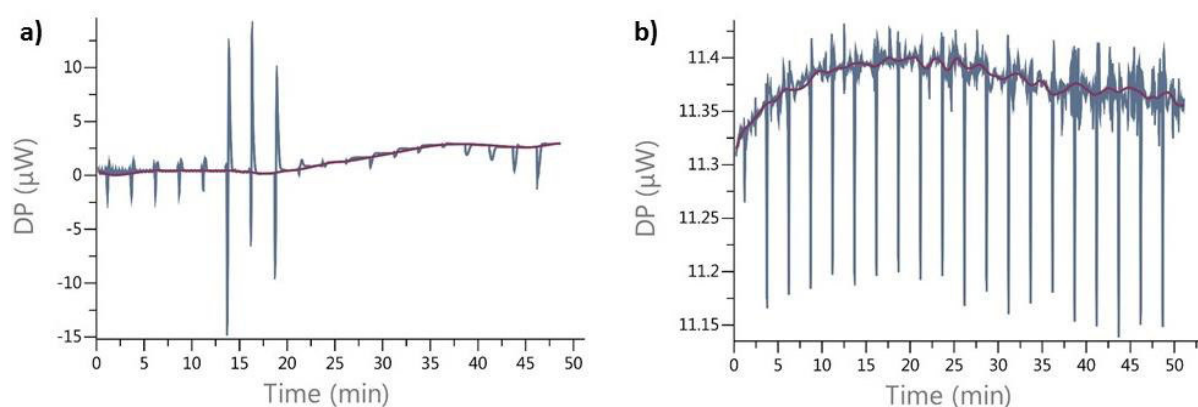


Figure A4 Heated dilution of 250 μM CREBBP titrated into HEPES buffer at 25 °C (a) and 15 °C (b).

Bibliography for Appendix A

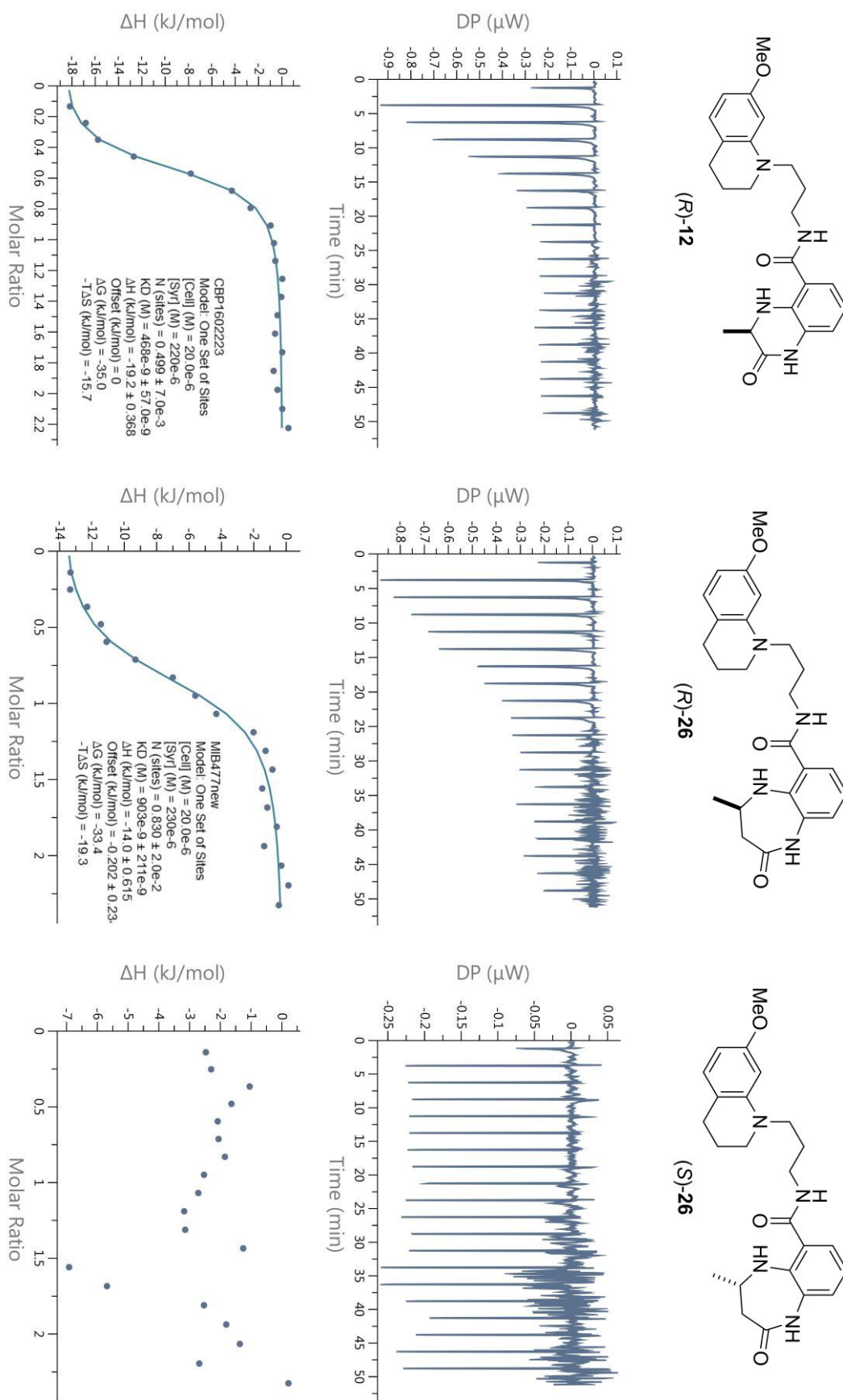
- (1) Pantoliano, M. W.; Petrella, E. C.; Kwasnoski, J. D.; Lobanov, V. S.; Myslik, J.; Graf, E.; Carver, T. E. D.; Asel, E.; Springer, B. A.; Lane, P.; Salemme, F. R. High-Density Miniaturized Thermal Shift Assays as a General Strategy for Drug Discovery. *J. Biomol. Screen.* **2001**, *6* (6), 1995–1998.
- (2) Niesen, F. H.; Berglund, H.; Vedadi, M. The Use of Differential Scanning Fluorimetry to Detect Ligand Interactions That Promote Protein Stability. *Nat. Protoc.* **2007**, *2* (9), 2212–2221.
- (3) Hewings, D. S.; Wang, M.; Philpott, M.; Fedorov, O.; Uttarkar, S.; Filippakopoulos, P.; Picaud, S.; Vuppusetty, C.; Marsden, B.; Knapp, S.; Conway, S. J.; Heightman, T. D. 3,5-Dimethylisoxazoles Act as Acetyl-Lysine-Mimetic Bromodomain Ligands. *J. Med. Chem.* **2011**, *54* (19), 6761–6770.
- (4) Hewings, D. S.; Fedorov, O.; Filippakopoulos, P.; Martin, S.; Picaud, S.; Tumber, A.; Wells, C.; Olcina, M. M.; Freeman, K.; Gill, A.; Ritchie, A. J.; Sheppard, D. W.; Russell, A. J.; Hammond, E. M.; Knapp, S.; Brennan, P. E.; Conway, S. J. Optimization of 3,5-Dimethylisoxazole Derivatives as Potent Bromodomain Ligands. *J. Med. Chem.* **2013**, *56* (8), 3217–3227.
- (5) Rooney, T. P. C.; Filippakopoulos, P.; Fedorov, O.; Picaud, S.; Cortopassi, W.; Hay, D.; Martin, S.; Tumber, A.; Rogers, C. M.; Philpott, M.; Wang, M.; Thompson, A. L.; Heightman, T. D.; Pryde, D. C.; Cook, A.; Paton, R. S.; Müller, S.; Knapp, S.; Brennan, P. E.; Conway, S. J. A Series of Potent CREBBP Bromodomain Ligands Reveals an Induced-Fit Pocket Stabilized by a Cation- π Interaction. *Angew. Chem. Int. Ed. Engl.* **2014**, *53* (24), 6126–6130.
- (6) Hay, D.; Fedorov, O.; Martin, S.; Singleton, D. C.; Tallant, C.; Wells, C.; Picaud, S.; Philpott, M.; Monteiro, O. P.; Rogers, C. M.; Conway, S. J.; Rooney, T. P. C.; Tumber, A.; Yapp, C.; Filippakopoulos, P.; Bunnage, M. E.; Müller, S.; Knapp, S.; Schofield, C. J.; Brennan, P. E. Discovery and Optimization of Small-Molecule Ligands for the CBP/p300 Bromodomains. *J. Am. Chem. Soc.* **2014**, *136* (26), 9308–9319.
- (7) Unzue, A.; Xu, M.; Dong, J.; Wiedmer, L.; Spiliotopoulos, D.; Ca, A.; Nevado, C. Fragment-Based Design of Selective Nanomolar Ligands of the CREBBP Bromodomain. *J. Med. Chem.* **2016**, *59* (1), 1350–1356.
- (8) Philpott, M.; Yang, J.; Tumber, T.; Fedorov, O.; Uttarkar, S.; Filippakopoulos, P.; Picaud, S.; Keates, T.; Felletar, I.; Ciulli, A.; Knapp, S.; Heightman, T. D. Bromodomain-Peptide Displacement Assays for Interactome Mapping and Inhibitor Discovery. *Mol. Biosyst.* **2011**, *7* (10), 2899–2908.
- (9) Eglén, R. M.; Reisine, T.; Roby, P.; Rouleau, N.; Illy, C.; Bossé, R.; Bielefeld, M. The Use of AlphaScreen Technology in HTS: Current Status. *Curr. Chem. Genomics* **2008**, *1*, 2–10.
- (10) Fish, P. V.; Filippakopoulos, P.; Bish, G.; Brennan, P. E.; Bunnage, M. E.; Cook, A. S.; Fedorov, O.; Gerstenberger, B. S.; Jones, H.; Knapp, S.; Marsden, B.; Nocka, K.; Owen, D. R.; Philpott, M.; Picaud, S.; Primiano, M. J.; Ralph, M. J.; Sciammetta, N.; Trzuppek, J. D. Identification of a Chemical Probe for Bromo and Extra C-Terminal Bromodomain Inhibition through Optimization of a Fragment-Derived Hit. *J. Med. Chem.* **2012**, *55* (22), 9831–9837.
- (11) Chen, P.; Chaikuad, A.; Bamborough, P.; Bantscheff, M.; Bountra, C.; Chung, C.; Fedorov, O.; Grandi, P.; Jung, D.; Lesniak, R.; Lindon, M.; Müller, S.; Philpott, M.; Prinjha, R.; Rogers, C.; Selenski, C.; Tallant, C.; Werner, T.; Willson, T. M.; Knapp, S.; Drewry, D. H. Discovery and Characterization of GSK2801, a Selective Chemical Probe for the Bromodomains BAZ2A and BAZ2B. *J. Med. Chem.* **2016**, *59*, 1410–1424.
- (12) Hay, D.; Fedorov, O.; Filippakopoulos, P.; Martin, S.; Philpott, M.; Picaud, S.; Hewings, D. S.; Uttarkar, S.; Heightman, T. D.; Conway, S. J.; Knapp, S.; Brennan, P. E. The Design and

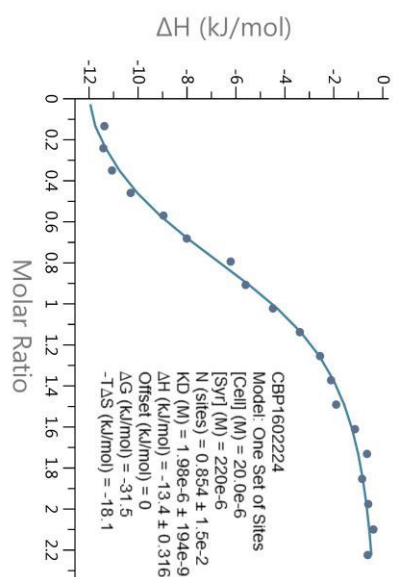
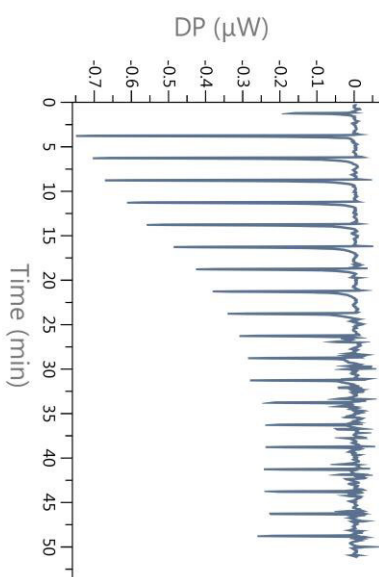
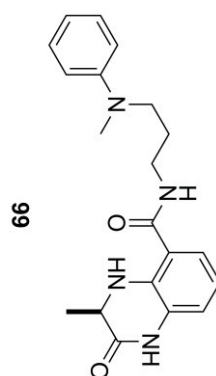
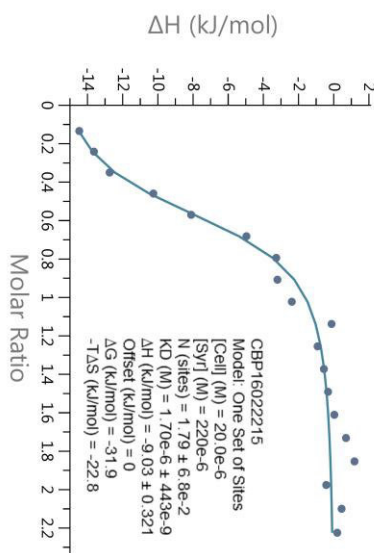
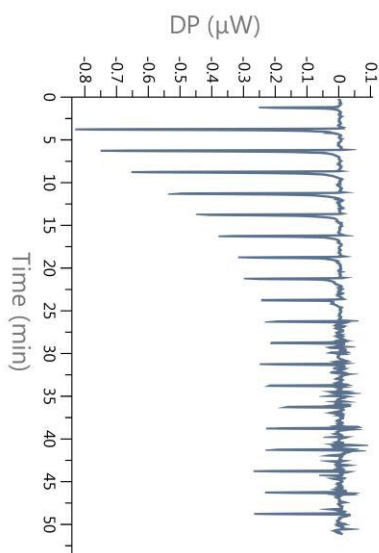
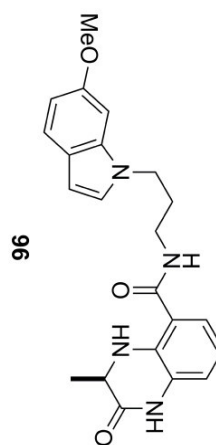
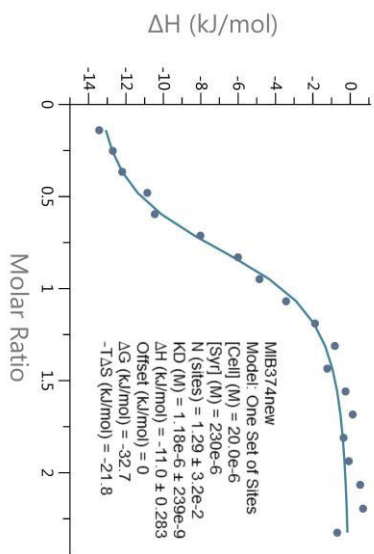
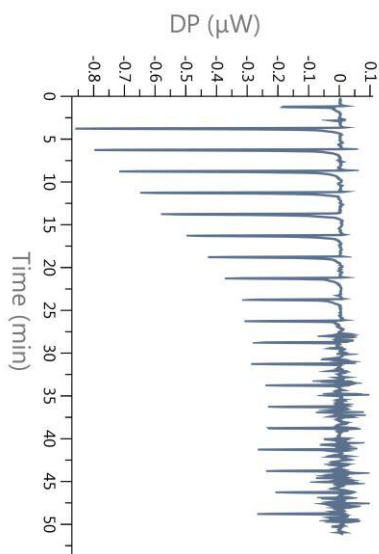
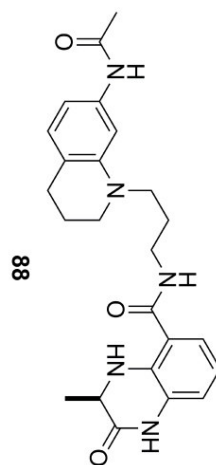
Appendix A

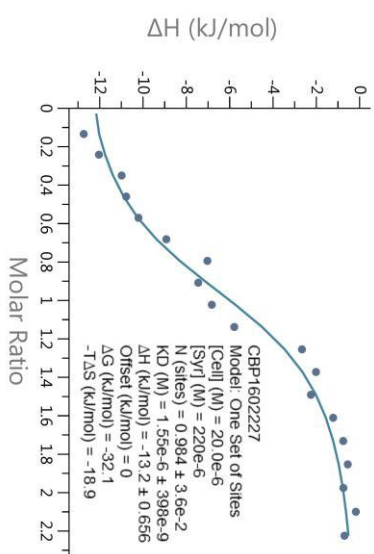
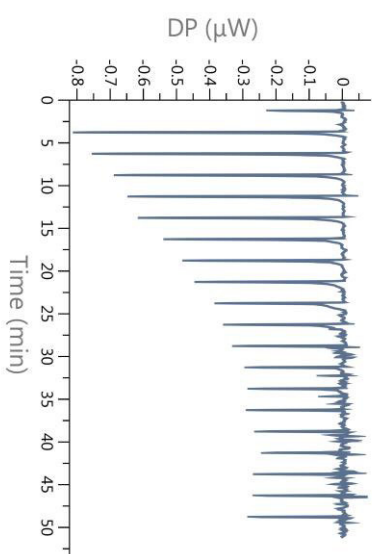
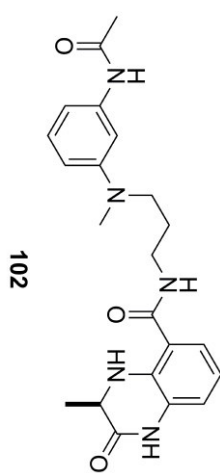
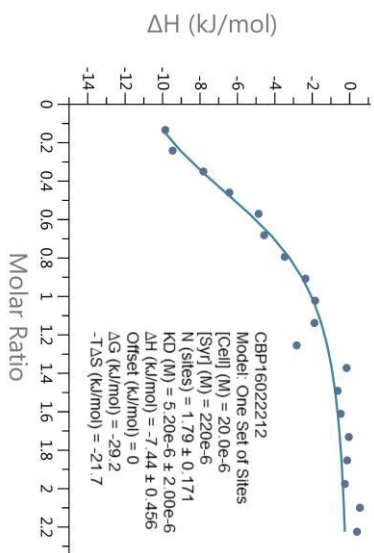
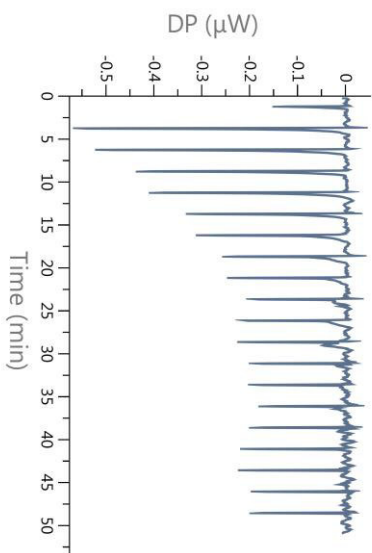
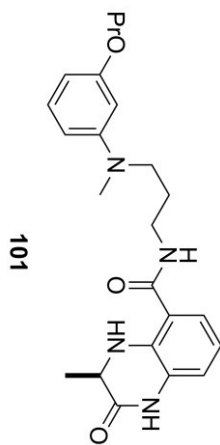
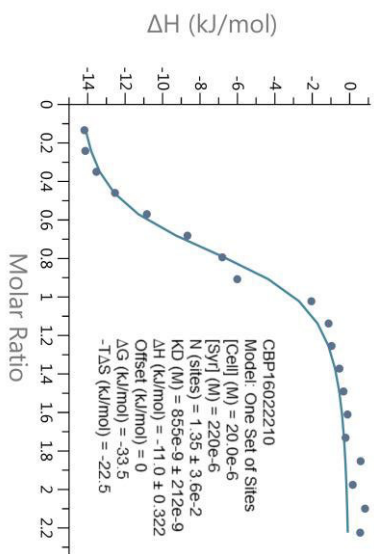
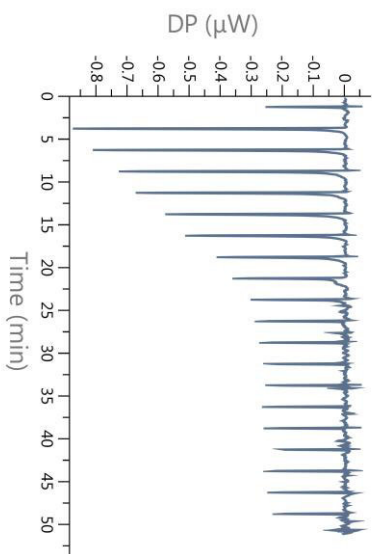
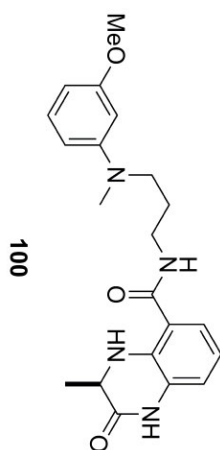
Synthesis of 5- and 6-Isoxazolylbenzimidazoles as Selective Inhibitors of the BET Bromodomains. *Medchemcomm* **2013**, *4* (1), 140–144.

- (13) Pierce, M. M.; Raman, C. S.; Nall, B. T. Isothermal Titration Calorimetry of Protein–Protein Interactions. *Methods* **1999**, *19*, 213–221.
- (14) Freyer, M. W.; Lewis, E. A. Isothermal Titration Calorimetry: Experimental Design, Data Analysis, and Probing Macromolecule/Ligand Binding and Kinetic Interactions. *Methods Cell Biol.* **2008**, *84*, 79–113.

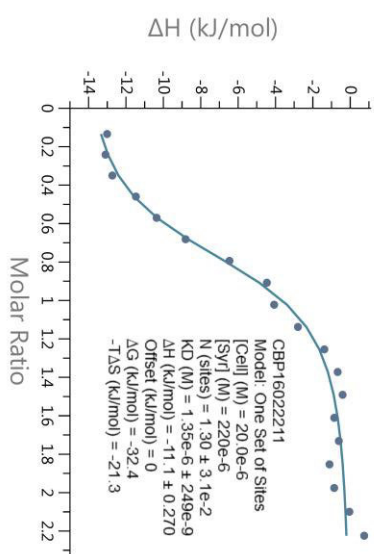
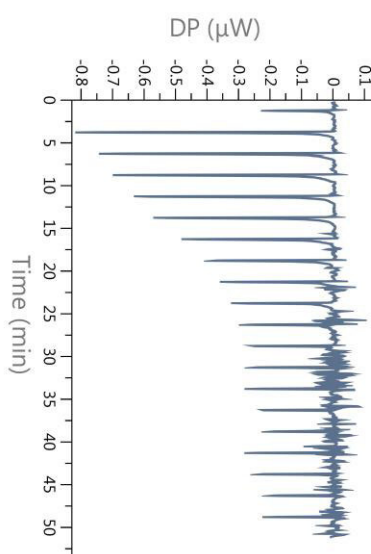
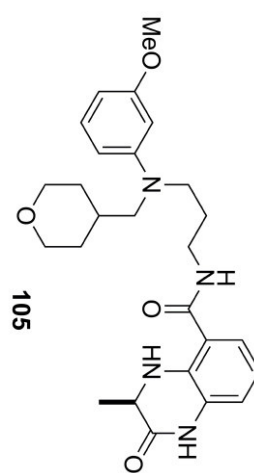
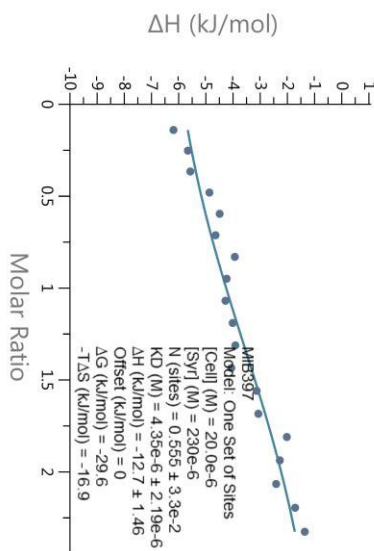
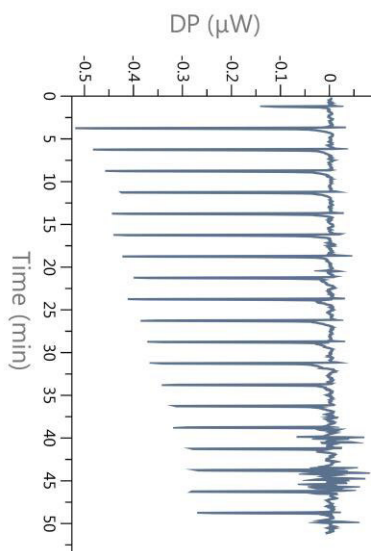
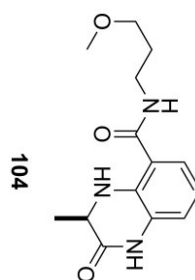
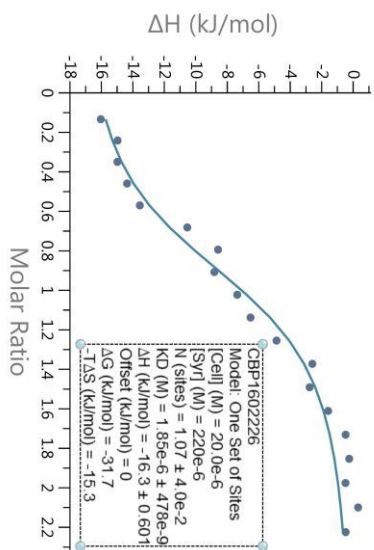
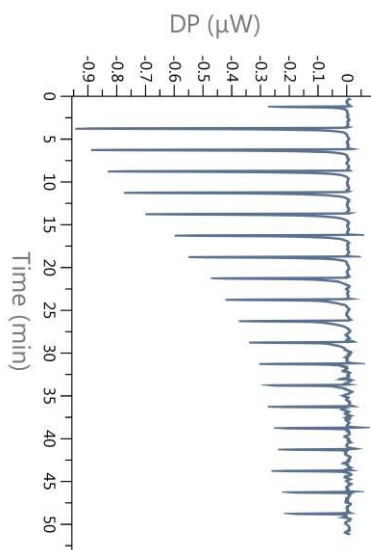
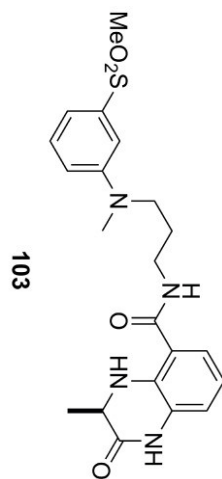
B1 ITC raw data on the CREBBP bromodomain



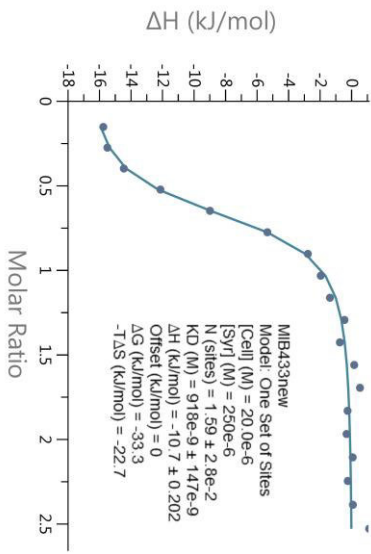
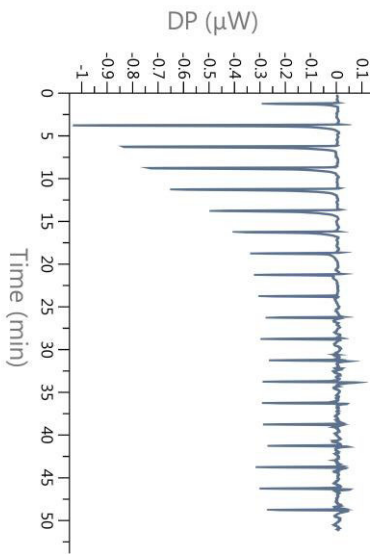
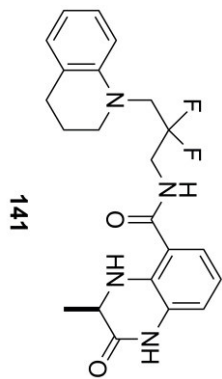
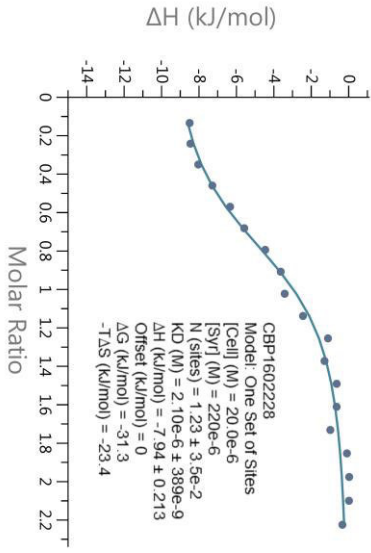
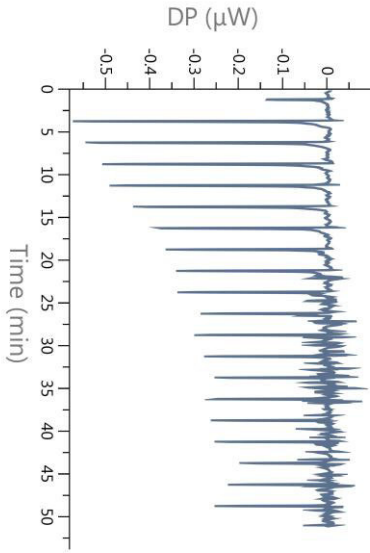
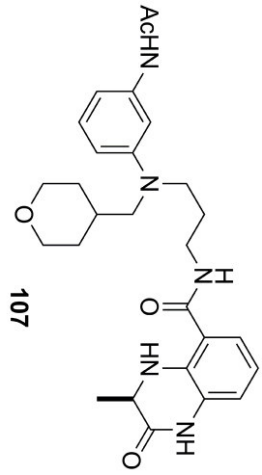
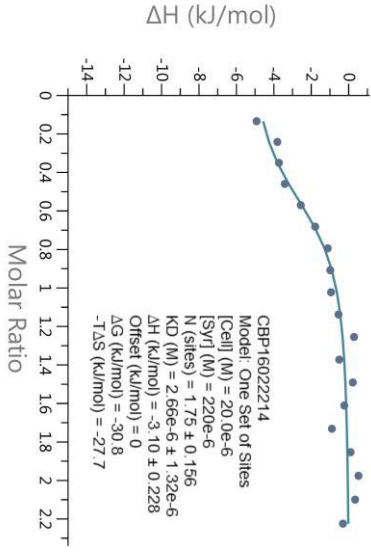
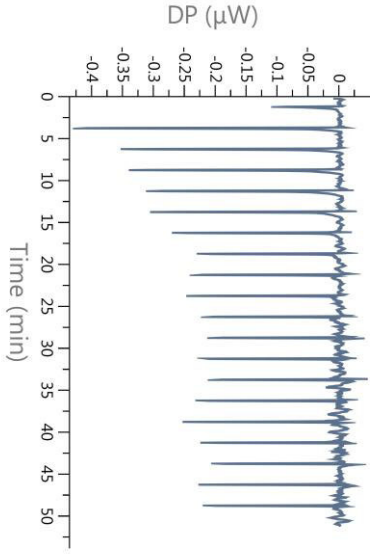
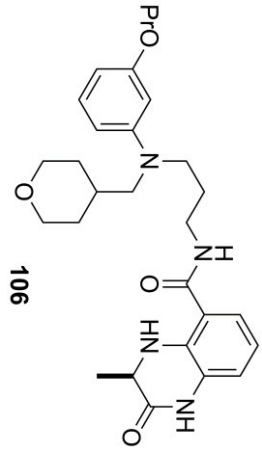




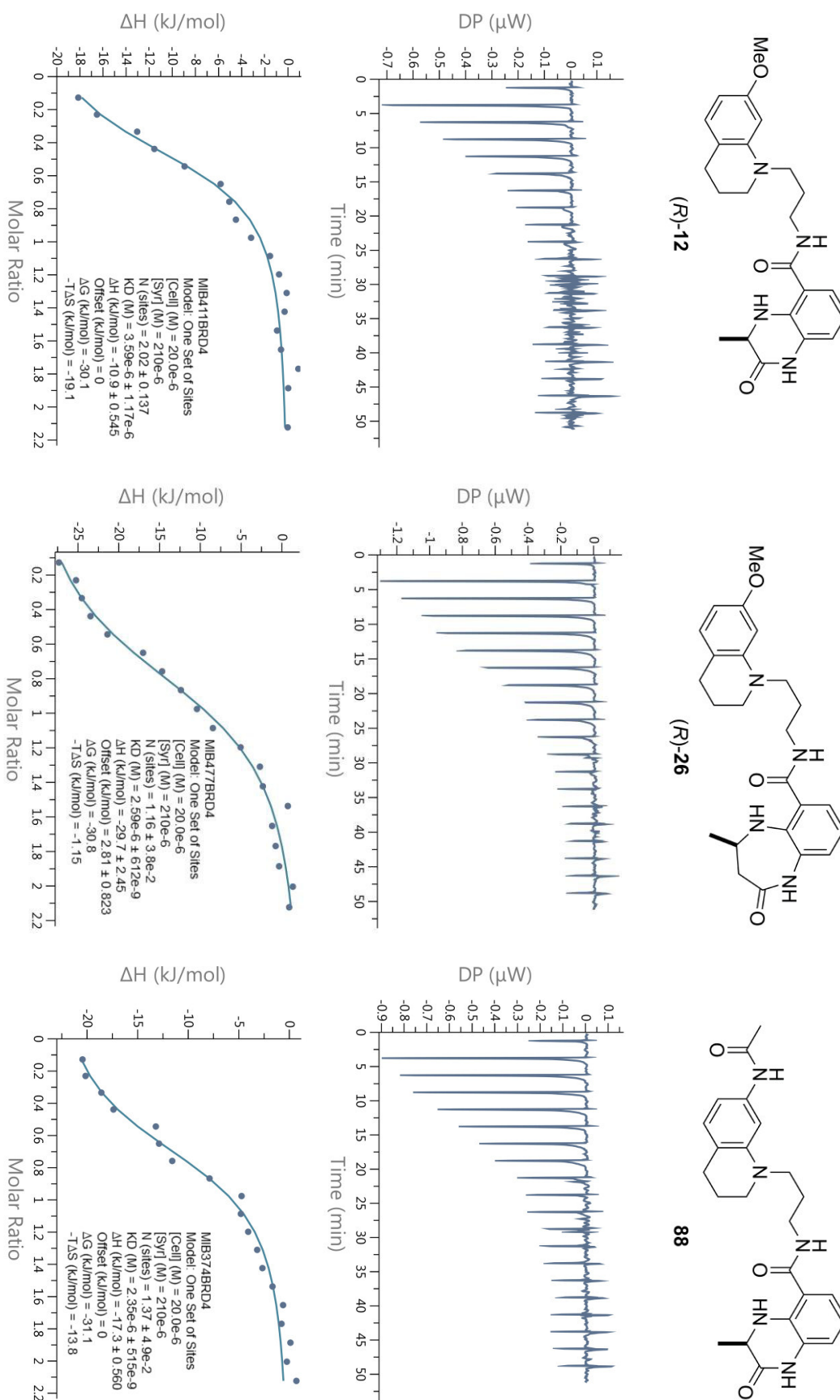
Appendix B: ITC



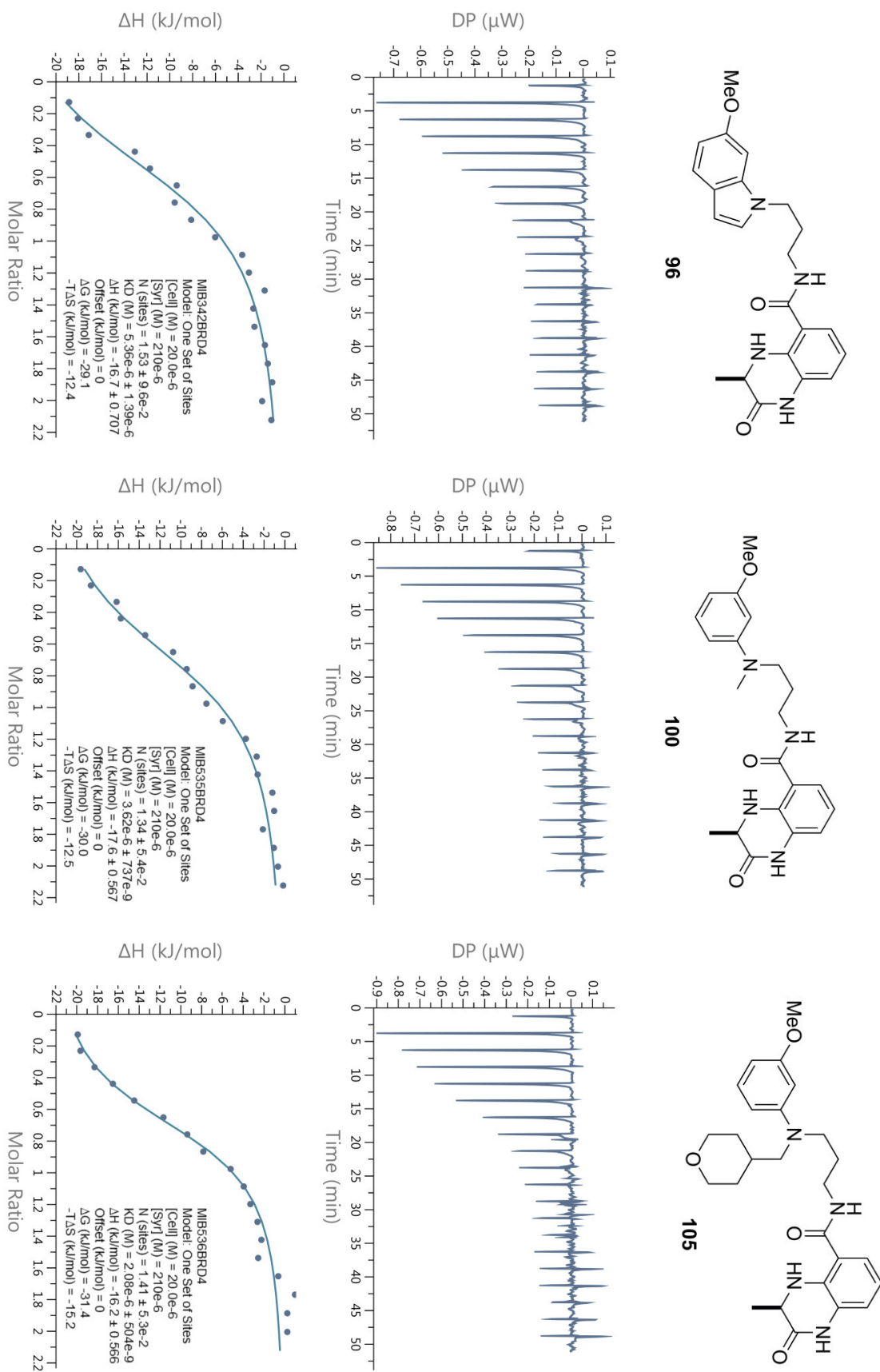
Appendix B: ITC



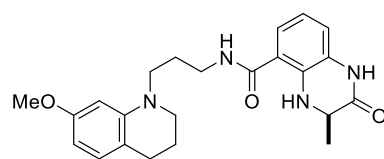
B2 ITC raw data on the BRD4(1) bromodomain



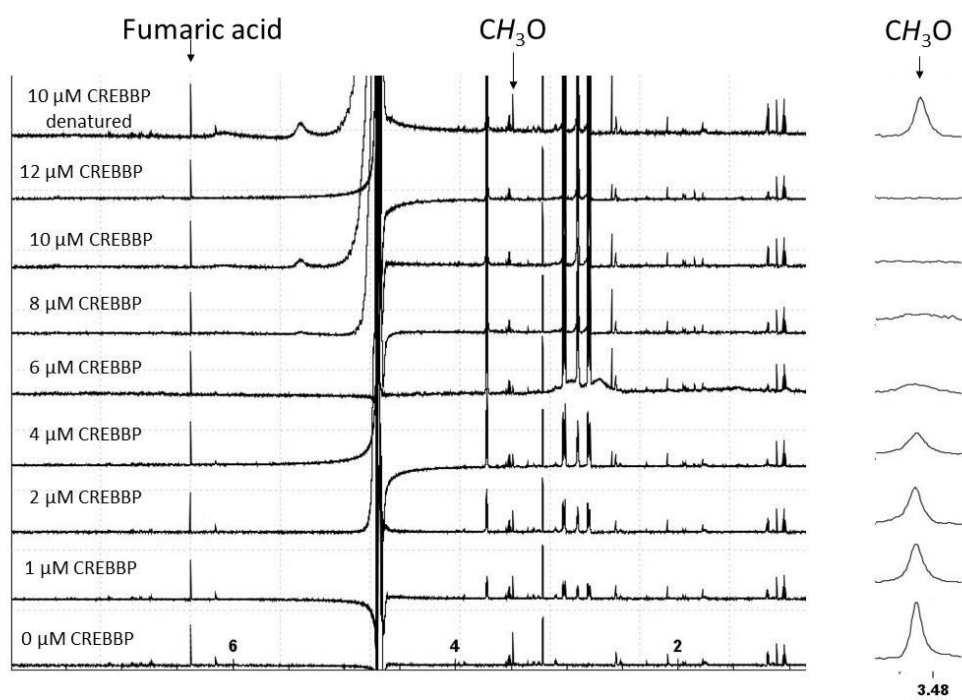
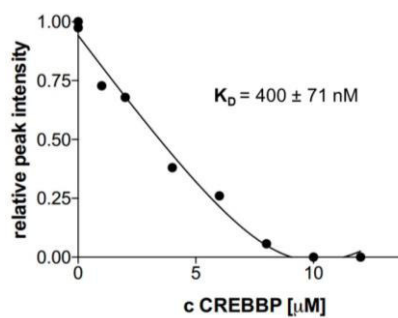
Appendix B: ITC



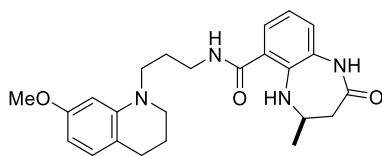
C CPMG-NMR raw data



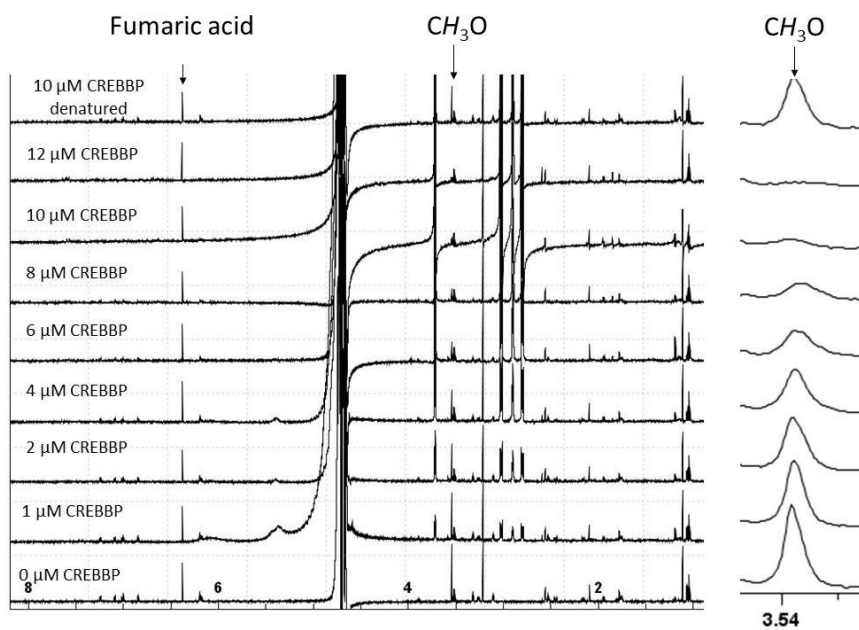
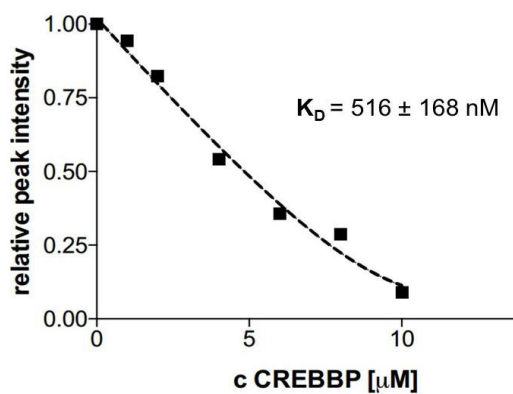
(R)-12



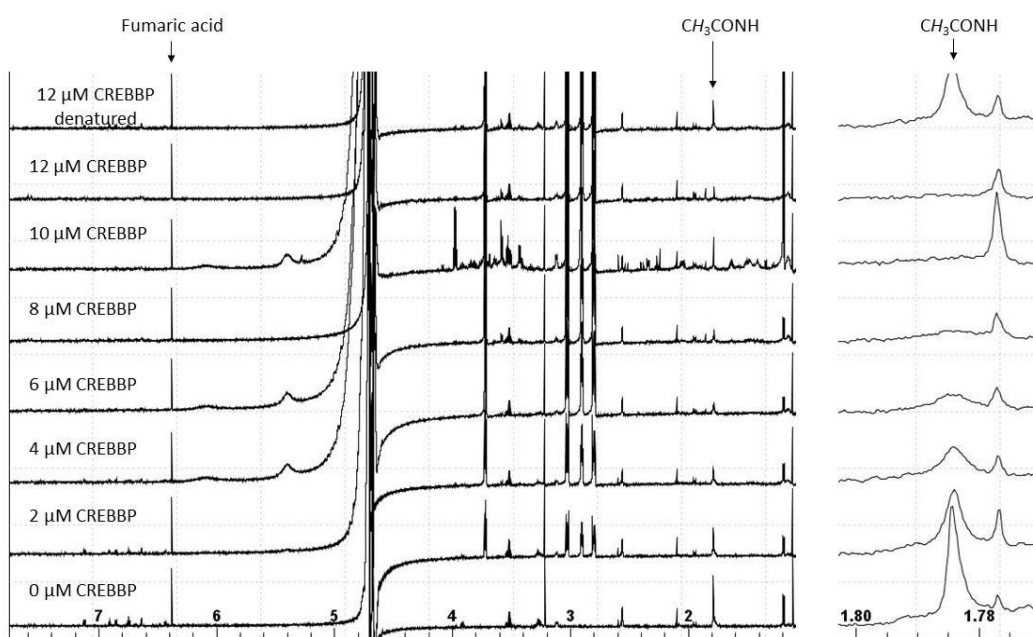
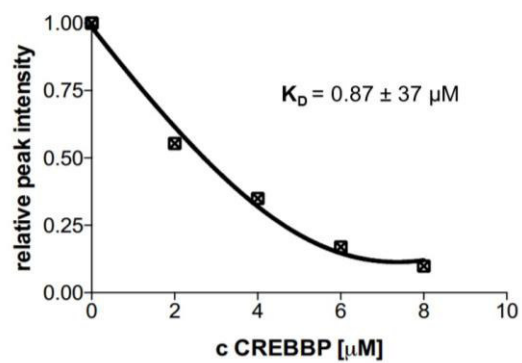
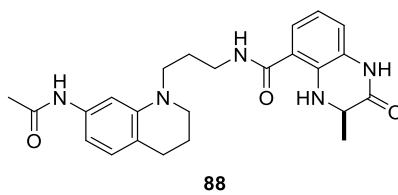
Appendix C: CPMG-NMR



(R)-26



Appendix C: CPMG-NMR

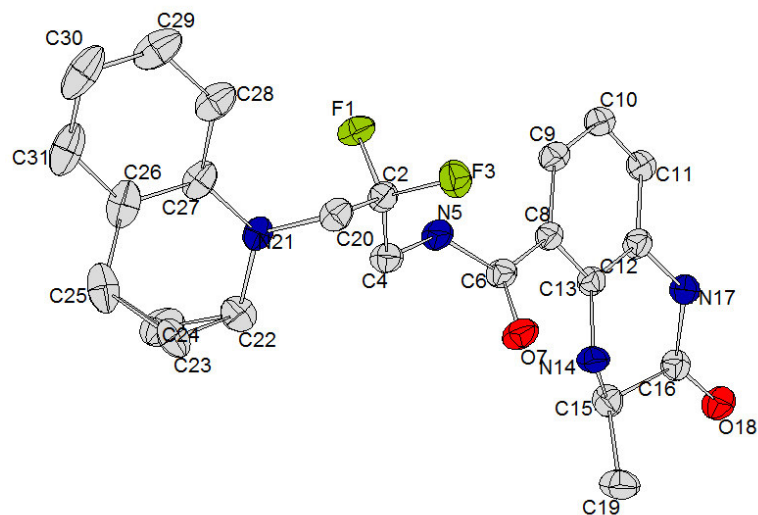


Appendix D: Crystallography

D1 Protein crystallisation data collection and refinement statistics

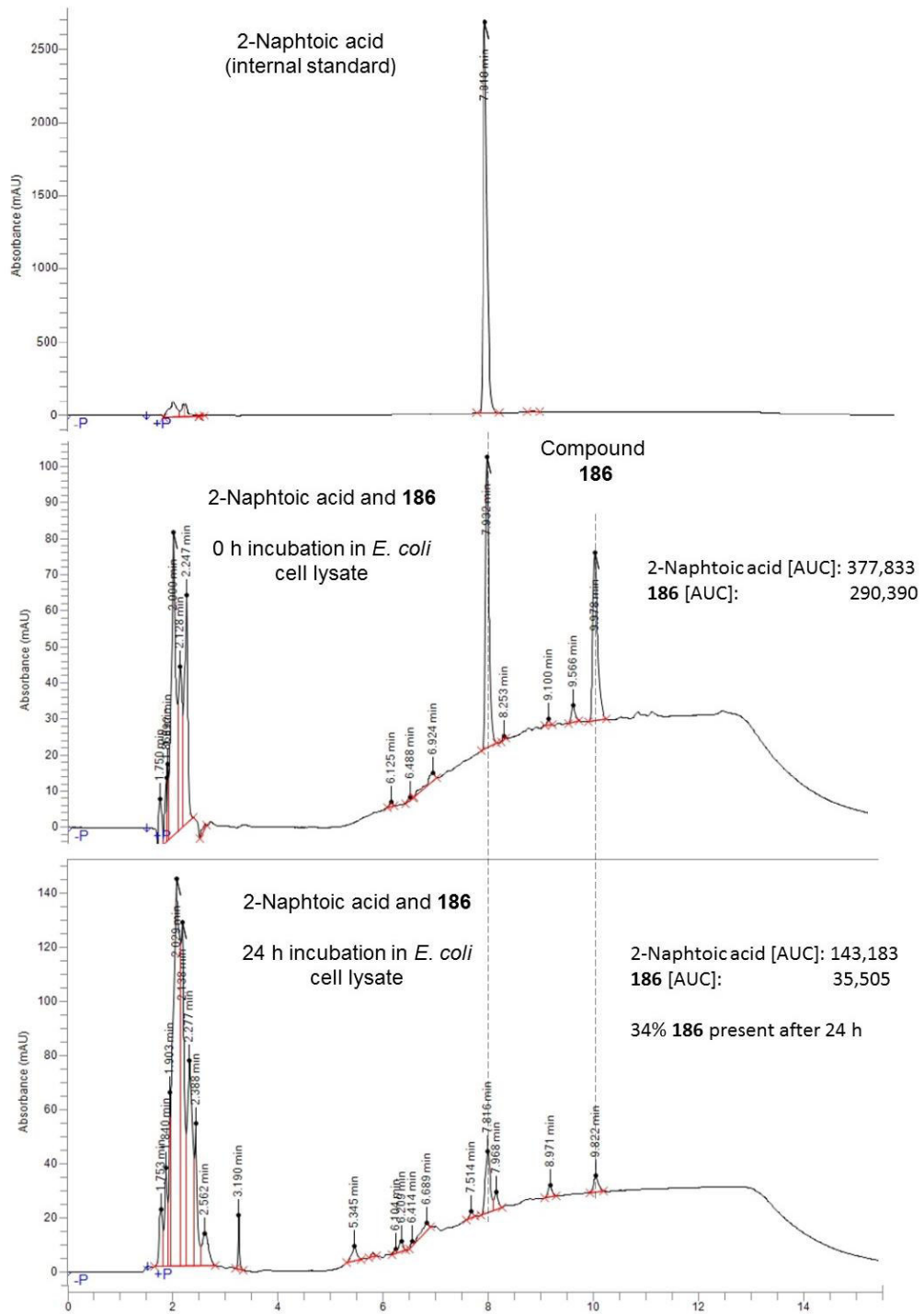
Data Collection			
	Figure 2.13	Figure 4.10	Figure 4.11
Protein/Ligand	CREBBP/(R)- 26	CREBBP/ 141	CREBBP/ 141
Space group	C2	C2	P2 ₁
Cell dimensions: a, b, c (Å)	94.38 34.68 40.05	94.26 34.62 40.11	80.23 43.91 88.27
α, β, γ (deg)	90.00 107.18 90.00	90.00 107.29 90.00	90.00 110.06 90.00
Resolution* (Å)	1.23 (1.30-1.23)	1.22 (1.29-1.22)	1.70 (1.79-1.70)
Unique observations*	36020 (5196)	35941 (5117)	63697 (8842)
Completeness* (%)	99.7 (99.3)	97.1 (95.1)	99.0 (96.1)
Redundancy*	2.9 (2.8)	3.0 (2.9)	3.4 (3.4)
Rmerge*	0.052 (0.059)	0.061 (0.072)	0.047 (0.429)
I/σI*	20.7 (13.7)	15.6 (10.7)	14.3 (2.9)
Refinement			
Resolution (Å)	1.23	1.22	1.70
R _{work} / R _{free} (%)	14.1/16.7	13.3/15.1	16.3/18.7
Number of atoms (protein/other/water)	980/163/31	976/154/30	2859/150/325
B-factors (Å ²) (protein/other/water)21.85	11.98/24.26/13.68	11.89/23.92/12.64	33.98/35.61/41.78
r.m.s.d bonds (Å)	0.014	0.013	0.017
r.m.s.d angles (°)	1.750	1.704	1.915
Ramachadran Favoured (%)	99.08	100.00	99.70
Allowed (%)	0.92	0.00	0.30
Disallowed (%)	0.00	0.00	0.00

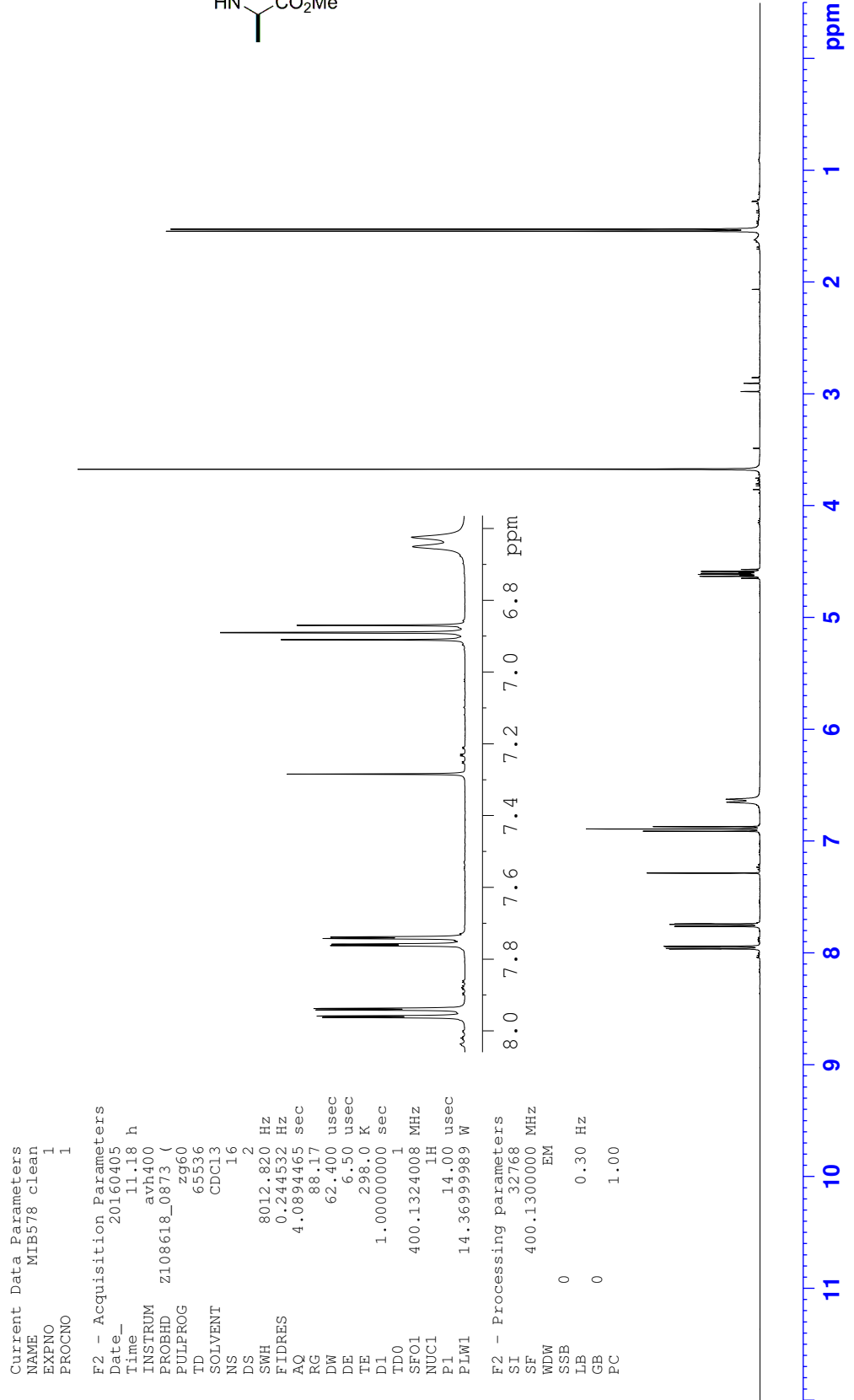
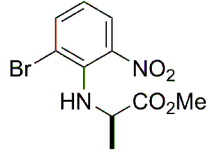
* Values in parentheses correspond to the highest resolution shell.

D2 Small molecule crystallisation data collection and refinement statistics.

X-ray crystal structure of **141**. Grey = carbon, blue = nitrogen, red = oxygen, green = fluorine. The C23 and C24 were disordered in a ratio of 23 to 77. Ellipsoids drawn at the 50% probability level. X-ray crystal structure data for **141** [$C_{22}H_{24}N_4O_2F_2$]: $M = 413.45$, orthorhombic, space group: $P 2_1 2_1 2_1$, $a = 8.98940(10)$ Å, $b = 16.2085(3)$ Å, $c = 13.5716(3)$ Å, $\alpha = 90^\circ$; $\beta = 90^\circ$, $\gamma = 90^\circ$, $V = 1977.45(6)$ Å³, $Z = 2$, $\mu = 0.71073$ mm.

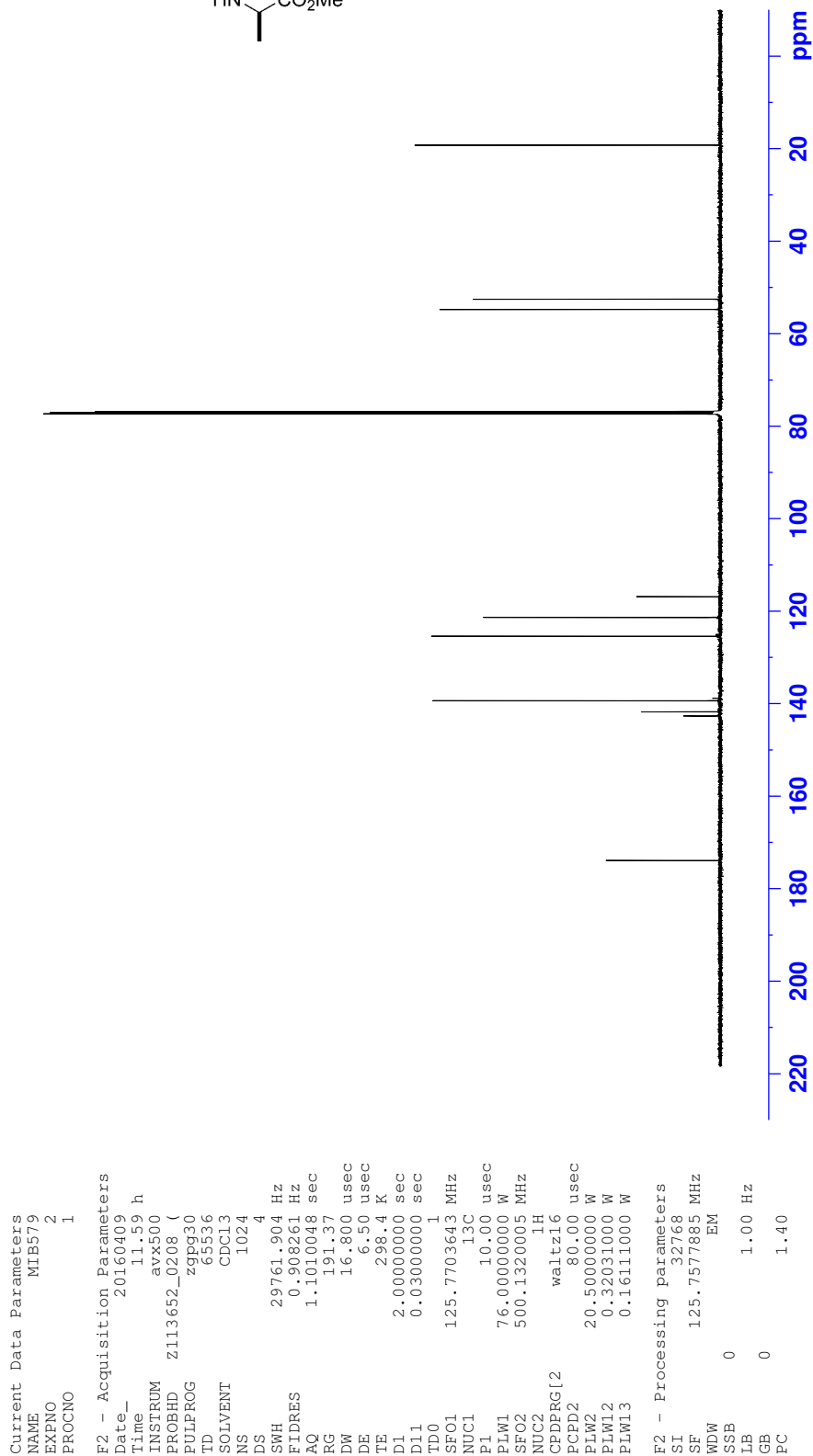
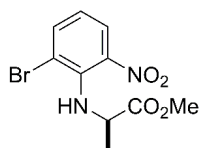
E Stability of compound 186 in cell lysate



¹H NMR Methyl (2-bromo-6-nitrophenyl)-D-alaninate ((*R*)-**34**)

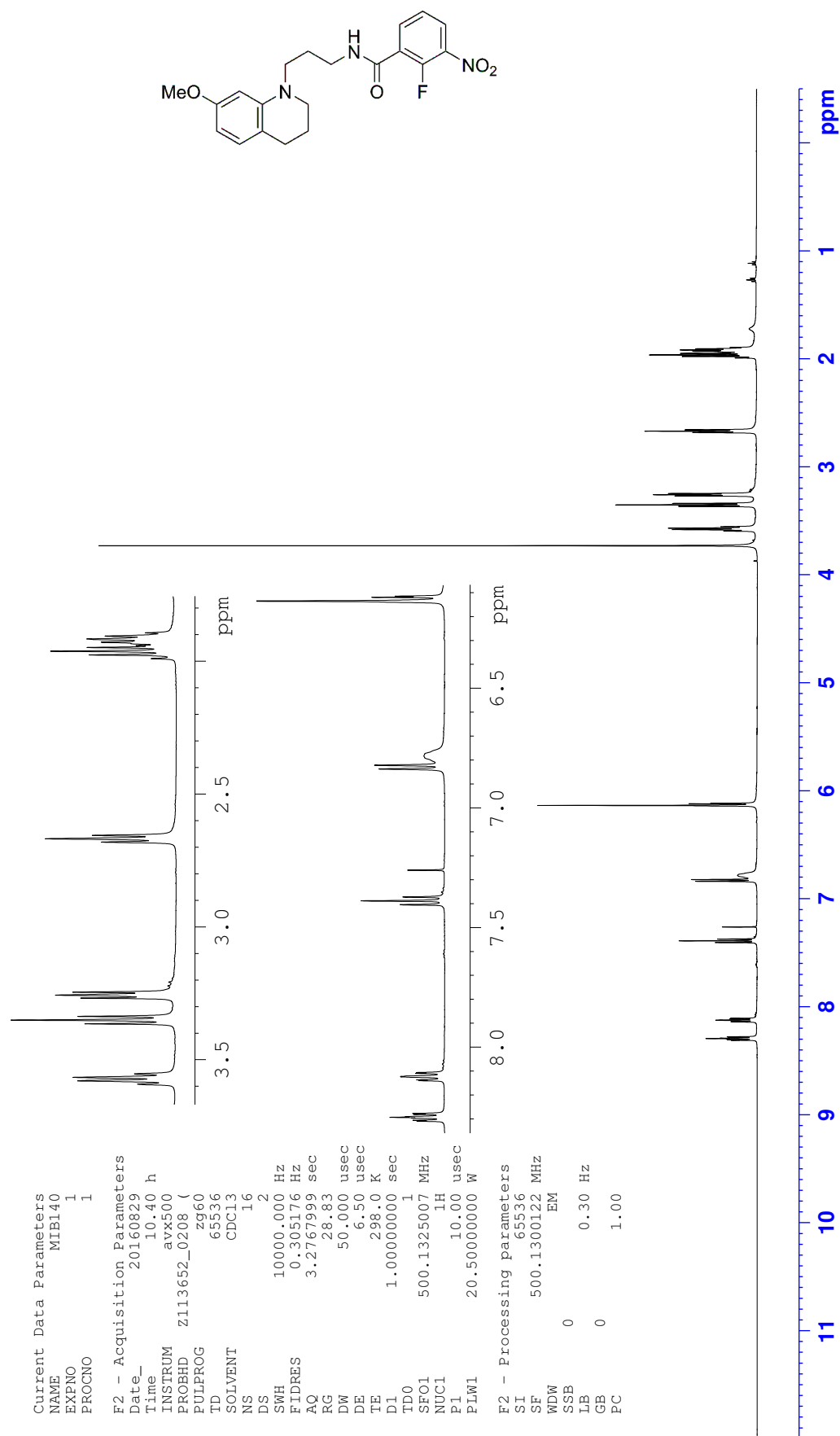
Appendix F: NMR spectra

¹³C NMR Methyl (2-bromo-6-nitrophenyl)-D-alaninate ((*R*)-**34**)



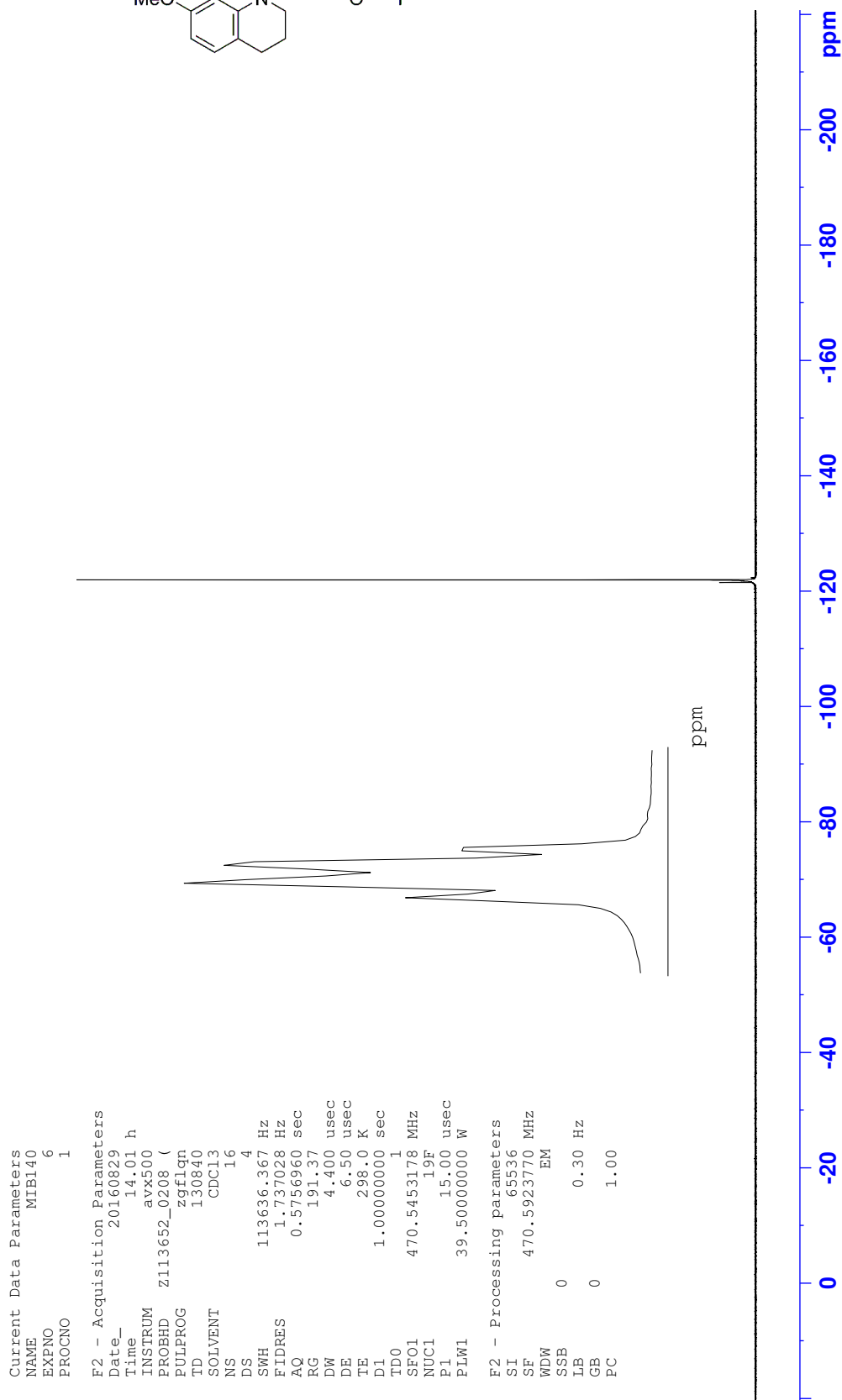
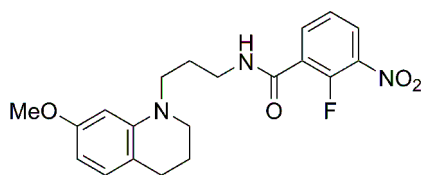
Appendix F: NMR spectra

¹H NMR 2-Fluoro-*N*-(3-(7-methoxy-3,4-dihydroquinolin-1(2*H*)-yl)propyl)-3-nitrobenzamide (46)



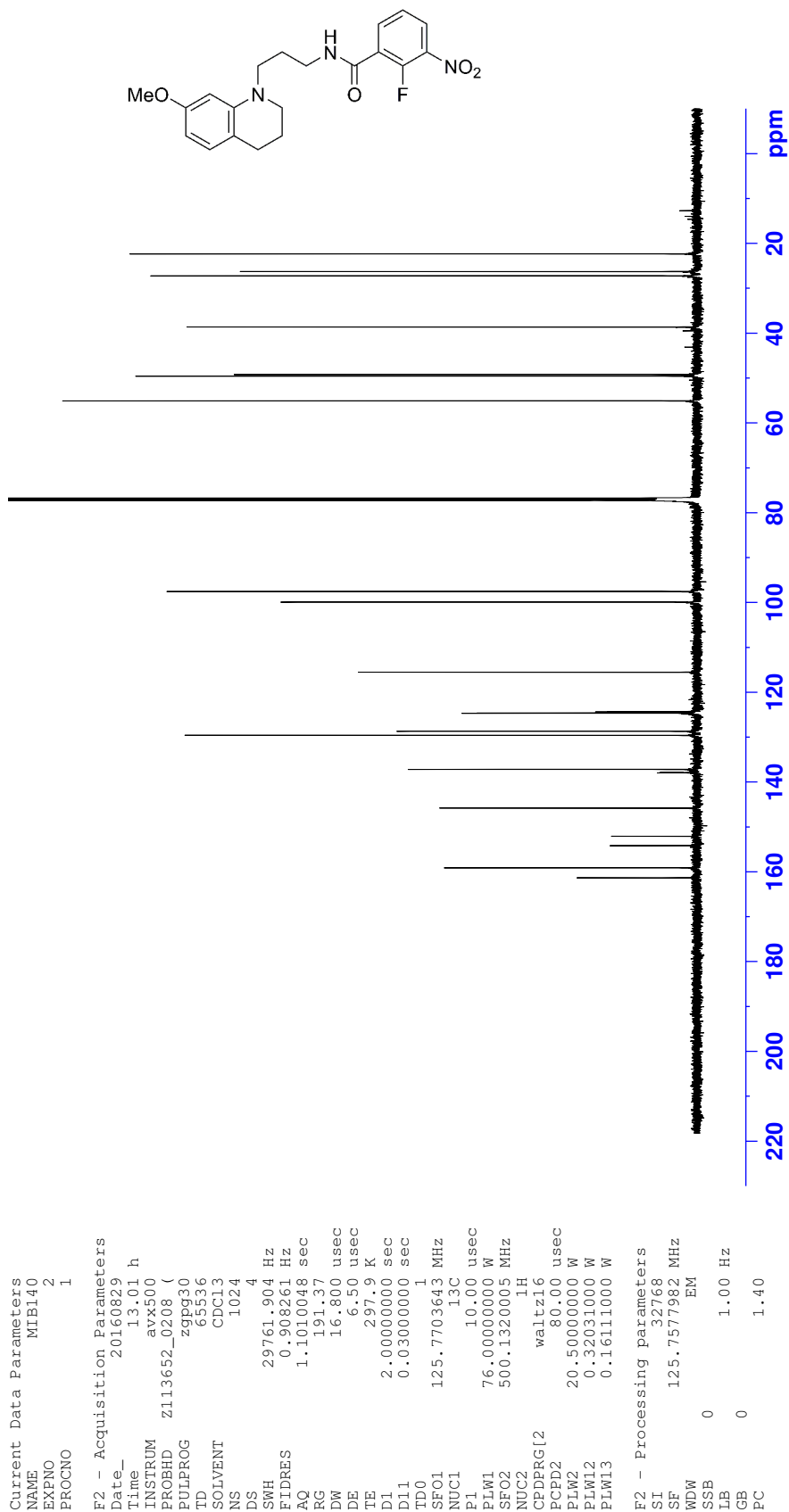
Appendix F: NMR spectra

¹⁹F NMR 2-Fluoro-*N*-(3-(7-methoxy-3,4-dihydroquinolin-1(2*H*)-yl)propyl)-3-nitrobenzamide (46)



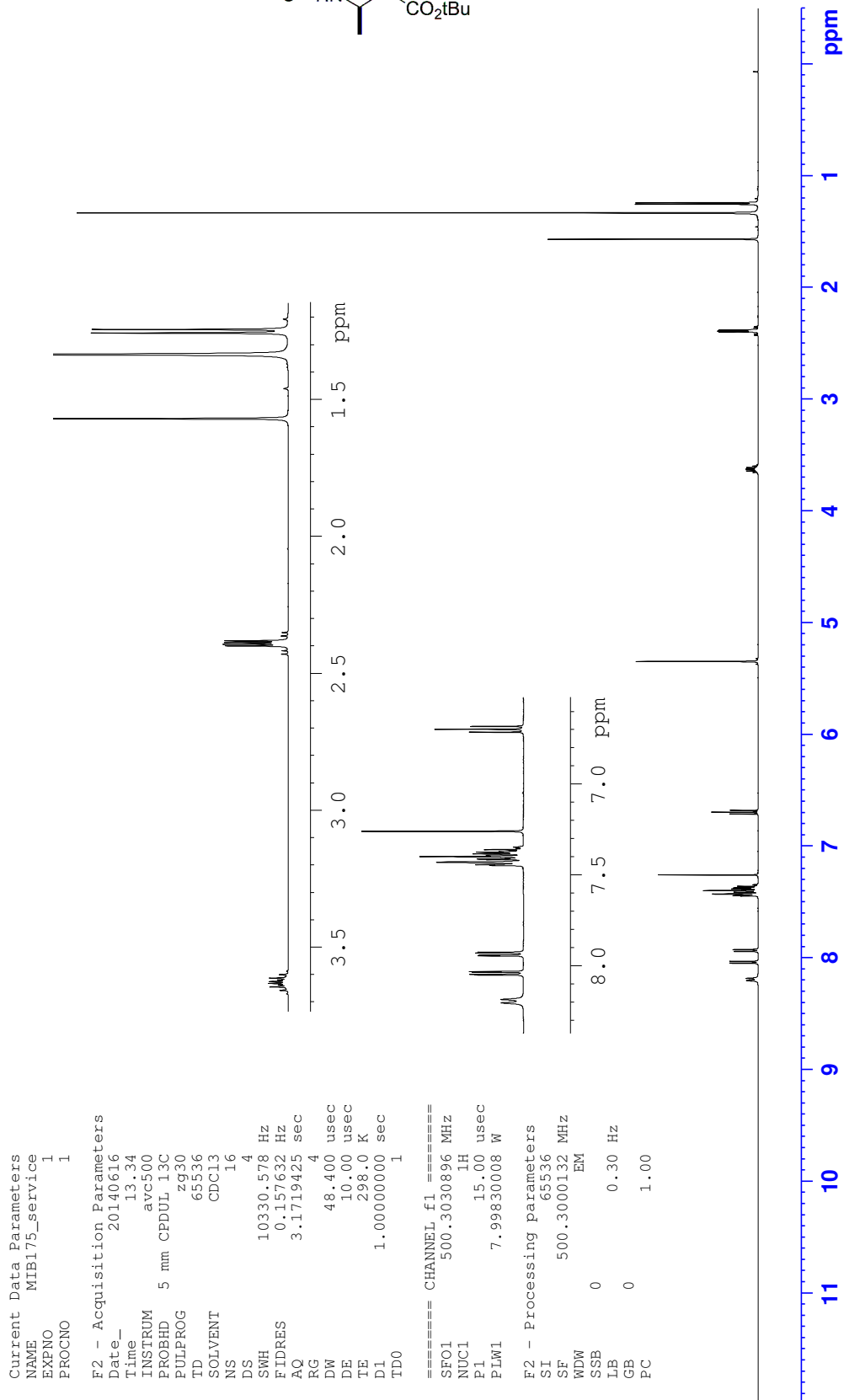
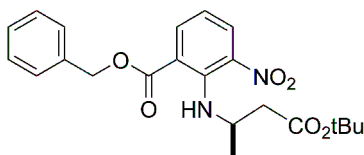
Appendix F: NMR spectra

¹³C NMR 2-Fluoro-N-(3-(7-methoxy-3,4-dihydroquinolin-1(2H)-yl)propyl)-3-nitrobenzamide (46)



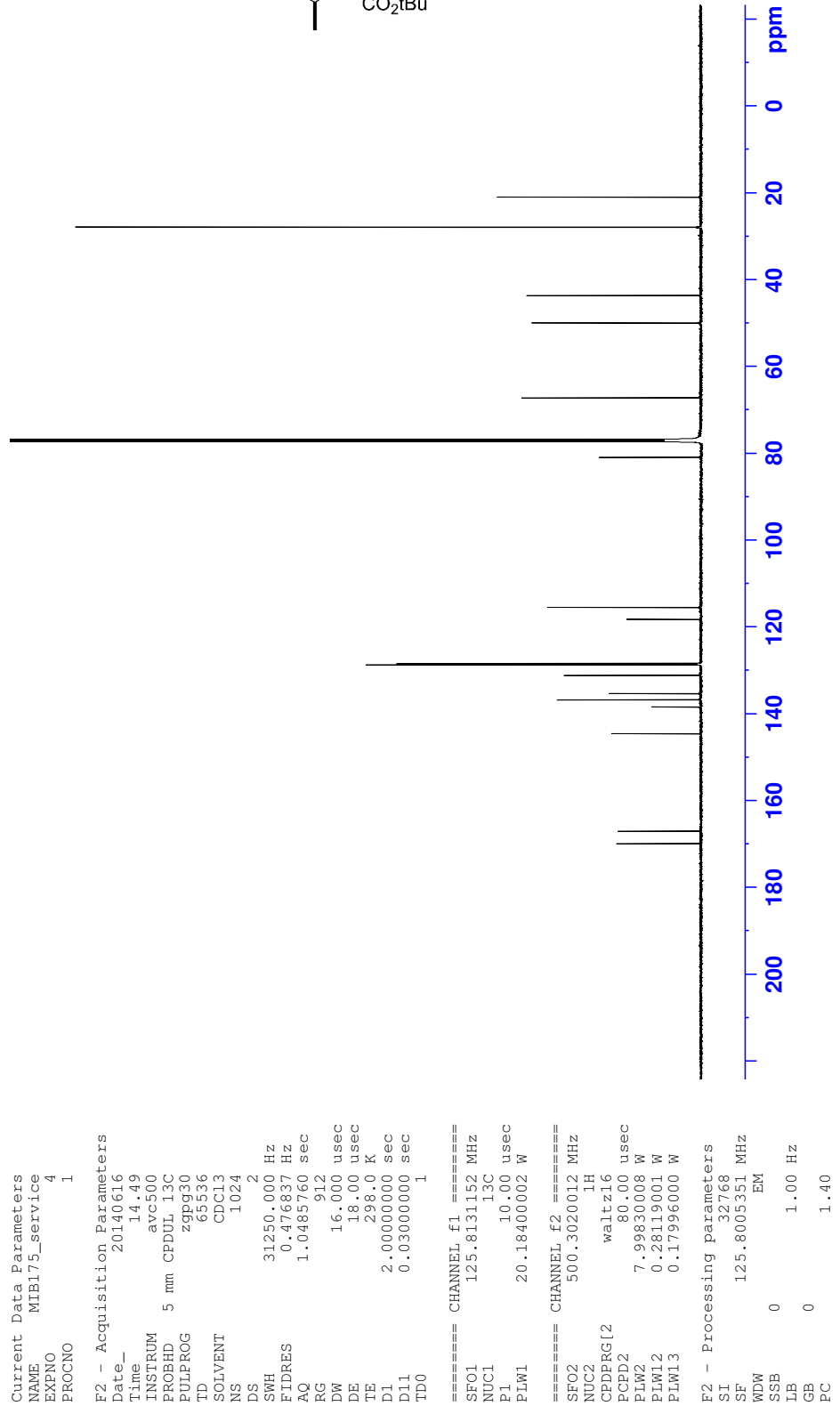
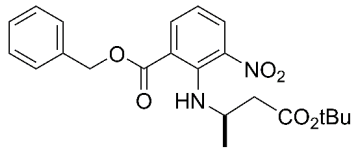
Appendix F: NMR spectra

¹H NMR (*R*)-Benzyl 2-(4-*tert*-butoxy-4-oxobutan-2-ylamino)-3-nitrobenzoate ((*R*)-**48**)



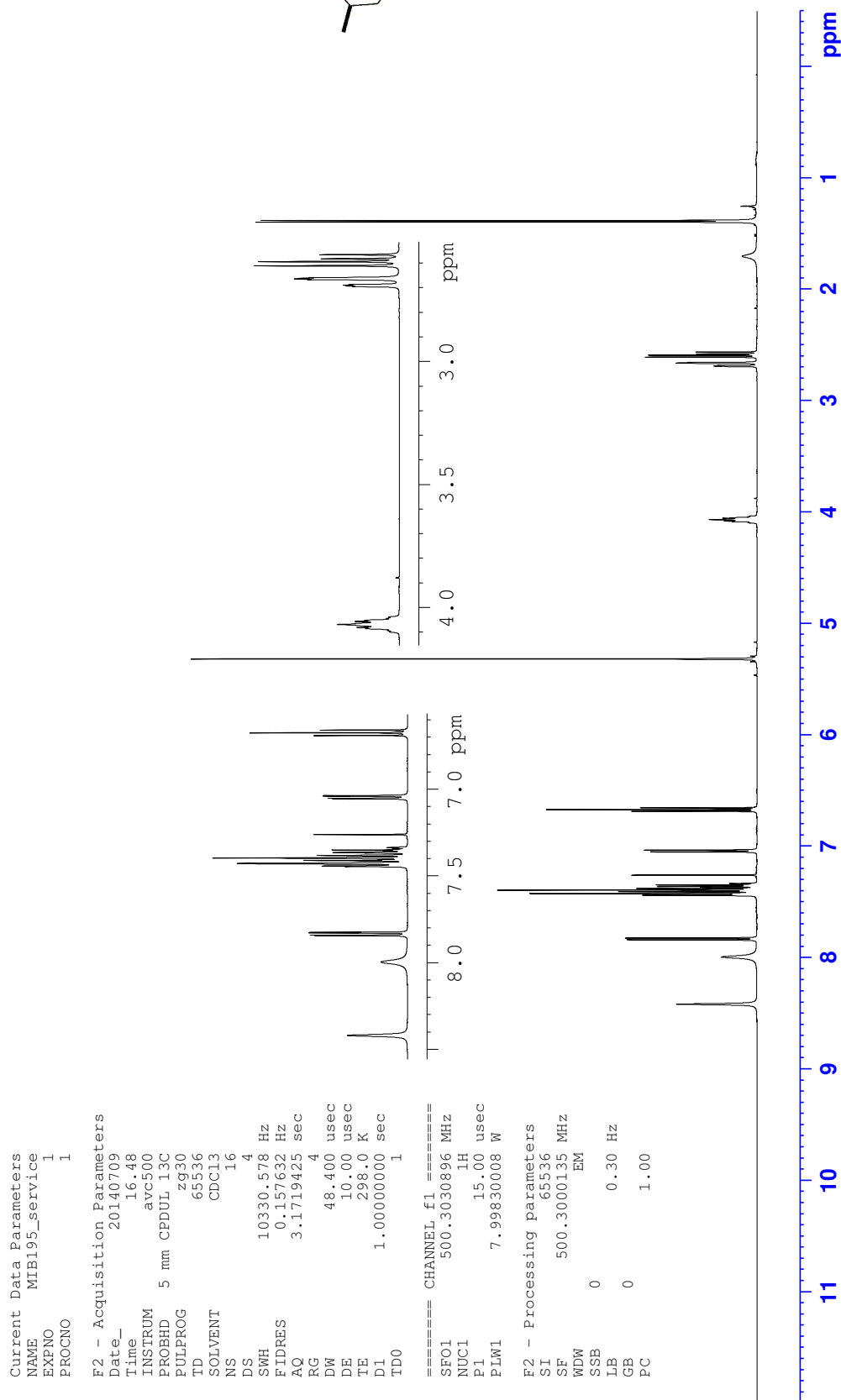
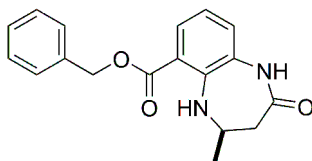
Appendix F: NMR spectra

¹³C NMR (*R*)-Benzyl 2-(4-*tert*-butoxy-4-oxobutan-2-ylamino)-3-nitrobenzoate ((*R*)-48)



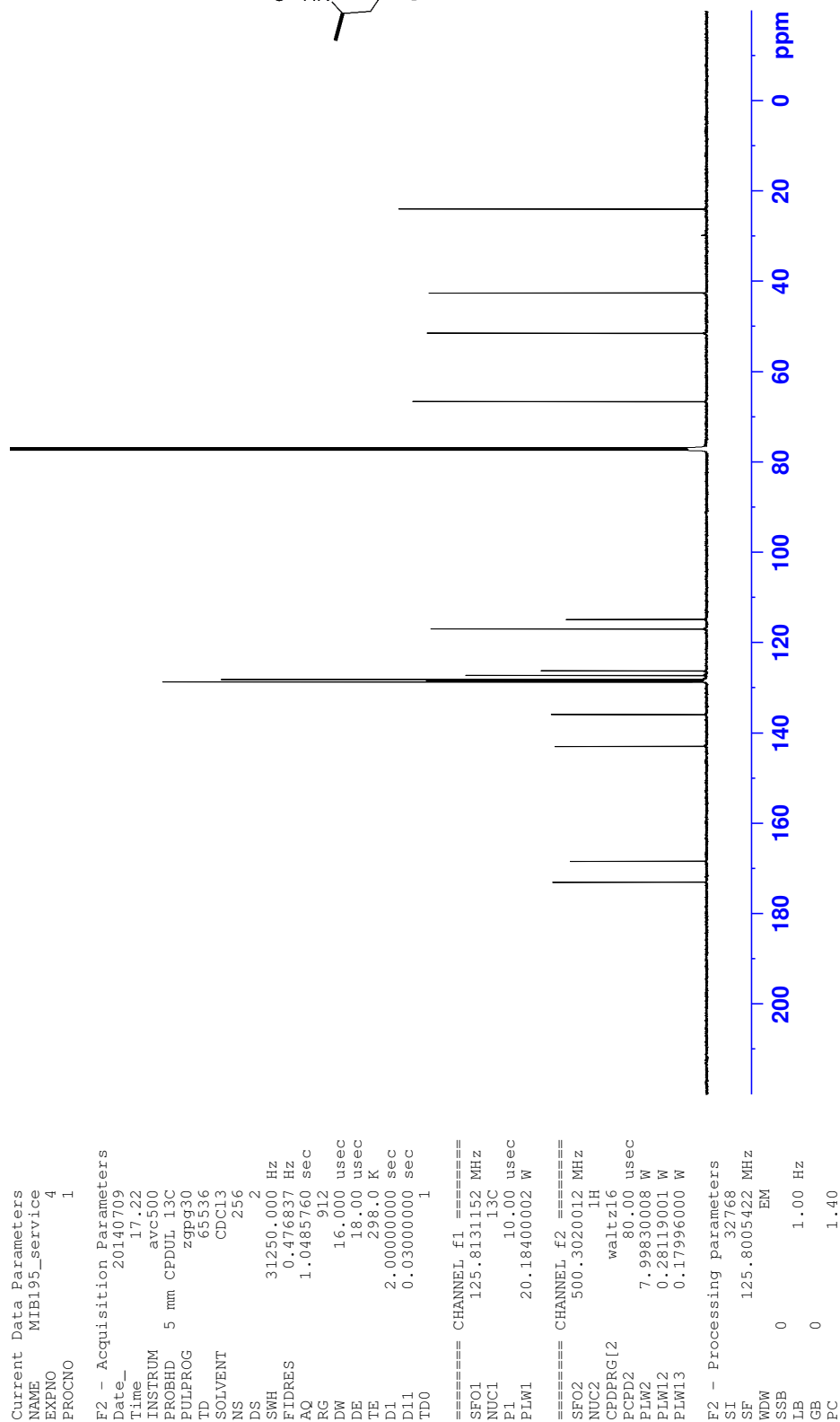
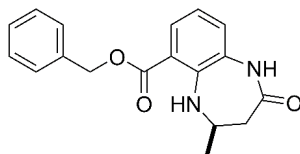
Appendix F: NMR spectra

¹H NMR (*R*)-Benzyl 4-methyl-2-oxo-2,3,4,5-tetrahydro-1*H*-benzo[*b*][1,4]diazepine-6-carboxylate ((*R*)-51)



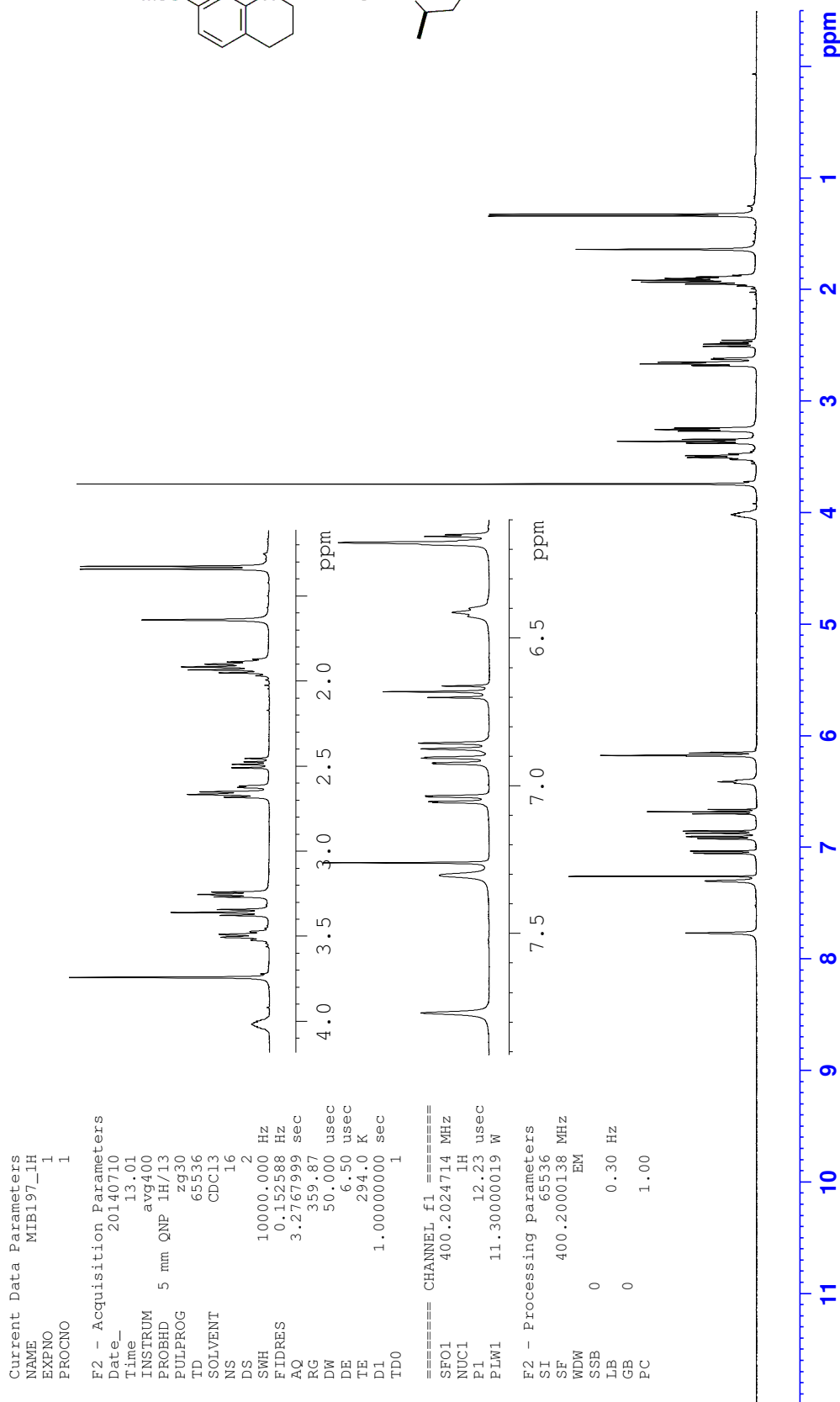
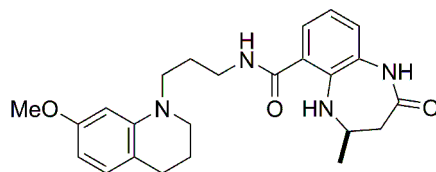
Appendix F: NMR spectra

¹³C NMR (R)-Benzyl 4-methyl-2-oxo-2,3,4,5-tetrahydro-1H-benzo[b][1,4]diazepine-6-carboxylate ((R)-51)



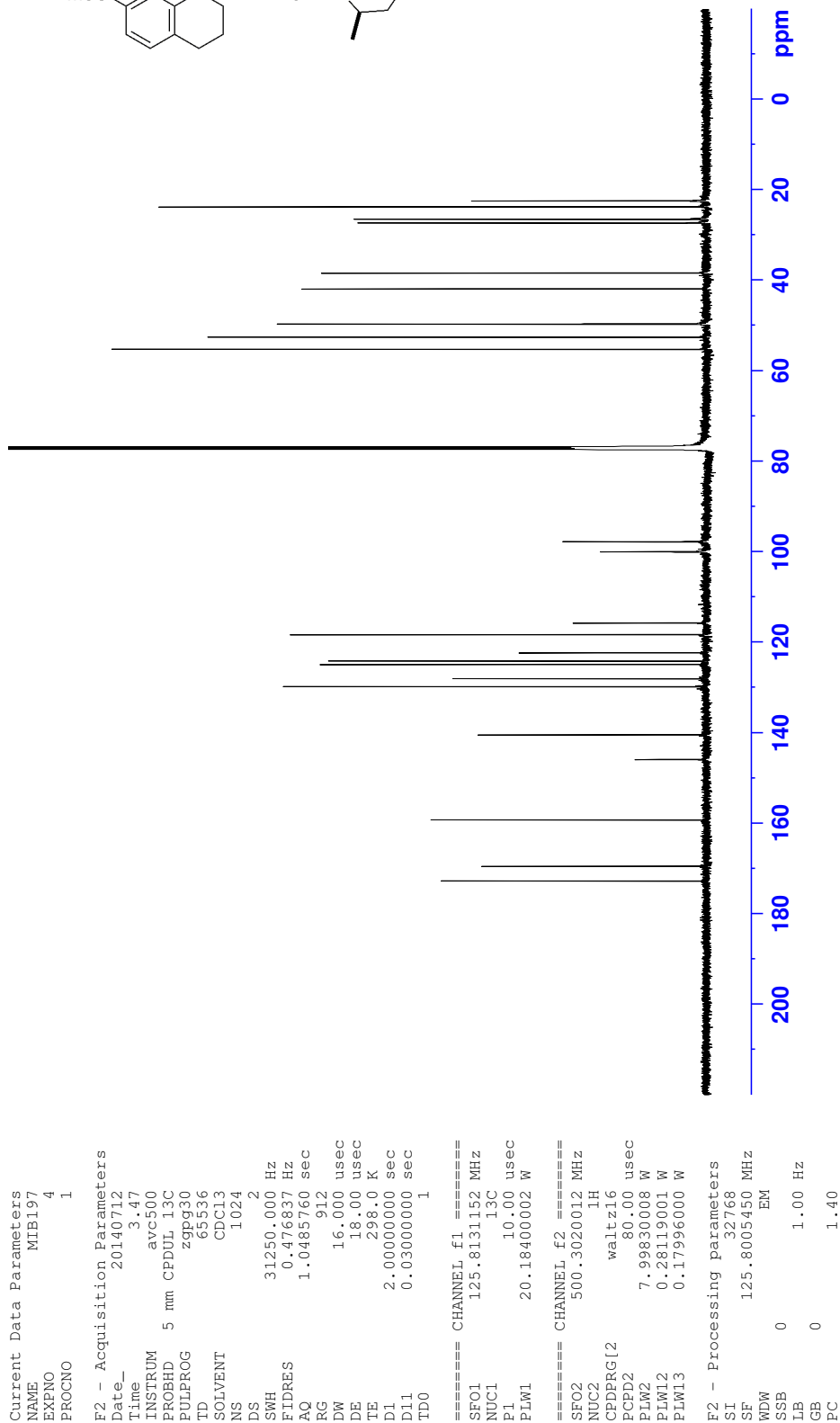
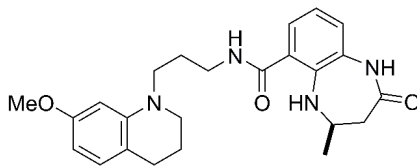
Appendix F: NMR spectra

^1H NMR (*R*)-3-(7-Methoxy-3,4-dihydroquinolin-1(2*H*)-yl)propyl 4-methyl-2-oxo-2,3,4,5-tetrahydro-1*H*-benzo[*b*][1,4]diazepine-6-carboxylate ((*R*)-**26**)



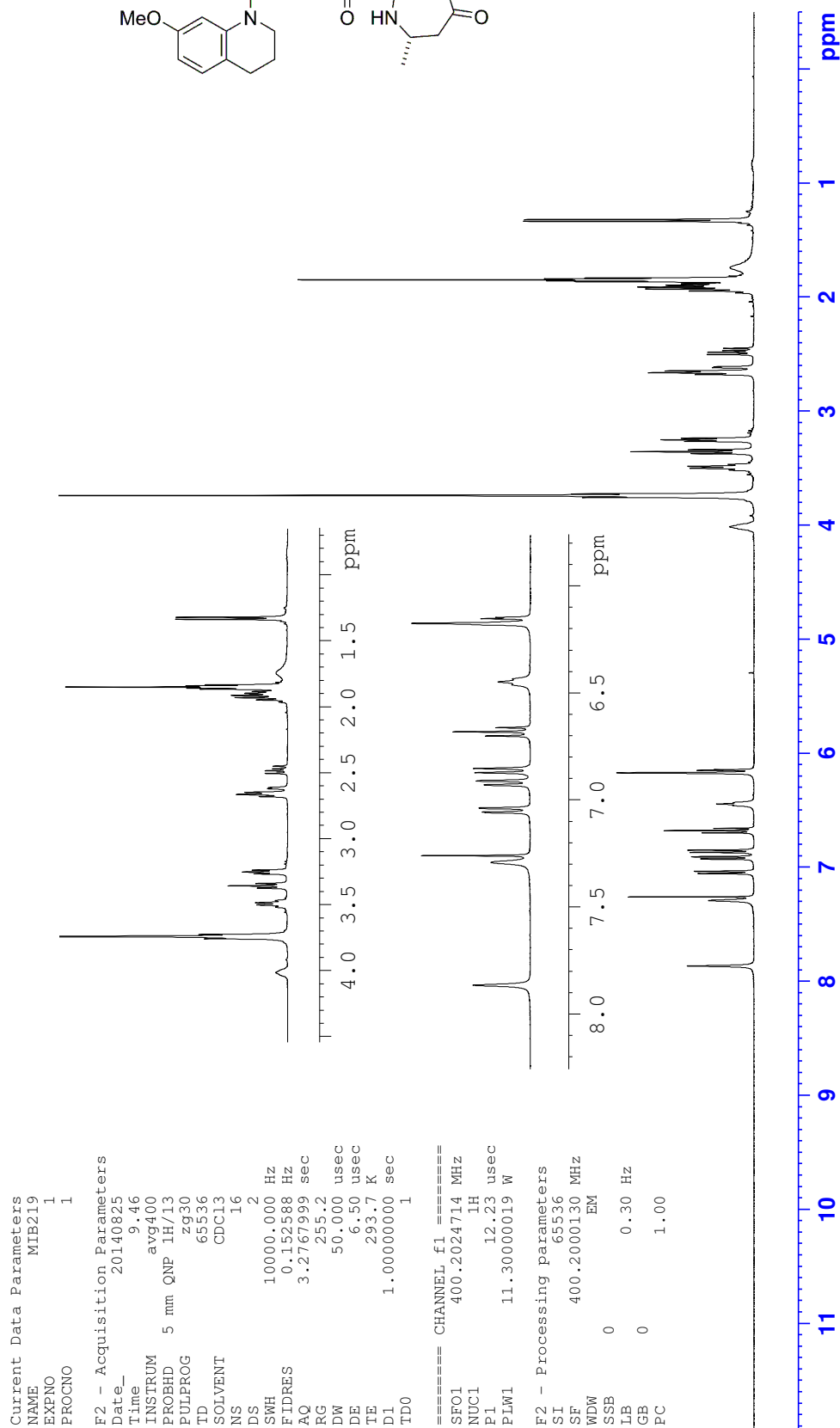
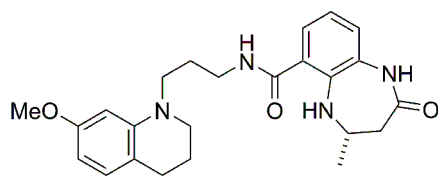
Appendix F: NMR spectra

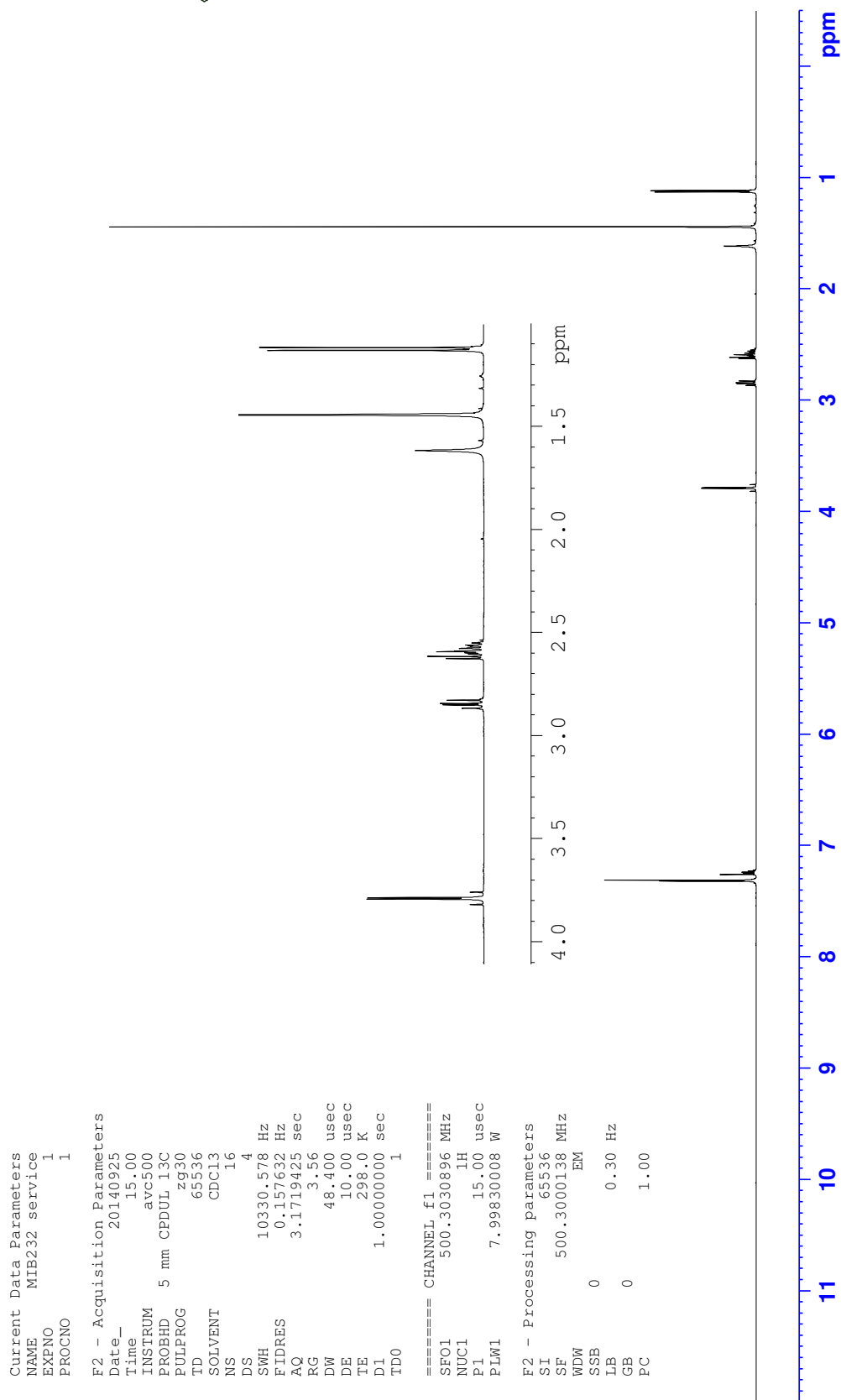
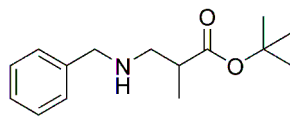
¹³C NMR (R)-3-(7-Methoxy-3,4-dihydroquinolin-1(2H)-yl)propyl 4-methyl-2-oxo-2,3,4,5-tetrahydro-1H-benzo[b][1,4]diazepine-6-carboxylate ((R)-26)

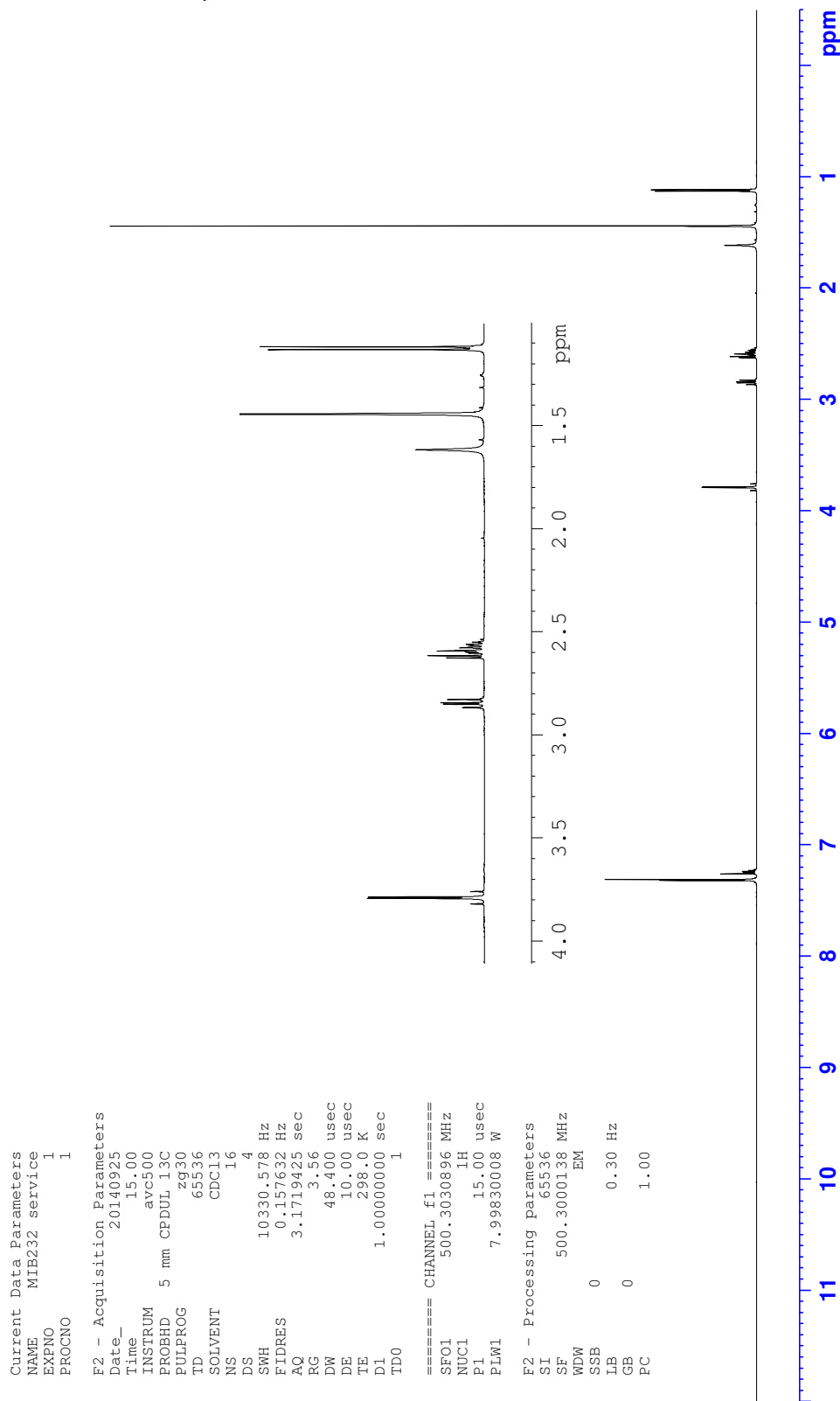
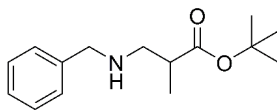


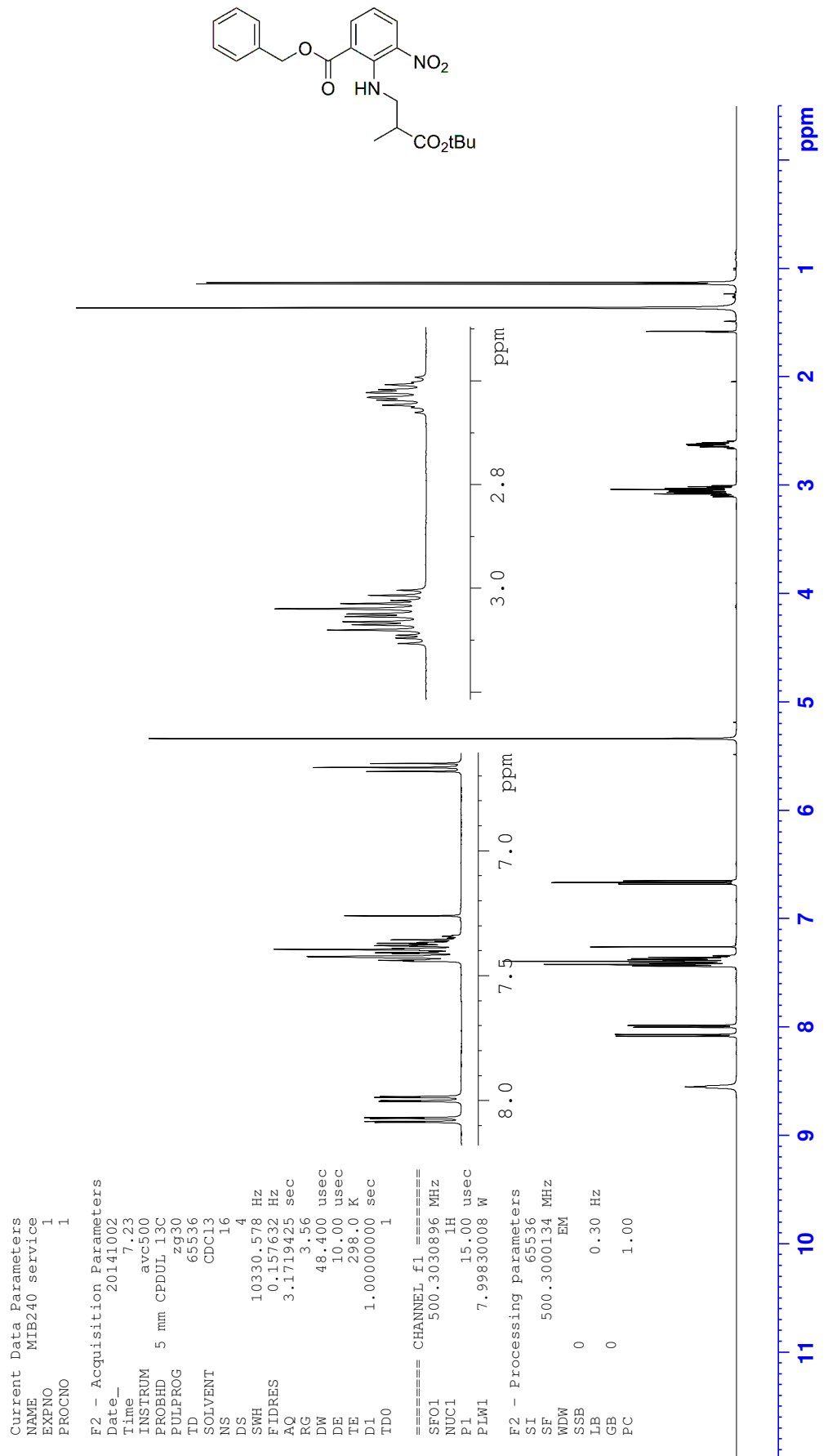
Appendix F: NMR spectra

^1H NMR (*S*)-3-(7-Methoxy-3,4-dihydroquinolin-1(2*H*)-yl)propyl 4-methyl-2-oxo-2,3,4,5-tetrahydro-1*H*-benzo[*b*][1,4]diazepine-6-carboxylate ((*S*)-**26**)



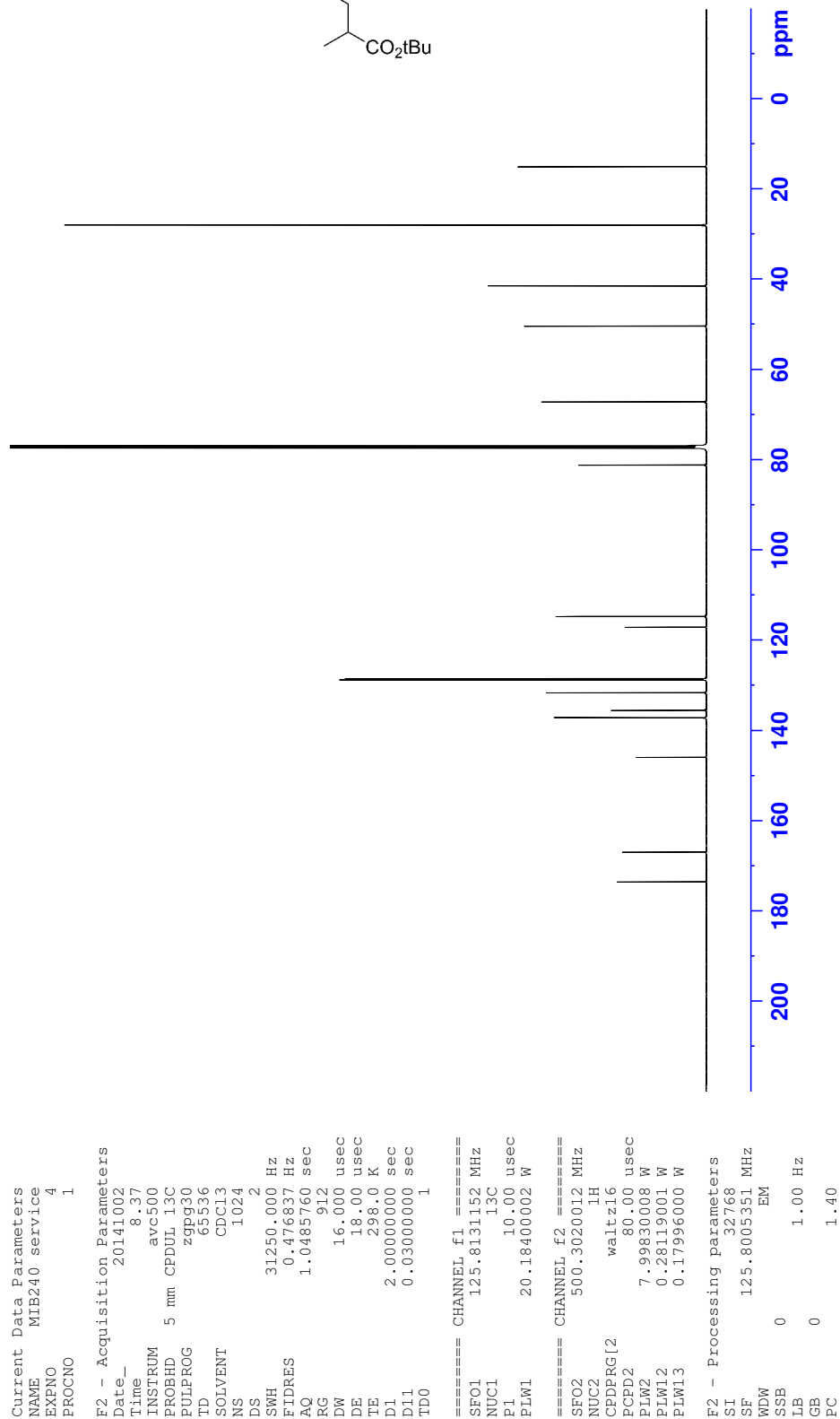
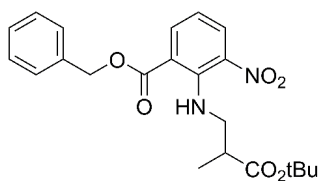
¹H NMR *tert*-Butyl 3-(benzylamino)-2-methylpropanoate (**54**)

^{13}C NMR *tert*-Butyl 3-(benzylamino)-2-methylpropanoate (**54**)

¹H NMR Benzyl 2-(3-*tert*-butoxy-2-methyl-3-oxopropylamino)-3-nitrobenzoate (**56**)

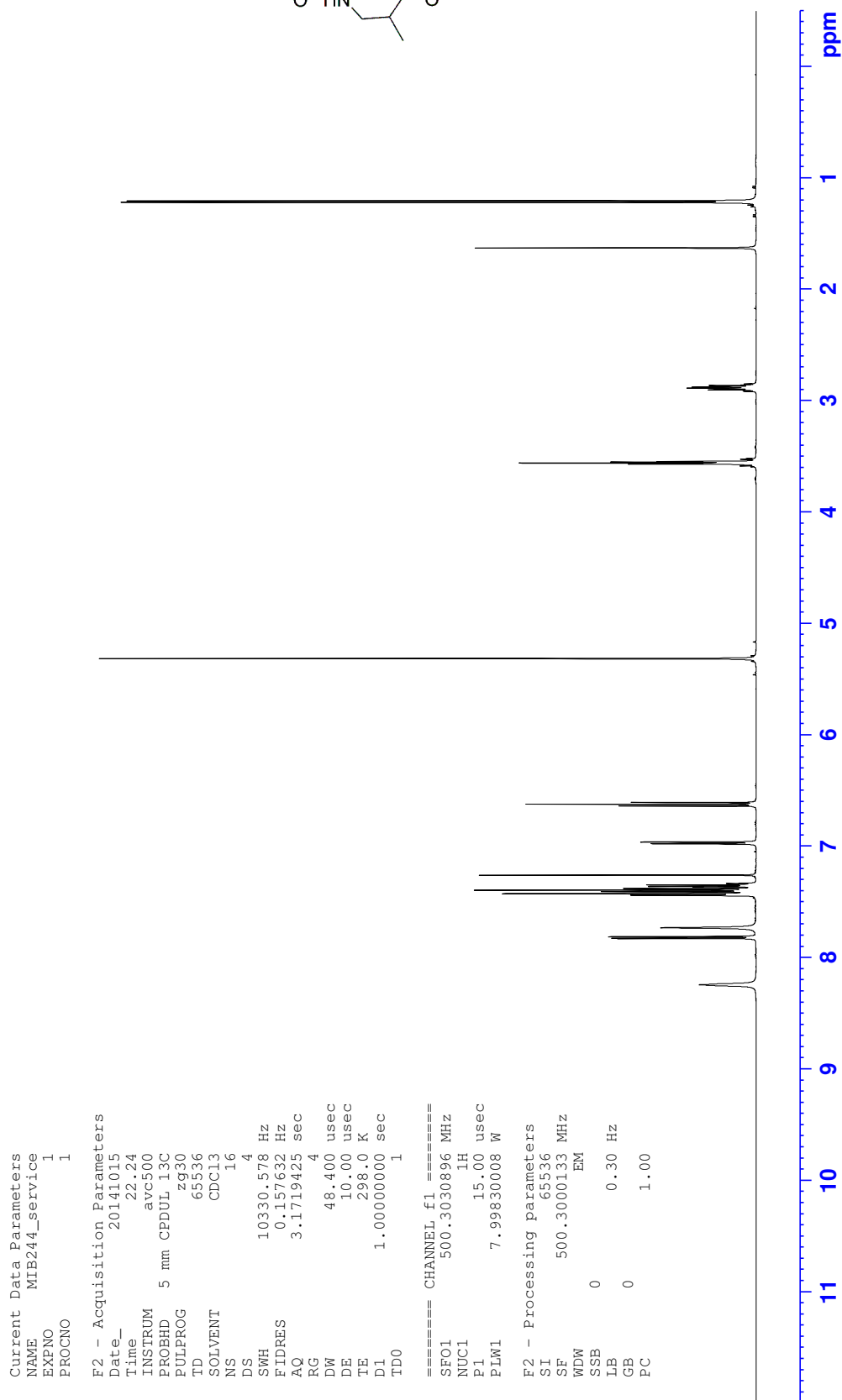
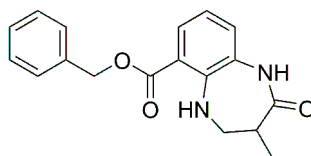
Appendix F: NMR spectra

¹³C NMR Benzyl 2-(3-*tert*-butoxy-2-methyl-3-oxopropylamino)-3-nitrobenzoate (**56**)



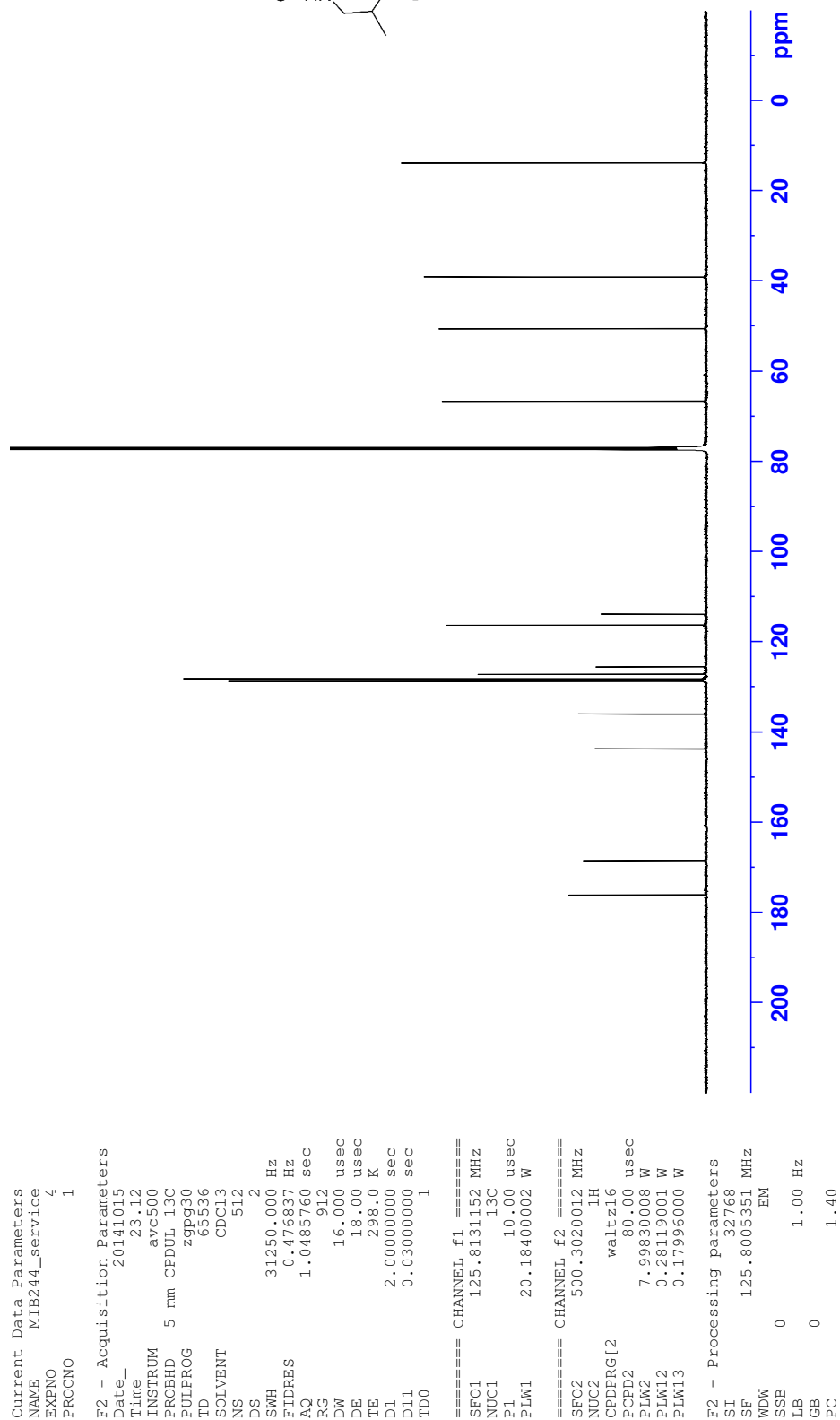
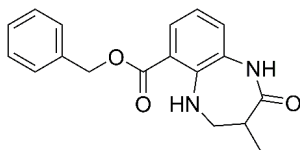
Appendix F: NMR spectra

¹H NMR Benzyl 3-methyl-2-oxo-2,3,4,5-tetrahydro-1H-benzo[b][1,4]diazepine-6-carboxylate (57)



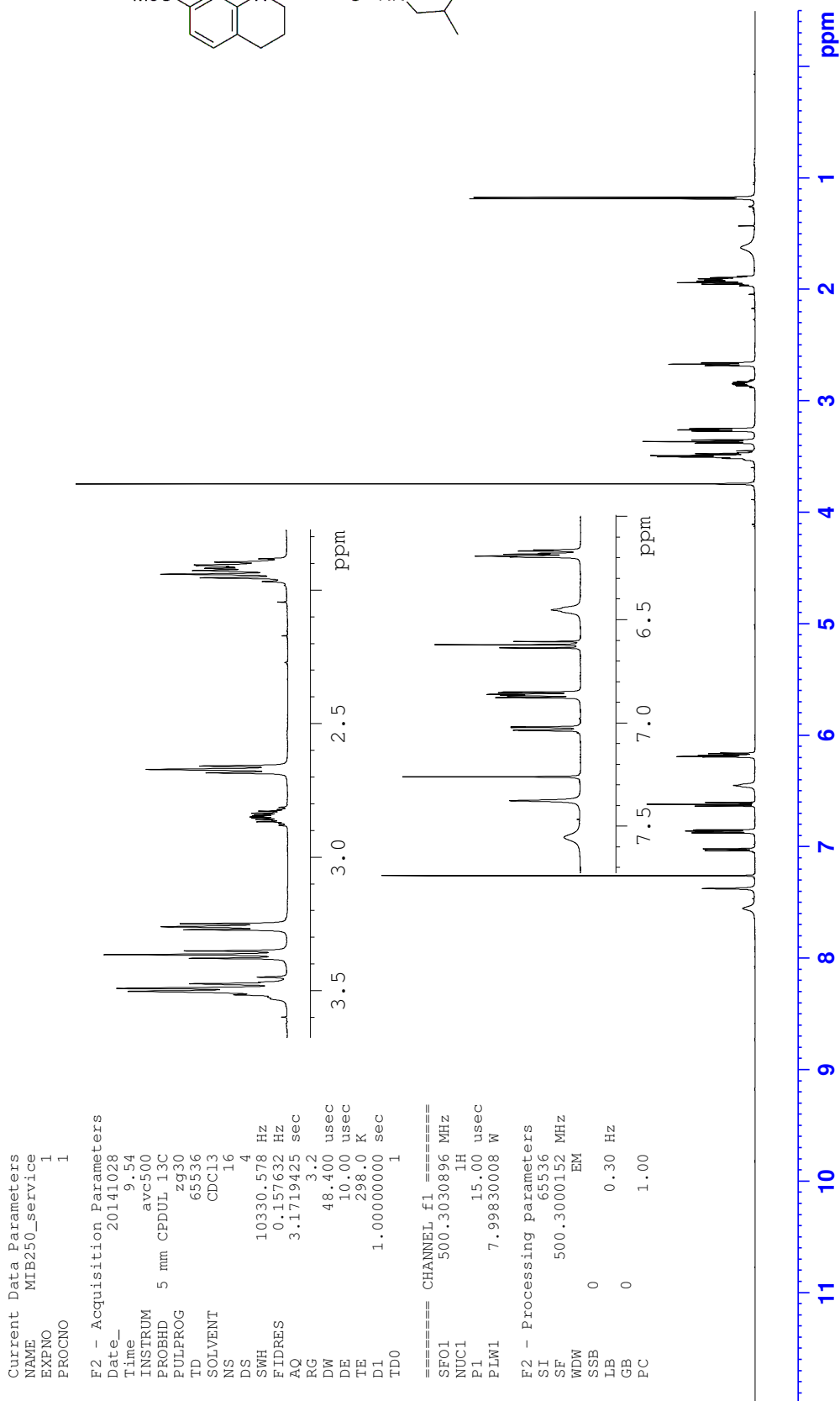
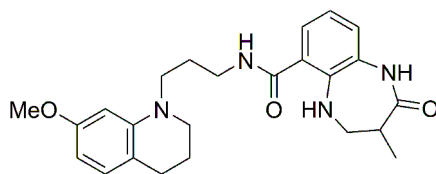
Appendix F: NMR spectra

¹³C NMR Benzyl 3-methyl-2-oxo-2,3,4,5-tetrahydro-1H-benzo[b][1,4]diazepine-6-carboxylate (57)



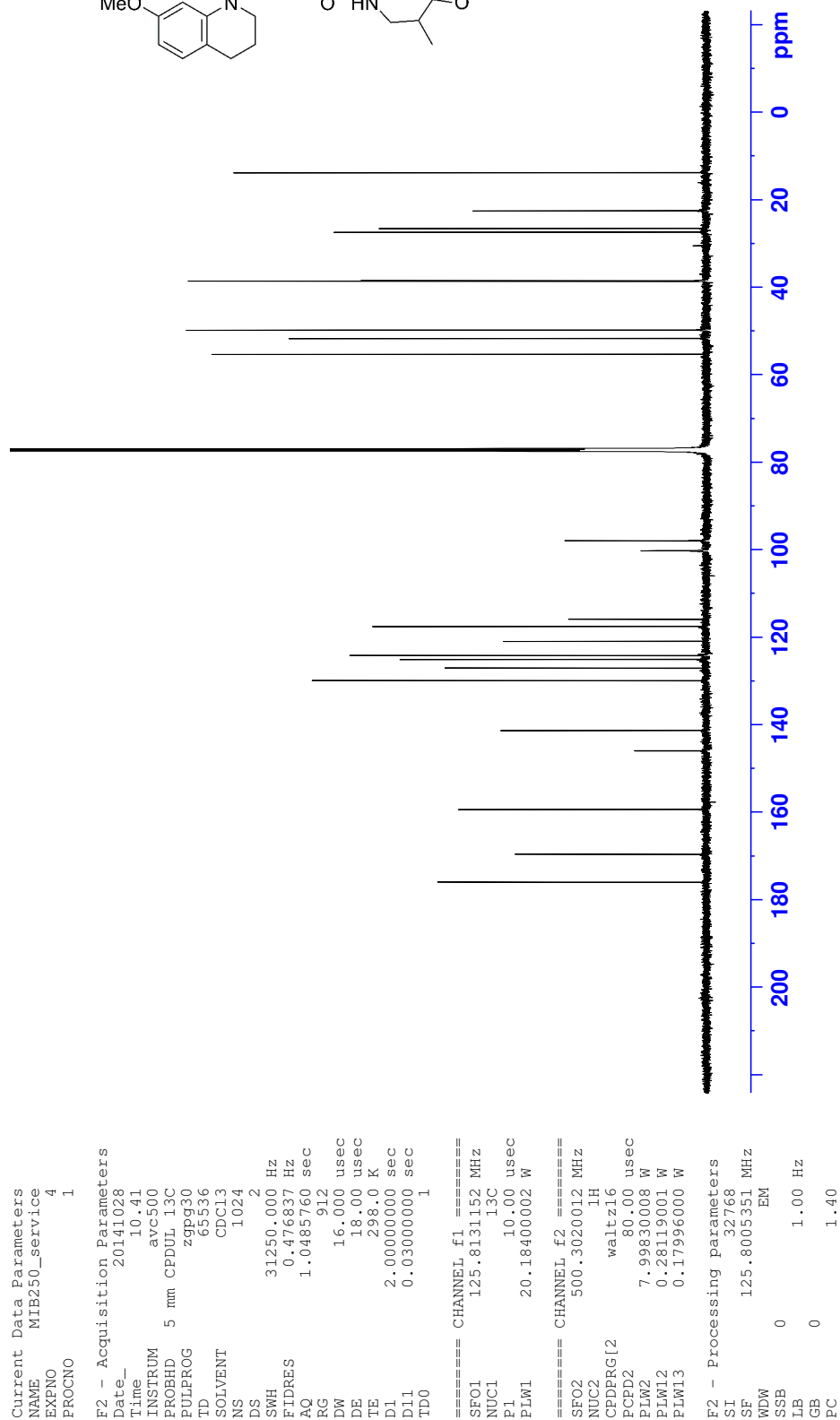
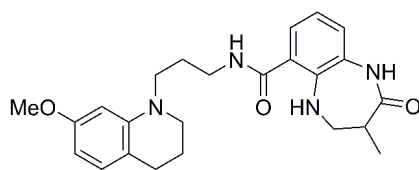
Appendix F: NMR spectra

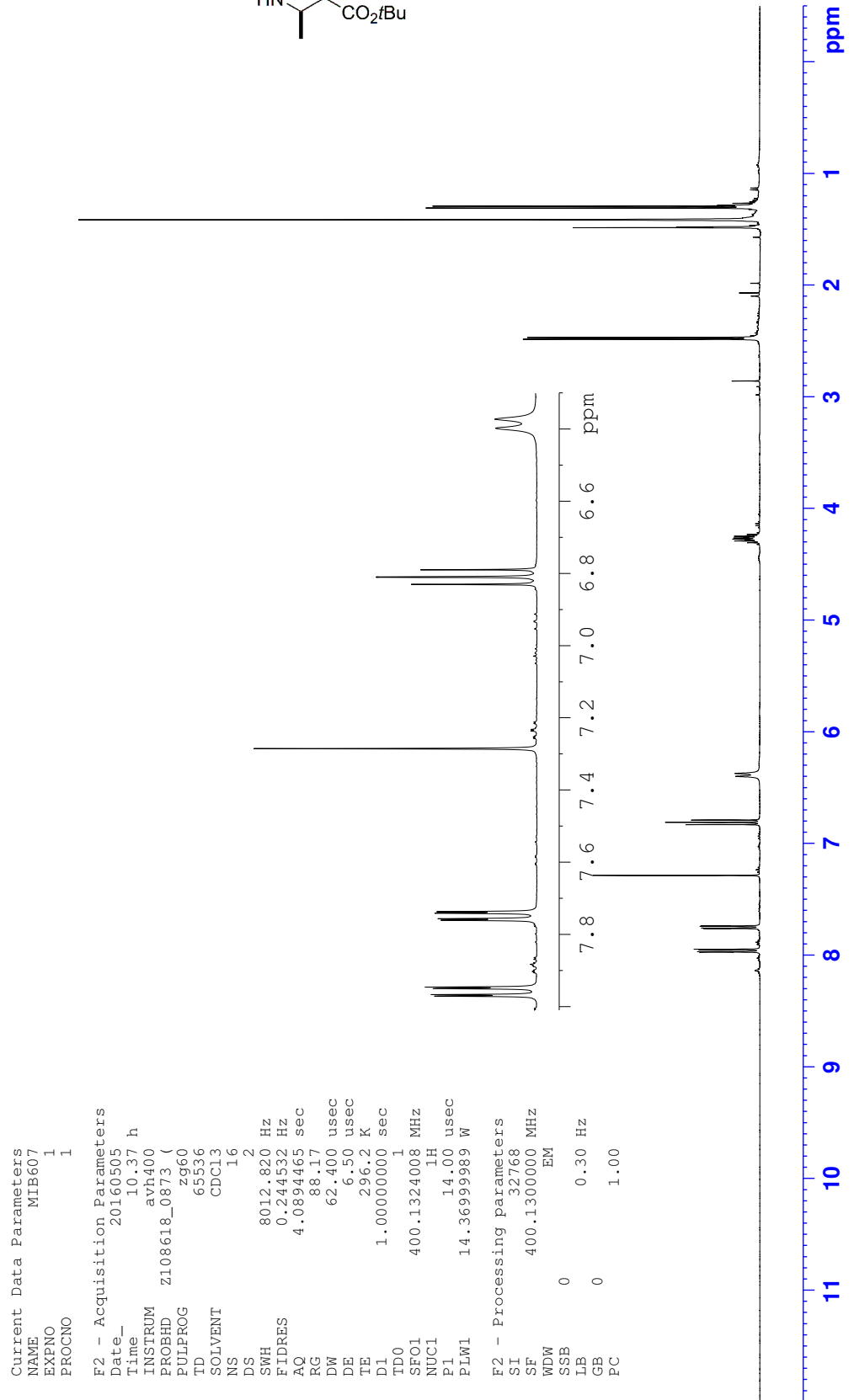
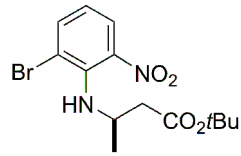
¹H NMR *N*-(3-(7-Methoxy-3,4-dihydroquinolin-1(2*H*)-yl)propyl)-3-methyl-2-oxo-2,3,4,5-tetrahydro-1*H*-benzo[*b*][1,4]diazepine-6-carboxamide (**27**)



Appendix F: NMR spectra

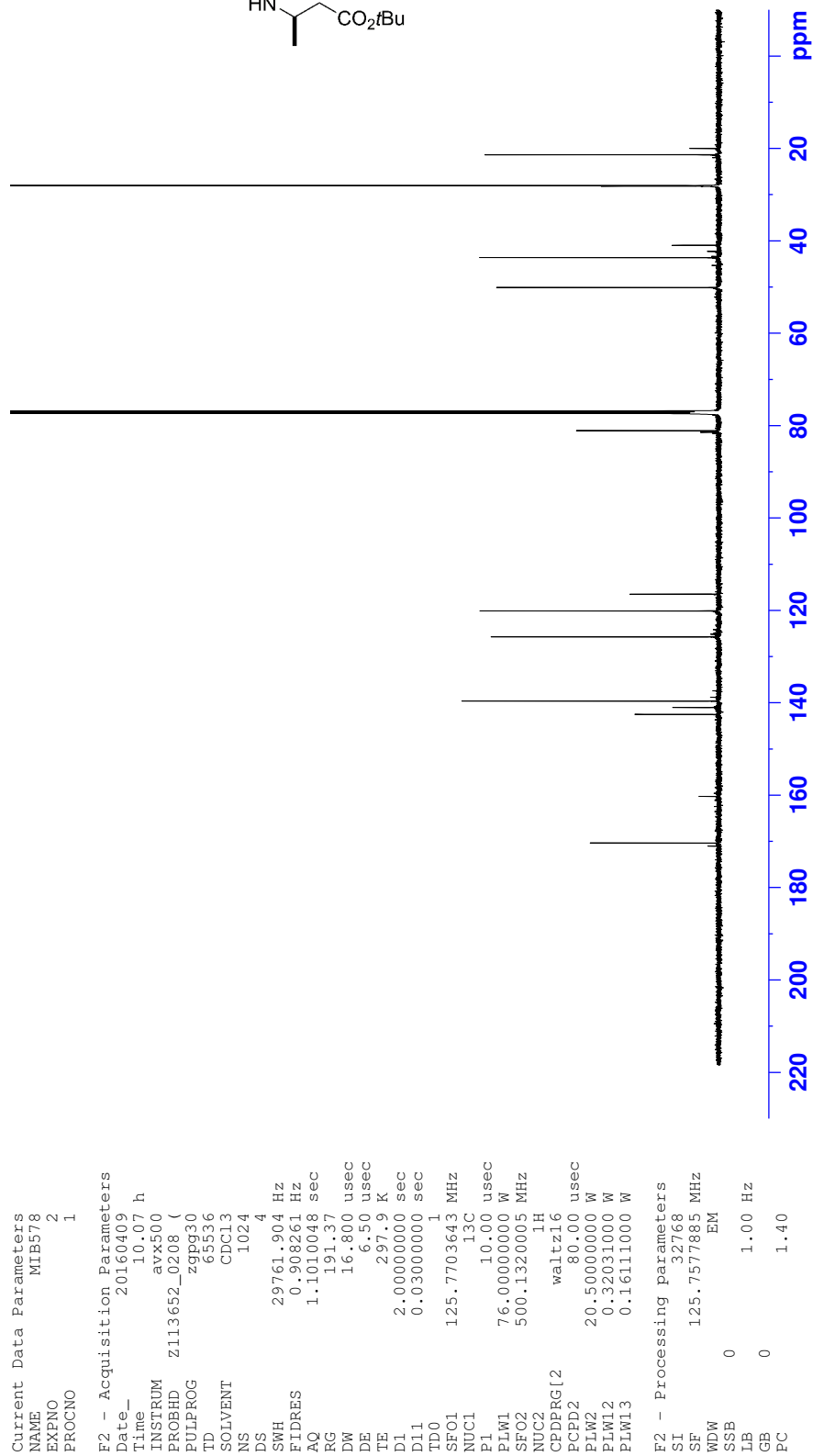
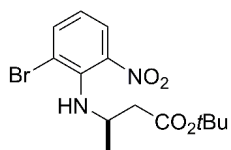
¹³C NMR *N*-(3-(7-Methoxy-3,4-dihydroquinolin-1(2*H*)-yl)propyl)-3-methyl-2-oxo-2,3,4,5-tetrahydro-1*H*-benzo[*b*][1,4]diazepine-6-carboxamide (**27**)



^1H NMR *tert*-Butyl (*R*)-3-((2-bromo-6-nitrophenyl)amino)butanoate ((*R*)-**57**)

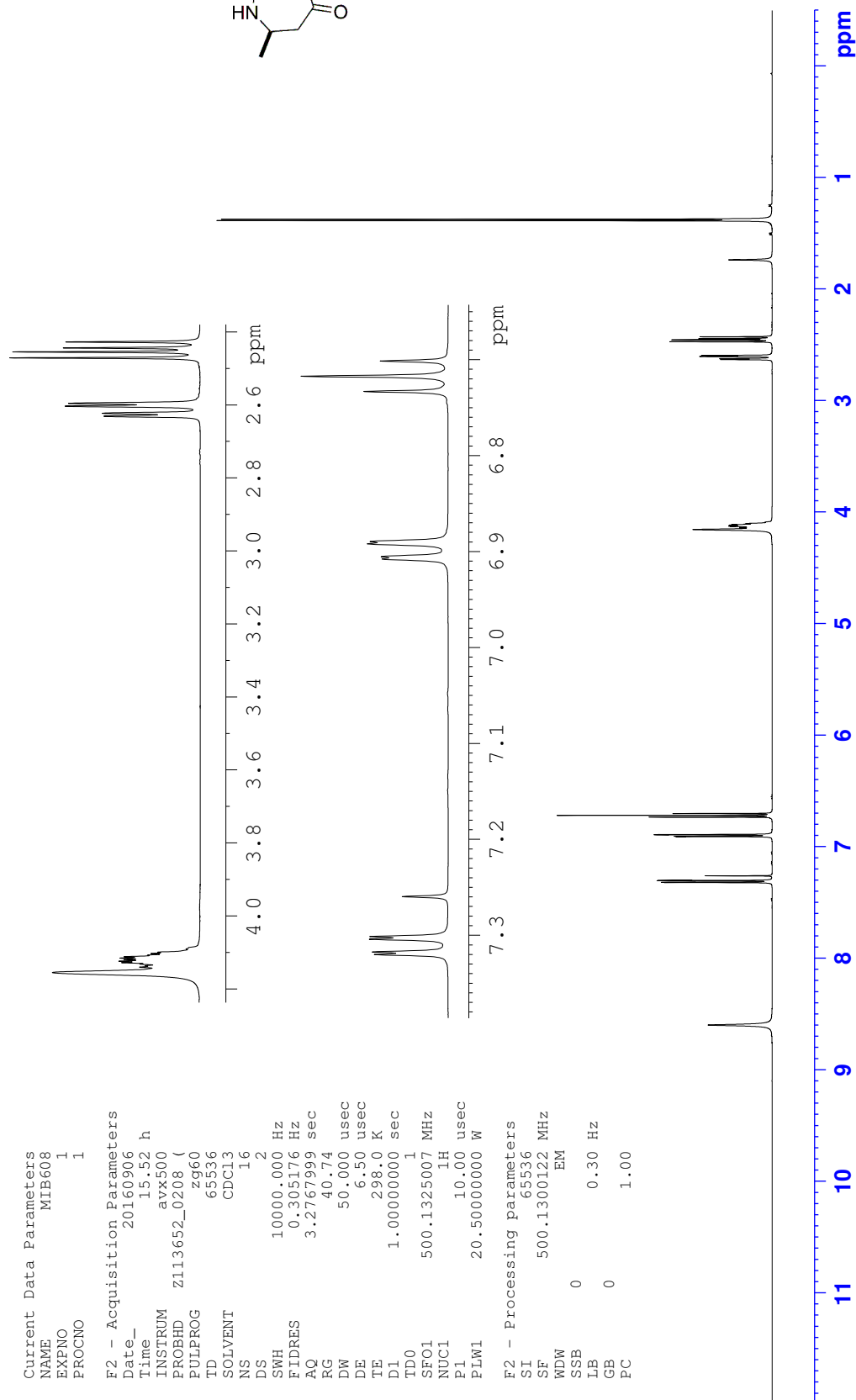
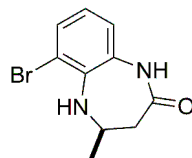
Appendix F: NMR spectra

¹³C NMR *tert*-Butyl (*R*)-3-((2-bromo-6-nitrophenyl)amino)butanoate ((*R*)-57)



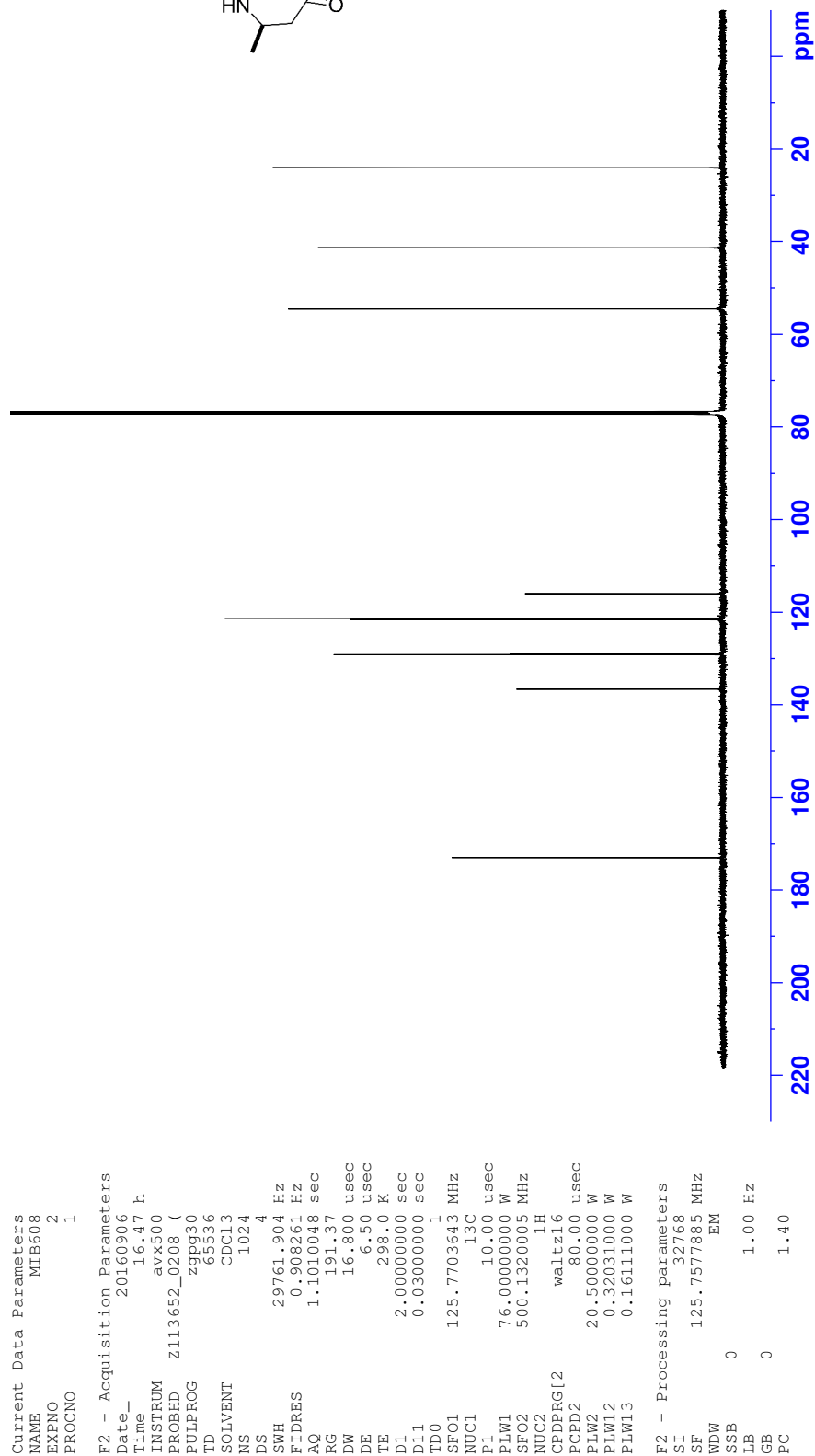
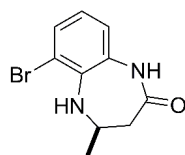
Appendix F: NMR spectra

^1H NMR (*R*)-6-Bromo-4-methyl-1,3,4,5-tetrahydro-2*H*-benzo[*b*][1,4]diazepin-2-one ((*R*)-**58**)



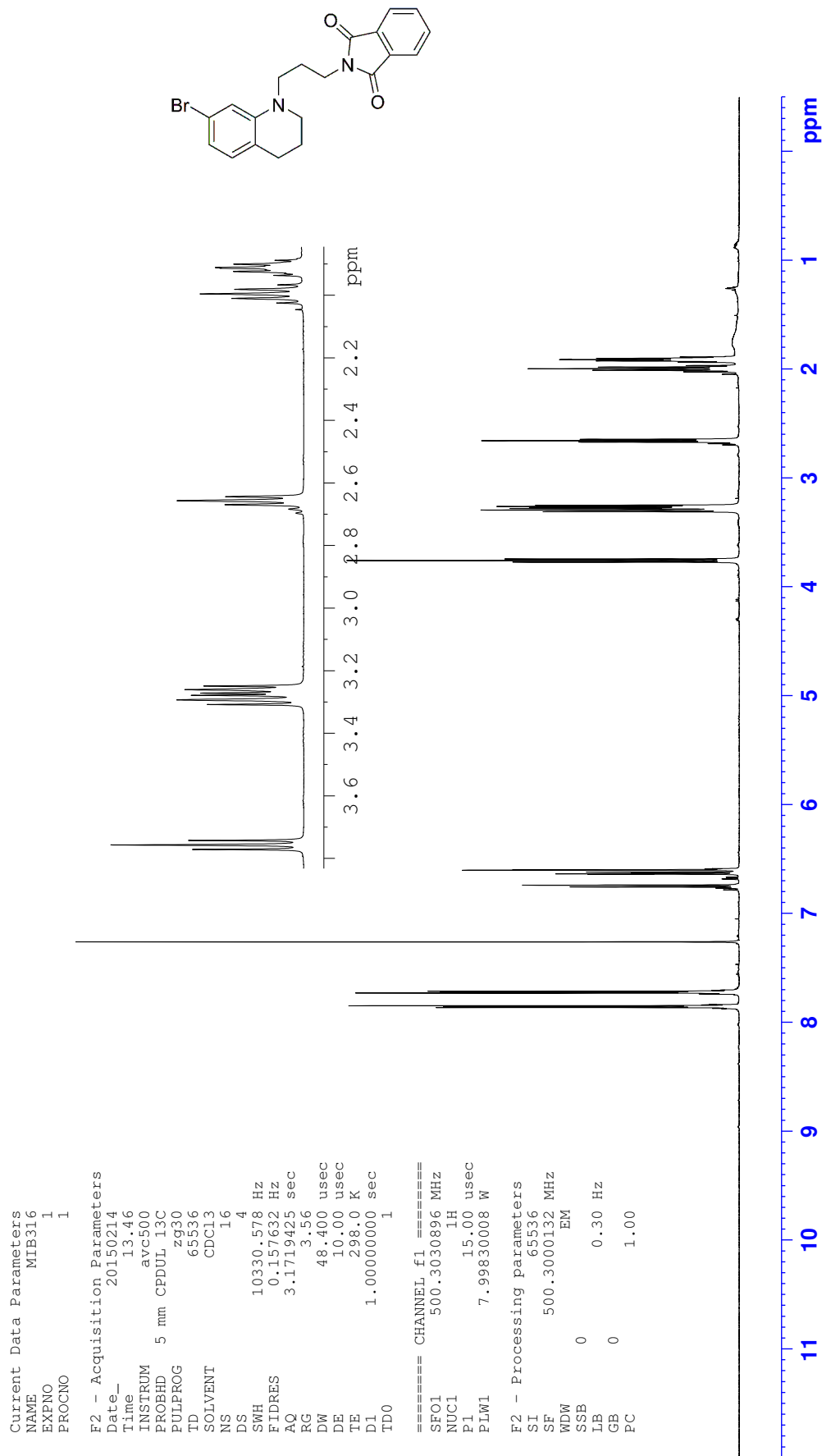
Appendix F: NMR spectra

¹³C NMR (*R*)-6-Bromo-4-methyl-1,3,4,5-tetrahydro-2*H*-benzo[*b*][1,4]diazepin-2-one ((*R*)-58)



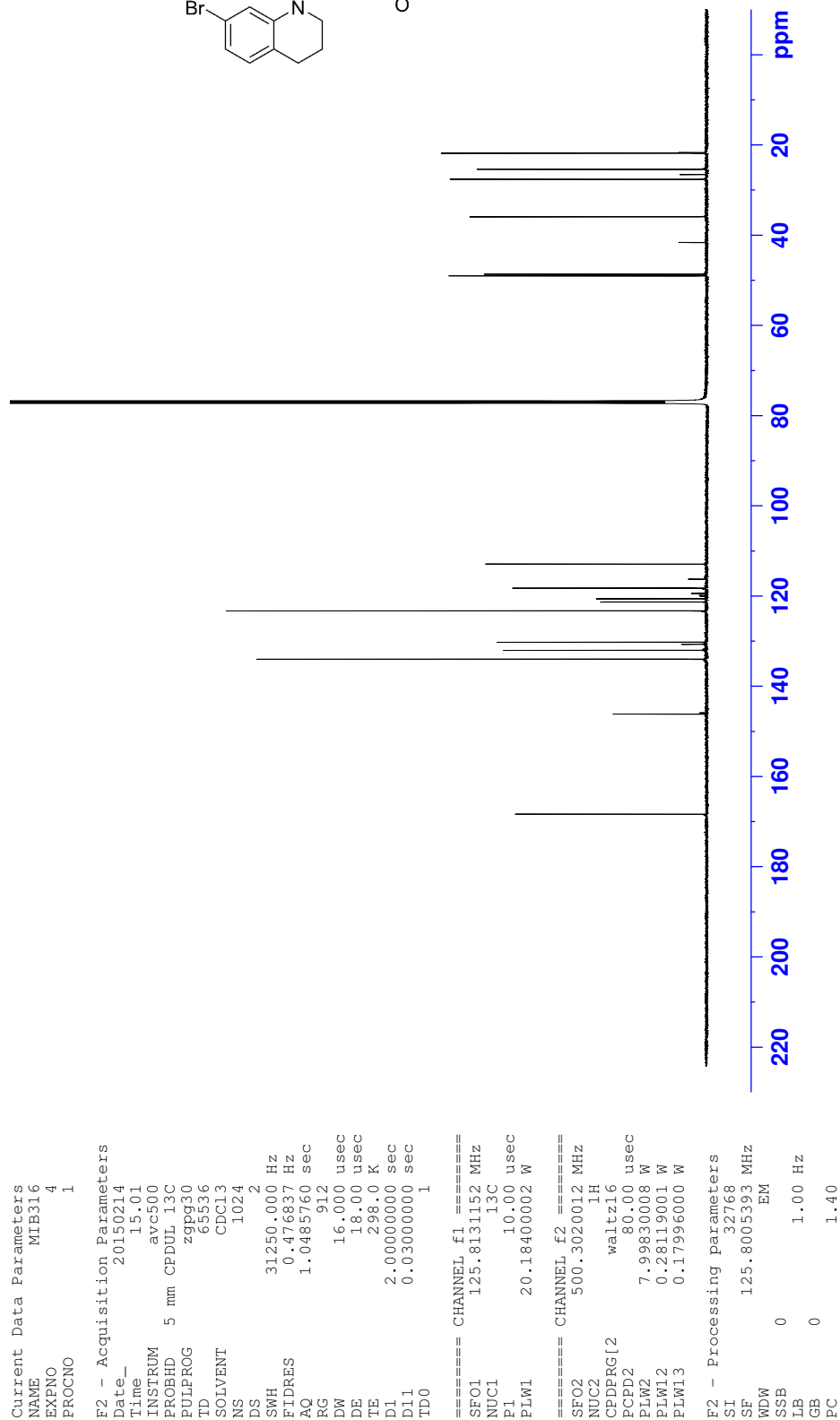
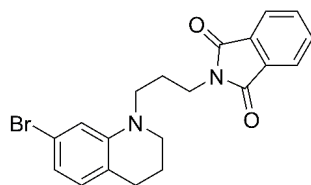
Appendix F: NMR spectra

¹H NMR 2-(3-(7-Bromo-3,4-dihydroquinolin-1(2*H*)-yl)propyl)isoindoline-1,3-dione (77)



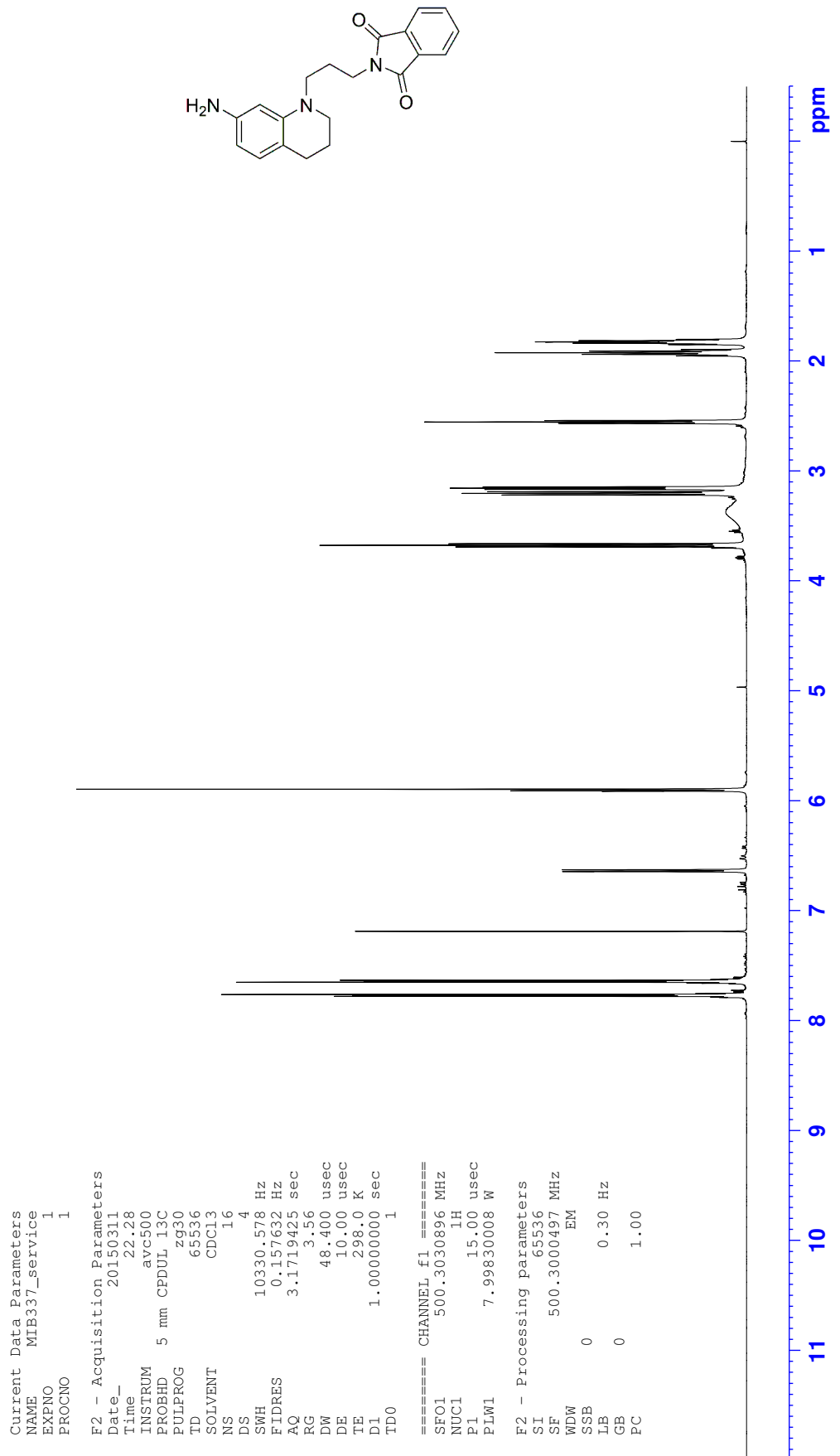
Appendix F: NMR spectra

^{13}C NMR 2-(3-(7-Bromo-3,4-dihydroquinolin-1(2*H*)-yl)propyl)isoindolin-1,3-dione (77)



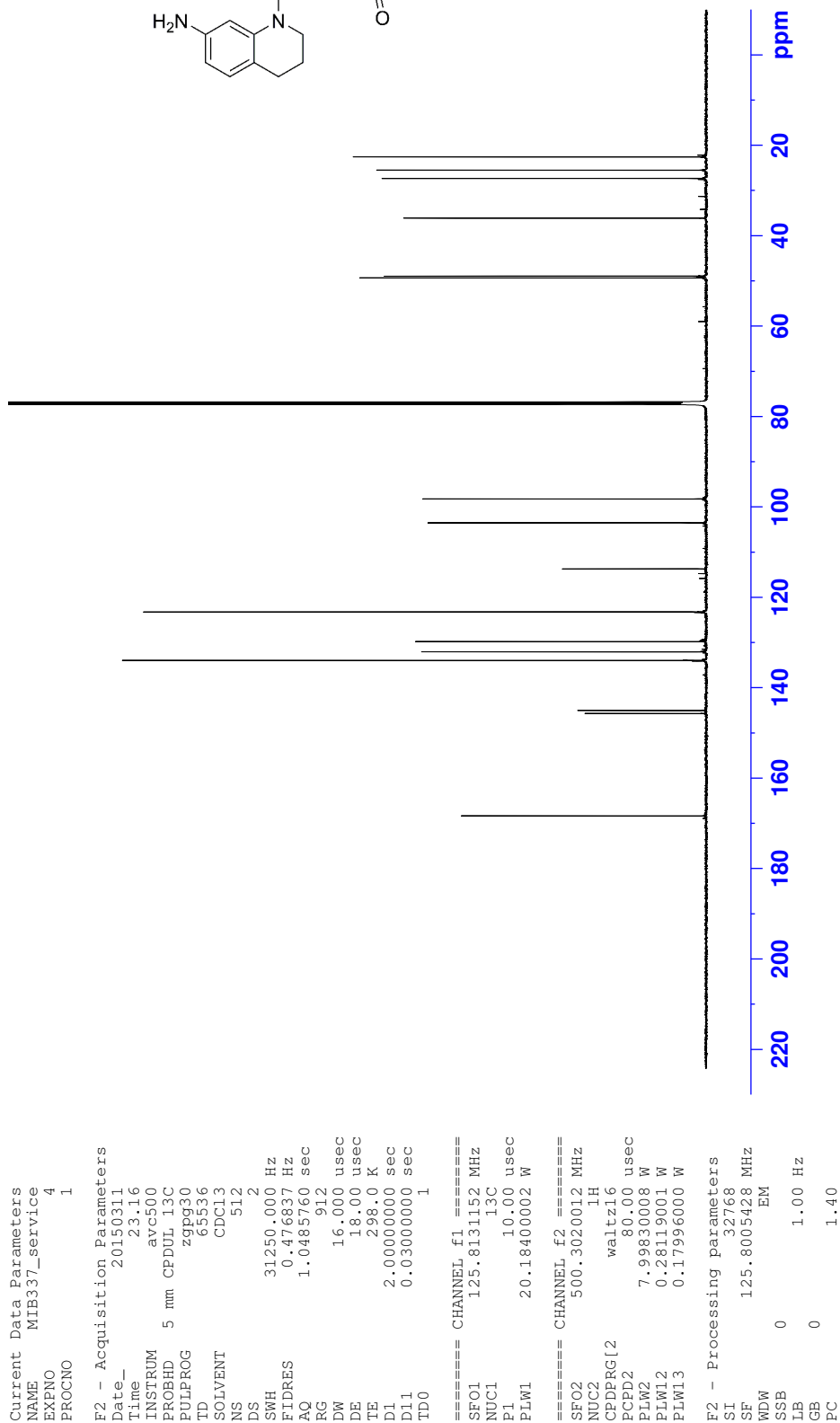
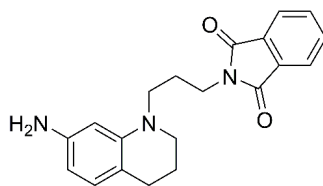
Appendix F: NMR spectra

¹H NMR 2-(3-(7-Amino-3,4-dihydroquinolin-1(2*H*)-yl)propyl)isoindoline-1,3-dione (**78**)



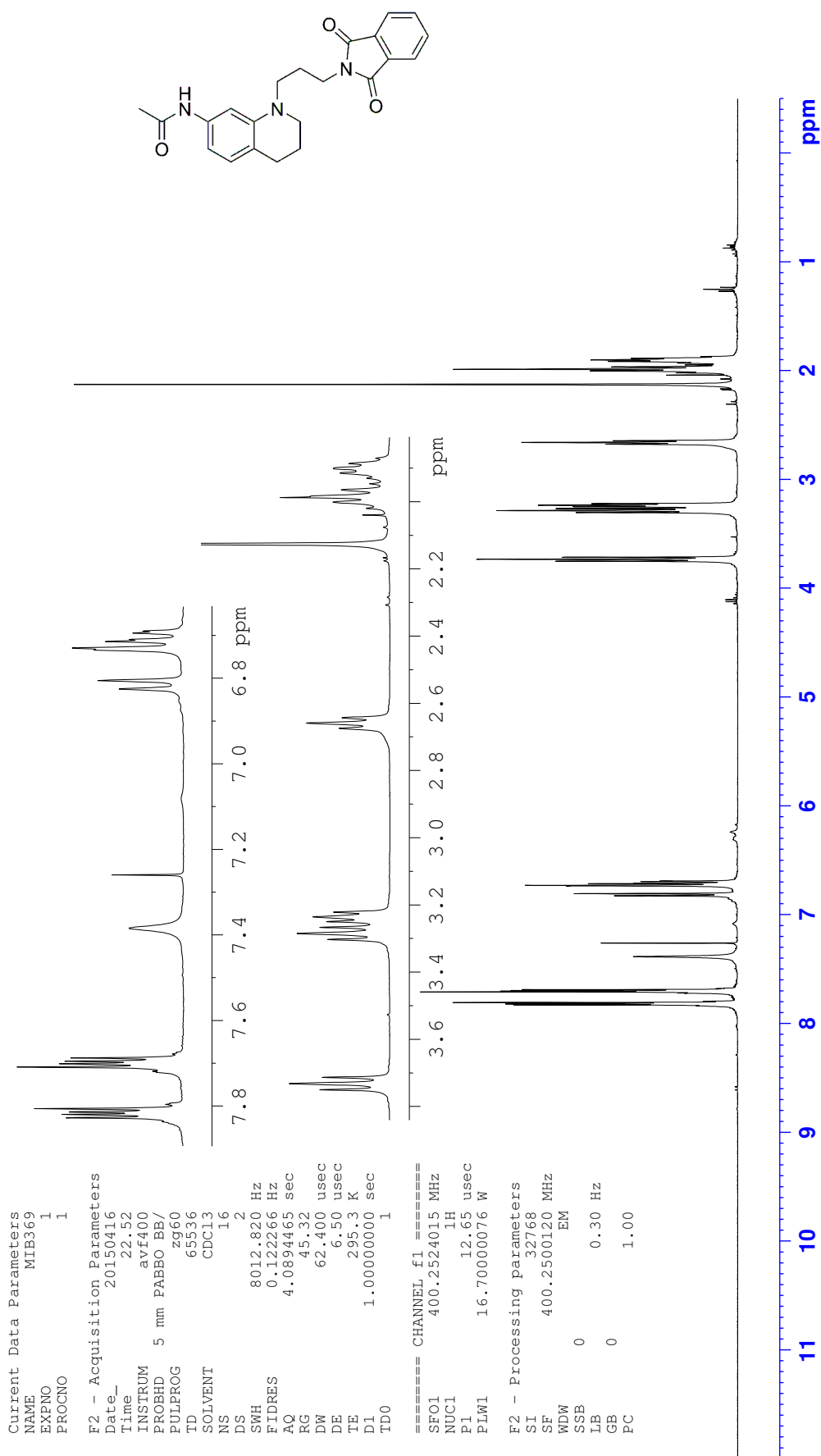
Appendix F: NMR spectra

¹³C NMR 2-(3-(7-Amino-3,4-dihydroquinolin-1(2*H*)-yl)propyl)isoindoline-1,3-dione (78)



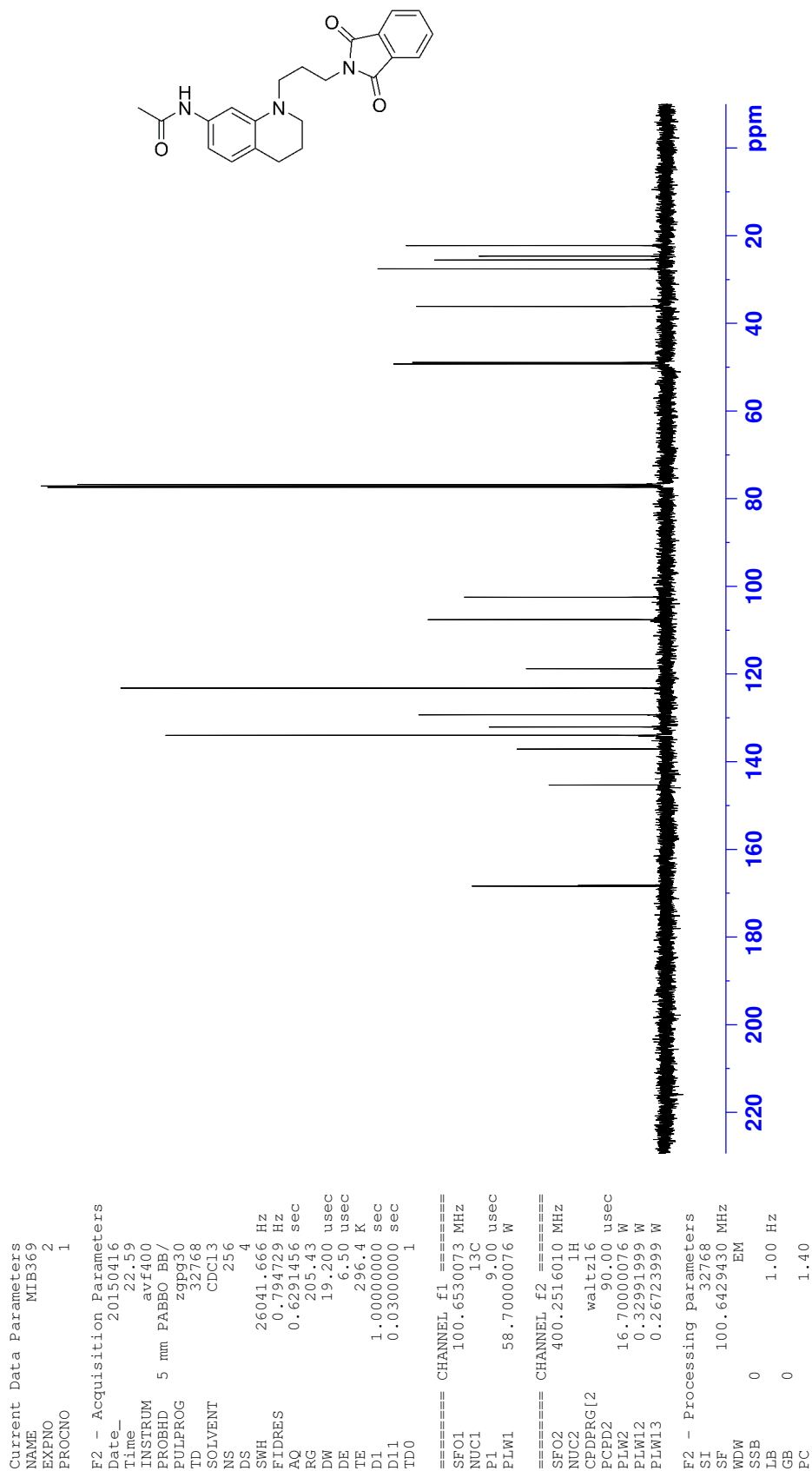
Appendix F: NMR spectra

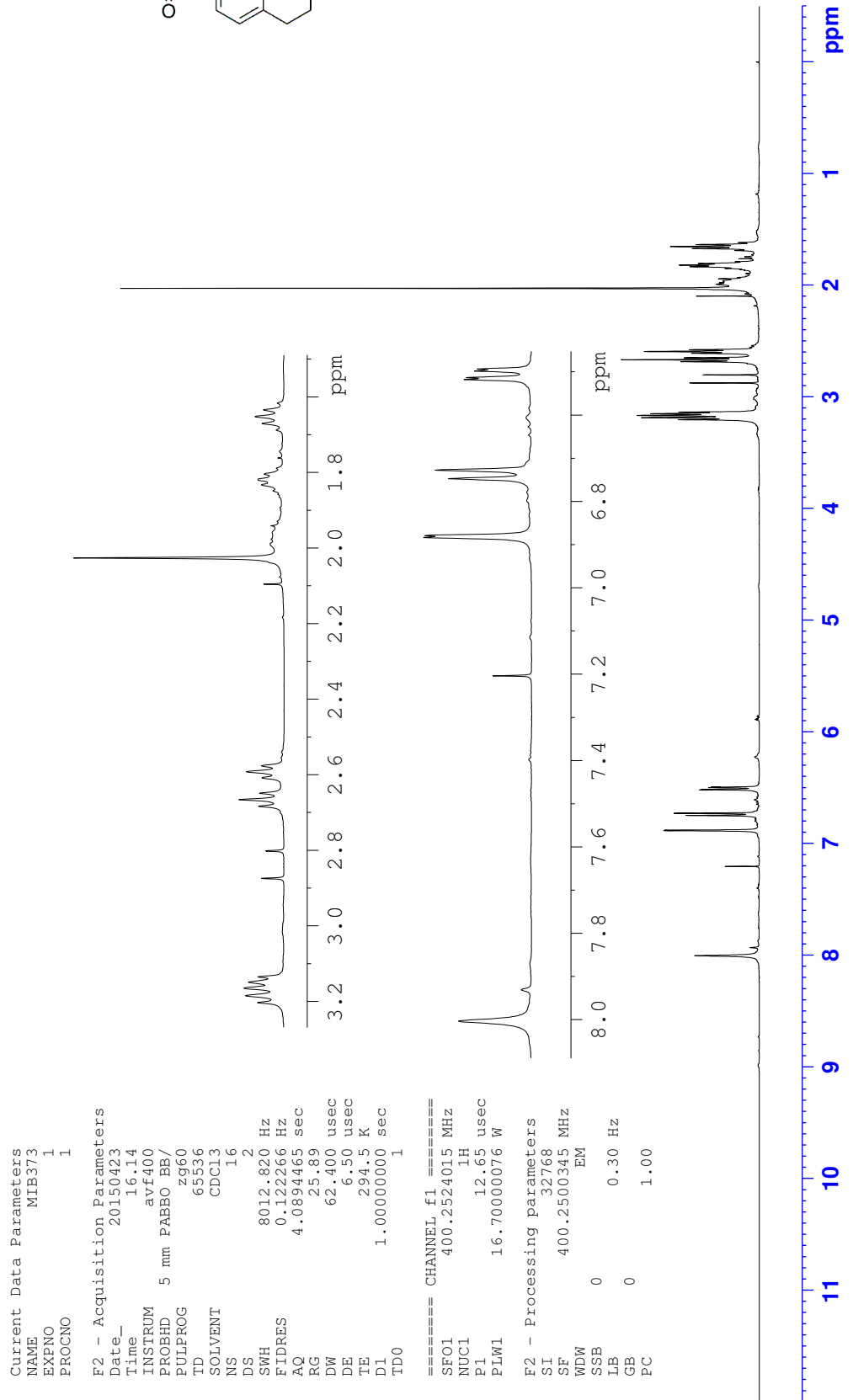
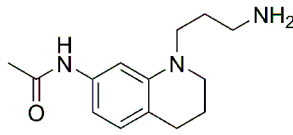
¹H NMR *N*-(1-(3-(1,3-dioxisoindolin-2-yl)propyl)-1,2,3,4-tetrahydroquinolin-7-yl)acetamide (79)



Appendix F: NMR spectra

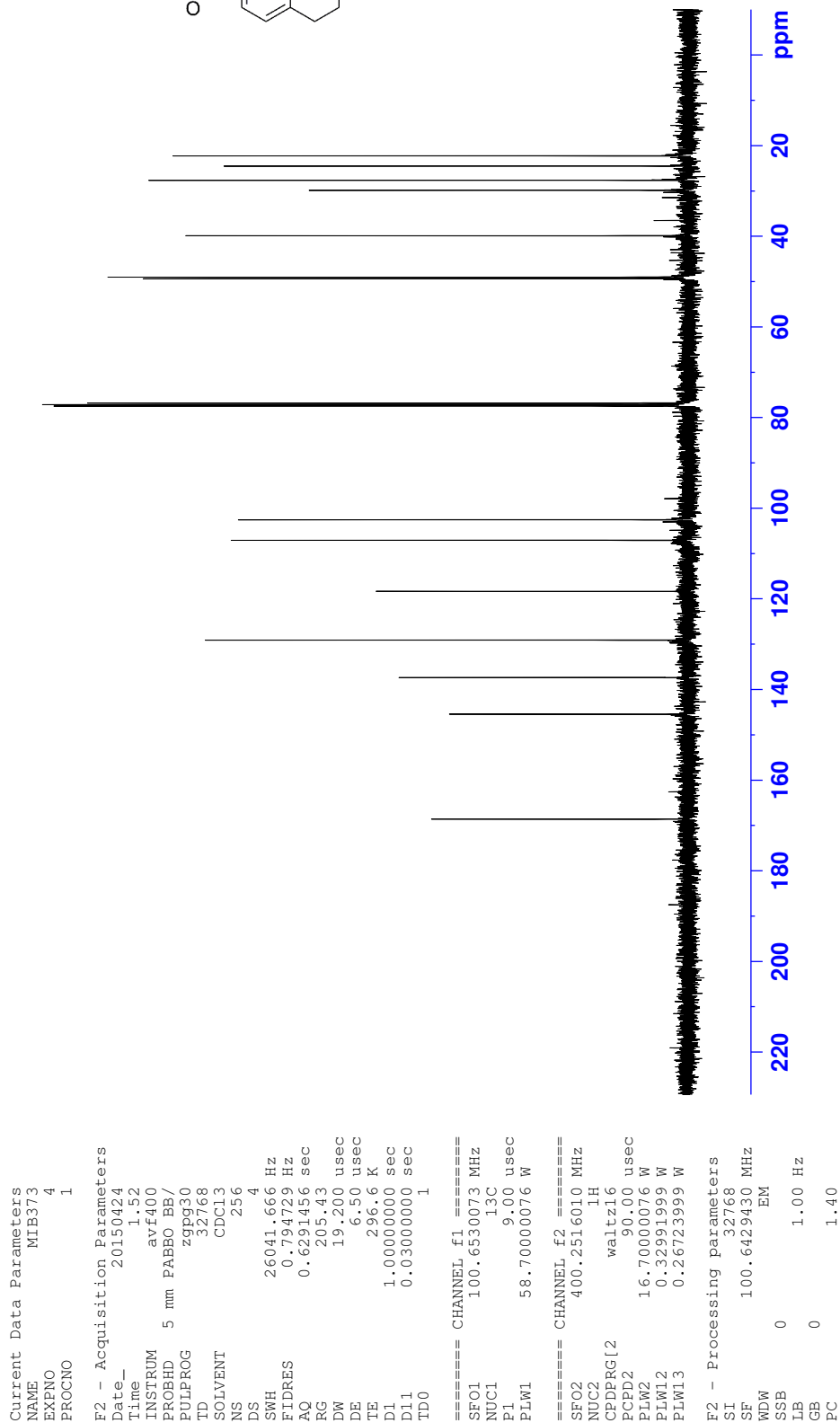
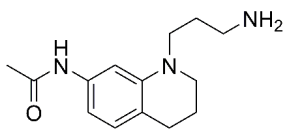
¹³C NMR *N*-(1-(3-(1,3-dioxisoindolin-2-yl)propyl)-1,2,3,4-tetrahydroquinolin-7-yl)acetamide (79)



¹H NMR *N*-(1-(3-aminopropyl)-1,2,3,4-tetrahydroquinolin-7-yl)acetamide (**85**)

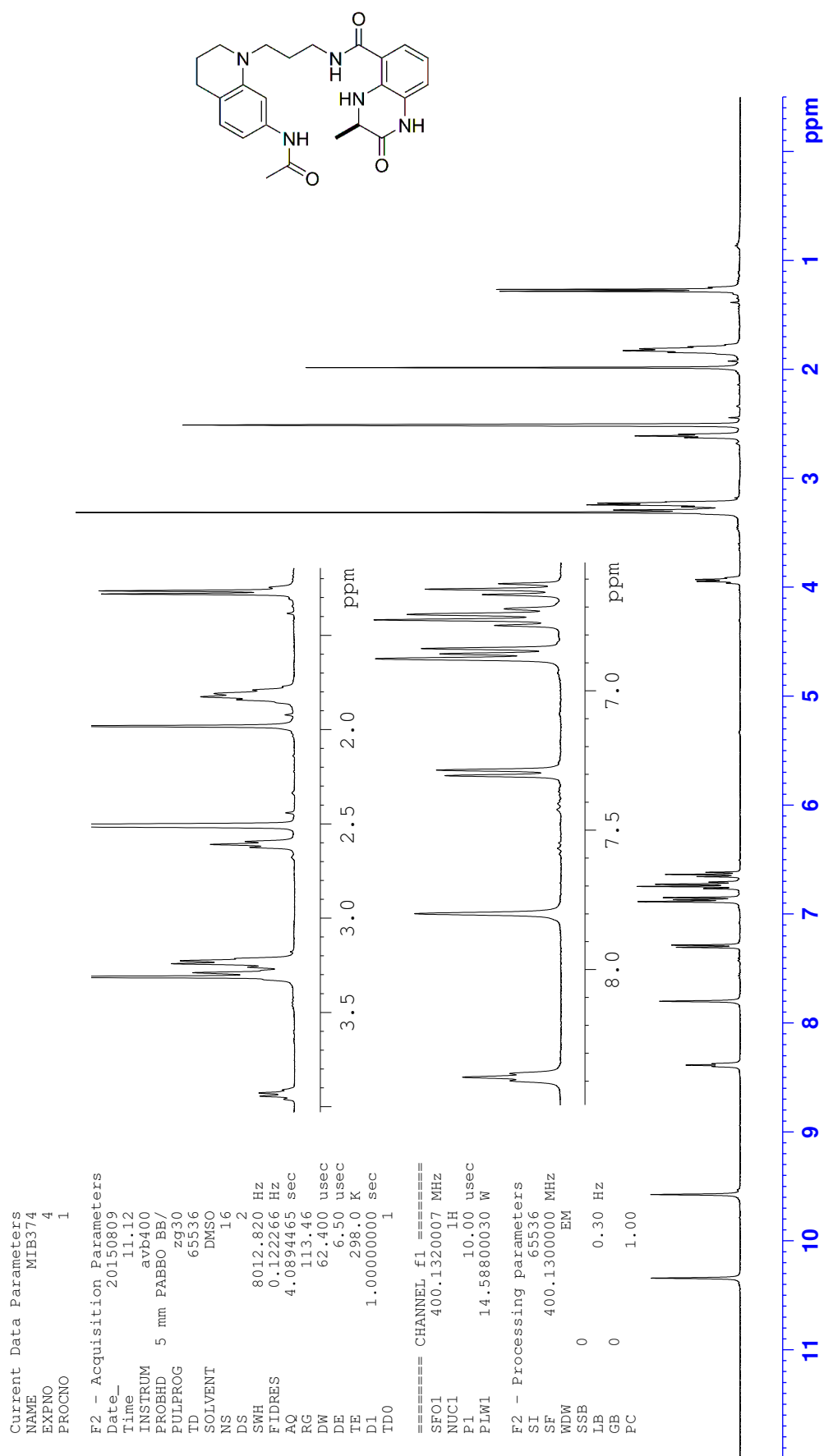
Appendix F: NMR spectra

¹³C NMR *N*-(1-(3-aminopropyl)-1,2,3,4-tetrahydroquinolin-7-yl)acetamide (85)



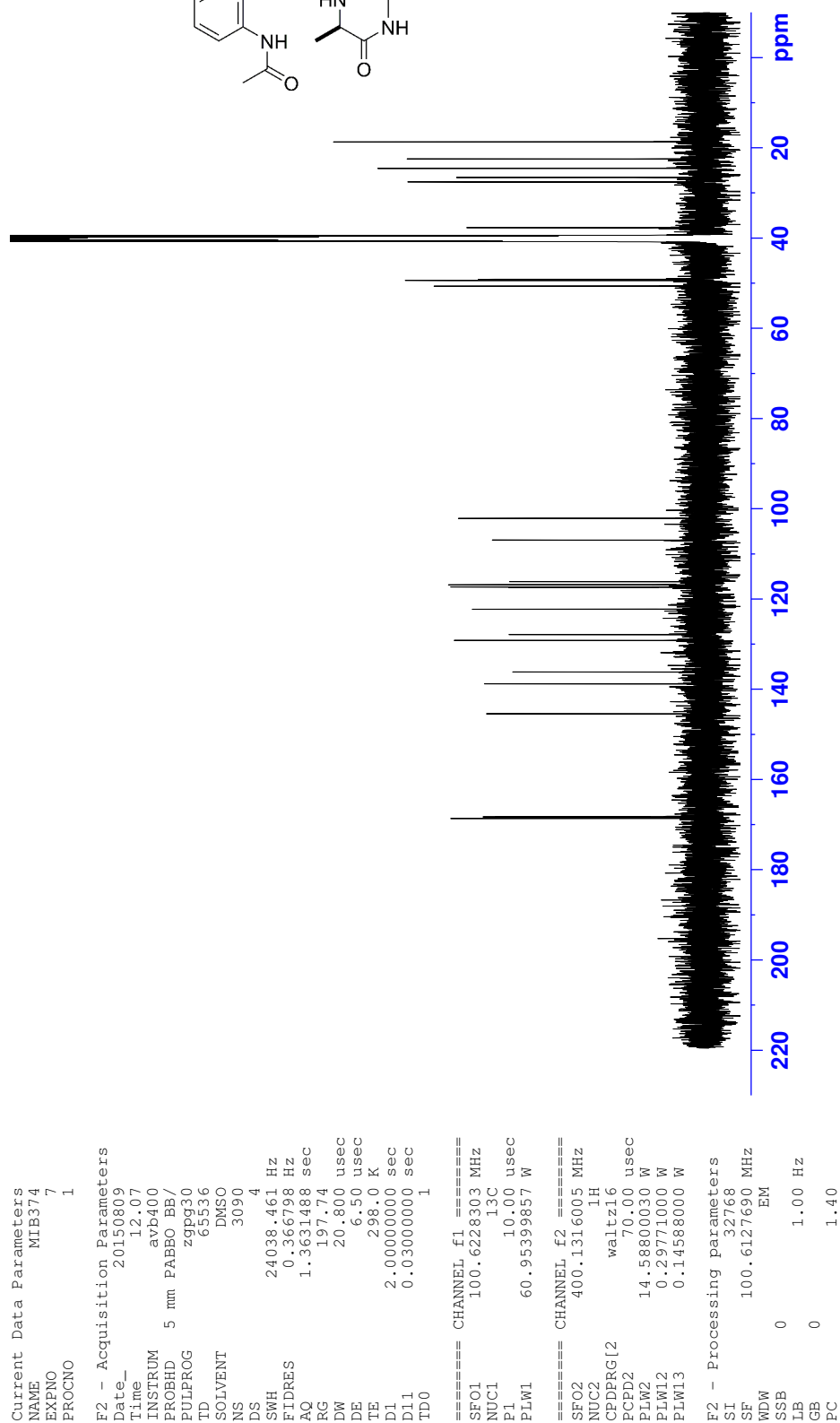
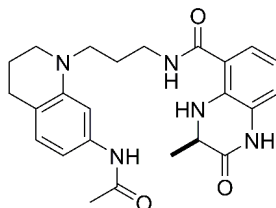
Appendix F: NMR spectra

^1H NMR (*R*)-*N*-(3-(7-Acetamido-3,4-dihydroquinolin-1(2*H*)-yl)propyl)-3-methyl-2-oxo-1,2,3,4-tetrahydroquinoxaline-5-carboxamide (**88**)



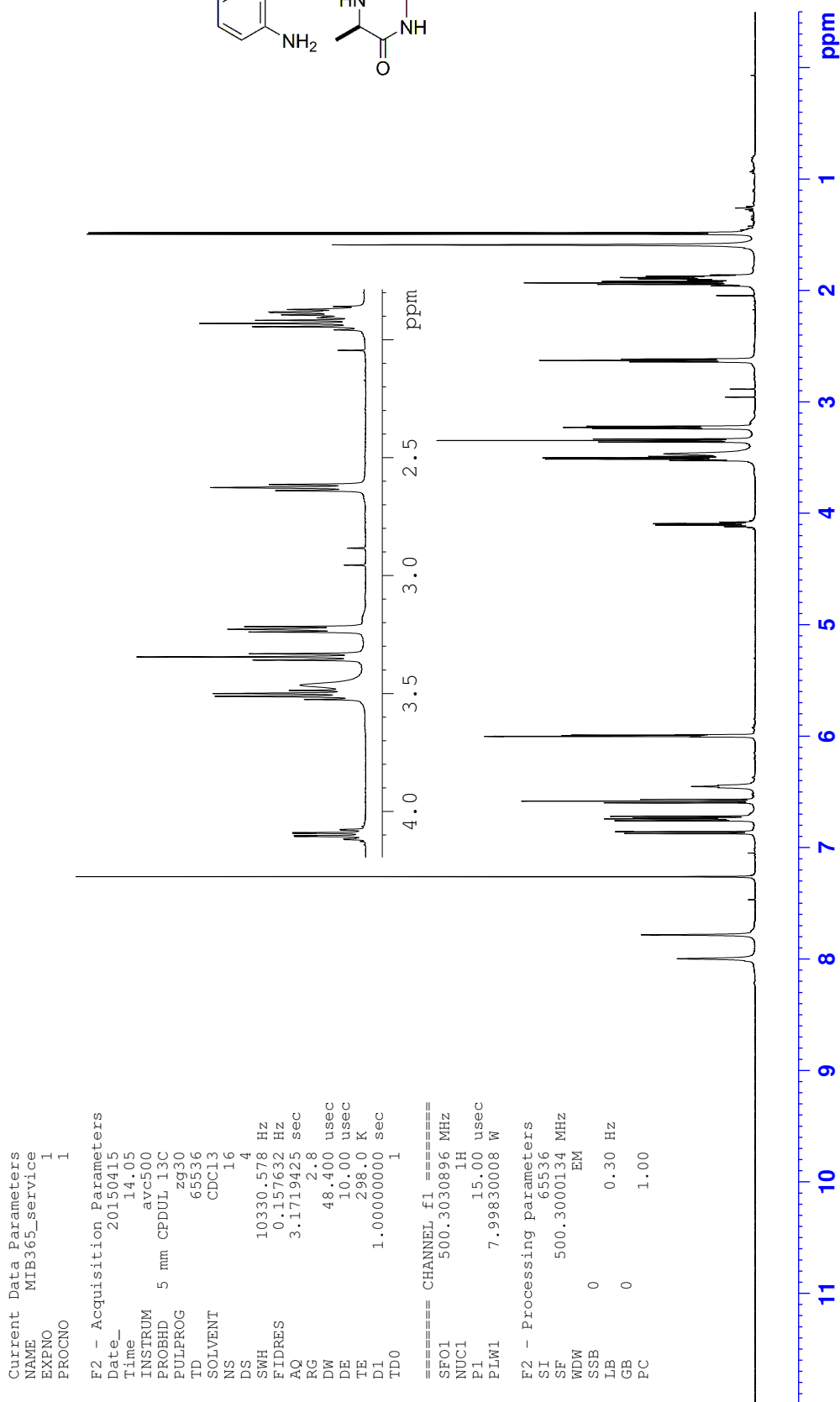
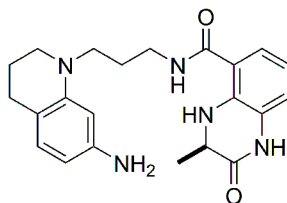
Appendix F: NMR spectra

¹³C NMR (*R*)-*N*-(3-(7-Acetamido-3,4-dihydroquinolin-1(2*H*)-yl)propyl)-3-methyl-2-oxo-1,2,3,4-tetrahydroquinoxaline-5-carboxamide (**88**)



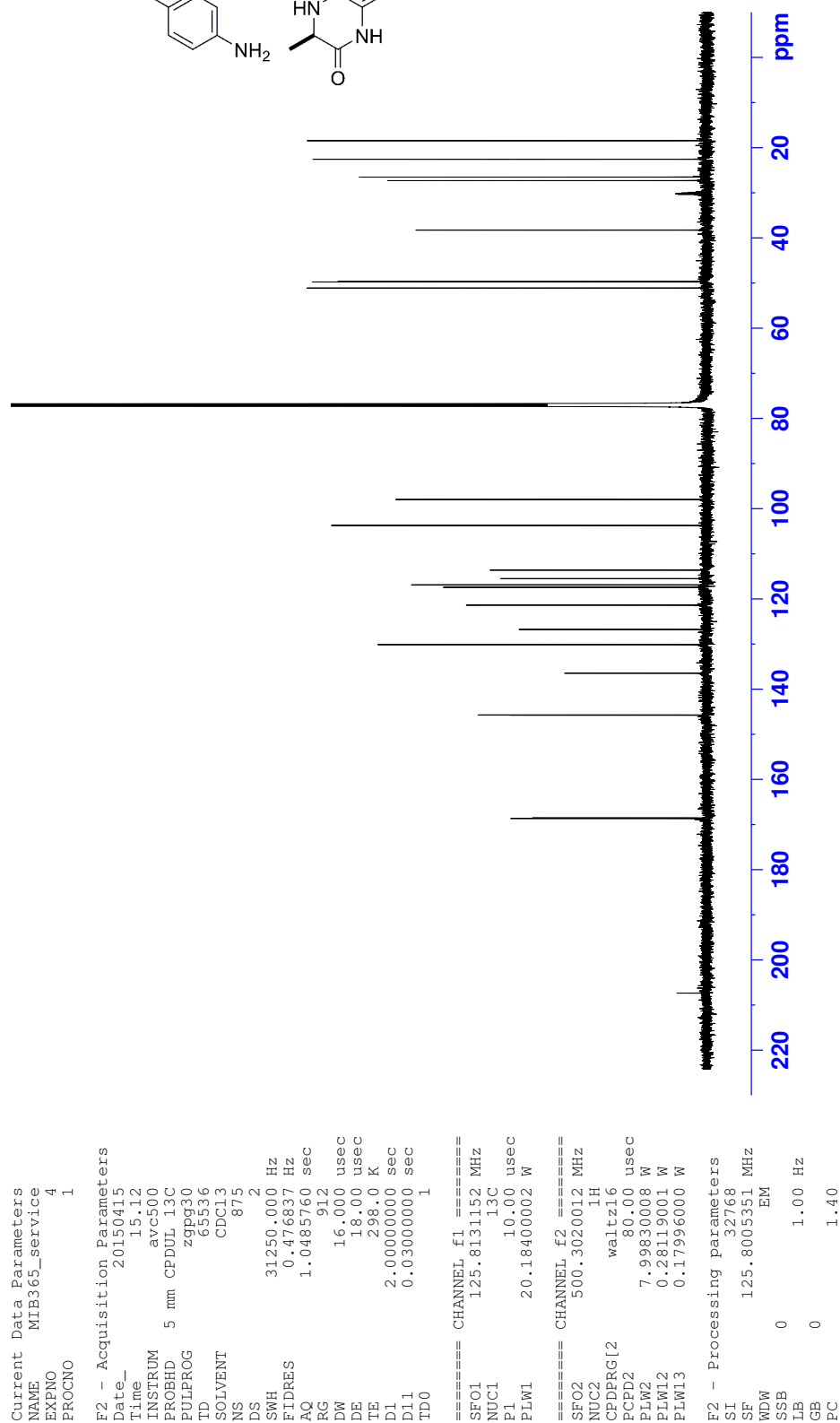
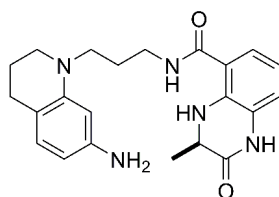
Appendix F: NMR spectra

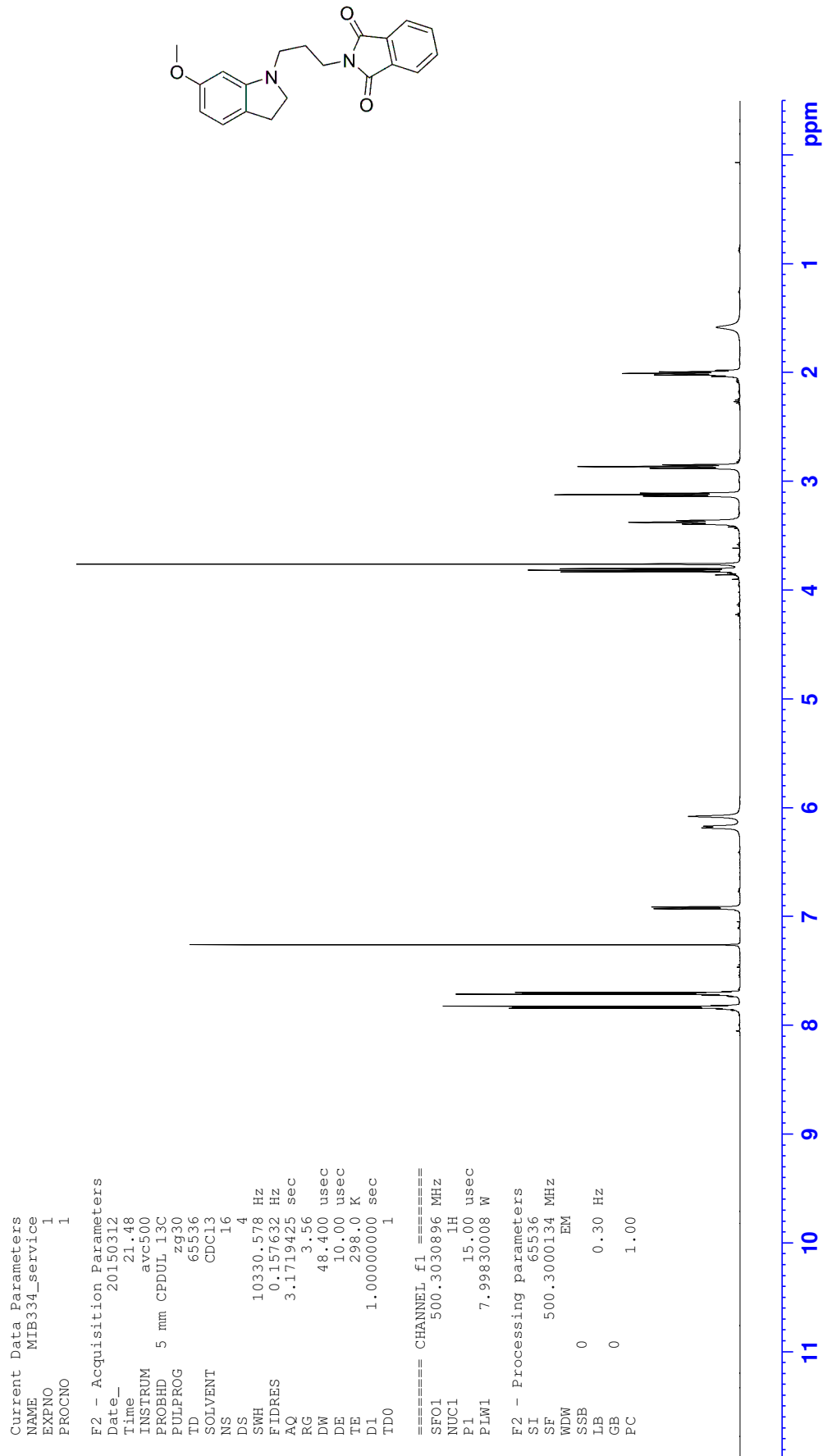
¹H NMR (*R*)-*N*-(3-(7-Amino-3,4-dihydroquinolin-1(2*H*)-yl)propyl)-3-methyl-2-oxo-1,2,3,4-tetrahydroquinoxaline-5-carboxamide (**89**)



Appendix F: NMR spectra

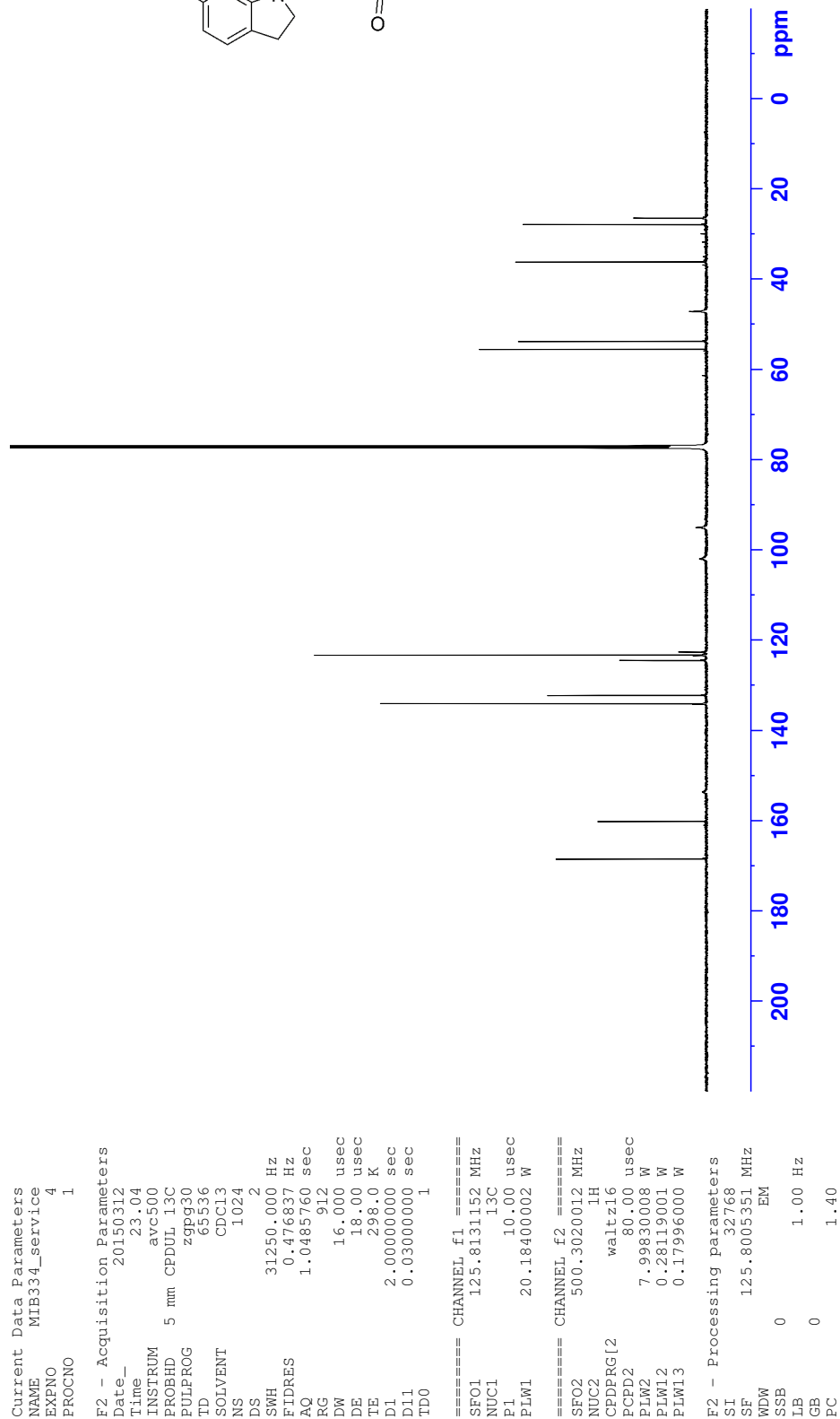
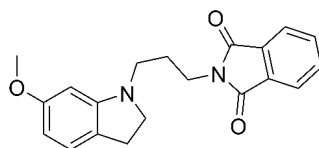
^{13}C NMR (*R*)-*N*-(3-(7-Amino-3,4-dihydroquinolin-1(2*H*)-yl)propyl)-3-methyl-2-oxo-1,2,3,4-tetrahydroquinoxaline-5-carboxamide (**89**)

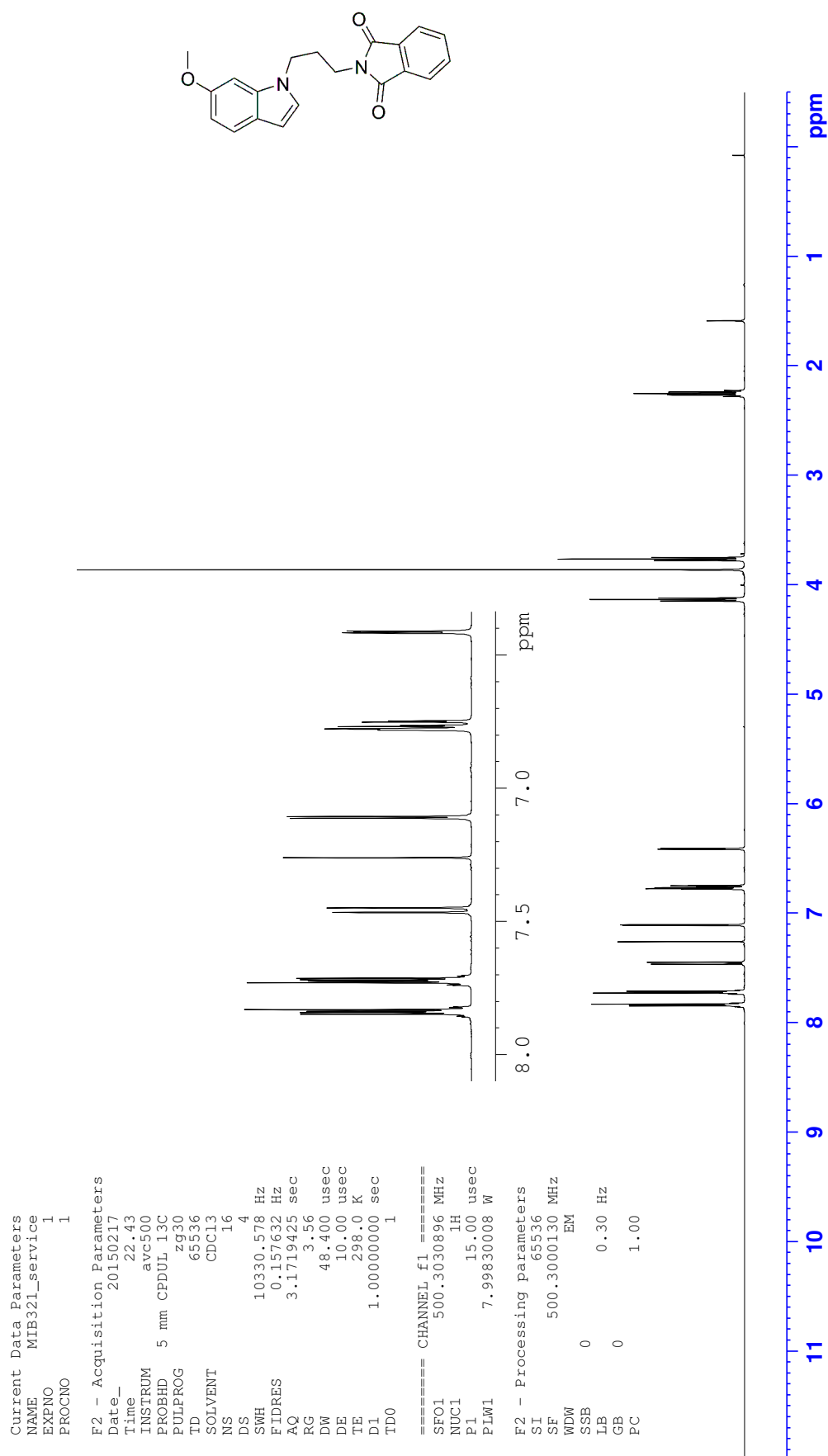


^1H NMR 2-(3-(6-Methoxyindolin-1-yl)propyl)isoindoline-1,3-dione (93)

Appendix F: NMR spectra

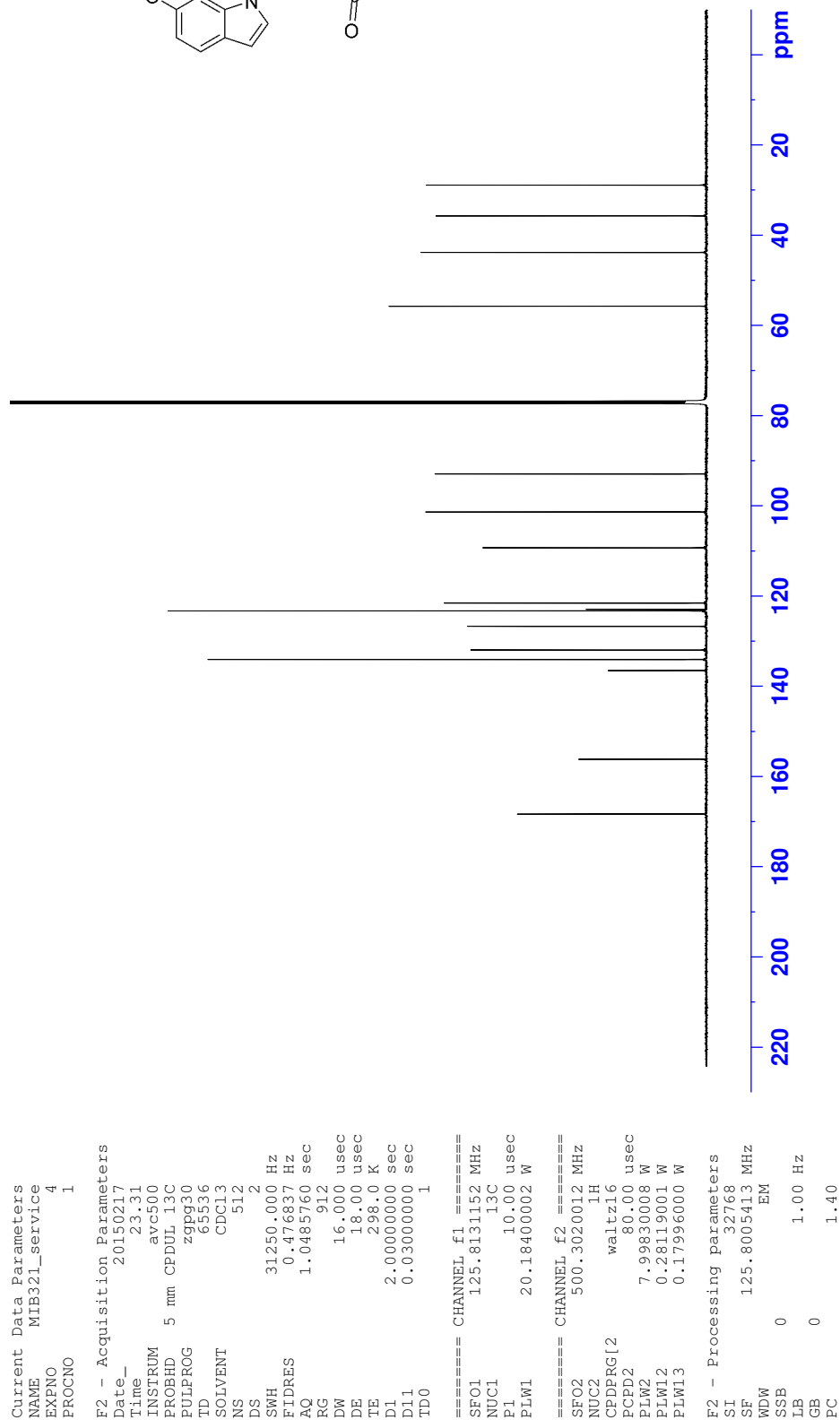
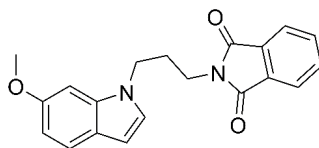
¹³C NMR 2-(3-(6-Methoxyindolin-1-yl)propyl)isoindoline-1,3-dione (93)

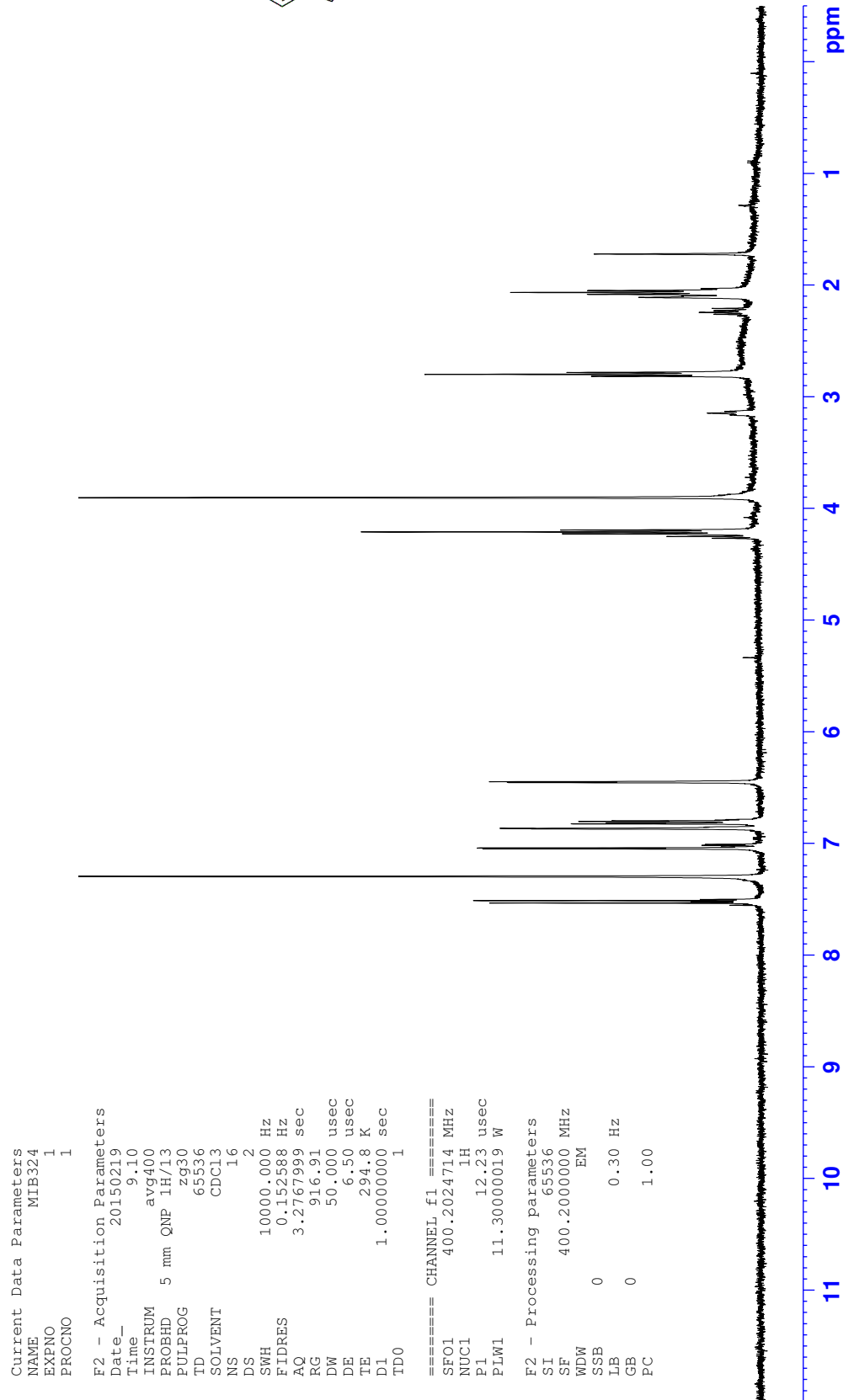
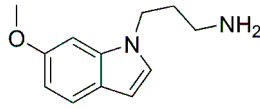


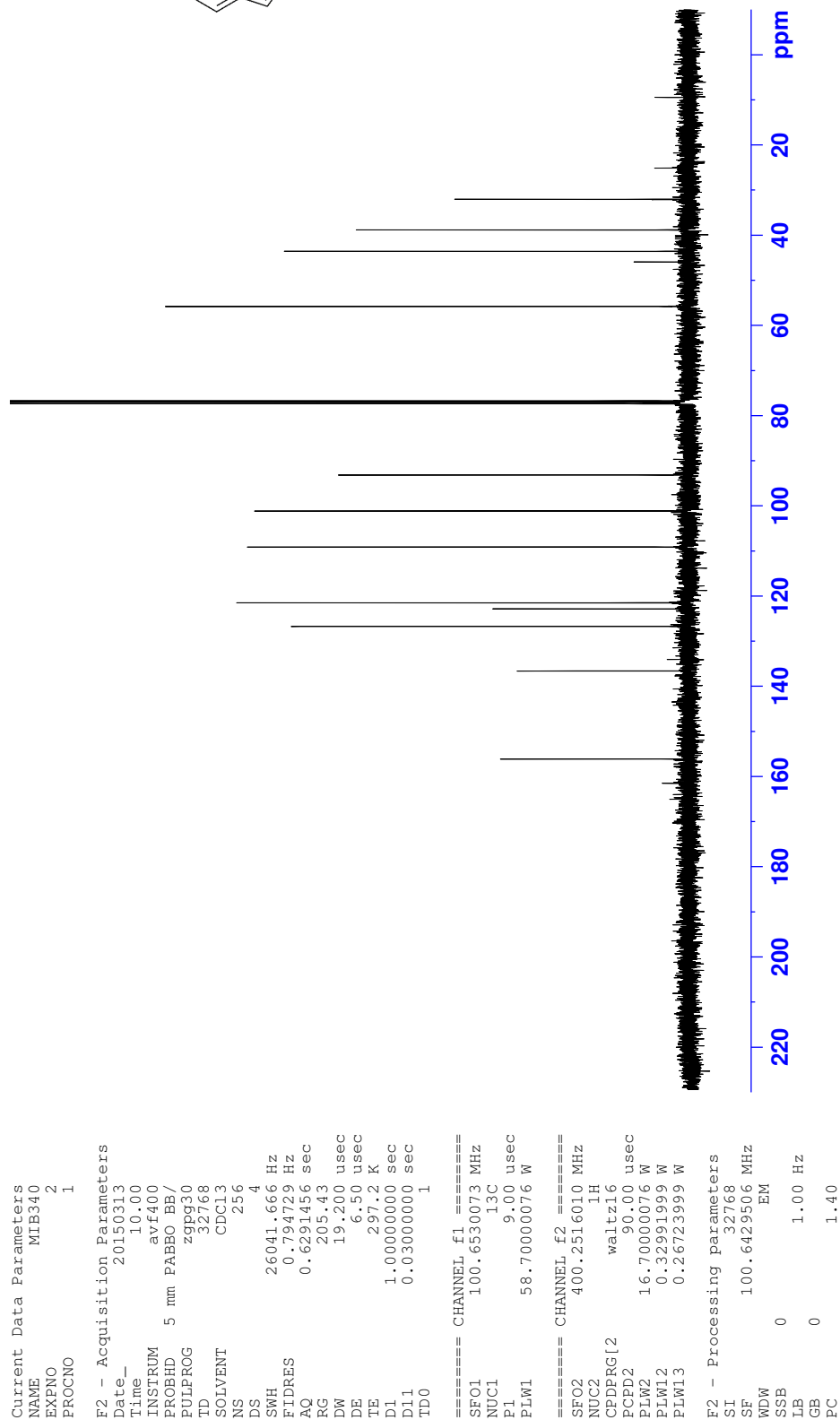
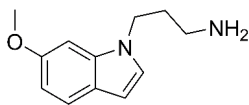
¹H NMR 2-(3-(6-Methoxy-1*H*-indol-1-yl)propyl)isoindoline-1,3-dione (**92**)

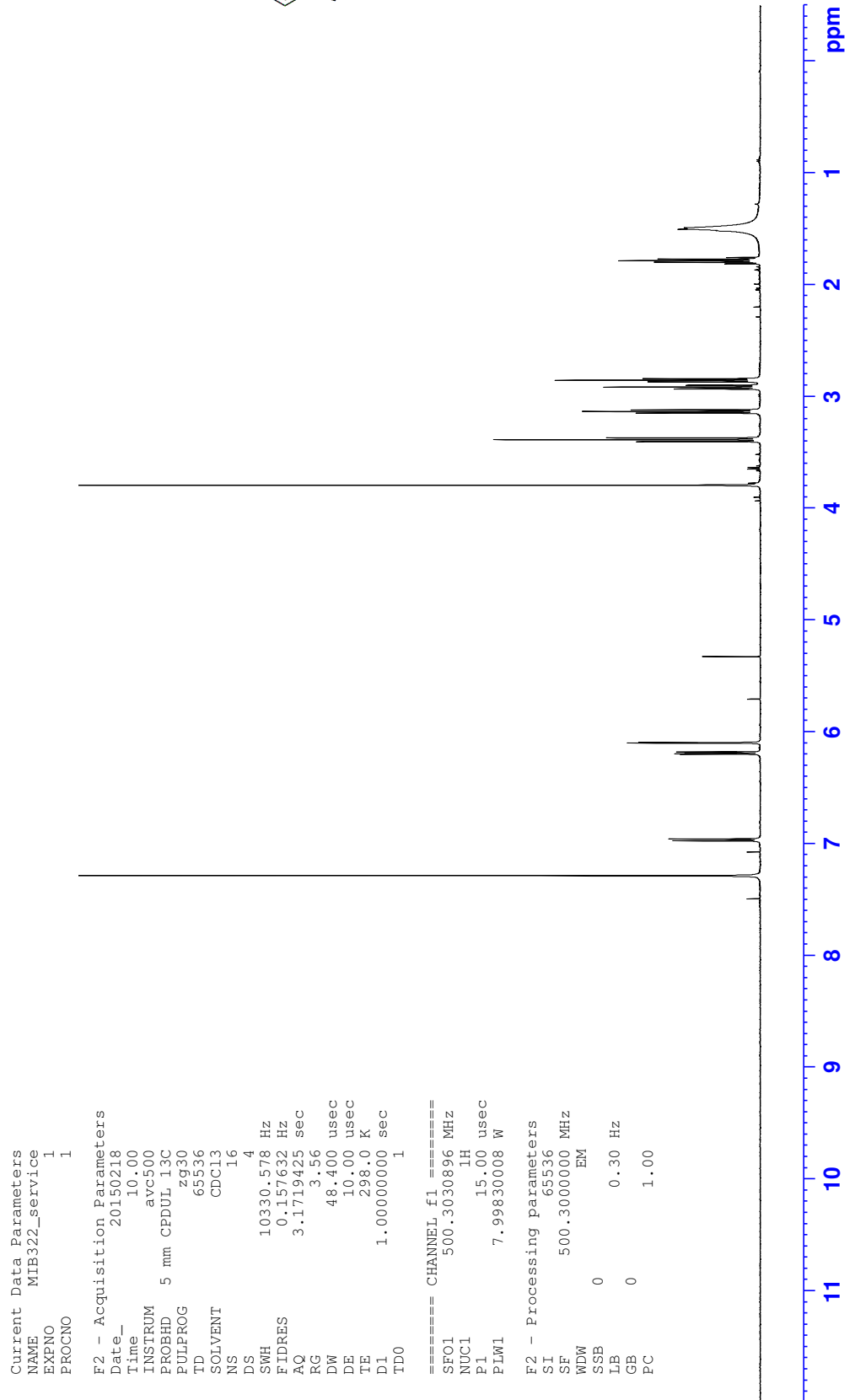
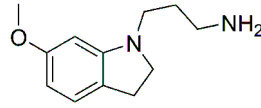
Appendix F: NMR spectra

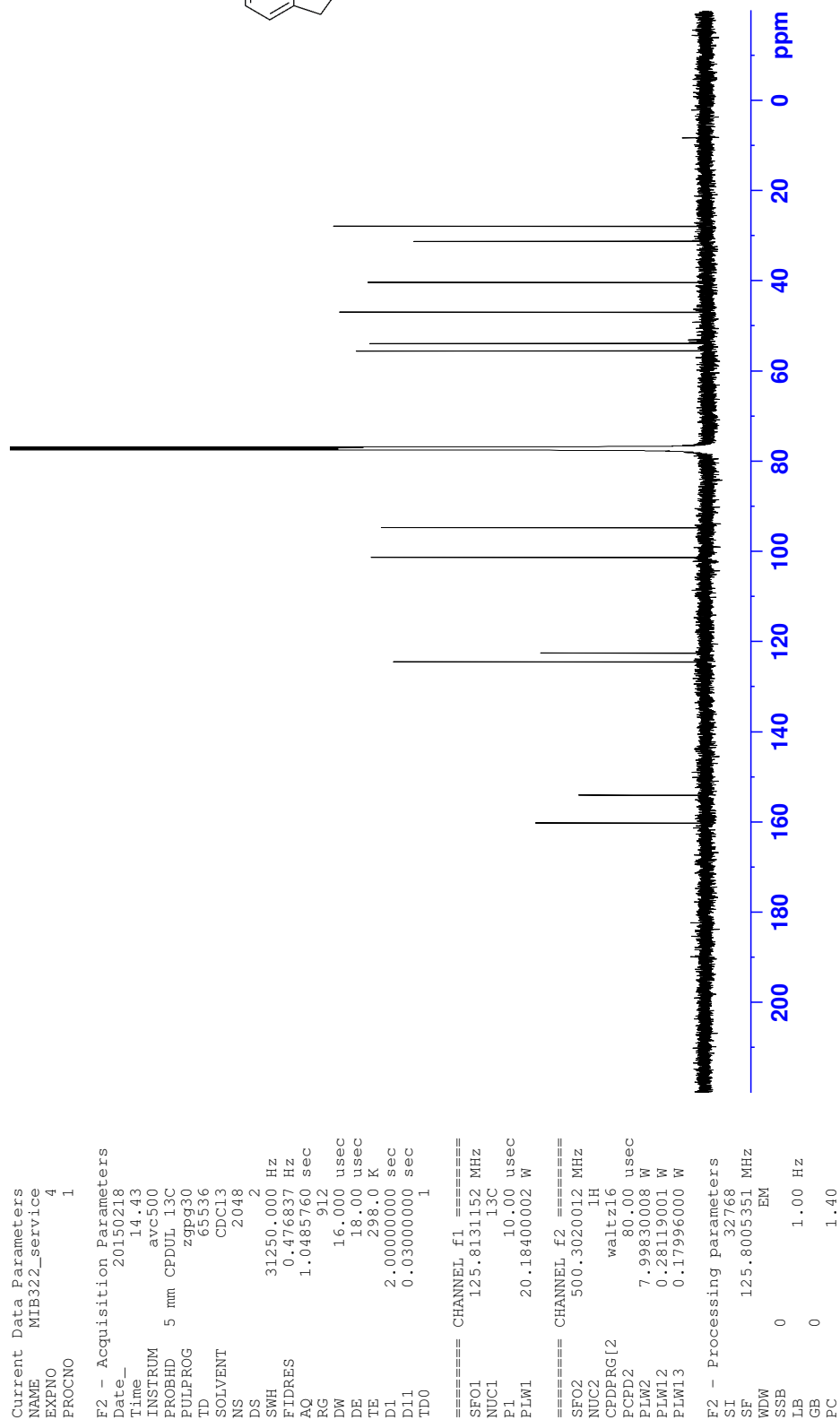
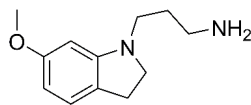
¹³C NMR 2-(3-(6-Methoxy-1*H*-indol-1-yl)propyl)isoindoline-1,3-dione (92)



¹H NMR 3-(6-Methoxy-1*H*-indol-1-yl)propan-1-amine (**94**)

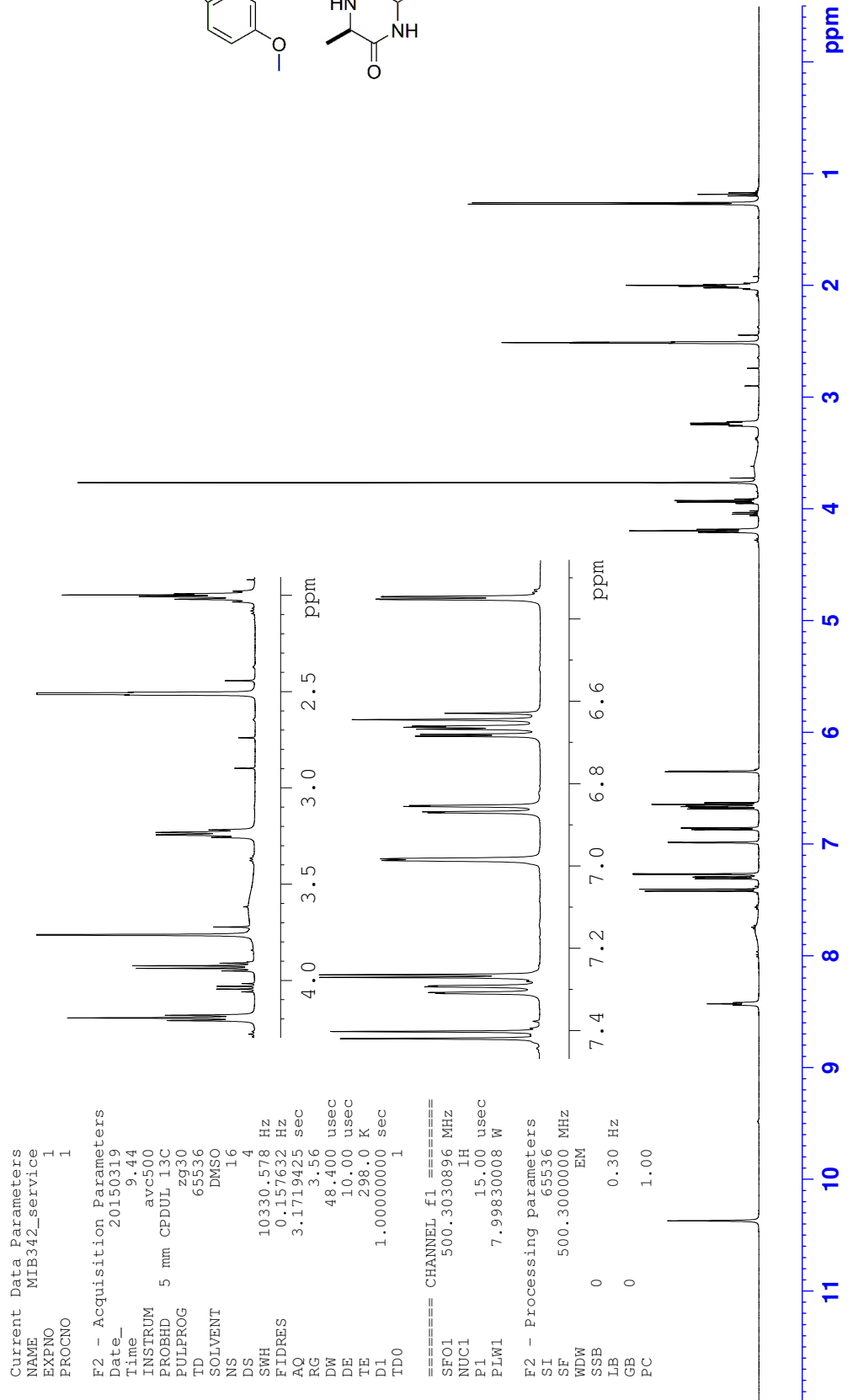
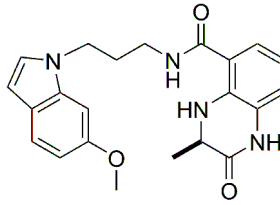
¹³C NMR 3-(6-Methoxy-1*H*-indol-1-yl)propan-1-amine (**94**)

¹H NMR 3-(6-Methoxyindolin-1-yl)propan-1-amine (**95**)

¹³C NMR 3-(6-Methoxyindolin-1-yl)propan-1-amine (**95**)

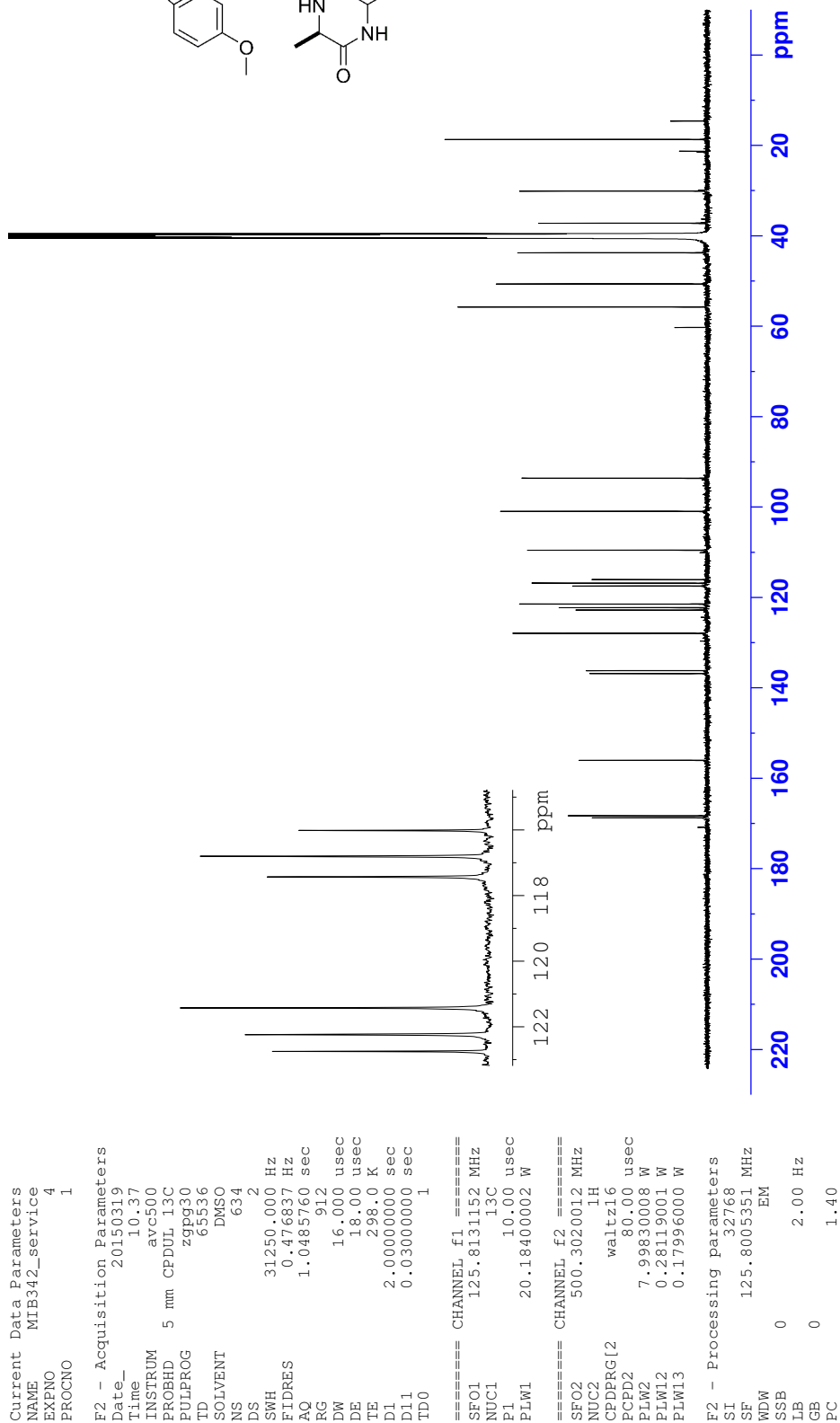
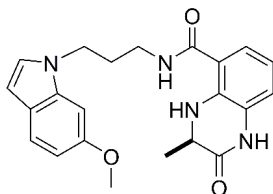
Appendix F: NMR spectra

¹H NMR (R)-N-(3-(6-Methoxy-1H-indolin-1-yl)propyl)-3-methyl-2-oxo-1,2,3,4-tetrahydroquinoxaline-5-carboxamide (**96**)



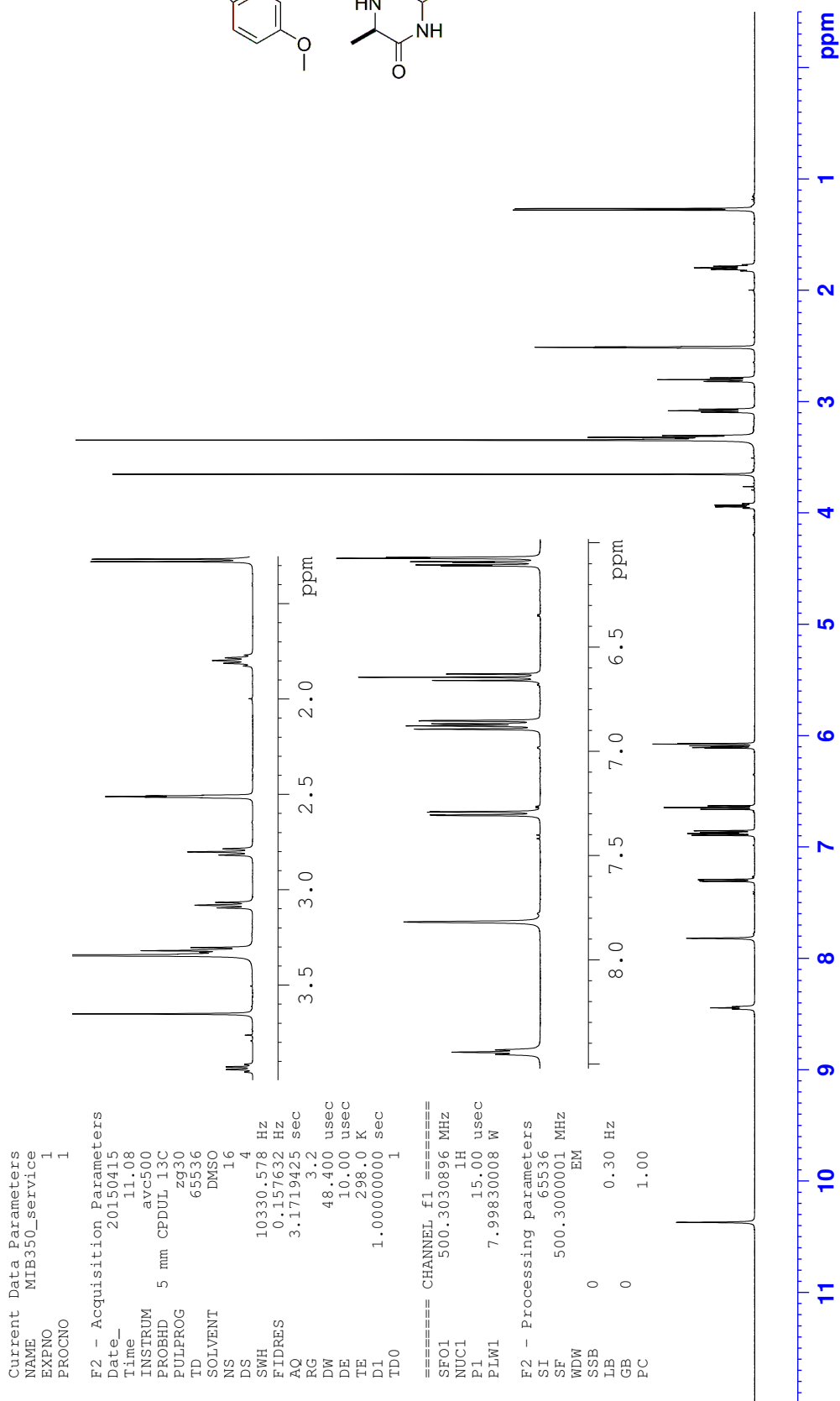
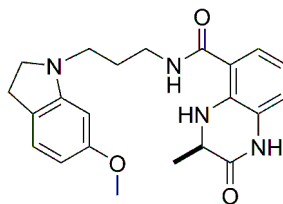
Appendix F: NMR spectra

¹³C NMR (R)-N-(3-(6-Methoxy-1H-indolin-1-yl)propyl)-3-methyl-2-oxo-1,2,3,4-tetrahydroquinoxaline-5-carboxamide (**96**)



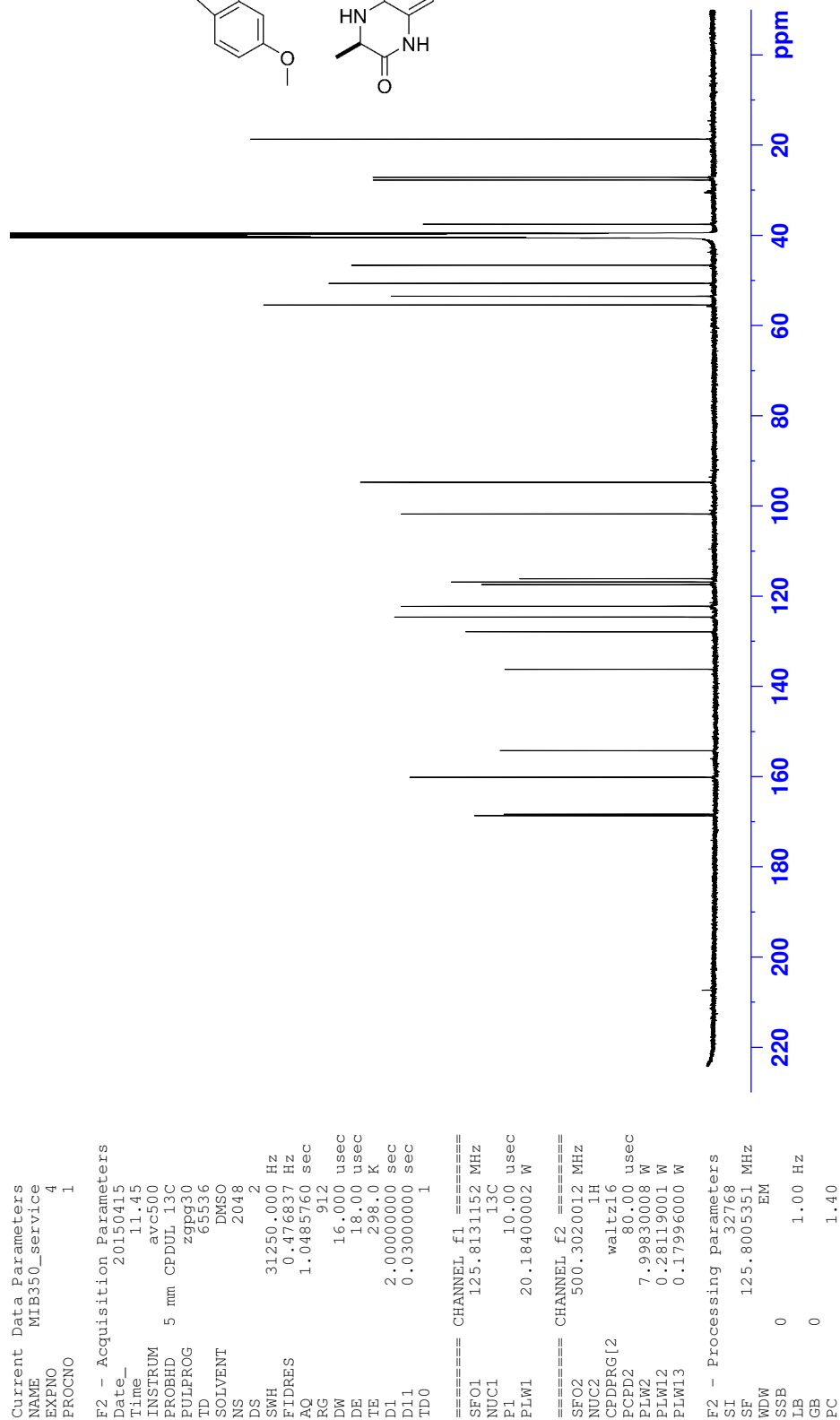
Appendix F: NMR spectra

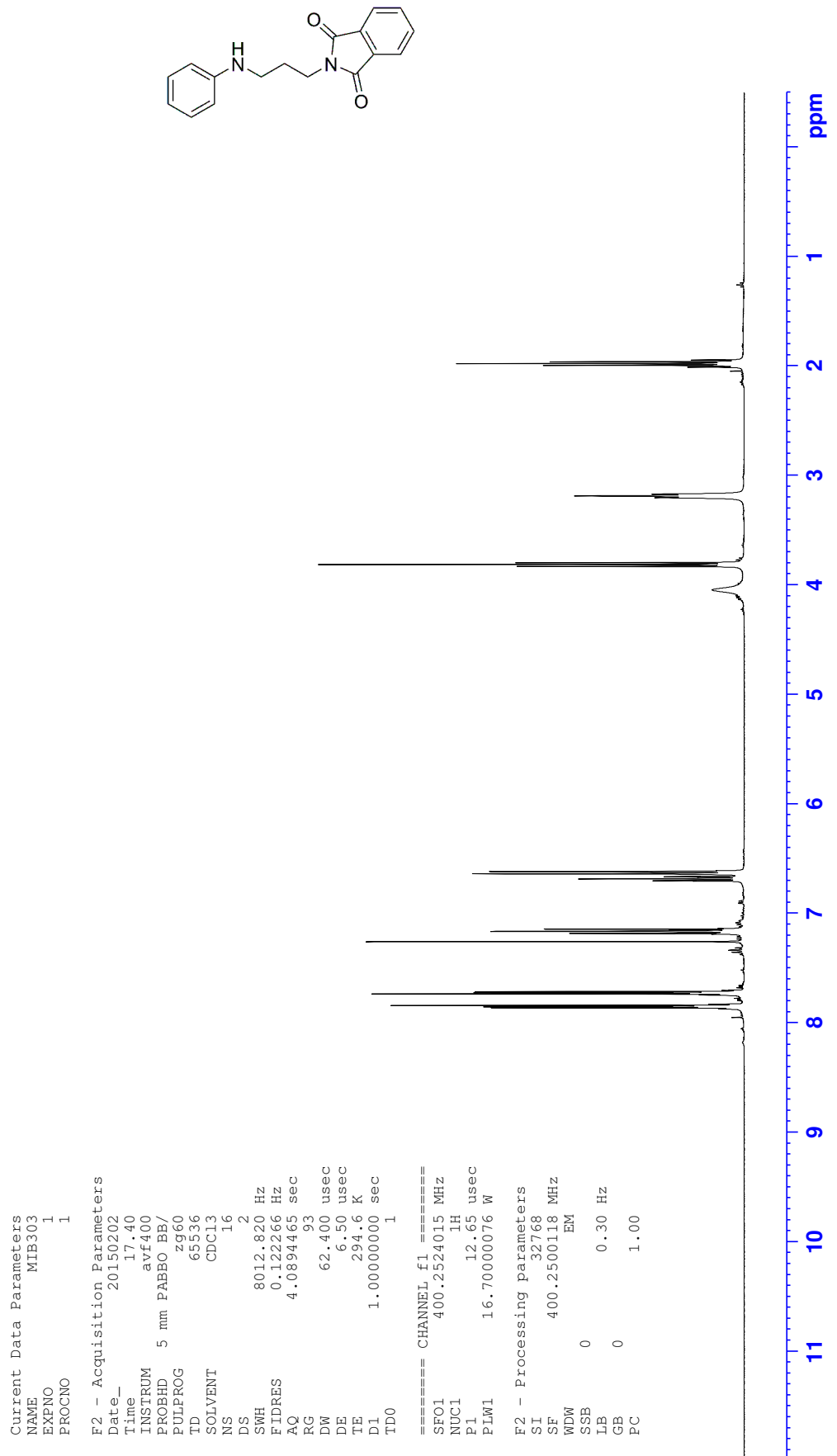
¹H NMR (R)-N-(3-(6-Methoxyindolin-1-yl)propyl)-3-methyl-2-oxo-1,2,3,4-tetrahydroquinoxaline-5-carboxamide (97)

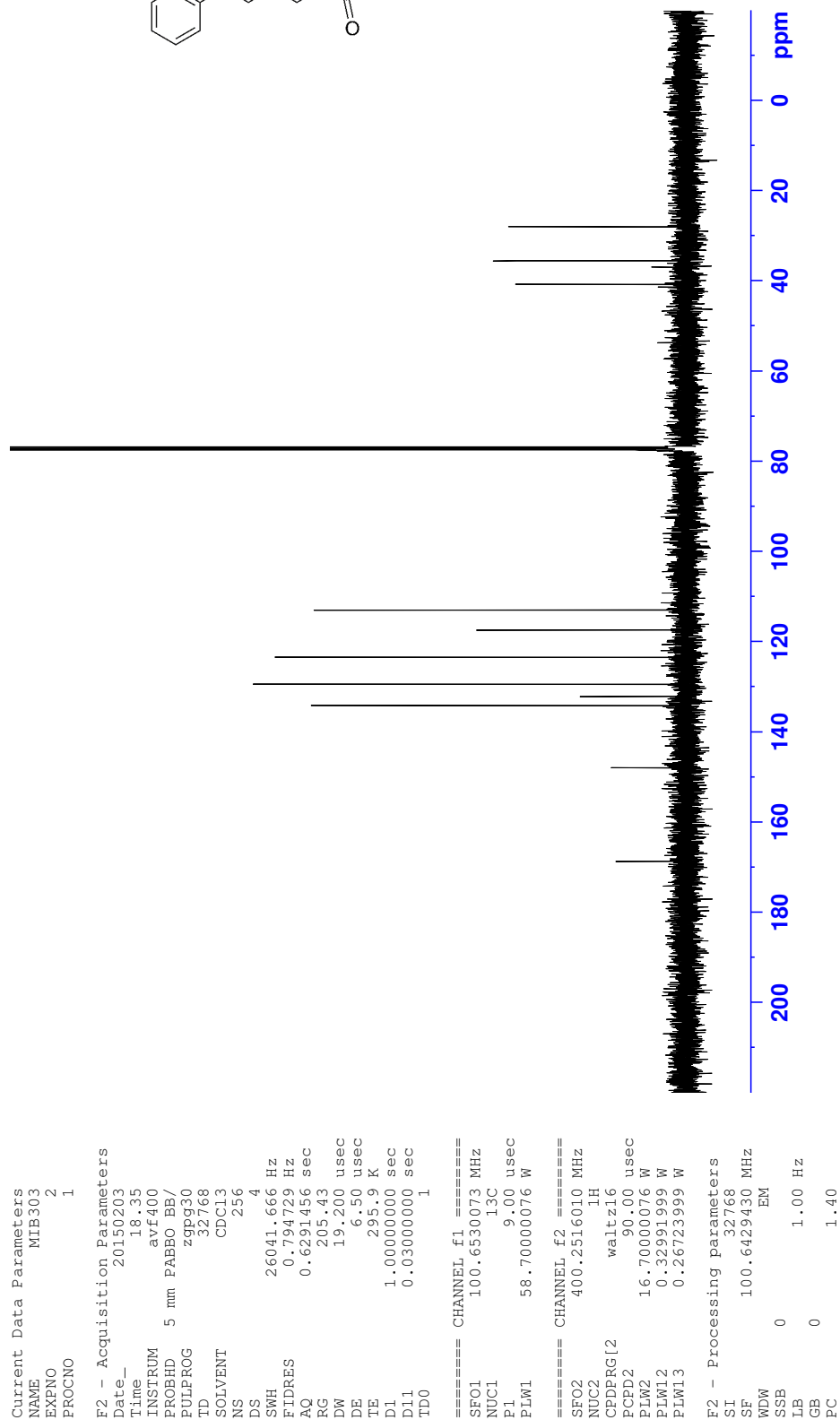
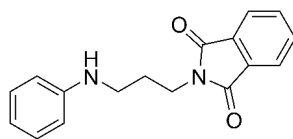


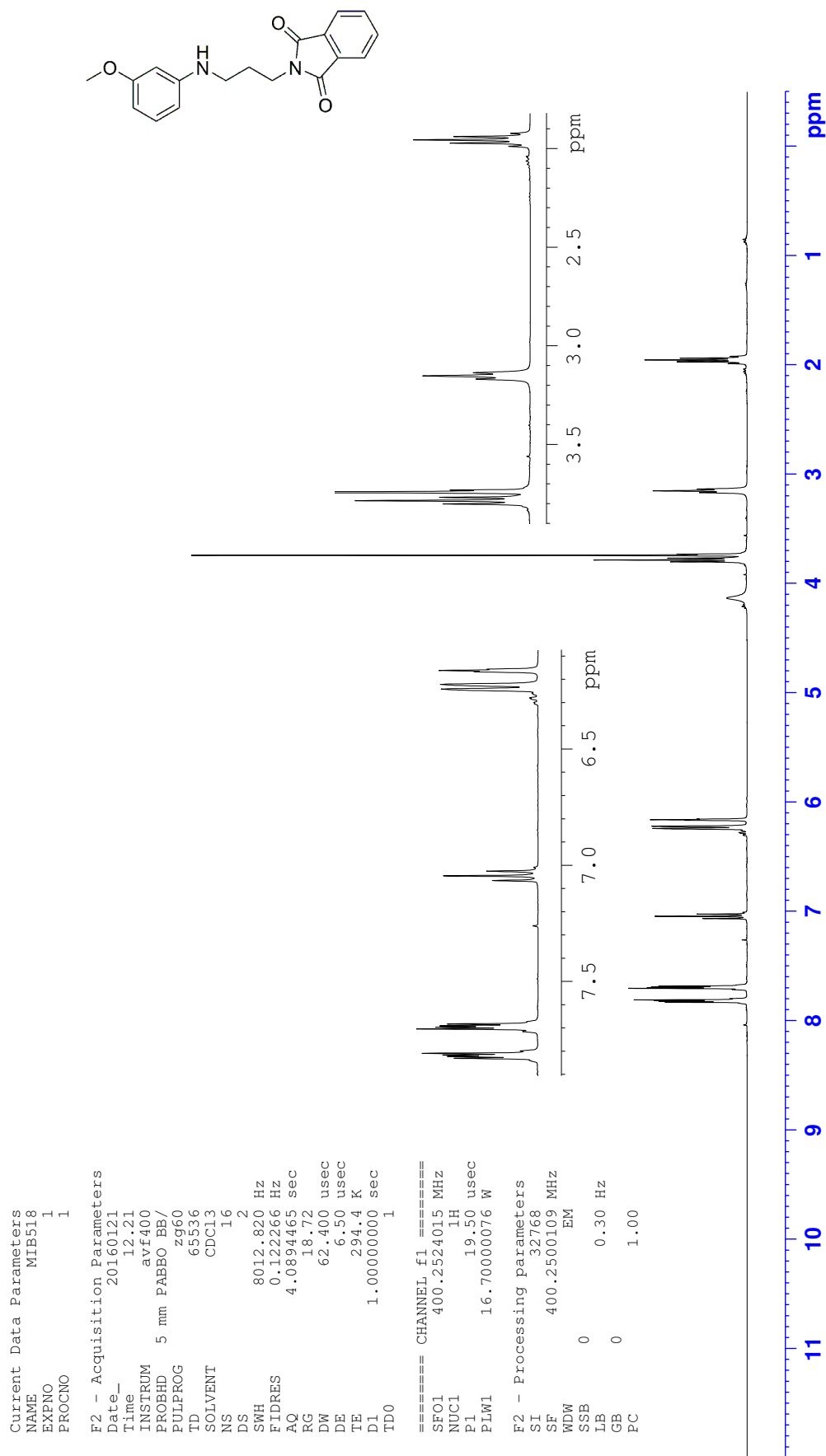
Appendix F: NMR spectra

¹³C NMR (R)-N-(3-(6-Methoxyindolin-1-yl)propyl)-3-methyl-2-oxo-1,2,3,4-tetrahydroquinoxaline-5-carboxamide (97)



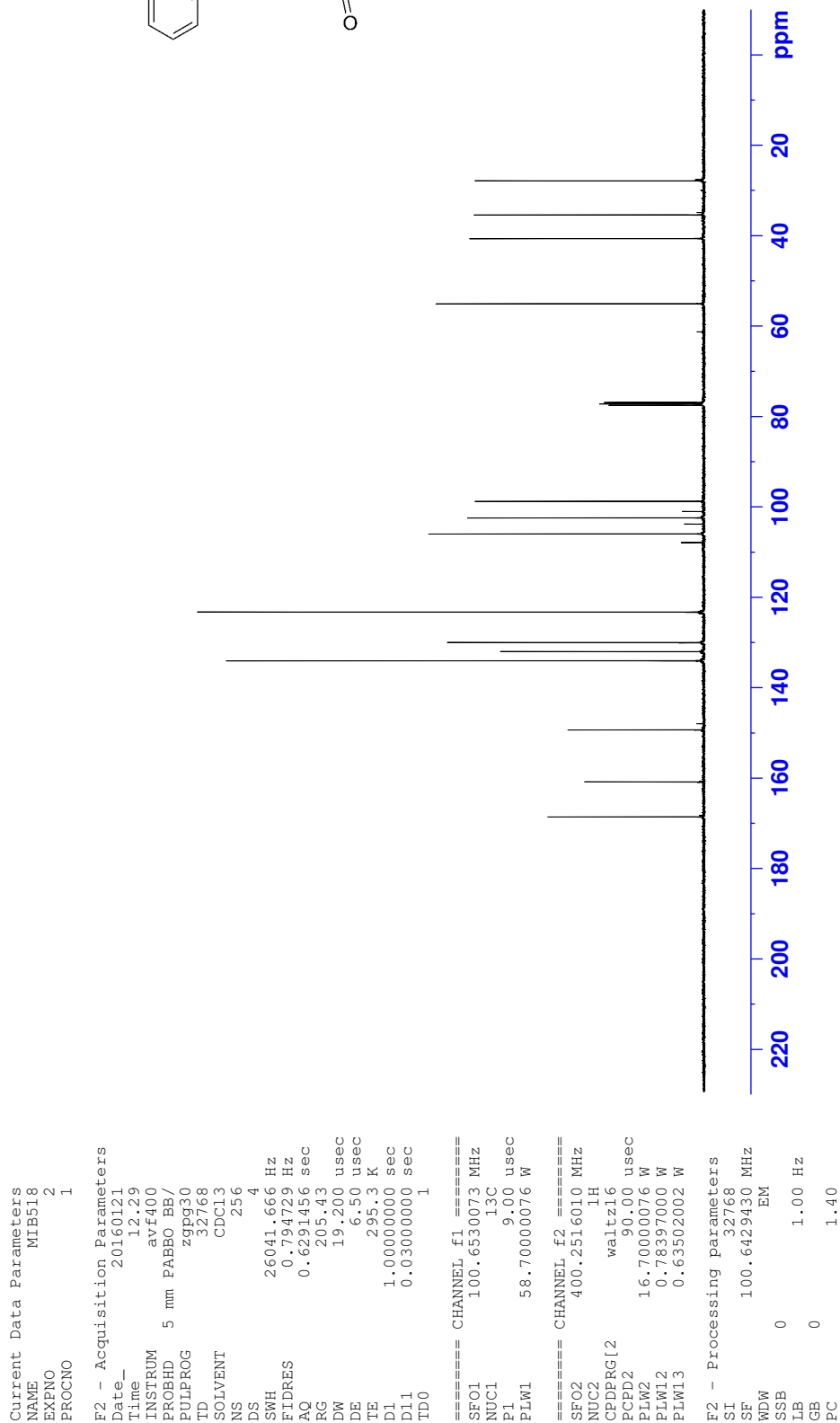
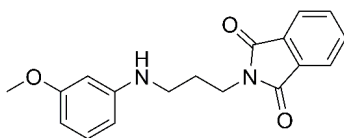
¹H NMR 2-(3-(Phenylamino)propyl)isoindoline-1,3-dione (**113**)

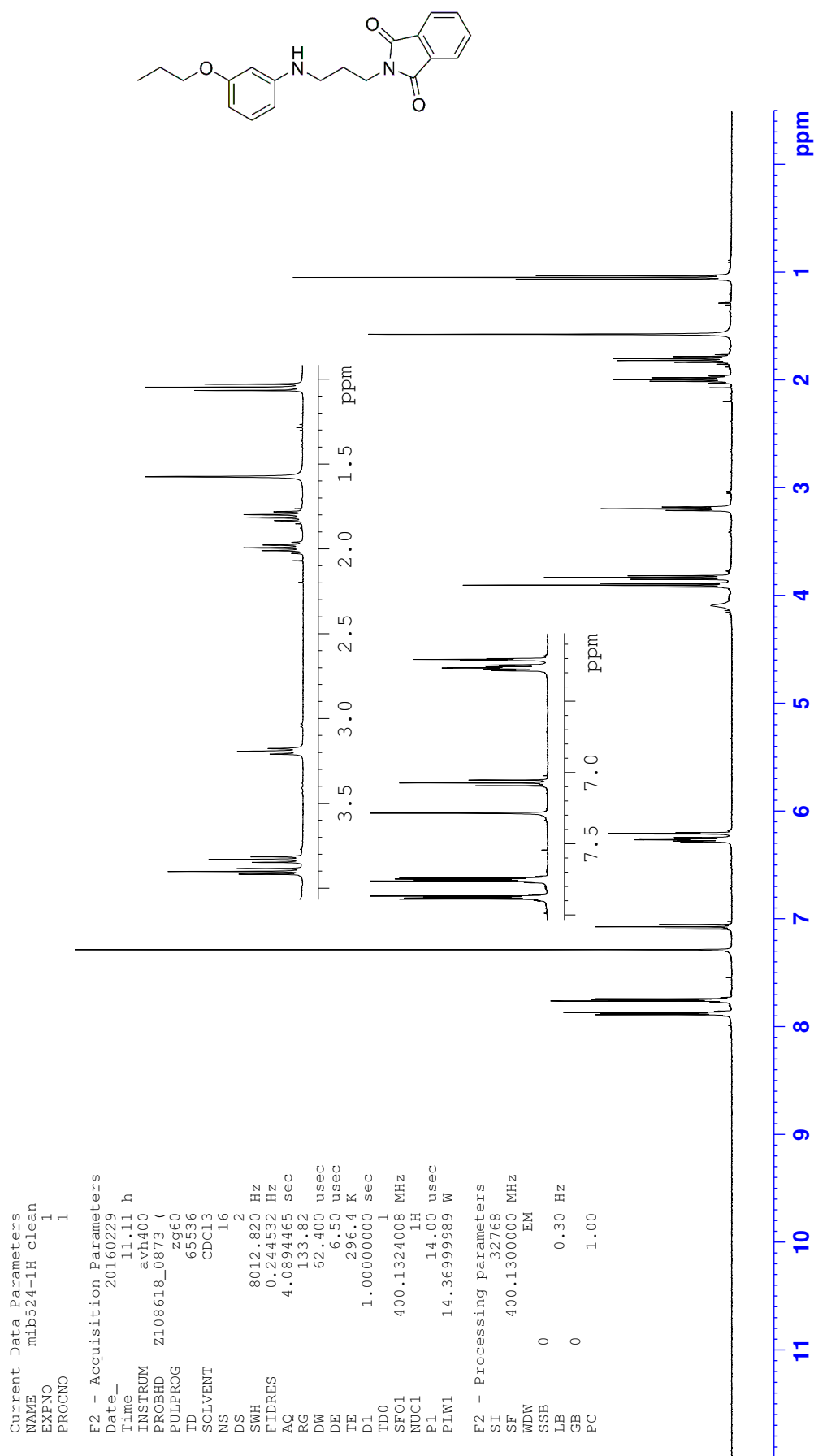
¹³C NMR 2-(3-(Phenylamino)propyl)isoindoline-1,3-dione (**113**)

¹H NMR 2-((3-(3-Methoxyphenyl)amino)propyl)isoindoline-1,3-dione (**114**)

Appendix F: NMR spectra

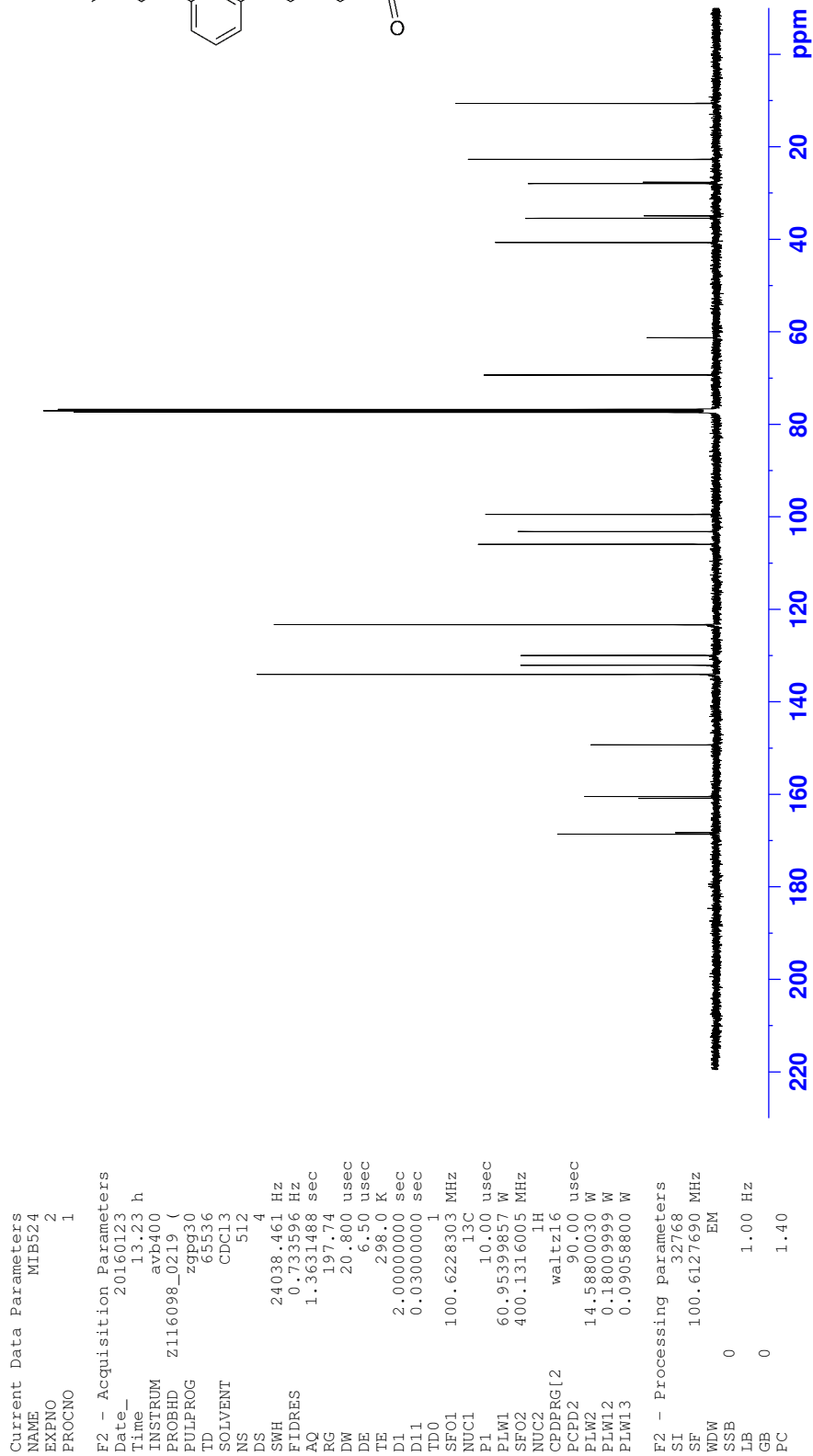
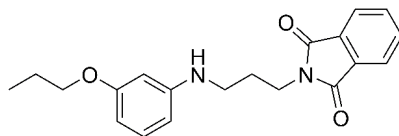
¹³C NMR 2-(3-((3-Methoxyphenyl)amino)propyl)isoindoline-1,3-dione (**114**)

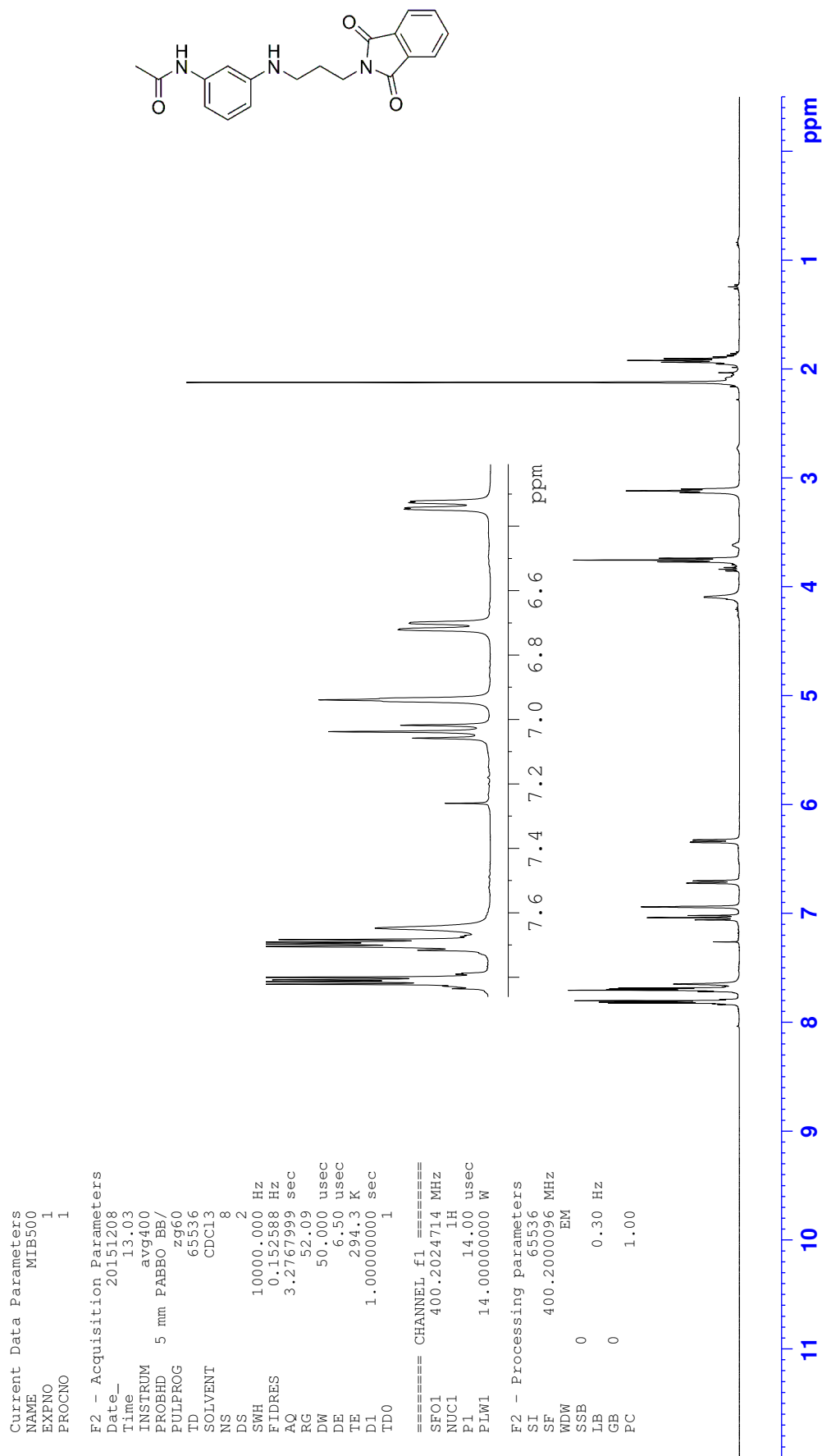


^1H NMR 2-((3-(3-Propoxyphenyl)amino)propyl)isoindoline-1,3-dione (**115**)

Appendix F: NMR spectra

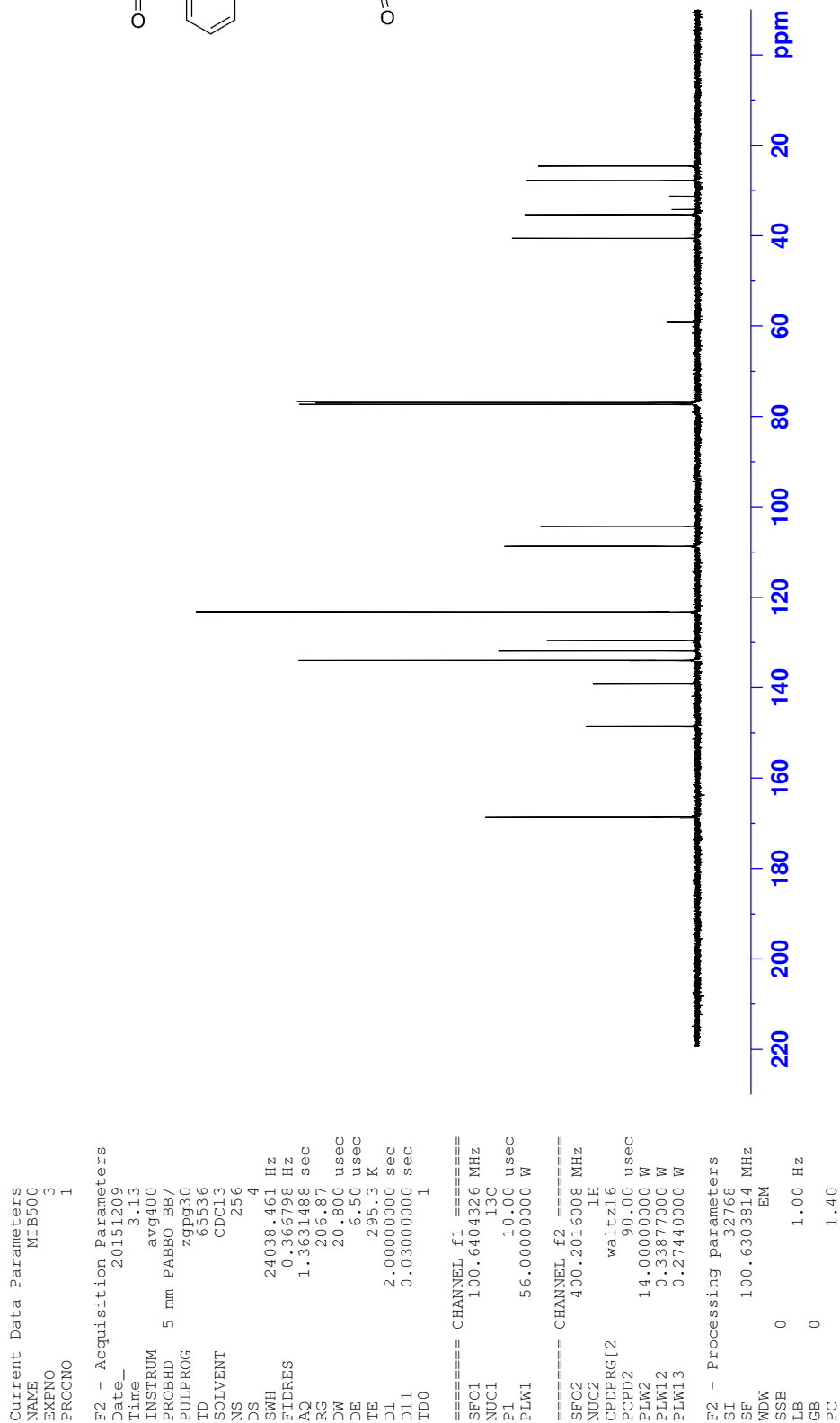
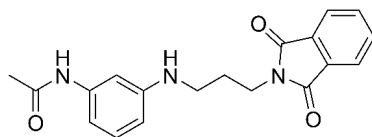
¹³C NMR 2-(3-((3-Propoxyphenyl)amino)propyl)isoindoline-1,3-dione (**115**)

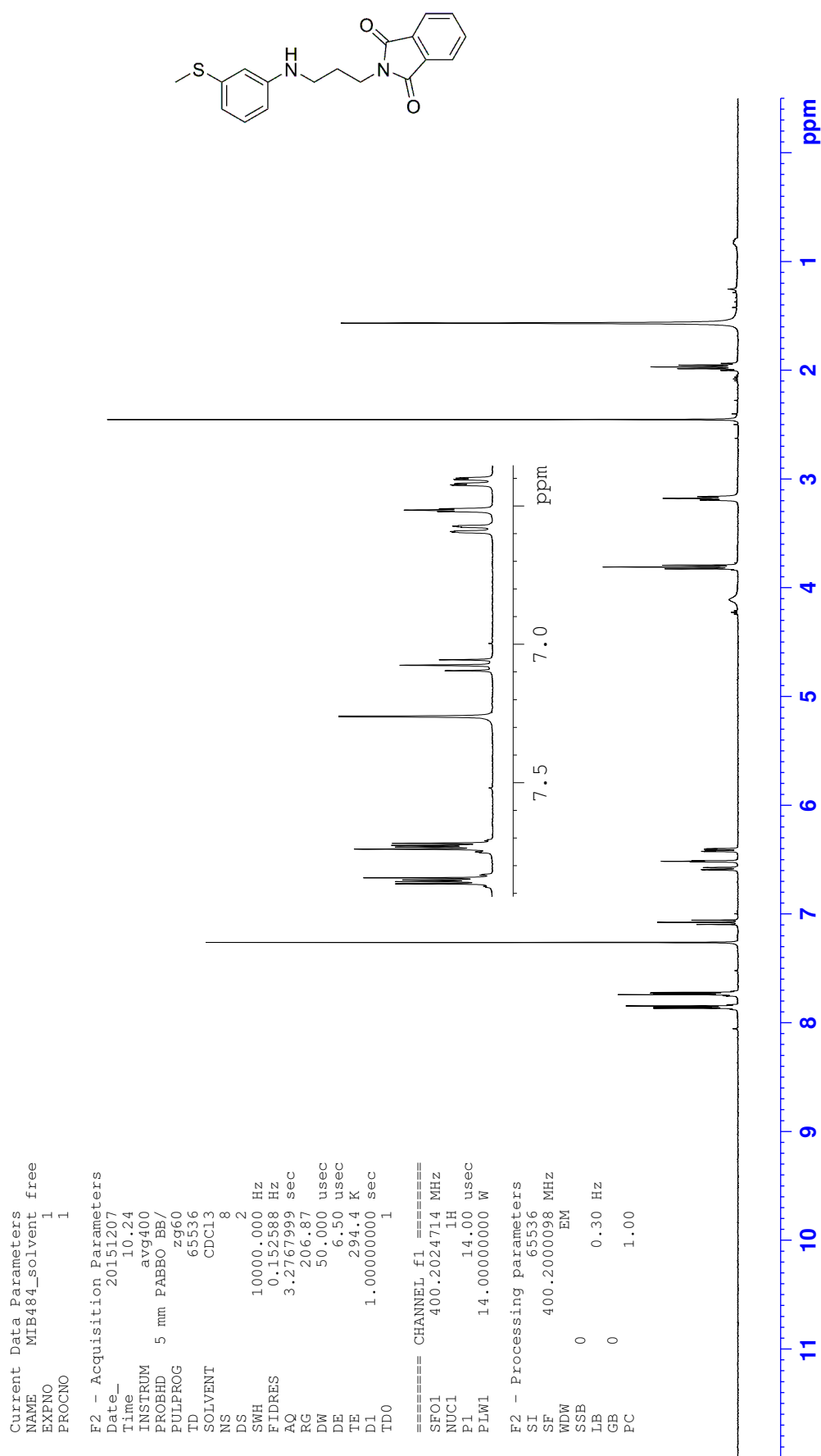


¹H NMR *N*-(3-((3-(1,3-Dioxisoindolin-2-yl)propyl)amino)phenyl)acetamide (**116**)

Appendix F: NMR spectra

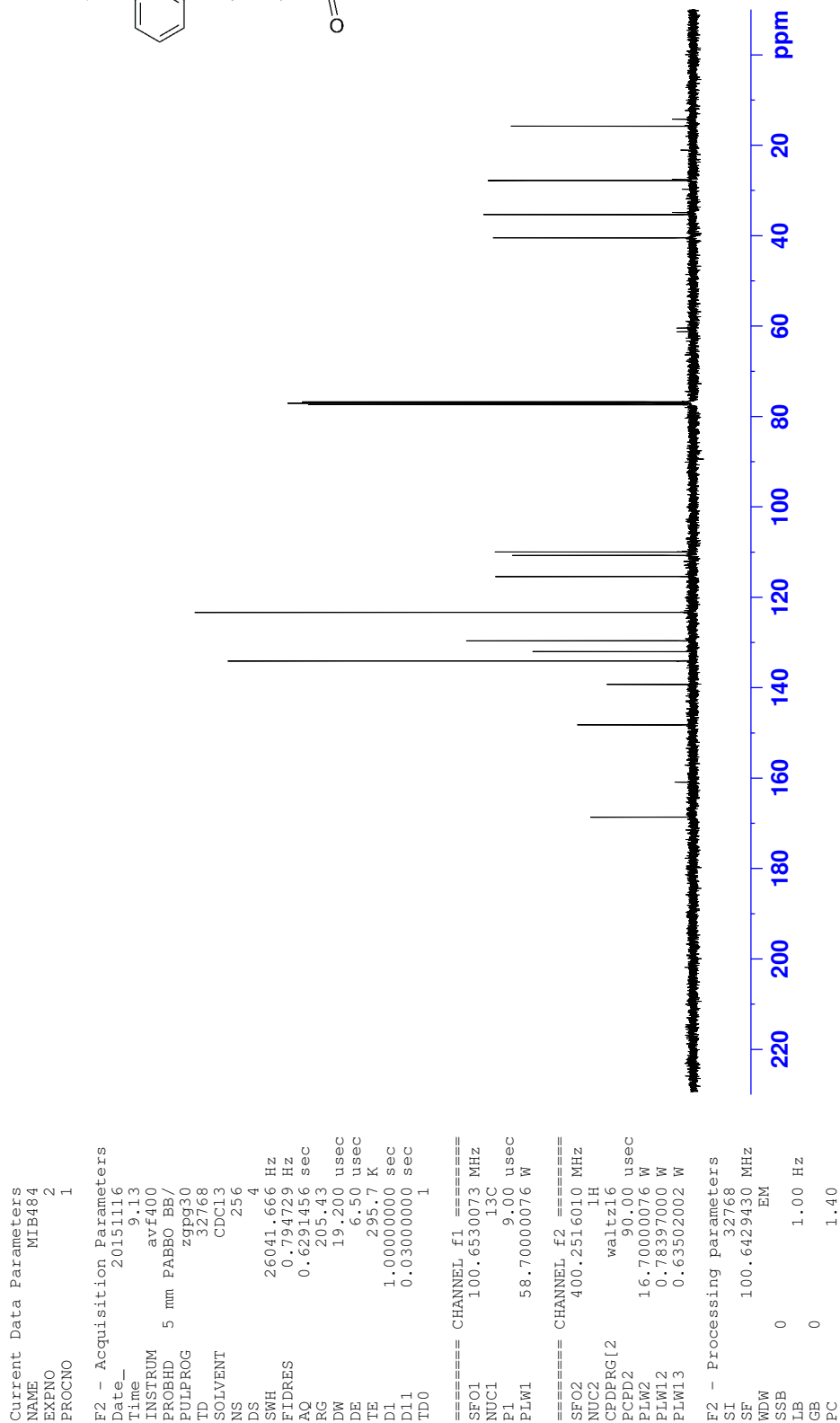
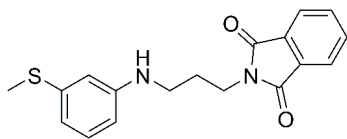
¹³C NMR *N*-(3-((3-(1,3-Dioxisoindolin-2-yl)propyl)amino)phenyl)acetamide (**116**)

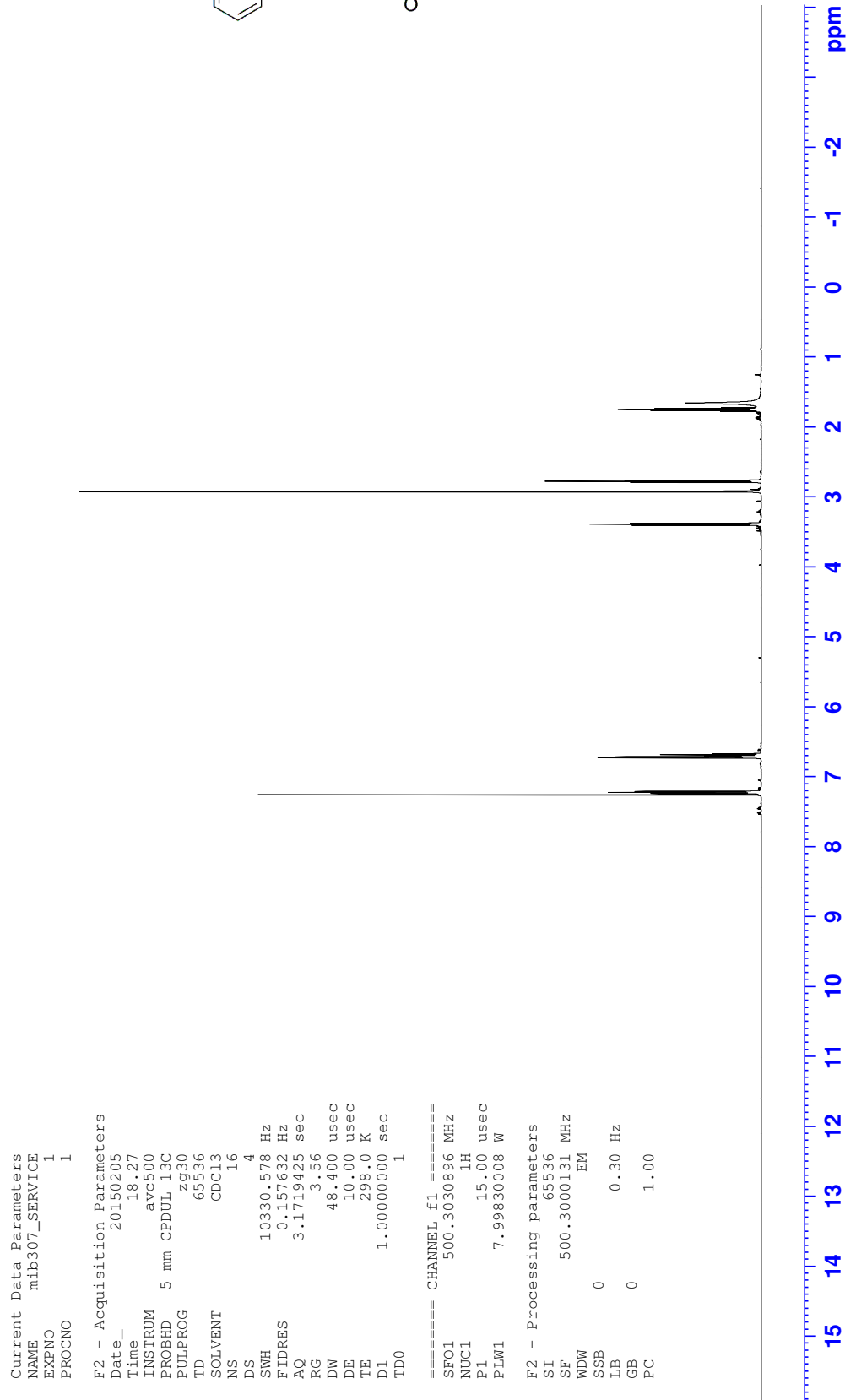
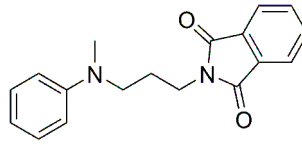


¹H NMR 2-((3-(Methylthio)phenyl)amino)propylisoindoline-1,3-dione (**117**)

Appendix F: NMR spectra

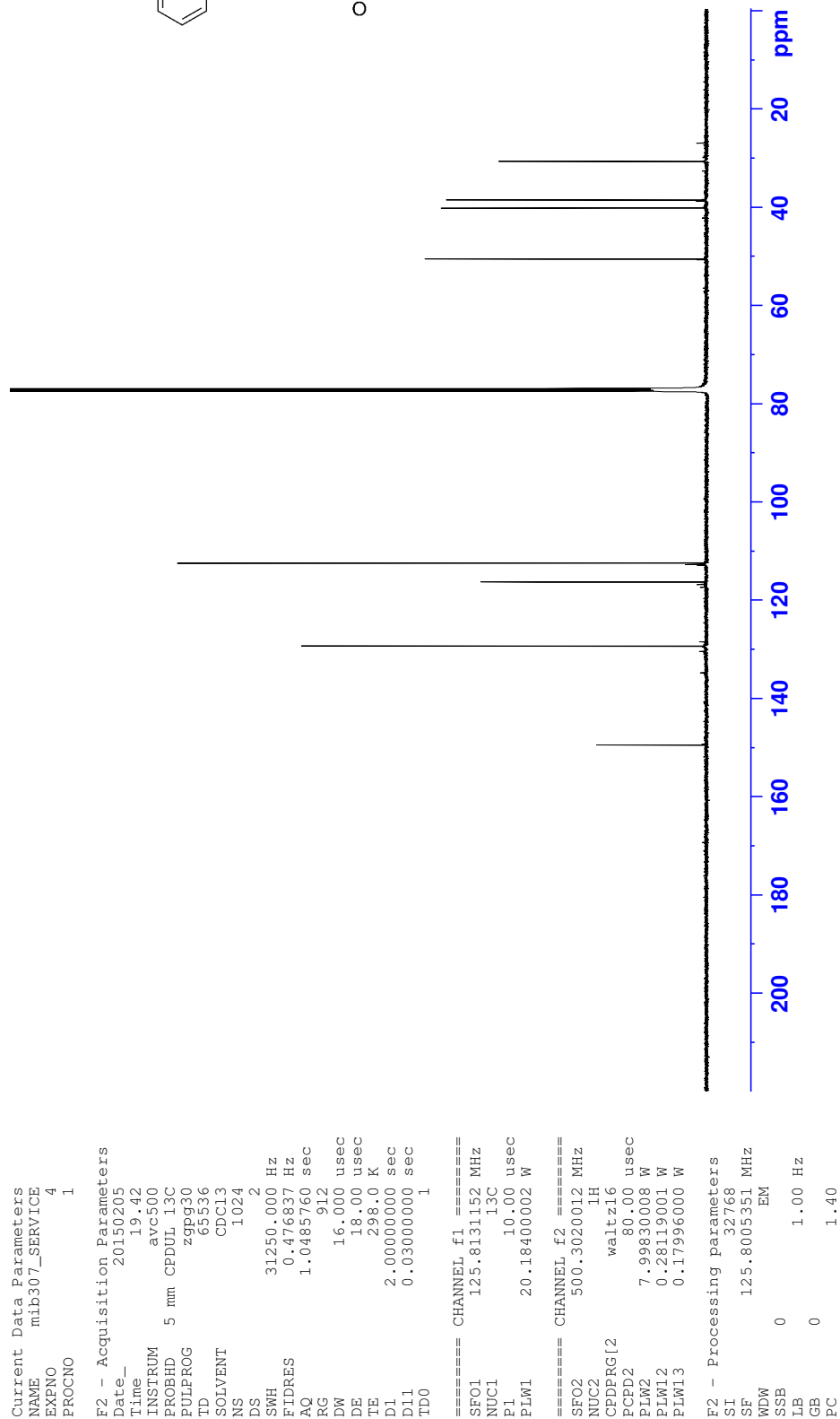
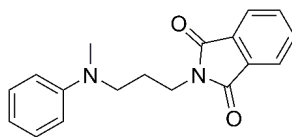
¹³C NMR 2-(3-((3-(Methylthio)phenyl)amino)propyl)isoindoline-1,3-dioneacetamide (**117**)

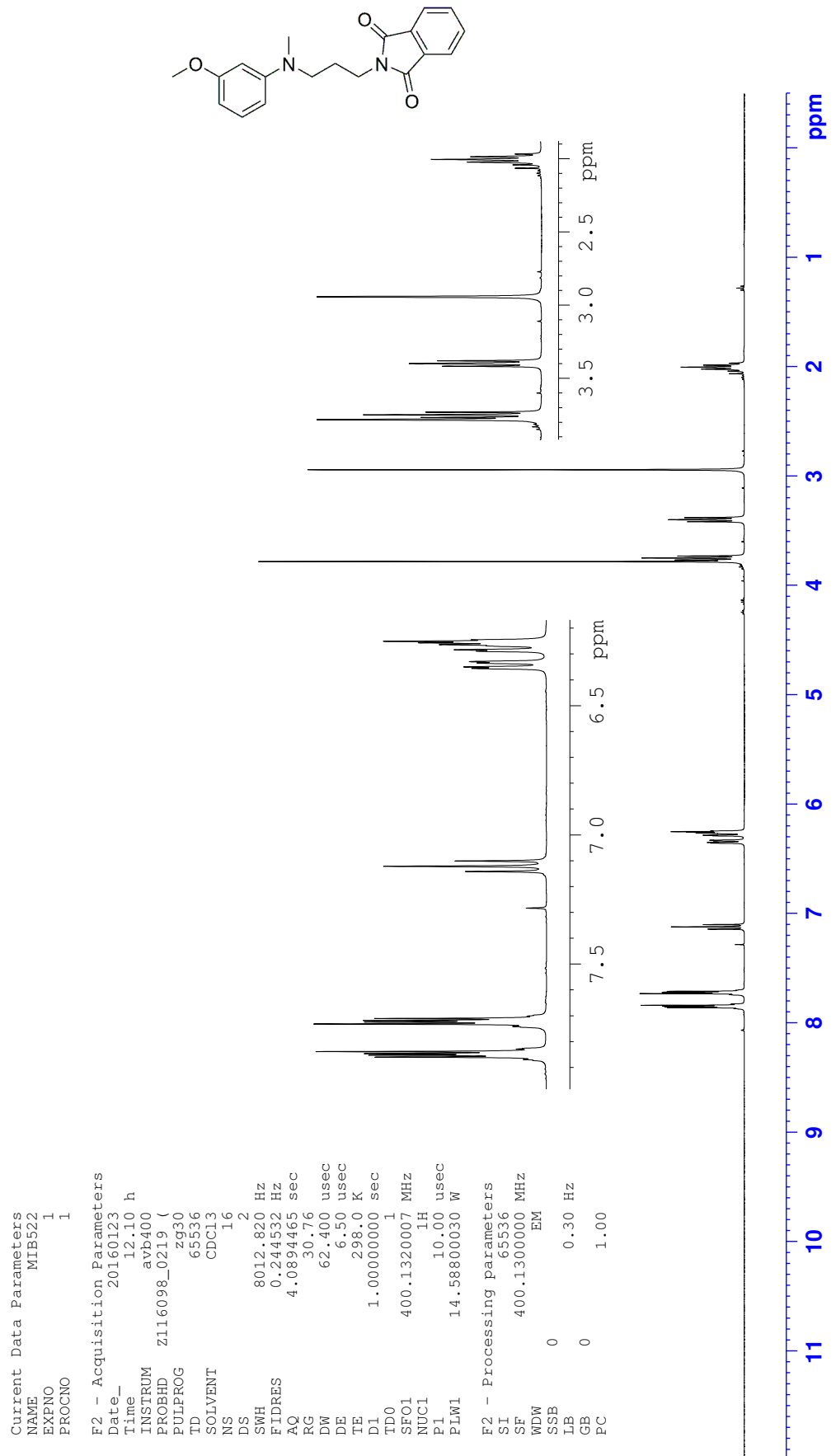


¹H NMR 2-(3-(Methyl(phenyl)amino)propyl)isoindoline-1,3-dione (**118**)

Appendix F: NMR spectra

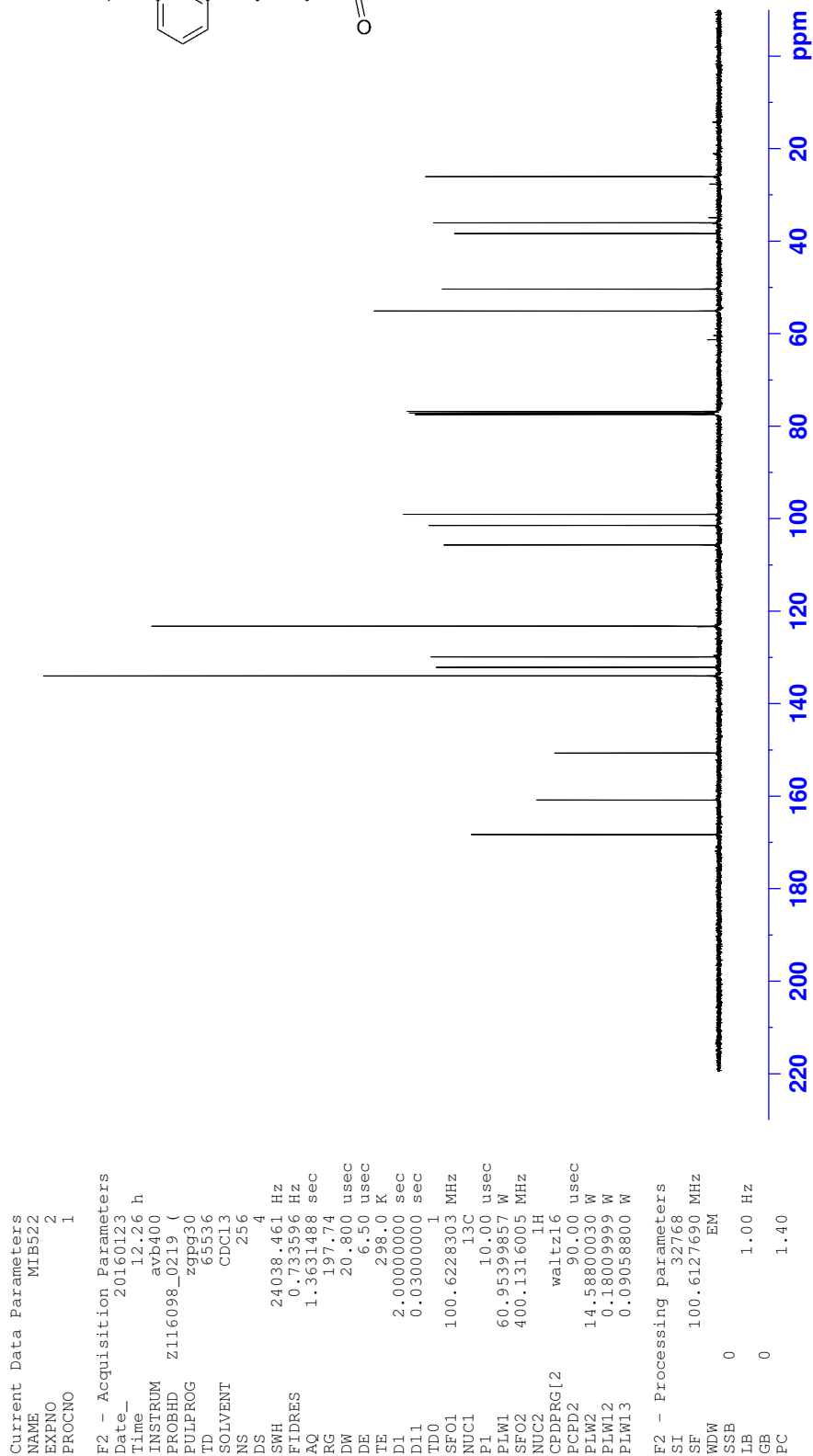
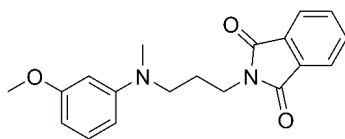
¹³C NMR 2-(3-(Methyl(phenyl)amino)propyl)isoindoline-1,3-dione (**118**)

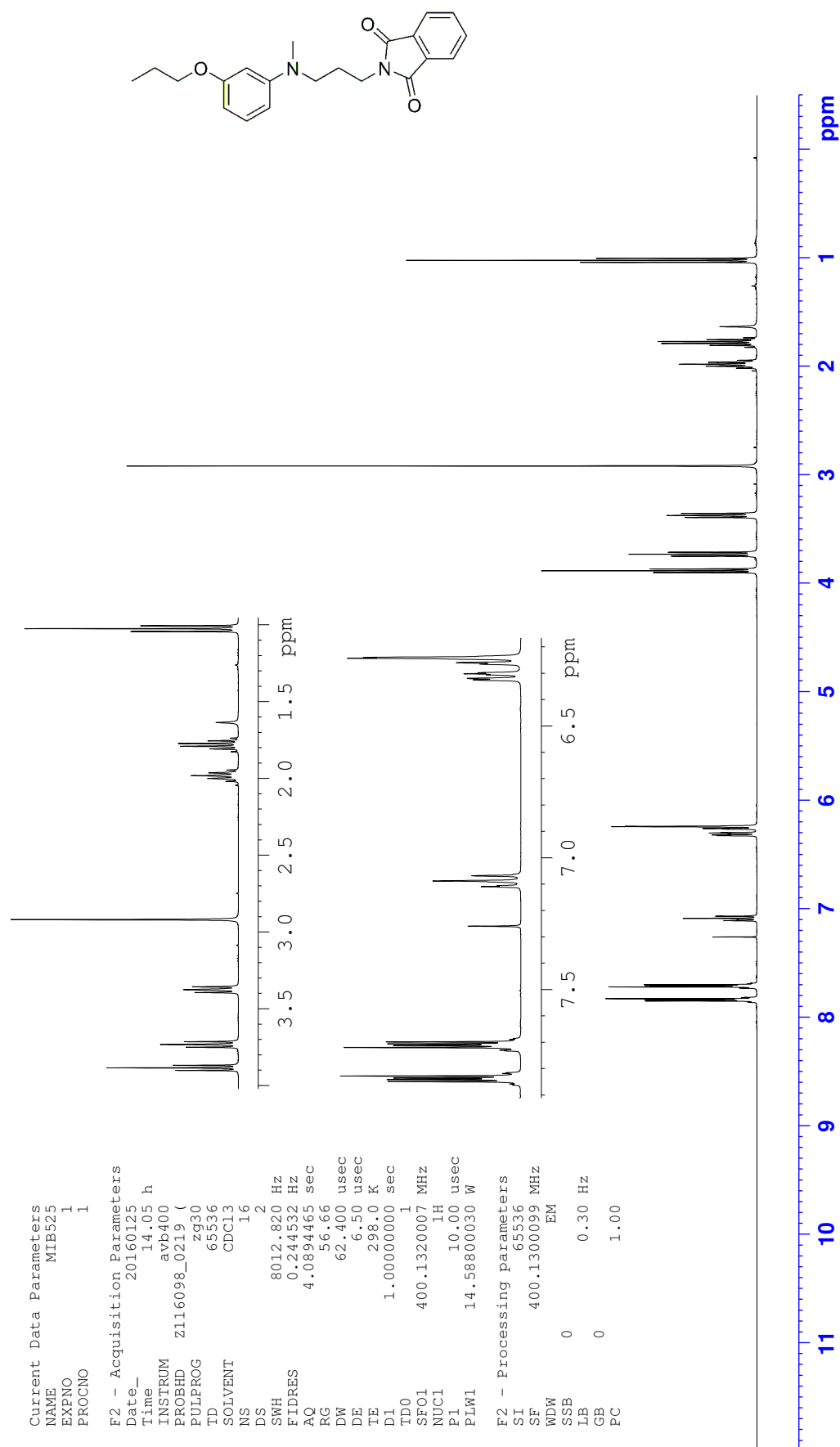


^1H NMR 2-((3-Methoxyphenyl)(methyl)amino)propyl)isoindoline-1,3-dione (**119**)

Appendix F: NMR spectra

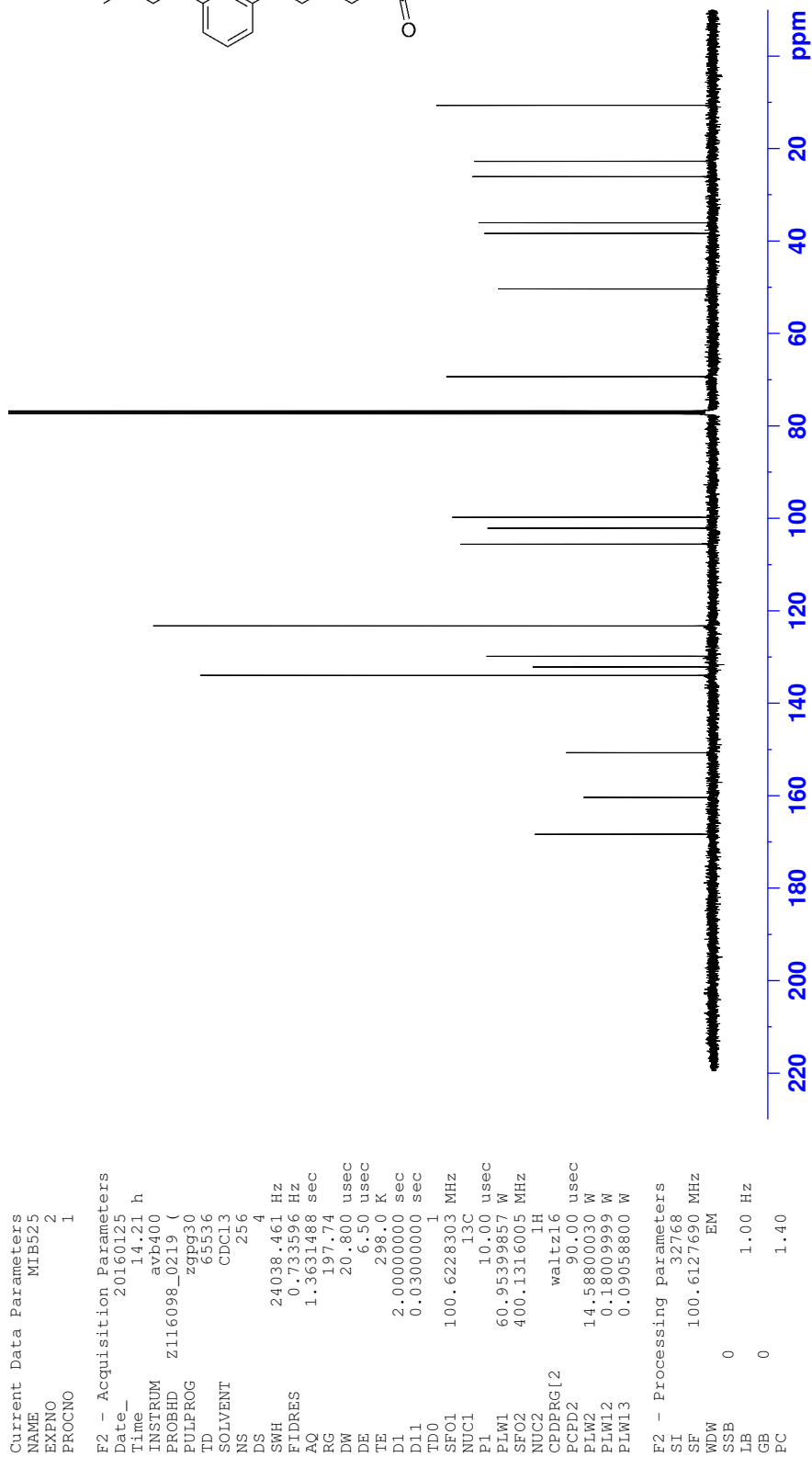
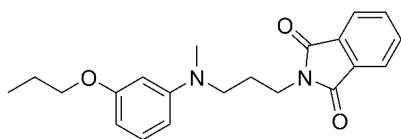
¹³C NMR 2-((3-Methoxyphenyl)(methyl)amino)propylisoindoline-1,3-dione (119)



^1H NMR 2-((3-(3-Propoxyphenyl)(methyl)amino)propyl)isoindoline-1,3-dione (**120**)

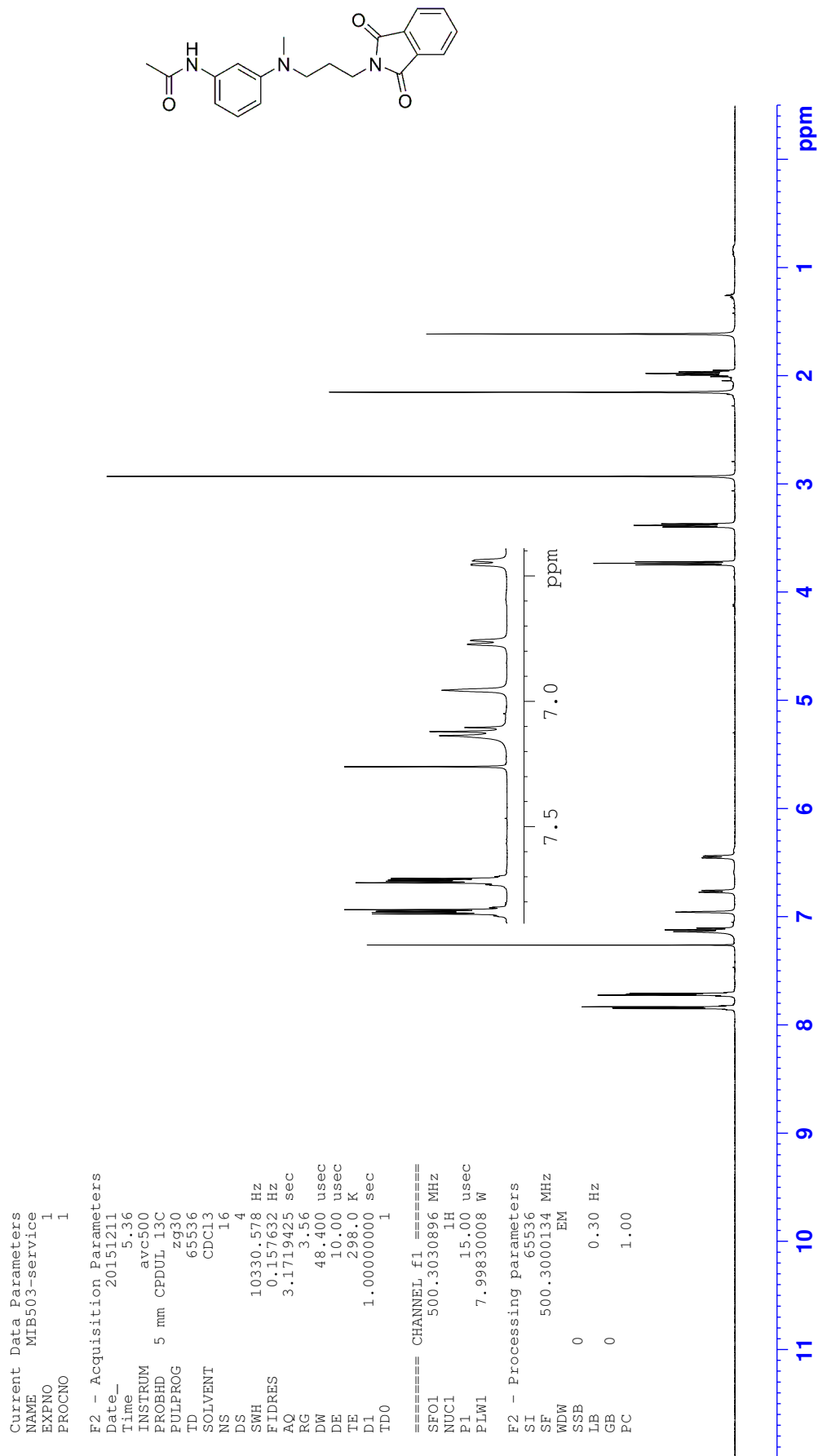
Appendix F: NMR spectra

¹³C NMR 2-(3-((3-Propoxyphenyl)(methyl)amino)propyl)isoindoline-1,3-dione (120)



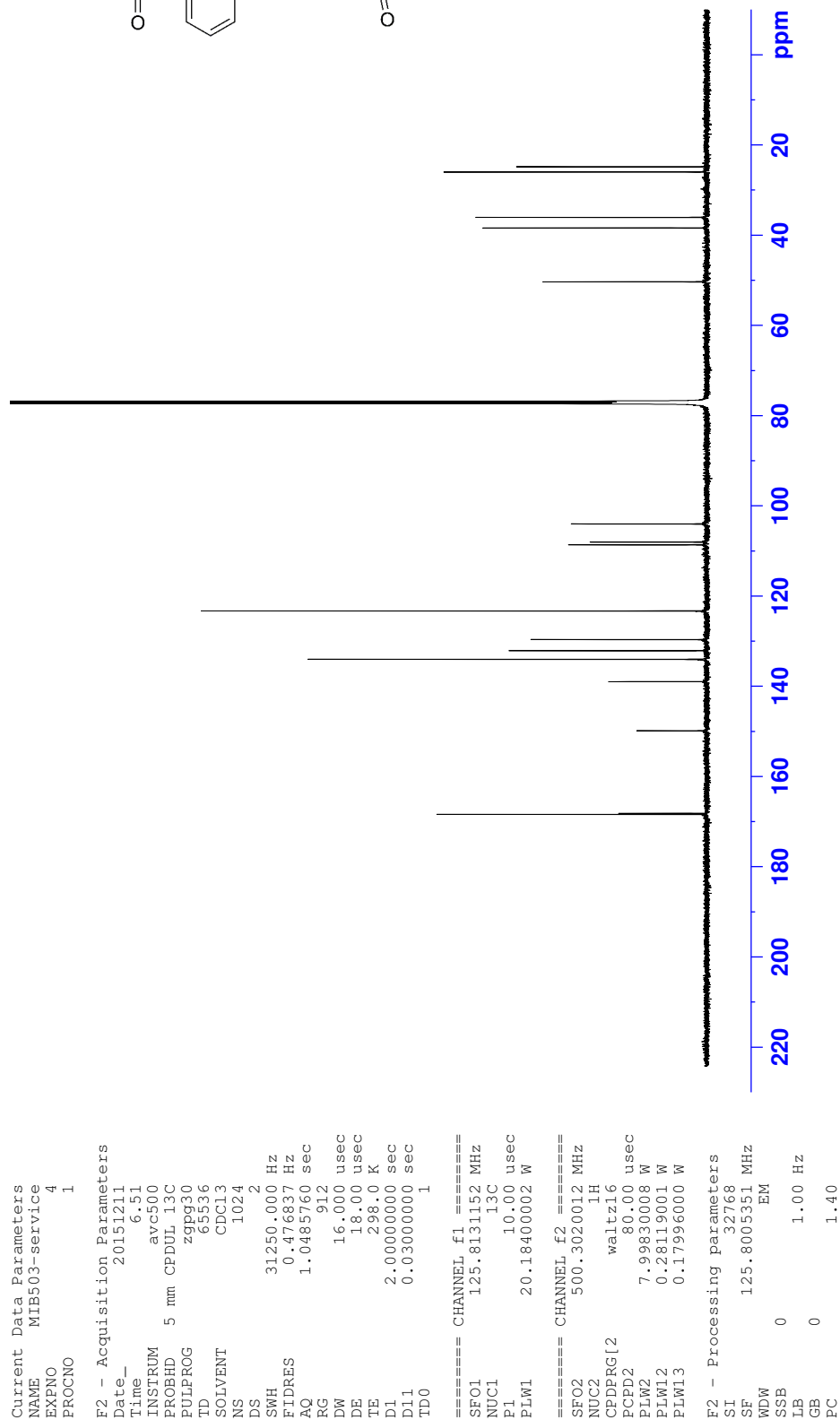
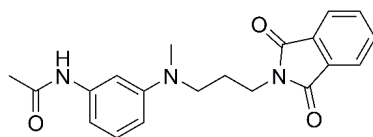
Appendix F: NMR spectra

¹H NMR *N*-(3-((3-(1,3-Dioxisoindolin-2-yl)propyl)(methyl)amino)phenyl)acetamide (**121**)



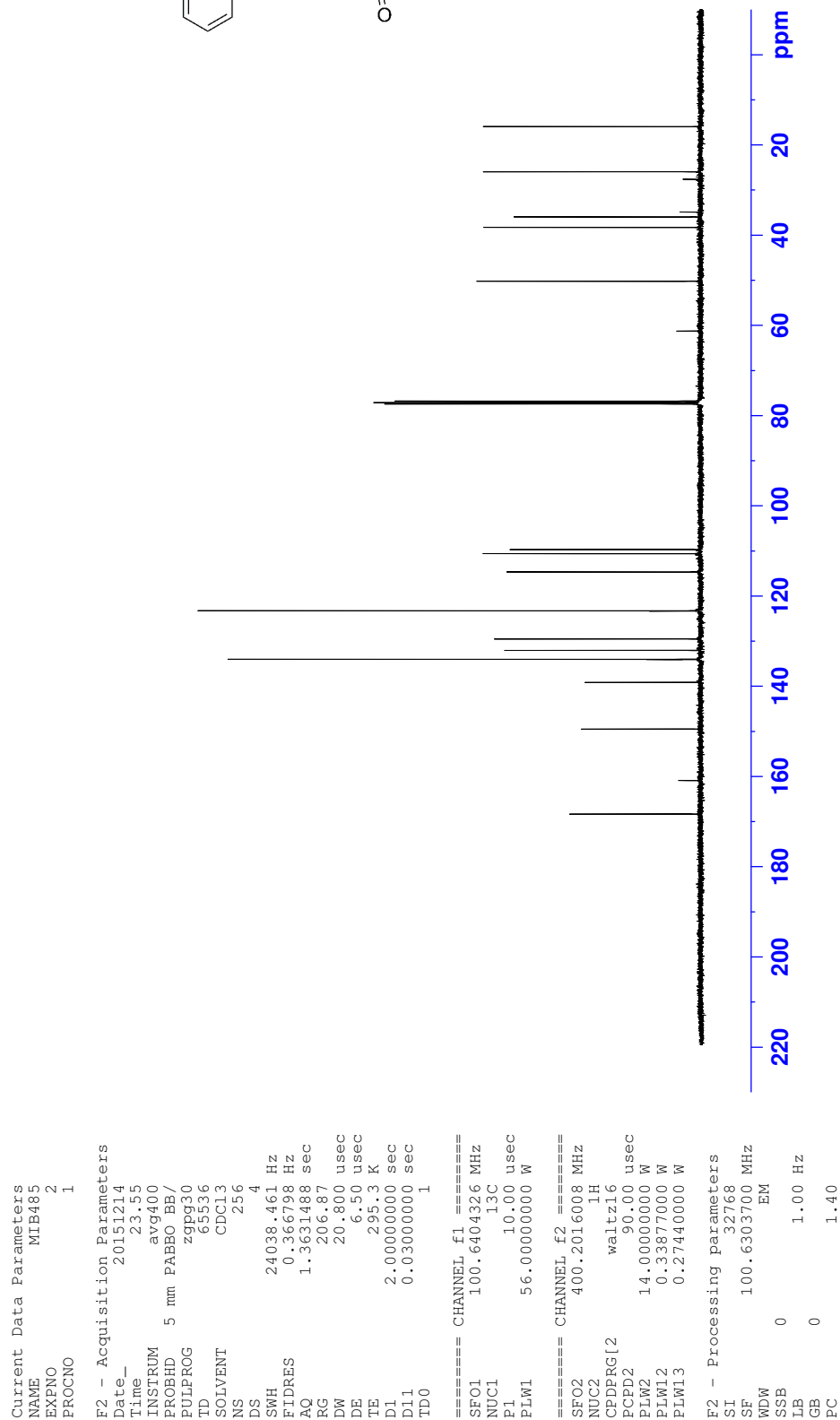
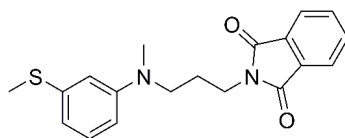
Appendix F: NMR spectra

¹³C NMR *N*-(3-((3-(1,3-Dioxisoindolin-2-yl)propyl)(methyl)amino)phenyl)acetamide (**121**)



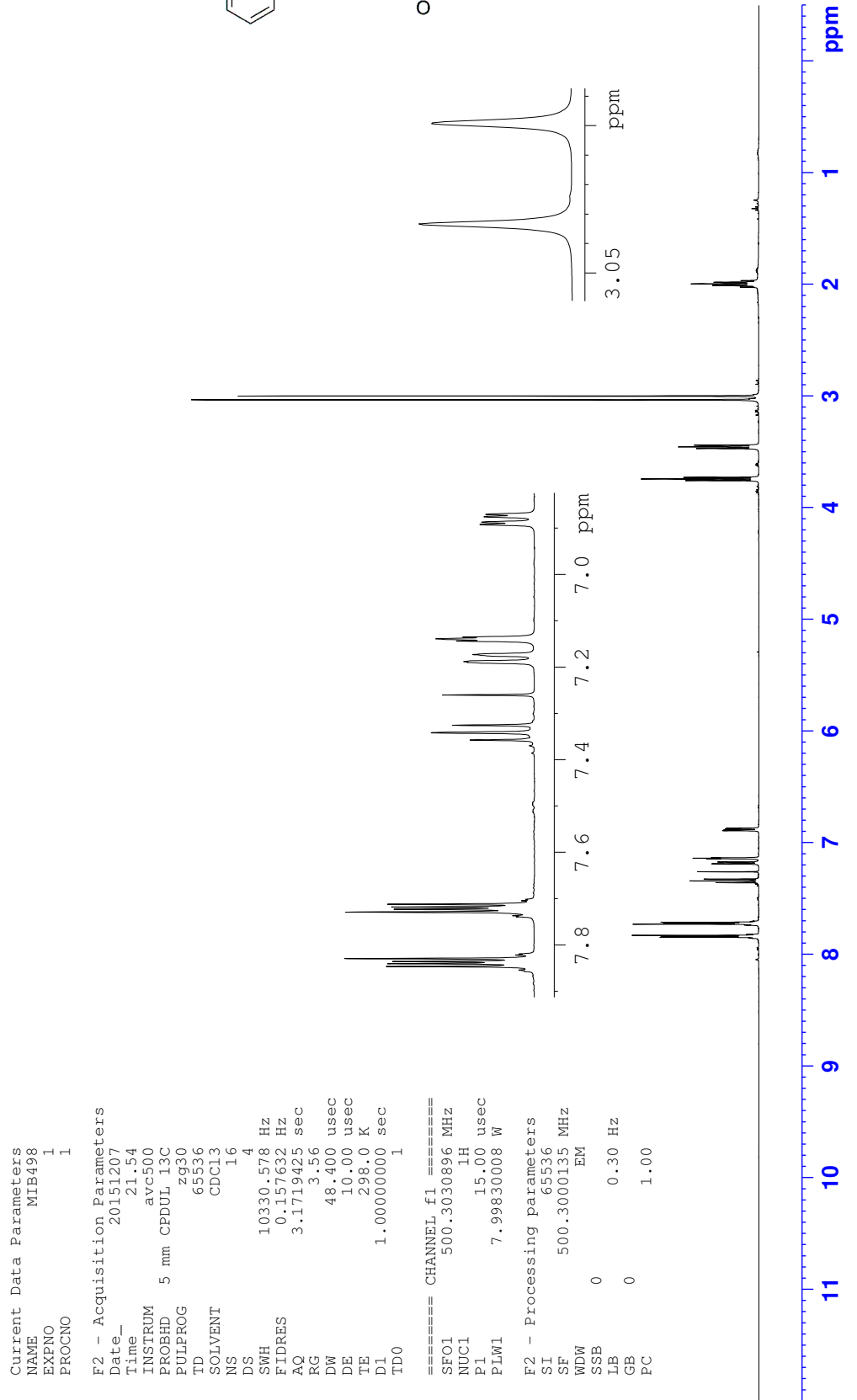
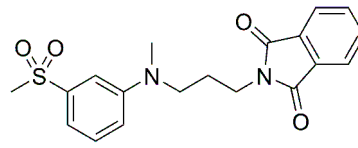
Appendix F: NMR spectra

¹³C NMR 2-(3-(Methyl(3-(methylthio)phenyl)amino)propyl)isoindoline-1,3-dione (122)



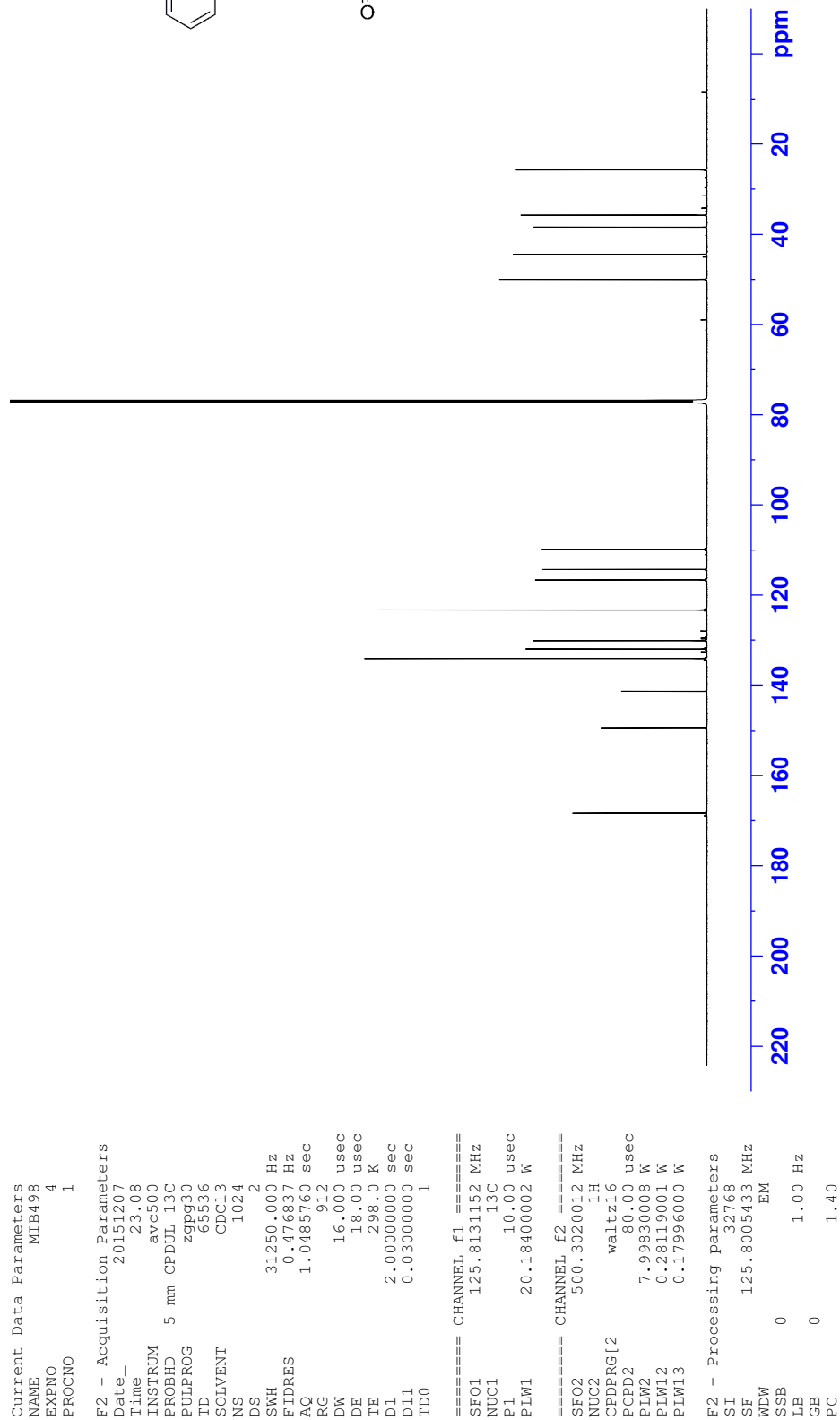
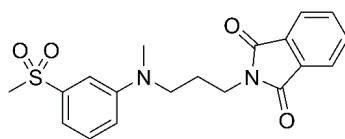
Appendix F: NMR spectra

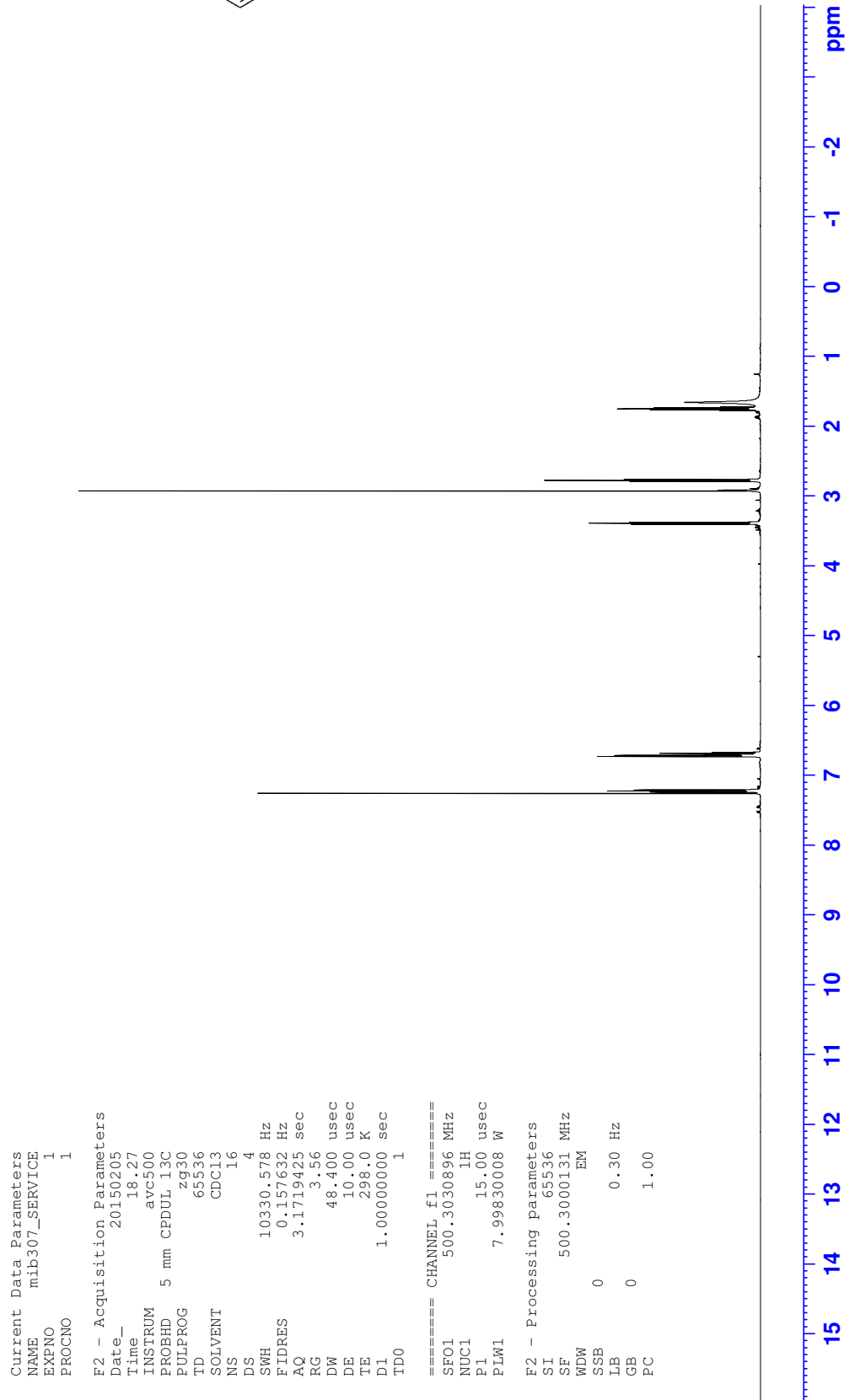
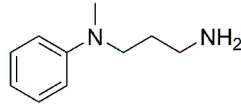
¹H NMR 2-(3-(Methyl(3-(methylsulfonyl)phenyl)amino)propyl)isoindoline-1,3-dione (**123**)



Appendix F: NMR spectra

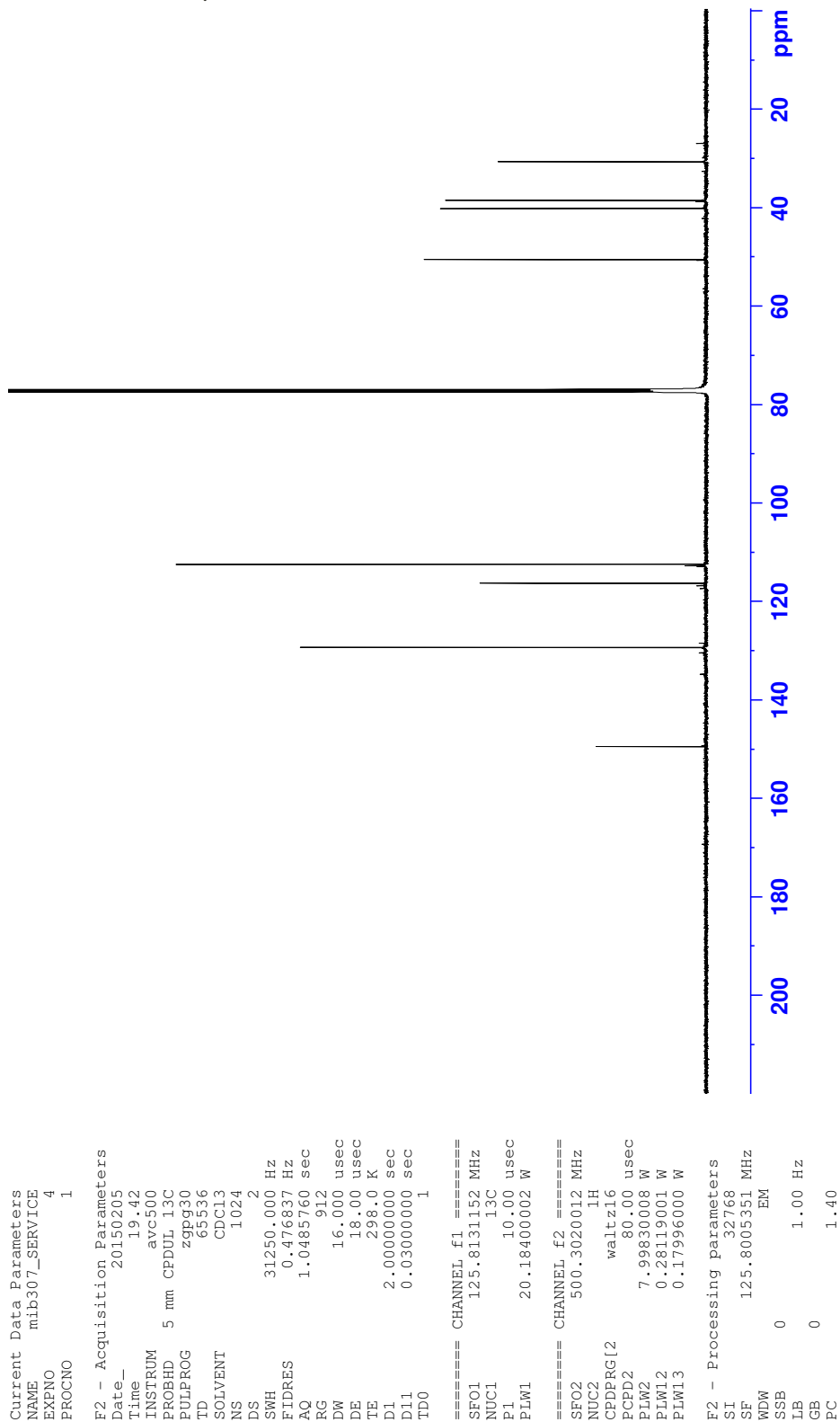
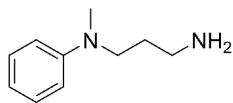
¹³C NMR 2-(3-(Methyl(3-(methylsulfonyl)phenyl)amino)propyl)isoindoline-1,3-dione (**123**)

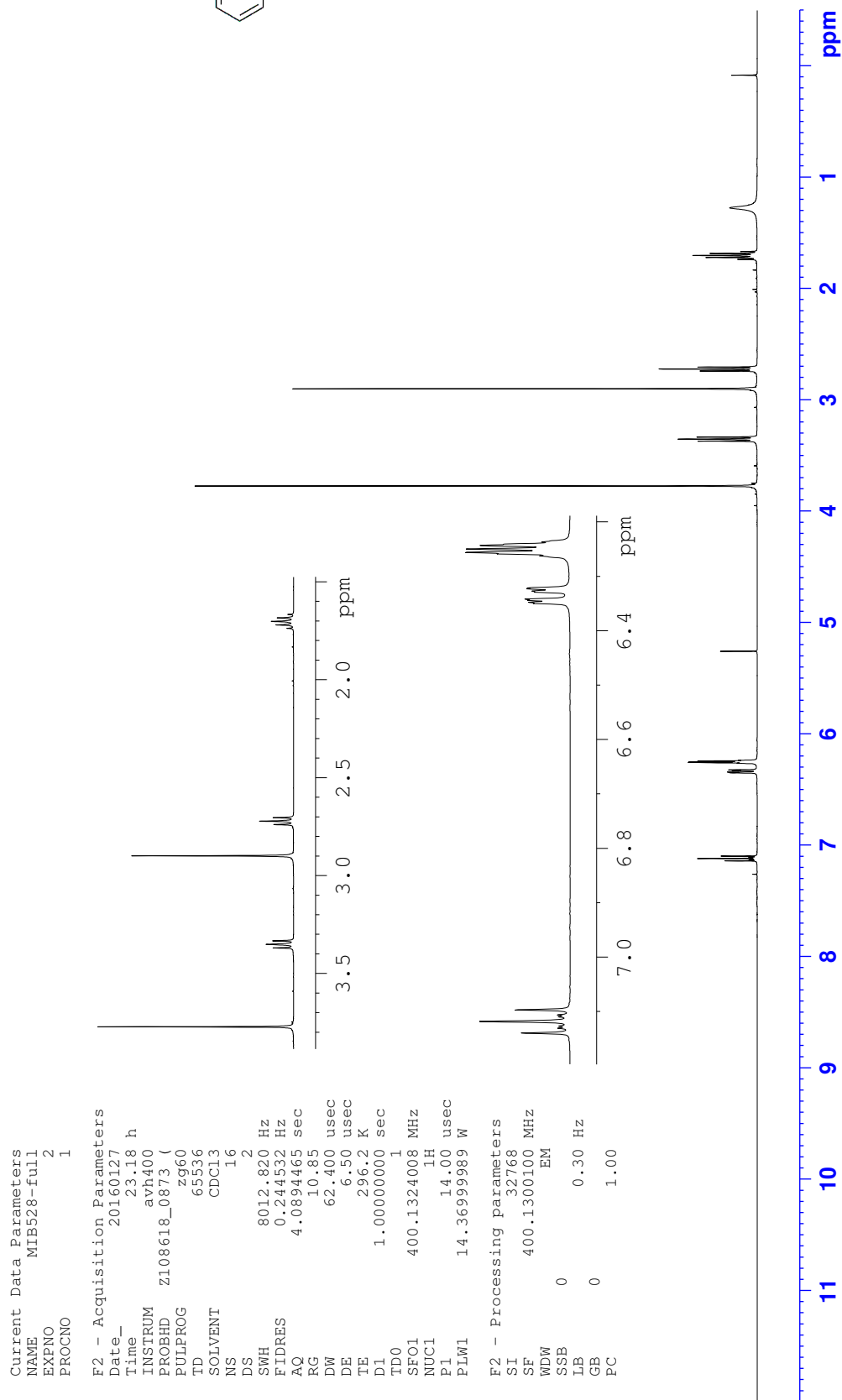
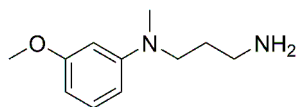


¹H NMR *N*-1-Methyl-*N*-1-phenylpropane-1,3-diamine (**126**)

Appendix F: NMR spectra

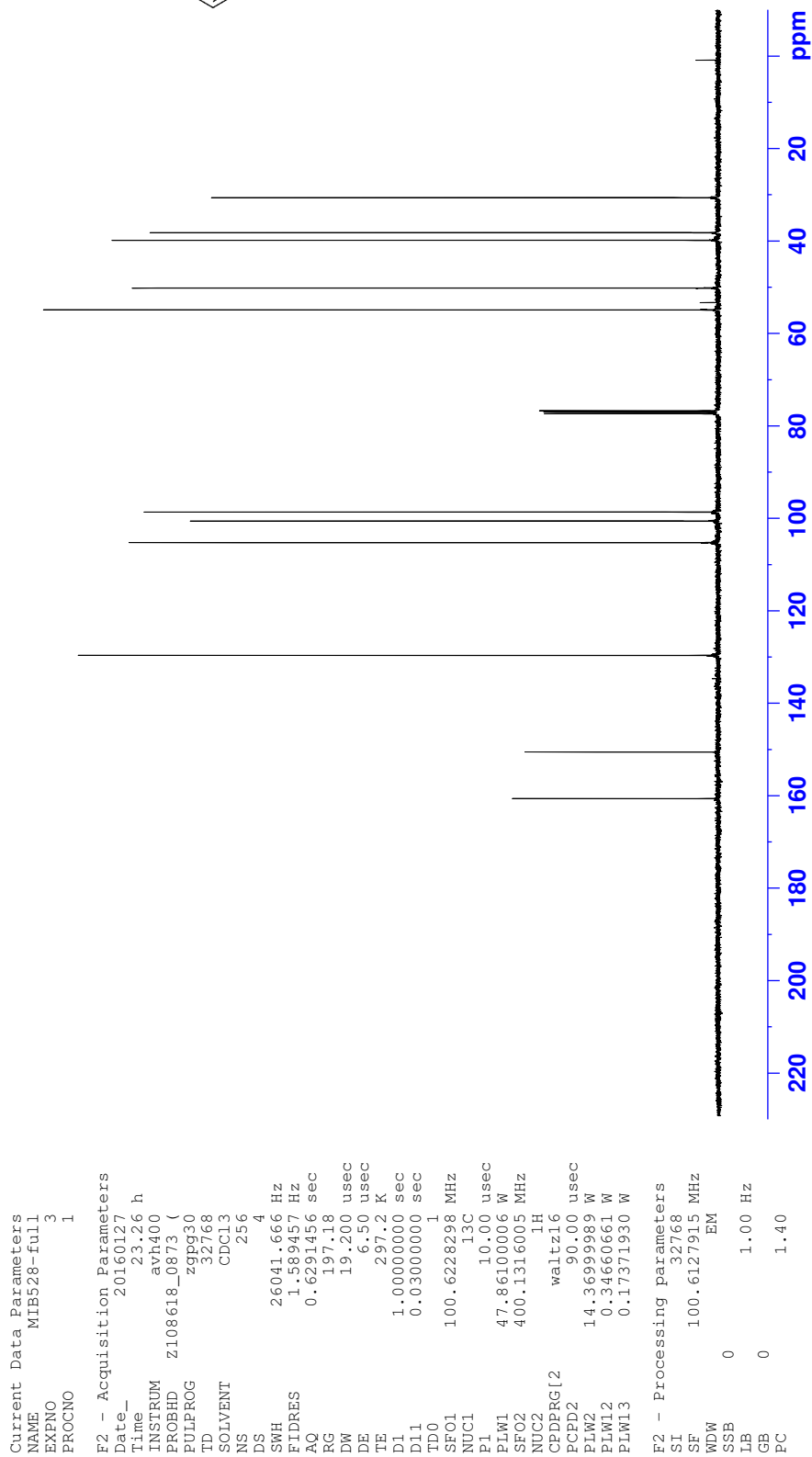
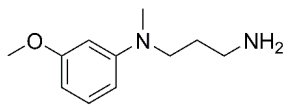
¹³C NMR *N*-1-Methyl-*N*-1-phenylpropane-1,3-diamine (**126**)

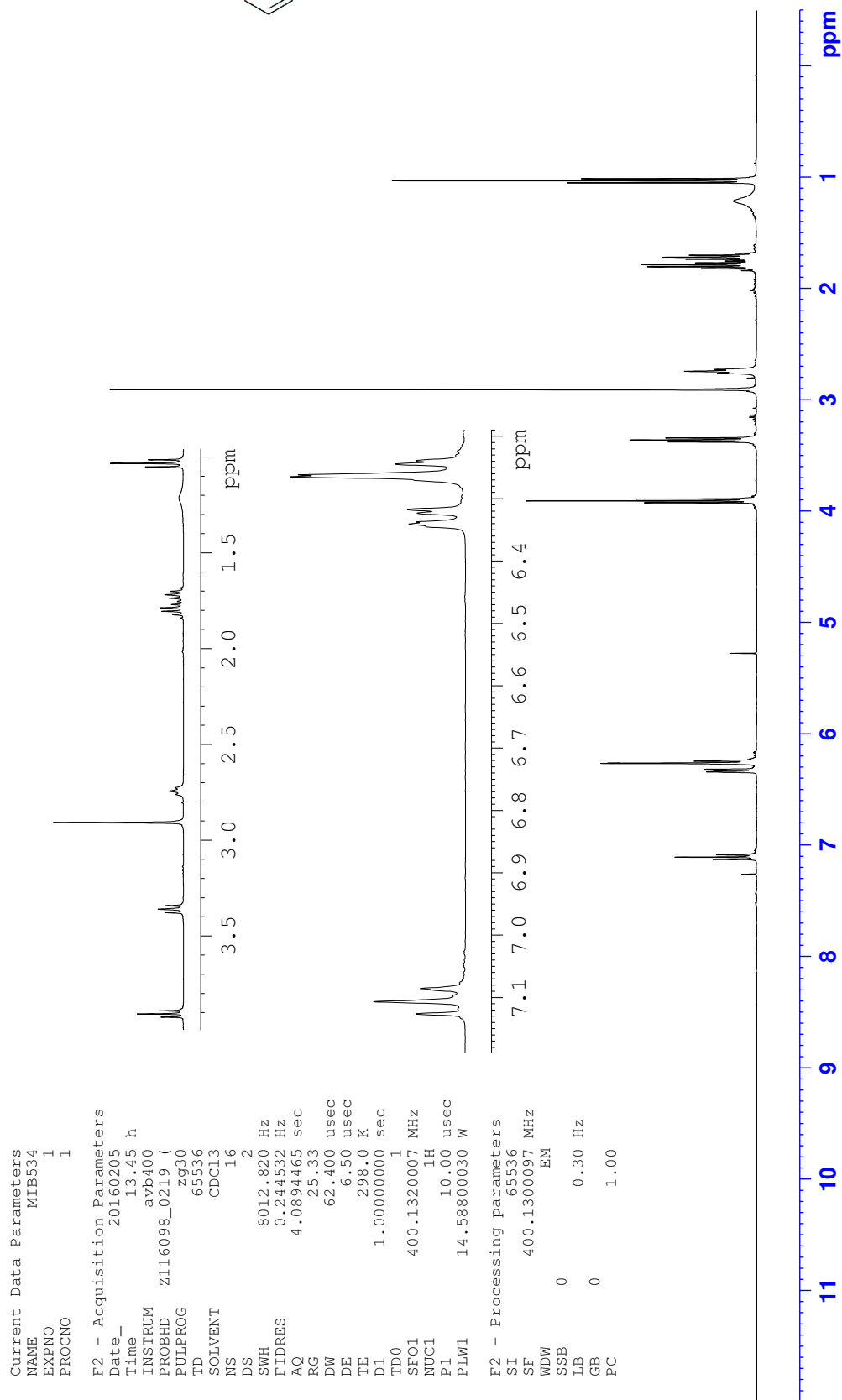
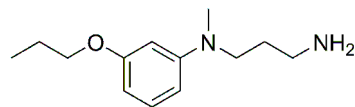


¹H NMR *N*1-(3-Methoxyphenyl)-*N*1-methylpropane-1,3-diamine (**127**)

Appendix F: NMR spectra

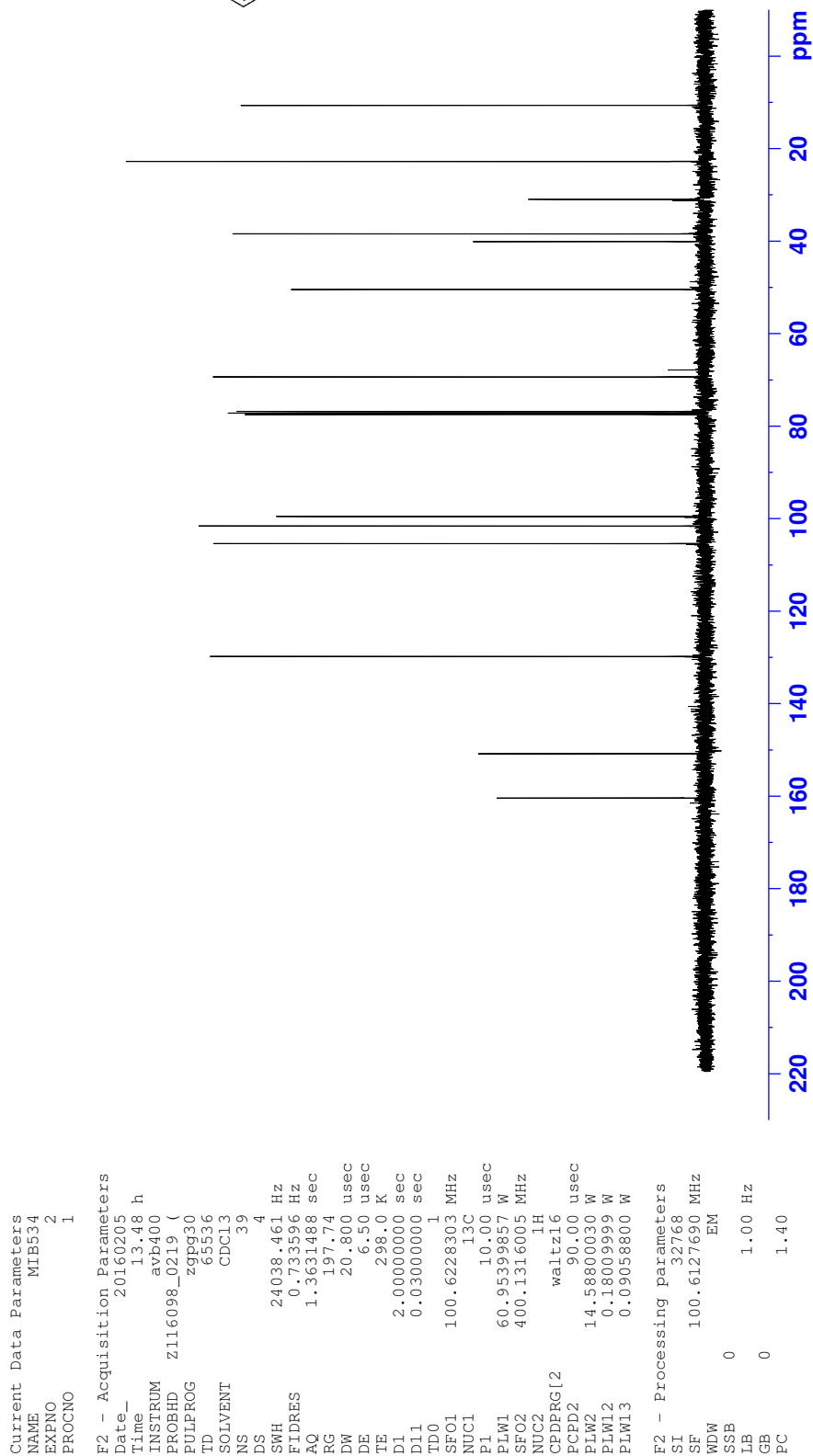
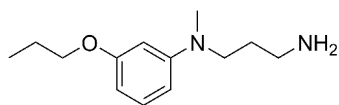
¹³C NMR N1-(3-Methoxyphenyl)-N1-methylpropane-1,3-diamine (127)

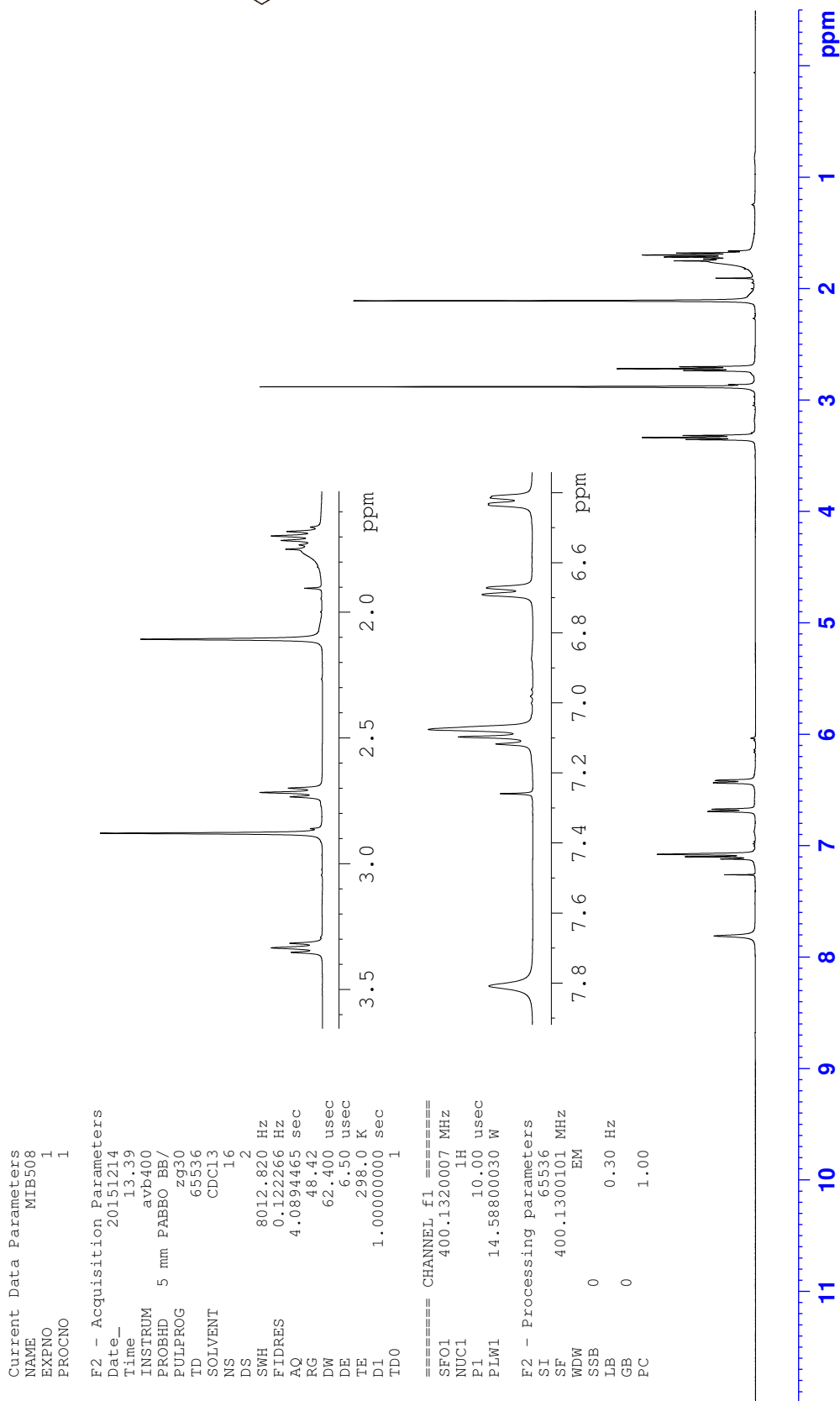
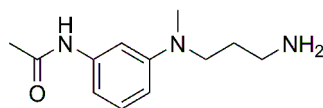


¹H NMR *N*1-(3-Propoxyphenyl)-*N*1-methylpropane-1,3-diamine (**128**)

Appendix F: NMR spectra

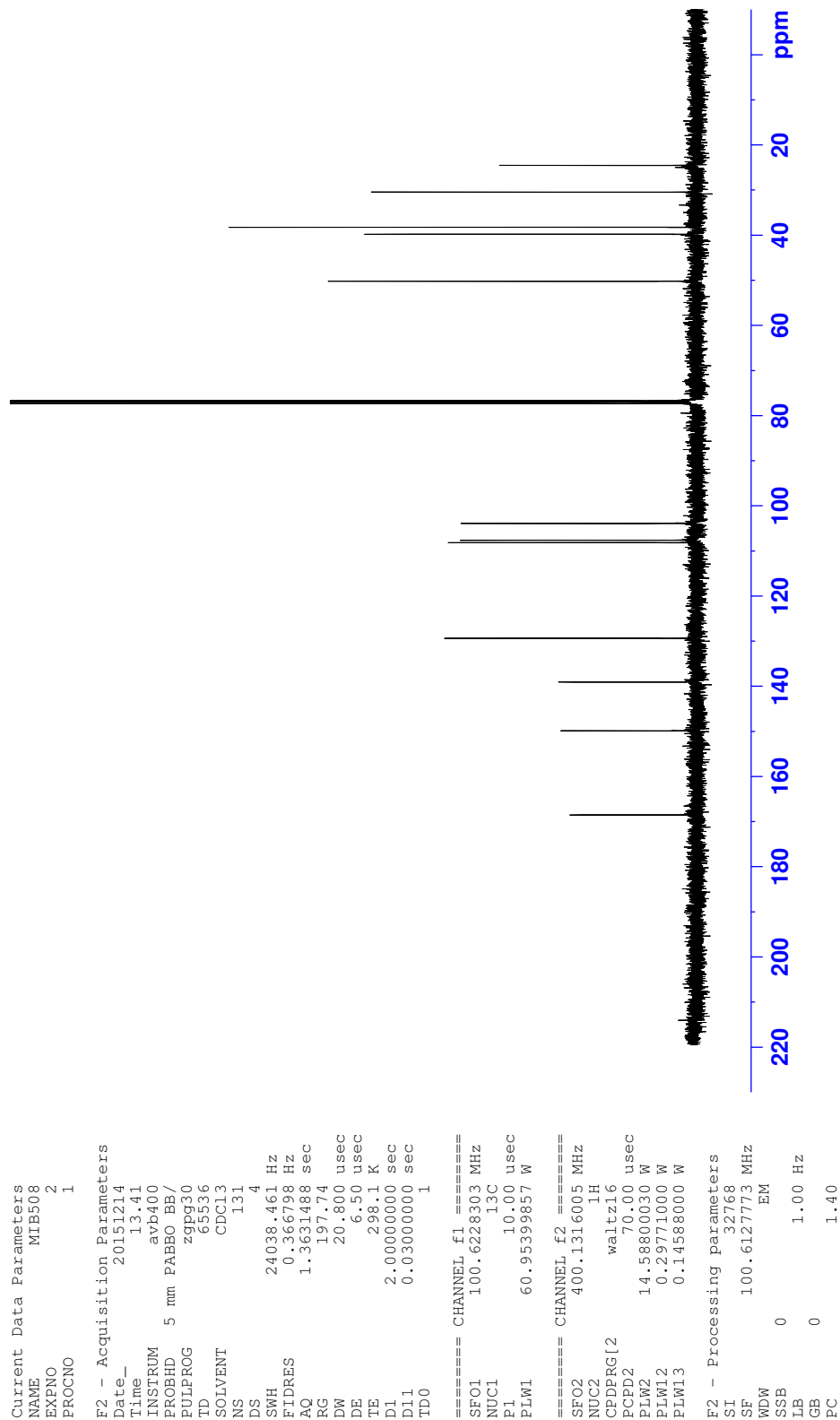
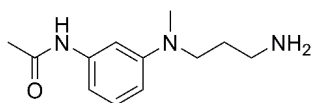
¹³C NMR *N*1-(3-Propoxyphenyl)-*N*1-methylpropane-1,3-diamine (**128**)

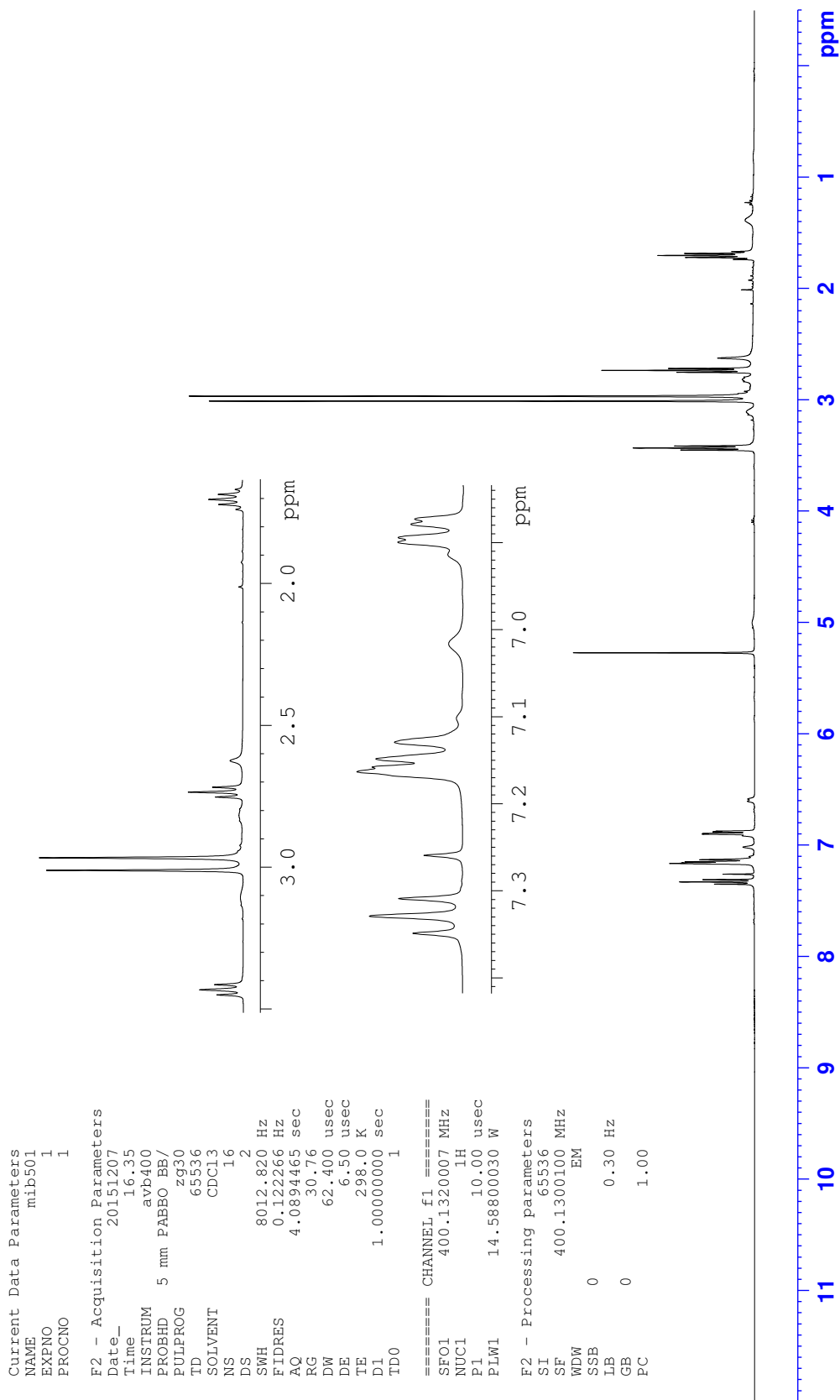
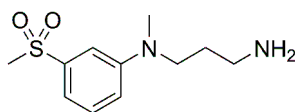


¹H NMR *N*-(3-((3-Aminopropyl)(methyl)amino)phenyl)acetamide (**129**)

Appendix F: NMR spectra

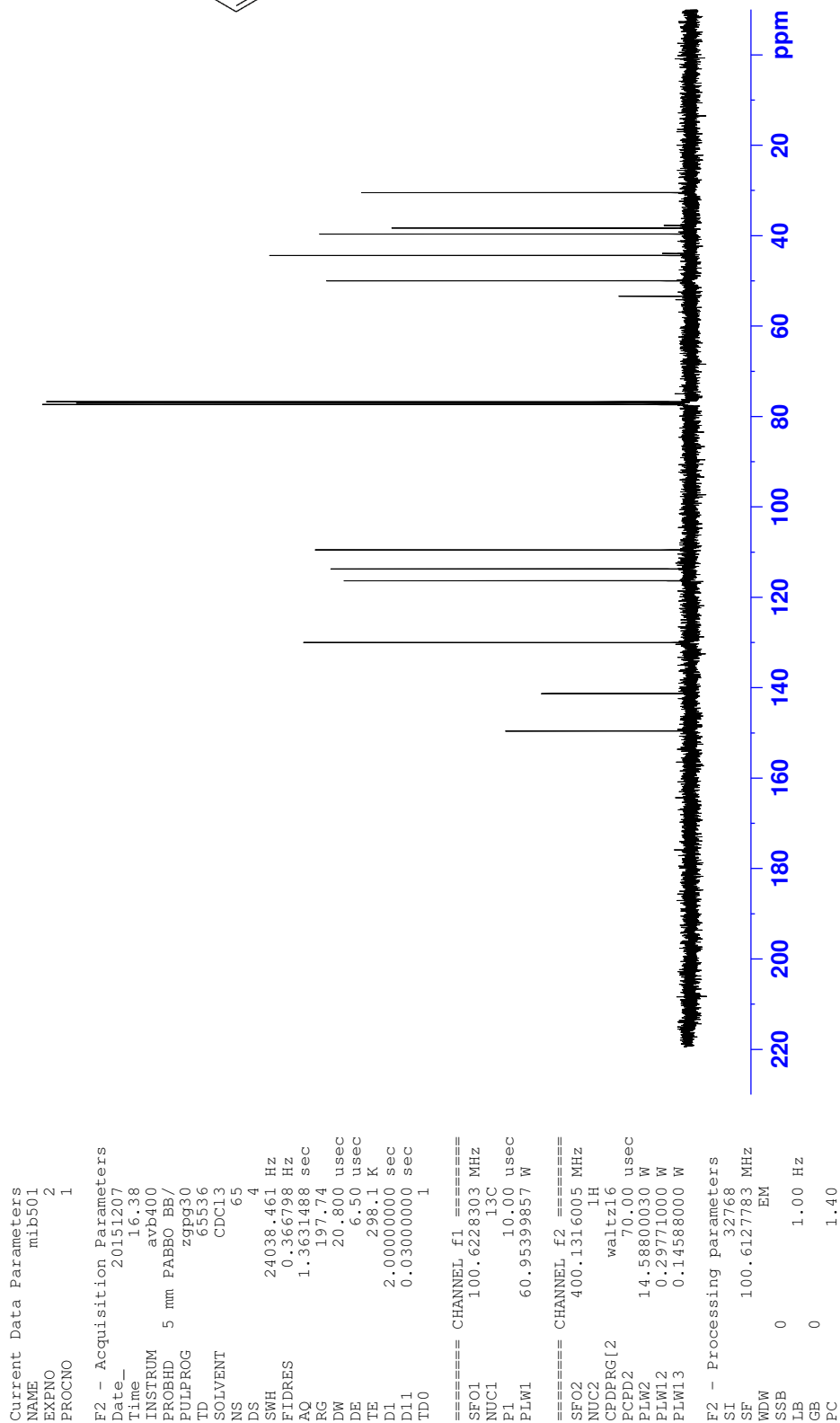
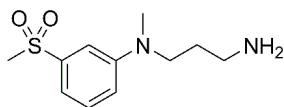
¹³C NMR *N*-(3-((3-Aminopropyl)(methyl)amino)phenyl)acetamide (**129**)



¹H NMR *N*-1-Methyl-*N*-(3-(methylsulfonyl)phenyl)propane-1,3-diamine (**130**)

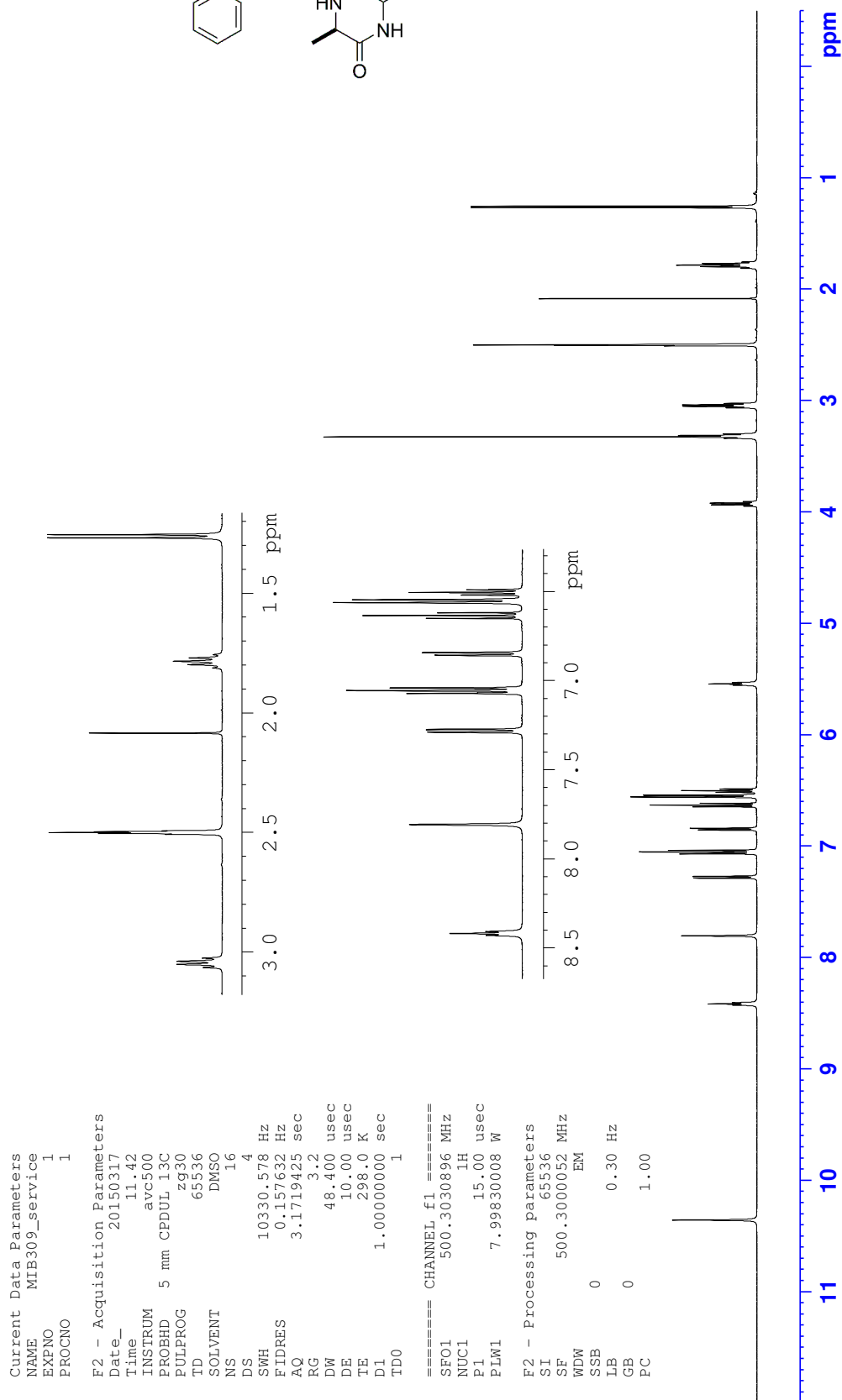
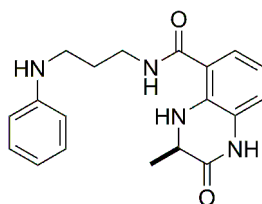
Appendix F: NMR spectra

¹³C NMR *N*-1-Methyl-*N*-(3-(methylsulfonyl)phenyl)propane-1,3-diamine (**130**)



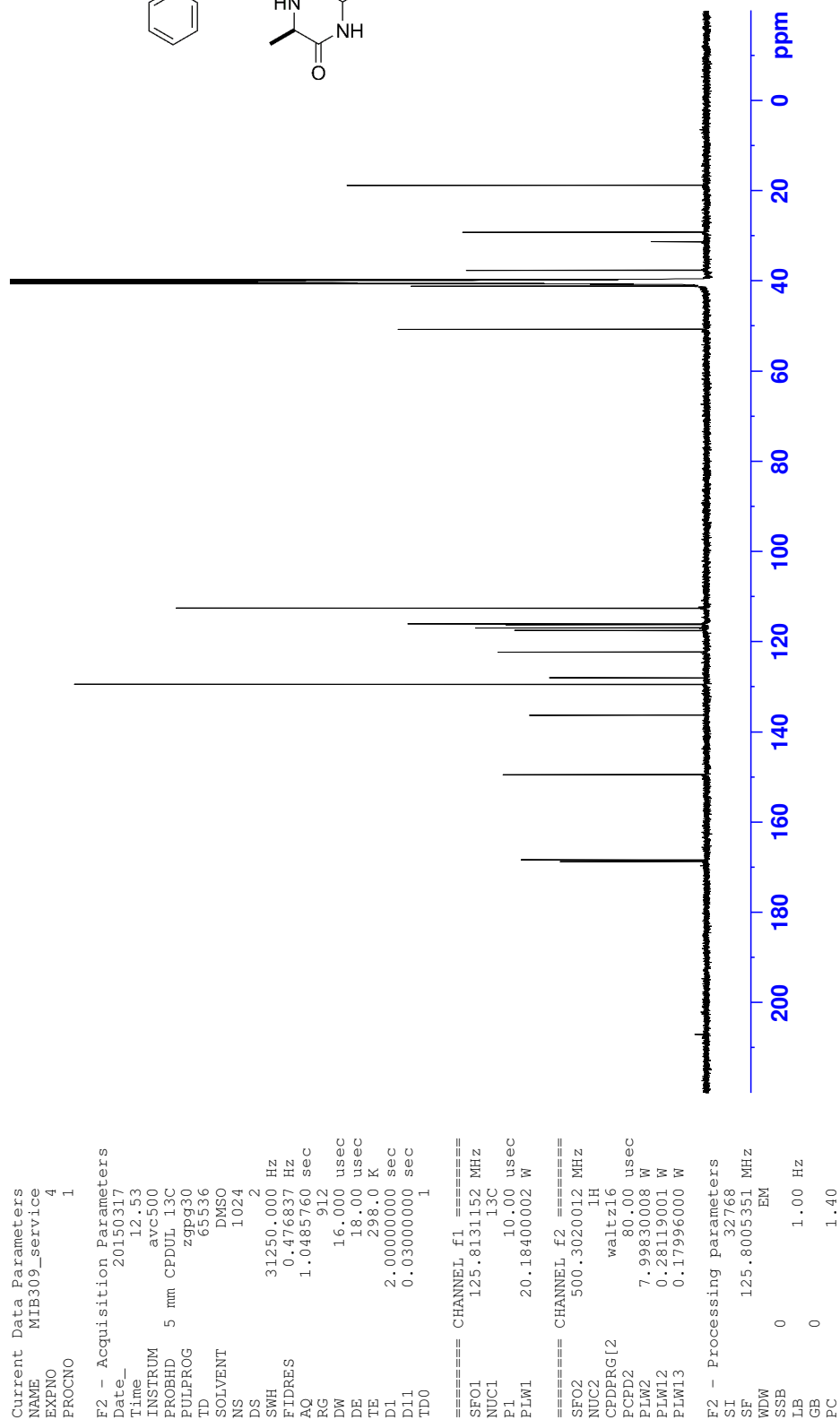
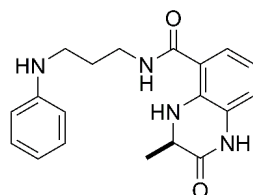
Appendix F: NMR spectra

¹H NMR (*R*)-3-Methyl-2-oxo-*N*-(3-(phenylamino)propyl)-1,2,3,4-tetrahydroquinoxaline-5-carboxamide (**98**)



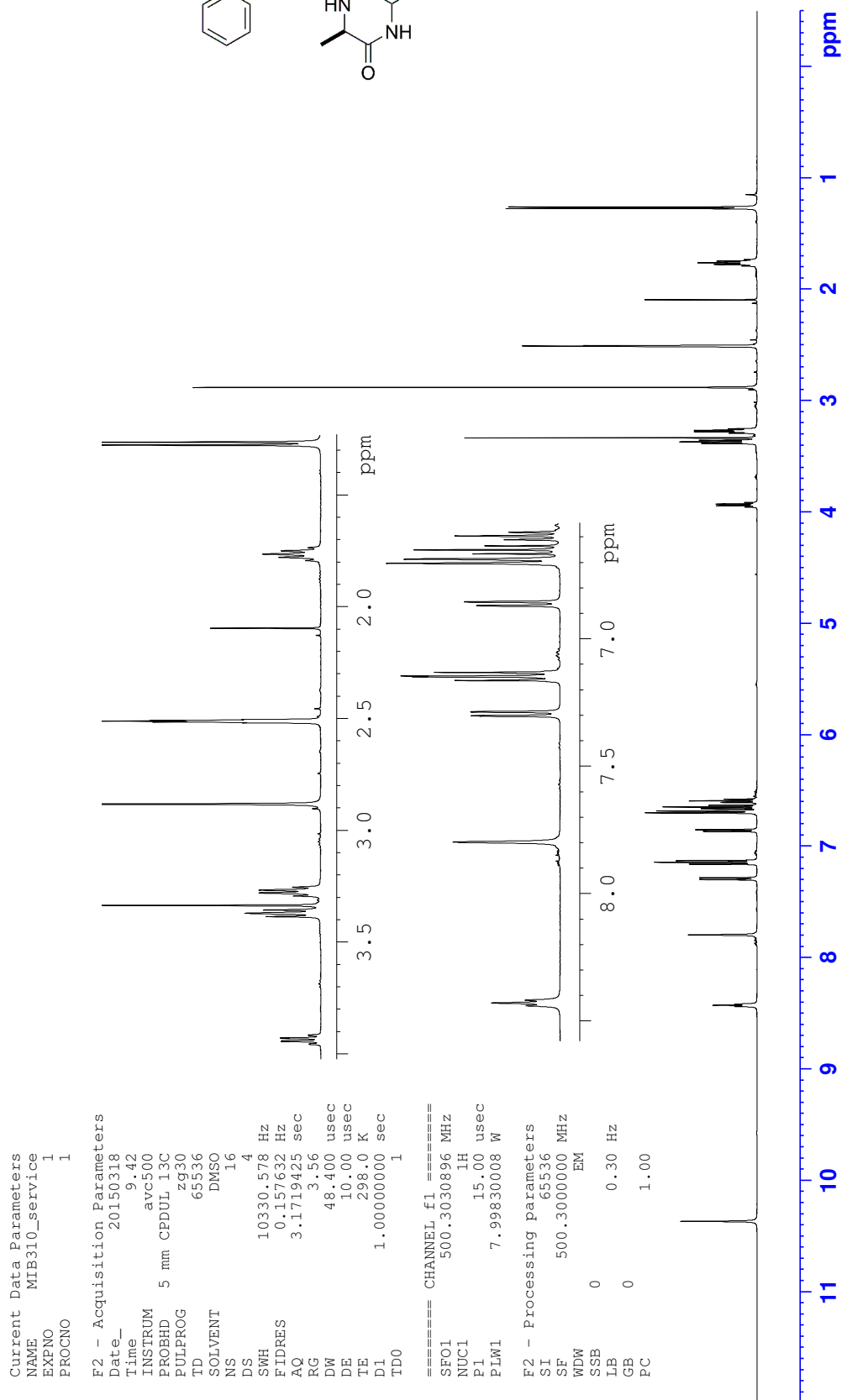
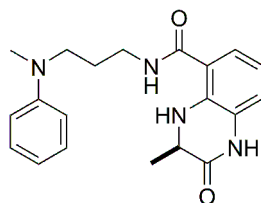
Appendix F: NMR spectra

¹³C NMR (*R*)-3-Methyl-2-oxo-*N*-(3-(phenylamino)propyl)-1,2,3,4-tetrahydroquinoxaline-5-carboxamide (**98**)



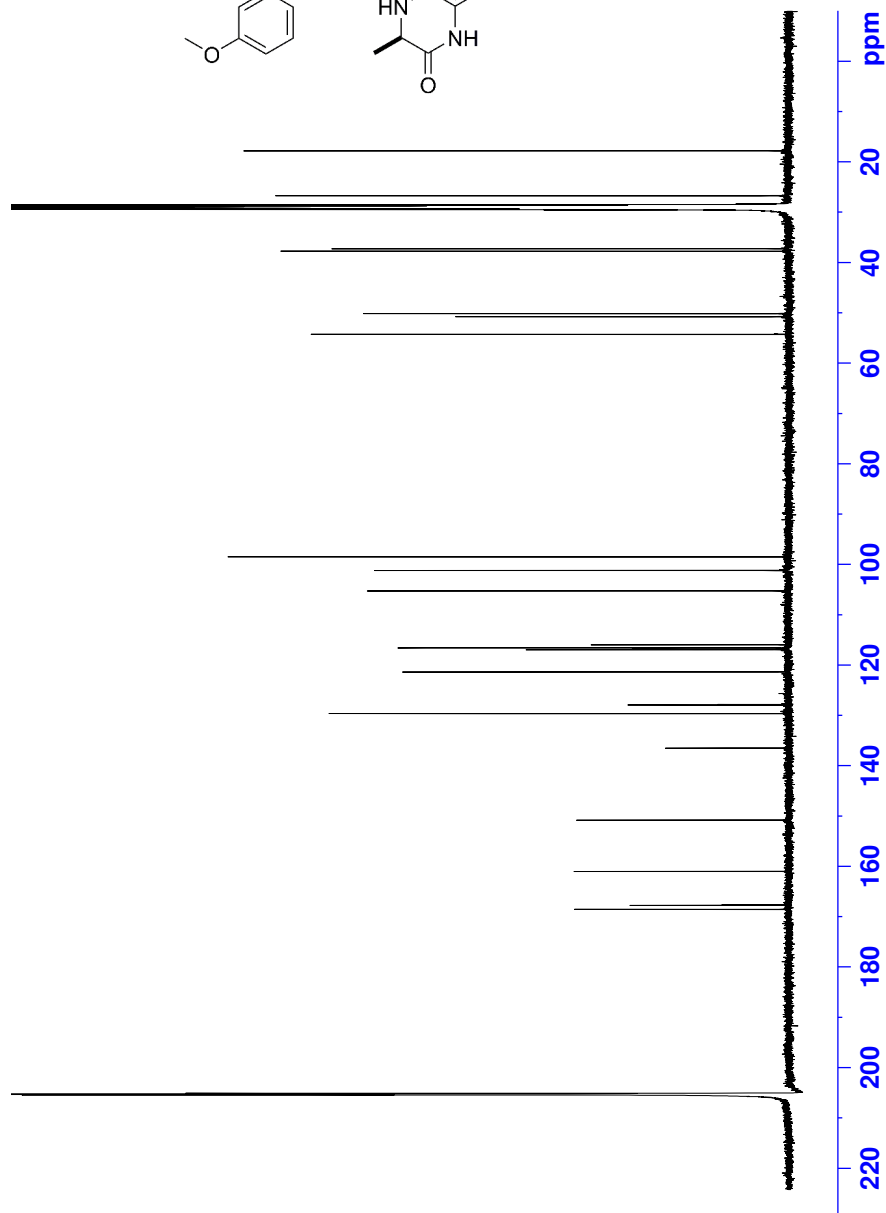
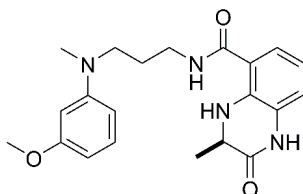
Appendix F: NMR spectra

¹H NMR (R)-3-Methyl-N-(3-(methyl(phenyl)amino)propyl)-2-oxo-1,2,3,4-tetrahydroquinoxaline-5-carboxamide (**99**)



Appendix F: NMR spectra

¹³C NMR (*R*)-*N*-(3-((3-Methoxyphenyl)(methyl)amino)propyl)-3-methyl-2-oxo-1,2,3,4-tetrahydroquinoxaline-5-carboxamide (**100**)



```

Current Data Parameters
NAME      MIB535-service
EXPNO     4
PROCNO    1

F2 - Acquisition Parameters
Date_     20160226
Time      12.48
INSTRUM   avc500
PROBHD    5 mm CPDUL 13C
PULPROG   zgpg30
TD         65536
SOLVENT    Acetone
NS         3072
DS         2
SWH        31250.000 Hz
FIDRES     0.476837 Hz
AQ         1.0485760 sec
RG         912
DM         16.000 usec
DE         18.000 usec
TE         298.0 K
D1         2.00000000 sec
D11        0.03000000 sec
TD0        1

===== CHANNEL f1 =====
SF01      125.8131152 MHz
NUC1       13C
P1         10.00 usec
PLW1       20.18400002 W

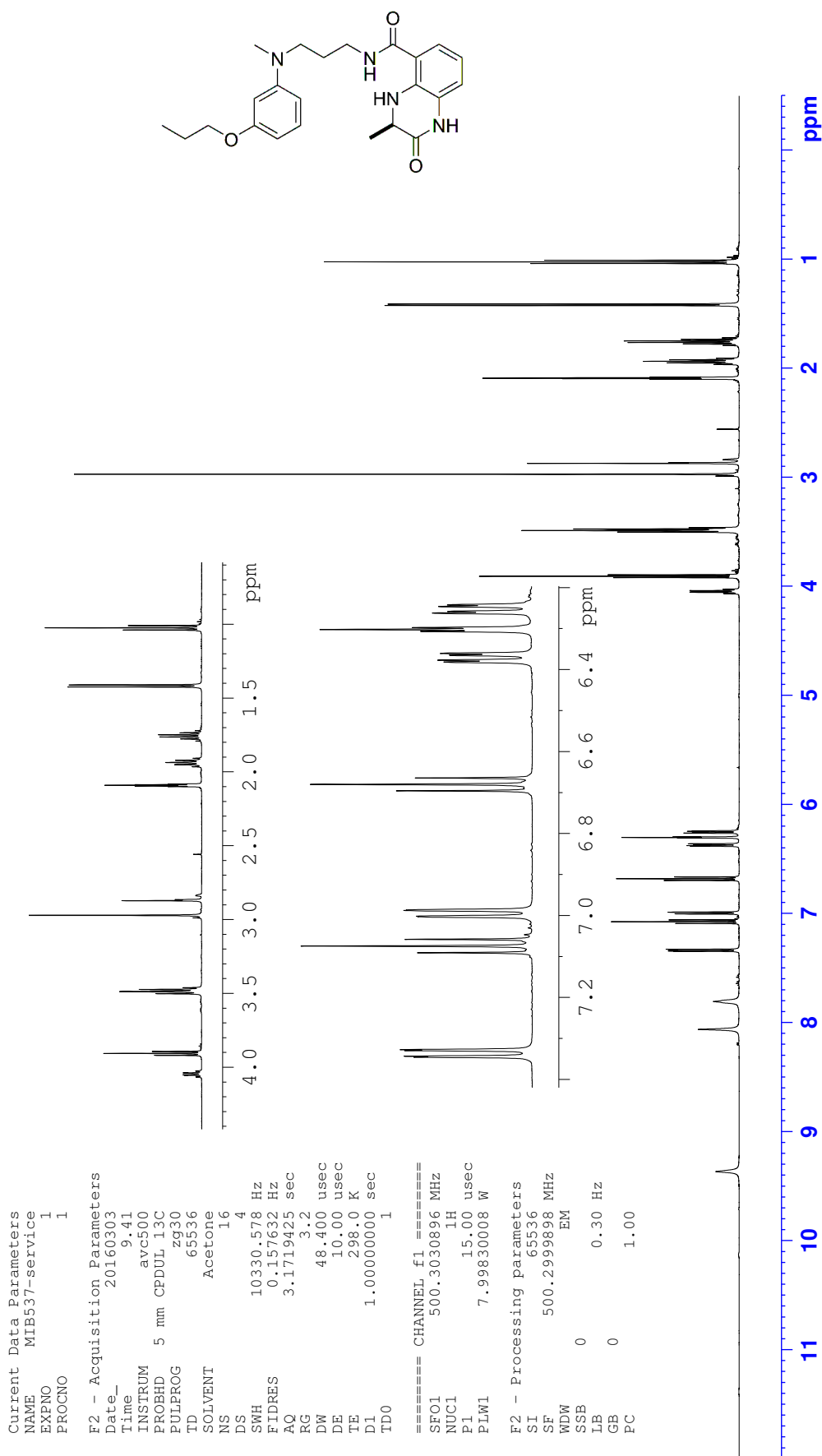
===== CHANNEL f2 =====
SF02      500.3020012 MHz
NUC2       1H
P2         10.00 usec
PLW2       20.18400002 W

===== CHANNEL f3 =====
SF03      7.99830008 W
NUC3       13C
P3         10.00 usec
PLW3       20.18400002 W

F2 - Processing parameters
SI         32768
SF         125.8005351 MHz
WDW        EM
SSB        0
LB         1.00 Hz
GB         0
PC         1.40
    
```

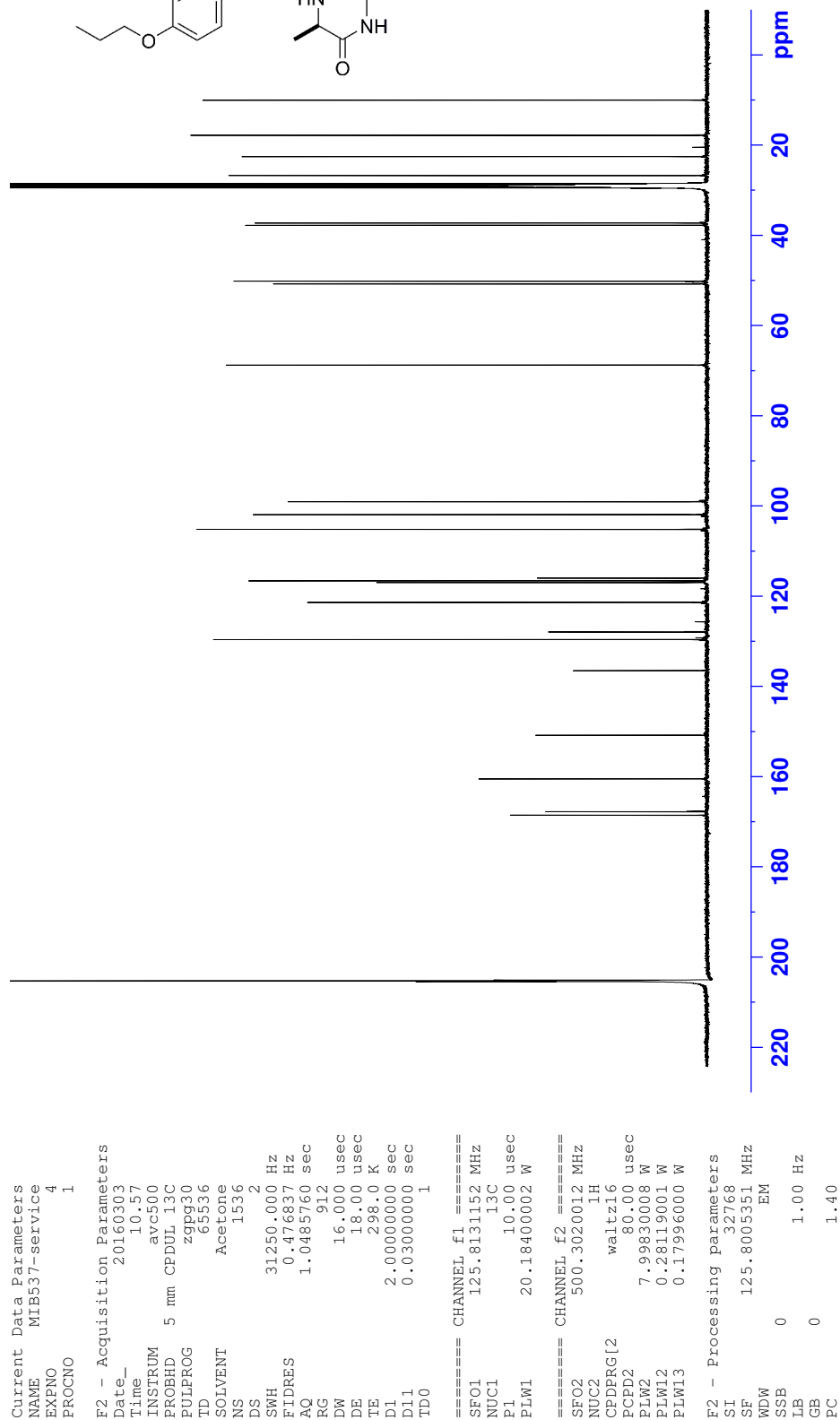
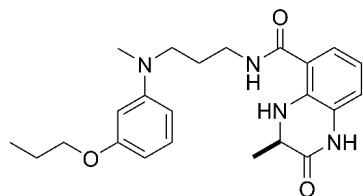
Appendix F: NMR spectra

¹H NMR (*R*)-*N*-(3-((3-Propoxyphenyl)(methyl)amino)propyl)-3-methyl-2-oxo-1,2,3,4-tetrahydroquinoxaline-5-carboxamide (**101**)



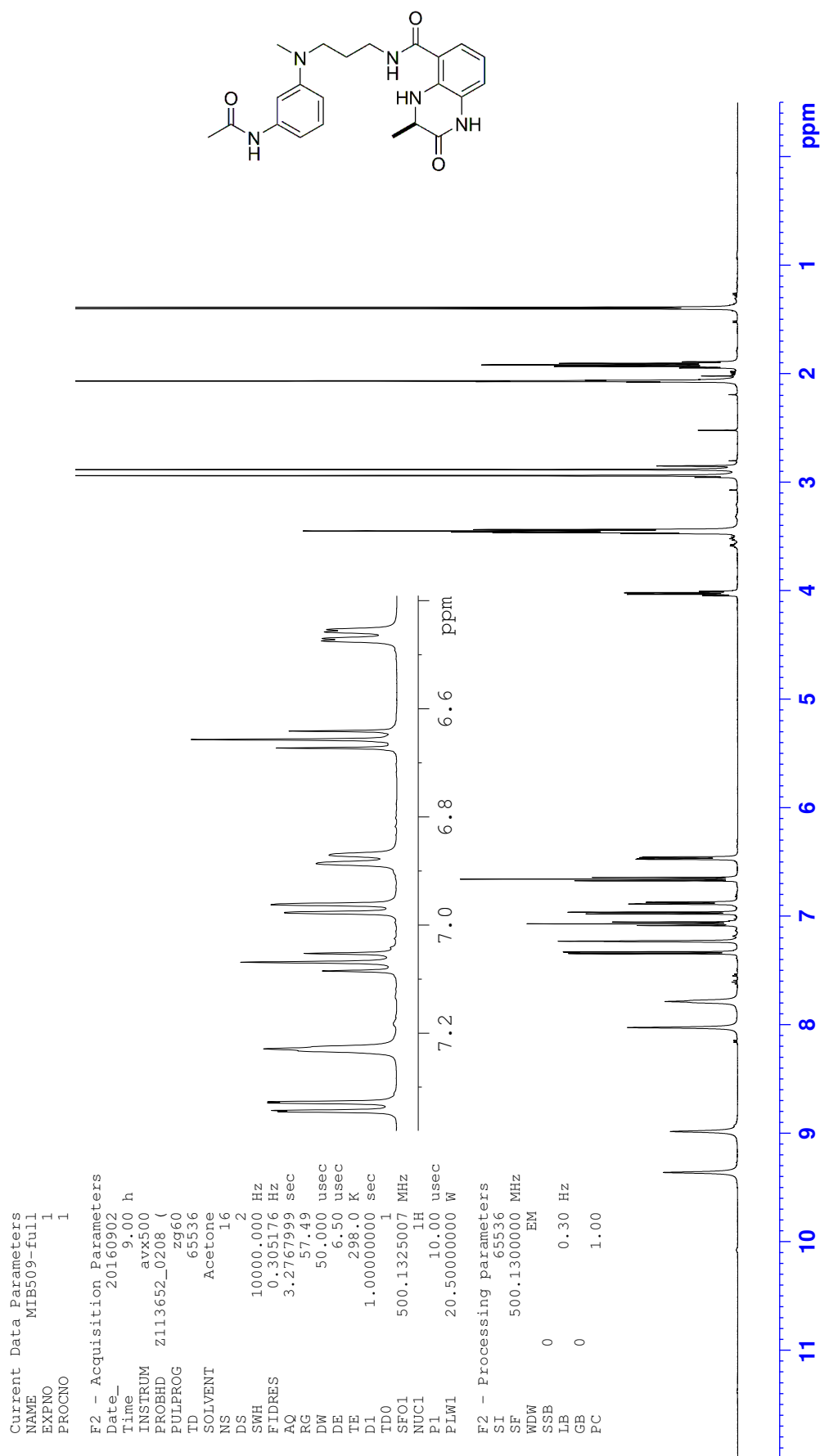
Appendix F: NMR spectra

¹³C NMR (R)-N-(3-((3-Propoxyphenyl)(methyl)amino)propyl)-3-methyl-2-oxo-1,2,3,4-tetrahydroquinoxaline-5-carboxamide (**101**)



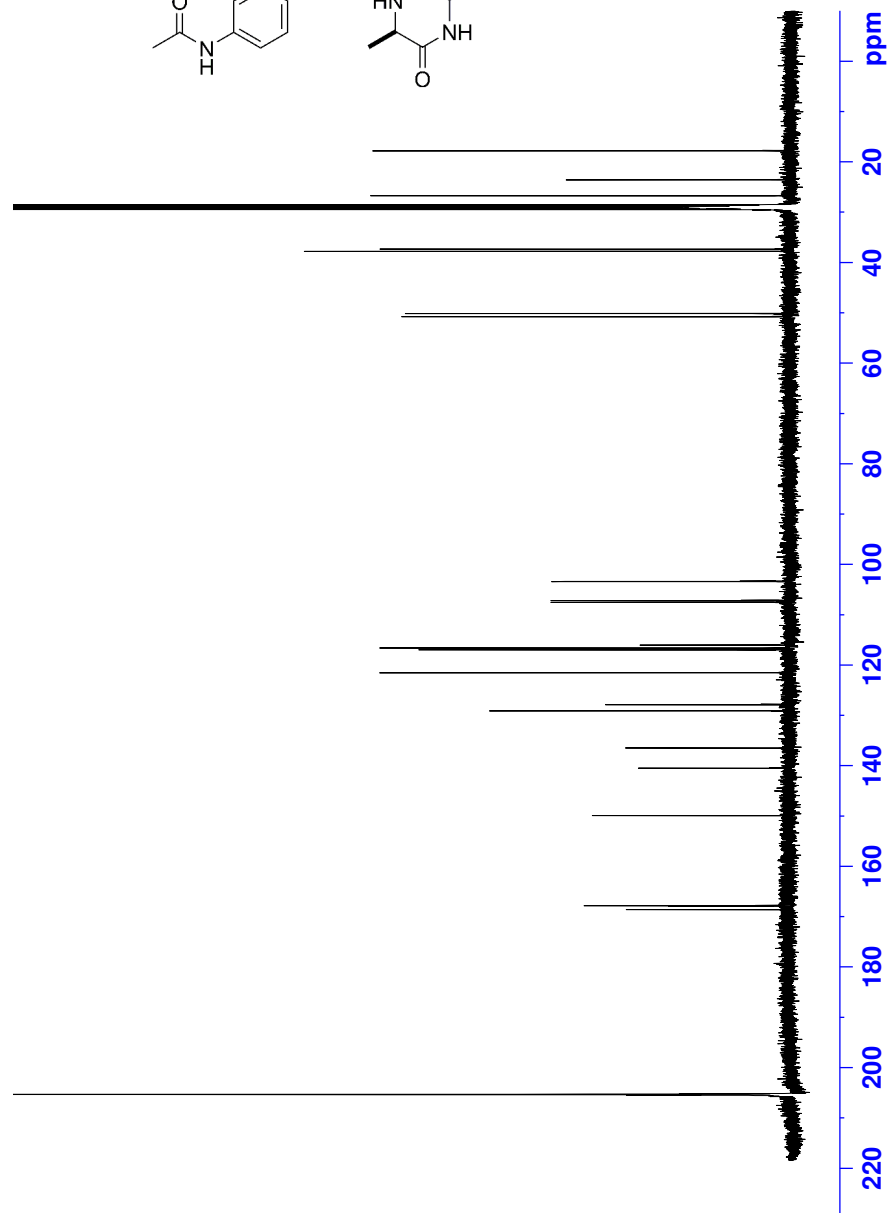
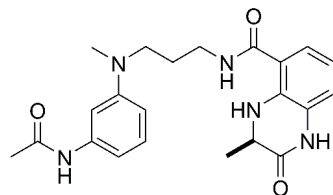
Appendix F: NMR spectra

¹H NMR (*R*)-*N*-(3-((3-Acetamidophenyl)(methyl)amino)propyl)-3-methyl-2-oxo-1,2,3,4-tetrahydroquinoxaline-5-carboxamide (**102**)



Appendix F: NMR spectra

¹³C NMR (*R*)-*N*-(3-((3-Acetamidophenyl)(methyl)amino)propyl)-3-methyl-2-oxo-1,2,3,4-tetrahydroquinoxaline-5-carboxamide (**102**)



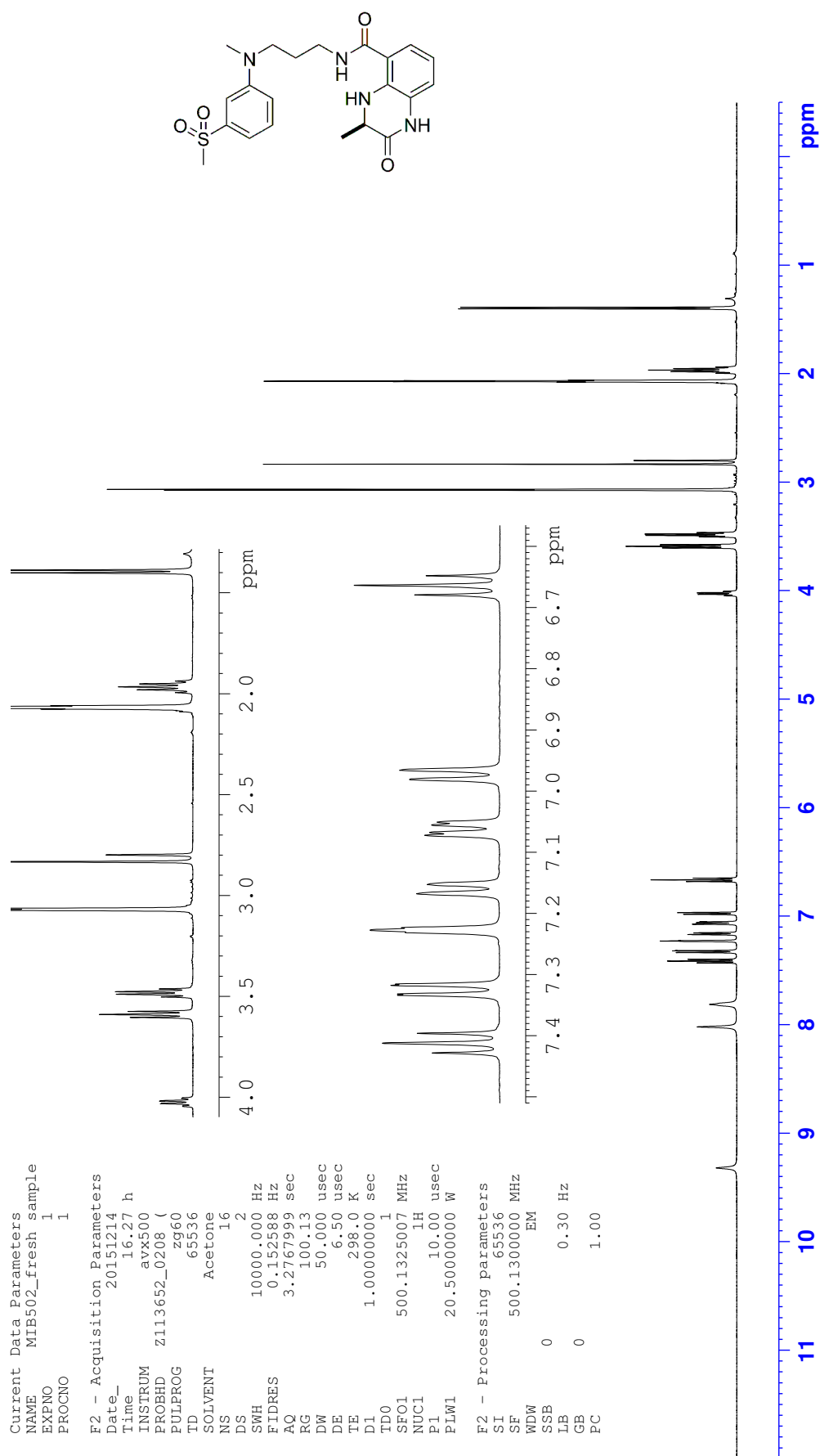
Current Data Parameters
 NAME MIB509-full
 EXPNO 2
 PROCNO 1

F2 - Acquisition Parameters
 Date_ 20160902
 Time 9.55 h
 INSTRUM avx500
 PROBHD z113652_0208 (zppg30
 FULPROG zppg30
 TD 65536
 SOLVENT Acetone
 NS 1024
 DS 4
 SWH 29761.904 Hz
 FIDRES 0.908261 Hz
 AQ 1.1010048 sec
 RG 191.37
 DM 16.800 usec
 DE 6.50 usec
 TE 298.0 K
 D1 2.00000000 sec
 D11 0.03000000 sec
 TD0 1
 SFO1 125.7703643 MHz
 NUC1 13C
 P1 10.00 usec
 PLW1 76.00000000 W
 SFO2 500.1320005 MHz
 NUC2 1H
 CPDPRG12 waltz16
 FCPD2 80.00 usec
 PLW2 20.50000000 W
 PLW12 0.32031000 W
 PLW13 0.16111000 W

F2 - Processing parameters
 SI 32768
 SF 125.7577885 MHz
 WDW EM
 SSB 0
 LB 1.00 Hz
 GB 0
 PC 1.40

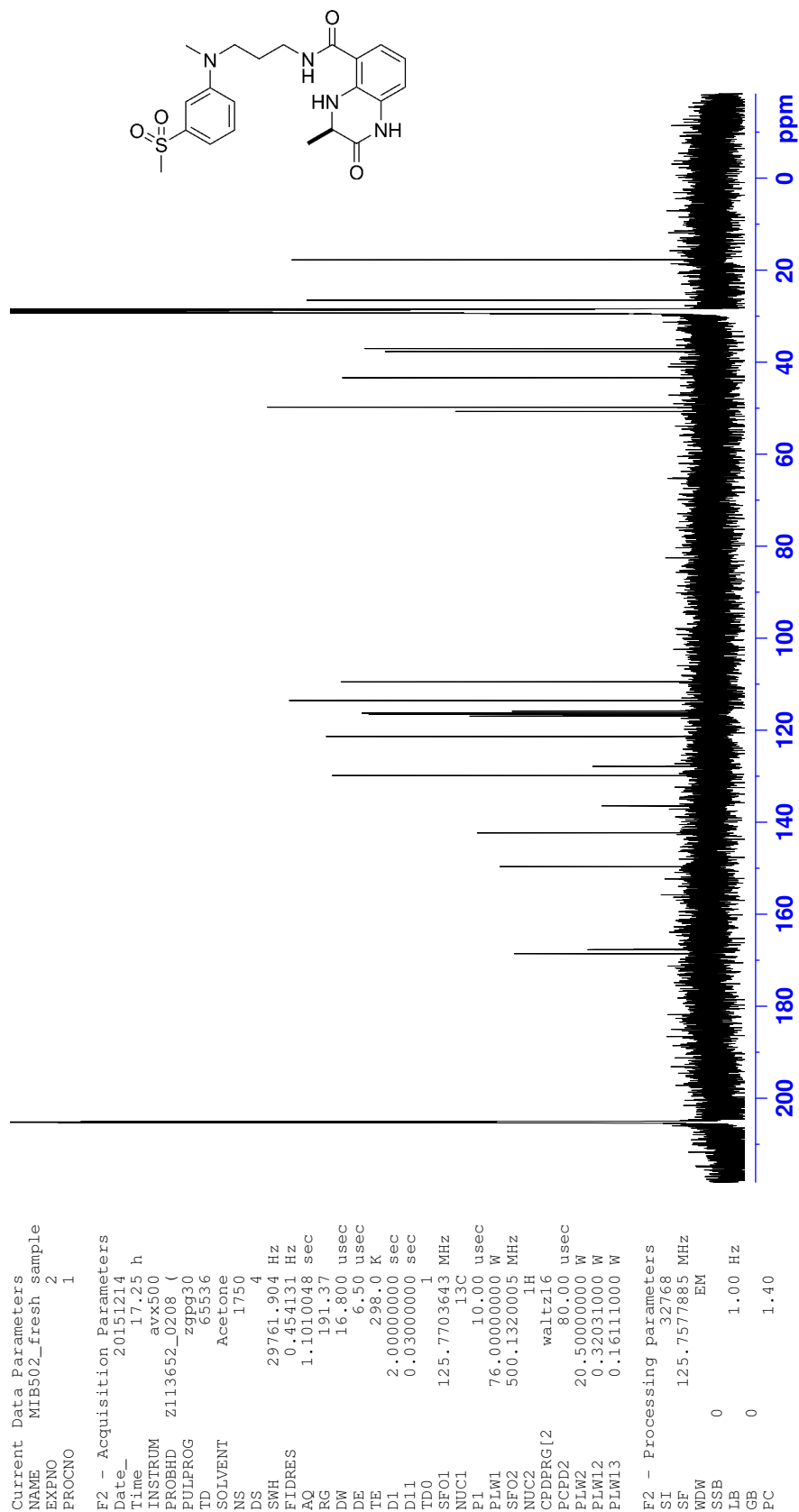
Appendix F: NMR spectra

¹H NMR (*R*)-3-Methyl-*N*-(3-(methyl(3-(methylsulfonyl)phenyl)amino)propyl)-2-oxo-1,2,3,4-tetrahydroquinoxaline-5-carboxamide (**103**)



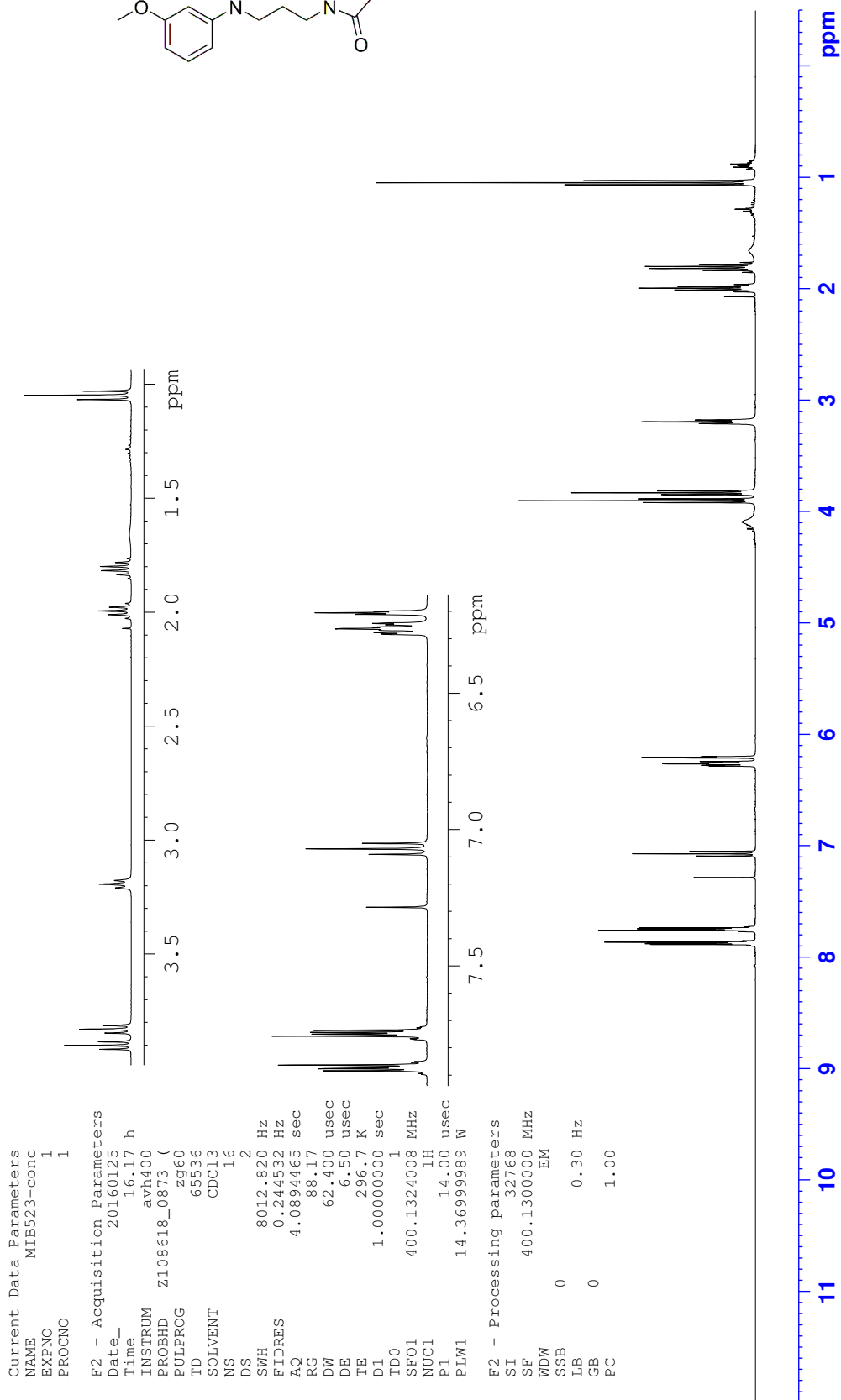
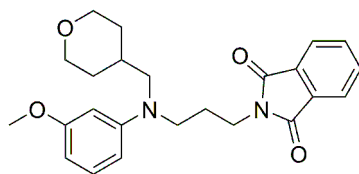
Appendix F: NMR spectra

¹³C NMR (*R*)-3-Methyl-*N*-(3-(methyl(3-(methylsulfonyl)phenyl)amino)propyl)-2-oxo-1,2,3,4-tetrahydroquinoxaline-5-carboxamide (**103**)



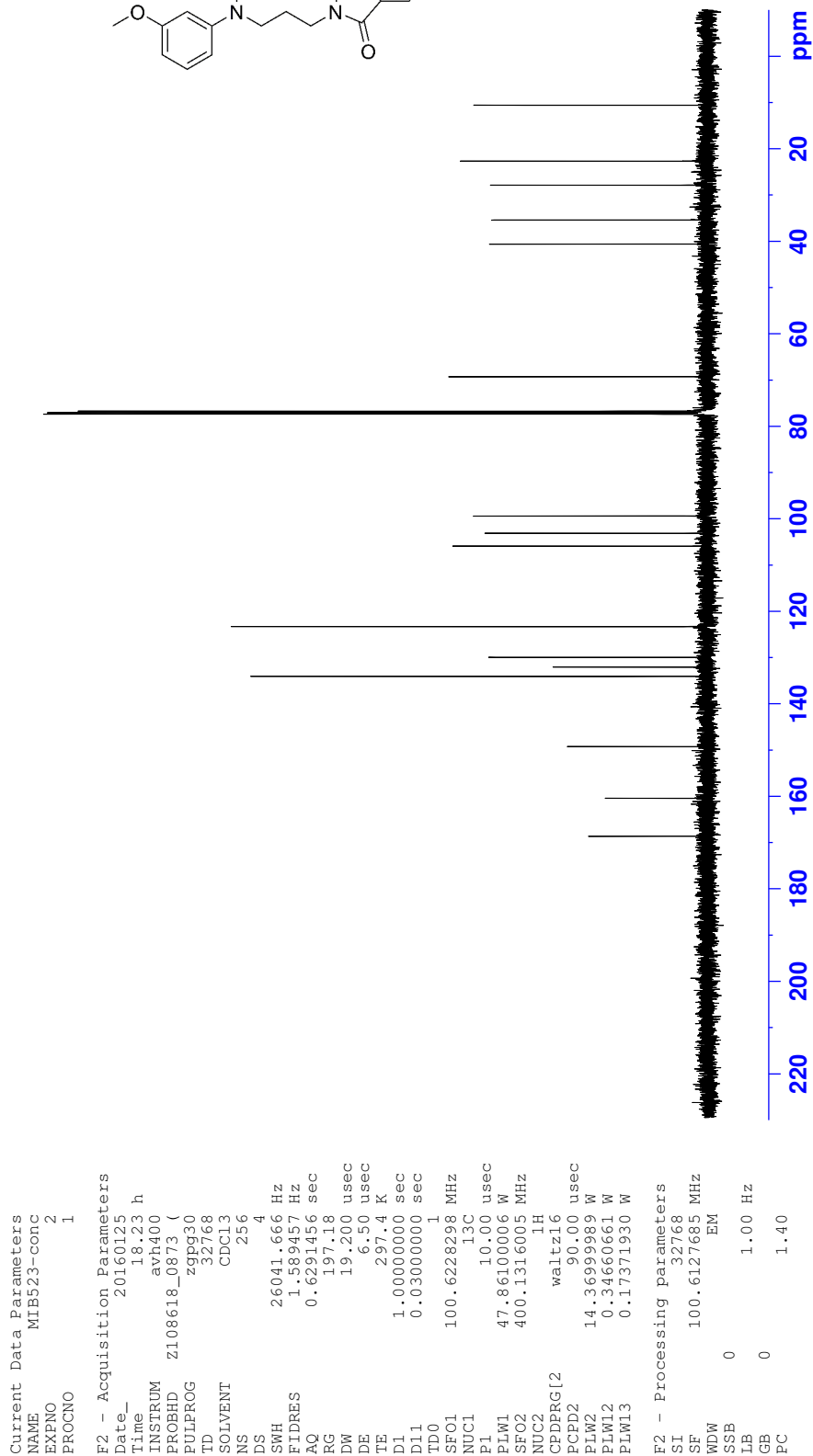
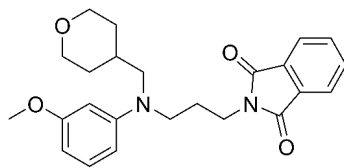
Appendix F: NMR spectra

¹H NMR 2-(3-((3-Methoxyphenyl)((tetrahydro-2H-pyran-4-yl)methyl)amino)propyl)-isoindoline-1,3-dione (**133**)



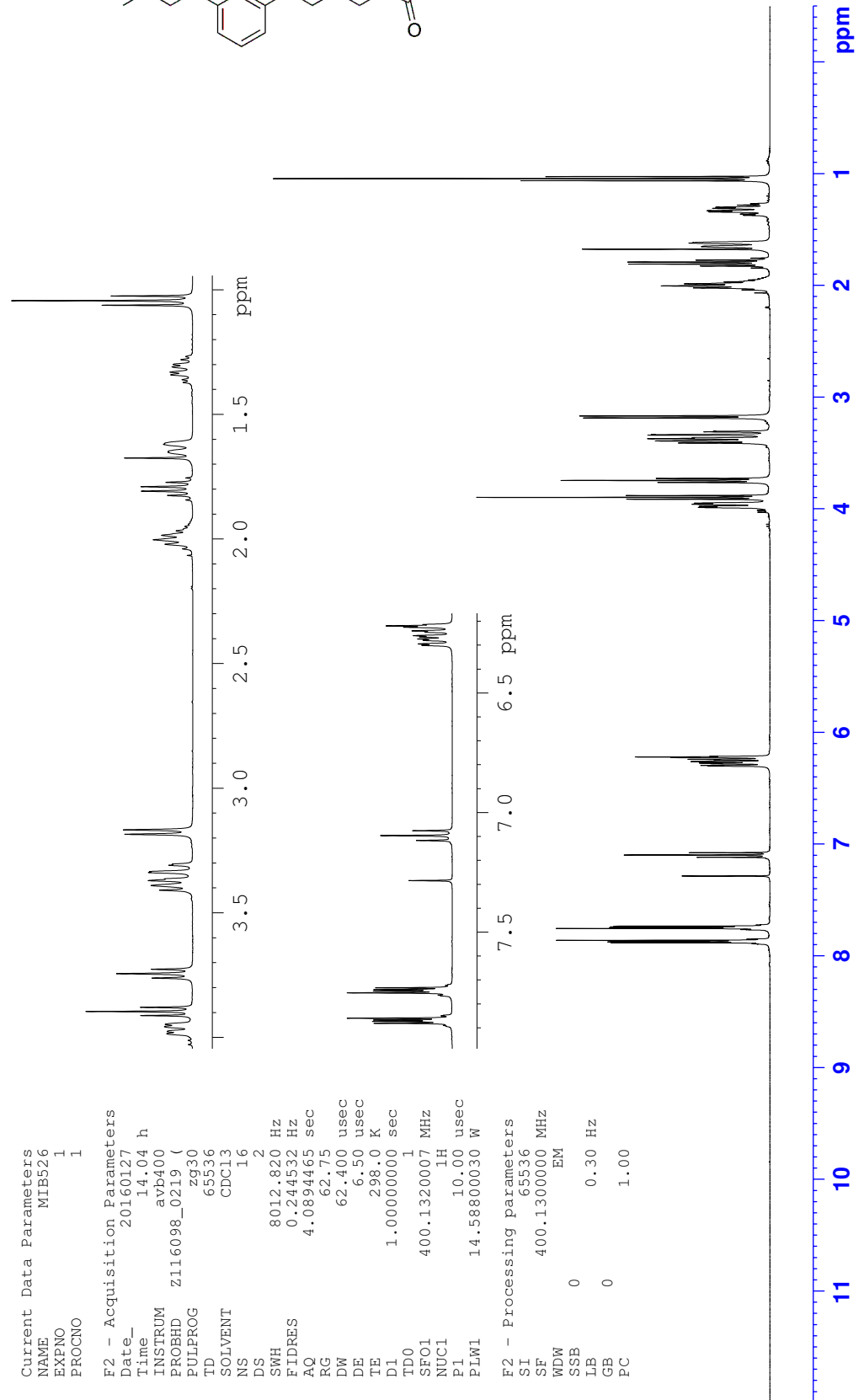
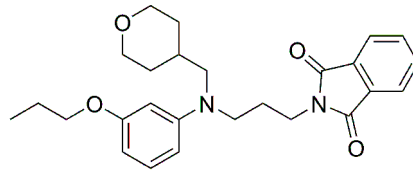
Appendix F: NMR spectra

¹³C NMR 2-(3-((3-Methoxyphenyl)((tetrahydro-2H-pyran-4-yl)methyl)amino)propyl)-isoindoline-1,3-dione (**133**)



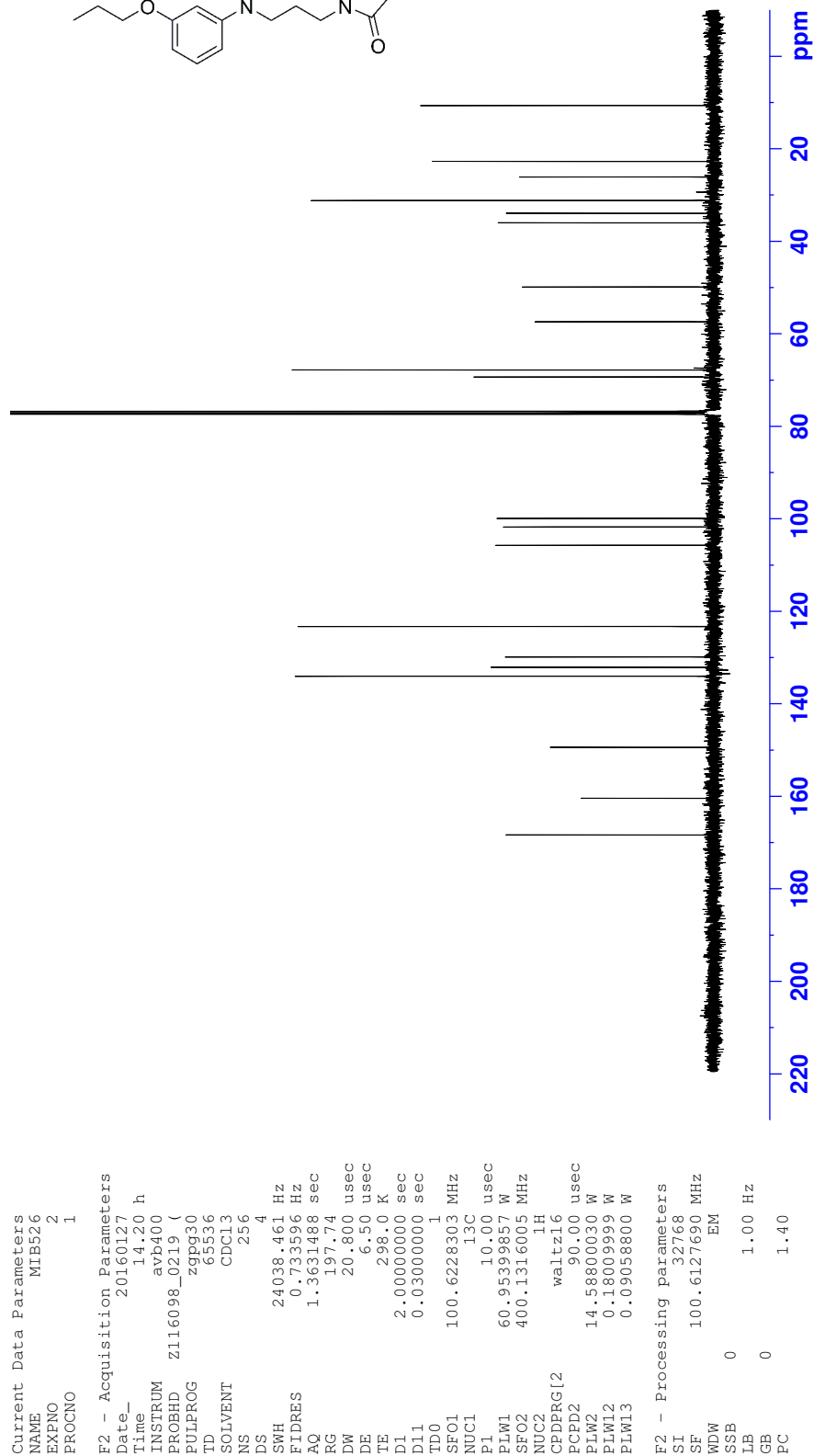
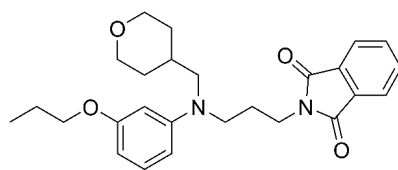
Appendix F: NMR spectra

¹H NMR 2-(3-((3-Propoxyphenyl)((tetrahydro-2H-pyran-4-yl)methyl)amino)propyl)-isoindoline-1,3-dione (**134**)



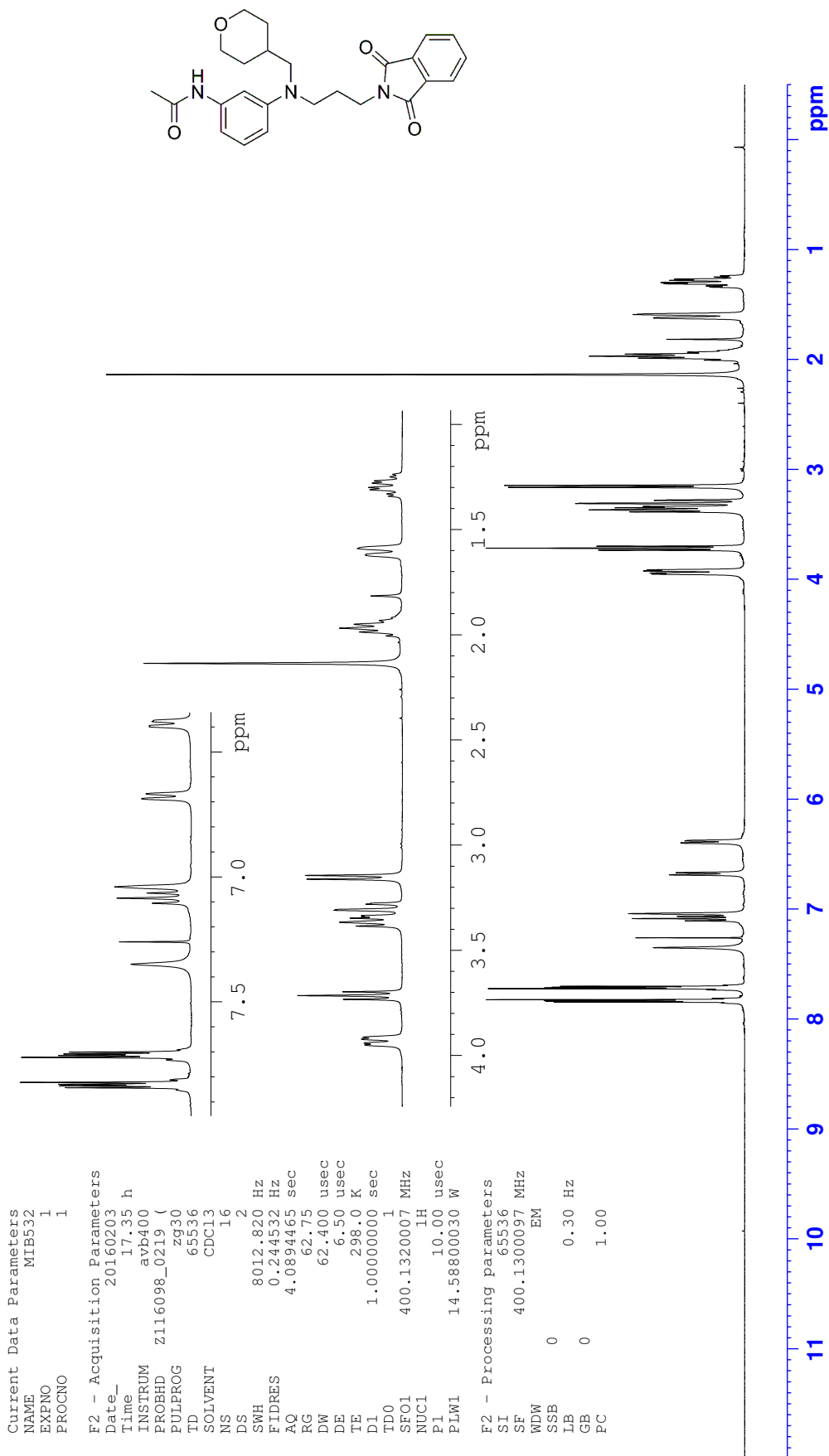
Appendix F: NMR spectra

¹³C NMR 2-(3-((3-Propoxyphenyl)((tetrahydro-2H-pyran-4-yl)methyl)amino)propyl)-isoindoline-1,3-dione (**134**)



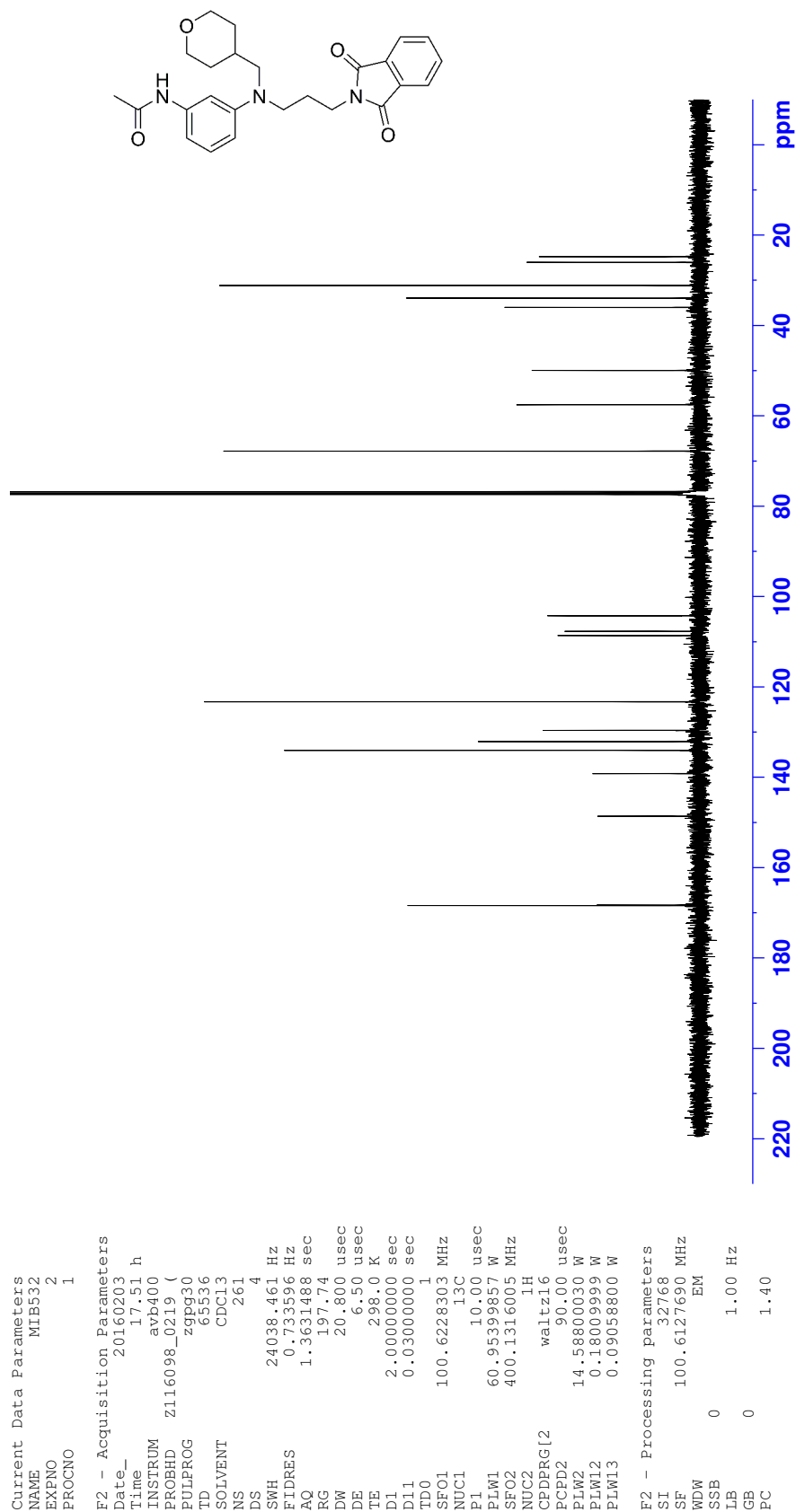
Appendix F: NMR spectra

¹H NMR *N*-(3-((3-(1,3-Dioxoisindolin-2-yl)propyl)((tetrahydro-2*H*-pyran-4-yl)methyl)-amino)phenyl)acetamide (**135**)



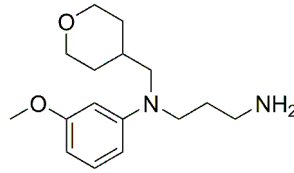
Appendix F: NMR spectra

¹³C NMR *N*-(3-((3-(1,3-Dioxisoindolin-2-yl)propyl)((tetrahydro-2*H*-pyran-4-yl)methyl)-amino)phenyl)acetamide (**135**)



Appendix F: NMR spectra

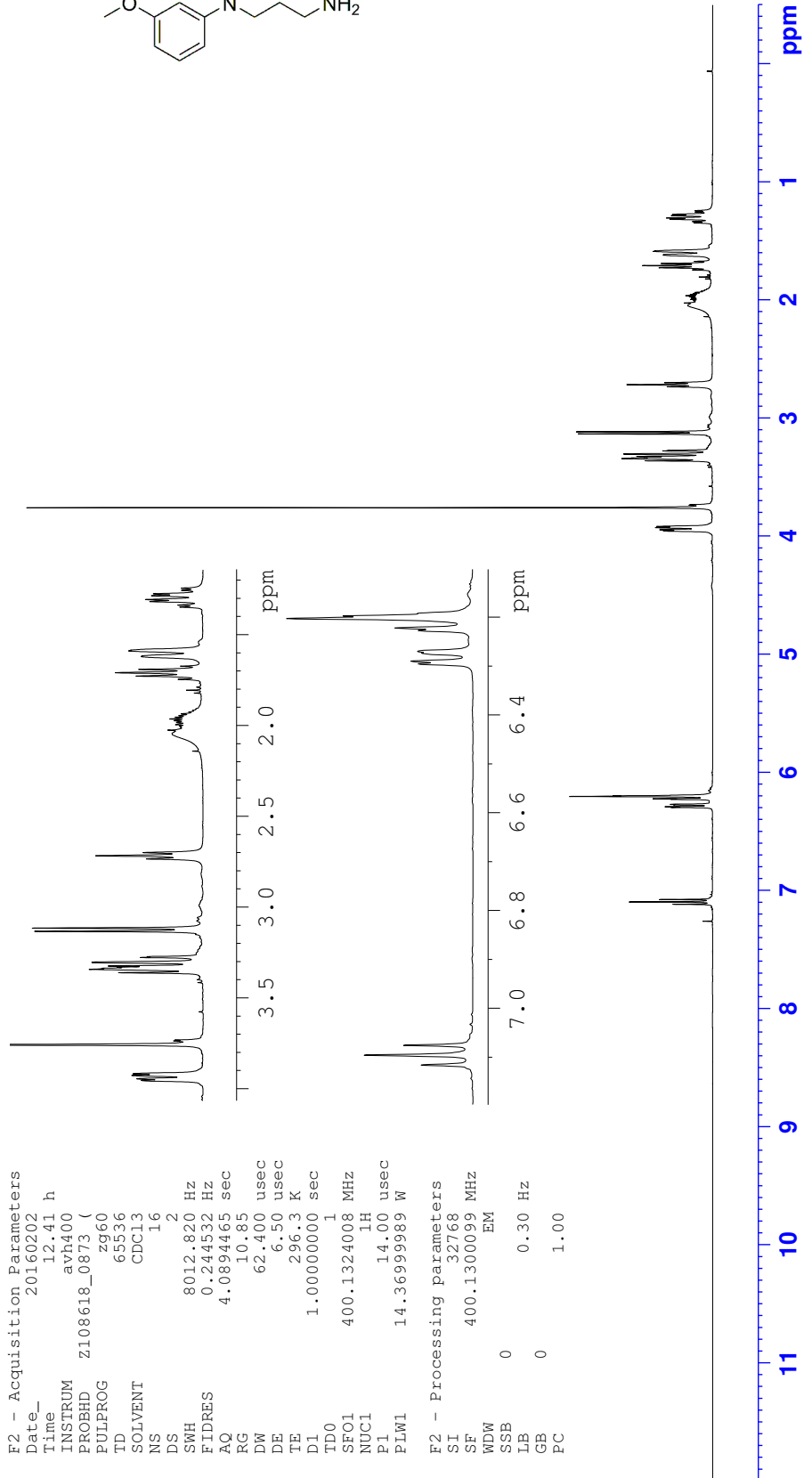
¹H NMR *N*1-(3-Methoxyphenyl)-*N*1-((tetrahydro-2*H*-pyran-4-yl)methyl)propane-1,3-diamine (136)



Current Data Parameters
 NAME MIB530_solvent free
 EXPNO 1
 PROCNO 1

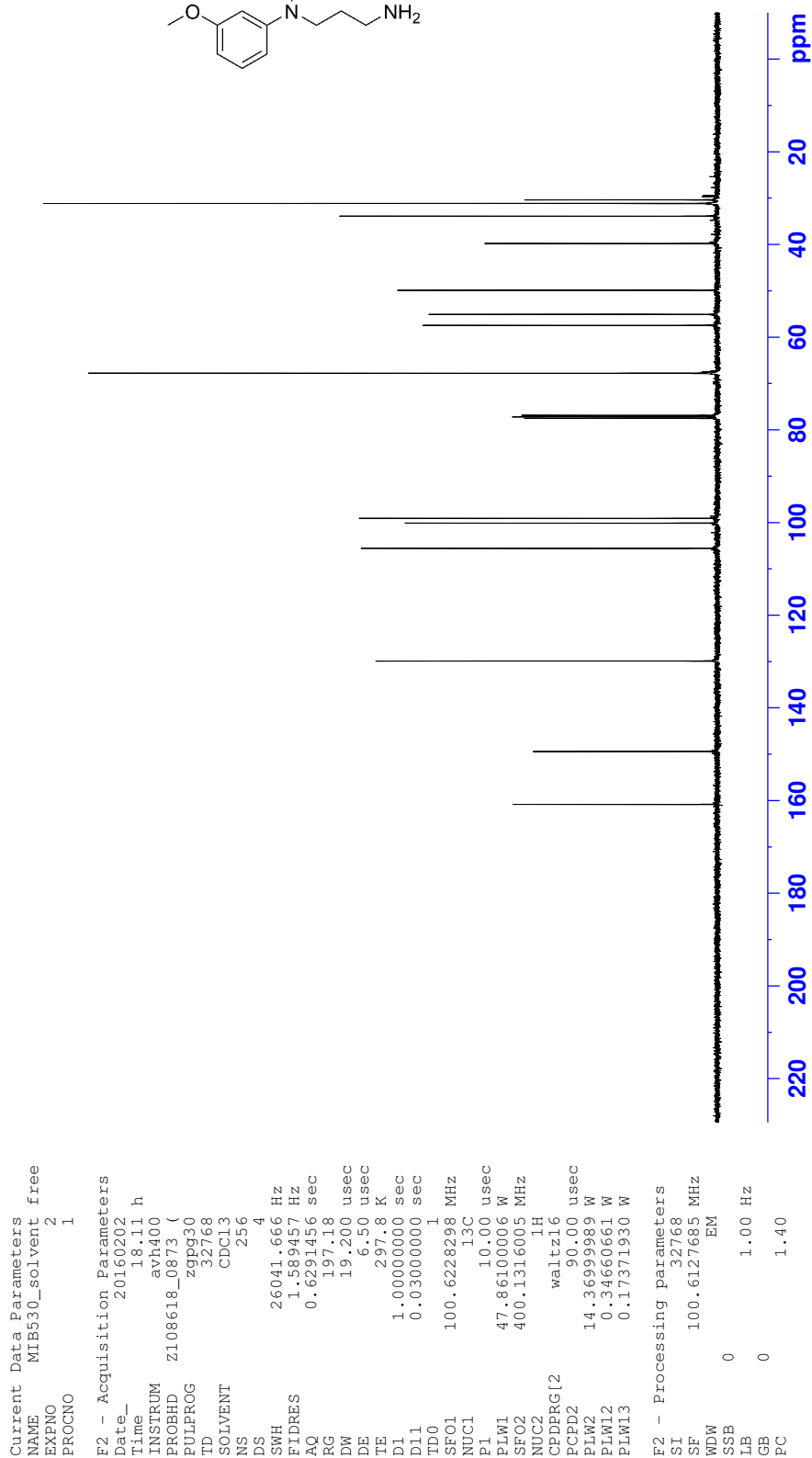
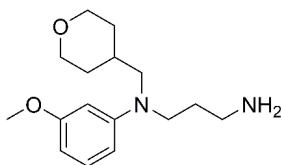
F2 - Acquisition Parameters
 Date_ 20160202
 Time 12.41 h
 INSTRUM avh400
 PROBHD z108618_0873 (
 PULPROG zg60
 TD 65536
 SOLVENT CDCl3
 NS 16
 DS 2
 SWH 8012.820 Hz
 FIDRES 0.244532 Hz
 AQ 4.0894465 sec
 RG 10.85
 DW 62.400 usec
 DE 6.50 usec
 TE 296.3 K
 D1 1.0000000 sec
 TD0 1
 SFO1 400.1324008 MHz
 NUC1 1H
 P1 14.00 usec
 PLW1 14.36999989 W

F2 - Processing parameters
 SI 32768
 SF 400.1300099 MHz
 EM
 WDW 0
 SSB 0
 LB 0.30 Hz
 GB 0
 PC 1.00



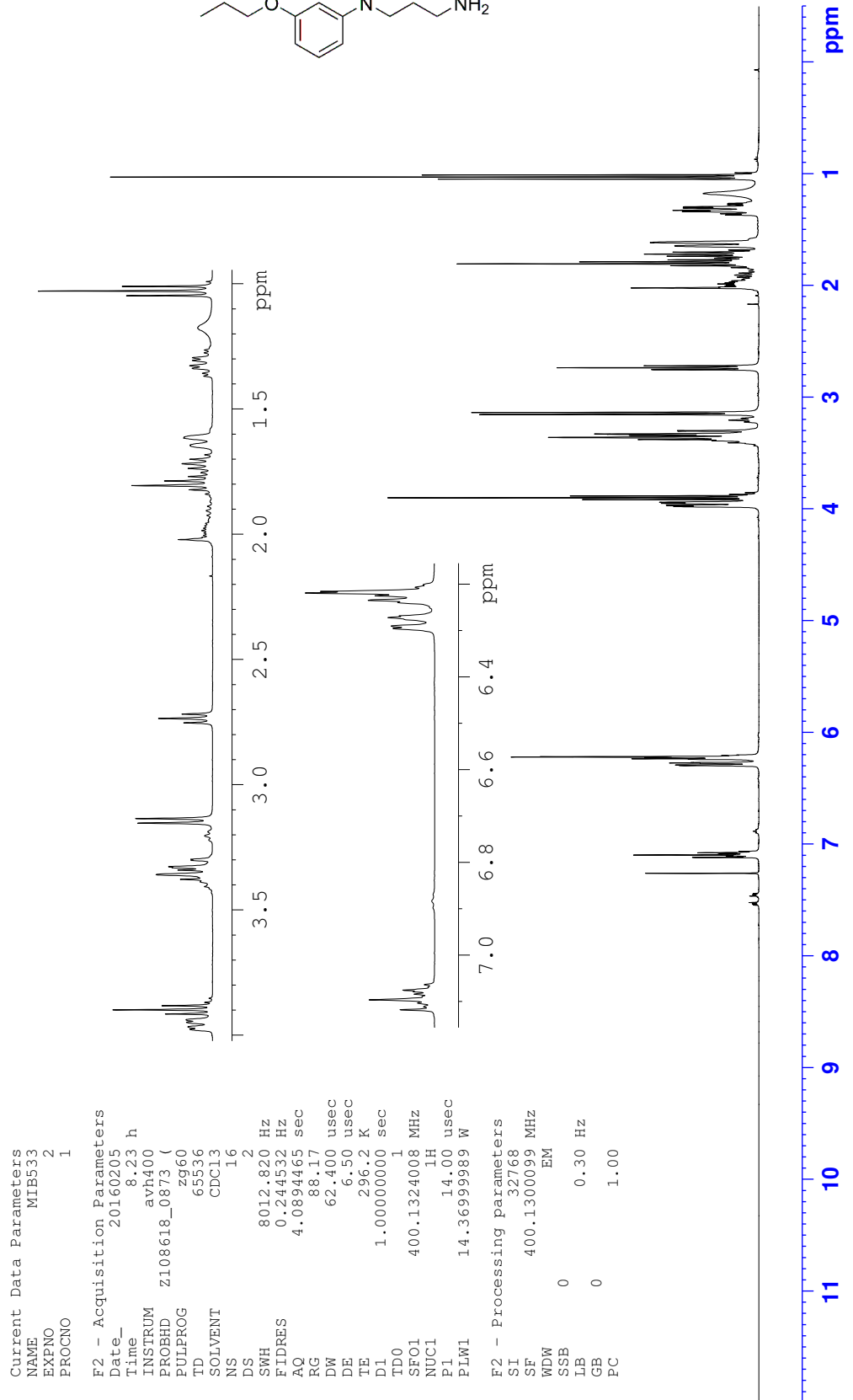
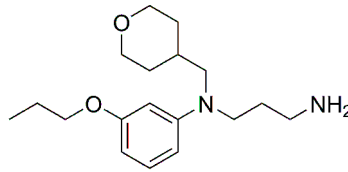
Appendix F: NMR spectra

¹³C NMR *N*1-(3-Methoxyphenyl)-*N*1-((tetrahydro-2*H*-pyran-4-yl)methyl)propane-1,3-diamine (136)



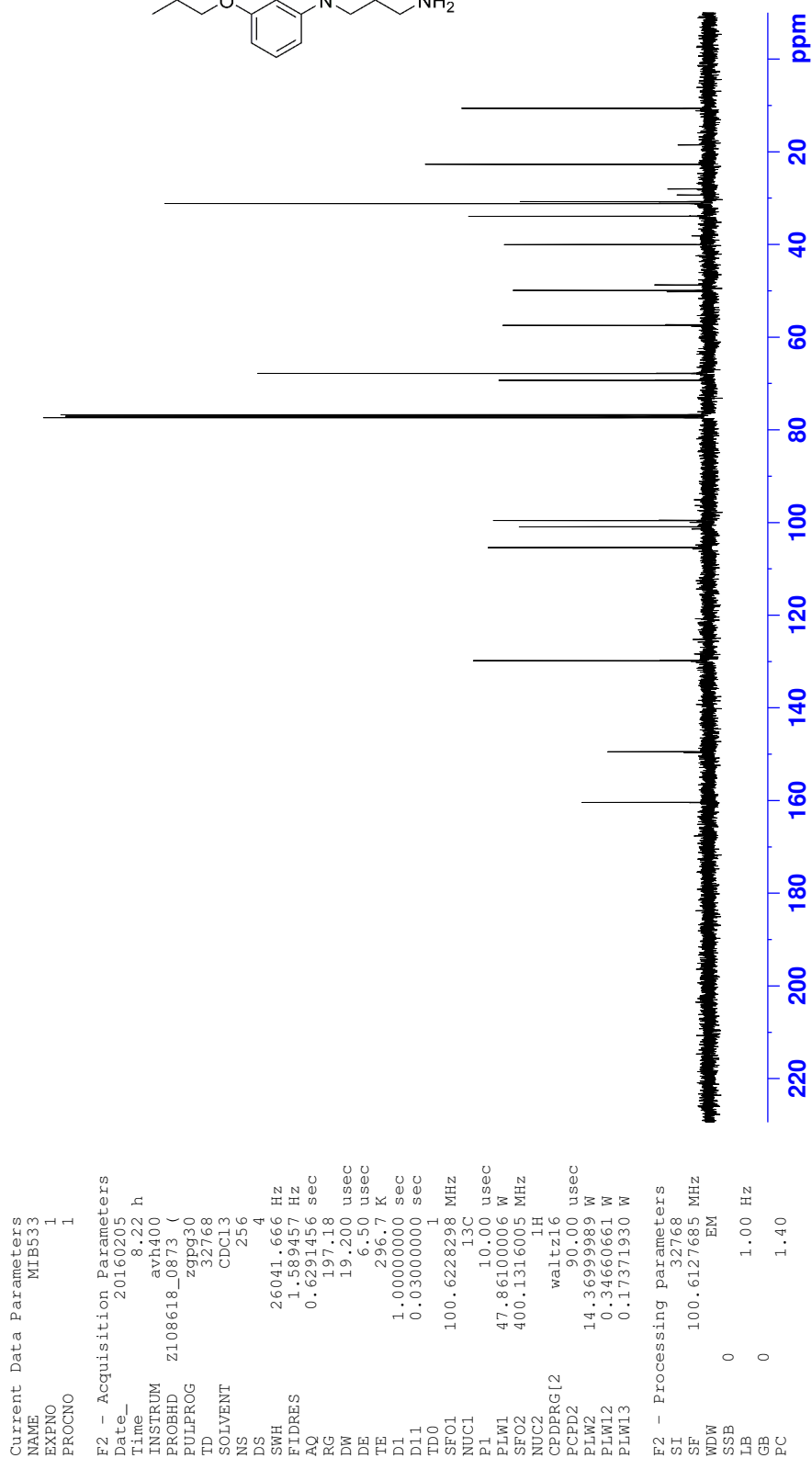
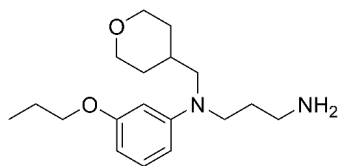
Appendix F: NMR spectra

¹H NMR *N*1-(3-Propoxyphenyl)-*N*1-((tetrahydro-2*H*-pyran-4-yl)methyl)propane-1,3-diamine (137)



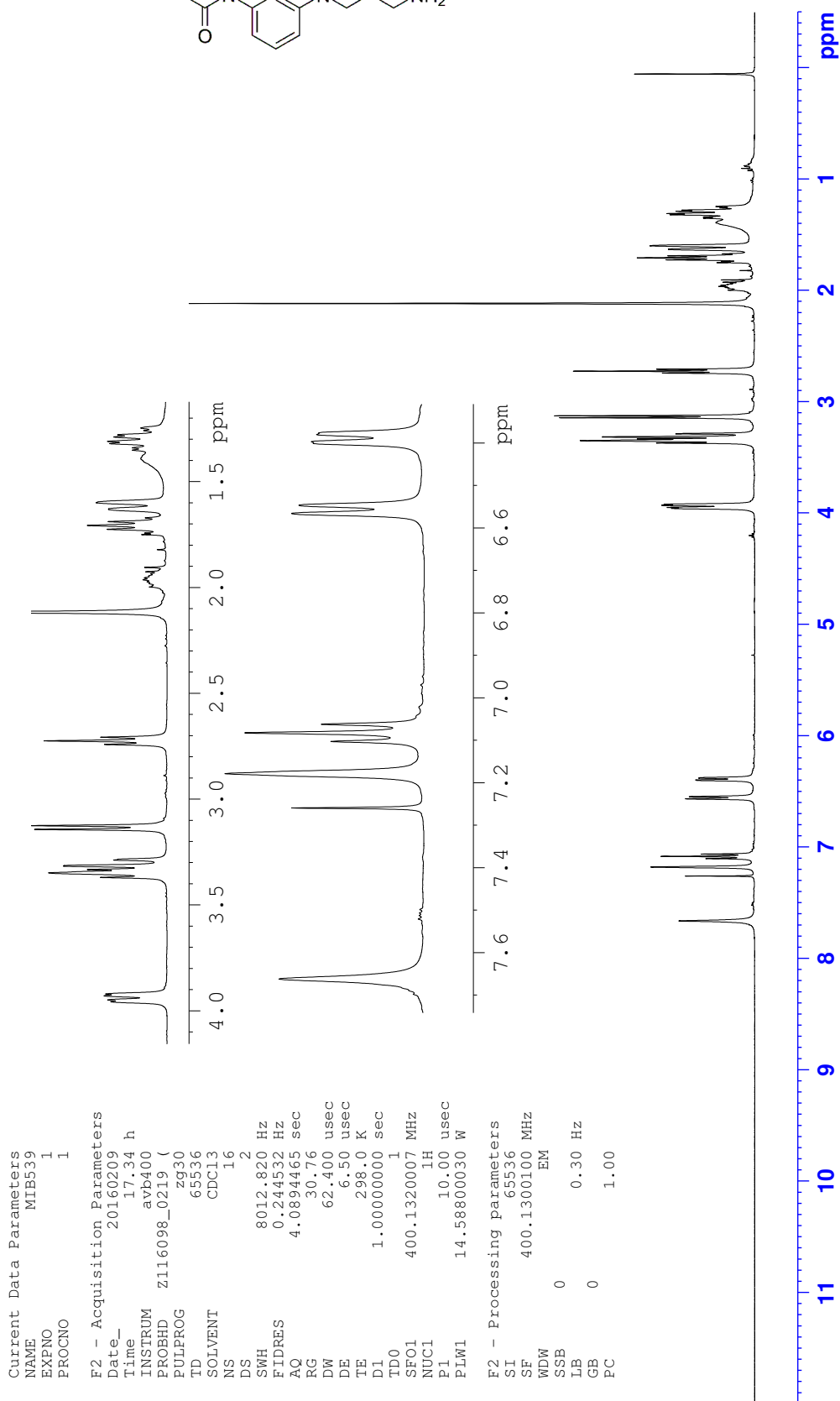
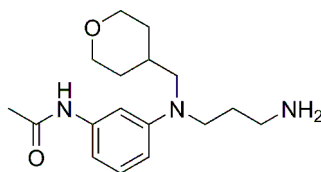
Appendix F: NMR spectra

¹³C NMR N1-(3-Propoxyphenyl)-N1-((tetrahydro-2H-pyran-4-yl)methyl)propane-1,3-diamine (137)



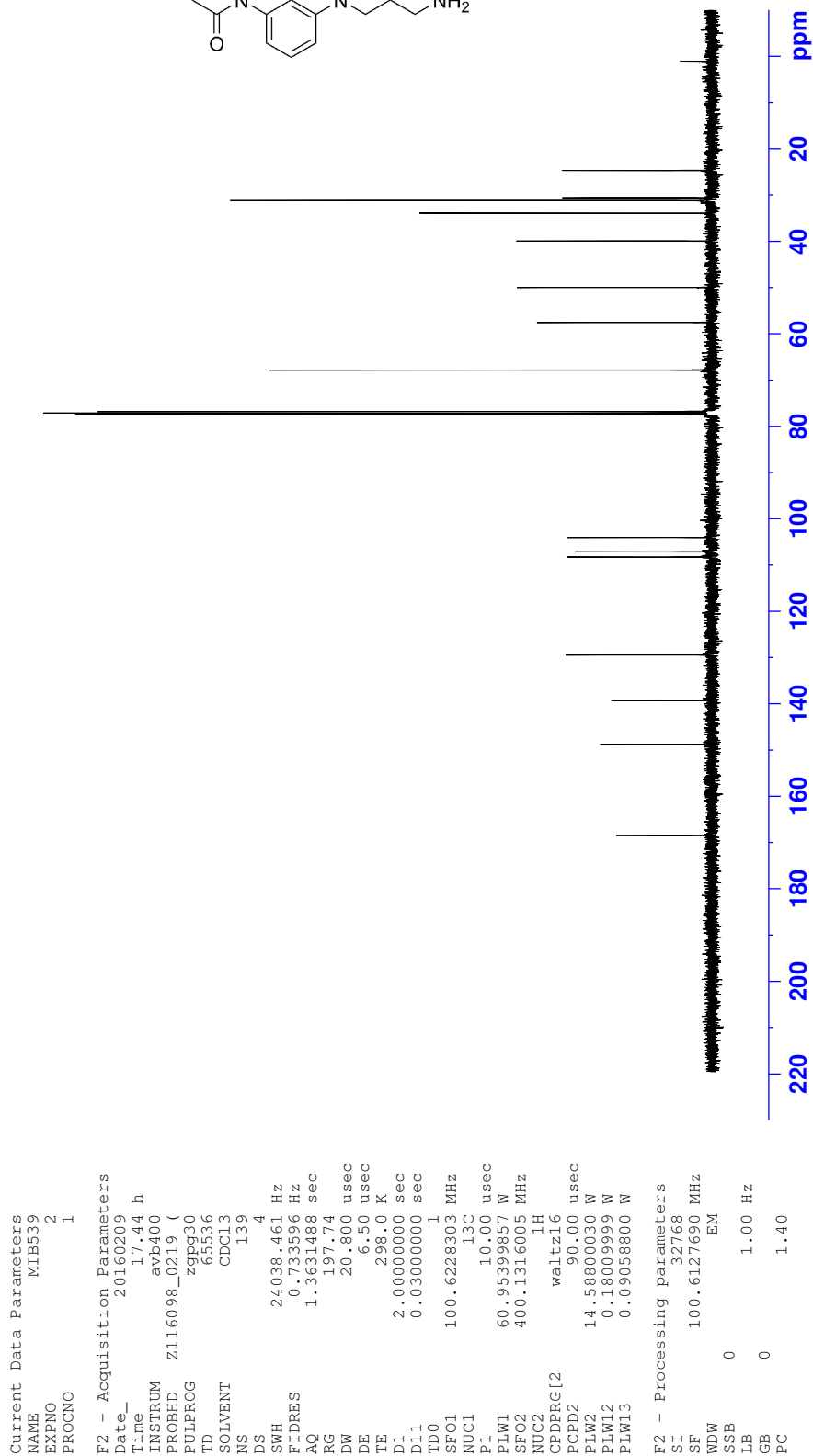
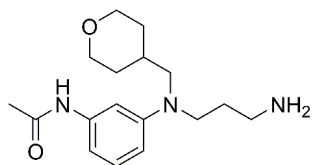
Appendix F: NMR spectra

¹H NMR *N*-(3-((3-aminopropyl)((tetrahydro-2*H*-pyran-4-yl)methyl)amino)phenyl)-acetamide (138)



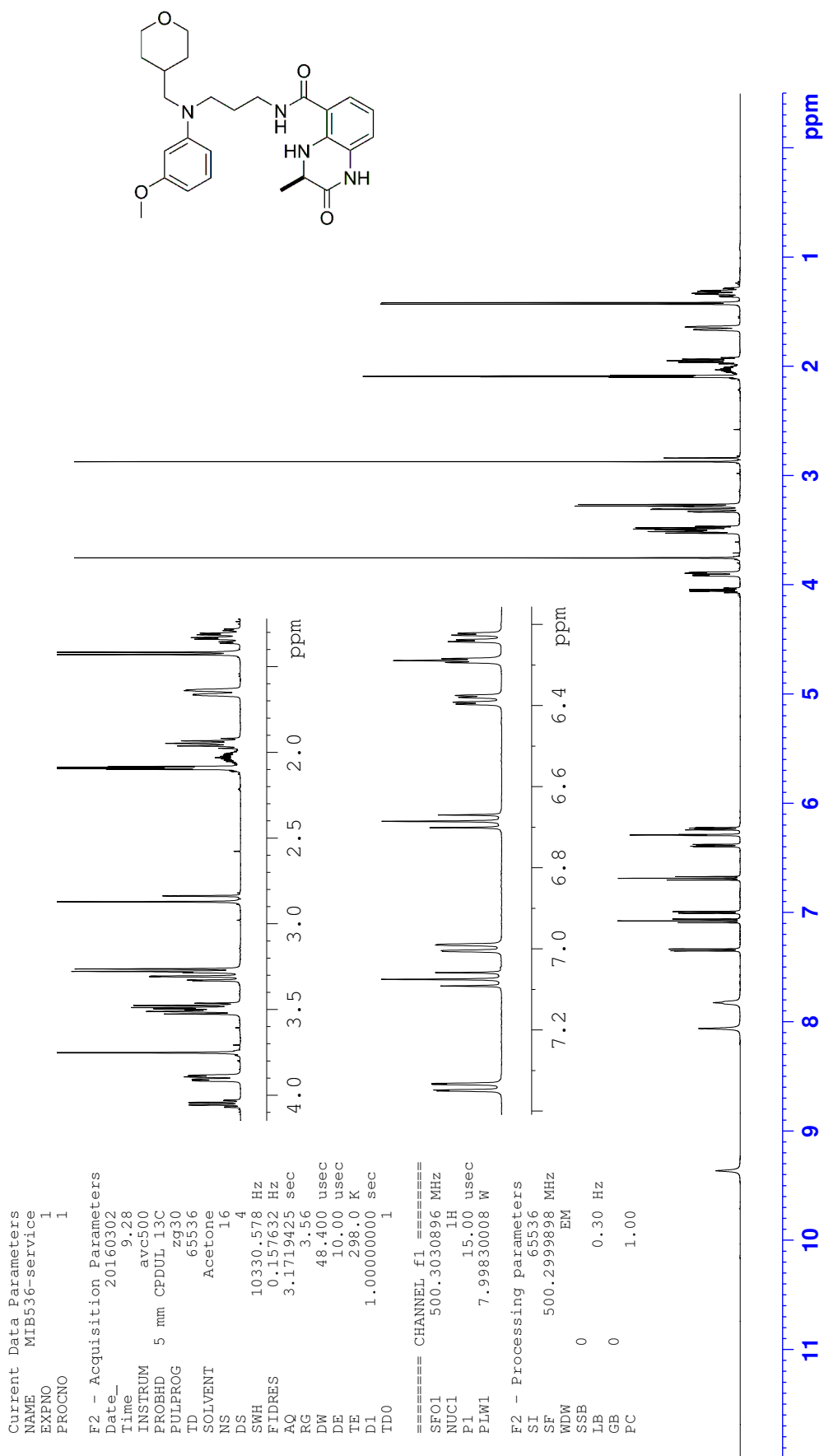
Appendix F: NMR spectra

^{13}C NMR *N*-(3-((3-aminopropyl)((tetrahydro-2*H*-pyran-4-yl)methyl)amino)phenyl)-acetamide (138)



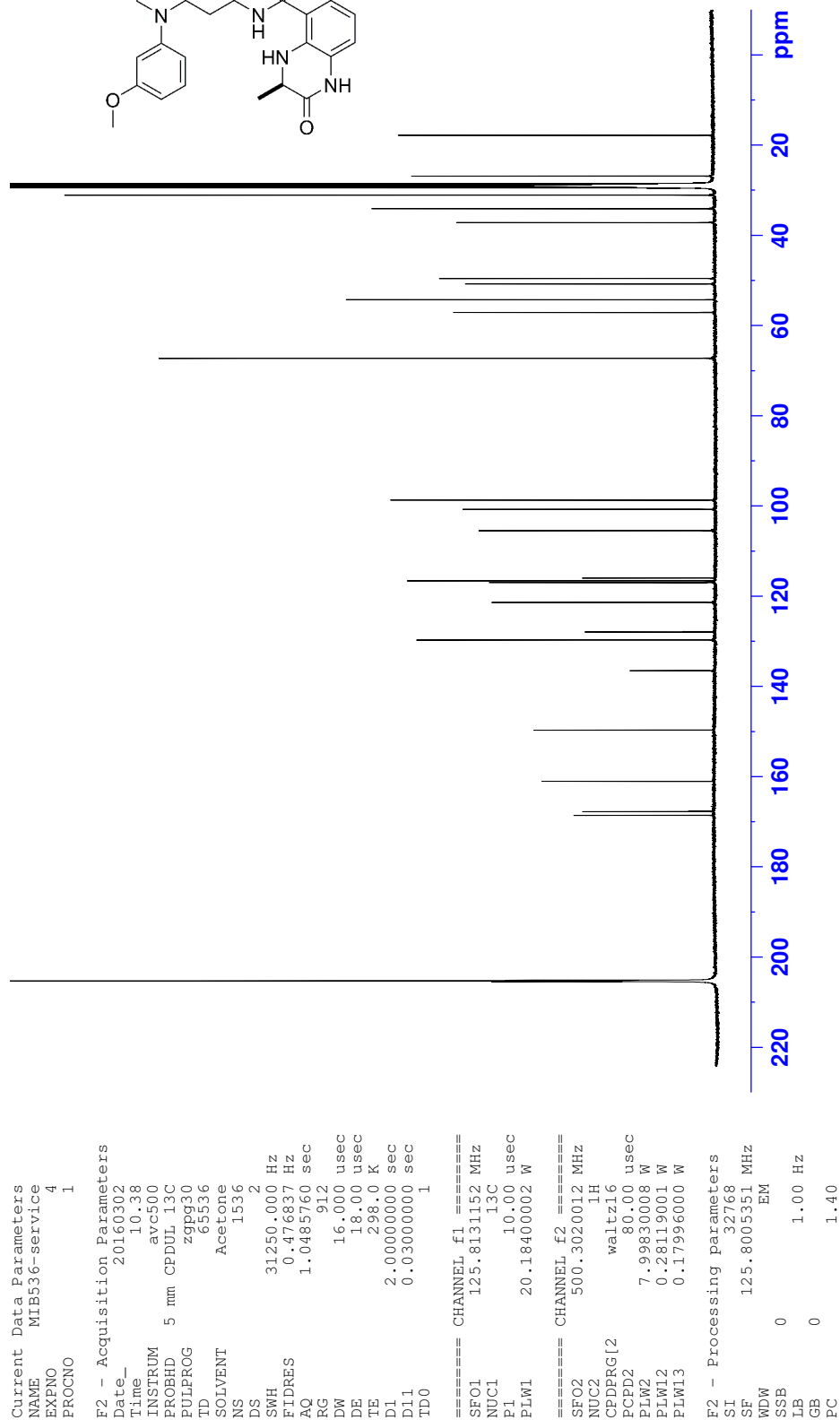
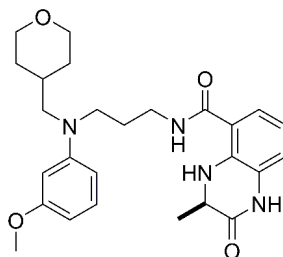
Appendix F: NMR spectra

¹H NMR (*R*)-*N*-(3-((3-Methoxyphenyl)((tetrahydro-2*H*-pyran-4-yl)methyl)amino)propyl)-3-methyl-2-oxo-1,2,3,4-tetrahydroquinoxaline-5-carboxamide (**105**)



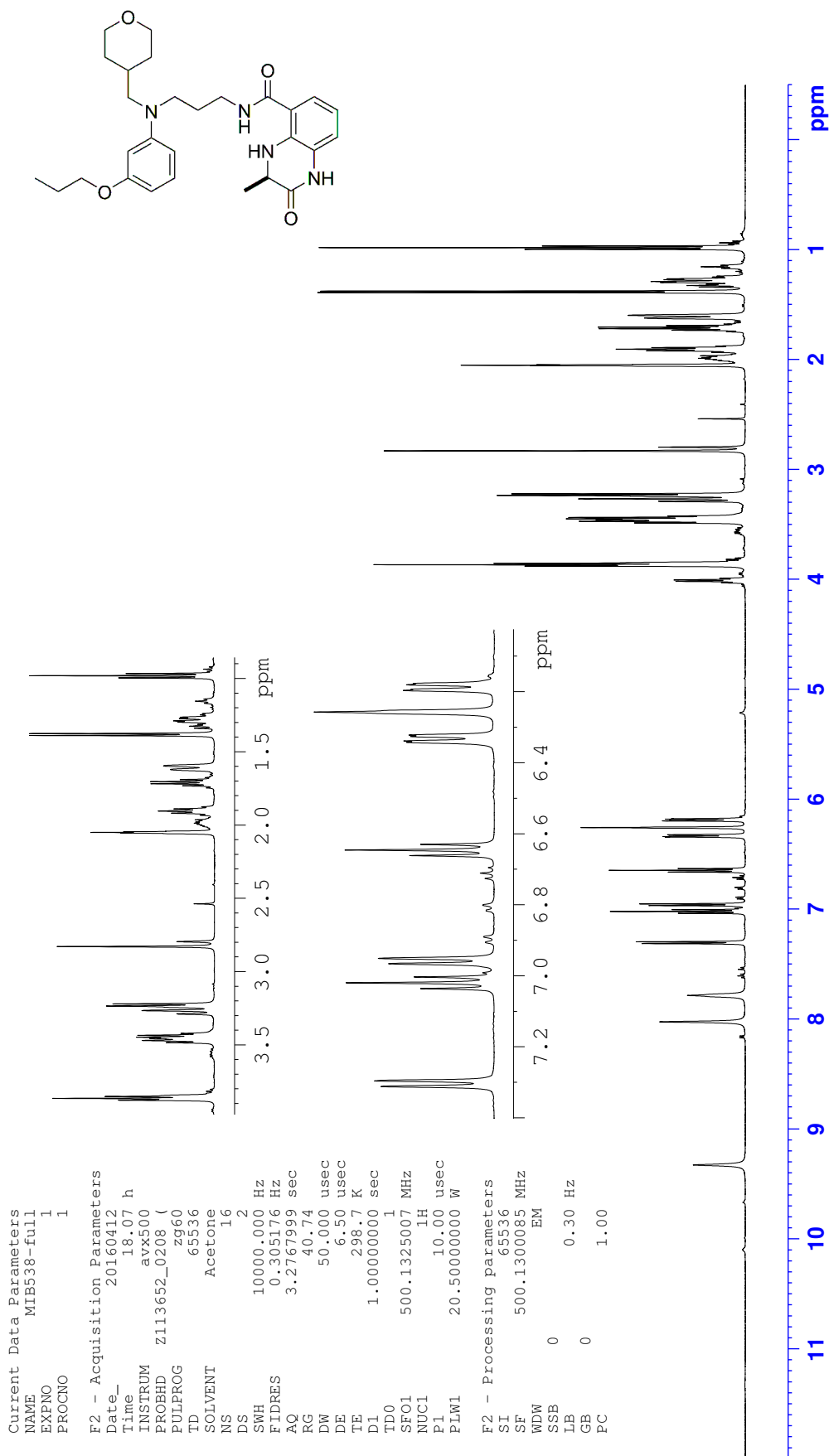
Appendix F: NMR spectra

^{13}C NMR (*R*)-*N*-(3-((3-Methoxyphenyl)((tetrahydro-2*H*-pyran-4-yl)methyl)amino)propyl)-3-methyl-2-oxo-1,2,3,4-tetrahydroquinoxaline-5-carboxamide (**105**)



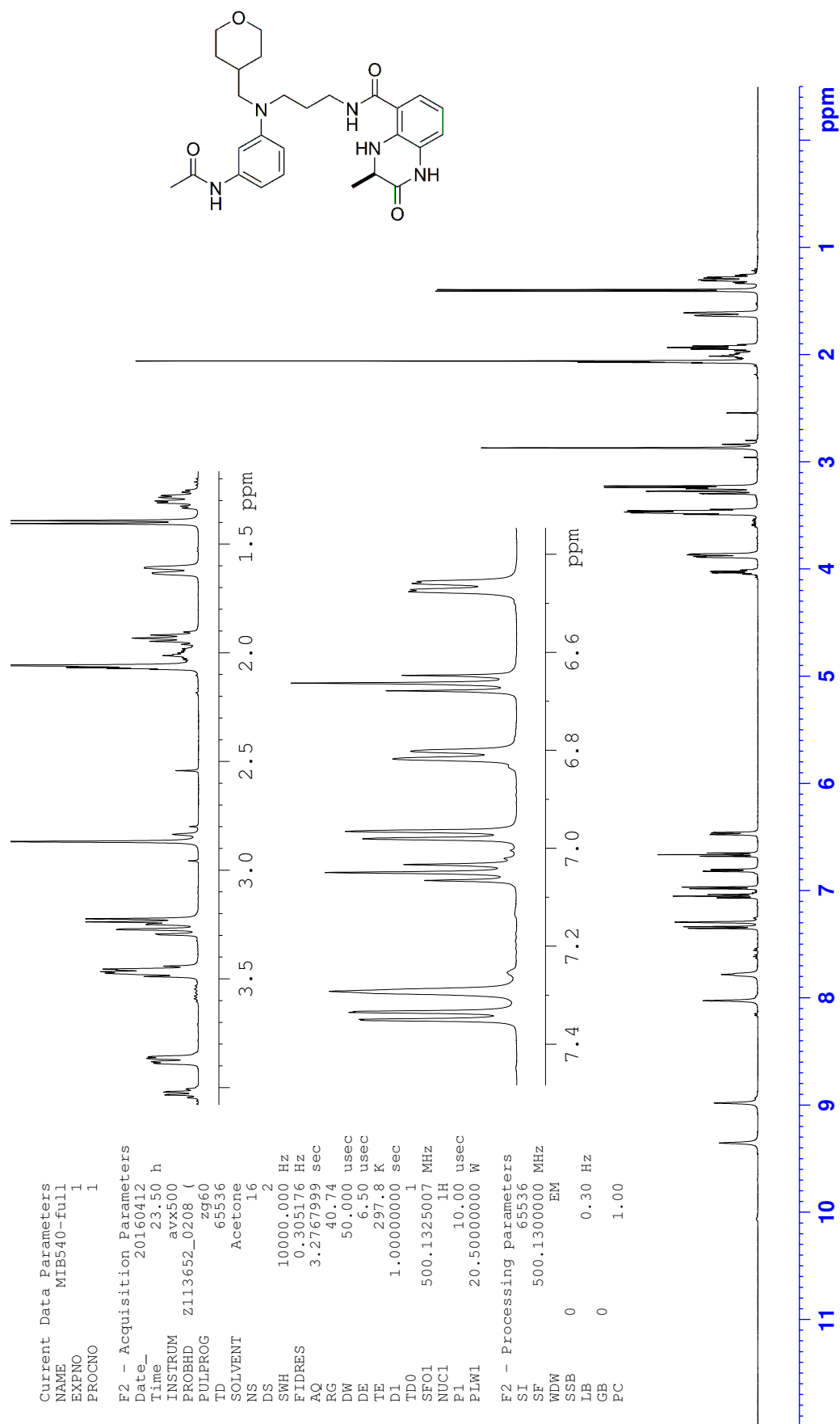
Appendix F: NMR spectra

^1H NMR (*R*)-*N*-(3-((3-Propoxyphenyl)((tetrahydro-2*H*-pyran-4-yl)methyl)amino)propyl)-3-methyl-2-oxo-1,2,3,4-tetrahydroquinoxaline-5-carboxamide (**106**)



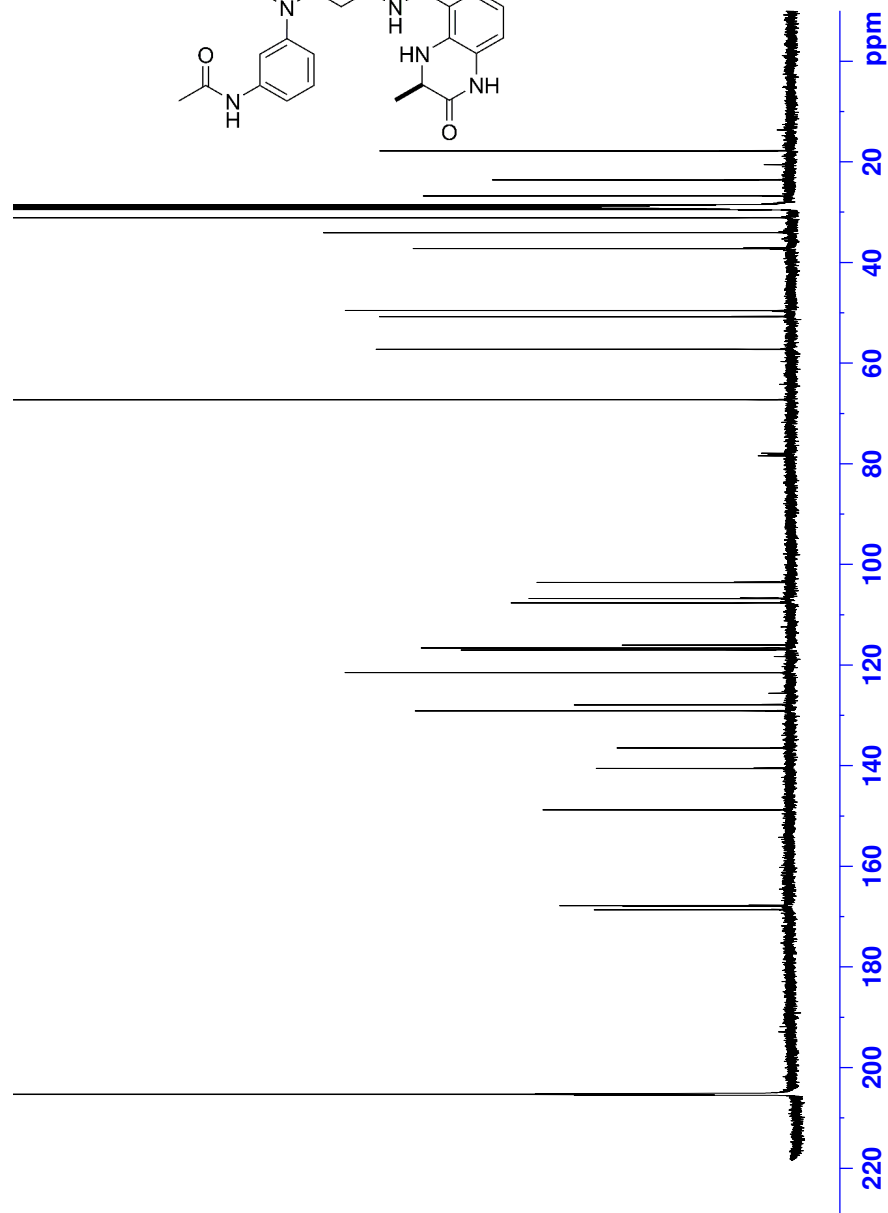
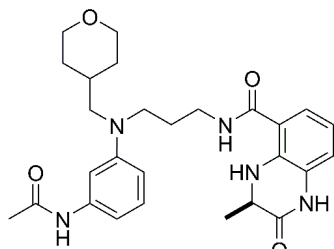
Appendix F: NMR spectra

¹H NMR (*R*)-*N*-(3-((3-Acetamidophenyl)((tetrahydro-2*H*-pyran-4-yl)methyl)amino)propyl)-3-methyl-2-oxo-1,2,3,4-tetrahydroquinoxaline-5-carboxamide (**107**)



Appendix F: NMR spectra

^{13}C NMR (*R*)-*N*-(3-((3-Acetamidophenyl)((tetrahydro-2*H*-pyran-4-yl)methyl)amino)propyl)-3-methyl-2-oxo-1,2,3,4-tetrahydroquinoxaline-5-carboxamide (**107**)



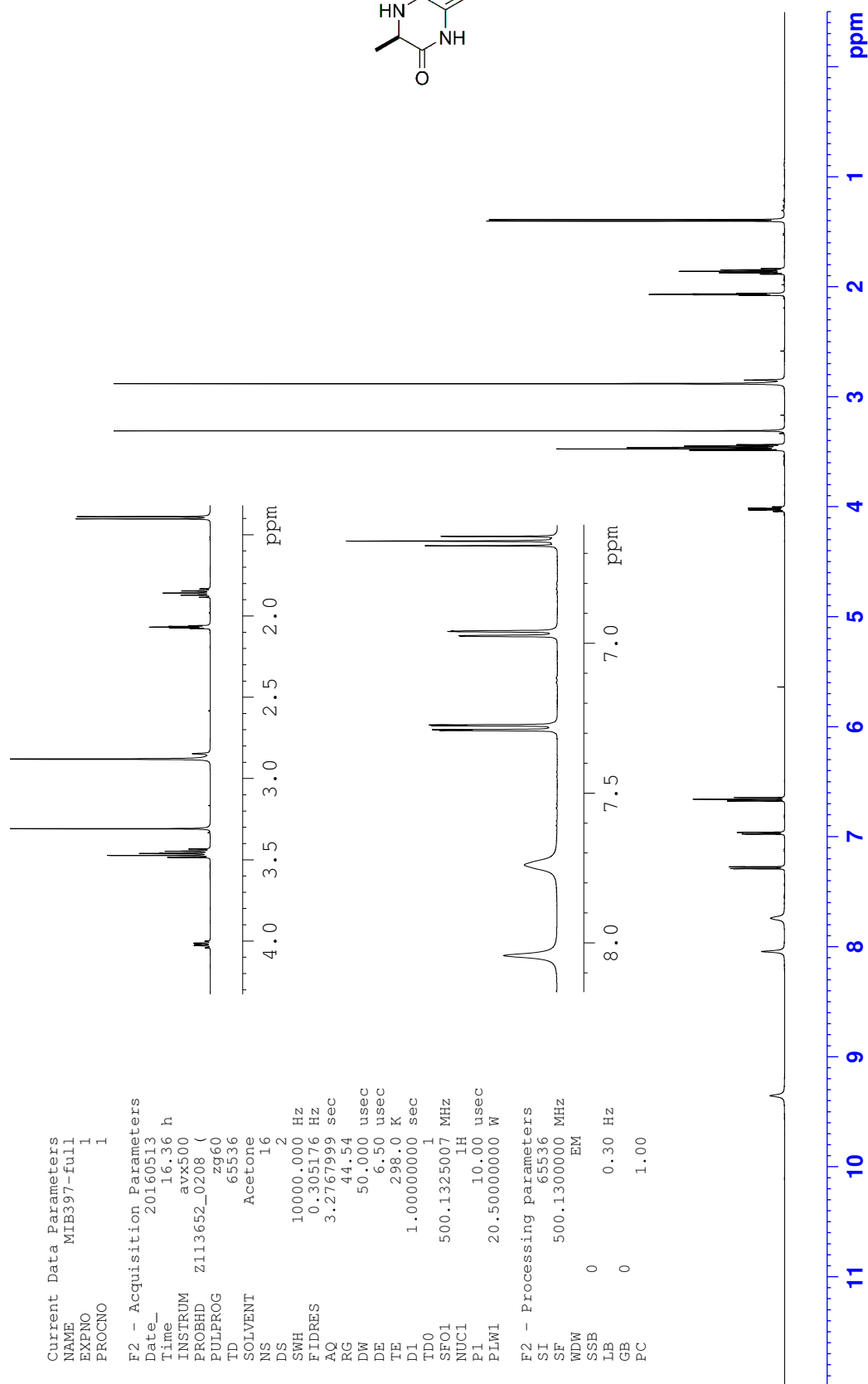
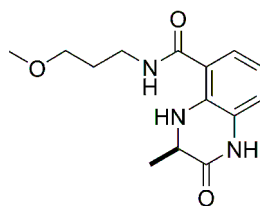
Current Data Parameters
 NAME MIB540-full
 EXPNO 5
 PROCNO 1

F2 - Acquisition Parameters
 Date_ 20160413
 Time 7.12 h
 INSTRUM avx500
 PROBHD z113652_0208 (zppg30
 FULPROG zppg30
 TD 65536
 SOLVENT Acetone
 NS 6144
 DS 4
 SWH 29761.904 Hz
 FIDRES 0.908261 Hz
 AQ 1.1010048 sec
 RG 191.37
 DM 16.800 usec
 DE 6.50 usec
 TE 298.0 K
 D1 2.0000000 sec
 D11 0.0300000 sec
 TD0 1
 SFO1 125.7703643 MHz
 NUC1 13C
 P1 10.00 usec
 PLW1 76.0000000 W
 SFO2 500.1320005 MHz
 NUC2 1H
 CPDPRG12 waltz16
 PCPD2 80.00 usec
 PLW2 20.5000000 W
 PLW12 0.3203100 W
 PLW13 0.1611100 W

F2 - Processing parameters
 SI 32768
 SF 125.7577885 MHz
 WDW EM
 SSB 0
 LB 1.00 Hz
 GB 0
 PC 1.40

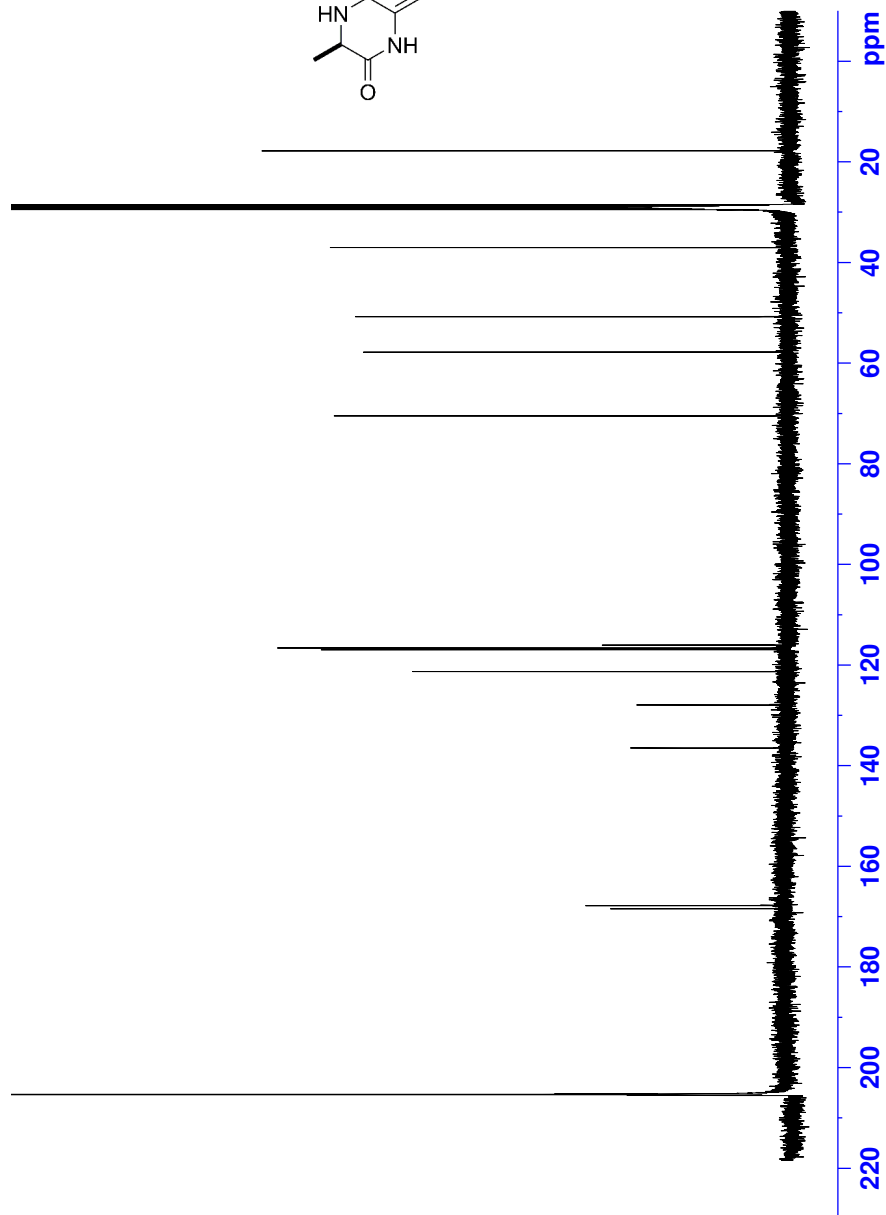
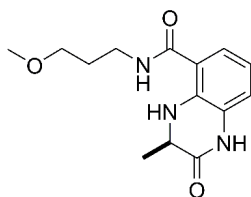
Appendix F: NMR spectra

¹H NMR (*R*)-*N*-(3-Methoxypropyl)-3-methyl-2-oxo-1,2,3,4-tetrahydroquinoxaline-5-carboxamide (**104**)



Appendix F: NMR spectra

¹³C NMR (R)-N-(3-Methoxypropyl)-3-methyl-2-oxo-1,2,3,4-tetrahydroquinoxaline-5-carboxamide (**104**)



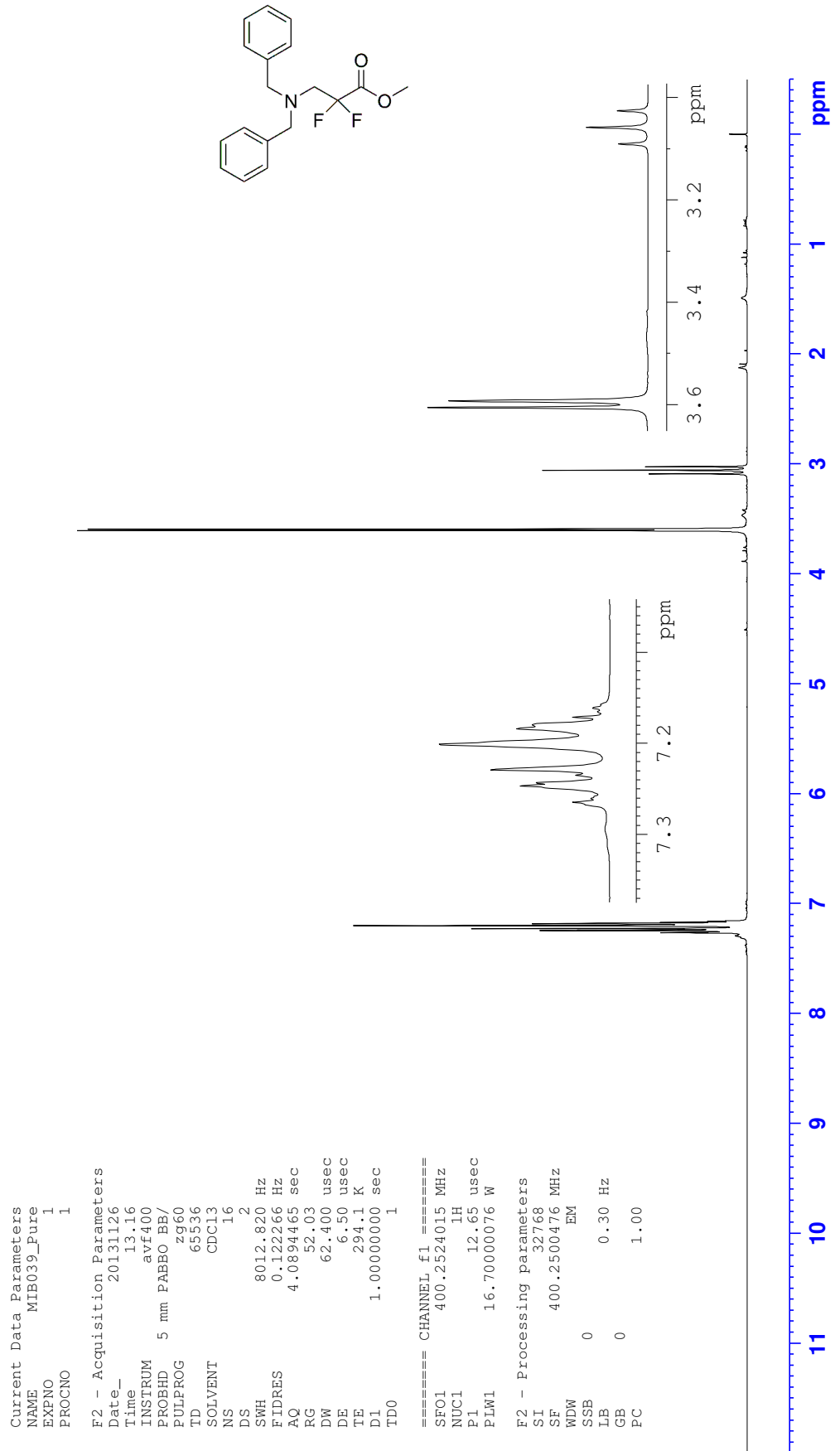
Current Data Parameters
 NAME MIB397-full
 EXPNO 2
 PROCNO 1

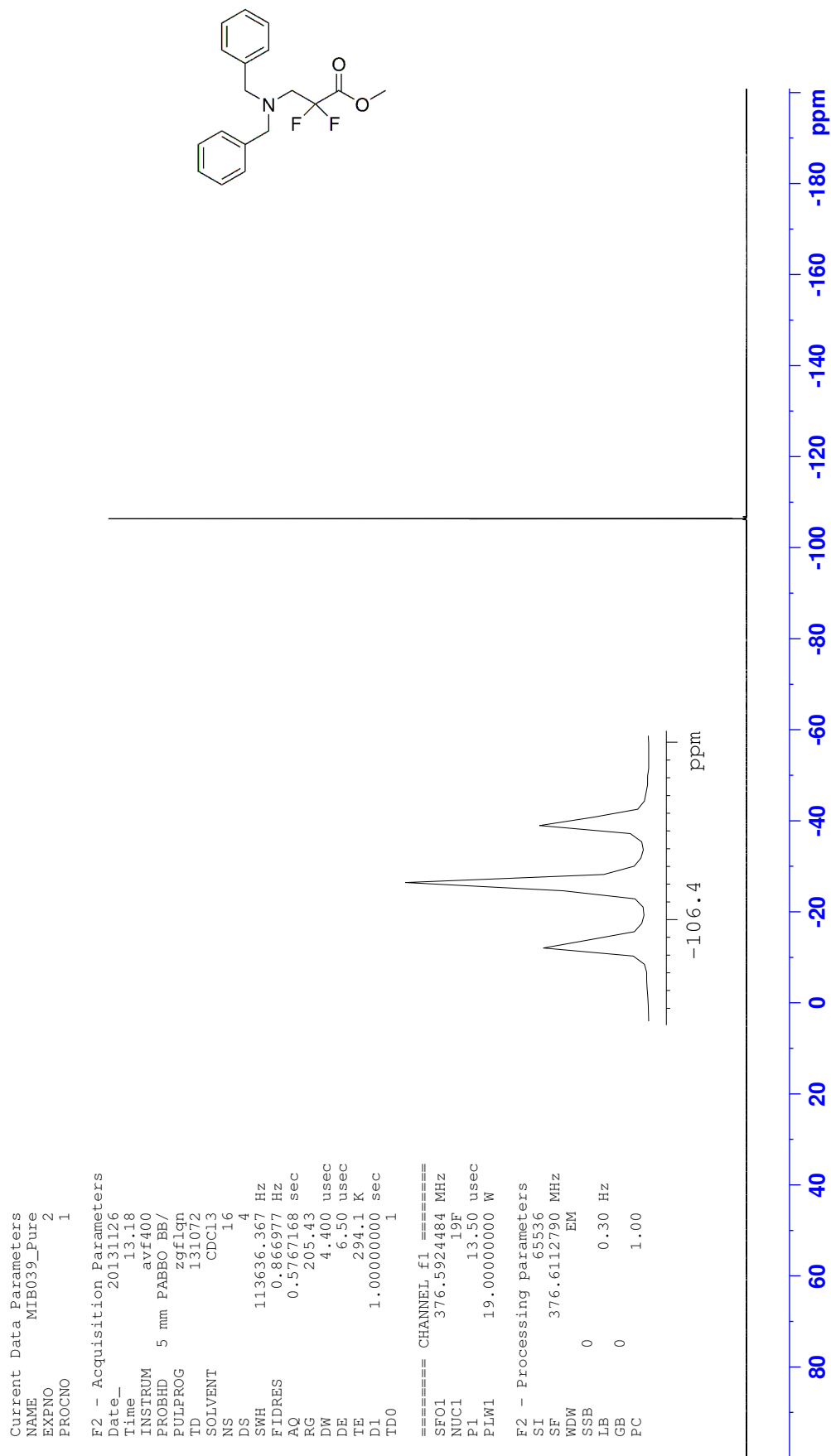
F2 - Acquisition Parameters
 Date_ 20160513
 Time 17.32 h
 INSTRUM avx500
 PROBHD z113652_0208 (zppg30
 FULPROG 65536
 TD 1024
 SOLVENT Acetone
 NS 4
 DS 29761.904 Hz
 SWH 0.908261 Hz
 FIDRES 1.1010048 sec
 AQ 191.37
 RG 16.800 usec
 DE 6.50 usec
 TE 298.2 K
 D1 2.0000000 sec
 D11 0.0300000 sec
 TD0 1
 SFO1 125.7703643 MHz
 NUC1 13C
 P1 10.00 usec
 PLW1 76.0000000 W
 SFO2 500.1320005 MHz
 NUC2 1H
 CPDPRG12 waltz16
 PCPD2 80.00 usec
 PLW2 20.5000000 W
 PLW12 0.3203100 W
 PLW13 0.1611100 W

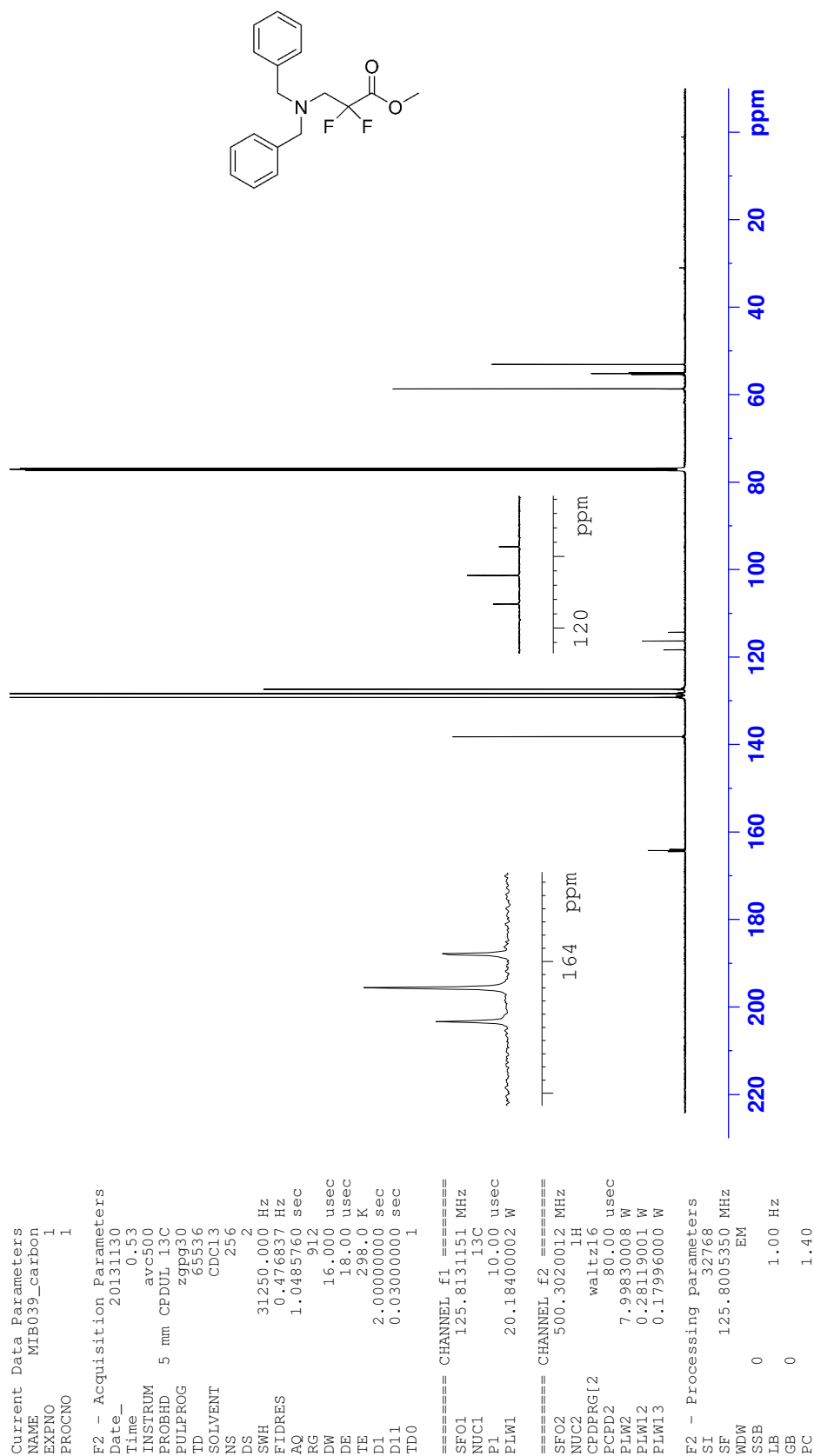
F2 - Processing parameters
 SI 32768
 SF 125.7577885 MHz
 WDW EM
 SSB 0
 LB 1.00 Hz
 GB 0
 PC 1.40

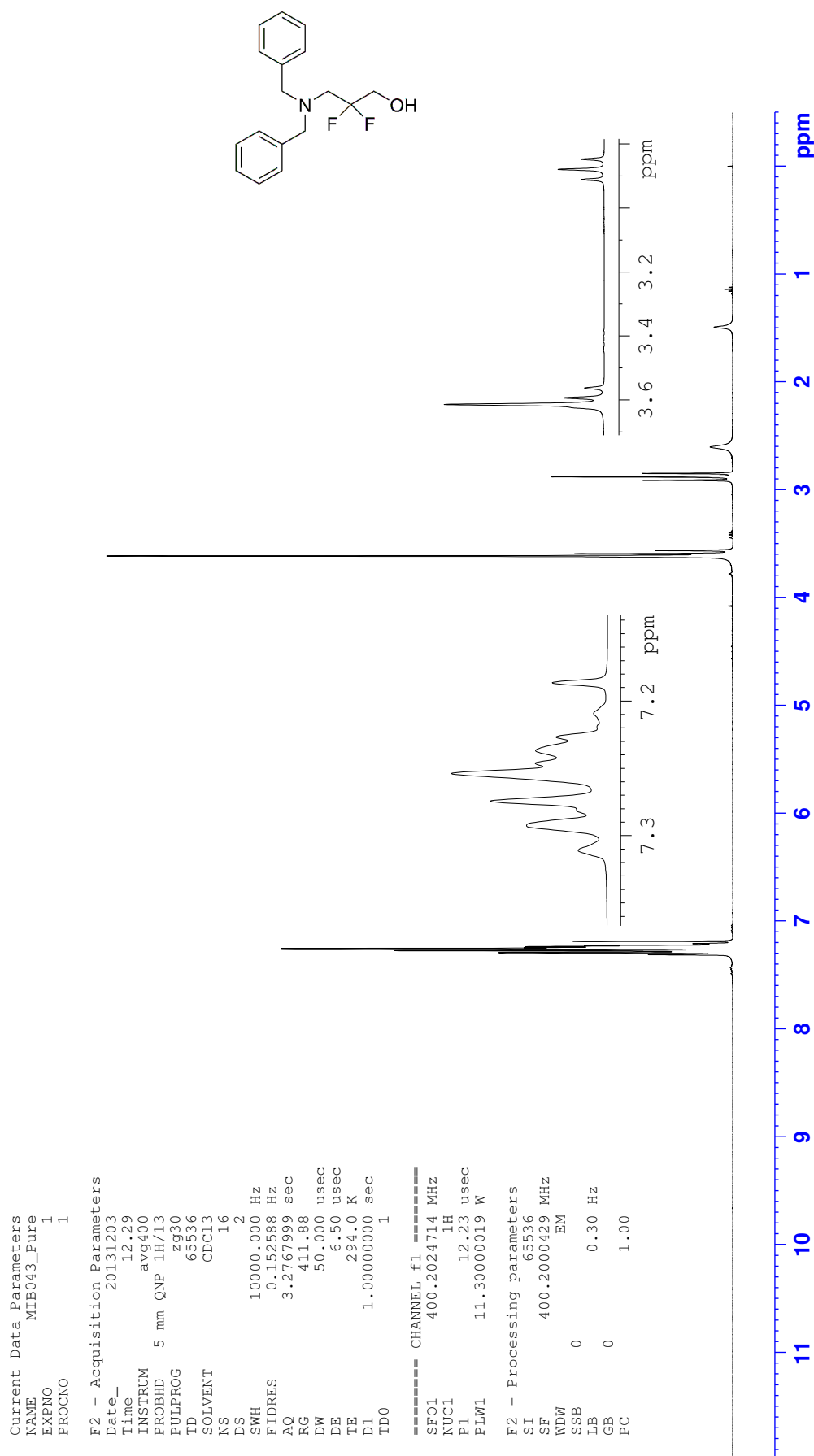
Appendix F: NMR spectra

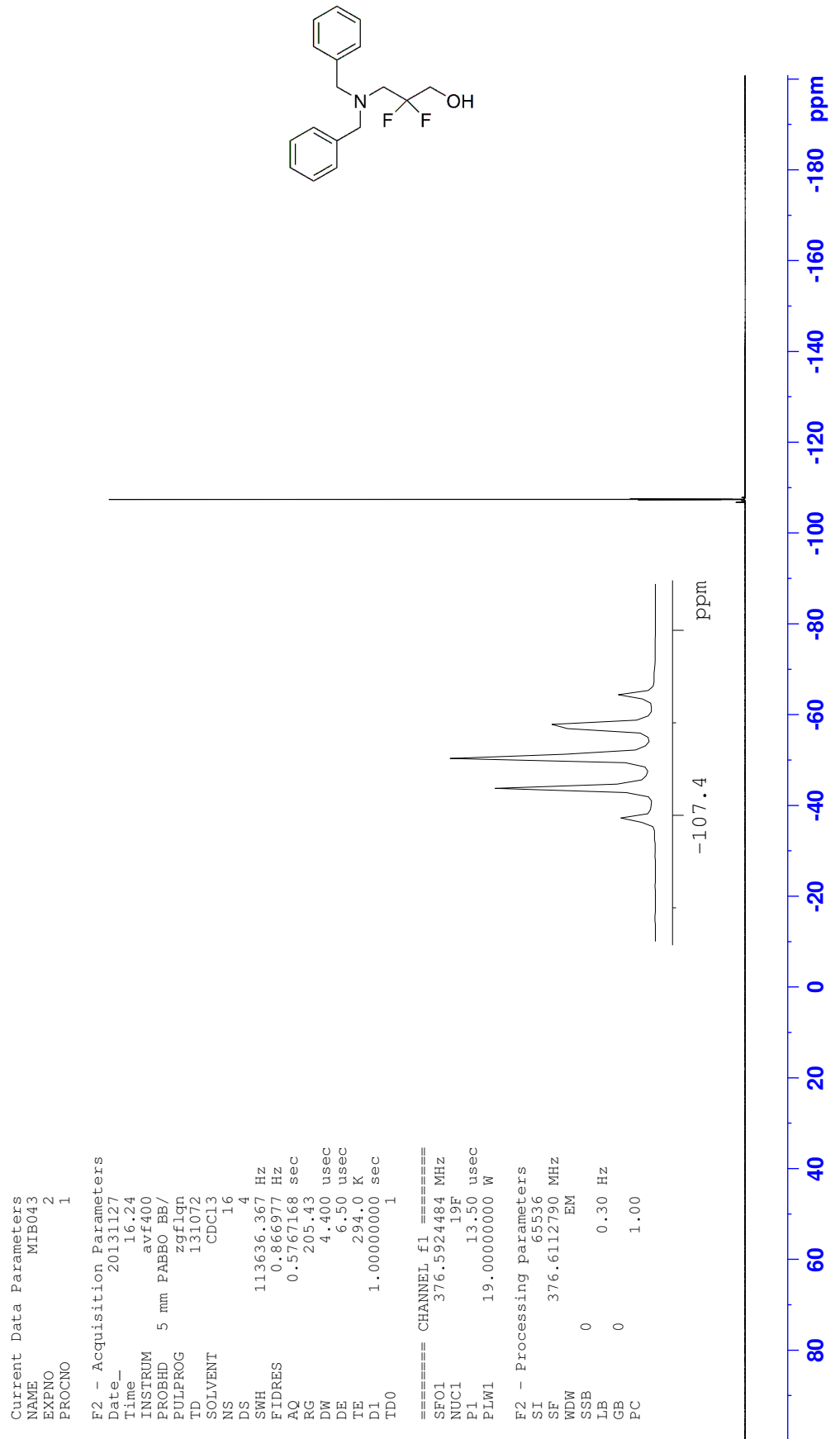
¹H NMR Methyl 3-(dibenzylamino)-2,2-difluoropropanoate (**144**)

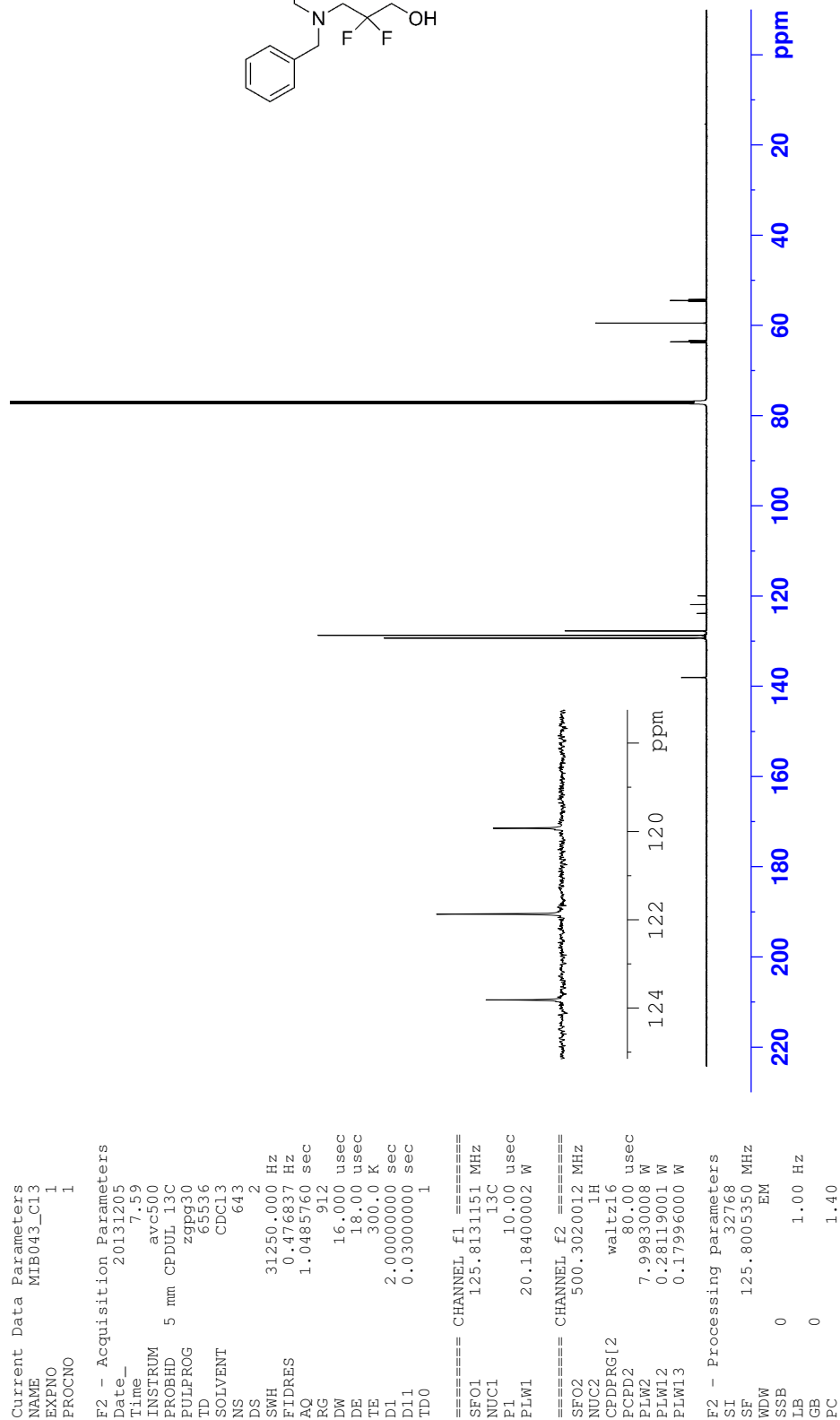
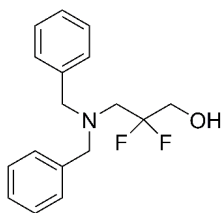


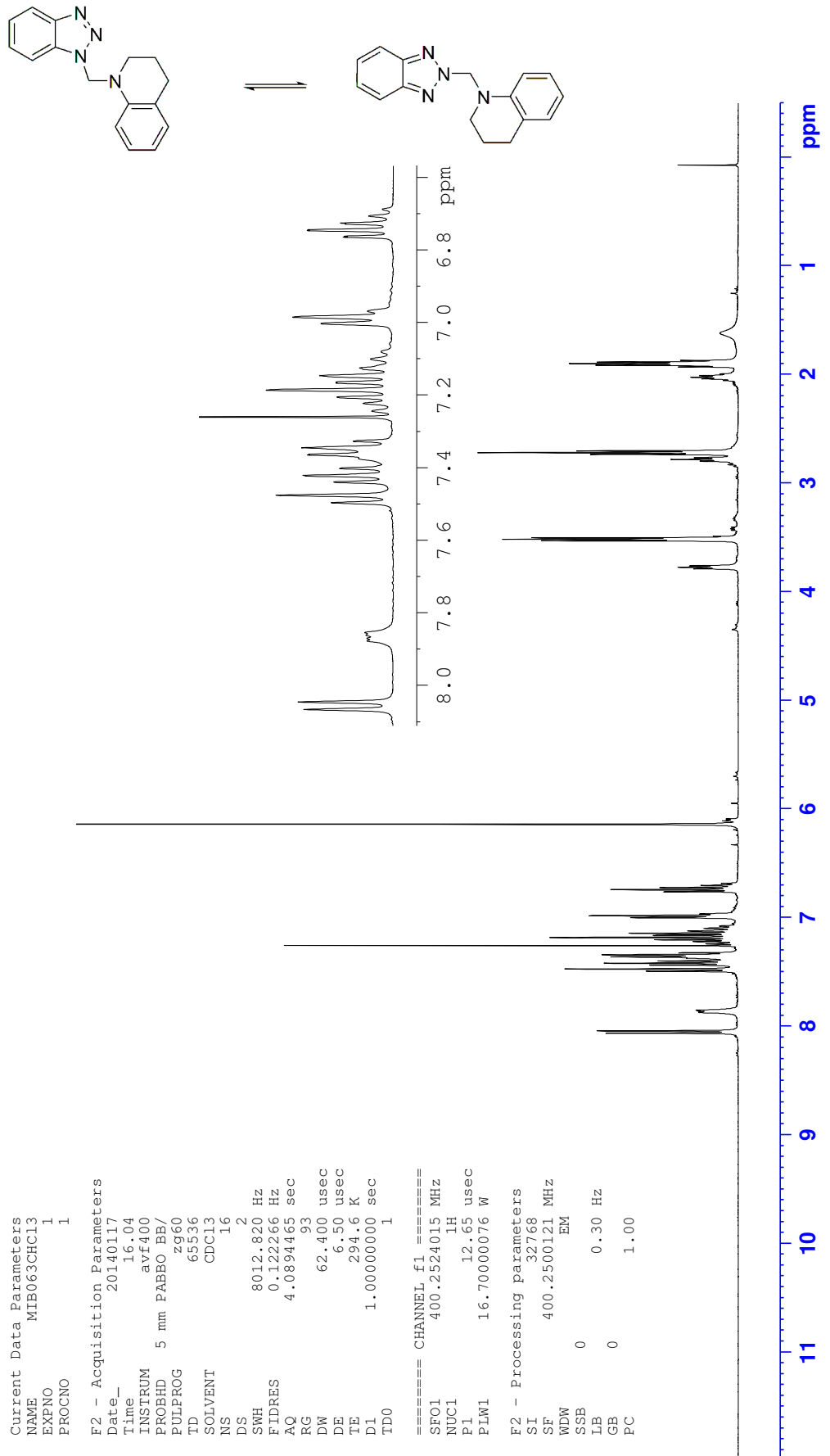
¹⁹F NMR Methyl 3-(dibenzylamino)-2,2-difluoropropanoate (**144**)

¹³C NMR Methyl 3-(dibenzylamino)-2,2-difluoropropanoate (**144**)

^1H NMR 3-(Dibenzylamino)-2,2-difluoropropan-1-ol (**150**)

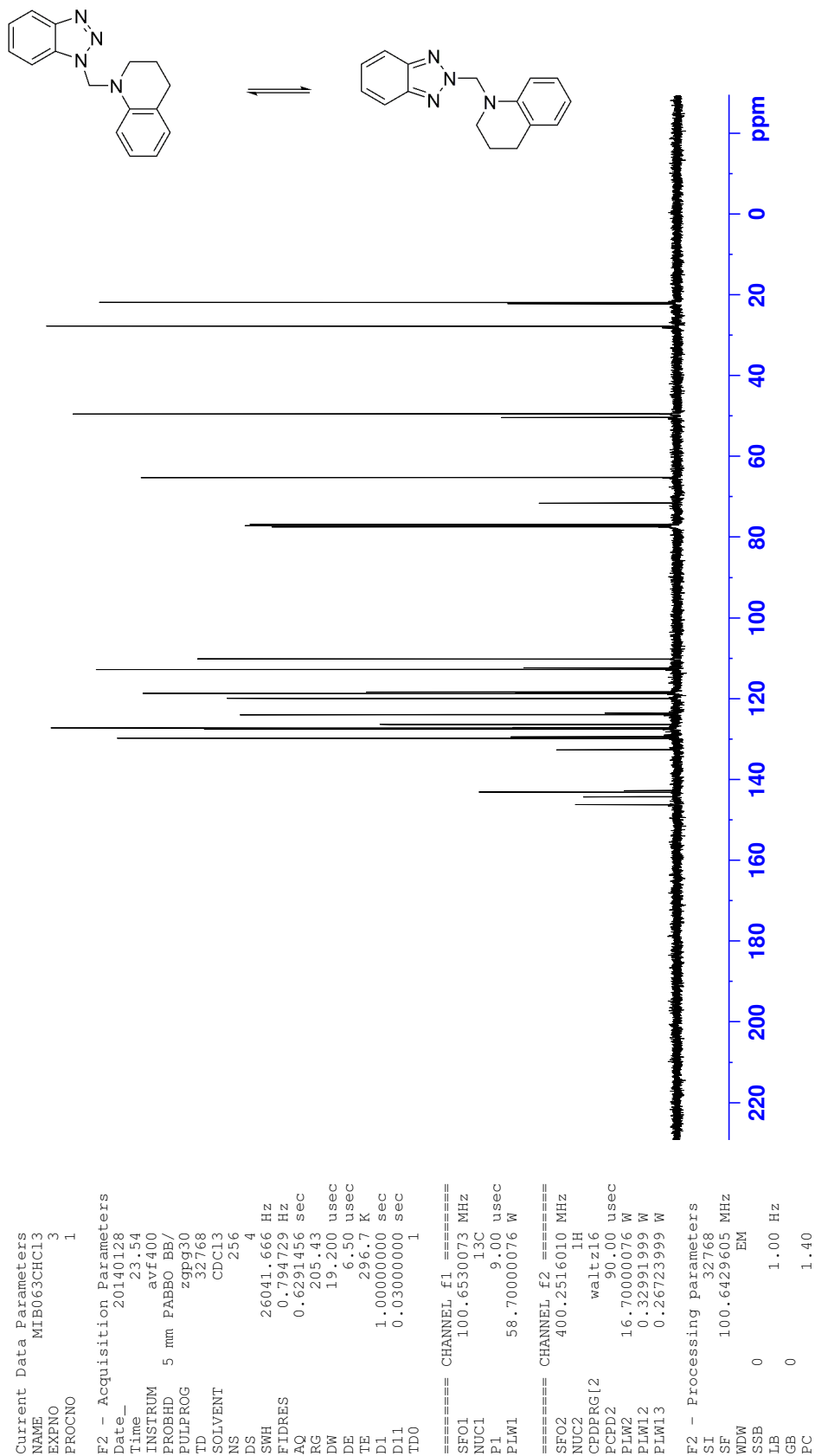
¹⁹F NMR 3-(Dibenzylamino)-2,2-difluoropropan-1-ol (**150**)

^{13}C NMR 3-(Dibenzylamino)-2,2-difluoropropan-1-ol (**150**)

¹H NMR 1-((1*H*-Benzo[d][1,2,3]triazol-1-yl)methyl)-1,2,3,4-tetrahydroquinoline **146**

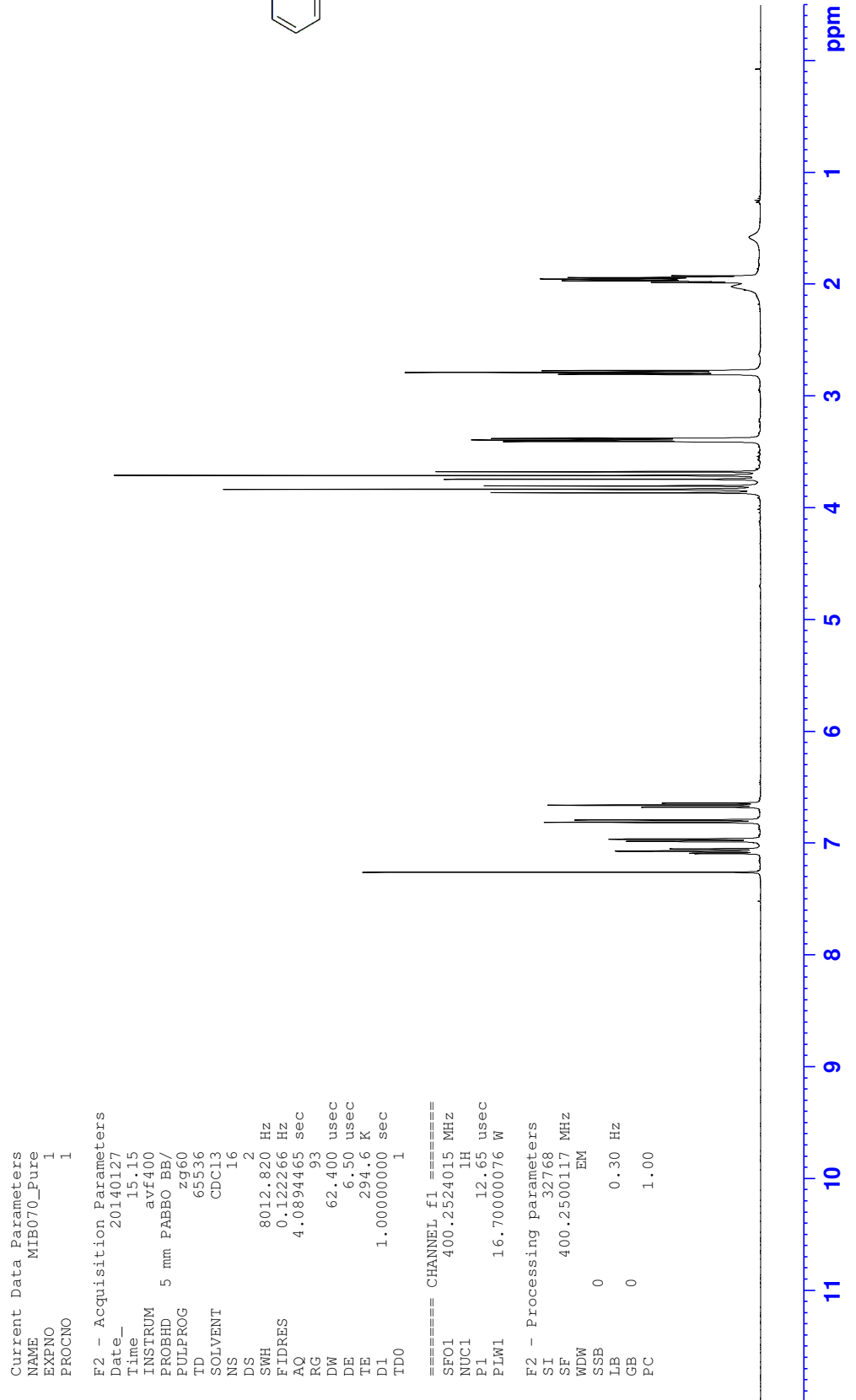
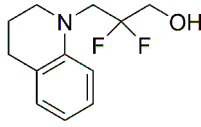
Appendix F: NMR spectra

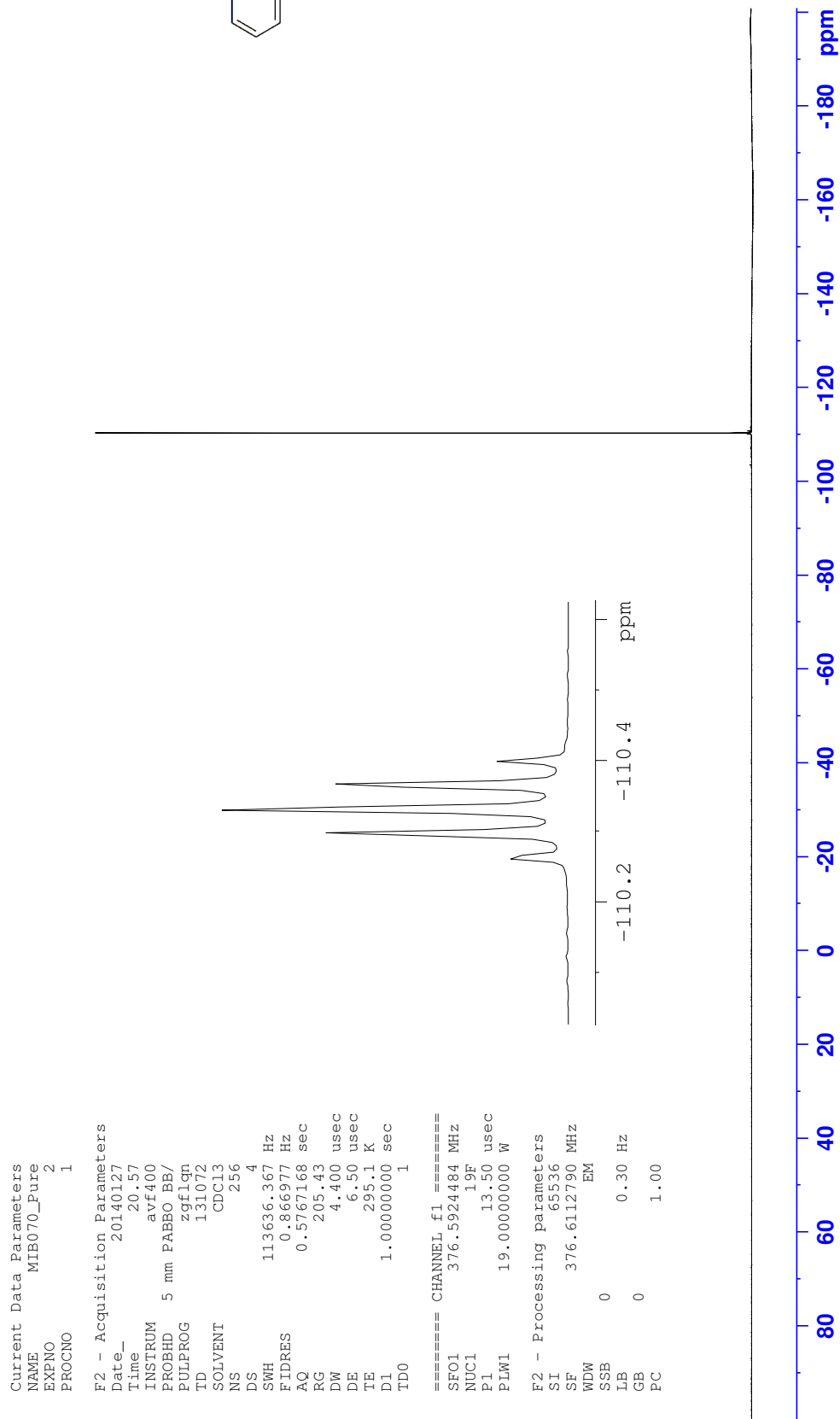
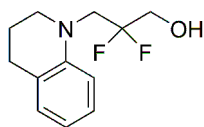
¹³C NMR 1-((1*H*-Benzo[d][1,2,3]triazol-1-yl)methyl)-1,2,3,4-tetrahydroquinoline **146**



Appendix F: NMR spectra

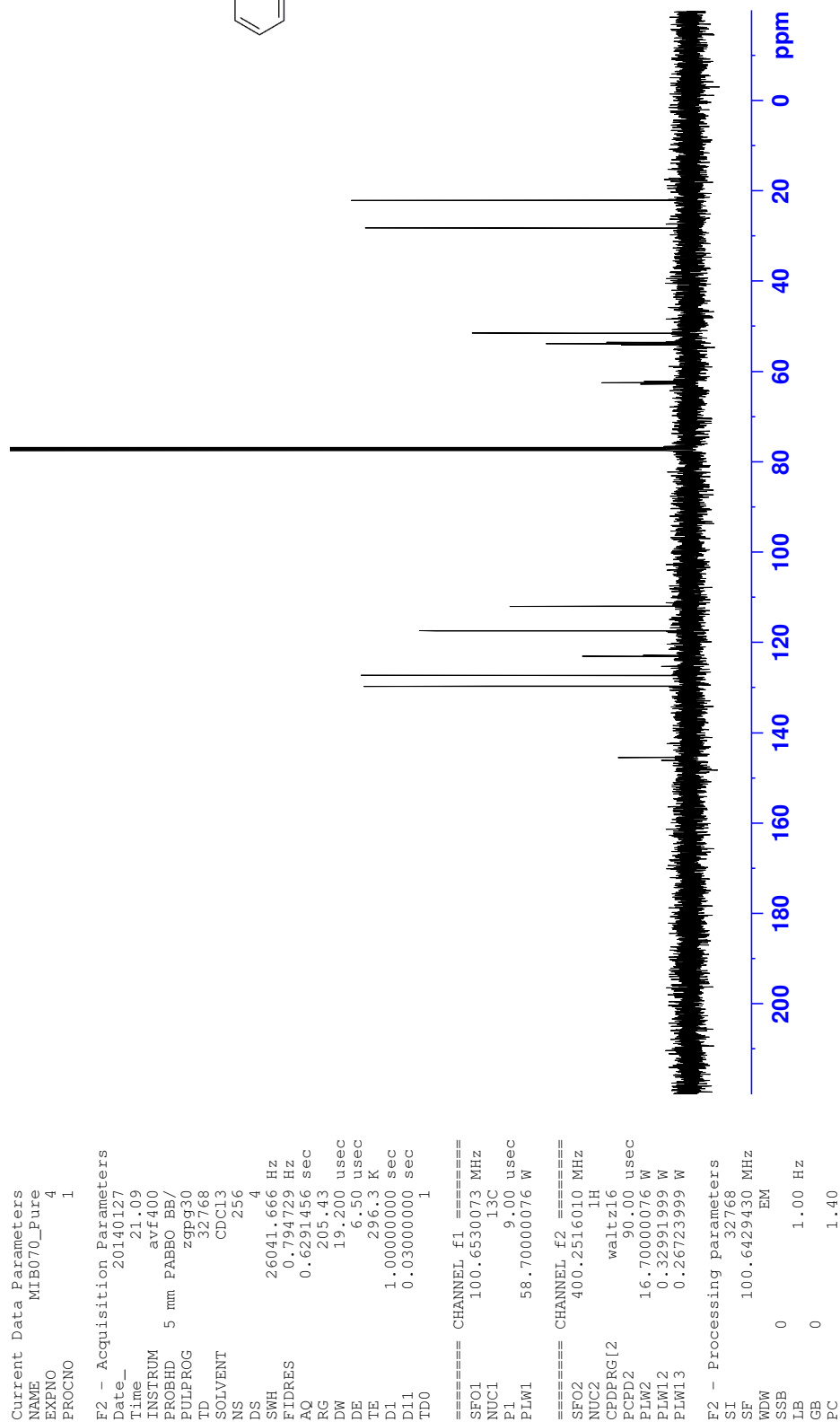
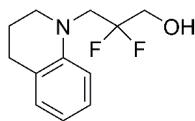
¹H NMR 3-(3,4-Dihydroquinolin-1(2H)-yl)-2,2-difluoropropan-1-ol (**149**)



^{19}F NMR 3-(3,4-Dihydroquinolin-1(2*H*)-yl)-2,2-difluoropropan-1-ol (**149**)

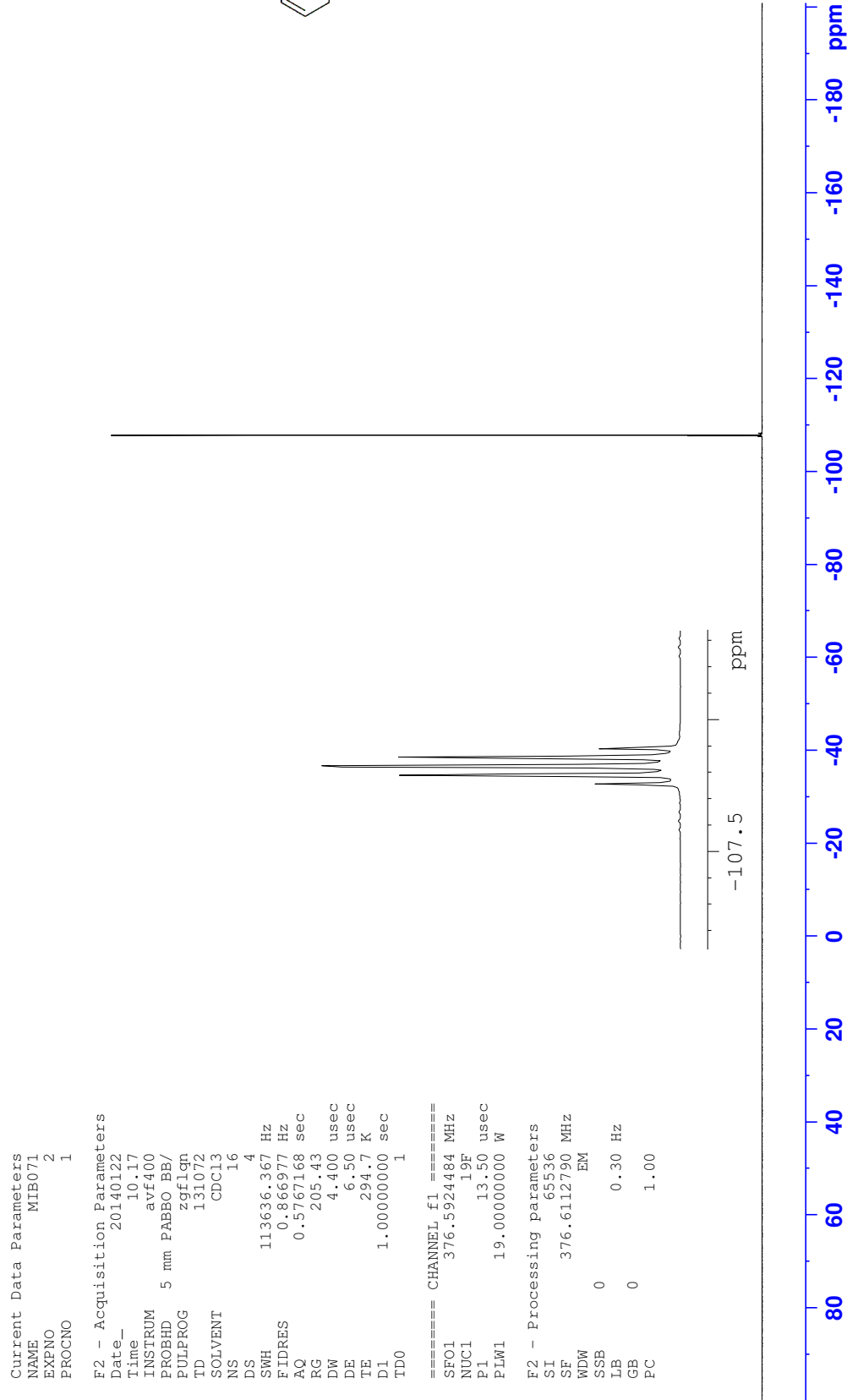
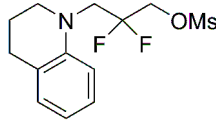
Appendix F: NMR spectra

¹³C NMR 3-(3,4-Dihydroquinolin-1(2*H*)-yl)-2,2-difluoropropan-1-ol (**149**)



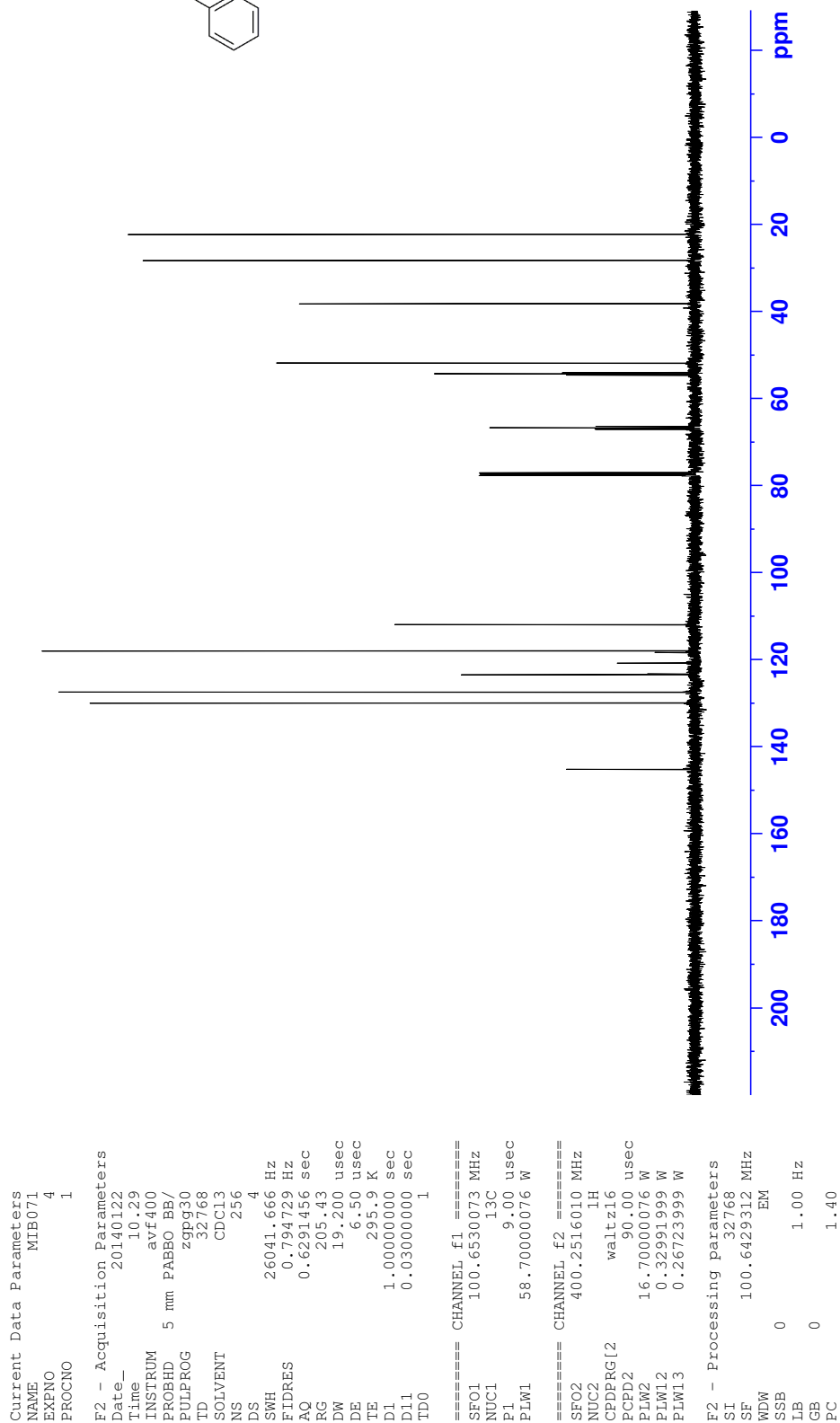
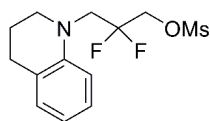
Appendix F: NMR spectra

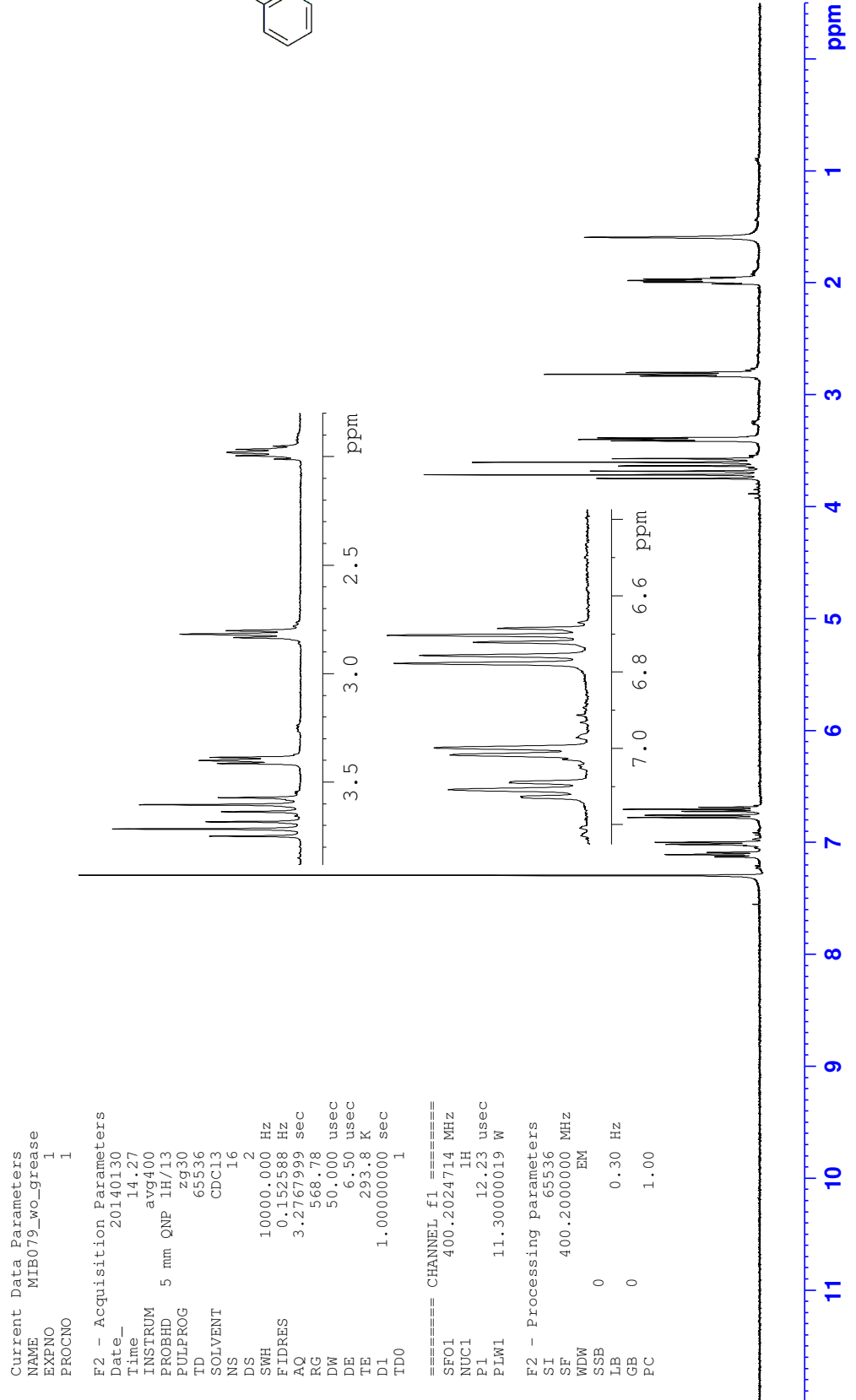
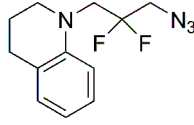
¹⁹F NMR 3-(3,4-Dihydroquinolin-1(2H)-yl)-2,2-difluoropropan methanesulfonate (**150**)

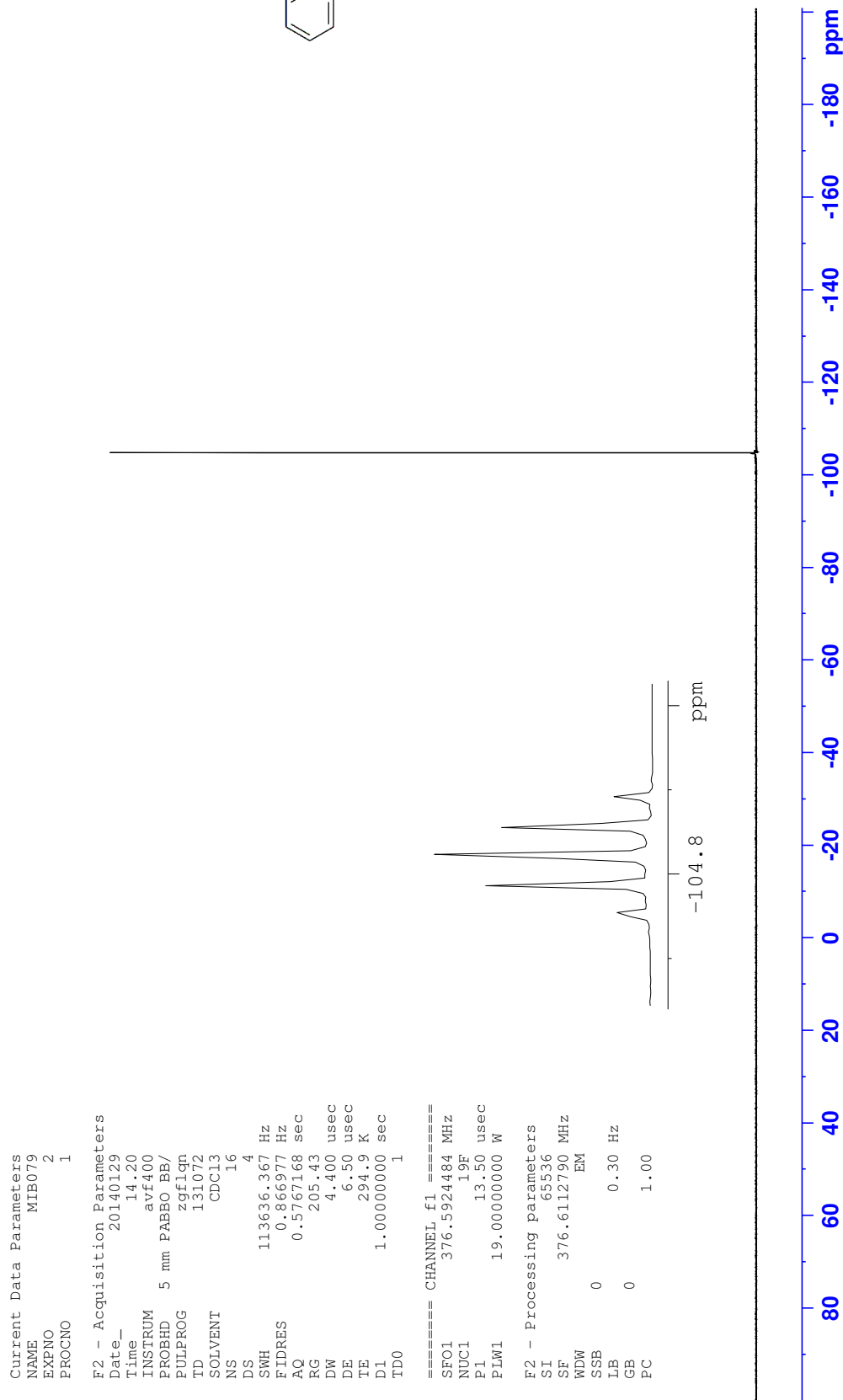
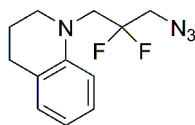


Appendix F: NMR spectra

¹³C NMR 3-(3,4-Dihydroquinolin-1(2*H*)-yl)-2,2-difluoropropan methanesulfonate (**150**)

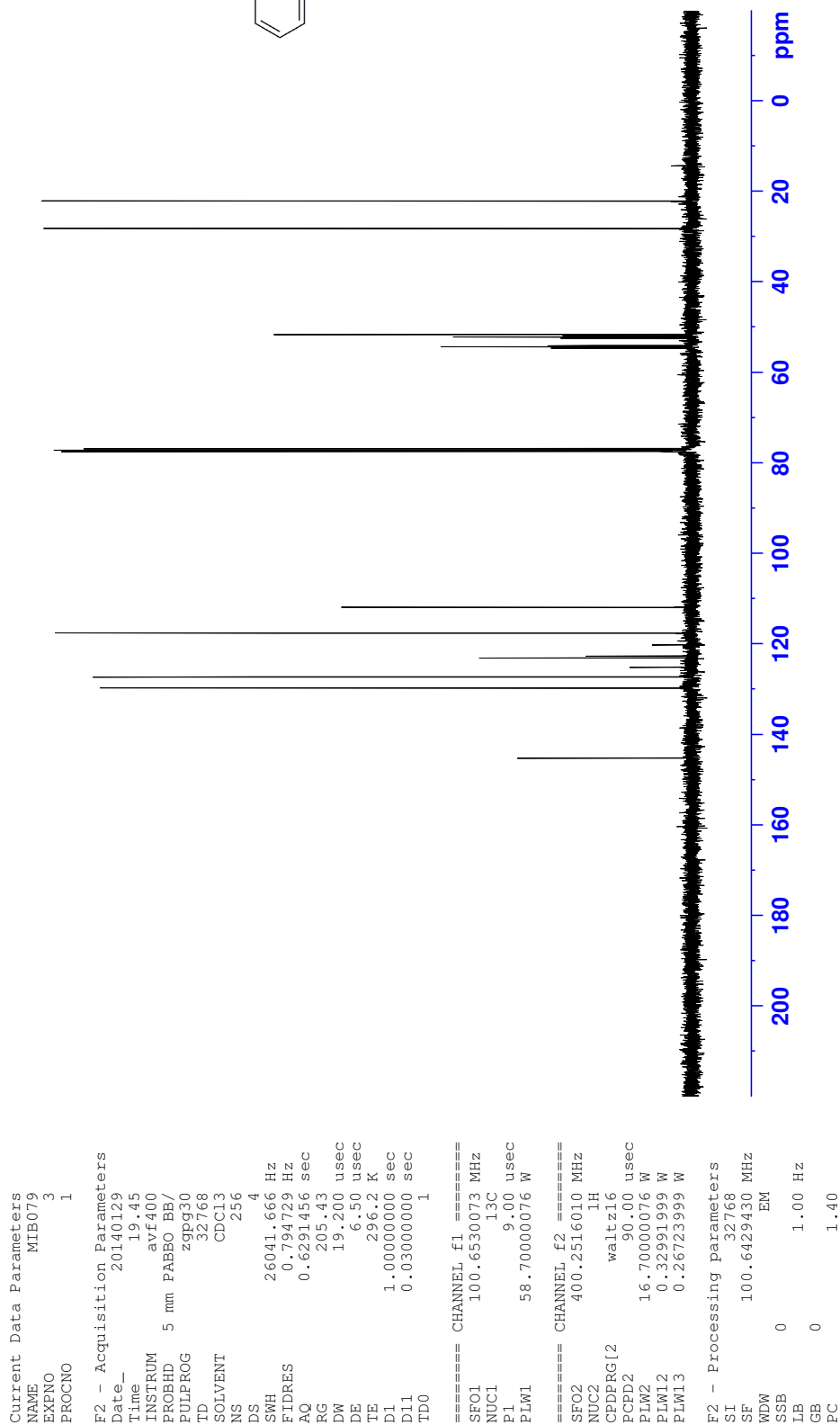
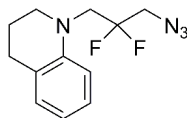


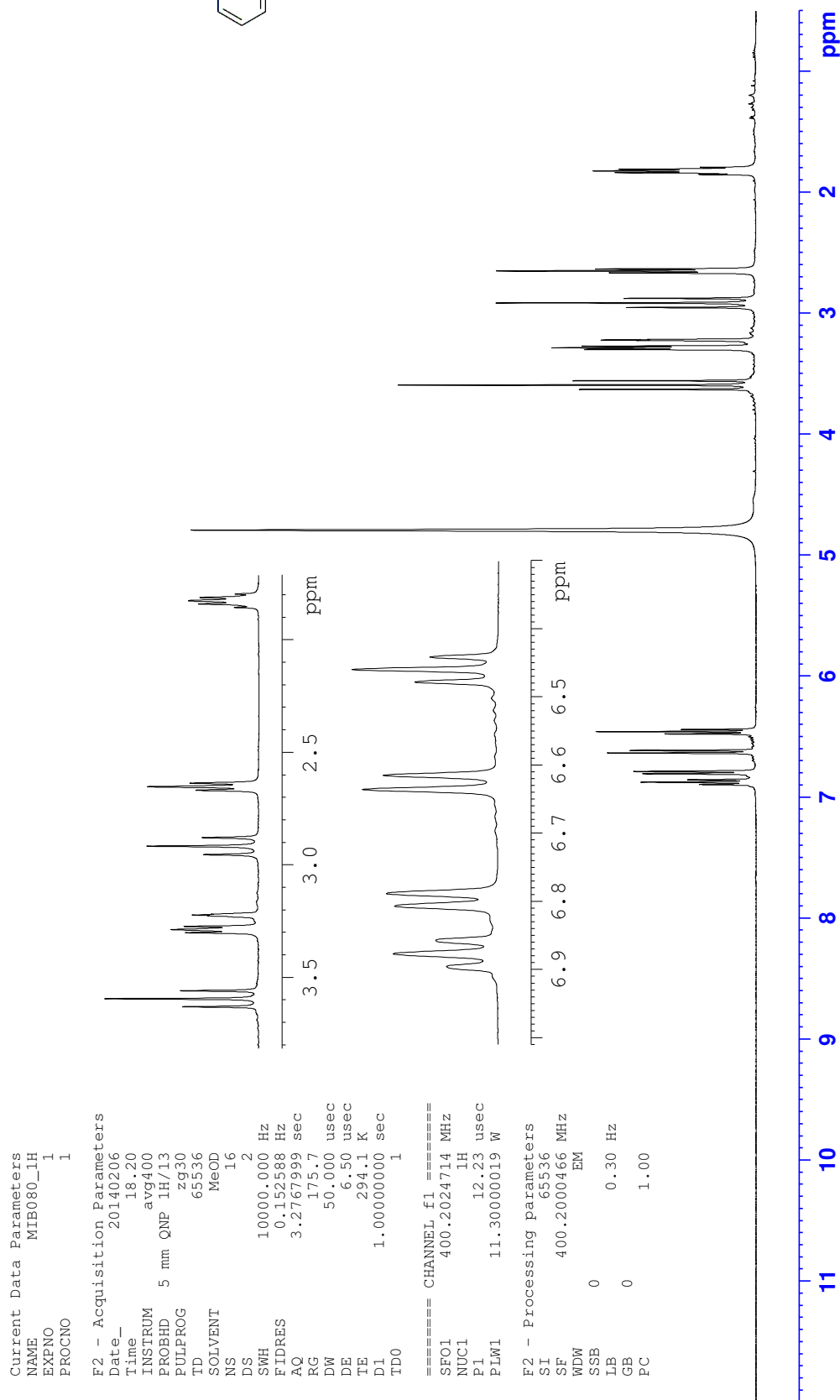
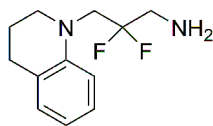
¹H NMR 1-(3-Azido-2,2-difluoropropyl)-1,2,3,4-tetrahydroquinoline (**151**)

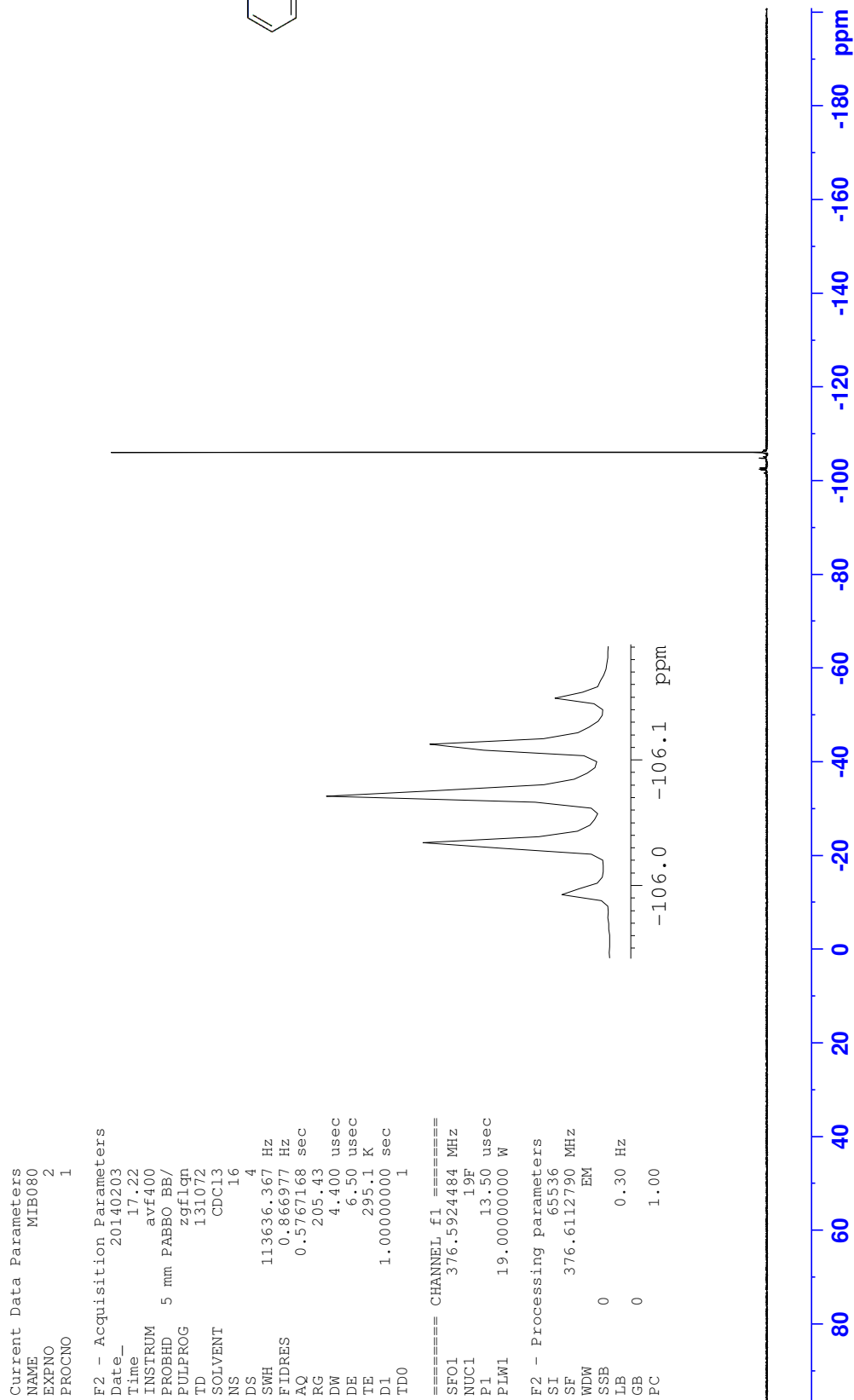
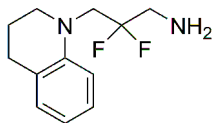
¹⁹F NMR 1-(3-Azido-2,2-difluoropropyl)-1,2,3,4-tetrahydroquinoline (**151**)

Appendix F: NMR spectra

¹³C NMR 1-(3-Azido-2,2-difluoropropyl)-1,2,3,4-tetrahydroquinoline (151)

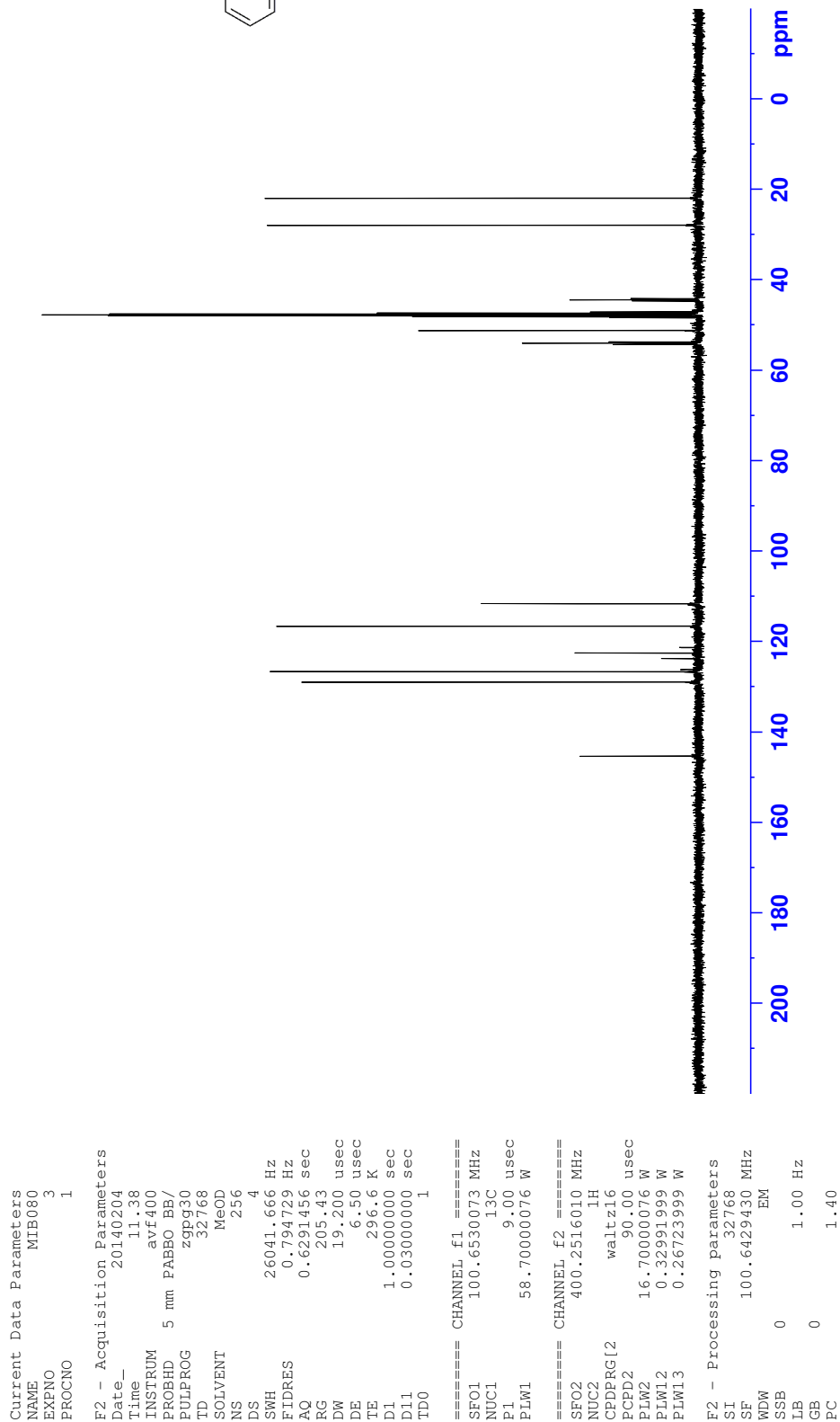
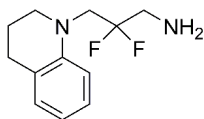


¹H NMR 3-(3,4-Dihydroquinolin-1(2*H*)-yl)-2,2-difluoropropan-1-amine (**142**)

^{19}F NMR 3-(3,4-Dihydroquinolin-1(2*H*)-yl)-2,2-difluoropropan-1-amine (**142**)

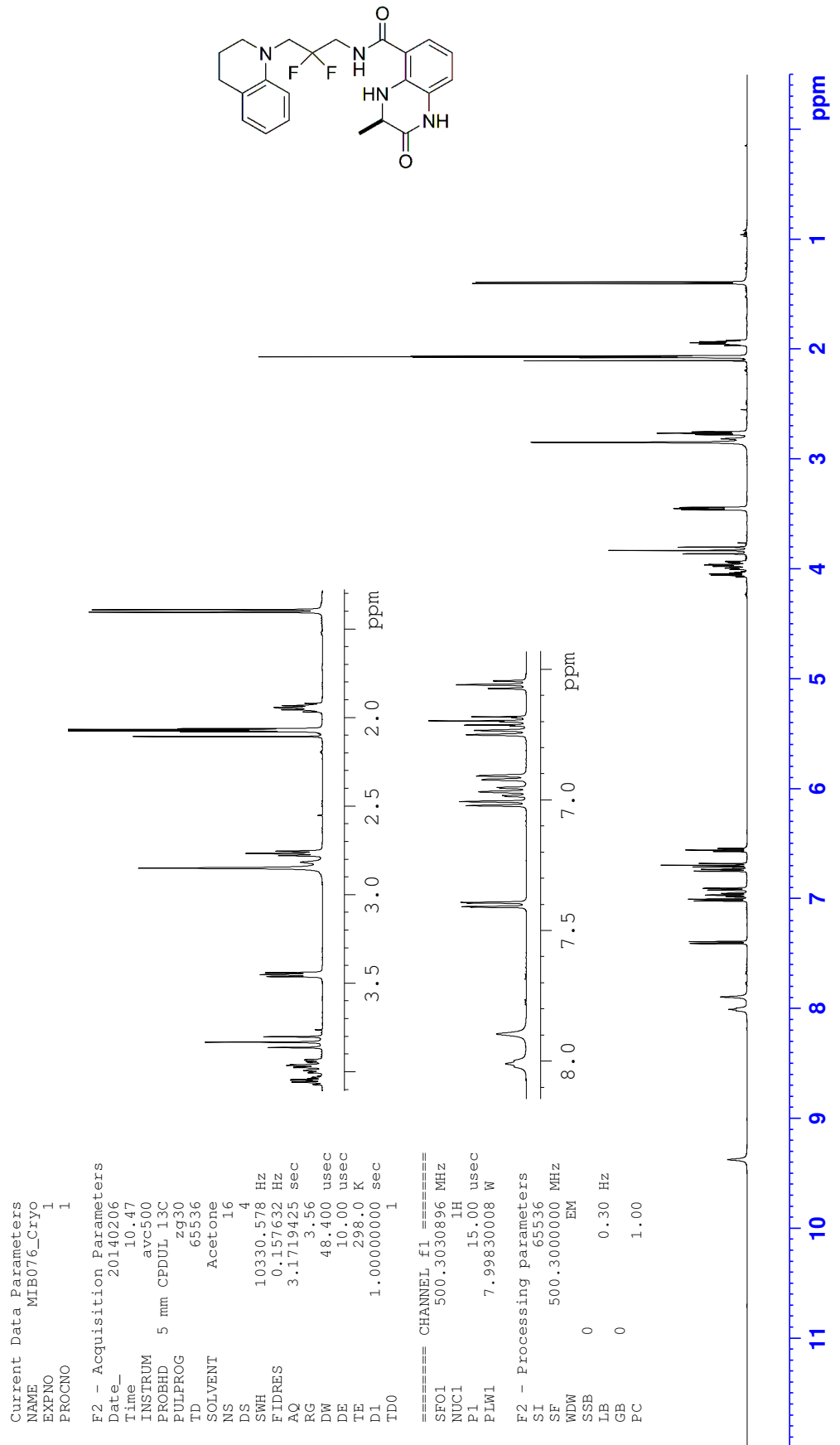
Appendix F: NMR spectra

¹³C NMR 3-(3,4-Dihydroquinolin-1(2H)-yl)-2,2-difluoropropan-1-amine (142)



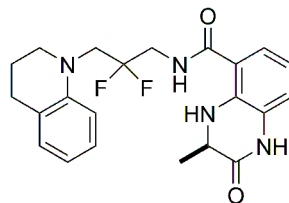
Appendix F: NMR spectra

¹H NMR (*R*)-*N*-(3-(3,4-Dihydroquinolin-1(2*H*)-yl)-2,2-difluoropropyl)-3-methyl-2-oxo-1,2,3,4-tetrahydroquinoxaline-5-carboxamide (**141**)



Appendix F: NMR spectra

^{19}F NMR (*R*)-*N*-(3-(3,4-Dihydroquinolin-1(2*H*)-yl)-2,2-difluoropropyl)-3-methyl-2-oxo-1,2,3,4-tetrahydroquinoxaline-5-carboxamide (**141**)



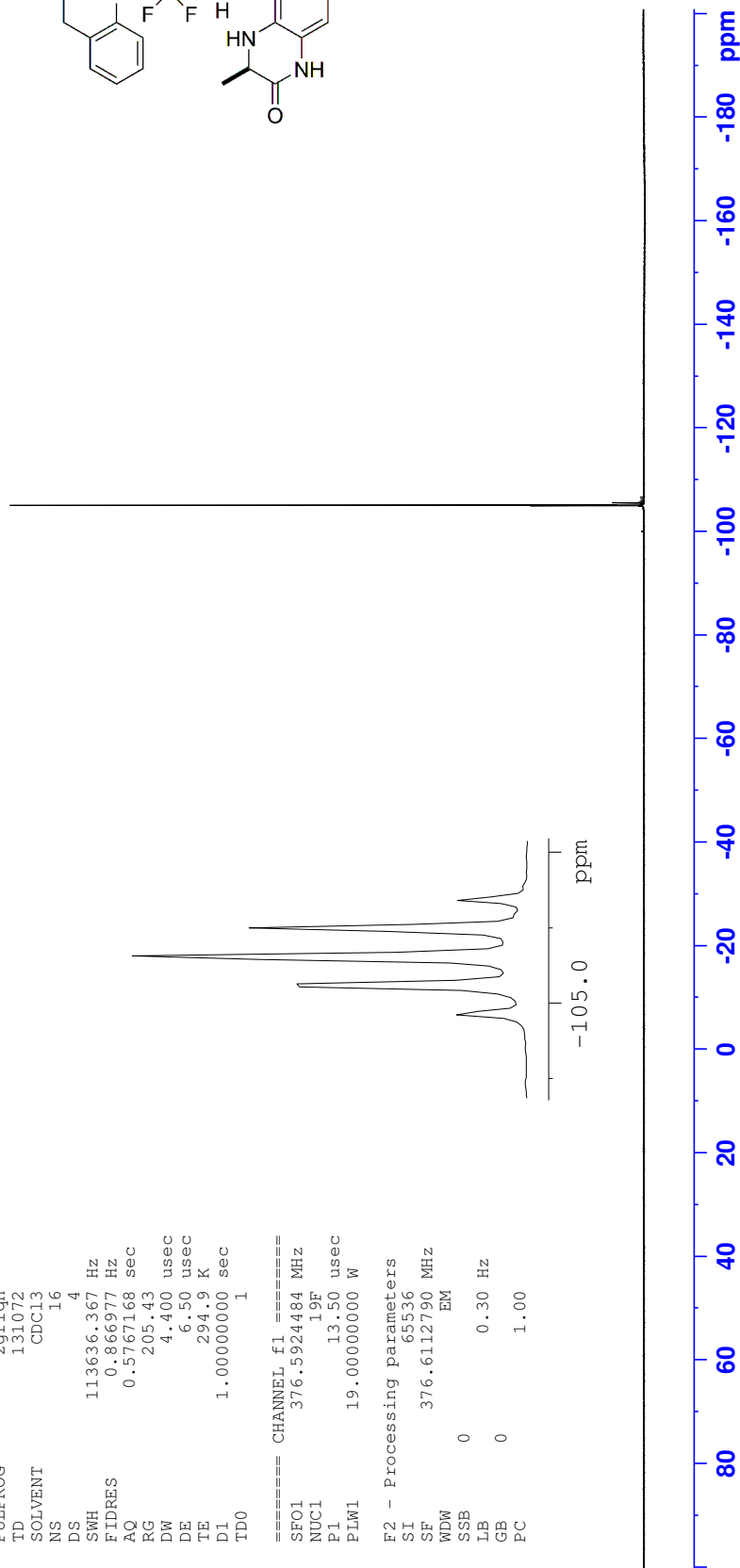
```

Current Data Parameters
NAME      MIB076
EXPNO    2
PROCNO   1

F2 - Acquisition Parameters
Date_    20140128
Time     13.09
INSTRUM  avf400
PROBHD   5 mm PABBO BB/
PULPROG  zgpg30
TD       131072
SOLVENT  CDCl3
NS       16
DS       4
SWH      113636.367 Hz
FIDRES   0.866977 Hz
AQ       0.5767168 sec
RG       205.43
DW       4.400 usec
DE       6.50 usec
TE       294.9 K
D1       1.00000000 sec
TD0      1

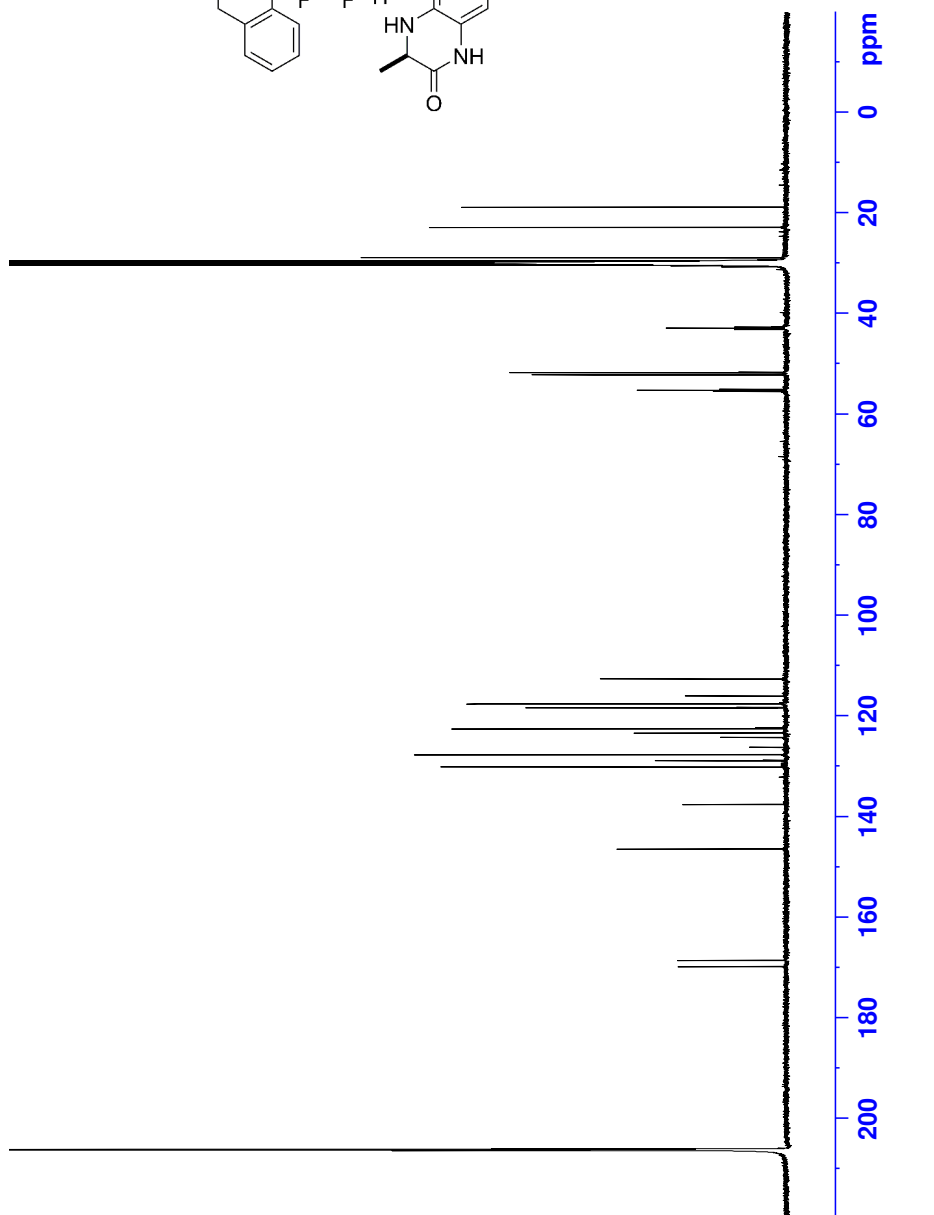
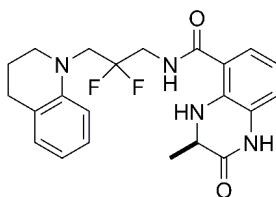
===== CHANNEL f1 =====
SFO1    376.5924484 MHz
NUC1    19F
P1      13.50 usec
PLW1    19.00000000 W

F2 - Processing parameters
SI      65536
SF      376.6112790 MHz
WDW     EM
SSB     0
LB      0.30 Hz
GB      0
PC      1.00
    
```



Appendix F: NMR spectra

^{13}C NMR (*R*)-*N*-(3-(3,4-Dihydroquinolin-1(2*H*)-yl)-2,2-difluoropropyl)-3-methyl-2-oxo-1,2,3,4-tetrahydroquinoxaline-5-carboxamide **141**



```

Current Data Parameters
NAME      MIB076_Cryo
EXPNO     4
PROCNO    1

F2 - Acquisition Parameters
Date_     20140206
Time      11_23
INSTRUM   avc500
PROBHD    5 mm CPDUL 13C
PULPROG   zgpg30
TD         65536
SOLVENT   Acetone
NS         1466
DS         2
SWH        31250.000 Hz
FIDRES     0.476837 Hz
AQ          1.0485760 sec
RG          912
DW          16.000 usec
DE          18.00 usec
TE          298.0 K
D1          2.00000000 sec
D11         0.03000000 sec
TD0         1

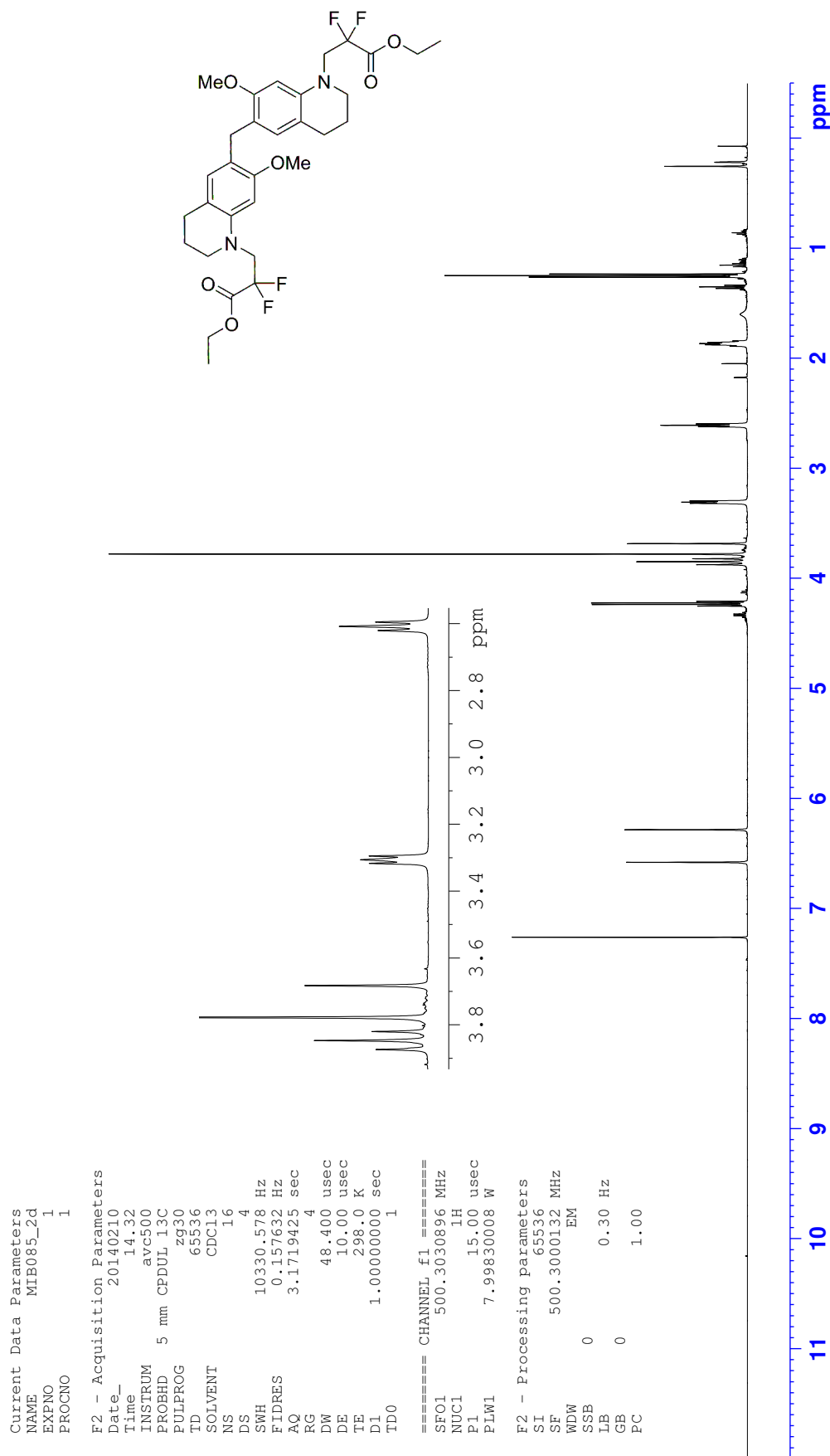
===== CHANNEL f1 =====
SF01      125.8131151 MHz
NUC1       13C
P1         10.00 usec
PLW1      20.18400002 W

===== CHANNEL f2 =====
SF02      500.3020012 MHz
NUC2       1H
CPDPRG12  waltz16
PCPD2     80.00 usec
PLW2     7.99830008 W
PLWI2    0.28119001 W
PLWI3    0.17996000 W

F2 - Processing parameters
SI         32768
SF         125.8004230 MHz
WDW        EM
SSB        0
LB         1.00 Hz
GB         0
PC         1.40
    
```

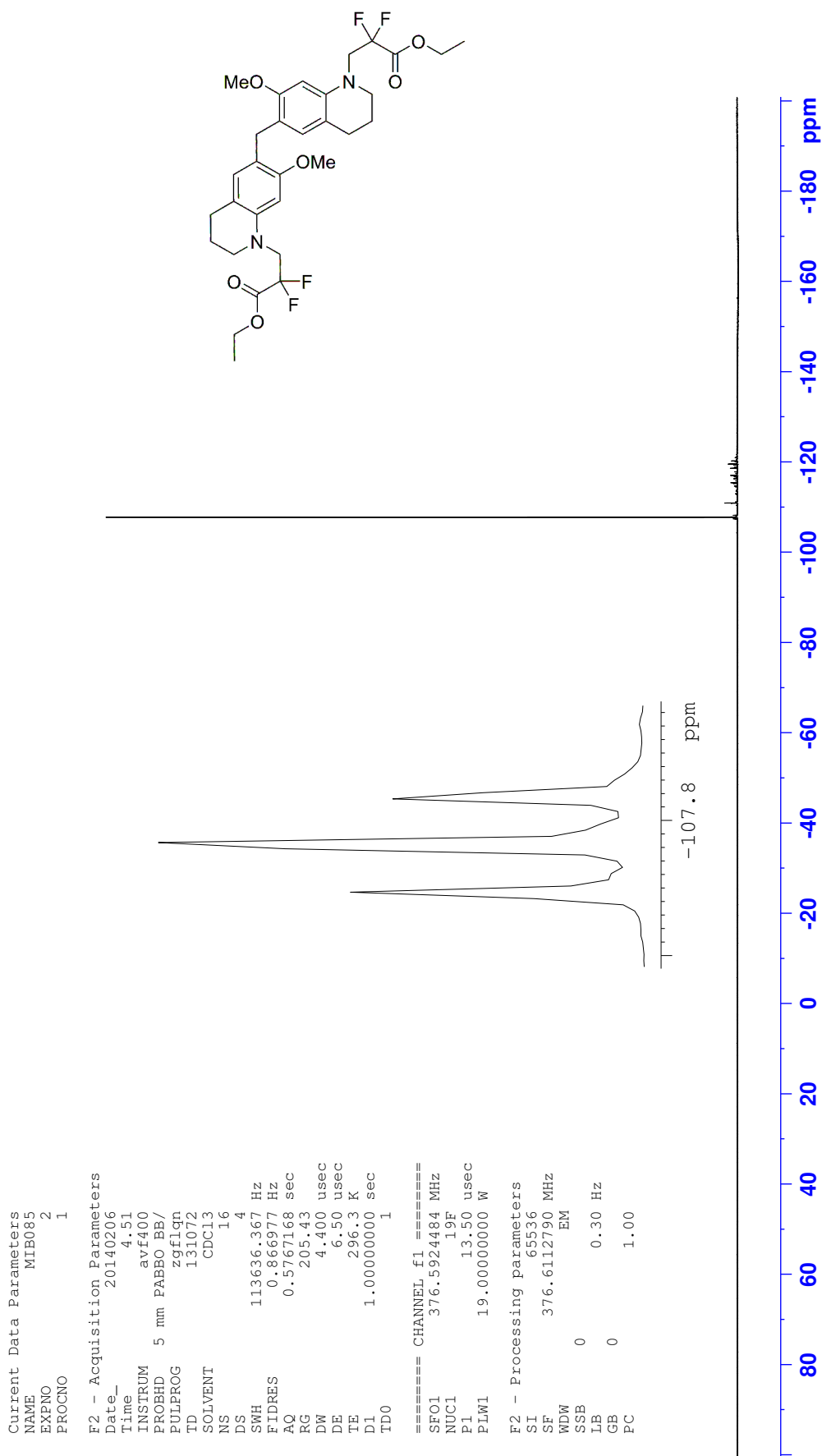
Appendix F: NMR spectra

¹H NMR Diethyl 3,3'-(methylenebis(7-methoxy-3,4-dihydroquinoline-6,1(2H)-diyl))bis(2,2-difluoropropanoate) (**152**)



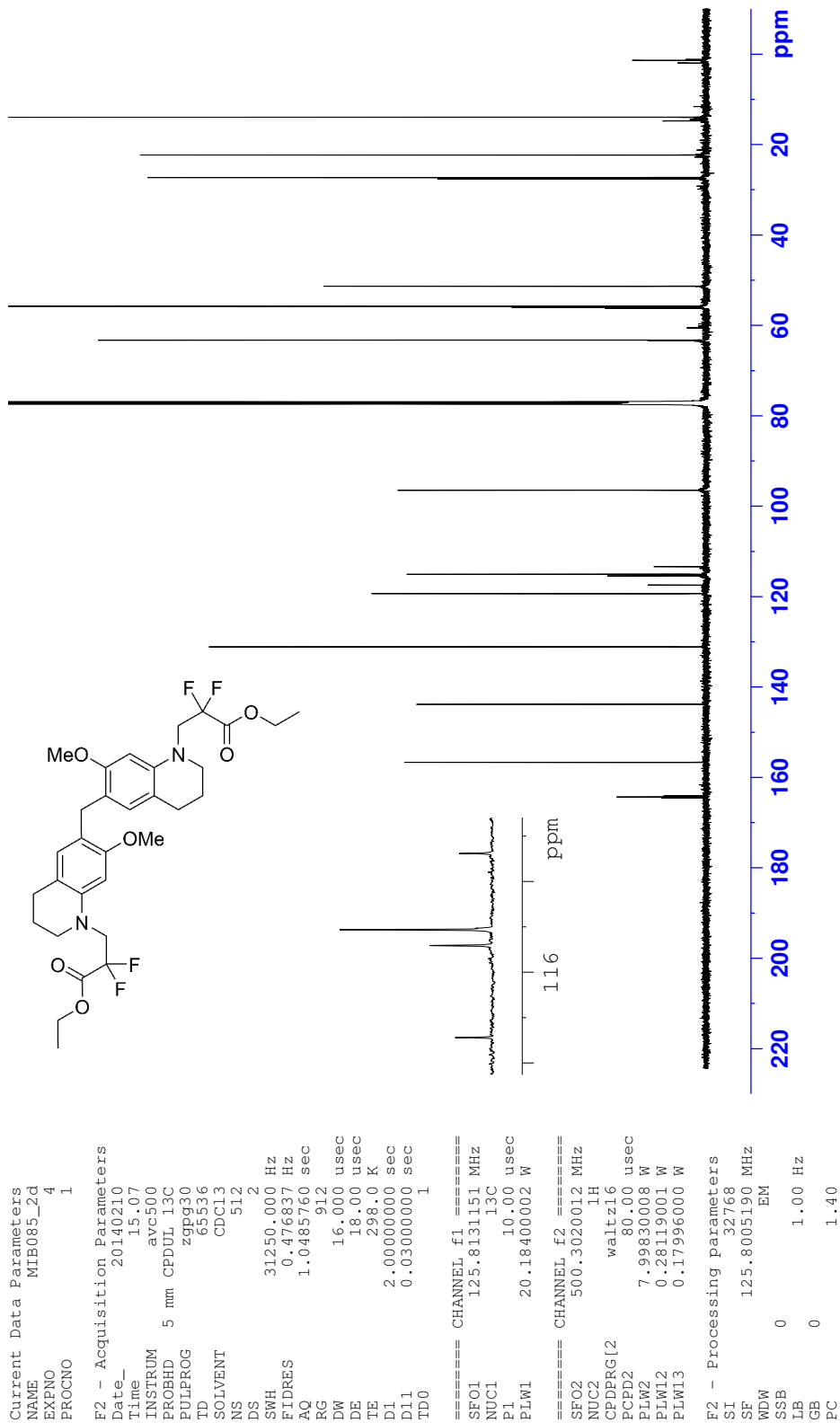
Appendix F: NMR spectra

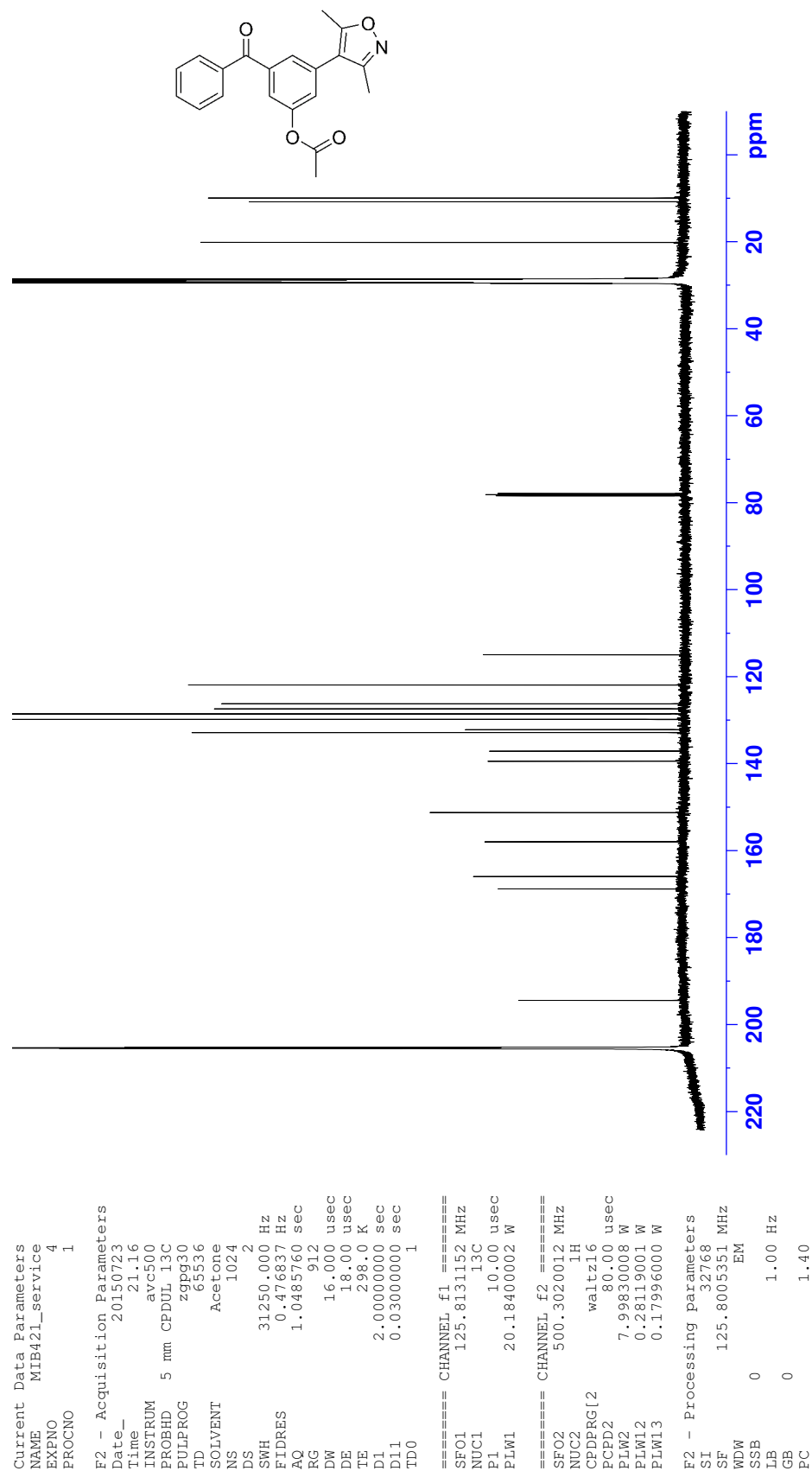
^{19}F NMR Diethyl 3,3'-(methylenebis(7-methoxy-3,4-dihydroquinoline-6,1(2H)-diyl))bis(2,2-difluoropropanoate) (**152**)

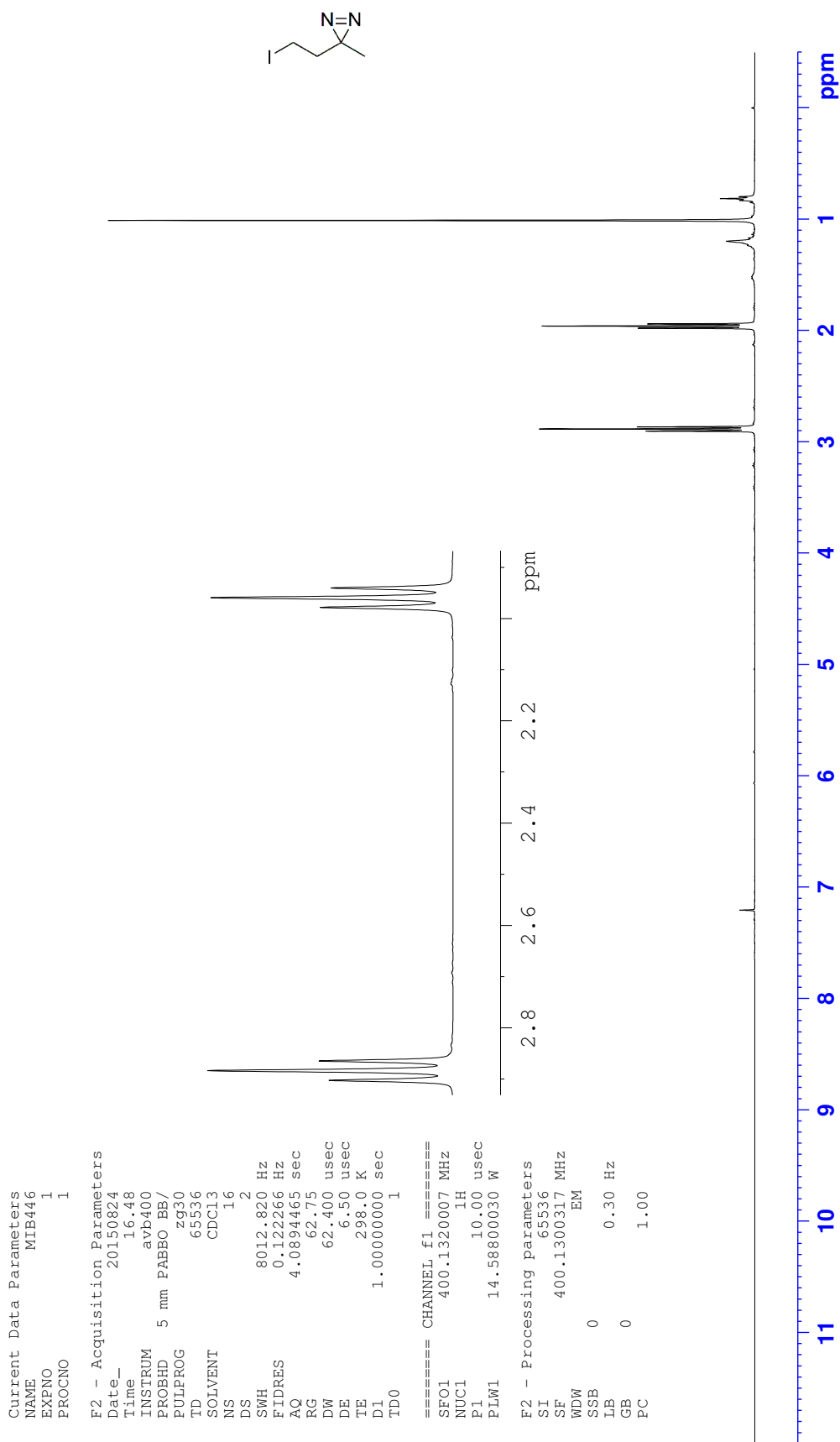


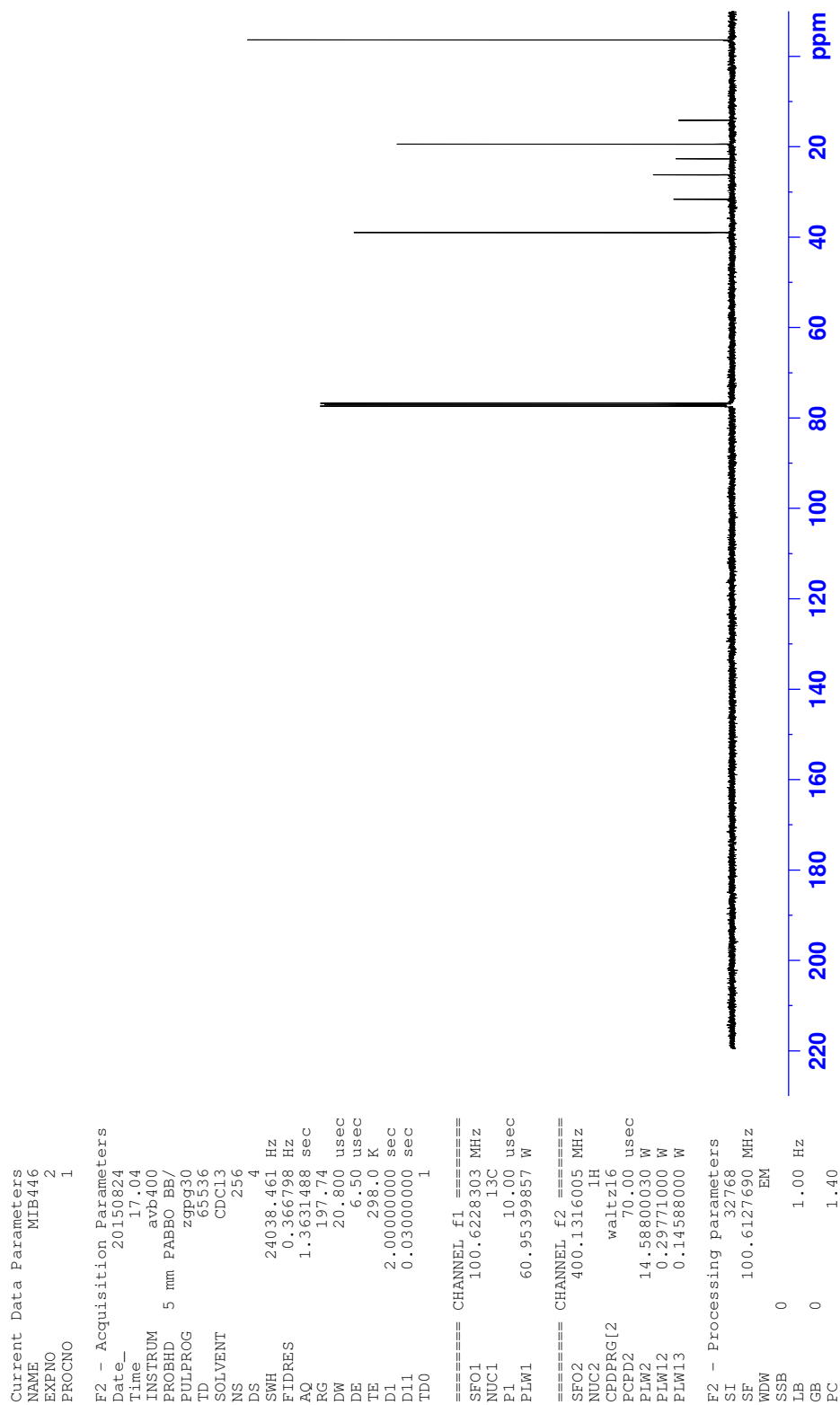
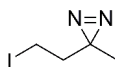
Appendix F: NMR spectra

¹³C NMR Diethyl 3,3'-(methylenebis(7-methoxy-3,4-dihydroquinoline-6,1(2H)-diyl))bis(2,2-difluoropropanoate) (**152**)



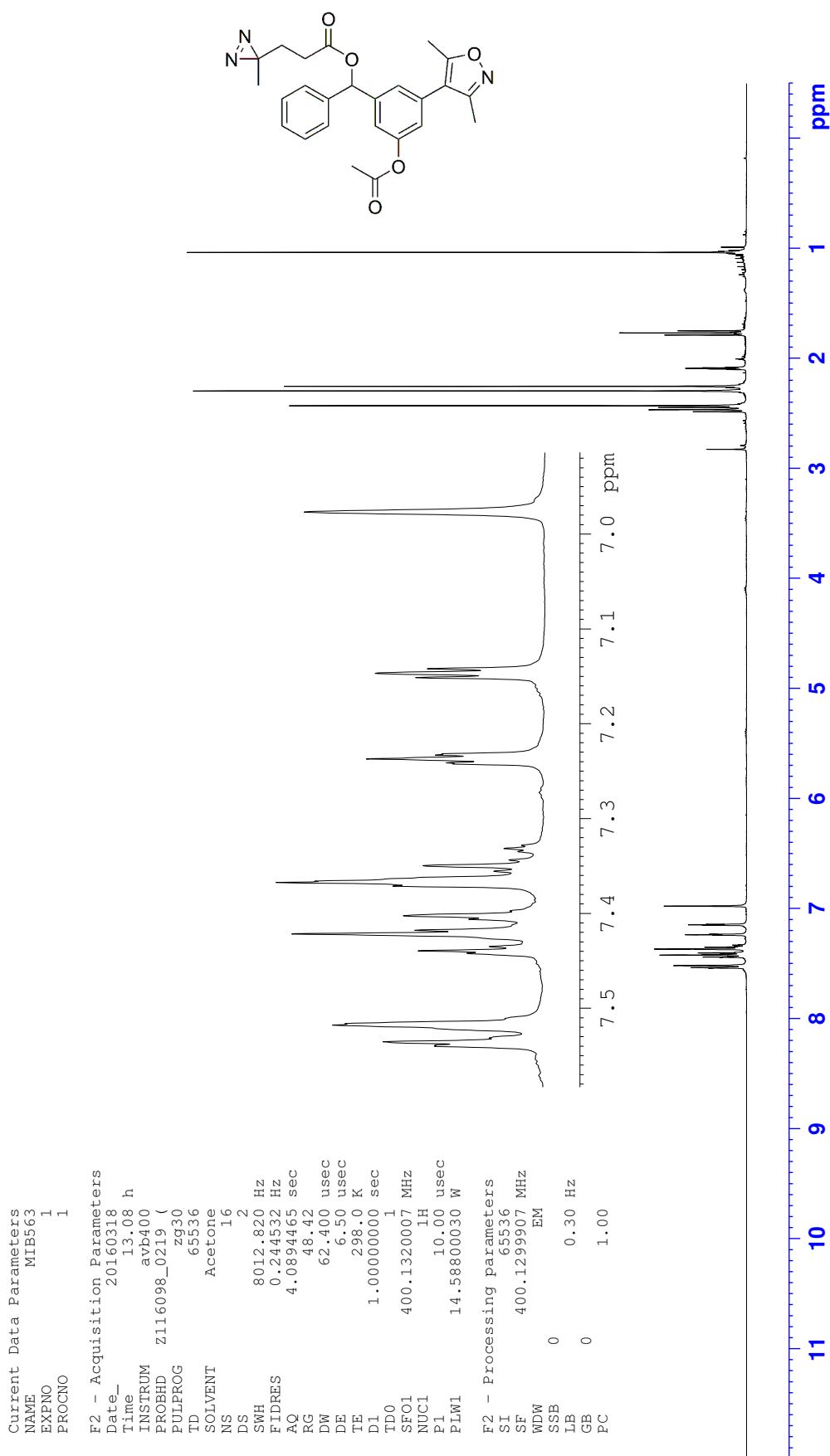
¹³C NMR 3-Benzoyl-5-(3,5-dimethylisoxazol-4-yl)phenyl acetate (**168**)

¹H NMR 3-(2-Iodoethyl)-3-methyl-3H-diazirine (**174**)

¹³C NMR 3-(2-Iodoethyl)-3-methyl-3H-diazirine (**174**)

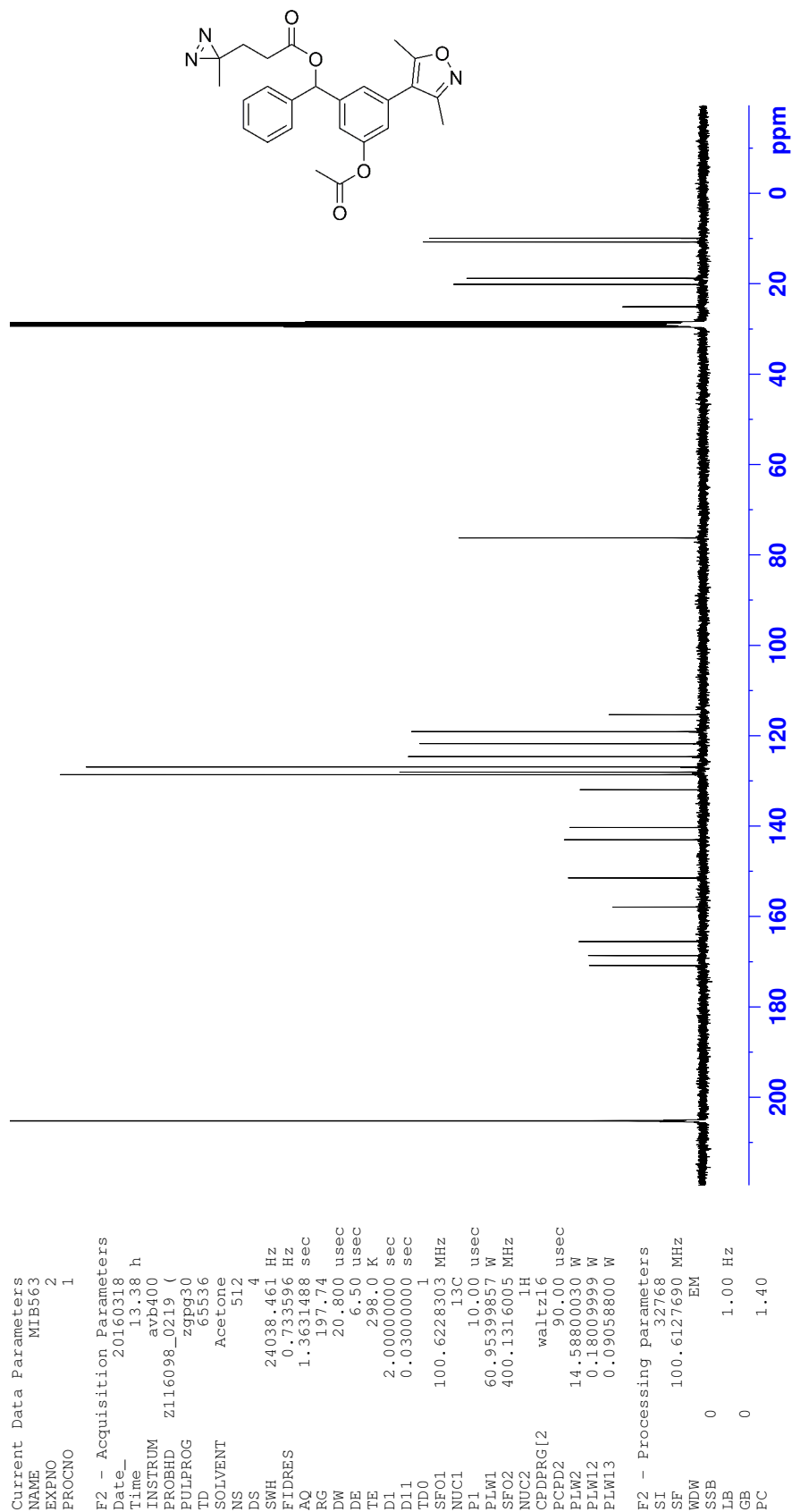
Appendix F: NMR spectra

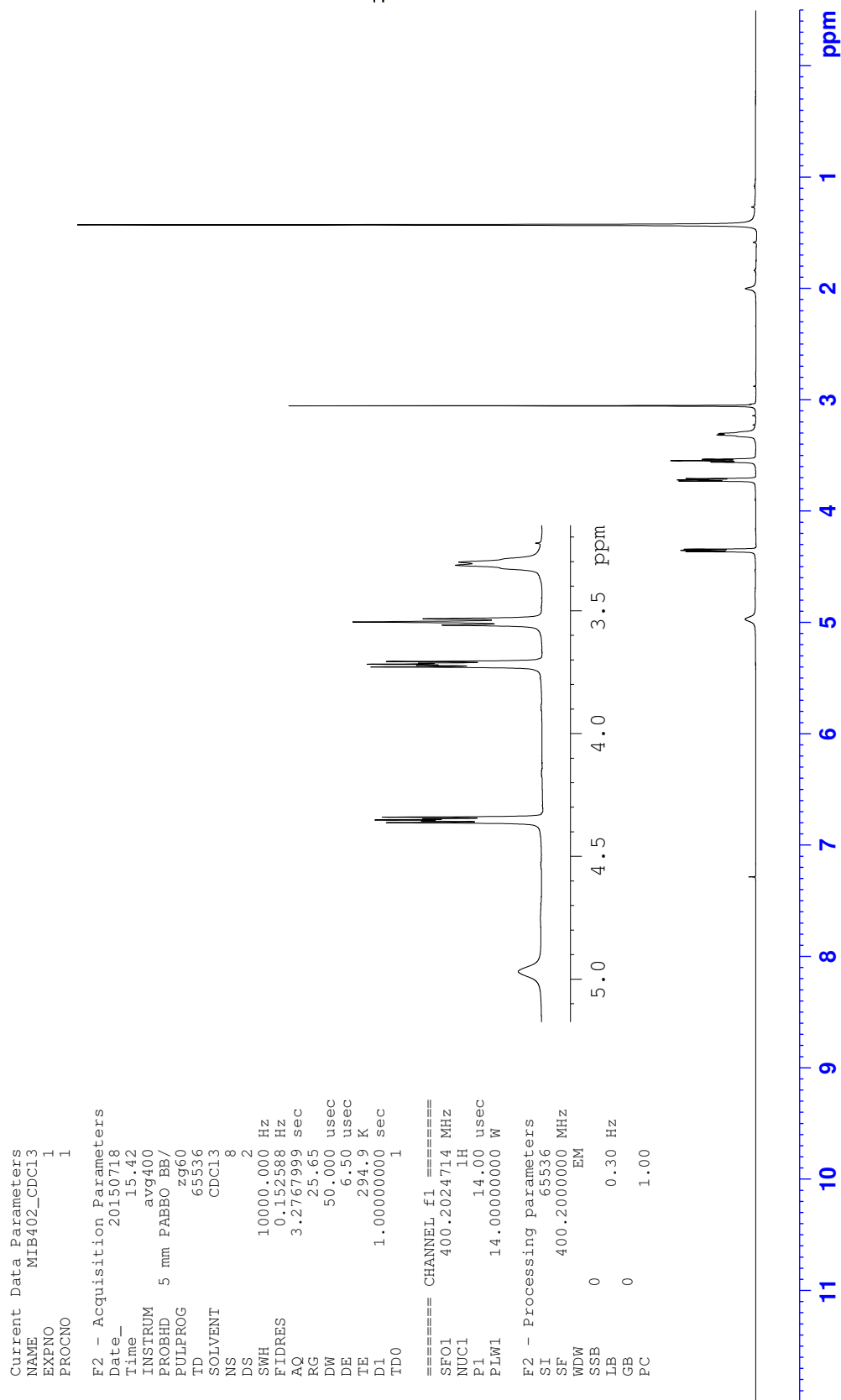
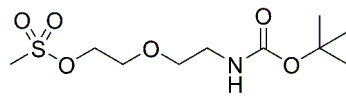
¹H NMR (3-Acetoxy-5-(3,5-dimethylisoxazol-4-yl)phenyl)(phenyl)methyl 3-(3-methyl-3H-diazirin-3-yl)propanoate (**181**)



Appendix F: NMR spectra

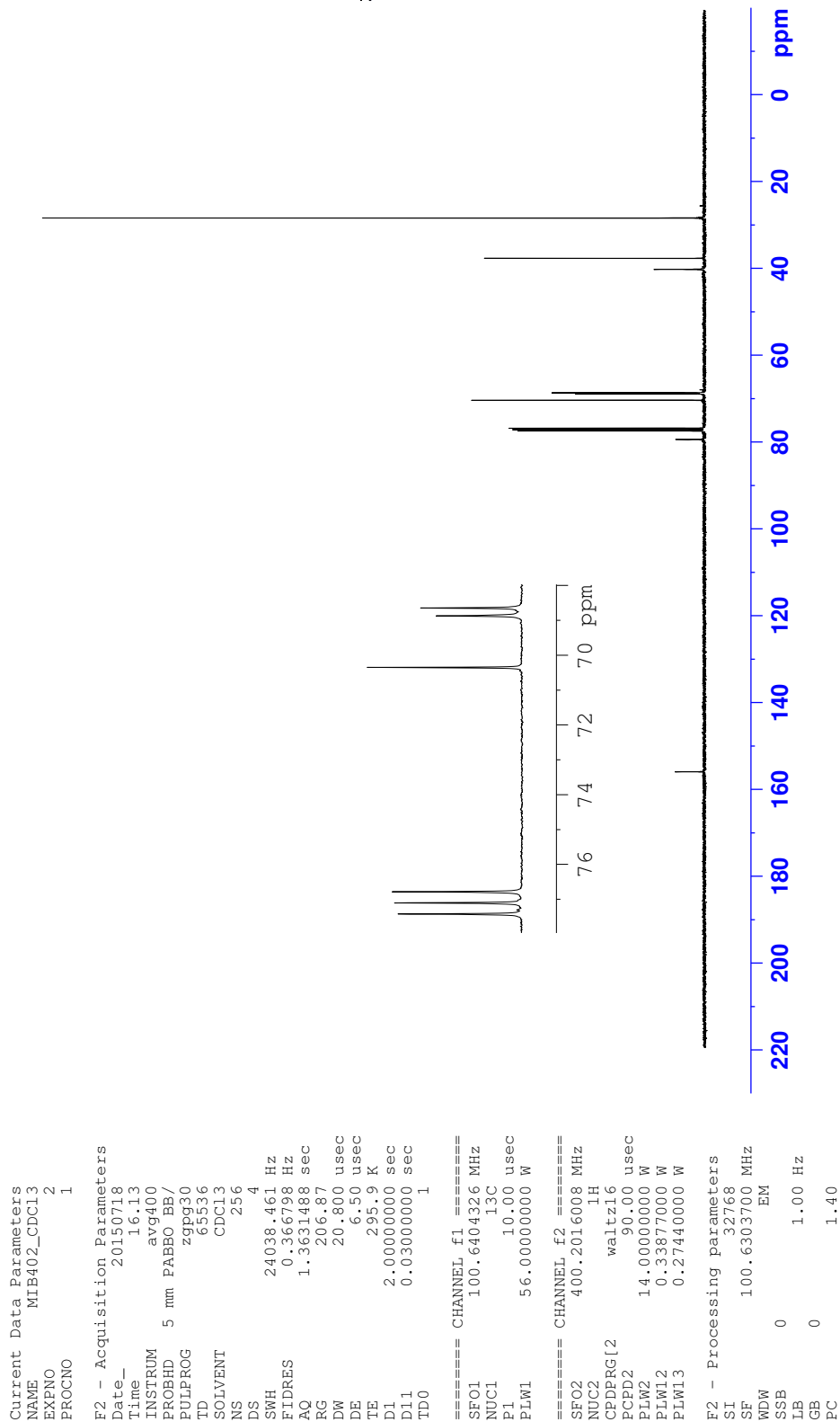
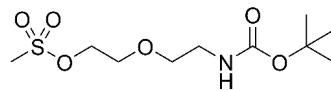
¹³C NMR (3-Acetoxy-5-(3,5-dimethylisoxazol-4-yl)phenyl)(phenyl)methyl 3-(3-methyl-3H-diazirin-3-yl)propanoate (**181**)



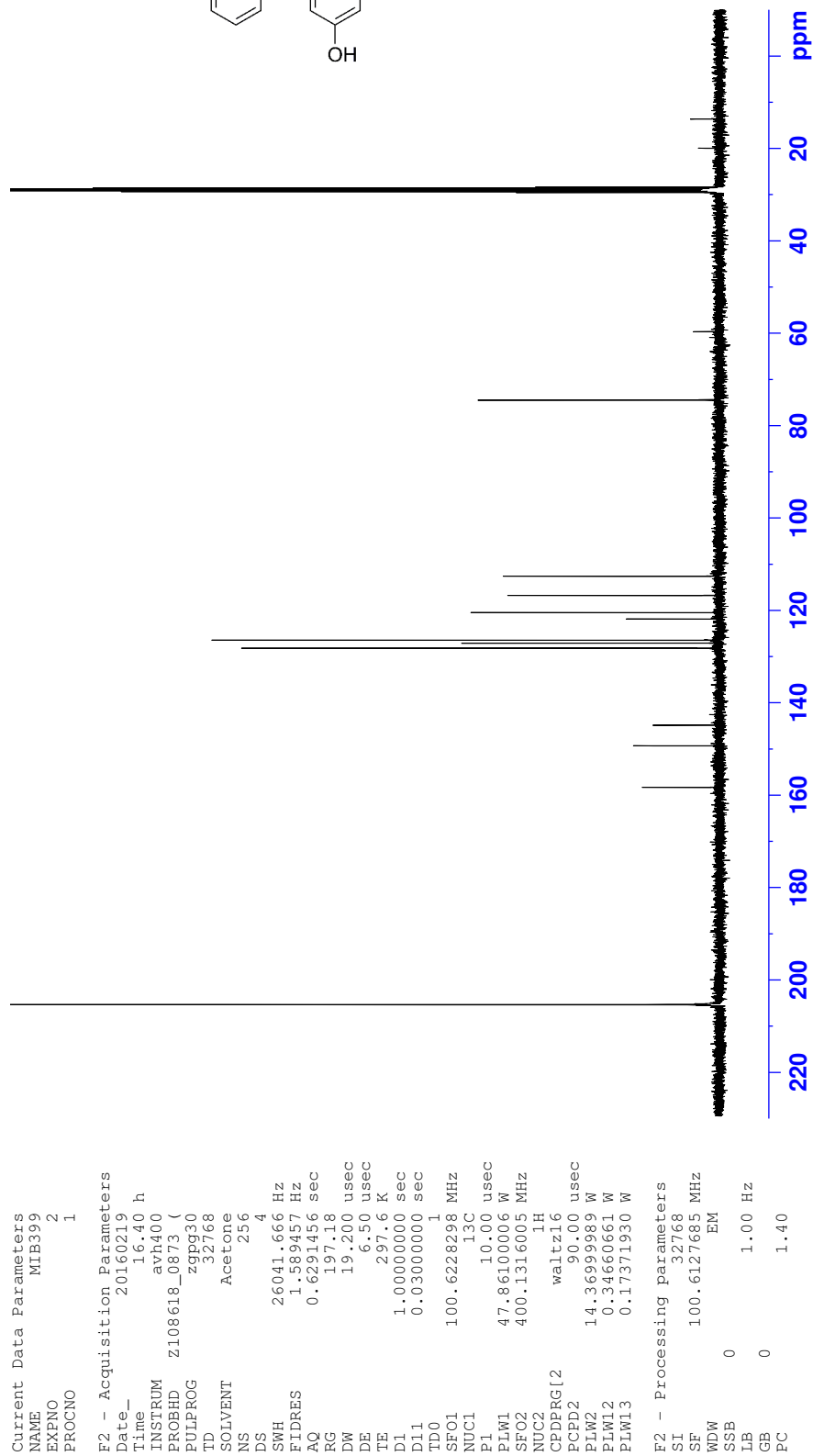
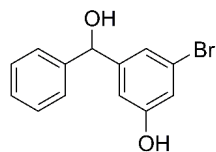
¹H NMR 2-(2-(*tert*-Butoxycarbonylamino)ethoxy)ethyl methanesulfonate (**189**)

Appendix F: NMR spectra

¹³C NMR 2-(2-(*tert*-Butoxycarbonylamino)ethoxy)ethyl (**189**) methanesulfonate

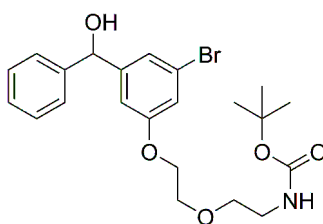


Appendix F: NMR spectra

 ^{13}C NMR 3-Bromo-5-(hydroxy(phenyl)methyl)phenol (**190**)

Appendix F: NMR spectra

¹H NMR *tert*-Butyl 2-(2-(3-bromo-5-(hydroxy(phenyl)methyl)phenoxy)ethoxy)ethylcarbamate (**191**)



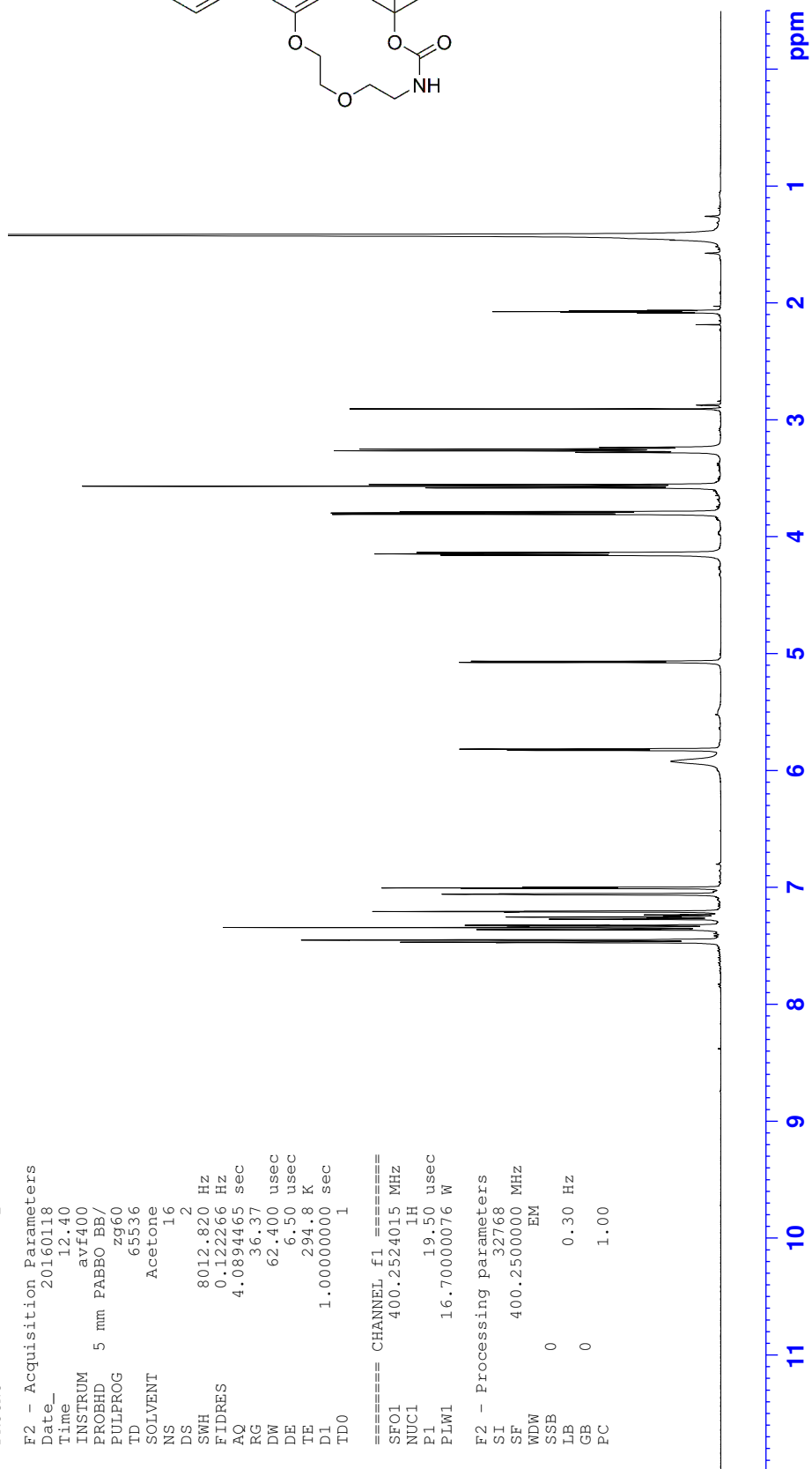
```

Current Data Parameters
NAME      MIB405-complete
EXPNO     1
PROCNO    1

F2 - Acquisition Parameters
Date_     20160118
Time      12.40
INSTRUM   avf400
PROBHD    5 mm PABBO BB/
PULPROG   zg60
TD         65536
SOLVENT   Acetone
NS         16
DS         2
SWH        8012.820 Hz
FIDRES     0.122266 Hz
AQ          4.0894465 sec
RG          36.37
DW          62.400 usec
DE          6.50 usec
TE          294.8 K
D1          1.00000000 sec
TD0        1

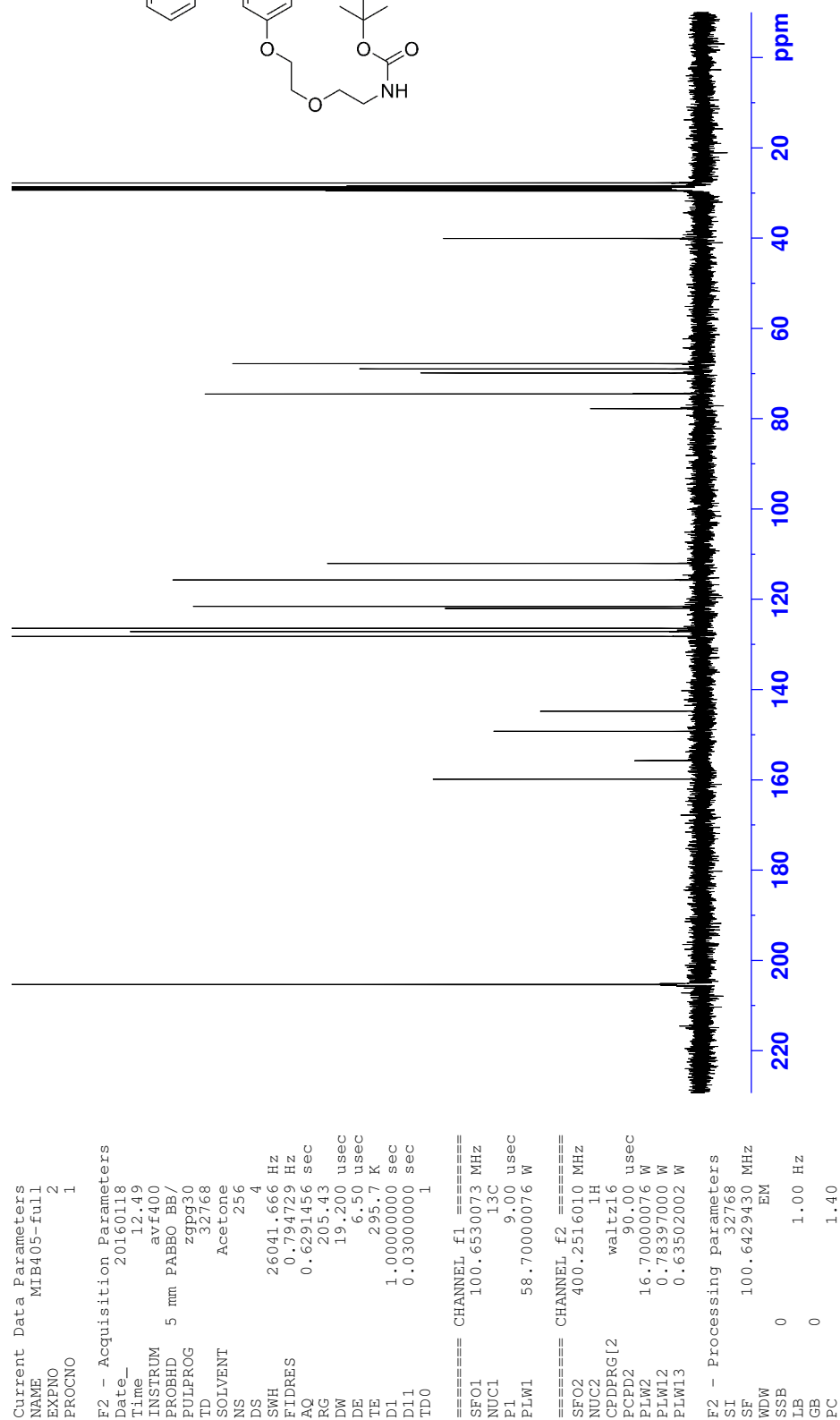
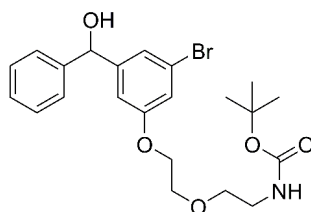
===== CHANNEL f1 =====
SFO1      400.2524015 MHz
NUC1       1H
P1         19.50 usec
PLW1      16.70000076 W

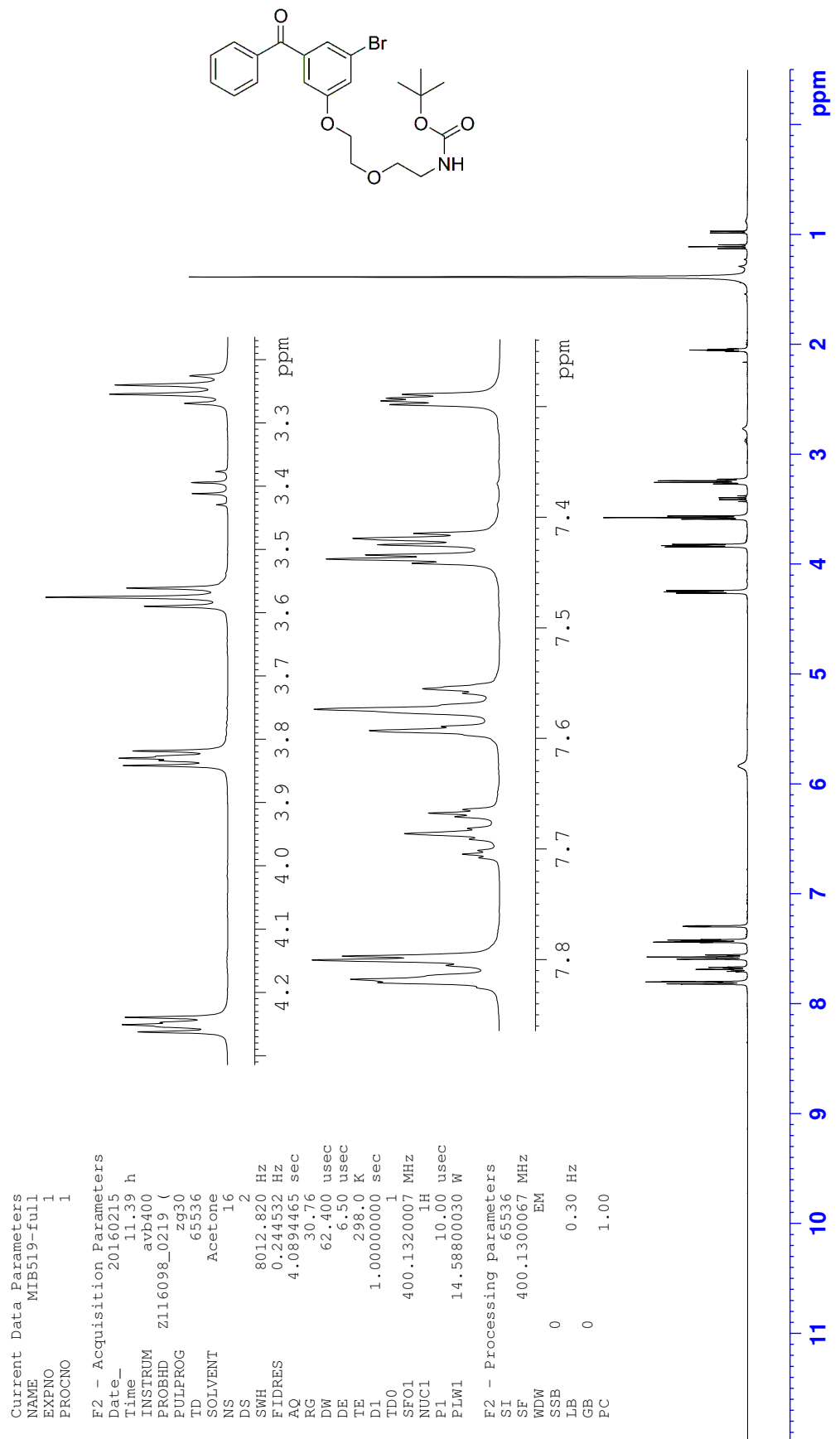
F2 - Processing parameters
SI         32768
SF         400.2500000 MHz
WDW        EM
SSB        0
LB         0.30 Hz
GB         0
PC         1.00
    
```



Appendix F: NMR spectra

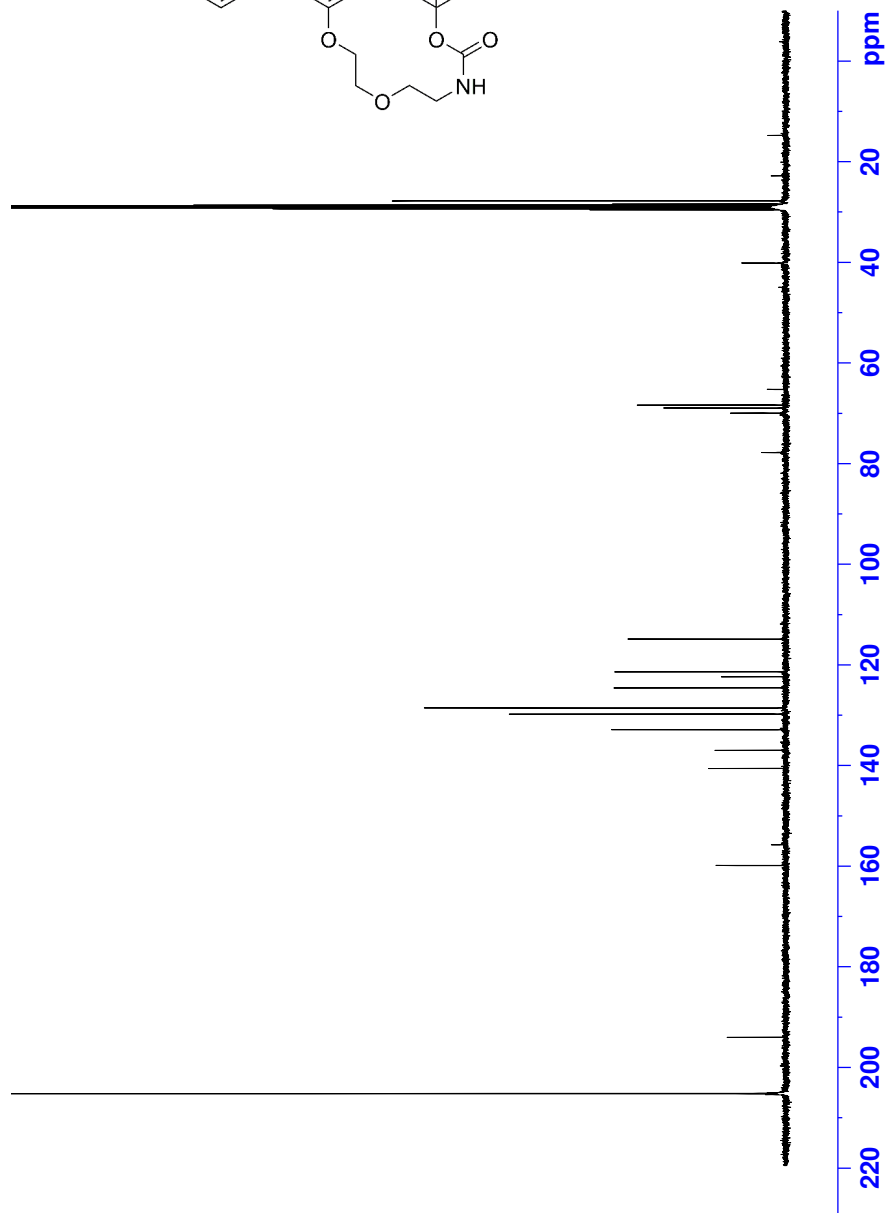
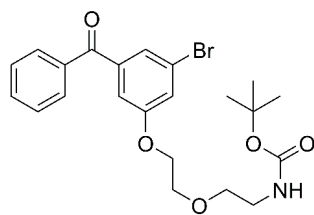
¹³C NMR *tert*-Butyl 2-(2-(3-bromo-5-(hydroxy(phenyl)methyl)phenoxy)ethoxy)ethylcarbamate (**191**)



¹H NMR *tert*-Butyl (2-(2-(3-benzoyl-5-bromophenoxy)ethoxy)ethyl)carbamate (**192**)

Appendix F: NMR spectra

¹³C NMR *tert*-Butyl (2-(2-(3-benzoyl-5-bromophenoxy)ethoxy)ethyl)carbamate (192)



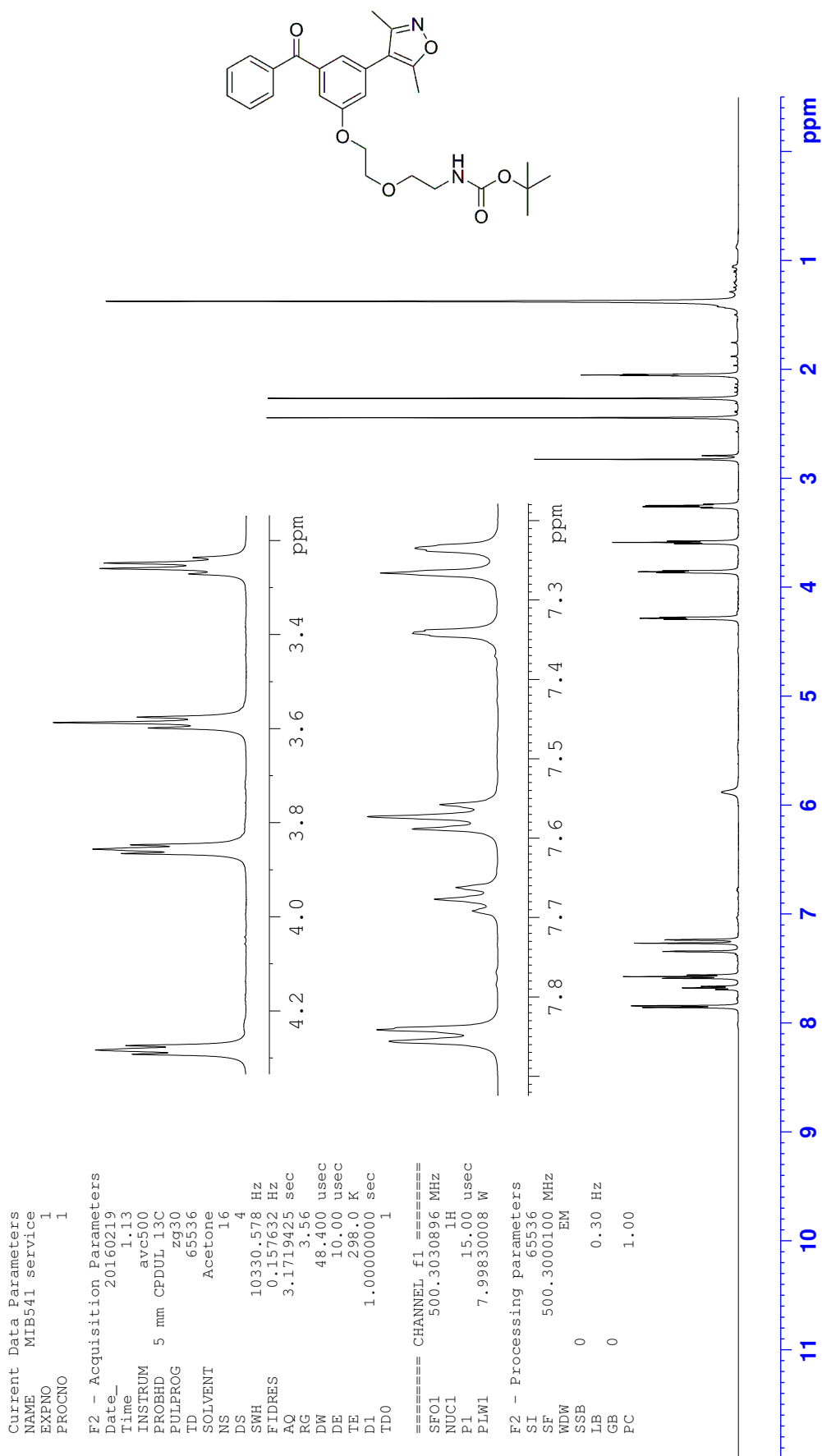
Current Data Parameters
 NAME MIB519-full
 EXPNO 2
 PROCNO 1

F2 - Acquisition Parameters
 Date_ 20160215
 Time 11.55 h
 INSTRUM avb400
 PROBRID Z116098_0219 (
 FULPROG zgpg30
 TD 65536
 SOLVENT Acetone
 NS 256
 DS 4
 SWH 24038.461 Hz
 FIDRES 0.733596 Hz
 AQ 1.3631488 sec
 RG 197.74
 DW 20.800 usec
 DE 6.50 usec
 TE 298.0 K
 D1 2.00000000 sec
 D11 0.03000000 sec
 TD0 1
 SFO1 100.6228303 MHz
 NUC1 13C
 P1 10.00 usec
 PLW1 60.95399857 W
 SFO2 400.1316005 MHz
 NUC2 1H
 CPDPRG2 waltz16
 PCPD2 90.00 usec
 PLW2 14.58800030 W
 PLW12 0.18009999 W
 PLW13 0.09058800 W

F2 - Processing parameters
 SI 32768
 SF 100.6127690 MHz
 WDW EM
 SSB 0
 LB 1.00 Hz
 GB 0
 PC 1.40

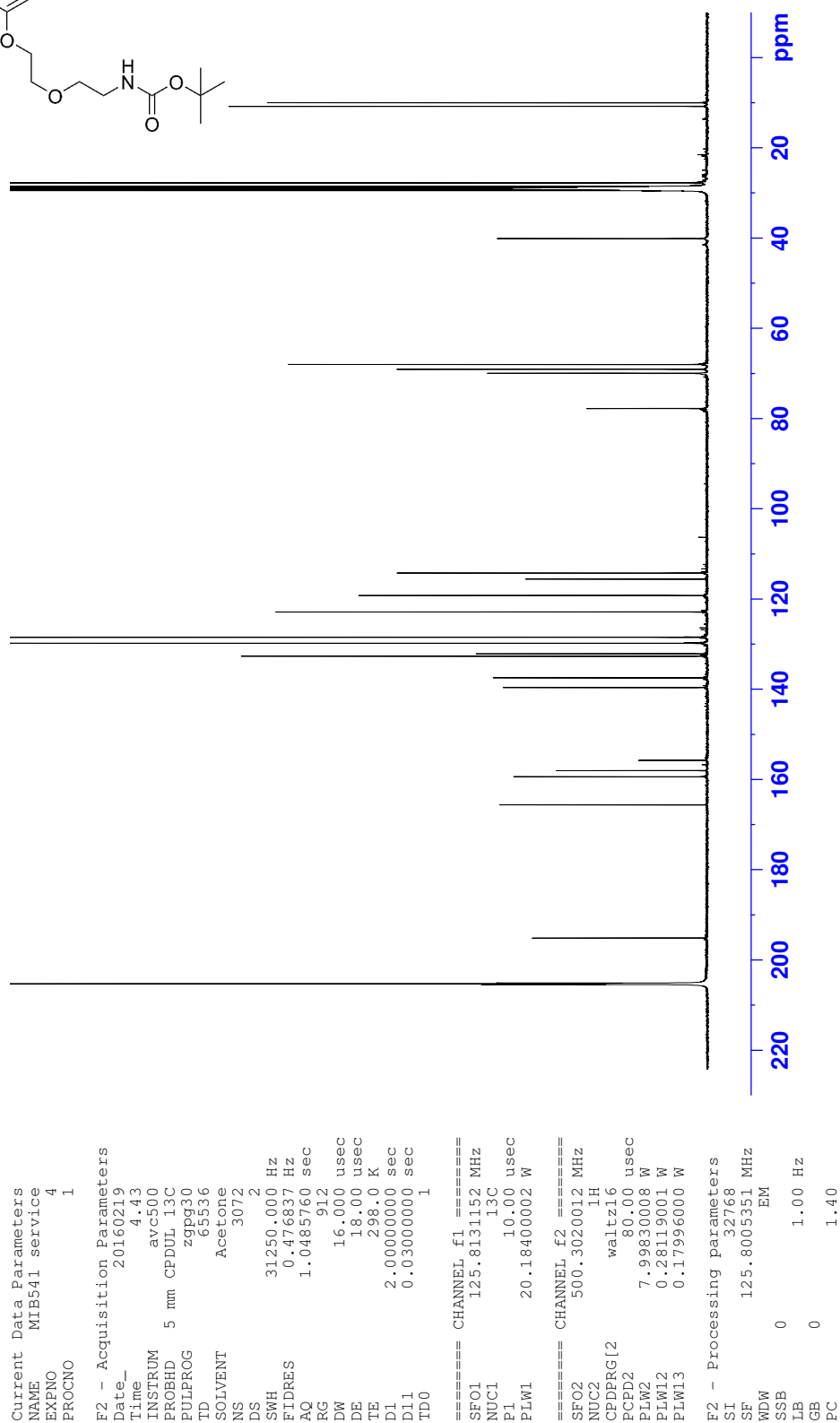
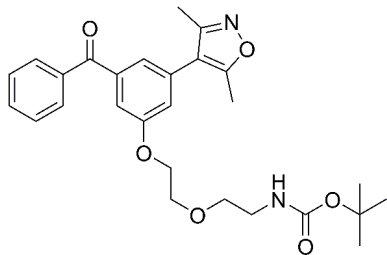
Appendix F: NMR spectra

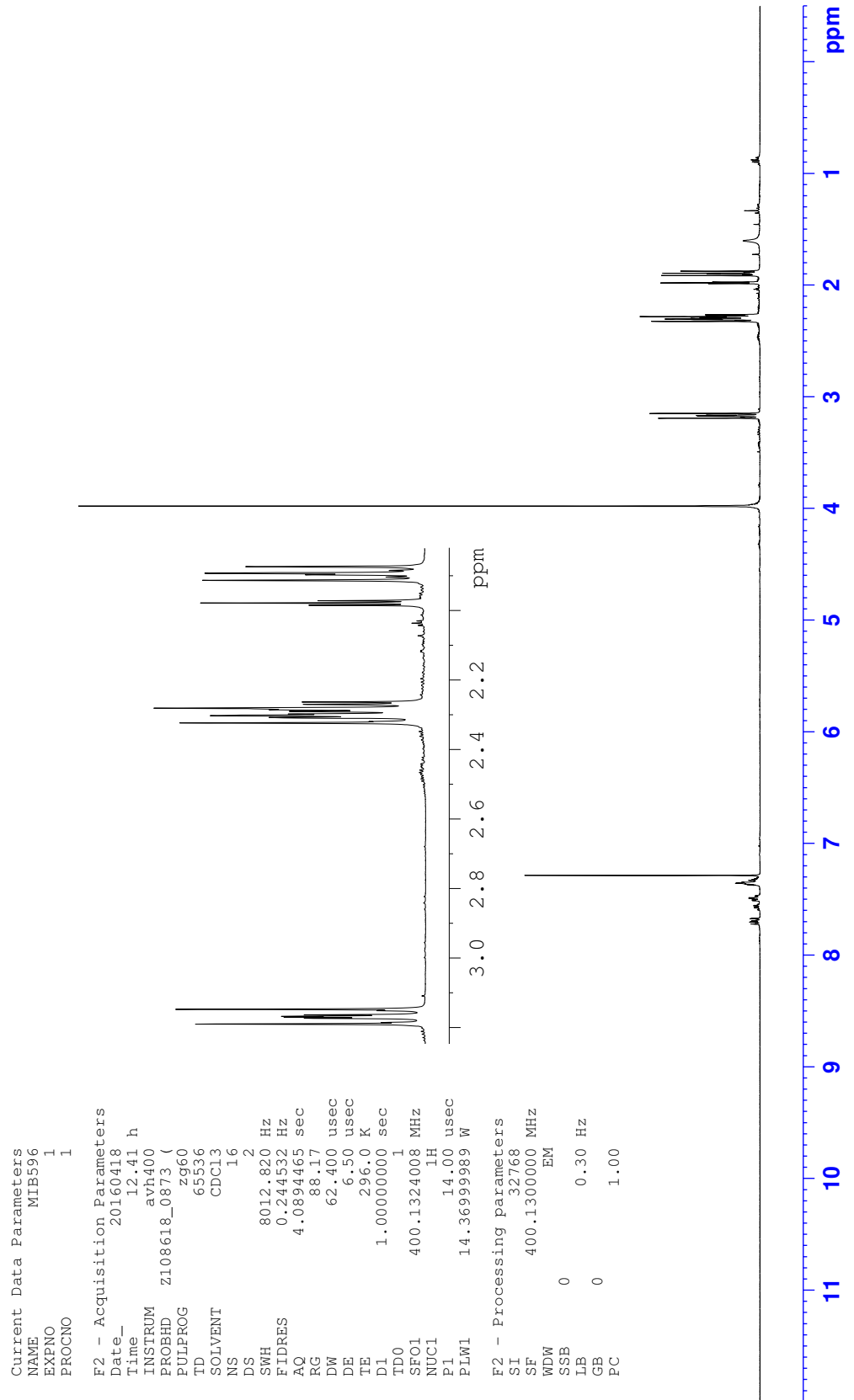
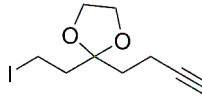
¹H NMR *tert*-Butyl (2-(2-(3-benzoyl-5-(3,5-dimethylisoxazol-4-yl)phenoxy)ethoxy)ethyl)-carbamate (**185**)



Appendix F: NMR spectra

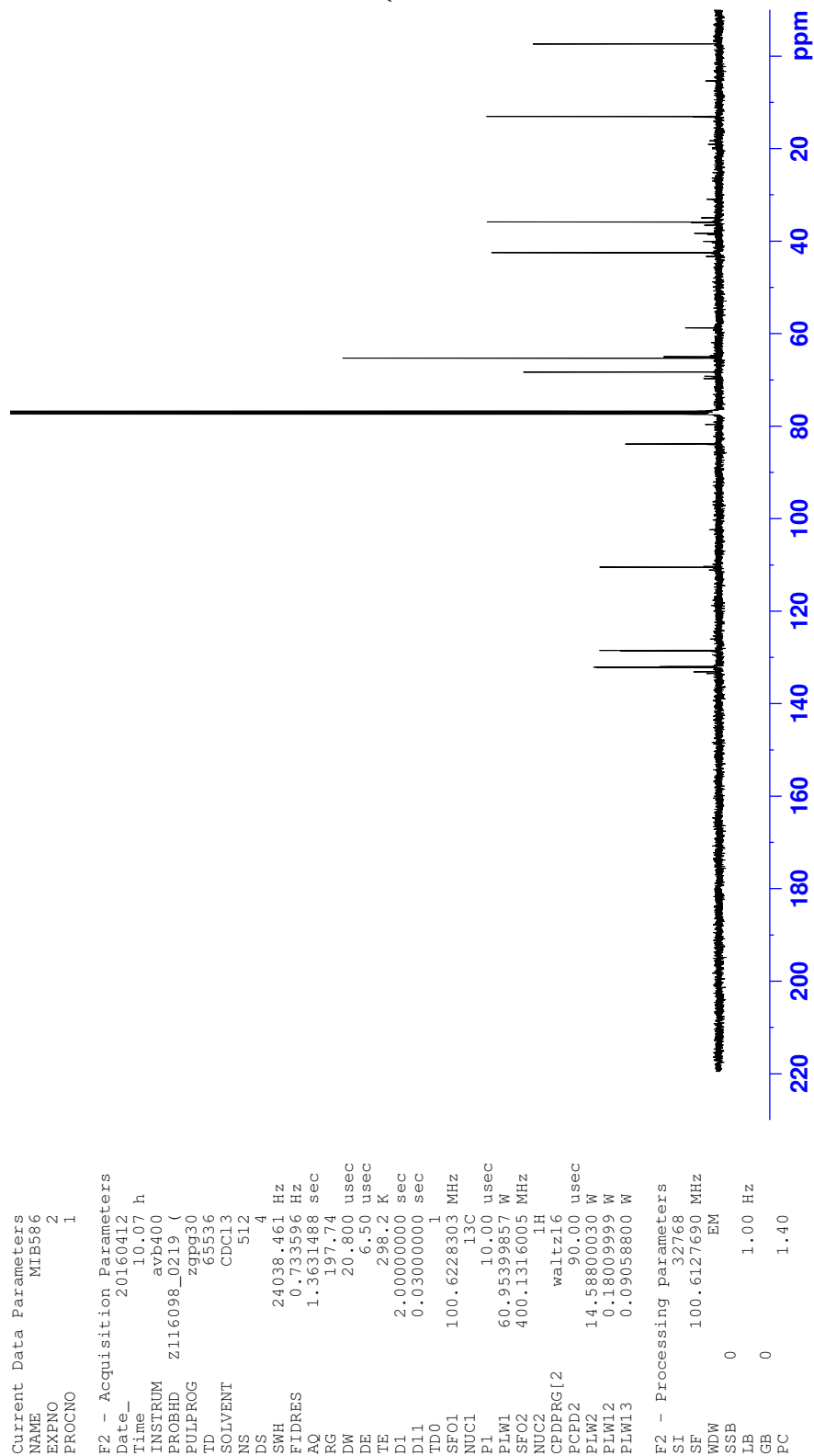
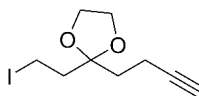
¹³C NMR *tert*-Butyl (2-(2-(3-benzoyl-5-(3,5-dimethylisoxazol-4-yl)phenoxy)ethoxy)ethyl)-carbamate (**185**)

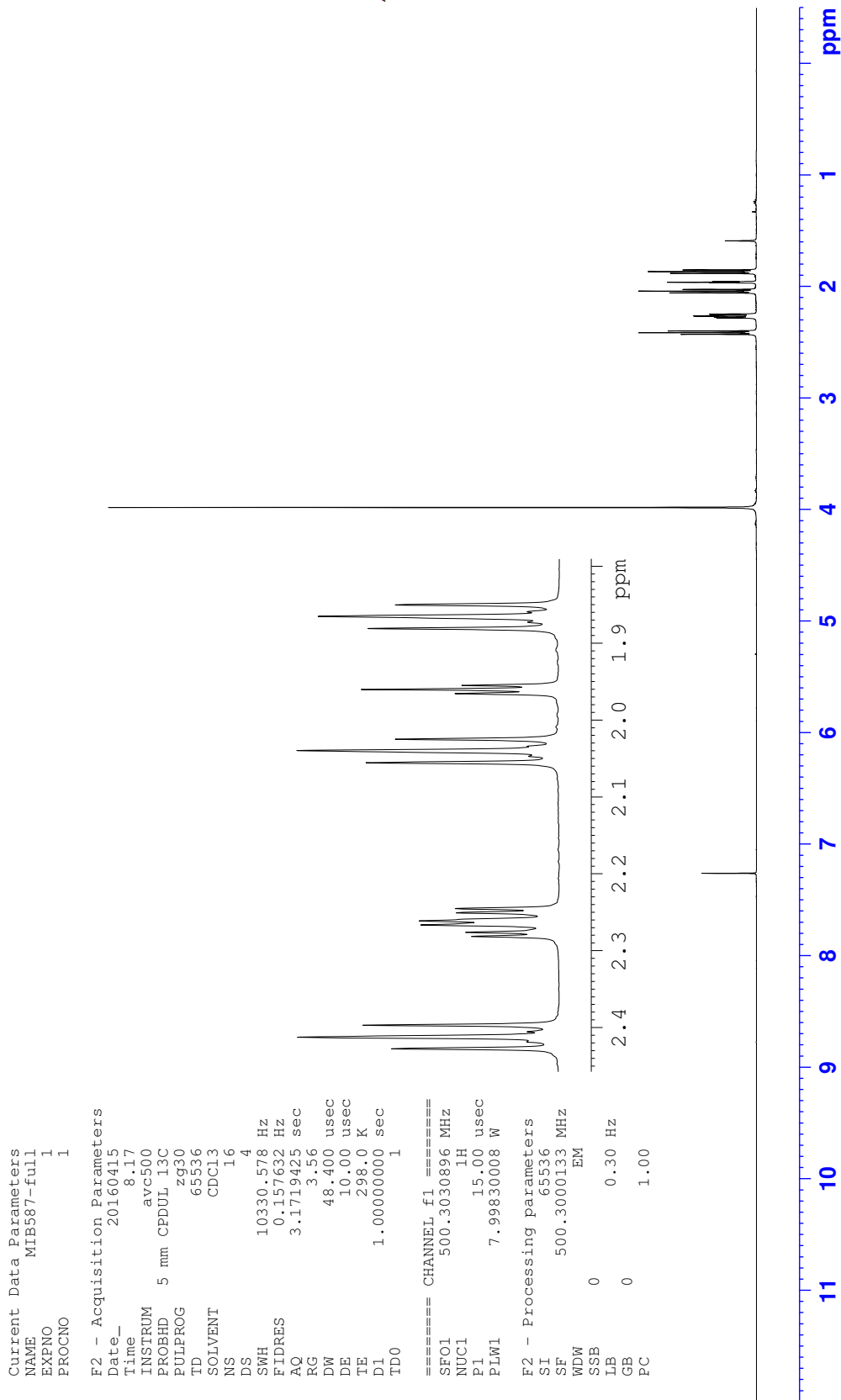
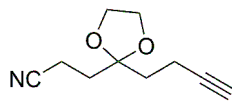


¹H NMR 2-(But-3-yn-1-yl)-2-(2-iodoethyl)-1,3-dioxolane (**197**)

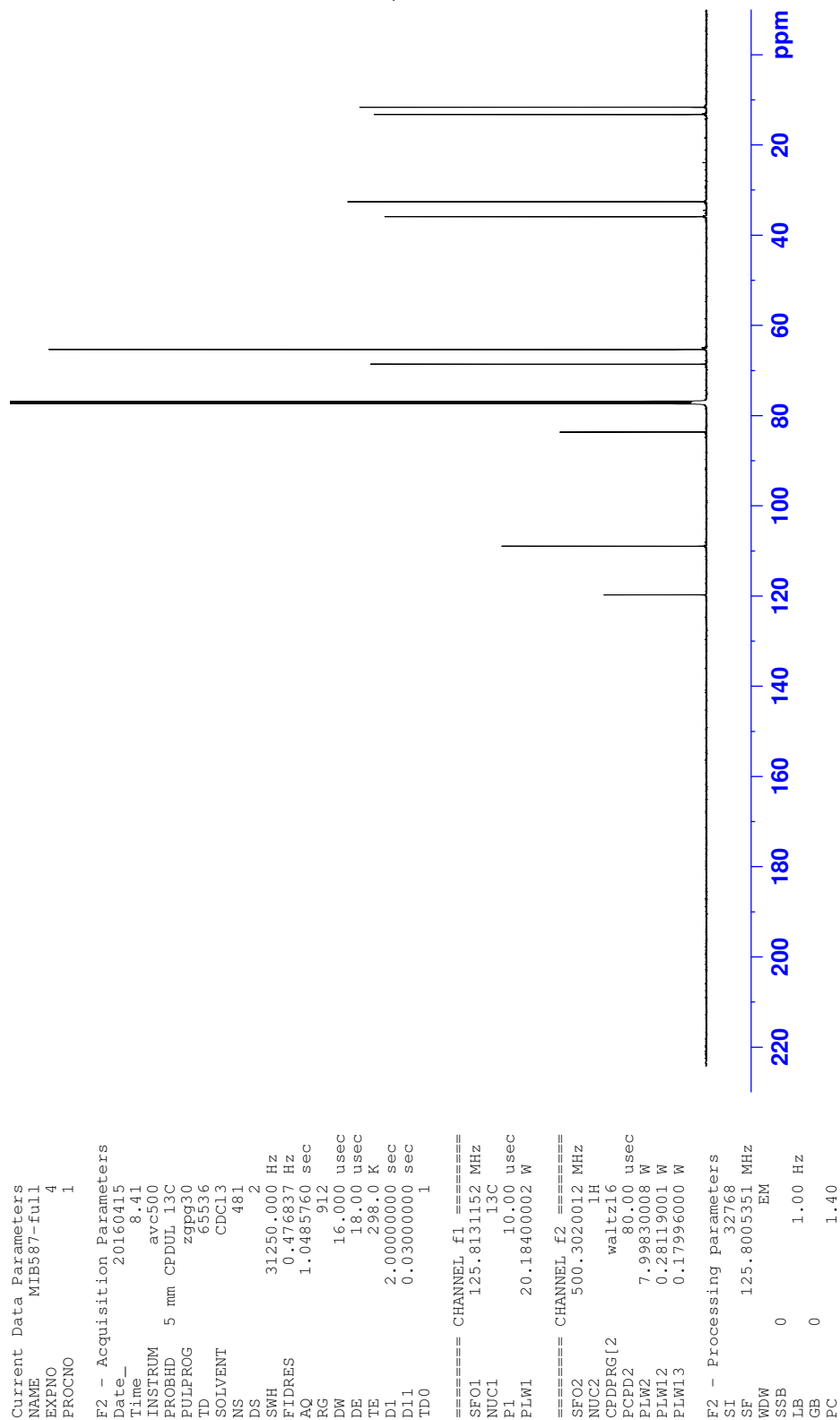
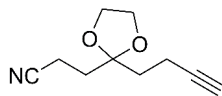
Appendix F: NMR spectra

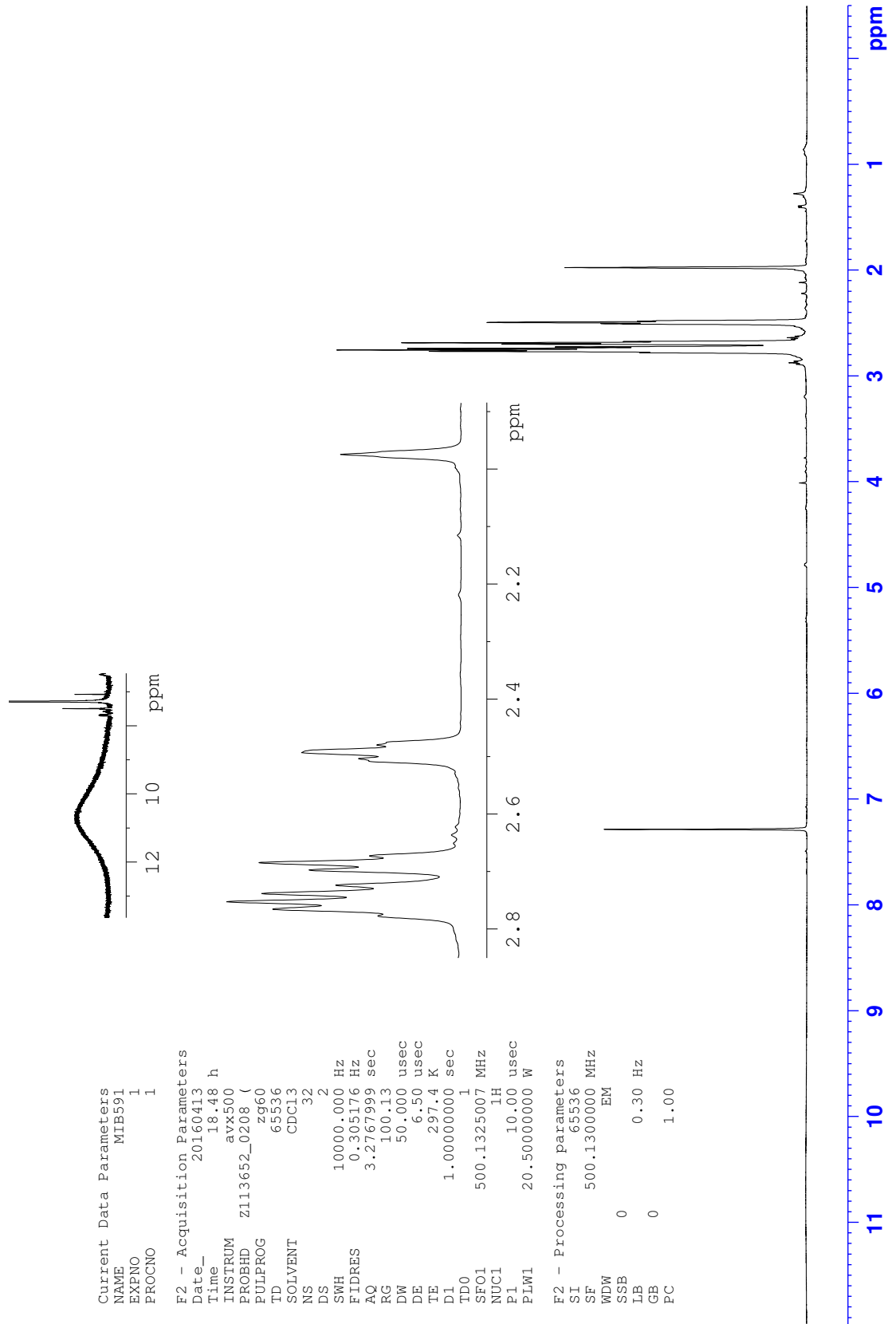
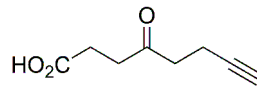
¹³C NMR 2-(But-3-yn-1-yl)-2-(2-iodoethyl)-1,3-dioxolane (**197**)



^1H NMR 3-(2-(But-3-yn-1-yl)-1,3-dioxolan-2-yl)propanenitrile (**198**)

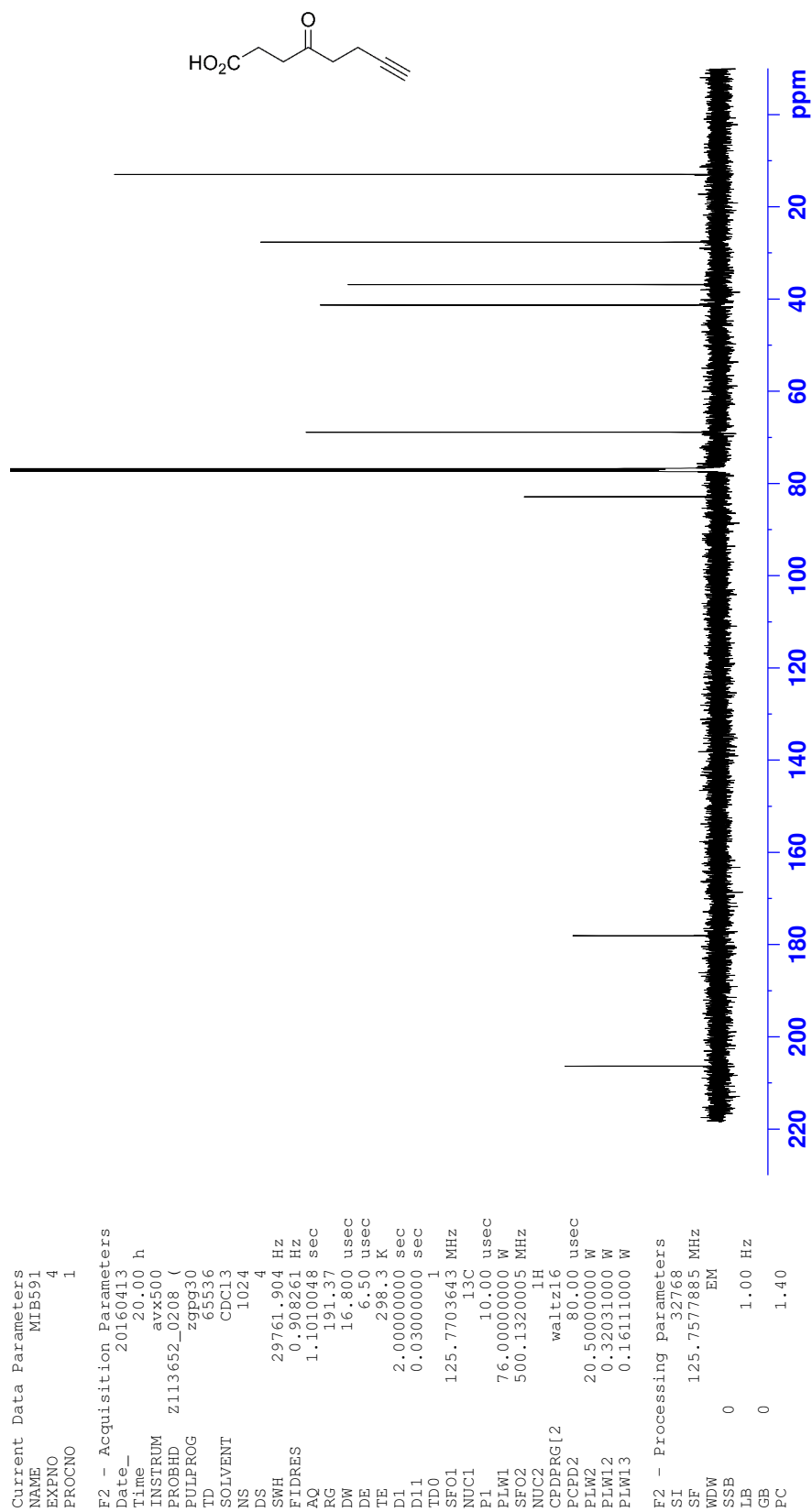
Appendix F: NMR spectra

 ^{13}C NMR 3-(2-(But-3-yn-1-yl)-1,3-dioxolan-2-yl)propanenitrile (**198**)

¹H NMR 4-Oxoct-7-ynoic acid (**199**)

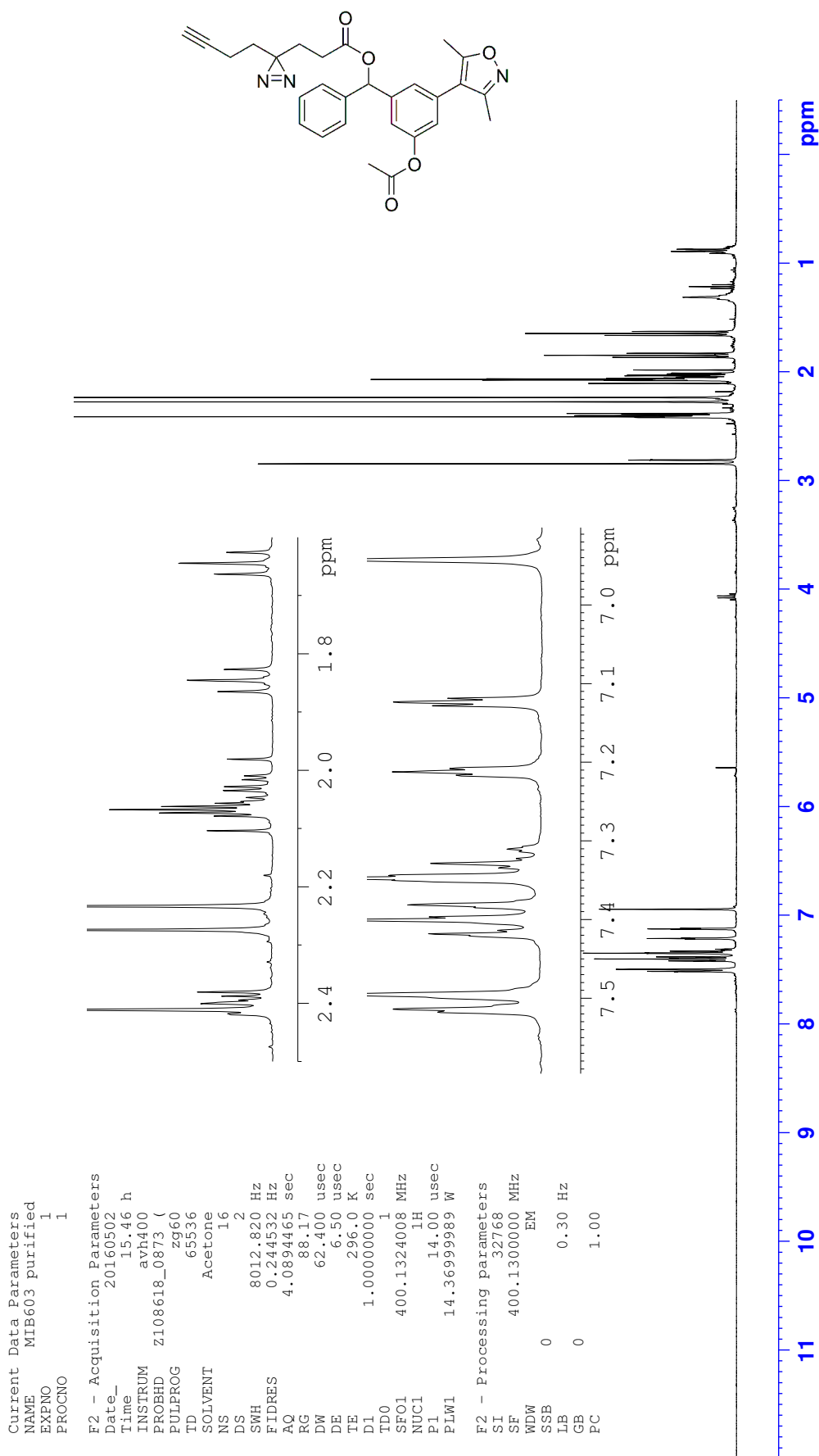
Appendix F: NMR spectra

¹³C NMR 4-Oxoct-7-ynoic acid (**199**)



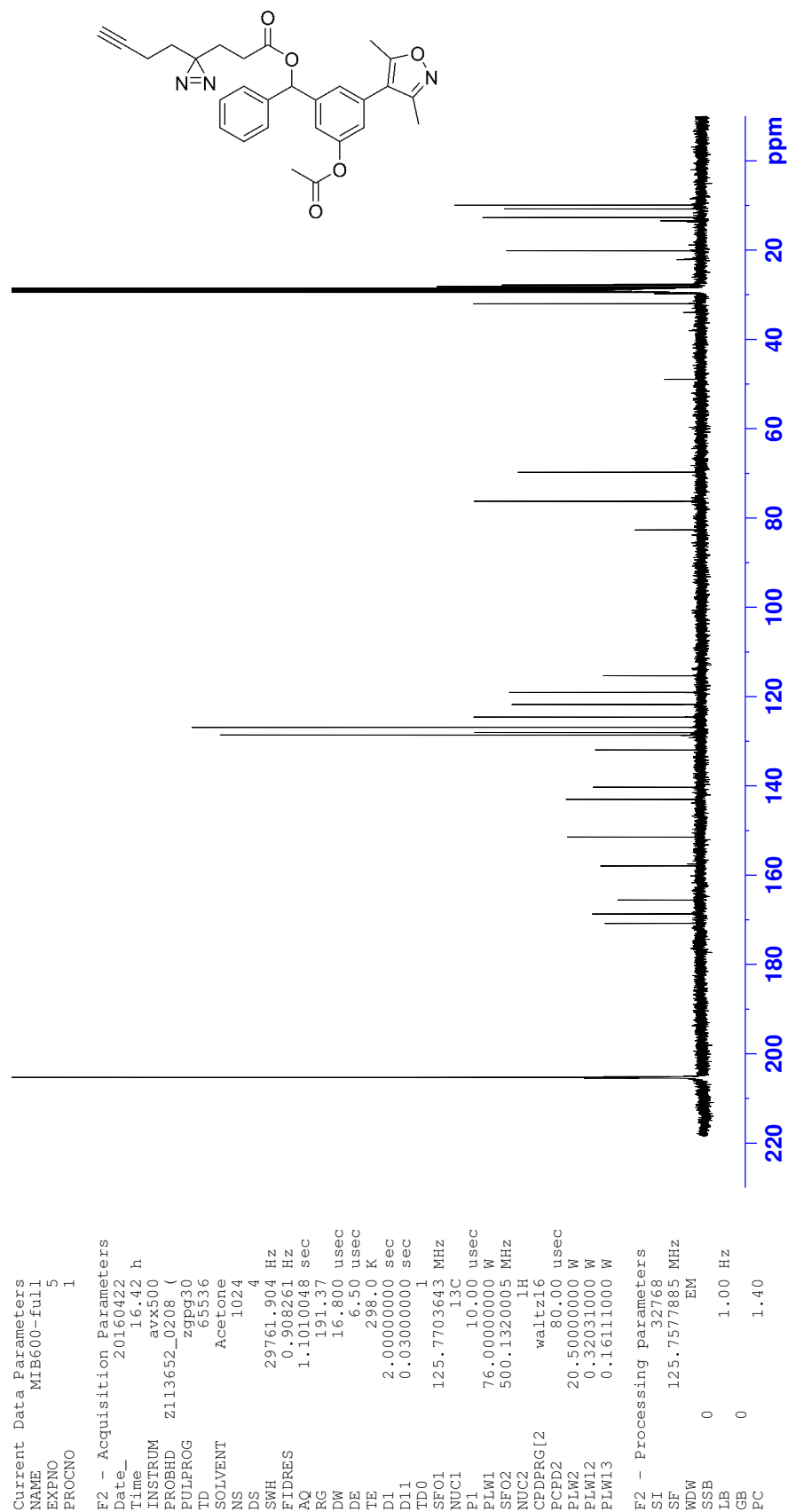
Appendix F: NMR spectra

¹H NMR (3-Acetoxy-5-(3,5-dimethylisoxazol-4-yl)phenyl)(phenyl)methyl 3-(3-(but-3-yn-1-yl)-3H-diazirin-3-yl)propanoate (**186**)



Appendix F: NMR spectra

¹³C NMR (3-Acetoxy-5-(3,5-dimethylisoxazol-4-yl)phenyl)(phenyl)methyl 3-(3-(but-3-yn-1-yl)-3H-diazirin-3-yl)propanoate (**186**)



G Permissions for reprinted/adapted figures

Figure 1.1a Chromosomes are compact structures comprising DNA wrapped around histone proteins forming electrostatic interactions.

RightsLink Printable License

<https://s100.copyright.com/App/PrintableLicenseFrame.jsp?publisher...>

NATURE PUBLISHING GROUP LICENSE TERMS AND CONDITIONS

Aug 16, 2016

This Agreement between Michael Brand ("You") and Nature Publishing Group ("Nature Publishing Group") consists of your license details and the terms and conditions provided by Nature Publishing Group and Copyright Clearance Center.

License Number	3930850681844
License date	Aug 16, 2016
Licensed Content Publisher	Nature Publishing Group
Licensed Content Publication	Nature
Licensed Content Title	Epigenetics: Unfinished symphony
Licensed Content Author	Jane Qiu
Licensed Content Date	May 11, 2006
Licensed Content Volume Number	441
Licensed Content Issue Number	7090
Type of Use	reuse in a dissertation / thesis
Requestor type	academic/educational
Format	print and electronic
Portion	figures/tables/illustrations
Number of figures/tables /illustrations	1
High-res required	no
Figures	The two main components of the epigenetic code
Author of this NPG article	no
Your reference number	
Title of your thesis / dissertation	DEVELOPING SMALL MOLECULE LIGANDS FOR THE STUDY OF BROMODOMAIN-HISTONE INTERACTIONS
Expected completion date	Oct 2016
Estimated size (number of pages)	250
Requestor Location	Michael Brand Lincoln College
	Oxford, OX13DR United Kingdom Attn: Michael Brand
Billing Type	Invoice
Billing Address	Michael Brand Lincoln College
	Oxford, United Kingdom OX13DR Attn: Michael Brand

Figure 1.1b Post-translational modifications of histone tails.

Rightslink® by Copyright Clearance Center

https://s100.copyright.com/AppDispatchServlet



RightsLink®

Account
Info

Help

Title: Future medicinal chemistry
Article ID: To be determined
Publication: Publication1
Publisher: CCC Reproduction
Date: Jan 1, 2009
 Copyright © 2009, CCC Reproduction

Logged in as:
 Michael Brand
 Account #:
 3001039526

LOGOUT

Order Completed

Thank you for your order.

This Agreement between Michael Brand ("You") and Future Science Ltd ("Future Science Ltd") consists of your order details and the terms and conditions provided by Future Science Ltd and Copyright Clearance Center.

License number	Reference confirmation email for license number
License date	Oct 05, 2016
Licensed content publisher	Future Science Ltd
Licensed content title	Future medicinal chemistry
Licensed content date	Jan 1, 2009
Type of use	Thesis/Dissertation
Requestor type	Academic institution
Format	Print, Electronic
Portion	image/photo
Number of images/photos requested	1
Title or numeric reference of the portion(s)	Figure 2: Post-translational modifications to histone proteins, displayed as amino acid sequences.
Title of the article or chapter the portion is from	Phenotypic screening and fragment-based approaches to the discovery of small-molecule bromodomain ligands.
Editor of portion(s)	Future Med Chem
Author of portion(s)	Laura J. Jennings et al.
Volume of serial or monograph	6
Issue, if republishing an article from a serial	2
Page range of portion	179-204
Publication date of portion	2014
Rights for	Main product
Duration of use	Current edition and up to 5 years
Creation of copies for the disabled	no
With minor editing privileges	yes
For distribution to in the following language(s)	U.K. and Commonwealth (excluding Canada) Original language of publication
With incidental promotional use	no
Lifetime unit quantity of new product	Up to 499
Made available in the following markets	Dissertation filed at the University of Oxford

Figure 1.3 Phylogenetic tree of the 61 bromodomains.

Rightslink® by Copyright Clearance Center

<https://s100.copyright.com/AppDispatchServlet>

The screenshot shows the RightsLink website interface. At the top left is the Copyright Clearance Center logo. In the center is the RightsLink logo. To the right are navigation buttons for Home, Account Info, and Help, along with a Live Chat icon. Below the logo is the ACS Publications logo with the tagline 'Most Trusted. Most Cited. Most Read.' The main content area displays the following information:

Title:	Progress in the Development and Application of Small Molecule Inhibitors of Bromodomain-Acetyl-lysine Interactions	Logged in as: Michael Brand Account #: 3001039526
Author:	David S. Hewings, Timothy P. C. Rooney, Laura E. Jennings, et al	LOGOUT
Publication:	Journal of Medicinal Chemistry	
Publisher:	American Chemical Society	
Date:	Nov 1, 2012	
Copyright © 2012, American Chemical Society		

PERMISSION/LICENSE IS GRANTED FOR YOUR ORDER AT NO CHARGE

This type of permission/license, instead of the standard Terms & Conditions, is sent to you because no fee is being charged for your order. Please note the following:

- Permission is granted for your request in both print and electronic formats, and translations.
- If figures and/or tables were requested, they may be adapted or used in part.
- Please print this page for your records and send a copy of it to your publisher/graduate school.
- Appropriate credit for the requested material should be given as follows: "Reprinted (adapted) with permission from (COMPLETE REFERENCE CITATION). Copyright (YEAR) American Chemical Society." Insert appropriate information in place of the capitalized words.
- One-time permission is granted only for the use specified in your request. No additional uses are granted (such as derivative works or other editions). For any other uses, please submit a new request.

If credit is given to another source for the material you requested, permission must be obtained from that source.

BACK**CLOSE WINDOW**

Copyright © 2016 Copyright Clearance Center, Inc. All Rights Reserved. [Privacy statement](#). [Terms and Conditions](#).
Comments? We would like to hear from you. E-mail us at customer-care@copyright.com

Figure 3.2b *Electrostatic surfaces of Trp and tetra fluorinated Trp.*

Rightslink® by Copyright Clearance Center

<https://s100.copyright.com/AppDispatchServlet#formTop>



Home Account Info Help  Live Chat


ACS Publications Most Trusted. Most Cited. Most Read.

Title: Cation- π Interactions in Ligand Recognition by Serotonergic (5-HT3A) and Nicotinic Acetylcholine Receptors: The Anomalous Binding Properties of Nicotine

Author: Darren L. Beene, Gabriel S. Brandt, Wenge Zhong, et al

Publication: Biochemistry
Publisher: American Chemical Society
Date: Aug 1, 2002
 Copyright © 2002, American Chemical Society

Logged in as: Michael Brand
 Account #: 3001039526
LOGOUT

PERMISSION/LICENSE IS GRANTED FOR YOUR ORDER AT NO CHARGE

This type of permission/license, instead of the standard Terms & Conditions, is sent to you because no fee is being charged for your order. Please note the following:

- Permission is granted for your request in both print and electronic formats, and translations.
- If figures and/or tables were requested, they may be adapted or used in part.
- Please print this page for your records and send a copy of it to your publisher/graduate school.
- Appropriate credit for the requested material should be given as follows: "Reprinted (adapted) with permission from (COMPLETE REFERENCE CITATION). Copyright (YEAR) American Chemical Society." Insert appropriate information in place of the capitalized words.
- One-time permission is granted only for the use specified in your request. No additional uses are granted (such as derivative works or other editions). For any other uses, please submit a new request.


If credit is given to another source for the material you requested, permission must be obtained from that source.

BACKCLOSE WINDOW


Copyright © 2016 [Copyright Clearance Center, Inc.](#) All Rights Reserved. [Privacy statement](#). [Terms and Conditions](#).
 Comments? We would like to hear from you. E-mail us at customerscare@copyright.com


Figure 5.2 Schematic overview of an activity based probe (ABP) and the target validation.

Rightslink® by Copyright Clearance Center https://s100.copyright.com/AppDispatchServlet



RightsLink®

[Home](#)
[Account Info](#)
[Help](#)




Title: Current Developments in Activity-Based Protein Profiling

Author: Lianne I. Willems, Herman S. Overkleeft, Sander I. van Kasteren

Publication: Bioconjugate Chemistry

Publisher: American Chemical Society

Date: Jul 1, 2014

Copyright © 2014, American Chemical Society

Logged in as:
Michael Brand

Account #:
3001039526

[LOGOUT](#)

PERMISSION/LICENSE IS GRANTED FOR YOUR ORDER AT NO CHARGE

This type of permission/license, instead of the standard Terms & Conditions, is sent to you because no fee is being charged for your order. Please note the following:

- Permission is granted for your request in both print and electronic formats, and translations.
- If figures and/or tables were requested, they may be adapted or used in part.
- Please print this page for your records and send a copy of it to your publisher/graduate school.
- Appropriate credit for the requested material should be given as follows: "Reprinted (adapted) with permission from (COMPLETE REFERENCE CITATION). Copyright (YEAR) American Chemical Society." Insert appropriate information in place of the capitalized words.
- One-time permission is granted only for the use specified in your request. No additional uses are granted (such as derivative works or other editions). For any other uses, please submit a new request.

If credit is given to another source for the material you requested, permission must be obtained from that source.

[BACK](#)
[CLOSE WINDOW](#)

Copyright © 2016 Copyright Clearance Center, Inc. All Rights Reserved. [Privacy statement](#). [Terms and Conditions](#). Comments? We would like to hear from you. E-mail us at customercare@copyright.com

Appendix G

Figure 7.1 Pulse sequence for the CPMG experiment.

RightsLink Printable License

<https://s100.copyright.com/CustomerAdmin/PLF.jsp?ref=6c3a69c3-54...>

ROYAL SOCIETY OF CHEMISTRY LICENSE TERMS AND CONDITIONS

Oct 25, 2016

This Agreement between Michael Brand ("You") and Royal Society of Chemistry ("Royal Society of Chemistry") consists of your license details and the terms and conditions provided by Royal Society of Chemistry and Copyright Clearance Center.

License Number	3975981439945
License date	Oct 25, 2016
Licensed Content Publisher	Royal Society of Chemistry
Licensed Content Publication	Chemical Communications (Cambridge)
Licensed Content Title	Spin echo NMR spectra without J modulation
Licensed Content Author	Juan A. Aguilar, Mathias Nilsson, Geoffrey Bodenhausen, Gareth A. Morris
Licensed Content Date	Nov 11, 2011
Licensed Content Volume Number	48
Licensed Content Issue Number	6
Type of Use	Thesis/Dissertation
Requestor type	academic/educational
Portion	figures/tables/images
Number of figures/tables /images	1
Format	print and electronic
Distribution quantity	3
Will you be translating?	no
Order reference number	
Title of the thesis/dissertation	DEVELOPING SMALL MOLECULE LIGANDS FOR THE STUDY OF BROMODOMAIN-HISTONE INTERACTIONS
Expected completion date	Oct 2016
Estimated size	250
Requestor Location	Michael Brand Lincoln College Oxford, OX13DR United Kingdom Attn: Michael Brand
Billing Type	Invoice
Billing Address	Michael Brand Lincoln College Oxford, United Kingdom OX13DR Attn: Michael Brand
Total	0.00 USD

Appendix AlphaScreen™ figure.

RightsLink Printable License

<https://s100.copyright.com/App/PrintableLicenseFrame.jsp?publisher...>**ROYAL SOCIETY OF CHEMISTRY LICENSE
TERMS AND CONDITIONS**

Jun 22, 2016

This Agreement between Michael Brand ("You") and Royal Society of Chemistry ("Royal Society of Chemistry") consists of your license details and the terms and conditions provided by Royal Society of Chemistry and Copyright Clearance Center.

License Number	3894280250623
License date	Jun 22, 2016
Licensed Content Publisher	Royal Society of Chemistry
Licensed Content Publication	Molecular BioSystems
Licensed Content Title	Bromodomain-peptide displacement assays for interactome mapping and inhibitor discovery
Licensed Content Author	Martin Philpott, Jing Yang, Tony Tumber, Oleg Fedorov, Sagar Uttarkar, Panagis Filippakopoulos, Sarah Picaud, Tracy Keates, Ildiko Felletar, Alessio Ciulli, Stefan Knapp, Tom D. Heightman
Licensed Content Date	Aug 1, 2011
Licensed Content Volume Number	7
Licensed Content Issue Number	10
Type of Use	Thesis/Dissertation
Requestor type	academic/educational
Portion	figures/tables/images
Number of figures/tables /images	1
Format	print and electronic
Distribution quantity	3
Will you be translating?	no
Order reference number	
Title of the thesis/dissertation	DEVELOPING SMALL MOLECULE LIGANDS FOR THE STUDY OF BROMODOMAIN-HISTONE INTERACTIONS
Expected completion date	Oct 2016
Estimated size	300
Requestor Location	Michael Brand Lincoln College Oxford, OX13DR United Kingdom Attn: Michael Brand
Billing Type	Invoice
Billing Address	Michael Brand Lincoln College Oxford, United Kingdom OX13DR Attn: Michael Brand

Appendix ITC figure.

RightsLink Printable License

<https://s100.copyright.com/CustomerAdmin/PLF.jsp?ref=76e9eff5-a0...>**ELSEVIER LICENSE
TERMS AND CONDITIONS**

Oct 25, 2016

This Agreement between Michael Brand ("You") and Elsevier ("Elsevier") consists of your license details and the terms and conditions provided by Elsevier and Copyright Clearance Center.

License Number	3898210399194
License date	Jun 29, 2016
Licensed Content Publisher	Elsevier
Licensed Content Publication	Elsevier Books
Licensed Content Title	Methods in Cell Biology
Licensed Content Author	Matthew W. Freyer, Edwin A. Lewis
Licensed Content Date	2008
Licensed Content Pages	35
Start Page	79
End Page	113
Type of Use	reuse in a thesis/dissertation
Portion	figures/tables/illustrations
Number of figures/tables /illustrations	1
Format	both print and electronic
Are you the author of this Elsevier chapter?	No
Will you be translating?	No
Order reference number	
Original figure numbers	Fig. 2 Representative diagram of a typical power compensation ITC.
Title of your thesis/dissertation	DEVELOPING SMALL MOLECULE LIGANDS FOR THE STUDY OF BROMODOMAIN-HISTONE INTERACTIONS
Expected completion date	Oct 2016
Estimated size (number of pages)	250
Elsevier VAT number	GB 494 6272 12
Requestor Location	Michael Brand Lincoln College Oxford, OX13DR United Kingdom Attn: Michael Brand
Total	0.00 USD
Terms and Conditions	

INTRODUCTION

1. The publisher for this copyrighted material is Elsevier. By clicking "accept" in connection with completing this licensing transaction, you agree that the following terms